UNIVERSIDAD AUTÓNOMA DE MADRID

Programa de Doctorado en Biociencias Moleculares

Estudio del Papel de PGC-1α en Senescencia Celular y Transformación Tumoral

Ignacio Prieto Arroyo

Madrid, 2018

Departamento de Bioquímica

Facultad de Medicina

UNIVERSIDAD AUTÓNOMA DE MADRID

Estudio del Papel de PGC-1α en Senescencia Celular y Transformación Tumoral

Ignacio Prieto Arroyo

Licenciado en Biología

Directora: Dra. María Monsalve Pérez

Instituto de Investigaciones Biomédicas "Alberto Sols"

AGRADECIMIENTOS

Quien me conozca un poco sabrá que aquí no voy a escribir mis mejores líneas. Avisados quedáis si persistís en continuar leyendo estos agradecimientos. Durante esta tesis ha pasado mucha gente por mi vida, parte ya estaban, otros llegaron después y algunos hicieron escala durante este tiempo. A todos, ¡gracias!

A la **Dra. María Monsalve Pérez** que me acogió en su laboratorio en el verano de 2011 para realizar mi proyecto de fin de carrera. Aquel año en el que terminé mi carrera dio paso a otra estancia en el laboratorio para realizar el trabajo fin de máster para luego comenzar el doctorado del que es fruto esta tesis. Han sido muchos años bajo tu tutela en los que he aprendido mucho y, creo, he mejorado como científico.

A mi tutor, el **Dr. Ignacio Palmero Rodríguez**, por su paciencia y estar siempre dispuesto a realizar todos los trámites que el programa de doctorado ha preparado para nosotros en estos últimos años.

Al **Dr. Alberto Zambrano**, por ayudarme con los experimentos de daño en el ADN; al **Dr. Antonio Martínez Ruiz** y al **Dr. Pablo Hernansanz**, por ayudarme con el Seahorse, al **Dr. Sebastián Cerdán**, por todas sus clases magistrales sobre metabolismo y RMN; a la **Dra. Mariona Jové**, por la ayuda con la espectrometría de masas; y a **Leti**, por su grandísima ayuda en el animalario.

A todos mis **compañeros de laboratorio** que han pasado durante todos estos años por el 1.3.2 aunque sea a compartir unas pocas semanas. Haciendo memoria me han salido 25 nombres, que no pondré a riesgo de dejarme alguno… Siempre ha reinado el buen ambiente en el laboratorio, y eso dice mucho de vosotros porque para aguantarme… ¡Gracias!

Aunque todos sois importantes, quiero agradecer individualmente a **Brigitte**, por ser quien me enseñó a trabajar por primera vez en un laboratorio. A **Cris**, mi gran compañera y amiga dentro del laboratorio, en este tiempo he compartido grandes momentos como tu tesis, tu boda y… ¡lo que está por venir! Y a **Carmen**, mi primera pikachu (llamada así por voluntad propia) y que parte de su trabajo está plasmado en esta tesis. ¡Muchas gracias y mucha suerte!

A mis **compañeros del IIBm**, los que siguen y los que ya se fueron del centro, por todos los buenos ratos dentro de estas paredes, las del Montoya y las del Karaoke. También es una larga lista de gente que incluye **Pistachos**, **Palmeritas**, el gran personal de servicios que hay en este centro y varios jugadores ocasionales de fútbol sala. ¡Muchas gracias!

A todos los amigos que hice en la facultad. A los seguidores, hooligans quizá, de **Rosalind Franklin** con los que compartí clases, prácticas, quedadas, un gran viaje al Algarve y muchas anécdotas; al gran **Bio 5.3**, aunque no nos acompañaron las victorias nos sobraron ganas de jugar juntos; y,

especialmente, al gran **Blastogrupo**, somos "especiales" en todas sus acepciones, pero cinco minutos con vosotros bastan para olvidarte de todo y reír durante horas. Sois la mejor terapia y espero manteneros en mi vida el mayor tiempo posible, aunque nos dispersemos por el globo. ¡Muchas gracias a todos!

A mis amigos **tricantinos**. El instituto es una de las mejores épocas de la vida, que nunca se olvida. Muchos recuerdos son en torno a un balón y como fuimos formando un verdadero equipo, primero en **Dycec** y luego **La Roma**. Nos hemos visto crecer y lograr objetivos marcados en nuestras vidas. ¡Seguid así! ¡Gracias!

A todos mis compañeros del club de corredores **IronSport 3c**, porque del deporte se aprende mucho y yo he aprendido con vosotros que con trabajo y sacrificio se pueden lograr los retos "imposibles" que te propongas. Eso sí, siempre es más fácil si te diviertes como en todos los entrenamientos y carreras compartidas con vosotros. ¡Muchas gracias! ¡Por más retos en el futuro!

A mi **familia**, por interesaros por cómo va mi doctorado y mi trabajo en el laboratorio, aunque muchas veces no sea fácil de entender todo lo que os cuento. A los que están y a los que nos han dejado, pero no olvidamos.

A mi **hermano**. Porque estás ahí desde que nací y estarás ahí hasta el final. Desde pequeño te seguía con admiración y tú te las ingeniabas para sacar provecho de la situación… Siempre hemos sido buenos hermanos y ojalá que continúe así muchos años. ¡Gracias!

A mis **padres**, por la educación que nos disteis, por el equilibrio perfecto entre libertad y exigencia que nos ha hecho como somos hoy en día siguiendo vuestro gran ejemplo. Espero que estéis orgullosos de vuestros hijos. ¡Muchas gracias!

A **Sara**, mi compañera de viaje, por aguantar esta tesis que se ha alargado más de lo que tú deseabas, pero que marca el principio de otra etapa de nuestro viaje juntos. ¡Que no acabe y que no deje de sorprendernos!

RESUMEN

Las células tumorales tienen marcadamente reducido el metabolismo oxidativo del piruvato en el ciclo de los ácidos tricarboxílicos y producen grandes cantidades de lactato a partir de la glucosa aun en condiciones aerobias, en contraposición con las células no tumorales. Este cambio es conocido como Efecto Warburg y se produce por una bajada en la capacidad de síntesis de ATP acoplada a la actividad de la cadena de transporte de electrones y, además, se genera una mayor producción mitocondrial de especies reactivas del oxígeno en células tumorales asociada a la baja actividad del metabolismo oxidativo. PGC-1α es un coactivador transcripcional y regulador clave de la biogénesis mitocondrial, el metabolismo oxidativo y los mecanismos en respuesta al estrés oxidativo mitocondrial.

Para valorar el papel de PGC-1α en el proceso de oncogénesis y analizar los posibles mecanismos implicados, se realizó un estudio *in vitro* en el que se replicó el proceso tumoral utilizando como modelo experimental Fibroblastos Embrionarios de Ratón. El modelo experimental consta de dos partes, en la primera se realizaron pases seriados de las células primarias hasta que estas indujeron la entrada en senescencia o la muerte celular y en la que se ha valorado el estrés oxidativo, el daño en el ADN y la inducción de marcadores de senescencia y el tiempo de inmortalización. La segunda parte del modelo se centró en estudiar las células inmortalizadas previamente en el contexto de Efecto Warburg y transformación tumoral, tanto *in vitro* como *in vivo*.

Los resultados obtenidos muestran que, en ausencia de PGC-1α, se produce una mayor inestabilidad genómica asociada a la oxidación del ADN por la generación de especies reactivas del oxígeno en la mitocondria. Esta mayor inestabilidad produce una entrada prematura en senescencia y una inmortalización temprana en ausencia de PGC-1α. Cuando se analizan los cultivos celulares inmortalizados, se observa que en ausencia de PGC-1α el metabolismo celular es más glucolítico y menos oxidativo respecto a los controles. Además, la deficiencia de PGC-1α induce la biosíntesis de macromoléculas, en especial de los ácidos grasos; y el uso anaplerótico de varios sustratos metabólicos, como la glucosa y la glutamina. Estas diferencias obtenidas al estudiar su metabolismo se correlacionan con un fenotipo tumoral más agresivo. En ausencia de PGC-1α aumenta la supervivencia, la capacidad de proliferar y la migración *in vitro* y se generan tumores más grandes y con más células proliferativas al ser inyectados los fibroblastos inmortalizados. También, se forman más nódulos pulmonares al ser inoculados junto a células de melanoma murino.

Estos resultados sugieren que PGC-1α juega un importante papel como supresor tumoral mediado por su función de regulador clave del metabolismo oxidativo y del estrés oxidativo.

SUMMARY

Tumor cells poorly oxidize pyruvate through tricarboxylic acids cycle but produce lactate from glucose even in aerobic conditions, in opposition with normal cells. This metabolic switch is named Warburg Effect and is caused by a drop in the ATP synthesis coupled to electronic transport chain and, in addition, higher amounts of reactive oxygen species are generated in tumor cells associated with a lower oxidative metabolism. PGC-1α is a transcriptional coactivator and master regulator of mitochondrial biogenesis, oxidative metabolism and oxidative stress response.

To elucidate the role of PGC-1α in oncogenesis and analyze possible mechanisms involved, we carried out an *in vitro* assay with Mouse Embryonic Fibroblast as an experimental model. The assay is composed of two defined parts. First, we made serial passages until cultures reach cellular senescence or cell death and we analyze oxidative stress, DNA damage, induction of senescence markers and immortalization time. The second part of the assay focuses in the previous immortalized cells in the context of Warburg Effect and tumor transformation, both *in vitro* and *in vivo*.

Our results show that, in absence of PGC-1α, higher genomic instability is produced and is associated with DNA oxidation by mitochondrial reactive oxygen species. Genomic instability causes a premature cellular senescence induction and earlier immortalization time in absence of PGC-1α. When immortalized cell cultures are analyzed, a more glycolytic and less oxidative metabolism is seen in fibroblast without PGC-1α. In addition, the absence of PGC-1α induces macromolecular biosynthesis, fatty acids primarily; and an anaplerotic use of different metabolic substrates, such as glucose and glutamine. These differences correlate with a more aggressive tumor phenotype. In absence of PGC-1α, survival, proliferation capacity and migration *in vitro* increases as well as bigger and more proliferative tumors when immortalized fibroblasts were injected in mice. Also, more lung metastases are generated when are coinoculated simultaneously with murine melanoma cells.

These results suggest that PGC-1α play an important role as tumor suppressor mediated by its role as a key regulator of oxidative metabolism and oxidative stress.

.

ÍNDICE

CLAVE DE ABREVIATURAS

Abreviatura	Significado
4-HNE	4-Hidroxinonenal
8-OH-dG	8-hidroxi-deoxiguanosina
AA	Ácido Araquidónico
ACC	Acetyl-CoA Carboxylase
Ac-CoA	Acetil-CoenzimaA
ACL	Longitud media de la cadena de carbonos
ACLY	ATP Citrate Lyase
AMPK	AMP-activated Protein Kinase
ATM	Ataxia-Telangiectasia Mutated
ATR	ATM- and Rad3-related
ATRX	ATP-dependent helicase
BAD	Bcl-2-associated death promoter
BRCA1	Breast Cancer 1
BSA	Albumina de Suero Bovino
BTLA	B and T lymphocyte attenuator
CDK	Cyclin-Dependent Kinase
cit C	citocromo C
CSC	Célula Madre del Cáncer
D_2O	Agua Deuterada
DAPI	4-6-diamino-2-fenilindol
DAXX	Death Domain Associated Protein
DBI	Índice de dobles enlaces
DDR	Focos de respuesta a daño en ADN
DGLA	Ácido Dihomo-γ-linolénico
DIC	Differential Interference Contrast
Dll4	Delta-like 4
DMEM	Medio de Eagle modificado por Dulbecco
EGFR	Epidermal Growth Factor Receptor
ERK	Extracellular signal-regulated Kinase
ERRα	Estrogen-related Receptor α
ETC	Cadena de Transporte de Electrones
FAS	Fatty Acid Sythase
FBS	Suero Bovino Fetal
FGFR	Fibroblast Growth Factor Receptor
FH	Fumarato Hidratasa
FOXO	Forkhead box O transcription factor
GFP	Proteína Verde Fluorescente
Gls1	Glutaminasa 1
Gls2	Glutaminasa 2
GLUT	Glucose Transporters
GS	Glutamina sintetasa
HCF	Host Cell Factor
HEK293T	Células embrionarias de riñón humano que contienen el antígeno T del virus SV40
HIF-1	Hypoxia Inducible Factor 1
HK	Hexoquinasa

IDH	Isocitrato Deshidrogenasa
IGFR	Insulin-like Growth Factor Receptor
IR	Insulin Receptor
JNK	c-Jun N-terminal Kinase
LDH	Lactato Deshidrogenasa
L-Gln	L-Glutamina
MAPK	Mitogen-activated Protein Kinase
MCT1	Monocarboxylate transporter 1
MDM2	Mouse double minute 2
ME	Enzima Málica
MEF	Fibroblastos Embrionarios de Ratón
M-MLV	Moloney-murine Leukemia Virus Reverse Transcriptase
MnSOD	Superóxido Dismutasa Manganésica
MON	Ácidos Grasos Monoinsaturados
mTOR	mammalian Target of Rapamycin
mTORC1	mTOR Complex 1
mTORC2	mTOR Complex 2
NFR	Nuclear Fast Red
NOD-SCID	Non-obese Diabetic portador de la mutación SCID
NOX	NADPH Oxidasa
NRF1	Nuclear Respirtory Factor 1
NRF2	Nuclear Respirtory Factor 2
O/N	Toda la noche
OA	Ácido Oleico
OAA	Oxalacetato
P/S	Penicilina/Estreptomicina
PBS	Tampón Fosfato Salino
PCx	Piruvato Carboxilasa
PDGFR	Platelet-derived Growth Factor Receptor
PDH	Piruvato Deshidrogenasa
PDK	PDH Quinasa
PDK1	Phosphoinositide-dependent Kinase 1
PFA	Paraformaldehido
PFK1	Fosfofructo Quinasa 1
PFKFB3	Fructosa-6-fosfato-2-Quinasa/Fructosa-2, 6-Bisfosfatasa
PGC-1α	Peroxisome Proliferator-Activated Receptor-γ Coactivator-1α
PGC-1β	Peroxisome proliferator-activated receptor gamma coactivator 1-beta
PGDH	Fosfoglicerato Deshidrogenasa
PGM1	Fosfoglicerato Mutasa 1
PI	Índice de Peroxibilidad
PI3K	Phosphatidylinositol-4,5-bisphosphate 3-kinase
PIP_3	Fosfatidilinositol-3-fosfato
PK	Piruvato Quinasa
PPP	Ruta de las Pentosas Fosfato
PRC	PGC-1-related coactivator
PTEN	Phosphatase and tensin homolog

PUFA	Ácidos Grasos Poliinsaturados
PVDF	Fluoruro de polivinilideno
qPCR	Reacción en cadena de la polimerasa cuantitativa
Rb	Retinoblastoma
RMN	Resonancia Magnética Nuclear
ROS	Especies Reactivas del Oxígeno
RT	Temperatura ambiente
RTK	Receptores Tirosina Quinasa
SAM	S-Adenosil Metionina
SASP	Senescence-associated Secretory Phenotype
SAT	Ácidos grasos Saturados
SA-β-Gal	Actividad β-Galactosidasa asociada a senescencia
SDH	Succinato Deshidrogenasa
SGLT	Sodium-Glucose Transporters
TALDO	Transaldolasa
TBS-T	Tris-Buffer Salino con Tween 20
TCA	Ciclo de los Ácidos Tricarboxílicos
TdT	Terminal Transferasa
TEM	Transición Epitelio-Mesénquima
TERT	Telomerase Reverse Transcriptase
TFAM	Factor de Transcripción mitocondrial A
TFB1M	Factor de Transcripción mitocondrial B1
TFB2M	Factor de Transcripción mitocondrial B2
TGFβ	Transforming Growth Factor β
TGFβR	TGFβ Receptor
TKT	Trasncetolasa
TME	Transición mesénquima-epitelio
TP53BP1	Tumor Protein 53 Binding Protein 1
VEGF	Vascular Endothelial Growth Factor
VEGFR	Vascular Endothelial Growth Factor Receptor
α-KG	α-cetoglutarato

INTRODUCCIÓN

El **cáncer** es la proliferación descontrolada de células, su acumulación evitando la muerte celular y su diseminación por el organismo. Es una de las principales causas de morbilidad y mortalidad en el mundo (Fig. 1). Según el estudio de la Organización Mundial de la Salud GLOBOCAN en 2012 hubo 14 millones de nuevos casos, estimándose un aumento del 70 % en los siguientes 20 años. Se estima que un tercio de los casos de cáncer se debe a uno de los siguientes factores de riesgo: índice de masa corporal elevado, nutrición inadecuada, falta de actividad física, consumo de tabaco y de alcohol (Collaborators 2016). En 2015, ocasionó 8,8 millones de defunciones, siendo el cáncer pulmonar el tipo de cáncer que más provoca. Además, el impacto económico de la enfermedad se estimó en 1,16 billones de dólares en el año 2010. Su elevado coste limita el acceso al tratamiento en muchos casos, principalmente en países en vías de desarrollo donde se registran las mayores tasas de mortalidad (McGuire 2016).

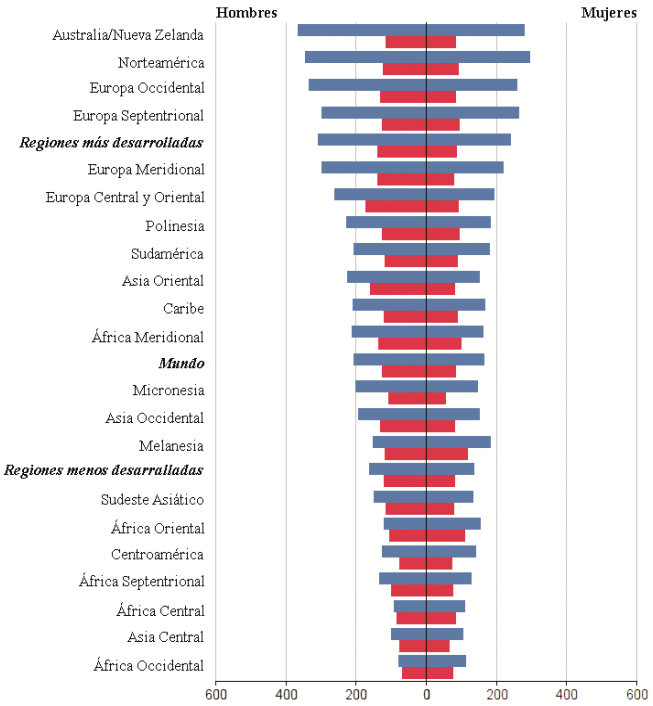

Figura 1. Morbilidad (barras azules) y mortalidad (barras rojas) en cáncer, separado por sexo en diferentes regiones geográficas. Representado como nuevos casos de cáncer o defunciones, respectivamente, por cada 10^5 habitantes. Fuente: Organización Mundial de la Salud.

Desarrollo Tumoral y Características de las células tumorales.

El **desarrollo tumoral** comienza con una mutación en una célula que hace que se divida de manera aberrante. Esto no implica que ésta adquiera todas las características de una célula tumoral desde el principio, sino que se trata de un proceso de varias etapas de mutación y selección clonal debido a la adquisición de ventajas adaptativas por las células descendientes. Frente a la proliferación aberrante existen mecanismos de respuesta, como son la senescencia celular, caracterizada por la parada irreversible de la división celular, o la inducción de la muerte celular. Sin embargo, una vez inducidos estos mecanismos, algunas células son capaces de sortearlos y proliferan libremente. La acumulación de dichas

células origina una hiperplasia, es decir, un aumento significativo del número de células en un tejido. A medida que ocurre la selección clonal en la población de células, éstas pierden su apariencia original y se genera una desestructuración tisular conocida como displasia, y finalmente, se origina un tumor primario. Cuando el tumor primario ha sido vascularizado y las células tumorales han sido objeto de un proceso de desdiferenciación, en el que las células epiteliales pierden polaridad y uniones adherentes entre células; y ganan la habilidad de migrar e invadir, llamado transición epitelio-mesénquima (TEM), las células tumorales pueden viajar por el torrente sanguíneo y originar un tumor secundario en otro tejido u órgano del organismo (Fig. 2).

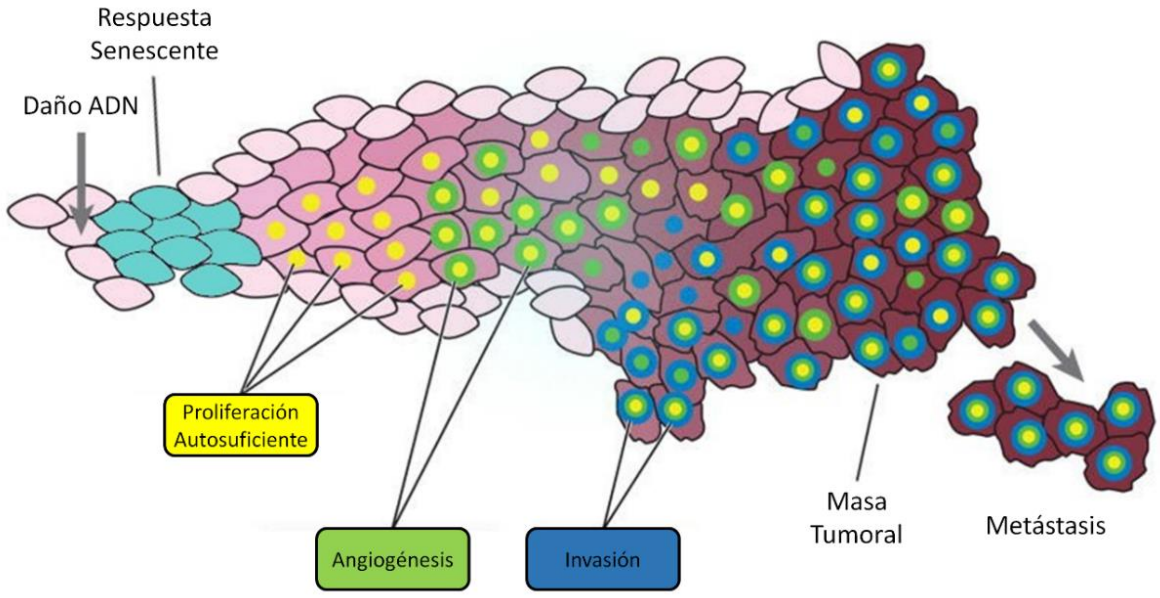

Figura 2. Esquema de la progresión tumoral. Editado de Salk et al., 2010.

Las células tumorales tienen varias **cualidades o características distintivas** respecto a las células normales, no tumorales: capacidad de proliferación ilimitada, crecimiento en ausencia de señales proliferativas, insensibilidad a las señales que normalmente inhiben el crecimiento, ausencia de respuesta a señales endógenas o exógenas de muerte celular (apoptosis), escape a la identificación por el sistema inmunitario, producción de factores proangiogénicos y alta capacidad de migración e invasión. Estas características se asocian, a través de mecanismos solo parcialmente comprendidos, a cambios notables en la actividad metabólica respecto a las células normales y a una gran inestabilidad genómica. Además, el organismo que soporta el crecimiento tumoral activa un programa de defensa inflamatorio que puede controlar a veces el crecimiento tumoral pero también favorecerlo por el aprovechamiento de las células tumorales de las señales proinflamatorias como estímulos proliferativos (Hanahan and Weinberg 2011).

La inestabilidad génica y la inflamación promueven la selección clonal durante la tumorogénesis.

Dos de estas características habilitan la aparición de las demás. La primera de las características habilitantes es la **inestabilidad genómica**. La inestabilidad se va estableciendo de manera gradual y pasa por varias etapas características en las que se van acumulando mutaciones (Mahale et al. 2008; Rangarajan et al. 2004) y modificaciones epigenéticas (Fraga et al. 2005; Paz et al. 2002) que tienen como resultado el establecimiento de cambios beneficiosos para el desarrollo tumoral. En general, las células tumorales presentan una mayor tasa de mutación debido, en parte, a una menor eficacia en la activación de los mecanismos de reparación, reduciéndose la sensibilidad al daño en el ADN, perdiéndose total o parcialmente la capacidad de activar cascadas de señalización como las que implican a las quinasas *Ataxia Telangiectasia-mutated* (ATM) y *ATM and Rad3 related* (ATR) (Darlington et al. 2012; Mandriota et al. 2015; Y. Xu et al. 1996); y a que se reducen, también, gran parte de los mecanismos de reparación del ADN (Escribano-Diaz et al. 2013). Es frecuente, por ejemplo, la perdida de la recombinación homóloga mediada por *Breast Cancer 1* (BRCA1) (Yun and Hiom 2009) lo que favorece la reparación no conservativa mediante recombinación no homóloga en la que participa *tumor protein 53 Binding Protein 1* (TP53BP1) (Bunting et al. 2010; Callen et al. 2013). Además, no inducen muerte celular ni parada del ciclo celular en respuesta a señales de daño al ADN (Z. Zhao et al. 2010), un contexto celular que en condiciones normales induciría apoptosis o la entrada en senescencia.

La segunda de las características tumorales habilitantes es que se establece un estado de **inflamación** inducido por el tumor que facilita la aparición del resto de las características distintivas tumorales. Múltiples evidencias indican que el infiltrado inflamatorio en tumores juega un importante papel promotor del desarrollo tumoral (Greten et al. 2004; He et al. 2012; Pikarsky et al. 2004). Las células infiltradas del sistema inmunitario producen citoquinas que actúan como factores de crecimiento y que promueven la proliferación de células tumorales (Garcia-Hernandez et al. 2002; He et al. 2012; Meng et al. 2006; Zhu et al. 2014) y su supervivencia (Garcia-Hernandez et al. 2002; Kulbe et al. 2007; Meng et al. 2006; Zeng et al. 2010). Además, colaboran en la producción e inducción de factores proangiogénicos necesarios para aumentar el acceso a los nutrientes del tumor en desarrollo (S. P. Huang et al. 2004; Kulbe et al. 2007; Zeng et al. 2010), así como en la producción de enzimas que modifican la matriz extracelular, favoreciendo la migración de las células tumorales y la aparición de la metástasis (Kinoshita et al. 2013; Zergoun et al. 2016) y señales que inducen la TEM (Ellenrieder et al. 2001).

Adquisición de ventajas proliferativas en progresión tumoral.

La **proliferación celular sostenida** es un factor clave en la progresión tumoral. Para mantener la proliferación de manera continuada, los tejidos tumorales necesitan de tres de las llamadas características

distintivas tumorales: capacidad de replicación ilimitada, mantenimiento de la señalización proliferativa aun en ausencia de factores de crecimiento y falta de respuesta a las señales supresoras de crecimiento.

El mantenimiento de la estabilidad génica depende de muchos factores, pero el más importante es el mantenimiento de los telómeros, estos son secuencias de nucleótidos repetidas en los extremos de los cromosomas, cuyo mantenimiento requiere de una maquinaria distinta a la de la replicación del resto del material genómico, siendo esencial la llamada enzima telomerasa, una proteína de unión a ARN, que sintetiza copias del llamado ADN telomérico usando su ARN molde como guía (Bodnar et al. 1998). La actividad de la telomerasa suele ser alta en células embrionarias y células madre de distintas estirpes, pero se inhibe con el proceso de diferenciación llegando su actividad a ser prácticamente indetectable en muchos tipos celulares diferenciados. Esto hace que con cada división celular se produzca un acortamiento telomérico (Harley et al. 1990). Cuando la longitud telomérica es tan corta que amenaza la estabilidad génica se inducen señales celulares de parada de ciclo (Harley et al. 1990) y de entrada en senescencia celular. El estado senescente puede ser sorteado debido a señales oncogénicas y las células pueden volver a proliferar, aunque los telómeros continúan siendo cortos y se produce un estado de crisis en el que se mezclan señales antagónicas: proliferativas y senescentes, que resultan en la inducción de la apoptosis. Finalmente, alguna de las células en estado de crisis puede superar dicho estado e inmortalizar, y para ello necesitan activar mecanismos que mantengan y elonguen los telómeros.

El mecanismo fundamental que permite la proliferación ilimitada en células tumorales es la reactivación de la actividad telomerasa (N. W. Kim et al. 1994). Observaciones realizadas en múltiples tipos tumorales (F. W. Huang et al. 2013; Killela et al. 2013), han llevado a proponer que la reactivación de la enzima telomerasa en cáncer se produce fundamentalmente gracias a la acumulación de mutaciones en el promotor del gen de la telomerasa (*Telomerase Reverse Transcriptase* (TERT)), que resultan en un aumento en sus niveles de expresión génica. Estas mutaciones aumentan el reclutamiento a las regiones promotoras de TERT de varios factores de trascripción activadores (Bell et al. 2015; Hsu et al. 2015), lo que resulta en un aumento de su expresión.

Es importante reseñar que, aunque todos los tumores consiguen reactivar mecanismos de mantenimiento telomérico, no en todos los casos estos dependen de la actividad telomerasa. Entre un 10 y un 15 % de los tumores no presentan expresión detectable de la telomerasa, lo que hace evidente la existencia de mecanismos alternativos involucrados en el mantenimiento telomérico (Heaphy et al. 2011b). Así, por ejemplo, se ha descrito la elongación de los telómeros mediante procesos de recombinación (Dunham et al. 2000) en tumores que presentan mutaciones en *ATP-dependent helicase* (ATRX) y *Death Domain Associated Protein* (DAXX) (Heaphy et al. 2011a; Lovejoy et al. 2012), dos proteínas que se requieren para el mantenimiento de la estructura de la cromatina en las regiones teloméricas.

En células no tumorales la respuesta ante señales proliferativas está firmemente regulada para mantener la homeostasis tisular. Sin embargo, en células tumorales se produce una **alteración en la regulación de las señales proliferativas**. Las señales de crecimiento están, generalmente, mediadas por

receptores de membrana tirosina quinasa (RTK). Los RTK son una familia de receptores de membrana, que actúan como receptores de factores de crecimiento, citoquinas y hormonas; entre otras señales extracelulares. Comprenden varias subfamilias entre las que se encuentran: *Epidermal Growth Factor Receptors* (EGFR), *Fibroblast Growth Factor Receptors* (FGFR), el receptor de insulina (IR), *Insulin-like Growth Factor Receptor* (IGFR), *Platelet-derived Growth Factor Receptors* (PDGFR) y *Vascular Endothelial Growth Factor Receptors* (VEGFR) entre otros. Se activan por dimerización inducida por ligando, que resulta en autofosforilación del receptor (Regad 2015). Los RTK activan vías de señalización relacionadas con proliferación, diferenciación, supervivencia y migración, entre las que se encuentran las vías de Ras/*Mitogen-activated Protein Kinase* (MAPK) y de *Phosphatidylinositol-4,5-bisphosphate 3-kinase* (PI3K)/Akt (Regad 2015).

Está descrito que en células tumorales existe una elevada producción de factores de crecimiento que actúan de manera autocrina (Hata et al. 2011; Hu et al. 2003; Z. Wei et al. 2015b) y paracrina, elevando también la producción de factores de crecimiento por células no tumorales de su entorno (Nickerson et al. 2013). Por otra parte, se acumulan mutaciones en distintos puntos de la cascada de señalización, apareciendo, por ejemplo, receptores constitutivamente activos, que mantienen las rutas activas en ausencia de señalización (Ding et al. 2008).

Ras es una GTPasa pequeña que se activa tras la dimerización de los RTK y, a su vez, activa a Raf, una serina/treonina quinasa que fosforila a las MAPK. La cascada de señalización de las MAPK termina con la activación de numerosas quinasas entre las que están *c-Jun N-terminal Kinase* (JNK), p38 o *Extracellular signal-regulated Kinase* (ERK) (Regad 2015). En cáncer, se estima que el 27 % de los casos están relacionados con una mutación en Ras. Comúnmente, se producen mutaciones que provocan la activación de Ras de manera constitutiva. Además, mutaciones en proteínas activadoras o inhibidoras permiten mantener la activación de Ras en cáncer (Hobbs et al. 2016).

Los RTK también provocan la activación de PI3K, una quinasa que genera fosfatidilinositol-3,4,5-trisfosfato (PIP_3) en la membrana celular. PIP_3 trasloca a Akt a la membrana donde es activada por fosforilación mediante *phosphoinositide-dependent protein kinase 1* (PDK1) y *mammalian Target of Rapamycin* (mTOR) *complex 2* (mTORC2). Tras su activación, Akt fosforila otras proteínas como *mTOR Complex 1* (mTORC1), principal responsable de la activación de las rutas de biosíntesis; *Forkhead box O transcription factors* (FOXO), *Mouse double minute 2* (MDM2), regulador negativo del supresor tumoral p53; y las proteínas apoptóticas BIM y *Bcl-2-associated death promoter* (BAD), inactivándolas; facilitando la supervivencia y la entrada en el ciclo celular. *Phosphatase and Tensin Homolog* (PTEN) al desfosforilar a PIP_3 actúa como un inhibidor de esta vía (Regad 2015). Múltiples trabajos evidencian que tanto PI3K como Akt presentan mutaciones asociadas a cáncer que provocan su hiperactivación. Además, también se han descubierto mutaciones en PTEN que producen su inhibición en tumores (Martini et al. 2014).

Aun con la capacidad de replicarse infinitamente y la amplificación de las señales proliferativas, las células tumorales tienen que **superar los mecanismos inhibidores del ciclo celular** para mantener el crecimiento tumoral. Las principales vías de señalización supresoras de entrada en ciclo celular son las que

implican a las proteínas p53 y Retinoblastoma (Rb) (Fig. 3). Ambos son considerados supresores tumorales, es decir, proteínas que con su acción inhiben la proliferación. p53 es un factor de transcripción que regula el ciclo celular, apoptosis, reparación de ADN y metabolismo. Rb es un importante inhibidor del factor de transcripción E2F, que regula genes involucrados en el ciclo celular.

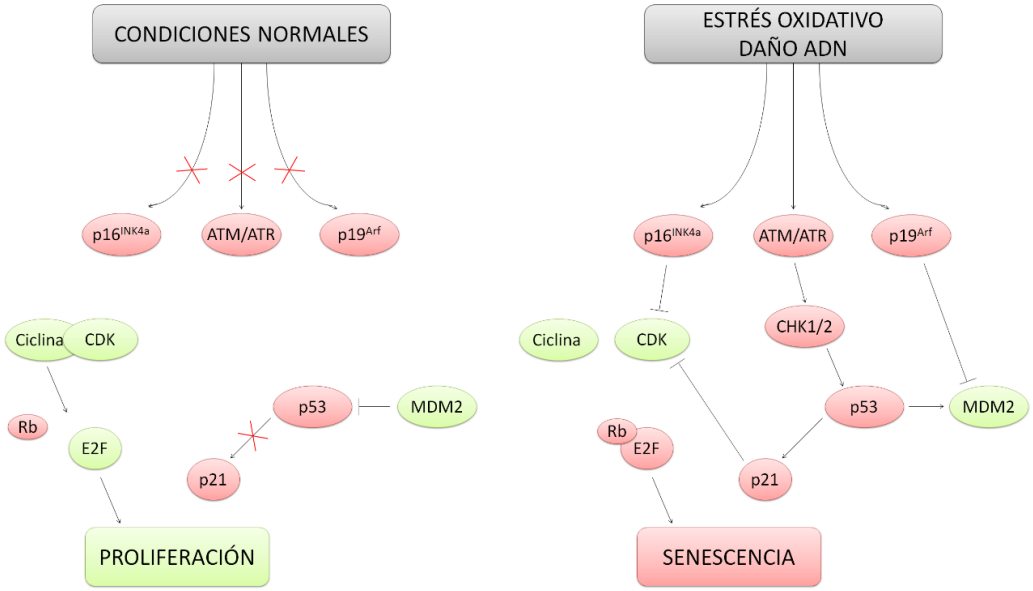

Figura 3. Esquema de la ruta de regulación del ciclo celular por parte de p53 y Rb. Izquierda: Condiciones basales de una célula en proliferación. Derecha: Regulación del ciclo celular en respuesta a estrés oxidativo o inestabilidad genómica.

p53 está regulada por varias proteínas, una de ellas es MDM2, que dirige la ubiquitinización de p53 para su degradación en el proteasoma (Honda et al. 1997). A su vez, MDM2 es regulada por p19, que se une a MDM2 evitando que realice su función (Honda and Yasuda 1999). Además, p53 necesita activarse por fosforilación, principalmente mediante la vía de señalización de ATM (Kodama et al. 2010).

Rb se une, inactivándolo, al factor de transcripción E2F, que normalmente induce la transcripción de genes implicados en la progresión del ciclo celular. Rb es sustrato de *Cyclin-dependent Kinases* (CDK), que fosforilan a Rb evitando su unión a E2F (Berthet et al. 2006). Las CDK están reguladas por varias proteínas, consideradas supresoras tumorales como son p15, p16, p27 o p21, está última ve regulada su expresión por p53, lo que une ambas rutas.

Estos inhibidores de CDK junto a p19 son expresados en condiciones de daño en el ADN o estrés oxidativo (Bieging-Rolett et al. 2016; D. Cheng et al. 2015; Jenkins et al. 2011; B. Liu et al. 2014; Muteliefu et al. 2012; M. Sasaki et al. 2014; Tung and Winn 2011; Y. Wang et al. 2013), para promover el arresto del ciclo celular en dichos contextos celulares.

Por ello, en cáncer aparecen mutaciones en uno o varios de estos supresores tumorales, p53, Rb, p15, p16, p19, p21 o p27 (Flores et al. 1996; Haidar et al. 1995; Hangaishi et al. 1996; Jackson et al. 2002; Oda et al. 2005; Omori et al. 2015; Pellegata et al. 2006); o bien se aumenta la expresión de algunos reguladores negativos, como puede ser MDM2 (Honda et al. 1997).

Supervivencia de las células tumorales ante señales de estrés.

p53 es un factor de transcripción que responde a distintas señales de estrés, como el daño en el ADN, activando genes de respuesta a estrés, entre ellos los de factores implicados en la parada de ciclo e inducción de procesos apoptóticos. Su papel central como supresor tumoral le ha proporcionado el sobrenombre de "guardián del genoma" (Lane 1992).

p53 puede inducir **apoptosis** por dos vías alternativas: la extrínseca que depende de la unión de un factor de muerte presente en el medio extracelular, o en una célula adyacente, a su receptor localizado en la membrana celular (*Death Receptor*) o la intrínseca, también llamada mitocondrial, en la que juega un papel fundamental la familia de los factores Bcl-2, a través de la regulación de la permeabilidad de la membrana mitocondrial externa. Distintos miembros de la familia de Bcl-2 funcionan como factores proapoptóticos, como Bax y Bak, o los miembros de la subfamilia *BH3-only*; y antiapoptóticos, como Bcl-2 y Bcl-xl. En respuesta a un estímulo apoptótico, los miembros de la subfamilia *BH3-only* antagonizan a los miembros antiapoptóticos y/o directamente activan a Bax y Bak, lo que tiene como resultado la formación de poros Bax/Bak en la membrana mitocondrial externa a través de los que se produce la liberación de citocromo C (cit C) al citoplasma, lo que a su vez resulta en la activación de la ruta de las caspasas y la inducción de muerte celular (C. C. Wu and Bratton 2013).

p53 regula la expresión de algunas de las proteínas de la subfamilia *BH3-only* (Nakano and Vousden 2001; Shibue et al. 2003) y miembros proapoptóticos como Bax (Chipuk et al. 2004), por lo que su ausencia en células tumorales favorece que las señales antiapoptóticas inhiban la formación del poro Bax/Bak. Además, la resistencia a la apoptosis en cáncer también está acompañada por una inducción en la expresión de miembros antiapoptóticos de la familia de Bcl-2, como el propio Bcl-2 (McDonnell and Korsmeyer 1991; Strasser et al. 1990); o por una inhibición en la ruta efectora de las caspasas (Gama et al. 2014; Muniz Lino et al. 2014).

Además de la entrada en senescencia celular y la inducción de la muerte celular, existe otro proceso para actuar en respuesta al crecimiento tumoral y es la actuación del sistema inmunitario del organismo, que reconoce las células tumorales y promueve su eliminación de los tejidos. Sin embargo, las células tumorales con baja inmunogenicidad terminan seleccionándose y promoviendo el desarrollo tumoral en un proceso conocido como **edición inmune**. Este proceso se desarrolla en tres fases: eliminación, cuando las células del sistema inmunitario eliminan con éxito las células tumorales; equilibrio,

cuando las células tumorales de baja inmunogenicidad se seleccionan; y escape, cuando las células tumorales acumulan diversas mutaciones que les permiten, evitando al sistema inmunitario, proliferar descontroladamente (Mittal et al. 2014).

El papel protector del sistema inmunitario se pone de manifiesto en la acentuada predisposición de los modelos murinos inmunodeficientes para desarrollar tumores, y de ahí el extensivo uso que se hace de estos modelos para estudios básicos de desarrollo tumoral (Shankaran et al. 2001). Así mismo, células tumorales que han crecido en ratones silvestres tienen mayor éxito formando un nuevo tumor al inyectarlas en otros ratones silvestres que aquellas células provenientes de tumores formados en ratones inmunosuprimidos (Shankaran et al. 2001), evidenciando que el contexto inmunitario en el que se forman los tumores tiene una incidencia en su crecimiento secundario.

Los mecanismos por los que las células tumorales seleccionadas superan la fase de equilibrio son diversos. Algunos guardan relación con otras características distintivas tumorales como el aumento de señales antiapoptóticas (McDonnell and Korsmeyer 1991), pero otros afectan directamente a la actividad inmunitaria, como el aumento en la secreción de citoquinas inmunosupresoras (Garcia-Hernandez et al. 2002; Kulbe et al. 2007), la perdida de expresión en la membrana de antígenos reconocibles por el sistema inmunitario (DuPage et al. 2012; Matsushita et al. 2012) o la sobreexpresión de proteínas con actividad inmunosupresoras como CD73 (Jin et al. 2010) o *B and T lymphocyte attenuator* (BTLA) (Hobo et al. 2012).

Vascularización del tejido tumoral e invasión de otros tejidos.

Las células tumorales, como todas las células del organismo, para su supervivencia necesitan tener **acceso al sistema vascular**, que proporciona nutrientes y elimina residuos. Los tumores iniciales, generalmente, no están vascularizados, por lo que se genera un núcleo apoptótico en la zona interna del nódulo, y el tumor prolifera en su zona superficial. La hipoxia que sufre el tumor induce la expresión del factor de transcripción *Hypoxia-inducible Factor-1* (HIF-1), que promueve la expresión de una gran cantidad de mediadores angiogénicos como *Vascular Endothelial Growth Factor* (VEGF) (Y. Yang et al. 2013).

La angiogénesis es dirigida por células endoteliales conocidas como *tip cells* capaces de migrar mediante estímulos químicos (Gerhardt et al. 2003). Siguiendo a dichas células aparecen las denominadas *stalk cells* capaces de proliferar para formar el nuevo vaso (Gerhardt et al. 2003). La formación de estos dos tipos de células endoteliales está regulada por la vía de VEGF y Notch, un receptor de membrana que activa genes de diferenciación, proliferación y supervivencia. Existe un gradiente de VEGF con mayor concentración en las *tip cells*. La cascada de señalización iniciada por VEGFR hace que se active *Delta-like 4* (Dll4), ligando del receptor Notch. Cuando Notch, presente en las *stalk cells*, se une a Dll4 se libera el dominio intracelular de Notch, que se trasloca al núcleo actuando como un regulador transcripcional (Blanco and Gerhardt 2013).

Como se ha mencionado antes, algunos tipos celulares del microambiente tumoral son capaces de secretar factores proangiogénicos (S. P. Huang et al. 2004; Kulbe et al. 2007) e incluso las células tumorales los producen de manera autocrina (Chatterjee et al. 2013) para promover la angiogénesis en respuesta a la hipoxia. La densidad de la microvasculatura aumenta y estos nuevos vasos suelen ser inmaduros y no presentan una cobertura normal de pericitos (Blanco and Gerhardt 2013).

Además de la formación de nuevos vasos, los tumores inducen alteraciones en la vasculatura preexistente en el tejido. Así, por ejemplo, se induce la cooptación de vasos (Passalidou et al. 2003; Sardari Nia et al. 2007), la formación de aneurismas (Oliveira de Oliveira et al. 2014) y la formación de estructuras parecidas a vasos por las propias células tumorales (El Hallani et al. 2010; W. Sun et al. 2012).

Esta vasculatura acelera el crecimiento del tumor al permitir su mejor acceso a nutrientes y eliminación de toxinas, pero además facilita los procesos de **migración e invasión** tumoral a otros tejidos. Es un proceso complejo y que comprende varias fases: invasión del tejido local, intravasación, circulación por el torrente sanguíneo, extravasación y colonización del nuevo tejido u órgano.

La capacidad de las células tumorales de invadir con éxito otros tejidos depende de la adquisición de una serie de características como capacidad migratoria, remodelado tisular y supervivencia en ausencia de anclaje a sustrato, que a nivel molecular se asocian a la TEM. En la fase de colonización este proceso se revierte, en la denominada transición mesénquima-epitelio (TME) que favorece la supervivencia de la célula tumoral y que pone de manifiesto la plasticidad característica de las células tumorales, necesaria para el éxito del proceso metastático.

La inducción de TEM en el entorno tumoral se estimula de manera paracrina mediante la producción aumentada de dos factores clave, la citoquina *Transforming Growth Factor* β (TGFβ) y las proteínas señalizadoras Wnt por parte de las células tumorales y por parte de las células del ambiente tumoral (Bonde et al. 2012; Labelle et al. 2011; Nishimura et al. 2012). Los receptores de TFGß (TGFβ-R) y de Wnt, inician cascadas de señalización que culminan en la inducción de varios factores de transcripción clave, como Snail (Cano et al. 2000), Slug (Savagner et al. 1997), SOX4 (Vervoort et al. 2013), ZEB1/deltaEF1 (Eger et al. 2005), ZEB2/SIP1 (Comijn et al. 2001), Twist (Howe et al. 2003; J. Yang et al. 2004). Además, la ruta de Wnt culmina con la translocación de β-catenina desde las uniones adherentes célula-célula, características de células epiteliales, al núcleo donde ejerce también como factor de transcripción (Hlubek et al. 2007), Estos factores tienen todos ellos un papel importante en el desarrollo embrionario, donde la migración juega un papel fundamental. Estos factores de transcripción reprimen la expresión de E-cadherina, un importante mediador de las uniones intercelulares (Cano et al. 2000; Fukagawa et al. 2015; Guaita et al. 2002; Shirakihara et al. 2007) e inducen la expresión de enzimas que degradan la matriz celular (Cui et al. 2014; L. Sun et al. 2008), N-cadherina, vimentina o fibronectina (Vervoort et al. 2013), proteínas presentes en las uniones entre la célula tumoral y la matriz extracelular o células del entorno tumoral (Hulit et al. 2007; C. Y. Liu et al. 2015) que promueven la migración celular .

Cambio metabólico característico de las células tumorales.

Las células diferenciadas, no proliferativas, dependen de la eficiencia en la producción de ATP para su supervivencia. Por ello, metabolizan la glucosa a piruvato mediante la glucolisis en el citoplasma y oxidan completamente la mayoría de este piruvato a CO_2 mediante el ciclo de los ácidos tricarboxílicos (TCA) de la mitocondria, donde el oxígeno es el aceptor final de una cadena de transporte de electrones (ETC) que genera un gradiente electroquímico que facilita la síntesis de ATP por la ATP sintasa.

Sin embargo, ya a mitad del siglo XX, Otto Warburg observó que las células tumorales producían grandes cantidades de lactato a partir de la glucosa, porque el piruvato no se metabolizaba de manera oxidativa en el ciclo TCA, aun en condiciones aerobias, a este efecto se le denominó Efecto Warburg (Warburg 1956a, 1956b). En los últimos años, la hipótesis de Warburg ha sido el foco de un enorme interés científico, y ha sufrido múltiples revisiones. Hasta donde llega el consenso, podemos decir que hay un importante cambio metabólico asociado a la progresión tumoral. Este cambio metabólico se caracteriza por una mayor entrada de nutrientes en la célula, especialmente de glucosa y glutamina, y que la glucolisis y el ciclo TCA sirven fundamentalmente para producir precursores biosintéticos. Además, algunos de los metabolitos generados participan tanto en la regulación génica como en interacciones con células del ambiente tumoral (Pavlova and Thompson 2016) (Fig. 4).

El primer cambio metabólico que se produce en el metabolismo de las células tumorales es la **inhibición de la ETC**. Existen varios mecanismos por los que la actividad de la ETC disminuye. Numerosos estudios relacionan mutaciones en el ADN mitocondrial, que contiene los genes más importantes de la cadena de transporte de electrones, relacionadas con una inhibición de la ETC con un mayor riesgo de padecer cáncer (K. Ishikawa et al. 2008; Parrella et al. 2001). También pueden producirse mutaciones en *Mitochondrial Transcription Factor A* (TFAM), regulador transcripcional de las proteínas involucradas en el metabolismo oxidativo (J. Guo et al. 2011; Han et al. 2011) y en proteínas clave en la replicación y transcripción del ADN mitocondrial como la helicasa SUV3 (Chen et al. 2013). Además, aparecen otras mutaciones en enzimas clave del metabolismo oxidativo mitocondrial, que forman parte del ciclo TCA, como son la Succinato Deshidrogenasa (SDH), que transforma el succinato en fumarato (Bardella et al. 2011; Baysal et al. 2002; Ricketts et al. 2012); la Fumarato Hidratasa (FH), que transforma el fumarato en malato (Castro-Vega et al. 2014; Frezza et al. 2011); y la Isocitrato Deshidrogenasa (IDH), que transforma el isocitrato en α-cetoglutarato (α-KG) (Dang et al. 2016).

Este bloqueo de la ETC hace que las células tumorales necesiten inducir rutas citosólicas menos eficientes en la producción de ATP como la glucolisis seguida por la reducción del piruvato a lactato. El primer efecto del uso obligado de estas rutas es un **incremento en el flujo metabólico**, incrementándose la entrada de glucosa y glutamina en la célula. Además, las células tumorales suelen mostrar signos de estrés metabólico debido a sus altas tasas proliferativas, lo que activa mecanismos oportunistas o alternativos, para la obtención de nutrientes como la macropinocitosis de proteínas (Commisso et al. 2013;

Kamphorst et al. 2015; Palm et al. 2015), exosomas (Nakase et al. 2015) y ATP (Qian et al. 2014; Qian et al. 2016); la entosis de células vivas (Krajcovic et al. 2013; Q. Sun et al. 2014); la fagocitosis de cuerpos apoptóticos (Krajcovic et al. 2013); e incluso pueden inducir procesos de autofagia para asegurar la supervivencia, aun comprometiendo la proliferación al no haber aumento de biomasa (J. Y. Guo et al. 2013; Karsli-Uzunbas et al. 2014; Strohecker et al. 2013).

La entrada de la glucosa en la célula se realiza mediante dos tipos de transportadores: un simportador de Na^+ y glucosa (SGLT) dependiente del gradiente de Na^+ y los transportadores específicos de glucosa (GLUT). Tanto la expresión de los transportadores SGLT (Casneuf et al. 2008; Helmke et al. 2004; N. Ishikawa et al. 2001) como los GLUT (F. R. Ayala et al. 2010; Carvalho et al. 2011; Chandler et al. 2003; Semaan et al. 2011) se encuentra comúnmente aumentada en diferentes tipos de cáncer, aunque los transportadores GLUT han sido los más ampliamente estudiados.

Así, por ejemplo, se han descrito al menos tres mecanismos que aumentan en tumores la expresión de GLUT1 por alteraciones en distintos puntos de las cascadas de respuesta a factores de crecimiento: la activación constitutiva de los receptores tirosina quinasa, la activación de Ras y la activación de la quinasa AKT dependiente de la quinasa PI3K, produciéndose tanto un aumento en los niveles de expresión de la proteína como su traslocación hacia la membrana celular (C. Y. Lin et al. 2013a; H. Sasaki et al. 2012; Wieman et al. 2007). La activación de las cascadas en respuesta a factores de crecimiento hace que se active mTORC1, componente clave en la señalización de la supervivencia y proliferación celular así como de las rutas de biosíntesis de macromoléculas (Populo et al. 2012). La activación de mTORC1 induce la expresión de GLUT1 (Buller et al. 2008) y, además, también es activado en respuesta a la ausencia de glucosa en la célula (Miniaci et al. 2015). Además, se producen cambios en los niveles o actividad de varias enzimas implicadas en el proceso glucolítico, como la inducción de la enzima hexoquinasa (HK) (Zhuo et al. 2015), que fosforila la glucosa entrante dando lugar a glucosa-6-P y permitiendo que continúe el flujo de glucosa hacia el interior celular a favor de concentración.

Tras su entrada en la célula, la glucosa es transformada en 2 moléculas de piruvato mediante las reacciones que forman parte de la glucolisis, obteniéndose un rendimiento neto de 2 moléculas de NADH y 2 de ATP a partir de 2 de NAD^+, 2 de ADP y 2 de Pi. La enzima responsable de la última reacción de la glucolisis, que media la transformación del fosfoenolpiruvato en piruvato, es la Piruvato quinasa (PK) y tiene cuatro isoformas. PKL, presente en el hígado; PKR, en eritrocitos; PKM1, en células diferenciadas de varios tejidos; y PKM2, en células en proliferación (P. Wang et al. 2015a). En células tumorales se expresa la isoforma PKM2 (Christofk et al. 2008; Mazurek et al. 2005), que necesita formar un tetrámero para realizar su actividad. La formación de este tetrámero está regulada por la acumulación de fructosa-1,6-P_2 o serina, que son inductores de la activación de PKM2 (Chaneton et al. 2012; Dombrauckas et al. 2005). En cáncer diversas modificaciones posttraduccionales como la acetilación, fosforilación, oxidación, hidroxilación de PKM2 inhiben la formación del tetrámero (Anastasiou et al. 2011; Hitosugi et al. 2009;

W. Luo et al. 2011; Lv et al. 2011; Lv et al. 2013; P. Wang et al. 2015a) así como varias mutaciones (Iqbal et al. 2014), produciendo una acumulación de metabolitos glucolíticos.

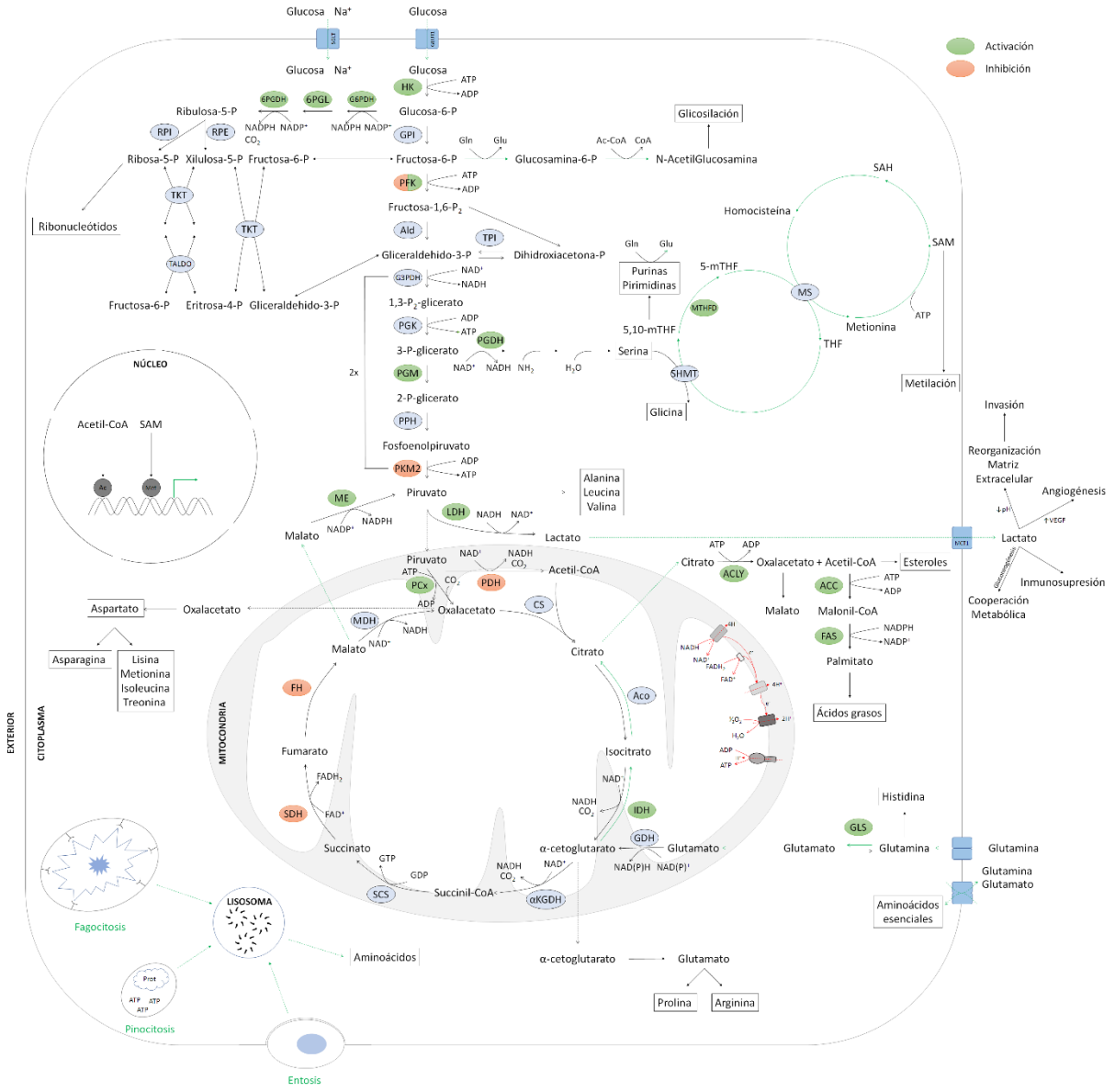

Figura 4. Esquema simplificado del metabolismo de la glucosa y la glutamina en células tumorales. **5,10-mTHF**, 5,10-metiltetrahidrofolato. **5-mTHF**, 5-metiltetrahidrofolato. **6PGDH**, 6-Fosfoglucanato Deshidrogenasa. **6PGL**, 6-Fosfoglucolactonasa. **ACC**, Acetil-CoA Carboxilasa. **ACLY**, ATP Citrato Liasa. **Aco**, Aconitasa. **CS**, Citrato Sintasa. **FAS**, Fatty Acid Synthase. **FH**, Fumarato Hidratasa. **G3PDH**, Gliceraldehido-3-Fosfato Deshidrogenasa. **G6PDH**, Glucosa-6-Fosfato Deshidrogenasa. **GLS**, Glutaminasa. **GPI**, Glucosa-6-Fosfato Isomerasa. **HK**, Hexoquinasa. **IDH**, Isocitrato Deshidrogenasa. **LDH**, Lactato Deshidrogenasa. **MDH**, Malato Deshidrogenasa. **ME**, Enzima Málica. **MS**, Metionina Sintasa. **MTHFD**, Metiltetrahidrofolato Deshidrogenasa. **PCx**, Piruvato Carboxilasa. **PDH**, Piruvato Deshidrogenasa. **PFK**, Fosfofructo Quinasa. **PGDH**, Fosfoglicerato Deshidrogenasa. **PGK**, Fosfoglicerato Quinasa. **PGM**, Fosfoglicerato Mutasa. **PKM2**, Piruvato Quinasa M2. **PPH**, Fosfopiruvato Hidratasa. **RPE**, Ribulosa-5-Fosfato Epimerasa. **RPI**, Ribulosa-5-Fosfato Isomerasa. **SAH**, S-Acetil-Homocisteina. **SAM**, S-Acetil-Metionina. **SCS**, Succinil-CoA Sintasa. **SDH**, Succinato Deshidrogenasa. **SHMT**, Serina Hidroximetil Transferasa. **TALDO**, Transaldolasa. **THF**, Tetrahidrofolato. **TKT**, Transcetolasa. **TPI**, Triosa Fosfato Isomerasa. **αKGDH**, α-Cetoglutarato Deshidrogenasa.

La Fosfofructoquinasa 1 (PFK1), que convierte la fructosa-6-P en fructosa-1,6-P_2 con la hidrólisis de una molécula de ATP en una reacción enzimática irreversible; es la principal enzima reguladora del flujo metabólico a través de la glucolisis. Tanto la inducción como la inhibición de su actividad son importantes para la célula tumoral ya que permiten una plasticidad metabólica según los requerimientos energéticos o anabólicos de la célula. Por ello, en células tumorales, la PFK1 puede aparecer fuertemente activada para mantener el flujo glucolítico (Bando et al. 2005; Kessler et al. 2008) o inhibida favoreciendo la entrada de intermediarios glucolíticos en las rutas de biosíntesis de macromoléculas (Yi et al. 2012). Una enzima importante en la regulación de PFK1 es PFKFB3 que produce fructosa-2,6-P_2 a partir de fructosa-6-P. La fructosa-2,6-P_2 es un activador de la PFK1 para la inducción del flujo glucolítico. La inhibición de PFKFB3 reduce el metabolismo de la glucosa y el crecimiento en células tumorales (O'Neal et al. 2016).

Se han propuesto diversas hipótesis para intentar entender el porqué de estos cambios en el metabolismo de la glucosa. Una de estas señala la importancia que tiene la glucolisis como **fuente de metabolitos precursores de rutas biosintéticas**, imprescindibles para mantener la proliferación.

El primero de los intermediarios de la glucolisis que actúa como precursor de una ruta biosintética es la glucosa-6-P. Este intermediario es el iniciador de la ruta de las pentosas fosfato (PPP). Esta ruta consta de una fase oxidativa, en el que se genera NADPH y ribosa-5-P, necesaria para la síntesis de nucleótidos; y una fase no oxidativa en el que se forma más ribosa-5-P a partir de otros metabolitos de la glucolisis como la fructosa-6-P y el gliceraldehido-3-P, en unas reacciones reguladas por la transcetolasa (TKT) y la transaldolasa (TALDO).

Los cambios en la expresión de enzimas glucolíticas que se producen en células tumorales favorecen la entrada de metabolitos en la ruta PPP. Como ya se ha mencionado antes, la inhibición de PKM2 y PFK1 hace que aumente el flujo de metabolitos hacia las rutas biosintéticas, en este caso la glucosa-6-P hacia la vía oxidativa de PPP para generar NADPH (Anastasiou et al. 2011; Yi et al. 2012). También se produce una sobreexpresión de la fosfoglicerato mutasa 1 (PGM1), que genera 2-P-glicerato a partir de 3-P-glicerato, evitando la acumulación de este metabolito que es un inhibidor de las enzimas de la PPP (Hitosugi et al. 2012). Además, algunas de las enzimas de la PPP se encuentran activadas o sobreexpresadas en cáncer (X. Rao et al. 2015; Ying et al. 2012), lo que favorece la síntesis de ribosa-5-P. Como regulador clave de las rutas de biosíntesis, mTORC1 induce la ruta PPP, así como el flujo de la glucosa a través de la glucolisis (Duvel et al. 2010).

Otro metabolito intermediario de la glucolisis, la fructosa-6-P, es precursor de la ruta de síntesis de las hexosaminas, a través de la que se forman los sustratos responsables de reacciones de O- y N-glicosilación. Estas reacciones producen un aumento de importantes modificaciones posttraduccionales de factores importantes en el control del metabolismo y la supervivencia tumoral (Ferrer et al. 2014; Itkonen et al. 2013).

Finalmente, el 3-P-glicerato es precursor de la síntesis de serina, un elemento esencial del ciclo del folato mediante el que se forman purinas y pirimidinas, así como NADPH y S-adenosilmetionina (SAM), sustrato de las metilasas de ADN. En algunos tipos de cáncer se ha descrito que aumenta la síntesis de serina (Possemato et al. 2011) por la inducción de la enzima Fosfoglicerato deshidrogenasa (PGDH) (Locasale et al. 2011), que es la primera enzima que actúa en la síntesis de serina a partir del 3-fosfoglicerato glucolítico. Además, varias de las enzimas que participan en el ciclo del folato aparecen frecuentemente sobreexpresadas en células tumorales (Nilsson et al. 2014; Tedeschi et al. 2015).

En tumores, el piruvato que se forma tras la glucolisis no entra en la mitocondria y **genera lactato**. Todas las enzimas que controlan este proceso están sobreexpresadas en cáncer. Hay una sobreexpresión de la enzima Lactato Deshidrogenasa (LDH), que produce lactato a partir de piruvato; del trasportador *Monocarboxylate transporter 1* (MCT1), que secreta el lactato al exterior celular; y una sobreexpresión de la enzima Piruvato Deshidrogenasa Quinasa (PDK), inhibidor mediante fosforilación de la enzima Piruvato Deshidrogenasa (PDH) que transforma el piruvato en acetil-CoA y que controla la entrada de piruvato en el ciclo TCA (J. W. Kim et al. 2006; J. W. Kim et al. 2007; Papandreou et al. 2006; Pate et al. 2014). Se sabe que la expresión varios de estos genes como los que codifican para LDH y PDK, está regulada por oncogenes como c-myc (J. W. Kim et al. 2007), β-catenina (Pate et al. 2014) y HIF1α (J. W. Kim et al. 2006; Papandreou et al. 2006).

El destino mayoritario del piruvato que entra en la mitocondria y se incorpora al ciclo TCA es la formación de citrato que se transporta al citoplasma para la **síntesis de ácidos grasos y esteroles**. El citrato en el citoplasma es convertido en oxalacetato (OAA) y acetil-Coa (Ac-CoA) por la *ATP Citrate Lyase* (ACLY). El OAA puede convertirse en malato y por medio de la enzima málica (ME) convertirse en piruvato generándose NADPH. El Ac-CoA sirve como precursor de la síntesis de ácidos grasos y esteroles convirtiéndose en malonil-CoA mediante la acción de la *Acetyl-CoA Carboxylase* (ACC). La condensación seriada mediante la *Fatty Acid Synthase* (FAS) de 7 malonil-CoA y 1 Ac-CoA, con el gasto de 14 moléculas de NADPH, genera una molécula de palmitato, un ácido graso saturado de 16 carbonos (16:0), que sirve como producto inicial sobre el que actúan diversas elongasas y desaturasas para dar lugar a diferentes ácidos grasos.

Las principales enzimas implicadas en la síntesis de ácidos grasos, ACLY, ACC y FAS se encuentran frecuentemente sobreexpresadas en celulares tumorales y su inhibición farmacológica suprime el crecimiento tumoral (Chajes et al. 2006; Migita et al. 2013; Saab et al. 2017; Zaidi et al. 2012), lo que pone de relevancia su importante papel en cáncer. Es importante señalar que la síntesis de lípidos no solo es necesaria para mantener la tasa proliferativa de las células tumorales, además son relevantes como moléculas de señalización de procesos como inflamación, migración o supervivencia tumoral (Rohrig and Schulze 2016). Nuevamente, mTORC1 es clave en la regulación de la síntesis de ácidos grasos activando enzimas clave de este proceso (Duvel et al. 2010).

Los metabolitos que forman parte del ciclo TCA también son precursores en la biosíntesis de aminoácidos no esenciales. Esto, unido a la perdida de citrato hacia el citoplasma y a la baja actividad de enzimas como la SDH y la FH, hace que haya un déficit de OAA para poder unirse al Ac-CoA y comenzar el ciclo TCA. Para regenerar el OAA, y teniendo en cuenta que la enzima PDH está inhibida normalmente en células tumorales, el piruvato formado en la glucolisis tiene que entrar en el ciclo TCA mediante una vía anaplerótica mediada por la enzima **Piruvato Carboxilasa** (PCx), en la que el piruvato incorpora un carbono del CO_2 para formar OAA gastando una molécula de ATP. En varios tipos de células tumorales, se ha descrito el aumento del flujo de entrada de piruvato en ciclo TCA mediante la acción de esta enzima (T. Cheng et al. 2011; Sellers et al. 2015) y, además, contribuye a mantener la síntesis de aminoácidos en células tumorales con el ciclo TCA comprometido (Cardaci et al. 2015).

La producción de citrato en el ciclo TCA también está sostenida por la **entrada anaplerótica de glutamina**. Como ocurre con la glucosa, los transportadores de glutamina ven aumentada su expresión en células tumorales. Su expresión es regulada mediante el factor de transcripción c-myc (Wise et al. 2008; X. Xu et al. 2015), que está altamente inducido en las células proliferativas. c-myc también induce la expresión de enzimas implicada en el catabolismo de la glutamina, como la glutaminasa 1 y 2 (Gls1 y Gls2) (Wise et al. 2008; D. Xiao et al. 2015; X. Xu et al. 2015). E2F es otro factor de transcripción frecuentemente activado en tumores y otras células proliferativas que regula la inducción de la expresión de los transportadores de glutamina y de Gls1 (Reynolds et al. 2014). El glutamato resultante se incorpora principalmente de manera anaplerótica al TCA convirtiéndose en α-KG (DeBerardinis et al. 2007; C. Yang et al. 2014). Además, la acumulación tanto de glutamina como de glutamato facilita la entrada de otros aminoácidos esenciales mediante antiportadores de aminoácidos (Hayashi et al. 2012; Thomas et al. 2015).

Con esta entrada de glutamina en el ciclo TCA se puede regenerar el OAA necesario para que el ciclo TCA no se vea comprometido por la salida de citrato al citoplasma. Además, durante la oxidación del α-KG a OAA se forman otros intermediarios importantes para el metabolismo tumoral (Mullen et al. 2014). Entre estos metabolitos destaca el malato, sustrato de la ME y que genera, como se mencionó anteriormente, NADPH, siendo la principal fuente de NADPH en células tumorales. La ausencia por deleción o inhibición de la enzima ME, es, de hecho, deletérea para el crecimiento y supervivencia tumoral (Dey et al. 2017; Murai et al. 2017; Zheng et al. 2012).

La aparición de mutaciones en enzimas que comprometen la función mitocondrial y la necesaria formación de intermediarios del ciclo TCA, hace que, para compensar esta deficiencia, las células tumorales, en algunos casos, sean capaces de producir citrato a partir del α-KG mediante **carboxilación reductiva** (Mullen et al. 2011), una vía que utiliza el ciclo TCA en reverso. Este proceso depende de un cambio en la isoforma activa de la IDH y es dependiente de NADPH (Metallo et al. 2011; Mullen et al. 2011; Yoo et al. 2008). La carboxilación reductiva requiere, por tanto, la oxidación del α-KG, ya que como se ha mencionado antes, permite la síntesis de NADPH por la acción de la ME (Mullen et al. 2014). Cabe

también reseñar que la entrada de glutamina en el ciclo TCA, no solo permite la generación de diversas macromoléculas sino también participa en la síntesis de ATP (Fan et al. 2013).

La glutamina, además de ser fuente de carbono en el metabolismo tumoral, también es **fuente de nitrógeno**. El nitrógeno es un elemento clave en la biosíntesis de diversas macromoléculas como pueden ser las purinas, las pirimidinas y los aminoácidos. Para producir uracilo y timina se necesita una molécula de glutamina que ceda su grupo amida, para la formación de adenina y citosina se necesitan dos y para la generación de guanina tres. El glutamato es también importante como donador de nitrógeno ya que es utilizado en reacciones de transaminación para formar otros aminoácidos, como la alanina o el aspartato. Este último es necesario en el proceso de ensamblaje de los anillos de las purinas y las pirimidinas (Patel et al. 2016). La importancia de este proceso viene evidenciada porque la inhibición de transaminasas en células tumorales pancreáticas inhibe el crecimiento tumoral (D. Li et al. 2015).

La dependencia de las células tumorales hacia la glutamina, bien sea por ser fuente de carbono o fuente de nitrógeno, es probablemente la causa por la que la vía de síntesis de este aminoácido se vea también aumentada en diversos tipos tumorales (Dal Bello et al. 2010; Kung et al. 2011; Marin-Valencia et al. 2012), que acumulan glutamina derivada de la glucosa y sobreexpresan la enzima limitante en el proceso de síntesis, la Glutamina Sintetasa (GS). Además, la inducción de esta vía de generación de glutamina contribuye también al aumento de la síntesis de nucleótidos (Tardito et al. 2015).

En las células tumorales, es c-myc el principal factor de transcripción responsable de la inducción de las rutas de síntesis de purinas y pirimidinas (Cunningham et al. 2014; Mannava et al. 2008), al mismo tiempo que, como ya se ha mencionado, induce la entrada de glutamina en la célula (Wise et al. 2008; X. Xu et al. 2015). Por tanto, es el responsable de la entrada y del destino de las moléculas de glutamina que entran en las células tumorales mientras que p53 es el principal inhibidor de estas rutas en células normales, por lo que las mutaciones en p53 tienen como resultado la inducción de estas rutas biosintéticas (Kollareddy et al. 2015).

Por todo ello, las alteraciones metabólicas asociadas a la transformación tumoral generan modificaciones en los niveles de numerosos metabolitos. Para un buen número de estas variaciones se ha demostrado un efecto directo sobre las características tumorales, afectando tanto en la propia célula tumoral como a las células que forman parte del ambiente tumoral. Así, por ejemplo, la sobreactivación de rutas biosintéticas genera, entre otros productos, niveles elevados de Ac-CoA y SAM, que son cofactores esenciales para la acetilación de histonas y la metilación de ADN respectivamente (Cai et al. 2011; Shyh-Chang et al. 2013; Wellen et al. 2009). Los cambios epigenéticos resultantes favorecen la progresión tumoral al activar oncogenes y silenciar la expresión de supresores tumorales. En células tumorales con una expresión baja o nula de SDH o FH se ha visto un aumento de la metilación del ADN debido a la inhibición de dioxigenasas dependientes de α-KG (Killian et al. 2013; Letouze et al. 2013; Tomlinson et al. 2002; M. Xiao et al. 2012). A este efecto contribuye, en varios tipos de cáncer, una mutación en la IDH recurrente que hace que se forme 2-hidroxiglutarato a partir de α-KG y que actúa como inhibidor

competitivo de las dioxigenasas dependientes de α-KG (W. Xu et al. 2011), favoreciendo la hipermetilación del ADN y las histonas (Figueroa et al. 2010; Turcan et al. 2012).

En relación al impacto sobre el ambiente tumoral de los metabolitos secretados por las células tumorales es especialmente importante el efecto del lactato. El lactato tiene una actividad inhibitoria sobre el sistema inmunitario (Colegio et al. 2014; Fischer et al. 2007; Goetze et al. 2011; Gottfried et al. 2006). Además, la acidificación del medio hipóxico, provocado por la secreción de lactato, parece contribuir a la inducción de la expresión de VEGF-A, dependiente de HIF-1, en células endoteliales del ambiente tumoral (Burns and Wilson 2003; Hunt et al. 2007) así como a la activación de enzimas implicadas en el remodelado de la matriz extracelular, lo que promueve la invasión (Estrella et al. 2013). Por último, algunas de las células del ambiente tumoral son capaces de incorporar el lactato secretado y sintetizar glucosa (Rattigan et al. 2012; L. Wei et al. 2015a) contribuyendo al reabastecimiento de la célula tumoral.

Papel del metabolismo oxidativo en la progresión tumoral.

Como hemos visto anteriormente, la perdida de actividades asociadas al ciclo TCA mitocondrial y la activación de rutas anapleróticas, mediada por la inducción de enzimas citosólicas, juega un papel central en las alteraciones metabólicas asociadas a los tumores. En este contexto, se produce además una bajada en la capacidad de síntesis de ATP acoplada a la actividad de la ETC. A pesar de que la pérdida de actividad mitocondrial parece que se vincula directamente a la agresividad tumoral, esto no es así, ya que la célula tumoral necesita la presencia de mitocondrias, de hecho, muchos tumores agresivos presentan proliferación mitocondrial. Aunque se han propuesto distintas hipótesis para explicar este fenómeno, la más aceptada señala el papel jugado por la producción mitocondrial de especies reactivas del oxígeno (ROS) en la inducción de la proliferación celular (Giampazolias and Tait 2016).

La cadena de transporte de electrones mitocondrial es, a nivel fisiológico, una importante fuente de ROS y se ha descrito que en patologías asociadas a disfunción mitocondrial se generan mayor cantidad de ROS. En cáncer, por ejemplo, se pueden formar mayor cantidad de ROS por el desacople entre la ETC y la síntesis de ATP debido a la sobreexpresión de inhibidores de la ATP sintasa (Formentini et al. 2012; Sanchez-Cenizo et al. 2010; Santacatterina et al. 2016).

Además de la ETC, existe una familia de enzimas asociadas a las membranas celulares, conocidas como NADPH oxidasas (NOX), cuya principal función es la producción de ROS. La sobreexpresión de estas enzimas está descrita en varios tipos de cáncer asociada con una mayor producción de ROS y una mayor progresión tumoral (Landry and Cotter 2014).

Los ROS son moléculas altamente reactivas con un papel dual en la fisiología de la célula. Si bien a altas concentraciones pueden ser tóxicos para la célula, juegan un papel esencial como elementos señalizadores en una gran cantidad de procesos fisiológicos, incluido el control de la proliferación celular y

los procesos de senescencia e inmortalización (Davalli et al. 2016). Por un lado, se ha visto que pueden activar a Ras favoreciendo la proliferación tumoral (Tai and Ascoli 2011). Por otro, los ROS actúan como mensajeros en muchos procesos fisiológicos que tienen un papel importante en cáncer, entre los que se encuentran la inflamación, ya que los elevados niveles de ROS producidos por las células tumorales promueven la secreción de citoquinas proinflamatorias por parte de macrófagos asociados a tumores (X. Lin et al. 2013b); la vascularización, ya que los ROS inducen y estabilizan a HIF-1α (Brunelle et al. 2005; Guzy et al. 2005) que como ya hemos visto es el principal factor de transcripción involucrado en procesos de vascularización; y la invasión, ya que los ROS pueden activar a las quinasas Src y Pyk2 que promueven la reorganización del citoesqueleto y la migración (Ku et al. 2015; H. Y. Li et al. 2014; S. K. Lim et al. 2012).

Como ya se ha mencionado, los ROS son altamente reactivos y pueden producir modificaciones oxidativas en diferentes tipos de macromoléculas, ya sea oxidando lípidos, proteínas o ácidos nucleicos (Rashid et al. 2013) alterando su actividad biológica. La oxidación de ácidos nucleicos puede provocar mutaciones puntuales y favorecer la aparición de roturas tanto de cadena simple como de doble cadena. Por ello, la oxidación del ADN es fuente de mutaciones e inestabilidad genómica (Shibutani et al. 1991) y promueve la adquisición de ventajas adaptativas a las células tumorales.

En células normales la sobreexposición a ROS es un potente inductor de la apoptosis (Giorgio et al. 2005). Dado que las células dependen de los ROS para mantener sus altas tasas proliferativas y su inestabilidad genómica, que facilita la continua adaptación de las células tumorales, debe suprimir las rutas que conducen a la muerte celular inducida por ROS. En células tumorales suele aparecer mutada o inactivada la proteína p53 o alguno de sus reguladores. p53 induce mediadores de parada de ciclo, entrada en senescencia y muerte celular en respuesta a ROS (Omori et al. 2015). Esto hace que el umbral de ROS que puede soportar una célula tumoral sea mayor, pero, como ya se ha mencionado, estas células generan mayor cantidad de ROS y permite que las terapias más utilizadas contra distintos tipos de cáncer, como la radiación o algunos agentes quimioterapéuticos, estén compuestas por agentes oxidantes (Glasauer and Chandel 2014).

Un regulador clave en el control de la actividad mitocondrial y la producción mitocondrial de ROS es ***Peroxisome Proliferator-Activated Receptor Gammma Coactivator 1α*** **(PGC-1α)**. PGC-1α, junto a *Peroxisome proliferator-activated receptor gamma coactivator 1β* (PGC-1β) y *PGC-1-related coactivator* (PRC), forma una familia de coactivadores transcripcionales que controla la proliferación mitocondrial (Andersson and Scarpulla 2001; J. Lin et al. 2002a).

PGC-1α es un coactivador transcripcional, y como tal, no puede unirse directamente a la cadena de ADN, por lo que necesita de la unión con factores de transcripción y receptores nucleares para realizar su función de regulación génica. Además, no presenta función acetiltransferasa de histonas, función que facilita la transcripción provocando cambios en la cromatina, por lo que requiere de otras proteínas, que sí presenten dicha actividad enzimática, para la regulación de la expresión génica como CBP/p300 o

miembros de la familia de coactivadores del receptor de esteroides (p160/SRC). Por ello, PGC-1α actúa fundamentalmente como anclaje en el acoplamiento de la maquinaria de transcripción (Villena 2015).

El hecho de unirse a varios factores de transcripción hace de PGC-1α un regulador maestro del metabolismo celular. PGC-1α es capaz de inducir la biogénesis mitocondrial mediante su unión con *Nuclear Respiratory Factor-1* (NRF-1) y *Nuclear Respiratory Factor-2* (NRF-2) (Z. Wu et al. 1999), con este último mediante la unión con *Host Cell Factor* (HCF) (J. Lin et al. 2002a). También regula la biogénesis mitocondrial a través de su interacción con *Estrogen-related Receptor α* (ERRα) (Huss et al. 2002; Mootha et al. 2004; Schreiber et al. 2004). De esta manera, aumenta la expresión de TFAM (LaGory et al. 2015; Y. Wang et al. 2015b), *Mitochondrial Transcription Factor B1* (TFB1M) y *Mitochondrial Transcription Factor B2* (TFB2M) (Falkenberg et al. 2002) al ser dianas de expresión de dichos factores de transcripción nucleares. La expresión de los factores de transcripción mitocondriales promueve la transcripción de gran parte de las proteínas necesarias para el metabolismo mitocondrial y la replicación del ADN mitocondrial (Litonin et al. 2010; Rohas et al. 2007; Shi et al. 2012; Stein et al. 2008; Z. Wu et al. 1999).

La expresión de PGC-1α es responsable de la respuesta específica de los tejidos a estímulos que indican un aumento en la demanda energética. Por ejemplo, en el tejido adiposo marrón se produce una respuesta termogénica regulada por PGC-1α en respuesta al frío (Puigserver et al. 1998), mientras que, en el hígado, se activa la gluconeogénesis respondiendo a periodos de ayuno (Yoon et al. 2001). En el musculo esquelético, a su vez, PGC-1α media la conversión hacia miofibras de contracción lenta tipo I o tipo IIa que son altamente oxidativas en respuesta al ejercicio (Baar et al. 2002; J. Lin et al. 2002b).

También se ha descrito que PGC-1α, además de inducir el metabolismo oxidativo, es capaz de inducir rutas anabólicas como la lipogénesis y la ruta PPP en músculo esquelético (Summermatter et al. 2010) y en hígado (Park et al. 2014) o la gluconeogénesis indicada más arriba.

Por otra parte, PGC-1α activa la expresión de genes relacionados con la detoxificación de ROS (St-Pierre et al. 2003; St-Pierre et al. 2006; Valle et al. 2005) mediante la unión al factor de transcripción FOXO3a (Olmos et al. 2009) y a ERRα (Rangwala et al. 2007). y requiere de la acción de la desacetilasa SirT1 y de la activación por *AMP-activated protein kinase* (AMPK) (X. Zhao et al. 2014) para inducir la respuesta antioxidante. Interesantemente, AMPK puede ser regulada, a su vez, directamente por ROS, induciéndose su expresión al incrementar la concentración de ROS en la célula (Irrcher et al. 2009), lo que demuestra la existencia de un mecanismo de regulación recíproca entre los ROS y PGC-1α. Esto hace de PGC-1α responsable de un programa de "energía limpia" en el que la generación de metabolitos altamente energéticos y la eliminación de los productos tóxicos derivados están reguladas de manera coordinada (Finkel 2006).

Teniendo sus diversas funciones presentes, y la importancia del control metabólico en cáncer, diversos estudios han intentado esclarecer el papel de PGC-1α en la progresión tumoral. Sin embargo, su contribución no está completamente esclarecida. Los estudios en los que se analizó la expresión de PGC-

1α en diversos tipos tumorales (Deblois et al. 2013), encontraron su expresión disminuida en algunos casos; como es el caso de tumores de mama (Watkins et al. 2004), colon (Feilchenfeldt et al. 2004) y ovario (Y. Zhang et al. 2007) mientras que en otros la expresión de PGC-1α se encontró aumentada, como es el caso de los tumores renales (Klomp et al. 2010) y de endometrio (Cormio et al. 2009). Uno de los primeros y más relevantes estudios funcionales mostró que el acortamiento de los telómeros produce disfunción mitocondrial al activar p53, que reprime la expresión de PGC-1α (Sahin et al. 2011), induciendo senescencia celular. Seguidamente, algunos trabajos apuntaron hacia un papel promotor de la oncogénesis mediante la inducción de la lipogénesis (Bhalla et al. 2011), pero la mayoría sugieren que la disminución del metabolismo oxidativo por supresión de PGC-1α es la verdadera función de este coactivador en oncogénsis (Haq et al. 2013; J. H. Lim et al. 2014; Sancho et al. 2015) llegando a relacionar niveles reducidos de PGC-1α con una mayor agresividad y peor prognosis (W. G. Jiang et al. 2003).

Algunos autores sostienen que mientras que las células tumorales son altamente glucolíticas, sus progenitoras, las células madre del cáncer (CSC), presentan un metabolismo oxidativo más activo y una mayor plasticidad metabólica, estableciendo una relación inversa en la expresión de c-myc y PGC-1α (Sancho et al. 2015). Otros estudios indican que la expresión de PGC-1α en células tumorales protege a la célula ante diferentes agentes terapéuticos por su función reguladora del estrés oxidativo (Vazquez et al. 2013), si bien es cierto que la supresión de PGC-1α en estas células resulta en un aumento del metabolismo glucolítico, que favorece el crecimiento tumoral, a pesar de ser más vulnerables a los agentes terapéuticos (J. H. Lim et al. 2014). Por tanto, la alta plasticidad metabólica que muestran en muchos casos las células tumorales y en particular las CSC puede ser importante en la formación de tumores secundarios. De hecho, existen evidencias de que el metabolismo oxidativo puede tener un papel promotor de la metástasis (LeBleu et al. 2014; Y. Li et al. 2016; Lou et al. 2016) con PGC-1α como regulador principal, ya que no es una etapa de la progresión tumoral que dependa de la biosíntesis de macromoléculas y si de la eficiencia metabólica.

Sin embargo, también hay estudios que apoyan que la supresión de PGC-1α facilita la metástasis (C. Luo et al. 2016b; Torrano et al. 2016). En este sentido son relevantes los estudios que muestran que la supresión de PGC-1α promueve la migración celular (Borniquel et al. 2010), y previene la formación de vasos inestables, como los que se encuentran en tumores (Garcia-Quintans et al. 2016). Además, la sobreexpresión de PGC-1α en células tumorales hepáticas, también, aumenta la expresión de E-cadherina y reduce la motilidad celular (Lee et al. 2009).

OBJETIVOS

El objetivo principal de la tesis fue evaluar el papel de PGC-1α, regulador del metabolismo oxidativo mitocondrial y de la homeostasis del estado redox, en el proceso de inmortalización y progresión tumoral. Por ello, se plantearon los siguientes objetivos concretos:

Objetivo 1: Valorar el papel de PGC-1α en el proceso de senescencia e inmortalización celular.

- Determinar si la ausencia de PGC-1α altera el estado oxidativo de los MEF.
- Valorar el impacto del estado oxidativo en el daño al ADN en MEF.
- Analizar si la ausencia de PGC-1α afecta al proceso de entrada en senescencia de los MEF.
- Estudiar si la ausencia de PGC-1α altera el proceso de inmortalización de los MEF.

Objetivo 2: Valorar el papel de PGC-1α en el proceso de progresión tumoral.

- Determinar si en ausencia de PGC-1α, existen diferencias en el metabolismo de azúcares, lípidos y aminoácidos en los MEF inmortalizados, respecto a los de genotipo silvestre.
- Analizar el efecto de PGC-1α en las posibles características tumorales de los MEF inmortalizados, realizando un estudio *in vitro* valorando distintos aspectos como supervivencia, proliferación y migración.
- Valorar, en modelos *in vivo*, el papel de PGC-1α en la capacidad de formar tumores primarios y metástasis de los MEF inmortalizados.

MATERIALES Y MÉTODOS

Animales.

Se utilizaron ratones C57BL/6j PGC-1α$^{+/+}$ y PGC-1α$^{-/-}$ para aislar de sus embriones, a día 13,5, fibroblastos embrionarios (MEF). Los ratones C57BL/6j PGC-1α$^{-/-}$ provienen originalmente del laboratorio del Dr. Bruce Spiegelman (Dana-Farber Cancer Institute, Harvard Medical School). A partir de estos animales se estableció una colonia por transferencia embrionaria en el animalario del IIBm.

Se utilizaron ratones C57BL/6j machos de 12 semanas de edad para estudios de xenotransplante. En un grupo de ratones se monitorizó el crecimiento celular de MEF inmortalizados embebidos en matrigel (BD Biosciences) y en un segundo grupo se evaluó la capacidad proliferativa de MEF inmortalizados que expresaban la Proteína Verde Fluorescente (GFP) para facilitar su seguimiento. También se utilizaron ratones inmunodeprimidos *non-obese diabetic* (NOD) portadores de la mutación SCID, que impide la maduración de los linfocitos T y B; y hace que la función de las células *natural killer* (NK) sea deficiente (NOD-SCID), machos de 12 semanas de edad para evaluar la capacidad de desarrollo tumoral de MEF inmortalizados. Se utilizaron dos modelos experimentales, en el primero, de tumor primario, se inyectaron subcutáneamente MEF inmortalizados en la zona dorsal. En el segundo modelo, de metástasis pulmonar, se coinocularon MEF inmortalizados y células de melanoma murino B16-V5 a través de la vena de la cola. Estos ratones procedieron de las líneas mantenidas en el animalario del IIBm.

Los protocolos animales están aprobados por los comités de Bioética y Bioseguridad del CSIC, y siguen las indicaciones de la declaración de Helsinki y las guías del NIH relativas al uso y cuidado de animales de experimentación (publicación NIH No. 85-23). Los animales fueron mantenidos a temperatura constante de 21 ± 1°C con un ciclo de 12h de luz-oscuridad y con acceso ilimitado a agua y comida.

Células.

Cultivos Primarios.

Los MEF silvestres y deficientes en PGC-1α se obtuvieron a partir de embriones de 13,5 días de desarrollo. Tras separar los embriones de la placenta y lavarlos con solución salina, se eliminó la cabeza y las vísceras; el resto del embrión se trituró y se incubó con tripsina (0,25 % / 1 mM EDTA, p/v) (Gibco), a 37ºC durante 45 min. Posteriormente, la preparación fue disgregada mecánicamente mediante pipeteo y diluida en medio de Eagle modificado por Dulbecco (DMEM) (Sigma-Aldrich) suplementado con 10 % de suero fetal bovino (FBS) (Gibco), 2 mM de L-Glutamina (L-Gln) (Gibco), 1 % de

penicilina/estreptomicina (P/S) (Gibco). Las células se cultivaron en placas p100 (Falcon) y se incubaron a 37ºC en una atmósfera humidificada con 5 % de CO_2 durante 24 h. Pasadas 24 h, se renovó el medio con el fin de eliminar restos celulares derivados del proceso de aislamiento. Las células se cultivaron en medio DMEM con 10 % de FBS, 1 % de L-Gln y 1 % P/S.

Estas células se sometieron a pases seriados para analizar su capacidad proliferativa hasta la llegada a senescencia. Para ello se cultivaron, en pases sucesivos, 10^6 células en placas de 10 cm de diámetro a 37ºC. Las células se mantuvieron en cultivo 72 h. En ese momento, se levantaron con *TrypLE Express* (Gibco) y se contaron con una cámara de *Neubauer* (Blau Brand) en presencia del colorante *Trypan Blue* (Sigma-Aldrich) que tiñe las células muertas. Cuando los cultivos llegaron a senescencia, se mantuvieron en las placas con cambios de medio cada 72 h. Los cultivos senescentes, eventualmente, escaparon del estado senescente y reiniciaron el crecimiento. Seguidamente, se reanudó el contaje celular en pases sucesivos para determinar la velocidad de proliferación, siguiendo el mismo protocolo que el seguido con los cultivos primarios. (Fig. 5). En cada pase se contabilizó el número de células por placa para la determinación de la velocidad de proliferación siguiendo la fórmula: $\Delta Crecimiento = \log_2(n_f - n_i)$, donde n_f es el número contado tras levantarlas y n_i es el número de células iniciales, en este caso 10^6.

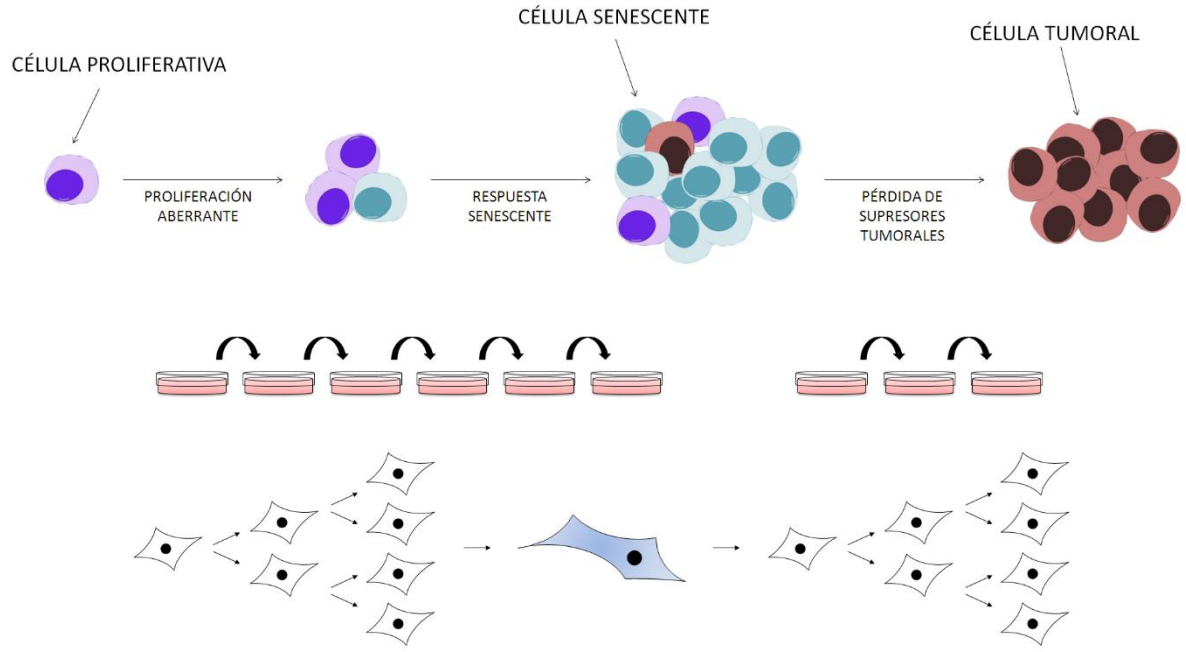

Figura 5. Modelo experimental *in vitro* de la progresión tumoral.

Líneas celulares establecidas.

Se utilizaron células embrionarias de riñón humano HEK293T, una línea celular establecida de células embrionarias de riñón humanas que contienen el antígeno T del virus SV40, para la producción de retrovirus y lentivirus. Las células HEK293T se mantuvieron en cultivo con medio DMEM con 10 % FBS, 1 % L-Gln y 1 % P/S.

Se utilizaron células B16-V5, una línea celular de melanoma de ratón, para el ensayo de metástasis pulmonar. Las células B16-V5 se mantuvieron en cultivo con medio DMEM con 10 % FBS, 1 % L-Gln y 1 % P/S.

Plásmidos.

Los plásmidos utilizados en este trabajo se describen a continuación, en la Tabla 1.

Plásmido	Característica	Referencia
pCL-Eco	Plásmido que complementa la expresión de genes retrovirales para la generación de partículas retrovirales.	
pCX4-GFP	Plásmido que contiene la secuencia codificante de GFP en un vector retroviral defectivo.	
VSVg	Plásmido que contiene el gen Env (glicoproteína de la envuelta) para generar partículas lentivirales (2ª generación).	
P8.9	Plásmido con el componente empaquetador (Gag--Pol, tat and rev) para generar partículas lentivirales (2ª generación).	
pHRSIN-CS-Luc-IRES-emGFP	Plásmido que contiene las secuencias codificantes de Luciferasa y GFP en un único operón.	(Garaulet et al. 2013)

Tabla 1. Plásmidos utilizados en la realización del trabajo presentado en esta tesis.

Infección con partículas virales.

Producción de Partículas virales e Infección.

Retrovirus.

Para la asegurar la trazabilidad de los MEF inmortalizados tras su inyección en ratones C57BL/6j, se utilizaron retrovirus recombinantes portadores de la secuencia codificante de GFP para generar líneas de MEF recombinantes que expresaban esta proteína de manera constitutiva.

Se empleó la línea celular HEK293T para la generación de retrovirus que contuvieran la secuencia de GFP. Las HEK293T se cultivaron en placas p100 con medio DMEM 10 % FBS, 1 % L-Gln y 1 % P/S manteniéndolas siempre en subconfluencia. Se cotransfectaron los plásmidos pCL-Eco, que tiene las secuencias codificantes de *gag*, *pol* y *env*, proteínas necesarias para el ensamblaje de las partículas virales; y pCX4-GFP, plásmido que contiene la secuencia de GFP.

La transfección ser realizó mediante la técnica del fosfato cálcico. Para ello, se prepararon dos tubos, en el primero se incluyó una mezcla con 12 µg de pCL-Eco, 12 µg de pCX4-GFP y $CaCl_2$ 0,25 M en un volumen final de 1,2 ml de H_20. En el segundo tubo se incluyó 1,2 ml de HBS 2x. Seguidamente, mientras se generaban burbujas en el segundo tubo utilizando una pipeta *pasteur* de vidrio acoplada a un pipeteador automático, se añadió la mezcla del primer tubo al segundo, gota a gota, a velocidad constante. Una vez preparada la mezcla, se incubó 20 min a temperatura ambiente (RT) y finalmente se añadió, gota a gota, a placas p100 de cultivos de HEK293T con un grado de confluencia del 60 %. Pasadas entre 12 y 16 h se cambió el medio del cultivo por medio fresco, y se comprobó la eficacia de la transfección mediante el seguimiento de la fluorescencia en verde en el microscopio invertido Axiovert 135 (Zeiss) de luz transmitida y epifluorescencia, acoplado a una cámara monocroma Nikon Ds-2MBWc controlada por el programa *NIS Elements F. 3.0*. Pasadas 24 h, se recogió el medio con una jeringa, se filtró con un filtro de 0,45 µm (Millipore) para eliminar restos celulares y se añadió polybreno (Millipore) a una concentración final de 8 µg/ml.

Las partículas retrovirales presentes en el medio recogido con polybreno se utilizaron para infectar MEF inmortalizados. Los MEF inmortalizados se cultivaron en placas de 6 pocillos y, tras añadir el medio con retrovirus, la placa se centrifugó a 1500 g durante 2 h y 30 min y se transfirió al incubador a 37 ºC. Pasadas 20 h, se cambió el medio de cultivo y se comprobó la eficacia de la infección mediante seguimiento de la fluorescencia en verde en el microscopio invertido Axiovert 135 (Zeiss).

Lentivirus.

Se utilizó la línea celular HEK293T para la generación de lentivirus recombinantes que contuvieran las secuencias codificantes de luciferasa y GFP en un mismo operón bajo el control de un promotor constitutivo. Las células HEK293T se cultivaron en placas p100 con medio DMEM con 10 % FBS, 1 % L-Gln y 1 % P/S manteniéndose siempre en subconfluencia. Se utilizó un sistema de empaquetamiento de lentivirus de segunda generación, formado por los plásmidos: VSVg, p8.9 y pHRSIN-CS-Luc-IRES-emGFP (Fig. 6), que contiene las secuencias codificantes de luciferasa y GFP en una construcción bicistrónica. La primera secuencia codificante (Luciferasa), situada junto al promotor CS, da lugar a mayores niveles de expresión que la segunda secuencia (GFP) situada tras la secuencia IRES, que permite la traducción del segundo gen del operón. Esta construcción nos permite, mediante el seguimiento de la fluorescencia en verde de la GFP la separación por *cell sorting* de las células infectadas que hayan integrado el transgén y lo expresen (GFP^+). En estas células, puede asumirse que también se expresa la luciferasa.

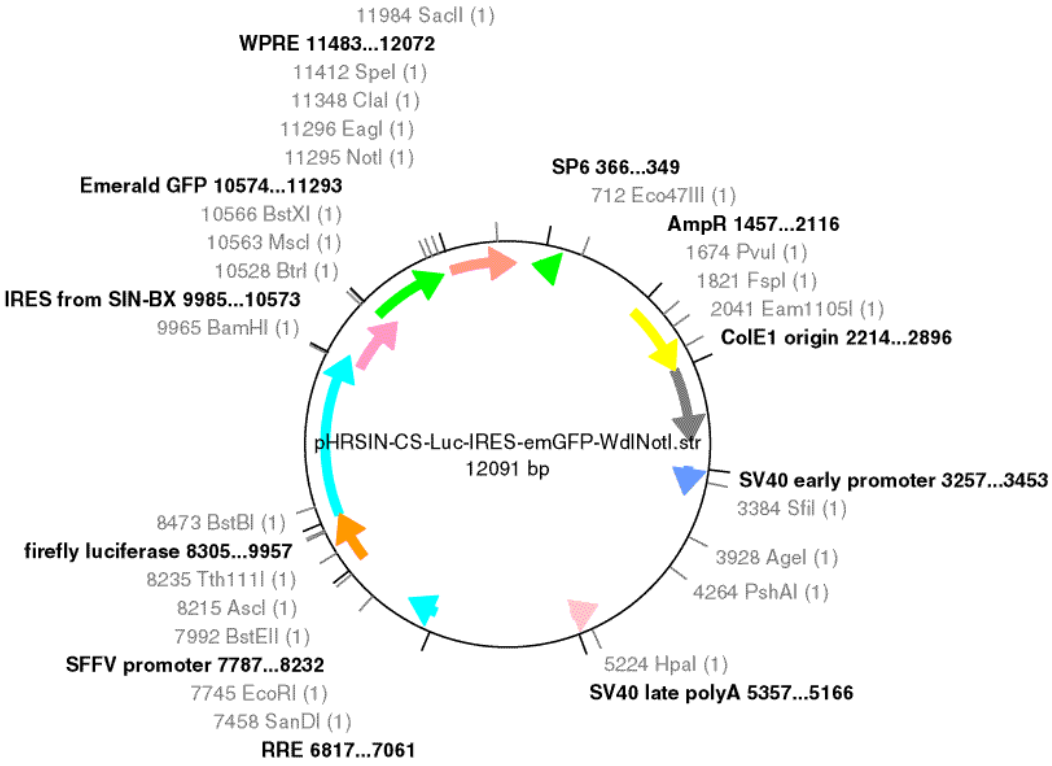

Figura 6. Plásmido pHRSIN-CS-Luc-IRES-emGFP utilizado para la generación de células que expresen luciferasa y emGFP para su tazabilidad *in vivo*.

La línea celular HEK293T fue transfectada con los tres plásmidos virales mediante la técnica del fosfato cálcico (descrita en la producción de retrovirus). Se comprobó la eficacia de la transfección siguiendo la fluorescencia en verde utilizando en el microscopio invertido Axiovert 135 (Zeiss) de luz

transmitida y epifluorescencia, acoplado a una cámara monocroma Nikon Ds-2MBWc controlada por el programa *NIS Elements F. 3.0*.

Pasadas 24 h, se recogió el medio portador de lentivirus con una jeringa, se filtró con un filtro de 0,45 µm (Millipore) para eliminar restos celulares y se añadió polybreno (Millipore) a una concentración final de 8 µg/ml.

El medio portador de lentivirus con polybreno se utilizó para infectar MEF inmortalizados y células de melanoma B16-V5. Las células se cultivaron en placas de 6 pocillos y, tras añadir el medio recogido con lentivirus, la placa se centrifugó a 1500 g durante 2 h y 30 min y se transfirió a un incubador a 37ºC. Pasadas 6 h, se cambió el medio por medio fresco y, a las 48 h, se comprobó la eficacia de la infección siguiendo la fluorescencia en verde en un microscopio invertido Axiovert 135 (Zeiss).

ARNm.

Aislamiento y purificación.

Para el aislamiento del ARN total de células se usó el reactivo *TRI Reagent* (Ambion), siguiendo las instrucciones del fabricante. Las células se lavaron dos veces con tampón fosfato salino (PBS) 1x frío y se lisaron con *TRI Reagent*. A continuación, mediante la adición de cloroformo (MERCK) seguida de centrifugación a 12000 g durante 15 min se separó la solución en tres fases, recuperando el ARN de la fase superior por precipitación con alcohol isopropílico (0,7 %) (Sigma-Aldrich). Tras el lavado con etanol al 70 % (MERCK), el ARN extraído se resuspendió en agua libre de ribonucleasas. Posteriormente, se cuantificó por espectrofotometría con el *spectophotometer ND1000* (Nanodrop).

Retrotranscripción.

La retrotranscripción a ADN complementario se realizó a partir de 1 µg de ARN total previamente calentado 2 min a 72ºC. Se utilizó la transcriptasa reversa M-MLV (*Moloney Murine Leucemia Virus Reverse Transcriptase,* Invitrogen) incubada en tampón de reacción a 37 ºC durante 45 min en presencia de una mezcla de hexámeros (GE Healthcare) cebadores.

Análisis cuantitativo de los niveles de ARNm.

Gen (HUGO)	Cebador	Secuencia 5'-3'
Sestrina1 (SESN1)	Directo	CAG GAA ATG CTT CGG TAA GTG
	Reverso	GTA ACT TCA TCA TCG TCC GA
Sestrina2 (SESN2)	Directo	CCA CTC TCT GGC CTC CTT TG
	Reverso	TTC AAA GCC CCC TGA GTT GT
Puma (BBC3)	Directo	GTA CGA GCG GCG GAG ACA AG
	Reverso	CTA GTT GGG CTC CAT TTC TGG
Noxa (PMAIP1)	Directo	GCA GAG CTA CCA CCT GAG TT
	Reverso	GAG TTG AGC ACA CTC GTC CT
Bax (BAX)	Directo	TTT GCT ACA GGG TTT CAT CC
	Reverso	CCA CGT CAG CAA TCA TCC T
ALDH4 (ALDH4)	Directo	TGA AGG TGA CCA ATG AGC CC
	Reverso	GTG CAT GGT TAA AGG GCG AC
GLS2 (GLS2)	Directo	AGC TCT TCC AAA AGT GTG TG
	Reverso	GGA TGT AGG CTG CCA CTT TG
Gadd45 (GADD45A)	Directo	CGT AGA CCC CGA TAA CGT GG
	Reverso	TTC GTC ACC AGC ACA CAG TG
Necdin (NDN)	Directo	AAG AAG GCC CTG GAG AGT TA
	Reverso	TAT TTA TGG TGG GGT TGC AT
Parkina2 (PARK2)	Directo	TGC ACA GAT GTC AGG AGC CC
	Reverso	CCT GTT GTA CTG CTC TTC TCC A
E. Málica1 (ME1)	Directo	CTG ACT TCG ACA GGT ATC TC
	Reverso	ACC ACA ATA GCC TTG ACG AC
E. Málica2 (ME2)	Directo	TGT TAA GGC TGT TGT GGT GAC
	Reverso	TAG TGC CAT GTT ATC AGT GCC
E. Málica3 (ME3)	Directo	TAA GGC TGT GGT GGT GAC TG
	Reverso	GGG TCT CTA AGA AGC TCC TC
PCx (PC)	Directo	CAG AGG TGA GAT TGC CAT CCG
	Reverso	CTA CAC CAT TTT CCT TGG CCA CC
IDH1 (IDH1)	Directo	GTG TGA GCC GGG TTA TTG AAG
	Reverso	AGC TAT GCA GAT CCA GTT CCA C
PDK3 (PDK3)	Directo	CTG GAC TTC GGA AGG GAT AAT G
	Reverso	AGT TAT CCA AAA CTC GTG GGT C
β-actina (ACTB)	Directo	CAC CTT CCA GCA GAT GTG GA
	Reverso	AGC ATT TGC GGT GGA CGA TGG

Tabla 2. Listado de cebadores utilizados.

El análisis cuantitativo de la expresión génica se realizó mediante la reacción en cadena de la polimerasa (qPCR) en *Realplex² Mastercycler* (Eppendorf). Para la mayor parte de los genes estudiados se diseñaron oligonucleótidos específicos (Tabla 2) que fueron sintetizados por Invitrogen, para la reacción de la qPCR se utilizó *SYBR Green I Dye* (Applied Biosystems). Las condiciones de amplificación fueron las siguientes:

- **50ºC durante 2 min**
- **95ºC durante 10 min**
- **95ºC durante 15 segundos**
  58ºC durante 30 segundos
  72ºC durante 30 segundos
  } **40 ciclos**

Los datos fueron analizados con el programa *Microsoft Excel* (Microsoft) por el método de la cuantificación relativa por comparación del umbral de detección establecido. Para la normalización de los niveles de expresión del gen de interés se utilizó la expresión de la β-actina como control de carga (Livak and Schmittgen 2001).

Proteínas.

Obtención de extractos celulares totales.

Para la obtención de los extractos celulares totales, se lavaron las células dos veces con PBS 1x frío y se lisaron en presencia de una solución que contiene 20 mM HEPES a pH 7.9, 125 mM NaCl, 1 % NP-40, 1 mM EDTA, 5 mM β-glicerolfosfato, 0,2 mM NaV, 0,2 mM NaF, 10 mM NaP e inhibidores de proteasas (Sigma-Aldrich). Los lisados se centrifugaron a 4 ºC y 13000 rpm durante 10 min. Los sobrenadantes se congelaron a -80 ºC.

Cuantificación e inmunodetección en soportes de membrana (Western Blot).

Las muestras de proteínas obtenidas se cuantificaron por colorimetría mediante una modificación del método de *Lowry* (Bio-Rad DC Protein Assay). Posteriormente, 35 µg de proteína desnaturalizada se separaron por electroforesis en geles de poliacrilamida-SDS (SDS-PAGE) y se transfirieron a membranas de fluoruro de polivinilideno (PVDF) *HybondTM-P* (Amersham Biosciences). Con el fin de evitar uniones

inespecíficas de los anticuerpos a las membranas, éstas se bloquearon durante 1 h con albúmina de suero bovino (BSA) (Sigma-Aldrich) en 5 % en Tris Buffer Salino con 0,1 % de Tween 20 (TBS-T).

Anticuerpo	Dilución	Especie	Marca comercial
p16	1/500	Conejo	Santa Cruz Biotechnology (sc-1207)
p19	1/500	Conejo	Cedido por Dr. Ignacio Palmero (IIB)
p21	1/500	Conejo	Santa Cruz Biotechnology (sc-397)
p53	1/1000	Ratón	Santa Cruz Biotechnology (sc-126)
Phospho-p53 (Ser15)	1/1000	Ratón	Cell Signaling (9286)
MnSOD	1/1000	Conejo	Enzo Life Sciences (ADI-SOD-110)
AMPK	1/1000	Conejo	Cell Signaling (2532)
Phospho-AMPK	1/1000	Conejo	Cell Signaling (2535)
PFKFB3	1/1000	Conejo	Proteintech (13763-1-AP)
Cit c	1/4000	Ratón	BD Biosciences (556433)
E. Málica	1/5000	Conejo	Cedido por Dra. Ángela Valverde (IIB)
c-myc	1/1000	Conejo	Santa Cruz Biotechnology (sc-764)
β-actina	1/5000	Ratón	Sigma-Aldrich (A 5441)

Tabla 3. Listado de anticuerpos utilizados para la inmunodetección de proteínas.

A continuación, se incubaron durante toda la noche (O/N) a 4ºC en agitación con los anticuerpos primarios específicos de las proteínas de interés (Tabla 3). Tras lavar las membranas tres veces con TBS-T, se realizó la incubación con los correspondientes anticuerpos secundarios conjugados a peroxidasa de rábano (HRP-conjugados), durante 1 h a RT. A continuación, se realizaron otros tres lavados con TBS-T de 5 min cada uno. Por último, el revelado se llevó a cabo mediante el sistema de detección quimioluminiscente ECL (Amersham Biosciences) y la exposición de películas autorradiográficas (AGFA).

Inmunofluorescencia indirecta de células.

Los MEF, primarios e inmortalizados (según el experimento), se cultivaron en portaobjetos de 8 pocillos (Nunc), se fijaron durante 10 min con 4 % paraformaldehido (PFA), se lavaron con PBS 1x y se permeabilizaron durante 5 min con solución de permeabilización (PBS 1x con 0,1 % Tritón X-100 y 0,1 % citrato de sodio). A continuación, se lavaron 20 min con PBS 1x y solución de lavado (PBS 1x con 0,25 % BSA y 0,1 % Tween-20), y se bloquearon 30 min con solución de bloqueo (solución de lavado con 2,5 **%** BSA). Los anticuerpos primarios (Tabla 4) diluidos en solución de bloqueo se incubaron en una cámara de

humedad O/N a 4 ºC. Después de esta incubación, se hicieron dos lavados de 10 min con solución de lavado. Los anticuerpos secundarios conjugados con diferentes fluorocromos se prepararon en solución de bloqueo y se incubaron durante 1 h en una cámara de humedad a RT. Finalmente, las células se incubaron 10 min con 4',6-diamino-2-fenilindol (DAPI) (Molecular Probes), se lavaron con PBS 1x y se montaron con *ProLong* (Molecular Probes).

Las fotos se tomaron con un microscopio Nikon 90i (Nikon), con una cámara refrigerada monocroma DS-Qi1Mc acoplada (Nikon) y con filtros para DAPI, FITC y TexasRed. El programa utilizado para la captura de imágenes fue el *NisElements 3.01* (Nikon). Las imágenes se analizaron con *ImageJ* (NIH).

Anticuerpo	Células	Dilución	Especie	Marca comercial
γH2AFX	MEF primarios	1/1000	Ratón	Millipore (05-636)
TP53BP1	MEF primarios	1/1000	Conejo	Novus Biologicals (NB100-304)
8-OH-dG	MEF primarios	1/200	Cabra	Novus Biologicals (NB600-1508)
β-catenina	MEF inmortalizados	1/500	Conejo	Santa Cruz (sc-1496)

Tabla 4. Listado de anticuerpos usados en las inmunofluorescencias de células.

Separación por *Cell Sorting*.

Para separar los MEF inmortalizados que, tras las infecciones con retrovirus o lentivirus, expresaban la proteína GFP de manera constitutiva, se utilizó el sistema *Cell Sorter* FACSVantage SE (BD Biosciences). Para ello, los cultivos de MEF inmortalizados e infectados se levantaron de las placas y, tras su sedimentación por centrifugación, se resuspendieron en PBS 1x a una concentración de $2*10^6$ células/ml. Tras el proceso de separación, se transfirieron a un tubo estéril de 15 ml con medio DMEM 10 % FBS, 1 % L-Gln y 1 % P/S.

En el caso de las infecciones con retrovirus, tras sembrar las células nuevamente en una placa p100, se comprobó la expresión de GFP en los MEF inmortalizados mediante el sistema de observación *in vivo* Cell Observer (Zeiss)

En el caso de las infecciones lentivirales, tras cultivar y expandir las células, y para comprobar que los cultivos expresaban tanto GFP como luciferasa se utilizó, por una parte, el sistema de observación *in vivo* Cell Observer (Zeiss), como con las infecciones con retrovirus; y, por otra parte, el luminómetro GloMax 96-microplate (Promega), para valorar la actividad emisora de luz de la luciferasa.

Caracterización de la entrada en senescencia.

Medida de especies reactivas de oxígeno (ROS).

Para la determinación de la producción mitocondrial de superóxido se realizó un marcaje con *MitoSOX Red* (Molecular Probes) según se ha descrito previamente (Borniquel et al. 2010). Este marcador se incorpora preferentemente a las membranas mitocondriales y al oxidarse en presencia de ion superóxido, emite fluorescencia en rojo. Los MEF primarios se cultivaron, en cada pase sucesivo, sobre cubreobjetos lenticulares en placas de 24 pocillos (Falcon). Tras lavarlos con PBS 1x, se incubaron 10 min a 37 ºC en oscuridad (se continuó trabajando en oscuridad a partir de este momento) con *MitoSOX Red* 3 µM en medio *Hank's balanced salt solution* (Sigma-Aldrich) se volvieron a lavar con PBS 1x y se fijaron 15 min con 4 % PFA (Sigma-Aldrich) a RT. Finalmente, se tiñeron con DAPI (Molecular Probes) los núcleos durante 10 min y se montaron con Mowiol. Las fotos se tomaron con un microscopio confocal espectral LSM710 (Zeiss), compuesto por un microscopio invertido de luz transmitida y epifluorescencia Observer.Z1 acoplado a un sistema confocal espectral con 6 líneas de láser (405, 488, 458, 514, 561, 633).

Actividad β-galactosidasa asociada a senescencia (SA-β-Gal).

El número de células senescentes se valoró mediante el contaje de células positivas para la actividad del enzima β-galactosidasa {Dimri, 1995 #760}. Para ello se incuban las células con X-gal, sustrato de la β-galactosidasa, que al degradarse produce un precipitado azul. Los MEF primarios, en cada pase sucesivo, se cultivaron sobre cubreobjetos lenticulares en placas de 24 pocillos (Falcon) y se procedió según las instrucciones del *Senescence β-Galactosidase Staining Kit* (Cell Signaling). Se montaron con glicerol al 70 % y se tomaron fotos en el microscopio Nikon 90i (Nikon) y con una cámara DS-Fi1 acoplada (Nikon), con la técnica de *Differential Interference Contrast* (DIC). Las imágenes se analizaron con el programa *ImageJ* (NIH).

Detección de roturas físicas en el ADN.

Se empleó la técnica ya descrita (Zambrano et al. 2014) utilizando la incorporación de dUTP biotinilado por la enzima terminal transferasa (TdT) para su posterior marcaje inmunocitoquímico. Los MEF primarios, de pases tempranos y tardíos, se cultivaron sobre un portaobjetos con 8 pocillos (Nunc), se fijaron con 4 % PFA durante 10 min, se permeabilizaron con solución de permeabilización (ver

inmunofluorescencia indirecta de células) durante 5 min y, tras un lavado con PBS 1x, se incubaron a 37 ºC O/N con 50 µl de la mezcla de reacción de la TdT (BioLabs) con 1 µl de dUTP biotinilado (Thermo Scientific). Posteriormente, se incubaron con estreptavidina-peroxidasa, del *Kit Vectastain ABC* (Vector Laboratories), según las instrucciones del fabricante. Se tiñeron los núcleos con *nuclear fast red* (NFR) (Sigma-Aldrich) y se montaron con *DPX Mountant* (Sigma-Aldrich). Las fotos se tomaron con el microscopio Nikon 90i (Nikon) con una cámara DS-Fi1 acoplada (Nikon). Las imágenes se analizaron con el programa *ImageJ* (NIH).

Medida de la reparación de roturas de doble cadena del ADN.

Para los experimentos de reparación de ADN con MEF primarios, estos se cultivaron en portaobjetos de 8 pocillos (Nunc) y se irradiaron con 3 Gy en un irradiador biológico Shepherd Mark I (J.L. Shepherd Mark) y se mantuvieron a 37 ºC el tiempo indicado. Entonces se procedió a valorar los complejos de reparación utilizando la técnica de inmunofluorescencia indirecta para células, anteriormente descrita.

Las fotos se tomaron con un microscopio Nikon 90i (Nikon), con una cámara refrigerada monocroma DS-Qi1Mc acoplada (Nikon) y con filtros para DAPI, FITC y TexasRed. El programa utilizado para la captura de imágenes es el *NisElements 3.01* (Nikon). Las imágenes se analizaron con el programa *ImageJ* (NIH).

Caracterización del fenotipo transformado *in vitro*.

Caracterización metabólica.

Medida de acidificación del medio.

Para valorar la diferencia de pH debido a secreciones de los MEF inmortalizados en cultivo, se cultivaron 10^6 células en placas p100 y, tras 72 h, se recogió el medio en un tubo de 15 ml (Falcon) y se midió el pH del medio de cultivo con un medidor de pH HI 2211 pH/ORP Meter (Hanna Instruments).

Medida de la Respiración celular.

Para obtener medidas de consumo de O_2 de nuestros cultivos, se utilizó el sistema *XF^{e}24 Analyzer* (Seahorse Biosciences). Se sembraron $6*10^4$ células en cada pocillo de una placa específica para la medida

de la respiración celular, *XF24 Cell Culture Microplates* (Seahorse Biosciences), y se mantuvieron en un incubador a 37 ºC O/N. Paralelamente, se incubaron los inyectores, *XF24 FluxPacks* (Seahorse Biosciences), con *XF Calibrant Solution* (Seahorse Biosciences) O/N en una estufa de CO_2 a 37 ºC.

Al día siguiente, se lavaron las células dos veces con PBS 1x y se cambió el medio por 675 µl de un medio DMEM sin tamponar, al que se le añadió 25 mM de Glucosa (Sigma-Aldrich) o 10 mM galactosa (Sigma-Aldrich), y se incubó 1 h en un incubador de CO_2 a 37 ºC. Durante este tiempo, se añaden a los inyectores (cuatro por pocillo), 75 µl de medio DMEM sin tamponar, 83,3 µl de Oligomicina (Sigma-Aldrich), 92,5 µl de FCCP (Sigma-Aldrich) y 102,8 µl de una mezcla de Rotenona (Sigma-Aldrich) y Antimicina A (Sigma-Aldrich) para obtener unas concentraciones finales de 6 µM de Oligomicina, 0,3 µM de FCCP, 0,1 µM de Rotenona y 0,1 µM de Antimicina A.

Los inyectores se introdujeron en el *XFe24 Analyzer* (Seahorse Biosciences) para comenzar el calibrado y al finalizar este, se introdujo, también, la placa con las células para iniciar las determinaciones. Se realizaron tres tipos de medidas de consumo de oxígeno tras añadir, en este orden, el medio DMEM sin tamponar, Oligomicina, FCCP y una mezcla de Rotenona y Antimicina A. Al finalizar las determinaciones, se recogieron las células y se prepararon extractos con el fin de determinar la cantidad de proteína por pocillo.

De esta forma, se obtuvieron determinaciones de la respiración basal, la respiración asociada a la síntesis de ATP, la respiración máxima, la capacidad de respiración reserva y la respiración no mitocondrial; y se calculó la eficiencia de respiración y de acoplamiento.

Análisis de flujos metabólicos mediante seguimiento de isotopos estables (^{13}C) por Resonancia Magnética Nuclear (RMN).

Para el estudio de flujos metabólicos a través de la glucolisis y el ciclo TCA, se cultivaron 10^6 MEF inmortalizados en placas de cultivo p100 con medio DMEM con 10 % FBS, 1 % L-Gln y 1 % P/S. Una vez alcanzada la confluencia, se cambió el medio por 15 ml de DMEM con 10 % FBS, 1 % P/S y con diferentes concentraciones de sustratos metabólicos con o sin marcaje con ^{13}C para su trazabilidad:

- 5 mM Glucosa y 2 mM Glutamina
- 5 mM (1-^{13}C) Glucosa.
- 5 mM (1-^{13}C) Glucosa y 2 mM Glutamina.
- 5 mM (1-^{13}C) Glucosa y 2 mM (U-$^{13}C_5$) Glutamina.
- 5 mM Glucosa y 2 mM (U-$^{13}C_5$) Glutamina.
- 2 mM Glucosa y 5 mM (U-$^{13}C_5$) Glutamina.

Se recogieron alícuotas de 400 µl en el tiempo 0 y pasadas 24 h, tras las cuales se lavaron los cultivos con PBS 1x, se realizó una lisis con N_2 líquido y una extracción de metabolitos solubles con ácido perclórico. Tras centrifugar la muestra, los pellets se guardaron y se utilizaron para cuantificar la cantidad de proteínas y los sobrenadantes se neutralizaron con KOH y se congelaron, para posteriormente liofilizarlos en un liofilizador *Telstar Cryodos* (Telstar). Seguidamente, se reconstituyeron con 800 µL de agua deuterada (D_2O) (Apollo Scientific), de los cuales 500 µl fueron transferidos a un tubo de RMN.

A las alícuotas recogidas del medio de cultivo se les añadieron 100 µl de D_2O y se pasaron 500 µl a un tubo de RMN. A todos los tubos se les añadió un capilar de 1 mm de diámetro con dioxano 10 mM como referencia.

Tanto las muestras de los extractos celulares como de los medios fueron analizados por el servicio de RMN del Servicio Interdepartamental de Investigación (SIdI) de la Universidad Autónoma de Madrid (UAM). Tras la obtención de los espectros por parte del servicio, se utilizó el programa *MestReNova* (MestreLab Research) para el análisis de los espectros y *Microsoft Excel* (Microsoft) para la cuantificación final de flujos metabólicos.

Análisis de aminoácidos intracelulares.

Los extractos celulares obtenidos en el experimento del estudio del flujo metabólico se enviaron al Servicio de Química de Proteínas del Centro de Investigaciones Biológicas (CIB) para realizar un análisis de aminoácidos. Los aminoácidos se separaron por cromatografía de intercambio catiónico y la derivatización se hizo postcolumna con ninhidrina.

Perfil de lípidos.

Se realizó un perfil de lípidos en colaboración con el grupo del Dr. José Ignacio Ruiz-Sanz de la Universidad del País Vasco (UPV).

Los lípidos se extrajeron con cloroformo/etanol (2:1, v/v) y los ácidos grasos individuales se obtuvieron e identificaron según estaba descrito previamente {Segarra, 2011 #1709}.

A partir de los datos de % de ácidos grasos obtenidos en el laboratorio del Dr. José Ignacio Ruiz-Sanz se calculó la cantidad de ácidos grasos saturados (SAT), monoinsaturados (MON) y poliinsaturados (PUFA); así como los ácidos grasos n-6 y n-3 y su relación n-6/n-3. También se calculó la longitud media de la cadena de carbonos (ACL), el índice de dobles enlaces (DBI) y el índice de peroxibilidad (PI) según se ha descrito anteriormente {Arranz, 2013 #1707}.

Finalmente, se calculó la actividad de desaturasas y elongasas concretas según se ha descrito anteriormente {Arranz, 2013 #1707}.

Muerte celular inducida por ausencia de factores de crecimiento.

Se cultivaron MEF inmortalizados en placas de seis pocillos (Falcon) con medio DMEM con 10 % FBS, 1 % L-Gln y 1 % P/S. Tras llegar a confluencia y detenerse la proliferación, se cambió el medio por medio DMEM fresco con distintas cantidades de FBS. Se contó el número de células viables en los pocillos a las 0, 24, 48, 72 y 96 h con una cámara de *Neubauer* (Blau Brand).

Crecimiento en baja densidad celular.

Para estudiar la capacidad de formación de colonias en cultivos celulares de baja densidad, se sembraron 2000 células en placas p100 (Falcon). Tras 11 días en cultivo, las células se fijaron mediante incubación durante 30 min con 4 % PFA y se tiñeron con cristal violeta (Sigma-Aldrich) 0,1 % preparado en PBS 1x. Tras 30 min de incubación, se lavaron con agua destilada, se contaron las colonias y se hicieron fotos de los bordes de las colonias con una cámara Nikon Digital Sight DS-L acoplada a una lupa MZ 16 F (Leica) y se analizaron con *ImageJ* (NIH). Las imágenes de toda la placa se obtuvieron escaneando las placas en un escáner hp scanjet 5590 (Hewlett-Packard).

Ensayos de sobreconfluencia.

Cultivos celulares de MEF inmortalizados se llevaron hasta confluencia en una placa p100 (Falcon) y se mantuvieron en estas condiciones 15 días más en cultivo con cambios de medio cada 48 h. Se hicieron fotos de los focos de sobrecrecimiento en tres dimensiones con una cámara Nikon Digital Sight DS-L acoplada a un microscopio Nikon TS100 (Nikon).

Formación de colonias en agar blando.

Se cubrió el fondo de los pocillos de una placa con seis pocillos (Falcon) con una primera capa de agarosa 0,6 % (Lonza) en medio DMEM con 10 % FBS, 1 % L-Gln y 1 % P/S precalentado y esterilizado en autoclave. Se dejó solidificar antes de añadir una segunda capa de agarosa 0,3 % en medio DMEM con 10 % FBS, 1 % L-Gln y 1 % P/S, que contenía $3*10^5$ células. Tras 15 min a 4 ºC, se mantuvieron a 37 ºC

durante 30 días, añadiendo 1 ml de medio fresco cada 72 h. Se monitorizó el crecimiento de colonias durante este tiempo, y a los 30 días las colonias se fijaron con 4 % PFA durante 30 min y se tomaron fotos con una cámara Nikon Digital Sight DS-L acoplada a una lupa MZ 16 F (Leica) que se analizaron posteriormente con el programa *ImageJ* (NIH).

Migración.

Se evaluó la velocidad de migración, el orden, la direccionalidad y la confluencia final adoptada por los cultivos tras la migración utilizando dos ensayos diferentes: un ensayo de cierre de herida *in vitro* y un ensayo de migración en cámara de Boyden.

Ensayo de cierre de herida *in vitro*.

Los MEF inmortalizados se cultivaron en placas de seis pocillos, y una vez llegados a confluencia, se realizó un surco en la monocapa celular con una punta de micropipeta p1000. Los pocillos se lavaron tres veces con PBS 1x para eliminar los restos celulares y se añadió medio fresco, con diferentes cantidades de FBS. Para monitorizar el cierre de herida se utilizó un sistema de observación *in vivo* Cell Observer (Zeiss), formado por un microscopio Observer.Z1 acoplado a un sistema de incubación con control de temperatura, CO_2 y humedad. Este sistema está acoplado a una cámara de alta resolución Cascade 1K (Photometrics). Se tomaron fotos cada 30 min, que se utilizaron para cuantificar el cierre de la herida con el programa *TScratch* {Geback, 2009 #652}. Los vídeos se montaron a partir de las fotos con el programa *Microsoft Windows MovieMaker* (Microsoft).

Ensayo de migración en cámara de Boyden.

Se sembraron $1{,}5*10^4$ MEF inmortalizados sobre la membrana porosa de una cámara de Boyden (Costar) con 100 µl de medio DMEM sin FBS. Se añadieron 500 µl de medio DMEM con 10 % de FBS en el fondo del pocillo, hacia donde migran las células. Tras 18 h en cultivo, las membranas se limpiaron con un hisopo para eliminar las células que no habían entrado en la membrana. Se lavaron las membranas con PBS 1x y se fijaron con etanol 70 % frío durante 15 min. Tras lavar 3 veces con PBS 1x, se incubó la membrana en oscuridad con medio de tinción nuclear (0,003 % yoduro de propidio, 0,1 mg/ml de ARNsa (Sigma-Aldrich) en PBS 1x), durante 30 min a 37 ºC y seguidamente durante 1 h y media a RT. Finalmente, se lavaron tres veces con PBS 1x, se recortó la membrana porosa y esta se montó en un portaobjetos con *ProLong* (Molecular Probes). Se tomaron imágenes con el microscopio confocal espectral LSM710 (Zeiss) de 6x6 campos y en 18 planos (*tile scan*), cubriendo toda la superficie y el grosor de la

membrana. Posteriormente, las imágenes se analizaron con el programa ZEN 2009 (Zeiss), que permite el montaje de las imágenes en tres dimensiones.

Experimentos *in vivo* de transformación tumoral.

Crecimiento celular *in vivo* sobre matriz (Matrigel).

Ratones C57BL/6j fueron inyectados subcutáneamente en el dorso con $2*10^6$ MEF inmortalizados obtenidos a partir de cultivos celulares en crecimiento exponencial, embebidas en 200 µl de una mezcla 2:1 de matrigel (BD Biosciences) y medio DMEM sin complementar, los ratones se mantuvieron anestesiados con isofluorano al 5 %. A los 60 días, los ratones fueron sacrificados y se extrajo el matrigel, se fijó con 4 % PFA y se incluyó en parafina (Casa Álvarez) para su posterior análisis histológico.

Crecimiento *in vivo* de MEF marcados con GFP en matrigel.

Los MEF inmortalizados GFP^+ obtenidos mediante infecciones con partículas retrovirales se cultivaron en placas p100, manteniéndose en crecimiento exponencial. Se inyectaron subcutáneamente $2*10^6$ células en el dorso de ratones C57BL/6j en 200 µl de matrigel (BD Biosciences) y medio DMEM sin complementar (relación 2:1).

A los 60 días, se sacrificaron los animales y se extrajeron las matrices. Estos se fijaron con 4 % PFA, durante 24 h, posteriormente se embebieron en sacarosa 30 % (Sigma-Aldrich) y, finalmente, se incluyeron en *Tissue-Tek OCT Compound* (Sakura) para su posterior análisis.

Formación de tumores primarios en ratones NOD-SCID.

Se inyectaron 10^7 MEF inmortalizados mediante inyección subcutánea en el dorso de ratones inmunodeprimidos NOD-SCID. Tras 15 días de evolución, se midieron los tumores con un calibre. La fórmula utilizada para obtener el volumen de los tumores fue: $V = \frac{4\pi}{3} abc$; donde a, b y c son los tres semiejes de un elipsoide. Se sacrificaron los animales y los tumores fueron fijados con 4 % PFA. Posteriormente, se incluyeron los tumores en parafina (Casa Álvarez) para su posterior análisis histológico.

Experimento *in vivo* de capacidad de formación de metástasis.

Inoculación de las células en ratones NOD-SCID.

Para valorar la capacidad de las células MEF inmortalizados de contribuir al desarrollo de metástasis, se realizó un ensayo de metástasis experimental *in vivo* mediante la coinoculación de MEF inmortalizados junto con células B16-V5, una línea celular de melanoma de ratón con capacidad metastática. Ambas líneas fueron previamente infectadas con lentivirus para generar variantes que expresaban constitutivamente los genes codificantes para GFP y luciferasa.

Tanto los MEF inmortalizados como las células de la línea tumoral de melanoma B16-V5 se crecieron en placas p100. Para la inoculación fueron resuspendidas, contadas y diluidas en *Hank's balanced salt solution* a una concentración de $5*10^5$ células por cada 100 µl.

100 µl de esta dilución fueron inoculados por la vena lateral de la cola en los ratones NOD-SCID. Para dilatar la vena de la cola, esta se calentó a 42 ºC.

Detección de luciferasa *in vivo*.

Se hizo un seguimiento semanal *in vivo* de la actividad luciferasa para monitorizar el desarrollo de metástasis. Para ello, se inyectaron intraorbitalmente 100 µl del sustrato de la luciferasa (15 µg/ml) (Cayman Chemical) por ratón y se detectó la emisión de luz mediante el sistema IVIS lumina (Perkin Elmer). A los 28 días de la inoculación, los ratones se sacrificaron y se extrajeron los pulmones, que fueron fijados con *Bouin's Solution* (Sigma). Los nódulos metastáticos se contaron manualmente en una lupa MZ 16 F (Leica). Finalmente, los pulmones se incluyeron en parafina (Casa Álvarez) para su posterior valoración histológica.

Histología.

Con las muestras de tejido que fueron incluidas en parafina, se realizaron cortes con un microtomo automático Leica RM 2255 (Leica) de 4 µm, que fueron posteriormente teñidas con hematoxilina-eosina o en las que se realizó una tinción inmunohistoquímica con los anticuerpos de interés.

Con las muestras que fueron incluidas en *Tissue-Tek OCT Compound*, se realizaron cortes de 10 µm de grosor con un criotomo y se utilizaron para los ensayos de inmunohistofluorescencia.

Tinción de hematoxilina-eosina.

Los cortes se desparafinaron durante 20 min en xilol, se hidrataron con pases sucesivos de 5 min en etanol absoluto, etanol 96 %, etanol 70 % y H_2O destilada. Una vez hidratados, se sumergieron en hematoxilina de Harris durante 4 min y se lavaron con agua corriente durante 5 min bajo el grifo (con flujo continuo). Seguidamente, se procedió a realizar la tinción con eosina alcohólica durante 3 min. Tras un lavado de agua corriente durante 5 min, se procedió a la deshidratación de los cortes, realizando pases sucesivos a etanol en concentraciones crecientes. Finalmente, las muestras se montaron con *DPX Mountant* (Sigma-Aldrich). Se adquirieron imágenes con el microscopio Nikon 90i (Nikon) acoplado a una cámara DS-Fi1 acoplada (Nikon). Las imágenes se analizaron con el programa *ImageJ* (NIH).

Inmunohistoquímica.

Los cortes se desparafinaron durante 20 min en Xilol y se hidrataron con pases sucesivos de 3 min en etanol absoluto, etanol 75 %, etanol 50 %, etanol 25 %, H_2O destilada y PBS 1x. El desenmascaramiento del antígeno se realizó en una olla a presión para microondas *Microwave Tender Cooker* (Nordic Ware) con tampón citrato pH 6.0 (10mM citrato de sodio, 0,05 % Tween 20) en cuna de plástico, durante 15 min a 700 W de potencia y durante otros 15 min a 350 W de potencia. Al restaurarse la presión ambiental, se sacaron los cortes a una cuna de cristal con PBS 1x y se procedió con la inhibición de la actividad peroxidasa endógena sumergiendo los cortes en Metanol/0,3 % H_2O_2 durante 25 min. A continuación, se realizó un bloqueo con permeabilización utilizando la solución de bloqueo del *Kit Vectastain ABC* (Vector Laboratories) y 0,1 % de Triton X-100, siguiendo las instrucciones del fabricante, durante 30 min en cámara de humedad a RT.

Seguidamente, se incubó con el anticuerpo primario O/N a 4 ºC en solución de bloqueo sin Triton X-100. La dilución empleada para el anticuerpo de Ki67 fue 1/200. El anticuerpo secundario (unido a biotina) se preparó según las instrucciones del *Kit Vectastain ABC* (Vector Laboratories), así como la estreptavidina-peroxidasa.

El sustrato de la peroxidasa se preparó siguiendo las instrucciones del *Peroxidase substrate Kit DAB* (Vector Laboratories) y se incubaron con él los cortes hasta que el control negativo (sin anticuerpo primario) comenzó a adquirir coloración marrón. Se tiñeron los núcleos con NFR durante 20 min, se lavaron con etanol absoluto y, a continuación, se transfirieron a xilol. Finalmente, se montaron con la solución *DPX Mountant* (Sigma-Aldrich). Se adquirieron imágenes con un microscopio Nikon 90i (Nikon) acoplado a una cámara DS-Fi1 acoplada (Nikon). Las imágenes se analizaron con el programa *ImageJ* (NIH).

Inmunohistofluorescencia.

Los cortes congelados e incluidos en OCT (guardados a -80 ºC) se depositaron en una cámara húmeda durante 30 min a RT, posteriormente se lavaron con PBS 1x y se incubaron durante 10 min con cloruro amónico 50 mM diluido en PBS pH 7,4 a RT para eliminar la autofluorescencia del propio tejido.

A continuación, se realizó una fase de bloqueo de antígenos y permeabilización celular incubando durante 1 h con una solución de bloqueo y permeabilización (5 % FBS, 0,3 % Triton X-100 en PBS 1x). Seguidamente, los cortes se lavaron 4 veces con PBS 1x durante 5 min antes de incubar con el anticuerpo primario diluido (Tabla 5) en la solución de bloqueo y permeabilización O/N a 4 ºC.

Anticuerpo	Dilución	Especie	Marca comercial
Ki67	1/200	Conejo	Thermo Scientific (RM-9106-S1)
GFP	1/200	Conejo	Santa Cruz (sc-8334)

Tabla 5. Anticuerpos utilizados en las inmunohistofluorescencias.

Tras lavar nuevamente el tejido con PBS 1x, se incubaron los cortes con un anticuerpo secundario unido a un fluoróforo, diluido en solución de bloqueo y permeabilización, durante 1 h a RT. Tras volver a lavar con PBS, los cortes se incubaron durante 15 min con DAPI diluido en PBS 1x.

Finalmente, se montaron con *ProLong* (Molecular Probes) y las fotos se tomaron con un microscopio confocal espectral LSM710 (Zeiss), compuesto por un microscopio invertido de luz transmitida y epifluorescencia Observer.Z1 acoplado a un sistema confocal espectral con 6 líneas de láser (405, 488, 458, 514, 561, 633).

Estadística.

Los datos que se representan en las gráficas son la media ± desviación estándar. El análisis estadístico utilizado fue una prueba T de Student para dos colas y datos con una varianza similar o una prueba T de Student para datos apareados cuando fue necesario. Se consideraron estadísticamente significativas las diferencias cuando el p-valor fue menor que el nivel de significancia $\alpha=0.05$. *, $p<0.05$; **, $p<0.01$; y ***, $p<0.005$.

RESULTADOS

Capítulo I: La ausencia de PGC-1α resulta en una inducción temprana de marcadores de senescencia celular y una rápida inmortalización en MEF.

Con el fin de valorar el papel de PGC-1α en el proceso de inducción de senescencia e inmortalización y analizar los mecanismos implicados se realizó un estudio *in vitro* utilizando como modelo experimental células MEF. Este protocolo consta de dos partes, en la primera se realizan pases seriados de las células primarias hasta que estas alcanzan su límite replicativo e inducen la entrada en senescencia o la muerte celular. En el organismo, cuando una célula entra en senescencia o muere, se activa el sistema inmunitario, reclutándose, al tejido afectado, monocitos circulantes. Los macrófagos activados son los responsables de eliminar los restos celulares y las células senescentes, lo que generalmente evita que se inicien procesos tumorales. Sin embargo, tanto *in vitro* como *in vivo*, algunas células son capaces de escapar de la senescencia e inmortalizar siendo el estudio de este proceso de inmortalización la segunda parte del protocolo llevado a cabo.

Para replicar este proceso *in vitro*, MEF silvestres y MEF deficientes en PGC-1α se crecieron en placas de cultivos y se realizaron pases seriados hasta que el cultivo llegó a senescencia, siguiendo el protocolo 3T3 clásico. Las células senescentes se mantuvieron en cultivo hasta que finalmente las células inmortalizaron espontáneamente (Todaro and Green 1963). En cada uno de los pases previos a la entrada a senescencia se valoró el estado de las células mediante diversas técnicas.

La ausencia de PGC-1α tiene un impacto en el metabolismo oxidativo y en la acumulación de ROS mitocondriales en MEF.

Como hemos referido anteriormente, PGC-1α es un coactivador transcripcional y regulador maestro del metabolismo oxidativo, regulando, entre otros, los genes responsables de la biogénesis mitocondrial, y de los sistemas que controlan la producción y eliminación de ROS mitocondriales. PGC-1α está presente en todos los tejidos del organismo, pero es más abundante en los tejidos que presentan una alta demanda energética, y se regula en respuesta a estímulos que indican cambios en la disponibilidad de nutrientes o en el gasto metabólico (Arany et al. 2005; Basu et al. 2013; Lehman et al. 2000; St-Pierre et al. 2006; Valle et al. 2005; Z. Wu et al. 1999). Diversos estudios muestran que la exposición a niveles elevados de ROS induce la entrada temprana en senescencia (Takahashi et al. 2006). Por ello, decidimos valorar el impacto de la ausencia de PGC-1α en la homeostasis redox y su impacto sobre la inducción de senescencia.

Empezamos por valorar como la ausencia de PGC-1α en MEF afectaba a los niveles de expresión de dos dianas génicas de PGC-1α (Valle et al. 2005), la enzima superóxido dismutasa mitocondrial

(MnSOD), una de las enzimas principales en la homeostasis redox mitocondrial y cit C, que forma parte de la ETC; mediante *western blot*.

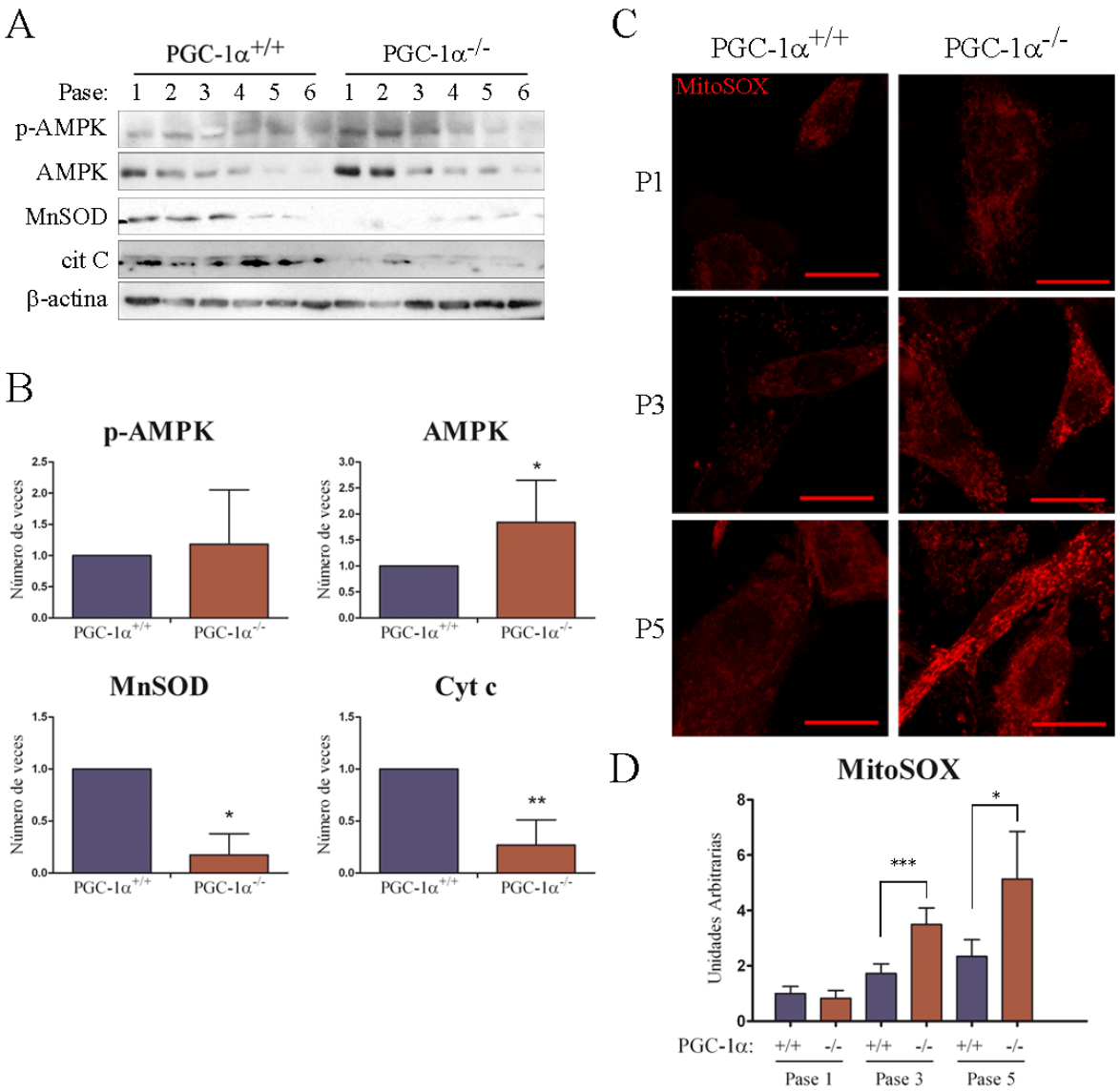

Figura 7. A) Nivel de expresión de proteínas de p-AMPK, AMPK, MnSOD y cit C. Control de carga: β-actina. **B)** Densitometrado del nivel de proteína por pase, relativizado con el control silvestre. N=3. **C)** Imágenes representativas de MEF primarios silvestres y deficientes en PGC-1α incubados con MitoSOX. P1, pase 1; P3, pase 3; P5, pase 5. Escala 20 μm. **D)** Cuantificación de los ROS mitocondriales en los MEF primarios silvestres y deficientes en PGC-1α. N=4. Los datos están representados como la media ± desviación típica. *, $p < 0.05$; **, $p \leq 0.01$; ***, $p \leq 0.005$.

Observamos como en MEF silvestres los pases sucesivos resultaban en un descenso gradual de la expresión de MnSOD, que se hacía más acusado cuando las células se acercaban a la senescencia. En ausencia de PGC-1α, la expresión de MnSOD resultó ser menor que en los MEF silvestres en todos los pases, llegando a ser prácticamente indetectable en los pases más altos (Fig. 7A-B).

Respecto a cit C, los niveles permanecieron prácticamente constantes en los distintos pases, siendo su expresión menor en MEF deficientes en PGC-1α que en los de genotipo silvestre (Fig. 7A-B).

Este resultado sugería, por una parte, que la entrada en senescencia se acompaña con una bajada en las defensas antioxidantes, al menos en la mitocondria, y por otra, que la ausencia de PGC-1α, al igual que en otros tipos celulares, tiene como resultado una disminución en la actividad mitocondrial y en la capacidad antioxidante de la célula.

Para valorar si la reducción en la actividad mitocondrial comprometía metabólicamente a las células, se analizaron los niveles de la proteína AMPK, tanto total como de su forma activa, fosforilada. AMPK es una quinasa que se activa en respuesta a un aumento en la relación AMP/ATP (Gowans et al. 2013). En MEF silvestres, los pases sucesivos resultaban en un descenso gradual de la expresión de AMPK y un aumento en su nivel de fosforilación (relación p-AMPK/AMPK). Los MEF deficientes en PGC-1α presentaron un nivel más alto de AMPK que los silvestres en todos los pases. Además, en los pases sucesivos, la fosforilación de AMPK también se redujo gradualmente. Como media, sin embargo, el nivel de p-AMPK fue similar en ambos genotipos, lo que sugería la ausencia de PGC-1α no generaba estrés metabólico en los MEF (Fig.7A-B).

La MnSOD es una enzima localizada en la matriz mitocondrial donde transforma al anión superóxido, producido en la ETC, en peróxido de hidrógeno. La observación de que el nivel de MnSOD disminuía con los pases en MEF silvestres, y estaban reducidos en ausencia de PGC-1α, nos llevó a valorar si esta reducción podría tener como consecuencia un aumento del nivel de anión superóxido en la mitocondria. Con este fin, se realizó una tinción de los cultivos a distintos pases con *MitoSOX Red,* un fluoróforo que se incorpora a favor de gradiente en la mitocondria y al oxidarse en presencia del anión superóxido emite fluorescencia en rojo.

Se observó que el nivel de fluorescencia del MitoSOX se va incrementando gradualmente a medida que los cultivos acumulan pases, tanto en MEF silvestres como deficientes en PGC-1α. Además, como era esperable, los MEF deficientes en PGC-1α mostraron mayor nivel de fluorescencia que los MEF silvestres, siendo la diferencia significativa a partir del tercer pase (Fig. 7C-D), cuando la cantidad de fluorescencia emitida en ausencia de PGC-1α fue 2 veces mayor y esta diferencia se mantuvo en los pases sucesivos hasta entrar en senescencia. Estos resultados son consistentes con los datos obtenidos para MnSOD, lo que apoya el papel esencial de esta proteína en el control del nivel de superóxido mitocondrial. Además, sugiere que la producción mitocondrial de superóxido puede contribuir de manera significativa al aumento del nivel celular de ROS que se asocia a la entrada en senescencia, y que se ha descrito como causa y efecto de la senescencia.

La mayor concentración de ROS detectados en ausencia de PGC-1α se asocia con mayor nivel de oxidación de ADN genómico y una mayor tasa de roturas en el ADN.

Dado que los MEF deficientes en PGC-1α parecían acumular más anión superóxido que los MEF silvestres durante los pases previos al estado senescente, decidimos valorar si la producción excesiva de ROS mitocondriales tenía como resultado un aumento en la oxidación del ADN. Para ello, realizamos un análisis por inmunofluorescencia de nuestros cultivos utilizando anticuerpos dirigidos contra la forma oxidada de la guanosina, la 8-hidroxi-deoxiguanosina (8-OH-dG), principal producto de la oxidación del ADN, y que es causa de la aparición de mutaciones en el ADN (Shibutani et al. 1991).

La primera observación reseñable fue la doble localización del marcaje del anticuerpo. Por un lado, se detectaron focos nucleares individuales fácilmente distinguibles y, por otro lado, un marcaje punteado citoplasmático que se atribuyó a la presencia de ADN mitocondrial (ADNmt) oxidado. El número de focos mitocondriales fue en todos los casos mucho mayor que el de focos nucleares, lo que se atribuye al hecho de que la mitocondria es una importante fuente de ROS, y el ADNmt es más susceptible de daño que el nuclear, en parte porque está menos protegido y en parte porque sus mecanismos de reparación son menos eficientes que los del ADN genómico (ADNg). Ambos tipos de señales se valoraron de manera independiente. Para valorar el marcaje mitocondrial se midió el nivel de fluorescencia y se relativizaron al número de células por campo. En cuanto al análisis de focos nucleares, se cuantificaron los focos por célula.

Se analizaron células de pase 2 y de pase 5 con el fin de determinar si existía una relación entre la inducción de senescencia y la presencia de ADN oxidado. Se observó que tanto la oxidación del ADNmt como del ADNg eran mayores en pase 5 que en pase 2, una observación consistente con los resultados previos que indicaban un aumento gradual del estrés oxidativo mitocondrial con los pases sucesivos.

Además, se valoró si el aumento de los ROS mitocondriales se correlacionaba con un incremento en la oxidación del ADNg, para lo que se contaron los focos que aparecían en el núcleo. En ausencia de PGC-1α, los MEF mostraron mayor cantidad de focos de oxidación de ADNg por célula (Fig. 8A-B) en pase 5, en el que mostraron 7,9 focos de oxidación por célula por los 4,1 focos de oxidación por célula en MEF silvestres. Sin embargo, no se observaron diferencias significativas en el nivel de ADNmt oxidado entre ambos genotipos.

Concluimos por tanto que, el aumento en el nivel de superóxido mitocondrial asociados a la bajada en el nivel de MnSOD podrían ser los responsables del mayor nivel de oxidación del ADN observado en los pases largos de los MEF y que estaba aumentado por la ausencia de PGC-1α.

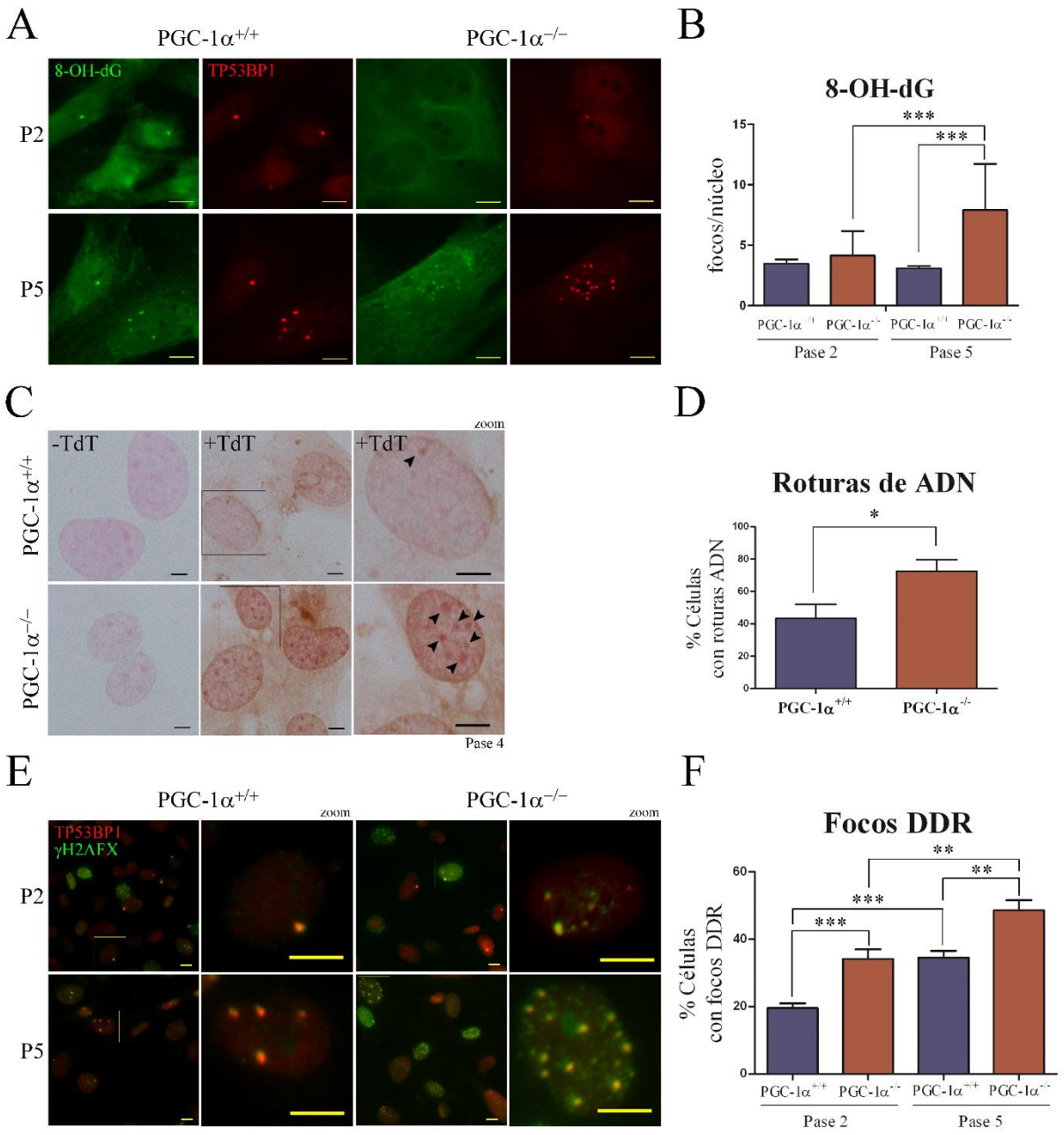

Figura 8. A) Imágenes representativas de MEF primarios silvestres y deficientes en PGC-1α incubados con 8-OH-dG y TP53BP1, marcando la oxidación del ADN. P2, pase 2; P5, pase 5. Escala 10 μm. **B)** Cuantificación de focos de ADN oxidado por núcleo. N=3. **C)** Imágenes representativas de la incorporación de dUTP biotinilado en las zonas de roturas de ADN en MEF primarios silvestres y deficientes en PGC-1α. La tercera columna muestra una vista ampliada de parte de la foto adyacente. Escala 10 μm. **D)** Cuantificación de las roturas de ADN en MEF primarios silvestres y deficientes en PGC-1α. N=3. **E)** Imágenes representativas de MEF primarios silvestres y deficientes en PGC-1α incubados con TP53BP1 y γH2AX, marcando los focos de reparación. La segunda y la cuarta columna muestran una vista ampliada de parte de la foto adyacente. P2, pase 2; P5, pase 5. Escala 10 μm. **F)** Cuantificación de los focos de reparación en MEF primarios silvestres y deficientes en PGC-1α. N=3. Los datos se muestran como la media ± desviación típica. *, $p < 0.05$; **, $p \leq 0.01$; ***, $p \leq 0.005$.

Seguidamente, dado que el ADN oxidado puede alterar la progresión de las horquillas de replicación y causar inestabilidad génica, se evaluó el número de roturas de doble cadena en MEF de pase 4. Para ello, realizamos un marcaje de las roturas, mediante la incorporación de nucleótidos biotinilados por la enzima TdT, una enzima capaz de incorporar nucleótidos en los extremos 3' libres de manera independiente de molde. La incorporación del nucleótido biotinilado dUTP permite revelar este marcaje tras incubación con estreptavidina unida a peroxidasa de rábano, utilizando los reactivos utilizados habitualmente en inmunohistoquímica. Se observó que el número de células que presentaba marcaje nuclear era significativamente mayor en los cultivos de MEF deficientes en PGC-1α que en los de MEF silvestres, un 43 % de los MEF silvestres mostraron marcaje de incorporación de dUTP mientras que en ausencia de PGC-1α este número se elevó hasta el 72 % de las células, lo que indicaba una mayor presencia de roturas de doble cadena en ausencia de PGC-1α (Fig. 8C-D), posiblemente asociada al mayor nivel de ADN oxidado, pero que podría estar también relacionada con una alteración en la eficacia de los sistemas de reparación.

Por tanto, decidimos evaluar la formación de complejos de reparación, para lo que se realizó un ensayo de inmunofluorescencia con anticuerpos dirigidos contra la proteína TP53BP1, que forma parte de los complejos de reparación (Manis et al. 2004; Ward et al. 2003a); y contra la histona γH2AX, que se recluta a zonas del ADN dañado (Burma et al. 2001; Stiff et al. 2004). Estas dos proteínas interaccionan y colocalizan en los llamados focos de reparación en respuesta al daño en el ADN (DDR) (Ward et al. 2003b). Se evaluó la colocalización de TP53BP1 y γH2AX con la presencia de marcaje para 8-OH-dG, observándose que el 80 % de los focos de reparación correspondían a focos positivos para 8-OH-dG, lo que apoyaba la idea de que la oxidación del ADN es la principal causa de la presencia de roturas en el ADN y que estas reclutan eficientemente los complejos de reparación incluso en ausencia de PGC-1α. Consistentemente, se observó un incremento gradual del número de células con focos de reparación tanto en MEF silvestres, del 19 % en pase 2 al 34 % en pase 5; como en ausencia de PGC-1α, del 34 % en pase 2 al 48 % en pase 5; y un mayor número de células con focos en MEF deficientes en PGC-1α que en MEF silvestres (Fig. 8E-F). Este resultado apoya, por tanto, la idea de que el aumento en el número de roturas se debe fundamentalmente al aumento en la oxidación del ADN en los cultivos de MEF. Sin embargo, no podíamos descartar una posible pérdida de actividad en los complejos de reparación en los MEF sin PGC-1α por lo que decidimos testar esta posibilidad en un experimento independiente.

Para ello, se sometieron a MEF de ambos genotipos, en pase 2, a una dosis subletal de radiación γ (3 Gy en un irradiador biológico) con el fin de evaluar la capacidad de reparación del ADN en ambos genotipos de manera independiente de la cantidad de daño a la que estaban expuestos. Teniendo en cuenta el grado de localización observado previamente entre TP53BP1 y γH2AX, los complejos de reparación se siguieron por inmunofluorescencia dirigida contra γH2AX a diferentes tiempos tras la irradiación de las células.

A los 15 min postirradiación, los cultivos de MEF de ambos genotipos presentaron más de 10 focos de marcaje de γH2AX en casi la totalidad de las células, lo que sugería que la cantidad de roturas inducidas por la radiación en ambos genotipos era similar. Sin embargo, a tiempos más largos postirradiación, empezaron a ser notables las diferencias entre los cultivos de ambos genotipos. A las 3 h, había significativamente menos focos de reparación en los MEF silvestres que en los deficientes en PGC-1α y esta diferencia seguía siendo evidente a las 6 h. A las 9 h, la mayor parte de los focos habían sido resueltos tanto MEF silvestres como MEF sin PGC-1α, llegando al estado basal preirradiación en torno a las 12 h en ambos cultivos (Fig. 9). Este resultado indica que la eficiencia de los procesos de reparación es menor en los MEF deficientes en PGC-1α y por tanto puede contribuir significativamente a la aparición de un mayor número de roturas de ADN en respuesta a la oxidación. Sin embargo, la magnitud de las diferencias observadas, en torno al 10 %, sugieren que la presencia de un mayor nivel de ADN oxidado es el factor fundamental en las diferencias observadas en el nivel de roturas de ADN detectables en MEF deficientes en PGC-1α.

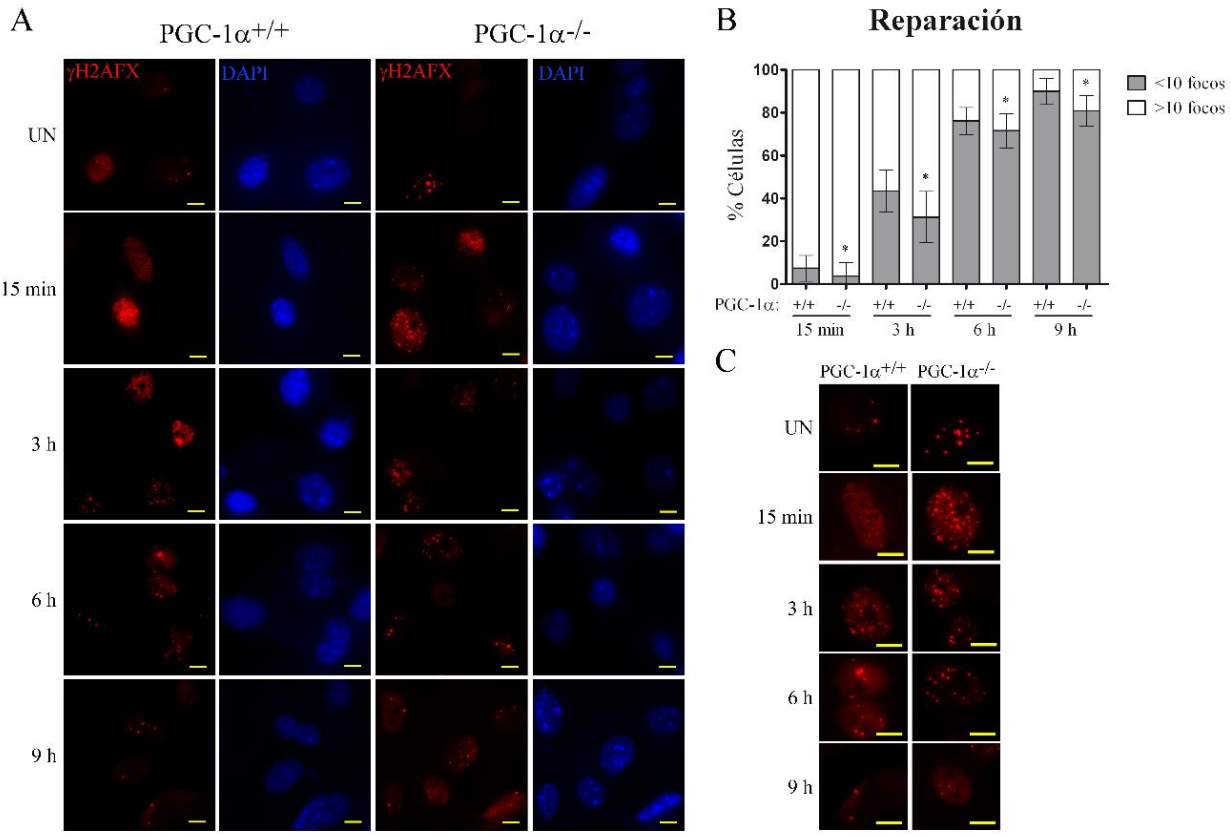

Figura 9. A) Imágenes representativas de la formación de focos de reparación tras 15 minutos, 3 horas, 6 horas y 9 horas postirradación; y sin irradiar (UN) de MEF primarios silvestres y deficientes en PGC-1α. Escala 10 μm. **B)** Gráfica que muestra el porcentaje de células con más de 10 focos de reparación y menos de 10 focos de reparación. N=3. **C)** Vista ampliada de los focos de reparación. Escala 10 μm. Los datos están representados como la media ± desviación típica. *, $p < 0.05$; **, $p \leq 0.01$; ***, $p \leq 0.005$.

El estrés genotóxico inducido por la ausencia de PGC-1α provoca la inducción temprana de marcadores de senescencia en MEF, pero no se induce de manera eficiente la parada de ciclo y la muerte celular, y se produce un proceso rápido de inmortalización.

Los resultados obtenidos resultaron, por tanto, ser consistentes con estudios anteriores en los que se había demostrado que la disfunción mitocondrial era un factor promotor de la entrada en senescencia al favorecer la acumulación del daño en el ADN y por tanto la inestabilidad génica (Hutter et al. 2004; Moiseeva et al. 2009) y sugerían que la ausencia de PGC-1α podía ser relevante en este proceso. Como ya se indicó en la introducción, son bien conocidos los mecanismos a través de los cuales el daño en el ADN y el estrés oxidativo inducen mediadores de parada de ciclo y apoptosis (Samper et al. 2003; Velarde et al. 2012). Los principales factores implicados en este proceso, y que se utilizan generalmente como marcadores moleculares de senescencia son p53, p16, p19 y p21 (Herbig et al. 2004; Serrano et al. 1993), siendo la inducción de p21 por p53 el principal ejecutor de la inducción de la parada de ciclo en respuesta a estrés genotóxico y ROS (Macip et al. 2003; Takahashi et al. 2006). En su conjunto, la activación del programa de entrada en senescencia se ha propuesto que permite mantener permanentemente activada la cascada de señalización por daño en el ADN (Passos et al. 2010).

Para evaluar como la ausencia de PGC-1α impacta en el proceso de entrada en senescencia, se evaluaron los niveles de estos factores en los distintos pases hasta la llegada a senescencia mediante *Western Blot*. En el caso de p53, se analizaron tanto el nivel total como el de su principal forma fosforilada (p-p53), que representa la forma activa de la proteína, pero no se encontraron diferencias significativas en el cociente p-p53/p53 ni de forma dependiente de pase ni de genotipo (Fig. 10A-B).

El análisis del patrón de inducción de p16, p19 y p21 sí mostró diferencias significativas entre ambos genotipos. En los MEF, estos inhibidores del ciclo celular mostraron una inducción más temprana y de mayor magnitud en ausencia de PGC-1α que en presencia de PGC-1α, aunque con patrones diferentes. En el caso de p16, la cantidad de proteína aumentó con el pase, tanto en los MEF silvestres como en MEF deficientes en PGC-1α (Fig. 10A-B). Por otra parte, el nivel de expresión de p19 en MEF silvestres resultó prácticamente indetectable, encontrándose elevado en MEF sin PGC-1α desde el primer pase para más tarde ir gradualmente decayendo (Fig. 10A-B). Finalmente, el nivel de expresión de p21 fue mayor en MEF deficientes en PGC-1α en todos los pases, aunque se observó un patrón descendente en ausencia de PGC-1α que no se vio en MEF silvestres, seguramente por el bajo nivel que se observó desde el primer pase. Estos resultados, en su conjunto sugerían una inducción temprana de los marcadores de senescencia en MEF deficientes en PGC-1α, consistente con la mayor presencia de ADN dañado en este genotipo.

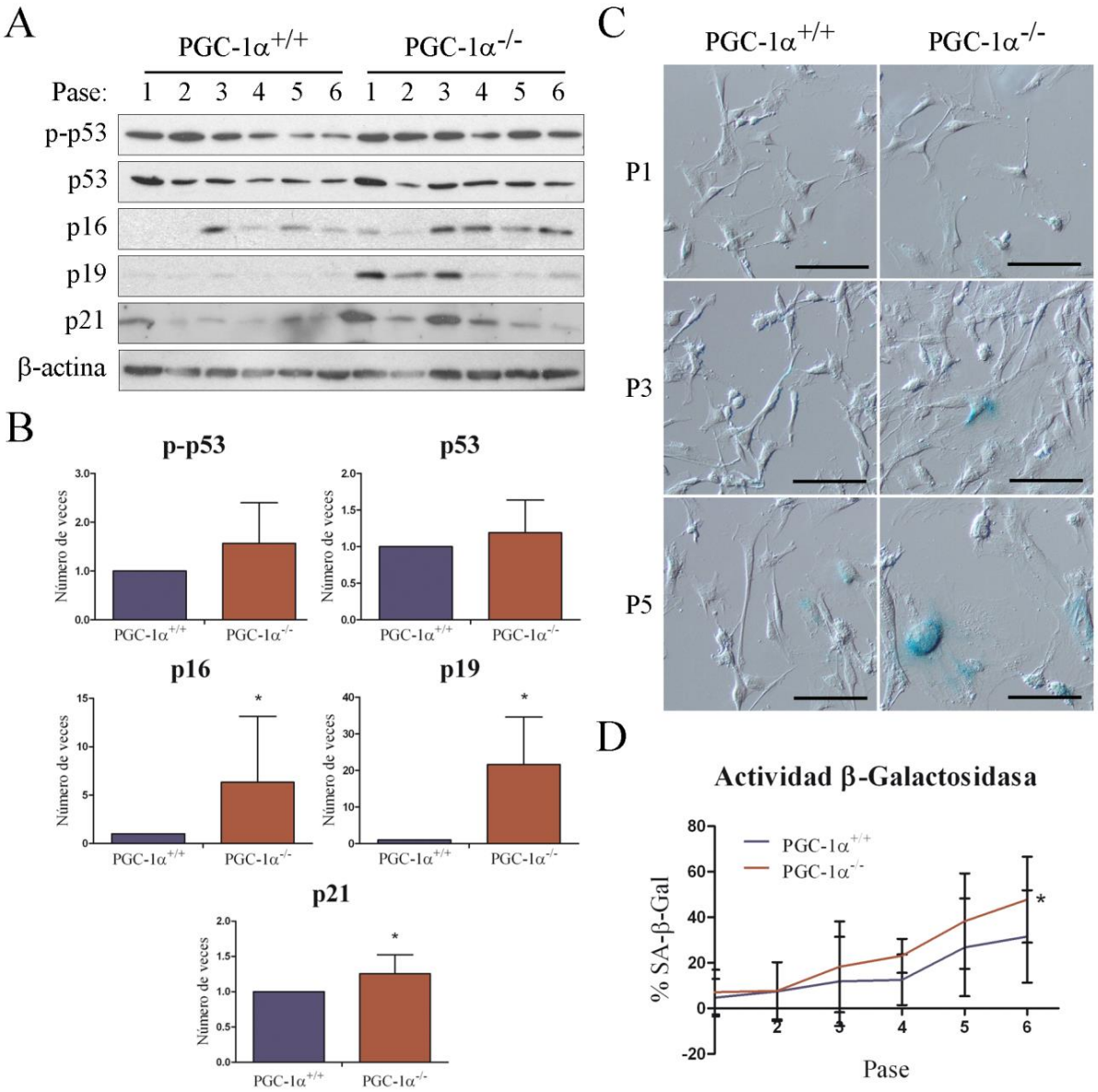

Figura 10. A) Nivel de expresión de proteína de p-p53, p53, p16, p19 y p21. Control de carga: β-actina. **B)** Densitometrado del nivel de proteína por pase, relativizado con el control silvestre. N=3. **C)** Imágenes representativas de la tinción con X-Gal de MEF primarios silvestres y deficientes en PGC-1α. P1, pase 1; P3, pase 3; P5, pase 5. Escala 100 μm. **D)** Cuantificación del porcentaje de células senescentes en cada pase antes de la entrada a senescencia. N=3. Los datos están representados como la media ± desviación típica. *, $p < 0.05$; **, $p \leq 0.01$; ***, $p \leq 0.005$.

Desde un punto de vista fenotípico, uno de los cambios más característicos de las células senescentes es la actividad SA-β-Gal, lo que permite diferenciar las células senescentes de las células proliferativas mediante un sencillo ensayo colorimétrico. Los cultivos son incubados con X-gal, que produce un precipitado azul al ser degradado por la β-Galactosidasa. Por tanto, para valorar si la inducción de marcadores moleculares se acompañaba de la inducción de un fenotipo senescente, realizamos un ensayo de actividad β-Galactosidasa en los cultivos de MEF a distintos pases. Como era de esperar, el

porcentaje de células senescentes presentes en las placas de cultivo aumentó a medida que los cultivos acumulaban pases en ambos genotipos. Sin embargo, los MEF sin PGC-1α presentaron un aumento significativamente mayor que los MEF silvestres (Fig. 10C-D), lo que indicaba una entrada en senescencia más temprana que en los MEF silvestres, un resultado consistente con la inducción temprana de marcadores de senescencia observada.

A la vista de estos resultados, cabía esperar que los cultivos de MEF deficientes en PGC-1α indujeran una parada de ciclo de manera más temprana que los MEF silvestres. Sin embargo, la evaluación de la velocidad de proliferación en ambos genotipos no mostró diferencias significativas con los pases, solamente una ligera tendencia a una menor velocidad de crecimiento en ausencia de PGC-1α en los MEF (Fig. 11A-B). La tasa de proliferación se calculó siguiendo la fórmula: $\Delta Crecimiento = \log_2(n_f - n_i)$, donde n_f es el número contado tras levantarlas y n_i es el número de células iniciales, en este caso 10^6.

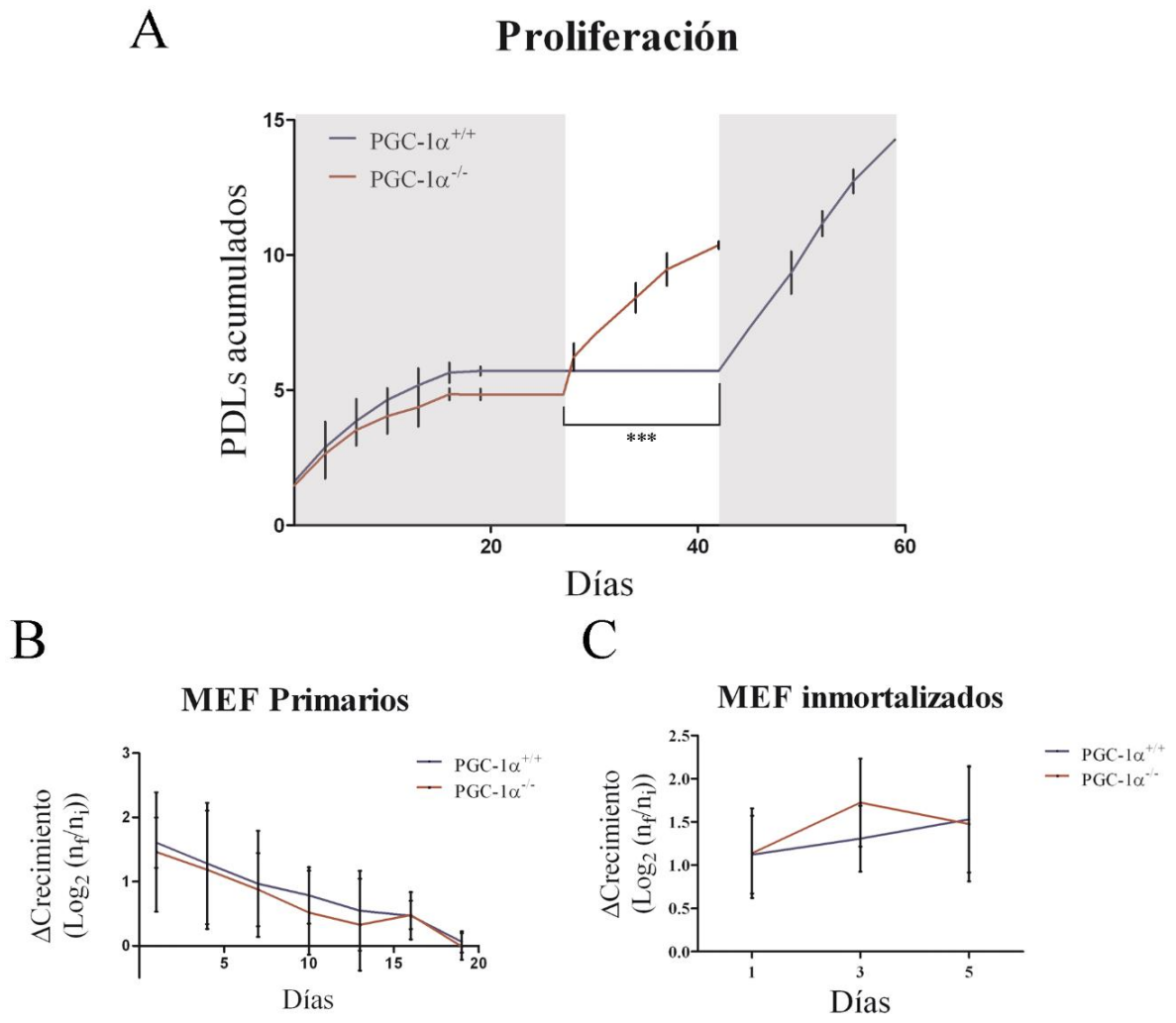

Figura 11. A) Proliferación acumulada en cultivo de MEF silvestres y MEF deficientes en PGC-1α, calculada como $\Delta_{Crecimiento} = \log_2(n_f - n_i)$ y agregándola a la del pase anterior. El espacio de fondo blanco se corresponde con la diferencia en el tiempo de inmortalización. N=8. **B)** Crecimiento de MEF primarios silvestres y deficientes en PGC-1α. N=8. **C)** Crecimiento de MEF inmortalizados silvestres y deficientes en PGC-1α. N=3. Los datos están representados como la media ± desviación típica. *, $p < 0.05$; **, $p \leq 0.01$; ***, $p \leq 0.005$.

Al no haber diferencias significativas en las tasas de proliferación, ambos genotipos indujeron la entrada en fase no proliferativa de manera simultánea. Los cultivos se mantuvieron en cultivo para evaluar el tiempo de inmortalización y, en este caso, sí se encontraron diferencias significativas, siendo más corto en ausencia de PGC-1α, que tardaron aproximadamente 8 días en inmortalizar mientras que los MEF de genotipo silvestre necesitaron 24 días para hacerlo (Fig. 11A). Finalmente, evaluamos en las células inmortalizadas las velocidades de proliferación y, de nuevo, no se encontraron diferencias significativas entre los dos genotipos (Fig. 11C).

Estos resultados sugerían una deficiencia en los MEF sin PGC-1α en la inducción de la parada de ciclo y/o la inducción de muerte celular. Teniendo en cuenta que PGC-1α interacciona y aumenta la actividad de p53 (Aquilano et al. 2013; Sahin et al. 2011; Sen et al. 2011), el principal inductor de parada de ciclo y muerte celular en respuesta a estrés oxidativo y genotóxico, decidimos evaluar la posibilidad de que una inducción defectiva en los genes diana de p53 pudiera estar mediando el efecto observado. Para determinar esto, se realizó un análisis de expresión mediante RT-qPCR de varios genes diana de p53, entre los que se encontraban genes proapoptóticos, como *Bbc3*, *Pmaip1* o *Bax*; reguladores del ciclo celular ante daño genómico o estrés oxidativo, como *Sesn1*, *Sesn2*, *Ndn* o *Gadd45a*; y enzimas metabólicas, como *Gls2* o *Aldh4*. El resultado de este experimento mostró una expresión reducida de 6, *Gls2*, *Aldh4*, *Sesn2*, *Bbc3*, *Pmaip1* y *Gadd45a*; de los 9 genes estudiados en ausencia de PGC-1α (Fig. 12), confirmando la reducida actividad transcripcional de p53 en este contexto, que podría justificar el fallo en la inducción de parada de ciclo, inducción de muerte y la rápida inmortalización de los MEF deficientes en PGC-1α.

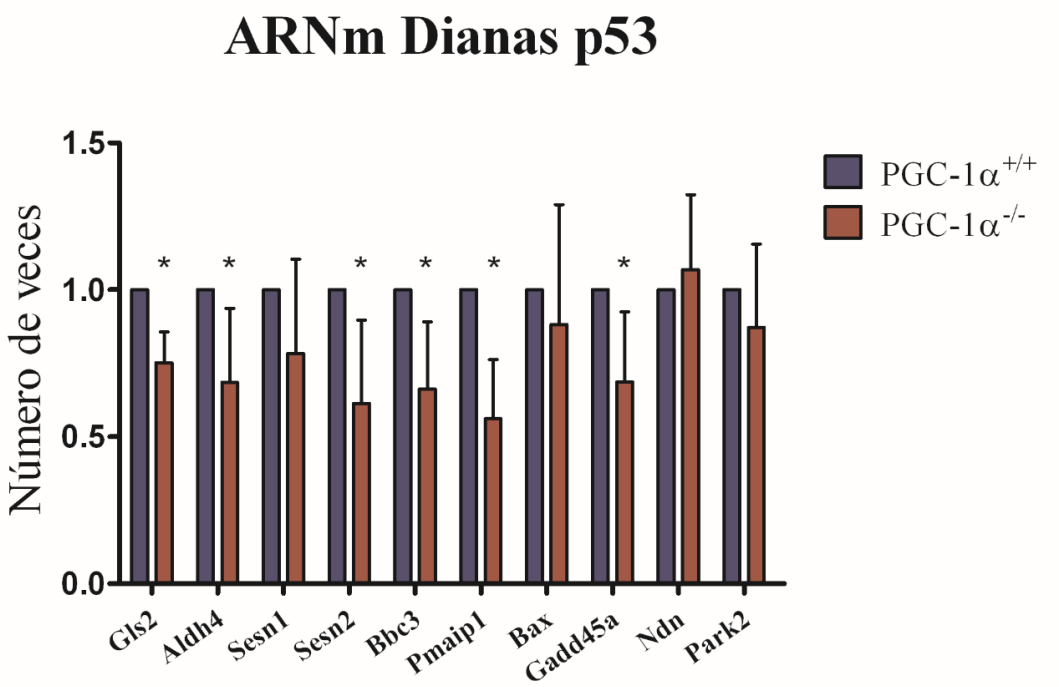

Figura 12. Nivel de expresión de ARNm de genes regulados por p53. Los datos están normalizados respecto al control silvestre y están representados como la media ± desviación típica. N=3. *, $p < 0.05$; **, $p \leq 0.01$; ***, $p \leq 0.005$.

Capitulo II: MEF inmortalizados deficientes en PGC-1α presentan cambios metabólicos y fenotípicos característicos de células tumorales.

Una vez que nuestros cultivos, tras alcanzar el estado senescente, inmortalizaron, quisimos valorar si el hecho de haber inmortalizado en un fondo genético u otro aportaba a estas células características distintivas que fueran relevantes en un contexto de desarrollo tumoral.

Teniendo en cuenta que PGC-1α es un regulador maestro del metabolismo debido a su papel de coactivador transcripcional de genes que controlan el metabolismo oxidativo (Villena 2015) y a la luz de las evidencias que indican que la reprogramación metabólica juega un importante papel en la agresividad tumoral, decidimos evaluar los cambios, a nivel metabólico, que se generaban en ausencia de PGC-1α en MEF inmortalizados que pudieran ser relevantes en este contexto.

Por otra parte, y de manera complementaria, dado que la transformación tumoral conlleva la adquisición de características distintivas por las células transformadas, tales como inestabilidad genómica, inducción de estado inflamatorio, capacidad de escapar a la activación de supresores de crecimiento, mantenimiento de la señalización proliferativa, resistencia a la muerte celular, inducción de angiogénesis, capacidad de invasión y escape a la detección por el sistema inmunitario; y que estas a su vez se relacionan con los cambios metabólicos que sufren las células tumorales (Hanahan and Weinberg 2011), decidimos analizar el fenotipo tumoral de los MEF inmortalizados de ambos genotipos *in vitro* para valorar las diferencias y sus posibles implicaciones en el desarrollo tumoral *in vivo*.

Los MEF inmortalizados deficientes en PGC-1α presentan un metabolismo más glucolítico y menos oxidativo que los MEF inmortalizados silvestres.

Dado el papel regulador del metabolismo oxidativo de PGC-1α, quisimos valorar si tras el proceso de inmortalización se preservaban las diferencias entre los dos genotipos en cuanto a la dependencia de la glucolisis y de la actividad oxidativa o si estas habían sido anuladas por el propio proceso de inmortalización, que actúa incrementando la dependencia de la glucolisis y en detrimento de la actividad de la fosforilación oxidativa y la actividad del ciclo TCA (Warburg 1956a).

Como primera aproximación para valorar el balance entre glucolisis y oxidación, empezamos por determinar mediante *Western blot* los niveles de la enzima PFKFB3, que regula positivamente el flujo glucolítico de la glucosa al piruvato, y de cit C, componente esencial de la ETC. Los resultados obtenidos mostraron que los MEF inmortalizados sin PGC-1α presentaban niveles más elevados de PFKFB3 y más reducidos de cit C que los MEF inmortalizados silvestres (Fig. 13A-B), lo que sugería una mayor actividad

oxidativa en los MEF inmortalizados silvestres que en los deficientes en PGC-1α, y por tanto indicaba que las diferencias en el control metabólico se mantenían tras el proceso de inmortalización.

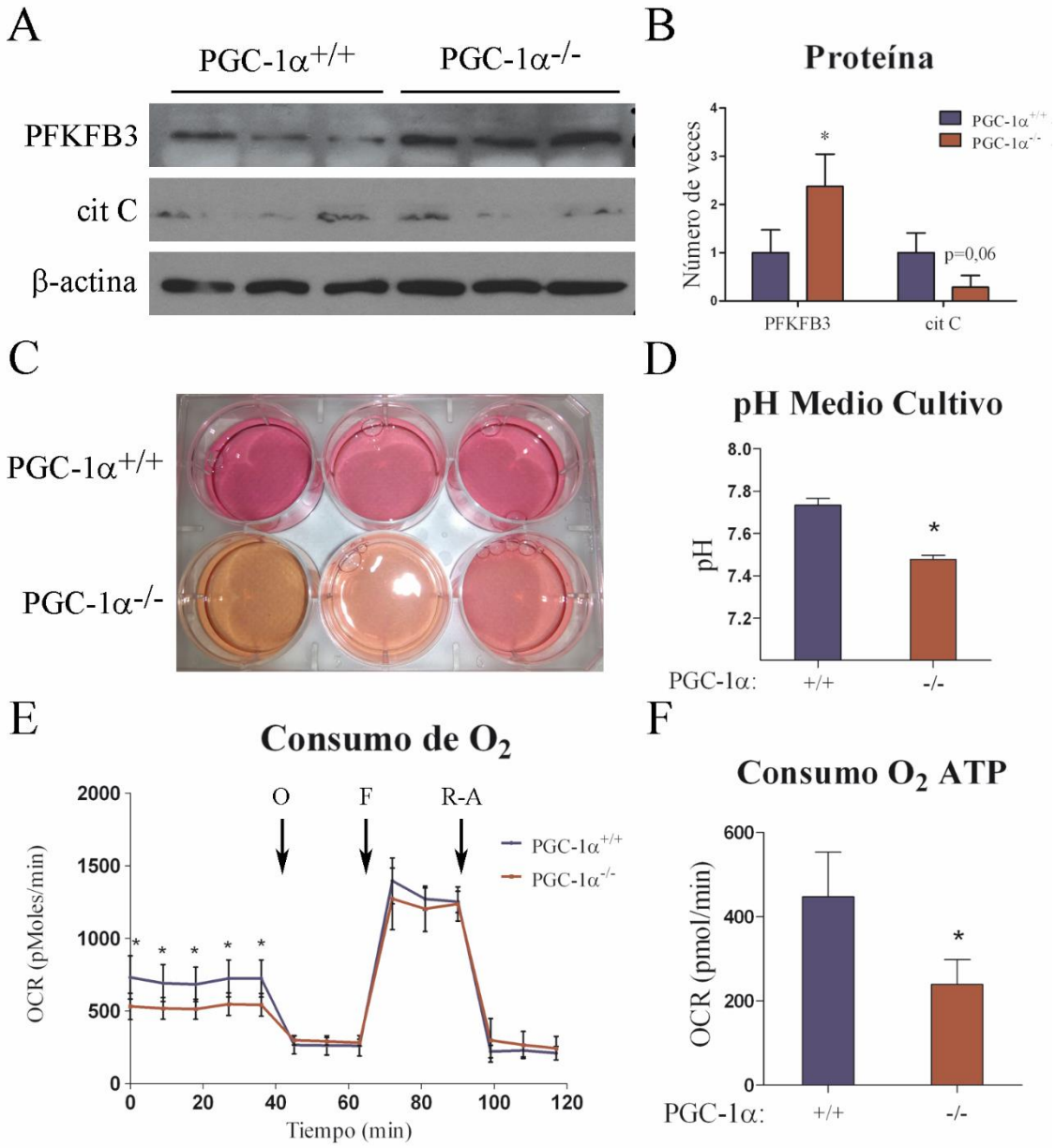

Figura 13. A) Medida mediante western blot del nivel de expresión de proteína de PFKFB3 y cit C en MEF inmortalizados silvestres y deficientes en PGC-1α. Control de carga: β-actina. **B)** Densitometrado del nivel de proteína, relativizado con el control silvestre. N=3. **C)** Imagen representativa de los medios de cultivo tras 3 días en cultivo. **D)** Medida de pH del medio de cultivo de MEF inmortalizados silvestres y deficientes en PGC-1α. N=3. E**)** Medida del consumo de O_2 basal y tras la adición de oligomicina 6 μM (O), FCCP 0,3 μM (F) y una mezcla de rotenona 0,1 μM y Antimicina A 0,1 μM (R-A) en MEF inmortalizados silvestres y deficientes en PGC-1α. N=3. F**)** Consumo de O_2 relacionado con la síntesis de ATP en MEF inmortalizados silvestres y deficientes en PGC-1α. N=3. Los datos están representados como la media ± desviación típica. *, $p < 0.05$; **, $p \leq 0.01$; ***, $p \leq 0.005$.

Para comprobar si esta diferencia a nivel de proteínas se correspondía con cambios fisiológicos realizamos una evaluación del cambio del pH del medio de cultivo tras 72 h de incubación, como medida indirecta de la acumulación de lactato, una medida que es, generalmente, indicativa del consumo anaerobio

de la glucosa, pero que, en nuestro caso, al ser utilizado un medio de cultivo tamponado, esta determinación no es adecuada para cuantificar la concentración de lactato en el medio. Los resultados obtenidos mostraron que el pH del medio de cultivo de los MEF inmortalizados deficientes en PGC-1α era 7,47 y era significativamente más ácido que el de MEF inmortalizados silvestres cuyo pH fue 7,73 tras 72 horas de incubación (Fig. 13C-D), lo que sugiere una mayor producción de lactato y, por tanto, una glucolisis anaerobia más activa en los MEF inmortalizados sin PGC-1α.

Seguidamente, decidimos evaluar directamente la capacidad oxidativa de los MEF inmortalizados utilizando un sistema de oximetría de alta resolución, para ello las células se incubaron en un medio de cultivo en el que se sustituyó la glucosa por la galactosa. Este cambio fuerza a las células en cultivo a utilizar el metabolismo oxidativo como fuente de ATP (Robinson et al. 1992), por lo que las células estrictamente glucolíticas no son viables en este tipo de medios. La evaluación del consumo de oxígeno se realizó tanto en condiciones basales como en presencia de inhibidores de la ATP sintasa (Oligomicina), de los complejos I (Rotenona) y III (Antimicina A) así como en presencia de un agente desacoplante (FCCP) con el fin de evaluar, entre otros parámetros, la capacidad respiratoria máxima, la capacidad de reserva, el nivel de acoplamiento entre el consumo de oxígeno y la producción de ATP, el "escape" de protones y el consumo de oxígeno no dependiente de la actividad de la ETC. Los resultados obtenidos mostraron que los MEF inmortalizados deficientes en PGC-1α tienen un consumo de oxígeno basal menor (Fig. 13E), así como un menor nivel de acoplamiento entre el consumo de oxígeno y la síntesis de ATP (Fig. 13F), un 50 % menor en MEF inmortalizados deficientes en PGC-1α, pero no se encontraron diferencias significativas en respiración máxima, capacidad de reserva ni respiración no mitocondrial. Estos resultados apoyaron por tanto la idea de que los MEF inmortalizados PGC-1α$^{-/-}$ tienen un metabolismo oxidativo menos activo que los silvestres.

Tras observar que los MEF inmortalizados deficientes en PGC-1α tenían un metabolismo oxidativo menor y una posible mayor producción de lactato, decidimos evaluar los flujos metabólicos utilizando (1-^{13}C) Glucosa y/o (U-$^{13}C_5$) Glutamina en el medio de cultivo para realizar estudios de seguimiento de moléculas marcadas con ^{13}C mediante RMN y espectrofotometría de masas, en extractos celulares y los correspondientes medios de cultivo a diferentes tiempos: antes de incubar las células con el medio y tras 24 horas de incubación.

El análisis por RMN de los medios de cultivo a tiempo 0 y a las 24 h de incubación, nos permitió determinar de manera directa el nivel de consumo de glucosa y la producción de lactato. De manera consistente con los resultados obtenidos mediante la medida del pH del medio de incubación, las células deficientes en PGC-1α produjeron más lactato, aunque no se encontraron diferencias significativas en el consumo de glucosa. La medida de consumo de glucosa y producción de lactato permitió la evaluación indirecta del consumo del O_2, que fue menor en los MEF inmortalizados sin PGC-1α, un resultado consistente con las medidas de consumo de oxígeno mediante oximetría (Fig. 14).

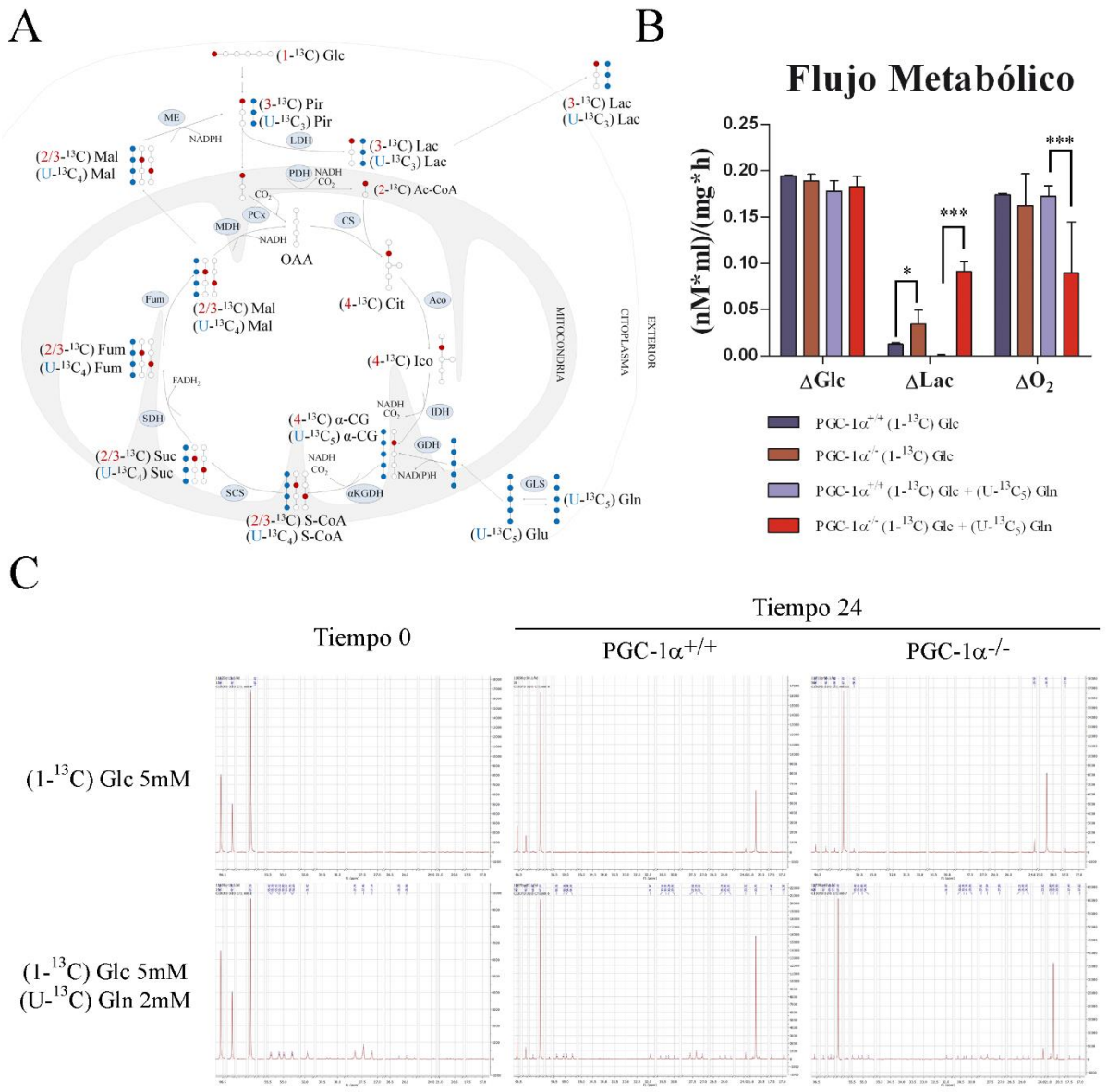

Figura 14. A) Esquema de la ruta seguida por la glucosa y la glutamina a través de la glucolisis y el ciclo TCA. En granate, la marca de ^{13}C con origen en la (1-^{13}C) glucosa. En azul, la marca de ^{13}C con origen en la (U-$^{13}C_5$) glutamina. α-CG, α-cetoglutarato; Ac-CoA, Acetil-CoA; Cit, Citrato; Fum, Fumarato; Glc, Glucosa; Glu, Glutamato; Gln, Glutamina; Ico, Isocitrato; Lac, Lactato; Mal, Malato; OAA, Oxalacetato; Pir, Piruvato; Suc, Succinato; S-CoA, Succinil-CoA. **B)** Medida del consumo de glucosa y O_2, y producción de lactato de MEF inmortalizados silvestres y deficientes en PGC-1α. N=4. **C)** Espectros de RMN representativos del medio de cultivo con (1-^{13}C) glucosa 5 mM y del medio de cultivo (1-^{13}C) glucosa 5 mM + (U-^{13}C) glutamina 2 mM de MEF inmortalizados silvestres y deficientes en PGC-1α a tiempo 0 y 24 horas. Referencia: dioxano 10 mM. Los datos están representados como la media ± desviación típica. *, $p < 0.05$; **, $p \leq 0.01$; ***, $p \leq 0.005$.

Como se ha indicado en la introducción, la salida del citrato de la mitocondria para su uso como precursor de la síntesis de ácidos grasos es una característica importante en el metabolismo tumoral. Con el experimento de trazabilidad de sustratos no conseguimos observar el citrato por lo que se realizó un perfil de ácidos grasos de los cultivos de MEF primarios e inmortalizados de ambos genotipos para valorar la regulación de la síntesis lipídica.

% nmol	PGC-1α$^{+/+}$ 1º	PGC-1α$^{-/-}$ 1º	PGC-1α$^{+/+}$ INM	PGC-1α$^{-/-}$ INM
SAT	47,92 ± 1,78	47,76 ± 1,55	50,11 ± 1,51	47,62 ± 0,75
MON	28,09 ± 1,74	21,14 ± 0,52^{a**}	25,19 ± 0,97	26,64 ± 4,00^{c*}
PUFA	23,98 ± 0,18	31,10 ± 1,03^{a**}	24,70 ± 0,77	25,75 ± 3,28^{c*}
n-6	17,28 ± 0,36	24,60 ± 0,37^{a**}	17,71 ± 0,94	19,59 ± 2,76^{c*}
n-3	6,44 ± 0,38	6,28 ± 0,61	6,52 ± 0,62	5,77 ± 0,53
n-6/n-3	2,69 ± 0,21	3,9 ± 0,32^{a**}	2,75 ± 0,36	3,39 ± 0,18
ACL	18,06 ± 0,05	18,29 ± 0,02	18,08 ± 0,15	18,12 ± 0,06
DBI	127,02 ± 2,40	149,17 ± 5,07^{a*}	125,67 ± 4,98	132,35 ± 11,35
PI	1,05 ± 0,02	1,35 ± 0,05^{a*}	1,06 ± 0,06	1,12 ± 0,17

Tabla 6. Porcentaje de lípidos saturados (SAT), insaturados, monoinsaturados (MON) y poliinsaturados (PUFA); y n-6 y n-3 en MEF primarios e inmortalizados silvestres y deficientes en PGC-1α. Con estos datos se han calculado las siguientes relaciones: el ratio n-6/n-3, el índice de dobles enlaces (DBI), el índice de peroxibilidad (PI) y la longitud media de los ácidos grasos (ACL). [a], PGC-1α$^{+/+}$ 1º vs PGC-1α$^{-/-}$ 1º; [b], PGC-1α$^{+/+}$ 1º vs PGC-1α$^{+/+}$ INM; [c], PGC-1α$^{-/-}$ 1º vs PGC-1α$^{-/-}$ INM; [d], PGC-1α$^{+/+}$ INM vs PGC-1α$^{-/-}$ INM. *, $p < 0.05$; **, $p \leq 0.01$; ***, $p \leq 0.005$.

No se encontraron diferencias significativas en el porcentaje de ácidos grasos saturados o insaturados presentes en los MEF. Sin embargo, dentro del grupo de ácidos grasos insaturados, si se encontraron diferencias en el porcentaje de ácidos grasos MON y PUFA, mostrando una mayor cantidad de PUFA en los MEF deficientes en PGC-1α (Tabla 6). Este aumento de PUFA puede ser consecuencia del cambio en los niveles de ácido araquidónico (20:4n-6) (AA) que mostró un aumento significativo de su nivel en ausencia de PGC-1α (Tabla 7). Este mayor nivel de AA en MEF deficientes en PGC-1α podría indicar, a su vez, una mayor actividad de la desaturasa Δ5(n-6) (Tabla 8) que es responsable de la formación de un doble enlace en el ácido dihomo-γ-linolenico (20:3n-6) (DGLA) para formar el AA.

% nmol	PGC-1α$^{+/+}$ 1º	PGC-1α$^{-/-}$ 1º	PGC-1α$^{+/+}$ INM	PGC-1α$^{-/-}$ INM
12:0	0,19 ± 0,09	0,10 ± 0,00	0,26 ± 0,15	0,10 ± 0,04
14:0	2,20 ± 0,43	0,92 ± 0,04	1,93 ± 0,41	1,27 ± 0,21
14:1n-5	0,02 ± 0,01	0,01 ± 0,00	0,02 ± 0,00	0,01 ± 0,01
15:0	0,61 ± 0,05	0,60 ± 0,02	0,55 ± 0,08	0,54 ± 0,04
16:0	22,48 ± 0,26	22,22 ± 0,74	24,15 ± 2,50	23,89 ± 0,70
16:1n-7(t)	0,08 ± 0,05	0,06 ± 0,05	0,11 ± 0,07	0,03 ± 0,02
16:1n-7(c)	2,54 ± 0,61	1,26 ± 0,15	2,05 ± 0,66	1,94 ± 0,50
16:1n-10	0,18 ± 0,02	0,15 ± 0,07	0,15 ± 0,02	0,14 ± 0,01
16:1n-10	0,21 ± 0,01	0,19 ± 0,04	0,19 ± 0,02	0,21 ± 0,02
16:1n-9(c)	2,00 ± 0,29	1,28 ± 0,15	2,15 ± 0,54	1,86 ± 0,35
17:0	0,91 ± 0,06	0,82 ± 0,02	0,80 ± 0,17	0,78 ± 0,05
18:0	15,67 ± 1,49	17,87 ± 1,39^{a**}	16,14 ± 1,70	15,42 ± 0,75^{c***}
18:1n-9(t)	0,07 ± 0,01	0,05 ± 0,01	0,06 ± 0,02	0,05 ± 0,01
18:1n-9(c)	15,29 ± 0,75	11,89 ± 0,78^{a***}	13,36 ± 1,18	15,34 ± 2,58$^{c***;d**}$
18:1n-7(c)	4,24 ± 0,60	3,72 ± 0,33	3,63 ± 0,52	4,20 ± 0,25
19:0	0,14 ± 0,01	0,11 ± 0,00	0,12 ± 0,01	0,11 ± 0,03
18:2n-6(t)	0,04 ± 0,01	0,02 ± 0,00	0,04 ± 0,00	0,02 ± 0,01
18:2n-6(c)	2,40 ± 0,21	2,40 ± 0,32	2,63 ± 0,25	2,40 ± 0,51
18:3n-6	0,09 ± 0,02	0,06 ± 0,00	0,13 ± 0,05	0,11 ± 0,06
20:0	0,26 ± 0,08	0,22 ± 0,07	0,34 ± 0,08	0,33 ± 0,14
18:3n-3	0,04 ± 0,01	0,03 ± 0,02	0,08 ± 0,03	0,03 ± 0,01
20:1n-9	0,18 ± 0,01	0,15 ± 0,03	0,38 ± 0,17	0,30 ± 0,15
21:0	0,05 ± 0,01	0,03 ± 0,02	0,04 ± 0,01	0,03 ± 0,01
20:2n-6	0,10 ± 0,01	0,10 ± 0,00	0,10 ± 0,00	0,10 ± 0,01
20:3n-9	0,26 ± 0,08	0,22 ± 0,06	0,47 ± 0,17	0,39 ± 0,06
20:3n-6	0,92 ± 0,07	1,00 ± 0,09	1,34 ± 0,43	0,75 ± 0,15
22:0	0,52 ± 0,06	0,58 ± 0,30	0,70 ± 0,05	0,74 ± 0,09
20:4n-6	10,79 ± 0,57	17,98 ± 0,11^{a***}	11,36 ± 0,62	13,47 ± 3,33$^{c***;d***}$
22:1n-9	1,00 ± 0,53	0,48 ± 0,15	1,55 ± 1,02	0,54 ± 0,23
23:0	0,12 ± 0,01	0,13 ± 0,06	0,12 ± 0,01	0,12 ± 0,02
20:5n-3	0,53 ± 0,06	0,50 ± 0,14	0,99 ± 0,38	0,40 ± 0,03
24:0	0,85 ± 0,05	0,76 ± 0,37	1,09 ± 0,23	0,84 ± 0,33
22:4n-6	2,53 ± 0,20	2,45 ± 0,23	1,76 ± 1,05	2,30 ± 0,16
24:1n-9	0,85 ± 0,08	0,82 ± 0,38	0,73 ± 0,05	0,92 ± 0,03
22:5n-6	0,41 ± 0,01	0,59 ± 0,07	0,35 ± 0,09	0,44 ± 0,04
25:0	0,06 ± 0,02	0,04 ± 0,02	0,15 ± 0,15	0,04 ± 0,02
22:5n-3	3,30 ± 0,14	2,59 ± 0,13	2,98 ± 0,36	2,45 ± 0,20
22:6n-3	2,57 ± 0,38	3,15 ± 0,58	2,47 ± 0,46	2,88 ± 0,37
26:0	0,04 ± 0,01	0,02 ± 0,00	0,04 ± 0,01	0,02 ± 0,02

Tabla 7. Porcentaje de ácidos grasos en MEF primarios e inmortalizados silvestres y deficientes en PGC-1α. [a], PGC-1α$^{+/+}$ 1º vs PGC-1α$^{-/-}$ 1º; [b], PGC-1α$^{+/+}$ 1º vs PGC-1α$^{+/+}$ INM; [c], PGC-1α$^{-/-}$ 1º vs PGC-1α$^{-/-}$ INM; [d], PGC-1α$^{+/+}$ INM vs PGC-1α$^{-/-}$ INM. *, $p < 0.05$; **, $p \leq 0.01$; ***, $p \leq 0.005$.

Además, el análisis comparativo de los distintos grupos de ácidos grasos mostró que el índice de dobles enlaces, el índice de peroxibilidad y la relación n-6/n-3 están aumentados en ausencia de PGC-1α, siendo las diferencias más marcadas en los cultivos primarios que en los inmortalizados (Tabla 6).

	Ratio	PGC-1α$^{+/+}$ 1º	PGC-1α$^{-/-}$ 1º	PGC-1α$^{+/+}$ INM	PGC-1α$^{-/-}$ INM
Δ9(n-7)	C16:1/C16:0	0,12 ± 0,03	0,06 ± 0,01	0,09 ± 0,02	0,08 ± 0,02
Δ9(n-9)	C18:1/C18:0	0,98 ± 0,13	0,67 ± 0,01	0,83 ± 0,06	1,00 ± 0,22
Δ8(n-6)	C20:3/C20:2	8,76 ± 0,46	10,02 ± 0,83	12,74 ± 3,92	7,42 ± 0,56^{d**}
Δ5(n-6)	C20:4/C20:3	11,79 ± 1,54	18,00 ± 1,60^{a**}	8,51 ± 6,05	18,04 ± 7,46^{d***}
ELOVL3 (n-9)	C20:1/C18:1	0,01 ± 0,00	0,01 ± 0,00	0,03 ± 0,01	0,02 ± 0,01
ELOVL6	C18:0/C16:0	0,70 ± 0,06	0,80 ± 0,09	0,67 ± 0,14	0,65 ± 0,01
ELOVL1/3/7	C20:0/C18:0	0,02 ± 0,00	0,01 ± 0,01	0,02 ± 0,00	0,02 ± 0,01
ELOVL1/3/7	C22:0/C20:0	2,00 ± 0,51	2,60 ± 0,53	2,06 ± 0,51	2,27 ± 0,65
ELOVL1/3/7	C24:0/C22:0	1,63 ± 0,11	1,31 ± 0,06	1,56 ± 0,37	1,14 ± 0,30
ELOVL5	C20:2/C18:2	0,04 ± 0,00	0,04 ± 0,00	0,04 ± 0,00	0,04 ± 0,00
ELOVL2/5 (n-6)	C22:4/C20:4	0,23 ± 0,02	0,14 ± 0,01	0,16 ± 0,09	0,17 ± 0,04
ELOVL2/5 (n-3)	C22:5/C20:5	6,18 ± 1,02	5,17 ± 1,75	3,02 ± 2,53	6,08 ± 0,97

Tabla 8. Actividad de las enzimas responsables de la formación de los diferentes ácidos grasos en MEF primarios e inmortalizados silvestres y deficientes en PGC-1α. [a], PGC-1α$^{+/+}$ 1º vs PGC-1α$^{-/-}$ 1º; [b], PGC-1α$^{+/+}$ 1º vs PGC-1α$^{+/+}$ INM; [c], PGC-1α$^{-/-}$ 1º vs PGC-1α$^{-/-}$ INM; [d], PGC-1α$^{+/+}$ INM vs PGC-1α$^{-/-}$ INM. *, $p < 0.05$; **, $p \leq 0.01$; ***, $p \leq 0.005$.

El hecho de observarse diferencias en la cantidad relativa de los ácidos grasos nos llevó a proponer que la síntesis de estos era diferente entre ambos genotipos, pudiendo haber una mayor síntesis en ausencia de PGC-1α. La mayor salida de citrato del ciclo TCA en MEF inmortalizados deficientes en PGC-1α puede provocar un déficit de OAA al no completarse el ciclo TCA. Además, la reducción general en la actividad de la ETC lleva consigo una baja actividad de la SDH o complejo II de la ETC. Esta baja actividad de la SDH produciría un bloqueo del ciclo reduciéndose los niveles de fumarato, malato y OAA. El OAA es un metabolito esencial para el inicio del ciclo TCA ya que se condensa con el Ac-CoA, formado por la PDH a partir del piruvato, y su déficit debe ser compensado por la activación de la vía anaplerótica de la enzima PCx, que cataliza la formación de OAA a partir de piruvato.

Con el fin de evaluar la vía de entrada en el ciclo TCA del piruvato analizamos el destino del marcaje de ^{13}C de la glucosa marcada en su C_1 midiendo los picos en los espectros de RMN del glutamato, tanto del C_2, C_3 y C_4; ya que los metabolitos del ciclo TCA formados por la vía de la PDH se marcan en su

carbono C_4, mientras que la entrada por la vía de la PCx da lugar a metabolitos marcados en su carbono C_2, y se pudo establecer el porcentaje de entrada por la vía anaplerótica respecto a la convencional (Fig. 15A).

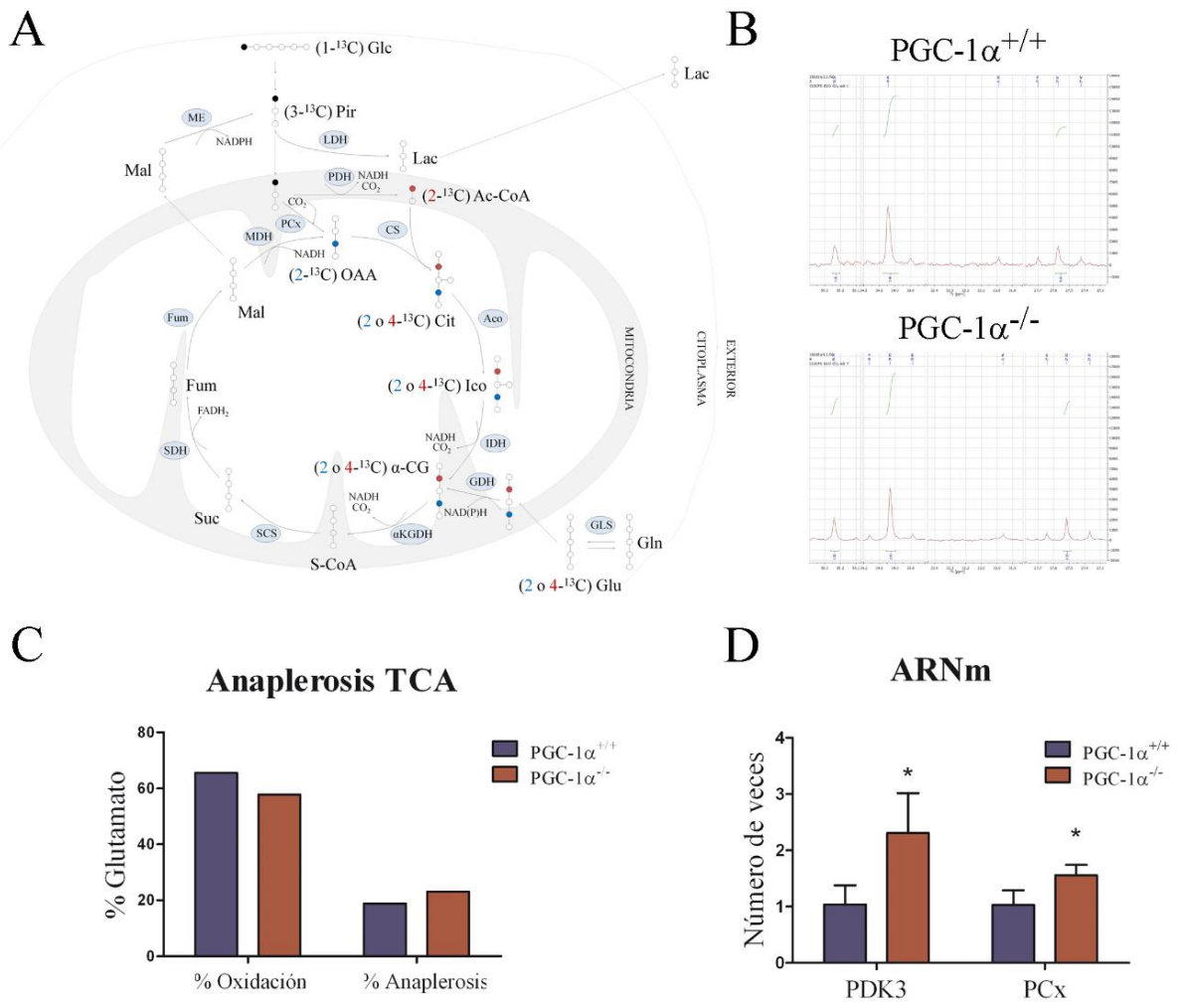

Figura 15. A) Esquema de la ruta seguida por la marca de ^{13}C de la (1-^{13}C) glucosa siguiendo la vía de entrada al ciclo TCA mediante la acción de la PDH (en granate) o mediante la acción de la PCx (en azul). α-CG, α-cetoglutarato; Ac-CoA, Acetil-CoA; Cit, Citrato; Fum, Fumarato; Glc, Glucosa; Glu, Glutamato; Gln, Glutamina; Ico, Isocitrato; Lac, Lactato; Mal, Malato; OAA, Oxalacetato; Pir, Piruvato; Suc, Succinato; S-CoA, Succinil-CoA. **B)** Espectros de RMN del C_2, C_3 y C_4 del glutamato en MEF inmortalizados silvestres y PGC-1α$^{-/-}$ incubados con (1-^{13}C) glucosa 5 mm. **C)** Cuantificación del porcentaje de uso de las dos vías de entrada de piruvato en el ciclo TCA en presencia o ausencia de PGC-1α. **D)** Nivel de expresión de ARNm de PCx y PDK3 en MEF inmortalizados silvestres y deficientes en PGC-1α. N=3. Los datos están representados como la media ± desviación típica. *, $p < 0.05$; **, $p \leq 0.01$; ***, $p \leq 0.005$.

En los cultivos de MEF inmortalizados en ausencia de PGC-1α, se observó un 5 % más de entrada de piruvato por la vía anaplerótica que en los MEF inmortalizados silvestres (Fig. 15B-C). Mientras que los MEF inmortalizados silvestres mostraron un 18,83 % del uso de la vía anaplerótica en ausencia de PGC-1α los MEF inmortalizados mostraron un 23,09 % de uso de dicha vía. Para comprobar

la validez de este resultado, se realizó un análisis de expresión mediante RT-qPCR de las enzimas implicadas y sus principales reguladores funcionales, observándose una mayor expresión de la PCx y de PDK3, un inhibidor de la actividad de PDH, en MEF inmortalizados sin PGC-1α (Fig. 15D), un resultado consistente con la propuesta mayor actividad de la vía de la PCx en MEF inmortalizados deficientes en PGC-1α.

Como se ha indicado anteriormente, además de la bajada en el consumo de oxígeno, las células tumorales acumulan otras alteraciones metabólicas, entre las que destaca el aumento en el consumo de glutamina (DeBerardinis et al. 2007). La mayor parte de los estudios realizados atribuyen esta dependencia de la glutamina a la reducción de los intermediarios del ciclo TCA por su utilización en vías biosintéticas (Svensson et al. 2016), además de la baja entrada de Ac-CoA proveniente del piruvato, por lo que se requiere la activación de vías complementarias, no mitocondriales, entre las que destaca el flujo de glutamina, que entra en el ciclo TCA como α-KG. Esta entrada evitaría la disminución de α-KG debida a la utilización del citrato en la síntesis de lípidos.

Para valorar la contribución de la supresión del metabolismo oxidativo mediado por PGC-1α, en el uso de la glutamina, decidimos valorar el efecto de la presencia de glutamina en la producción de lactato y el consumo de O_2, y se observó que la glutamina aumentaba la producción de lactato y disminuía el consumo de O_2, siendo el efecto mayor en células deficientes en PGC-1α (Fig. 14B). Esta observación podría indicar que la glutamina hace que las células sean menos dependientes del metabolismo oxidativo.

A continuación, decidimos estudiar si la pérdida del metabolismo oxidativo aumentaba la dependencia de las células hacia la glutamina. Para ello, se crecieron células hasta llegar a confluencia, y en este momento se sustituyó el medio normal por un medio sin glutamina y se valoró la supervivencia celular, contando las células adherentes a distintos tiempos. Cómo se observa en la gráfica, 24 h después de la retirada de la glutamina del medio, los cultivos de MEF inmortalizados deficientes en PGC-1α mostraron una bajada significativa, del 30 %, del número de células viables, mientras que en presencia de PGC-1α la bajada en la viabilidad no fue detectable hasta 48 h después de la retirada de glutamina del medio de cultivo, cuando disminuyó un 10 % la viabilidad celular, mientras que los MEF inmortalizados deficientes en PGC-1α mostraron un descenso del 65 % de la viabilidad celular a las 48 h (Fig. 16A). Este resultado sugería un impacto directo de la bajada en la capacidad oxidativa celular sobre la dependencia de la glutamina.

Con el objetivo de identificar el origen de esta dependencia, analizamos las diferencias en la concentración de aminoácidos entre los MEF inmortalizados en presencia o ausencia de PGC-1α. Se observó que había una concentración menor de glutamina y una mayor concentración de glutamato en MEF inmortalizados deficientes en PGC-1α (Fig. 16B). Este resultado es concordante con la mayor dependencia de la presencia de glutamina en el medio de cultivo observada en ausencia de PGC-1α y con la hipótesis de que la dependencia de glutamina debe compensar una teórica bajada en la concentración de

α-KG. Dado que la constante de equilibrio entre el glutamato y el α-KG es cercana a la unidad, un aumento en la cantidad de glutamato esta normalmente asociado a un incremento en la cantidad de α-KG. Además, se observaron, en MEF inmortalizados sin PGC-1α, niveles aumentados de otros aminoácidos que apoyan esta idea. Así, por ejemplo, se observó mayor nivel de aspartato en los MEF inmortalizados deficientes en PGC-1α (Fig. 16B), lo que podría derivarse del equilibrio generalmente existente entre el nivel de este aminoácido y el glutamato, mediado por transaminasas y que facilita los flujos anapleróticos; y el aumento de la concentración de alanina (Fig. 16B) que puede deberse a la aminación del piruvato con grupos amino procedentes tanto de la glutamina como del glutamato. Este aumento de la concentración de alanina pone, también, de manifiesto la mayor disponibilidad de piruvato, y es funcionalmente muy relevante dado que el nivel de alanina controla de forma fundamental los reguladores de la síntesis de otros aminoácidos y la síntesis proteica en general. Por tanto, estos datos son consistentes con la idea de que la dependencia de la glutamina puede deberse, también, a la necesidad de la célula tumoral de grupos amonio para promover la síntesis proteica.

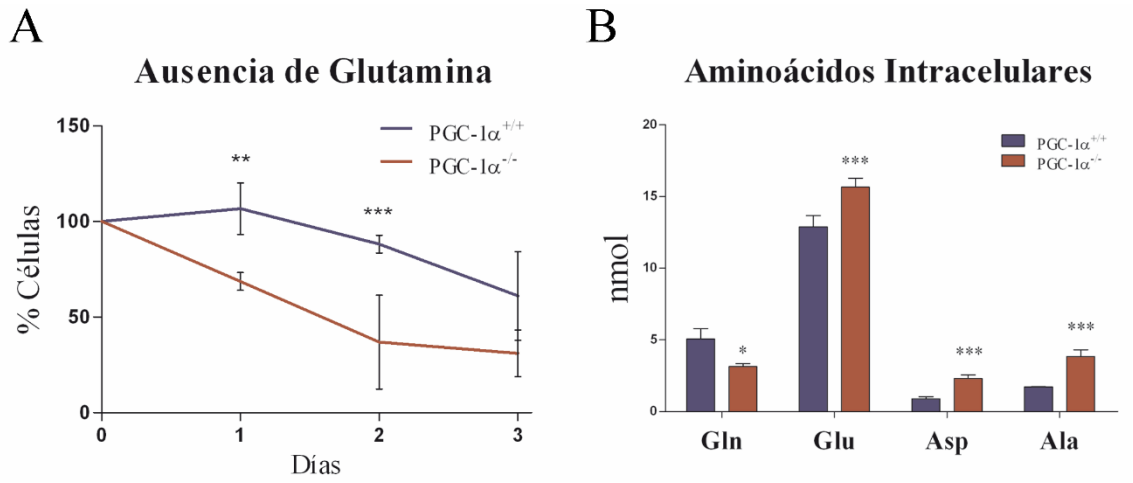

Figura 16. A) Supervivencia de MEF inmortalizados silvestres y deficientes en PGC-1α a 1, 2 y 3 días después de incubarlos con medio en ausencia de glutamina. N=3. **B)** Cantidad de aminoácidos detectados en extractos celulares de MEF inmortalizados silvestres y deficientes en PGC-1α. N=4. Los datos están representados como la media ± desviación típica. *, $p < 0.05$; **, $p \leq 0.01$; ***, $p \leq 0.005$.

La entrada de glutamina en el ciclo TCA tiene una importante función compensatoria del déficit de intermediarios del ciclo TCA, como ya se ha indicado. Además, la síntesis de ácidos grasos es un proceso que requiere una gran cantidad de poder reductor. Por ello, las células tumorales activan rutas que puedan generar este poder reductor. Así, por ejemplo, la salida de malato, uno de los intermediarios del ciclo TCA, de la mitocondria para su posterior transformación en piruvato mediante la ME, reacción en la que se genera poder reductor, se ve inducida (Dey et al. 2017; Murai et al. 2017). Además, este poder reductor es necesario para el mantenimiento del nivel normal de glutatión reducido, que evita la inducción de muerte celular en un contexto general de estrés oxidativo.

Con el fin de evaluar la actividad de la ME, se incubaron los MEF inmortalizados con glucosa y glutamina marcada con ^{13}C. El uso de glucosa marcada en su C_1 y glutamina uniformemente marcada permite discriminar el origen de varios de los metabolitos identificables por RMN, ya que la marca de un solo ^{13}C da lugar a un único pico en los espectros de RMN, mientras que la marca de ^{13}C contiguos da lugar a picos múltiples (dobletes, tripletes o multipletes). Esto permite que el análisis de los picos del lactato detectado sirva para valorar la actividad de la ME, ya que la presencia de dobletes solo pude explicarse por tener su origen en la glutamina uniformemente marcada y llegar a convertirse en lactato mediante la entrada al ciclo TCA por glutaminolisis, la posterior salida del malato de la mitocondria al citoplasma donde se transforma en piruvato por la ME y, finalmente, en lactato por la LDH.

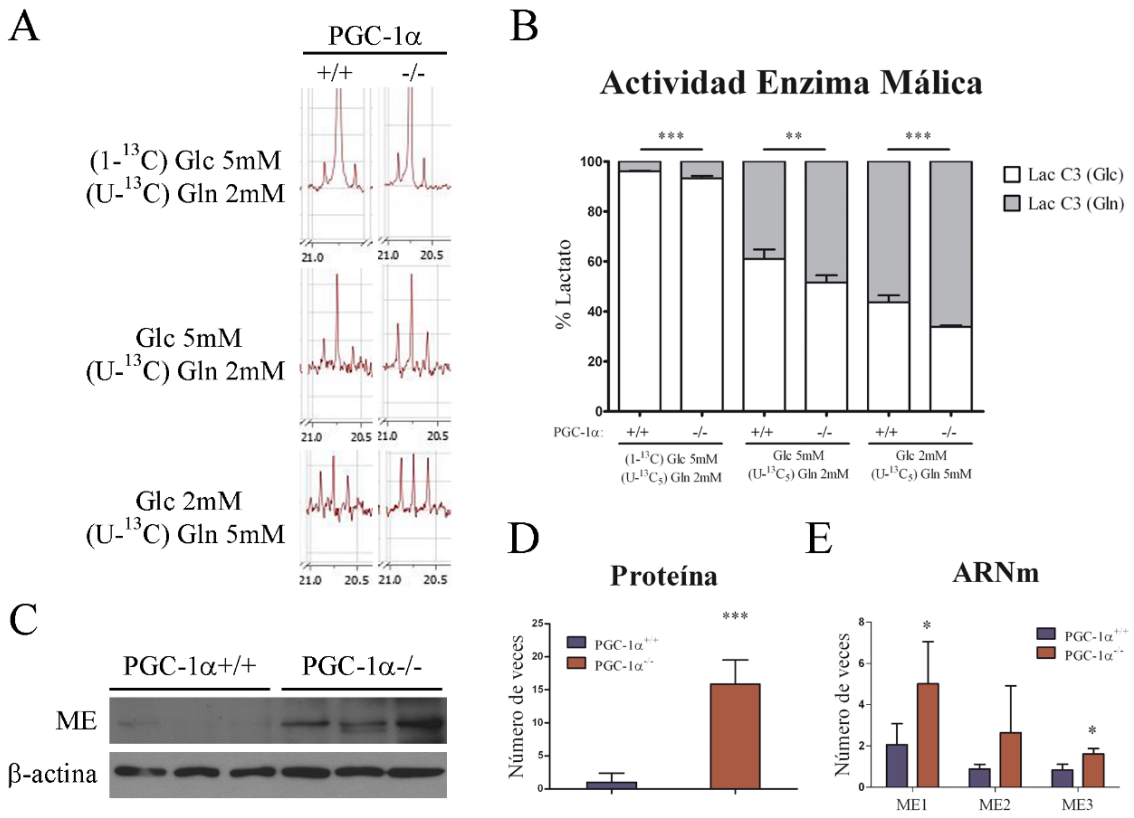

Figura 17. A) Espectros representativos de RMN del C_3 del lactato en los medios de cultivo mostrados (Tiempo 24 horas). **B)** Porcentaje de doblete en la señal del C_3 del lactato en los espectros de RMN como medida de la actividad de la ME MEF inmortalizados silvestres y deficientes en PGC-1α. N=4. **C)** Nivel de expresión de proteína de la ME en MEF inmortalizados silvestres y deficientes en PGC-1α. Control de carga: β-actina. **D)** Densitometrado del nivel de expresión de proteína, relativizado con el control silvestre. N=3. **E)** Nivel de expresión de ARNm de las tres isoformas de la ME en MEF inmortalizados silvestres y deficientes en PGC-1α. Los datos están representados como la media ± desviación típica. N=3. *, $p < 0.05$; **, $p \leq 0.01$; ***, $p \leq 0.005$.

Tanto en MEF inmortalizados con presencia de PGC-1α como en ausencia de PGC-1α se observó la formación de dobletes de lactato en los espectros de RMN, lo que indica la presencia de actividad de la ME en MEF inmortalizados de ambos genotipos (Fig. 17A). Sin embargo, el doblete que se formó en la señal del lactato resultó ser significativamente mayor en los MEF inmortalizados deficientes

en PGC-1α (Fig. 17B), que reveló un 10 % más de actividad de la ME en ausencia de PGC-1α. Este resultado se vio confirmado por el análisis de los niveles de ME, tanto a nivel de proteína como de ARNm, observándose mayores niveles en MEF inmortalizados sin PGC-1α (Fig. 17C-D-E).

Como se ha mencionado en la introducción, el regulador clave del metabolismo de la glutamina es el oncogen c-myc (Wise et al. 2008; X. Xu et al. 2015), para el cual se ha descrito su relación inversa con PGC-1α en la regulación del metabolismo tumoral (Sancho et al. 2015). Para valorar la posible contribución de c-myc al fenotipo observado realizamos un análisis de esta proteína mediante *western blot*. El nivel de c-myc resultó ser 2 veces mayor en los cultivos de MEF inmortalizados deficientes en PGC-1α que en los de MEF inmortalizados silvestres (Fig. 18).

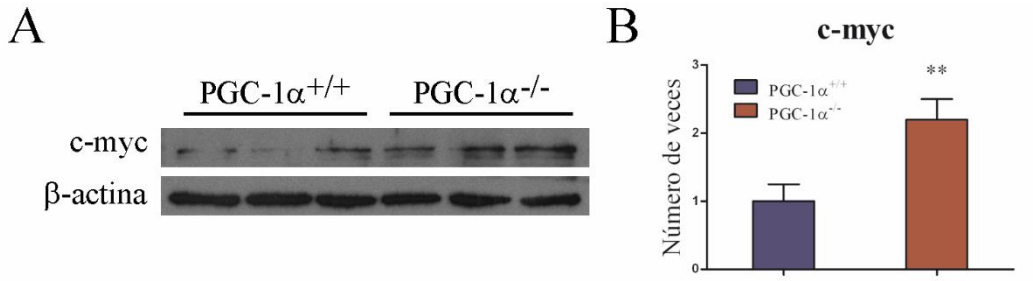

Figura 18. A) Nivel de expresión de proteína de c-myc. **B)** Densitometrado del nivel de expresión de proteína, relativizado con el control silvestre. N=3. Los datos están representados como la media ± desviación típica. *, $p < 0.05$; **, $p \leq 0.01$; ***, $p \leq 0.005$.

Además de la utilización de la glutamina para mantener la concentración de OAA y evitar el colapso del ciclo TCA, se ha propuesto que en algunos tipos tumorales avanzados la glutamina favorece la aparición de un flujo reverso en el ciclo TCA. En este contexto, se ha propuesto que puede funcionar la carboxilación reductiva, por la que el α-KG daría lugar a isocitrato (Mullen et al. 2011). Este fenómeno estaría facilitado por un cambio de isoenzima de la isocitrato deshidrogenasa, lo que aumentaría la concentración de citrato, necesario para la biosíntesis lipídica. Si este citrato sale de la mitocondria, mediante la enzima citrato liasa puede dar lugar a OAA y acetato, precursor de la síntesis de ácidos grasos.

Con el fin de evaluar la presencia de carboxilación reductiva se analizó mediante RMN la incorporación de ^{13}C en el acetato. Como ya se ha mencionado, los metabolitos con origen en la glucosa marcada en su C_1 o la glutamina uniformemente marcada son distinguibles entre sí en los espectros de RMN, lo que permite discriminar el origen del acetato. Así, la presencia de dobletes en la señal del acetato puede tener su origen en la glutamina que entra en el ciclo TCA transformándose en α-KG y que, siguiendo el ciclo en reverso, da lugar a citrato marcado con ^{13}C en sus 5 carbonos y, mediante la acción de la enzima citrato liasa, produciría el acetato doblemente marcado (Fig.19A). El análisis de los espectros de los medios de cultivo en los que habíamos añadido la glutamina uniformemente marcada con ^{13}C,

permitió identificar el doblete en la marca de acetato solamente en los medios de cultivo de MEF inmortalizados deficientes en PGC-1α (Fig. 19B).

Para contrastar la relevancia de este resultado, medimos el nivel de expresión de ARNm de la IDH1, normalmente elevada en los sistemas en los que se ha propuesto la existencia de carboxilación reductiva, observándose un aumento significativo en la expresión de esta enzima en los MEF inmortalizados deficientes en PGC-1α (Fig. 19C).

Este resultado no es, sin embargo, totalmente concluyente, dado que el acetato puede formarse también a partir de glutamina, pero siguiendo el ciclo canónico de los ácidos tricarboxílicos hasta dar lugar a malato que, al salir de la mitocondria, puede dar lugar a piruvato por medio de la ME, una enzima que como hemos visto aparece sobreexpresada en los MEF inmortalizados sin PGC-1α. Este piruvato que estaría uniformemente marcado podría dar también lugar a acetato uniformemente marcado tras la salida de citrato de la mitocondria.

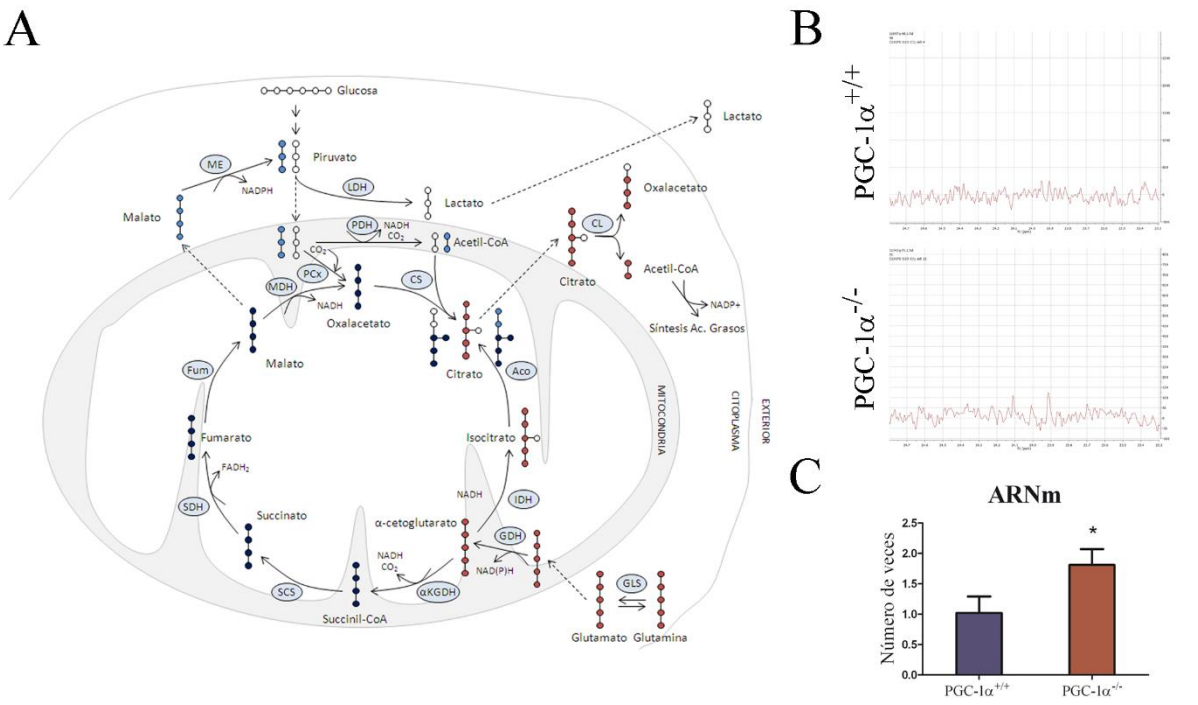

Figura 19. A) Esquema de la ruta seguida por la marca de ^{13}C de la (U-$^{13}C_5$) glutamina siguiendo las diferentes vías para la formaciónde citrato: la carboxilación reductiva (en granate), el ciclo TCA canónico (en azul marino) y la formación de Ac-CoA a partir de piruvato originado por la ME (en azul claro). **B)** Espectros representativos de RMN del acetato en el medio de cultivo con Glucosa 2 mM y (U-$^{13}C_5$) Glutamina 5 mM (Tiempo 24 horas) en MEF inmortalizados silvestres y deficientes en PGC-1α. **C)** Nivel de expresión de ARNm de IDH1 en MEF inmortalizados silvestres y deficientes en PGC-1α. Los datos están representados como la media ± desviación típica. N=3. *, $p < 0.05$; **, $p \leq 0.01$; ***, $p \leq 0.005$.

Los MEF inmortalizados deficientes en PGC-1α muestran un fenotipo transformado *in vitro*.

Como ya se ha expuesto anteriormente, las células tumorales presentan unas características distintivas que incluyen la capacidad de evitar la apoptosis, proliferar aun en presencia de supresores del crecimiento, mantener una señal proliferativa y migrar e invadir otros tejidos, entre otras (Hanahan and Weinberg 2011). Para valorar como las alteraciones metabólicas identificadas en los MEF inmortalizados impactaban en las características fenotípicas tumorales, se realizó un estudio *in vitro* de estos.

Para valorar la resistencia a la inducción de muerte celular, se realizó un experimento de deprivación de suero. Generalmente, los MEF se mantienen en cultivo en presencia de 10 % de FBS, que contiene una gran cantidad de factores de crecimiento. Para valorar la respuesta ante la privación de estos factores de crecimiento, llevamos los cultivos a confluencia y se sustituyó el medio normal por medio con distintas cantidades de FBS, 5 %, 2 %, 0,5 % y 0 %; y se valoró el número de células viables en días sucesivos.

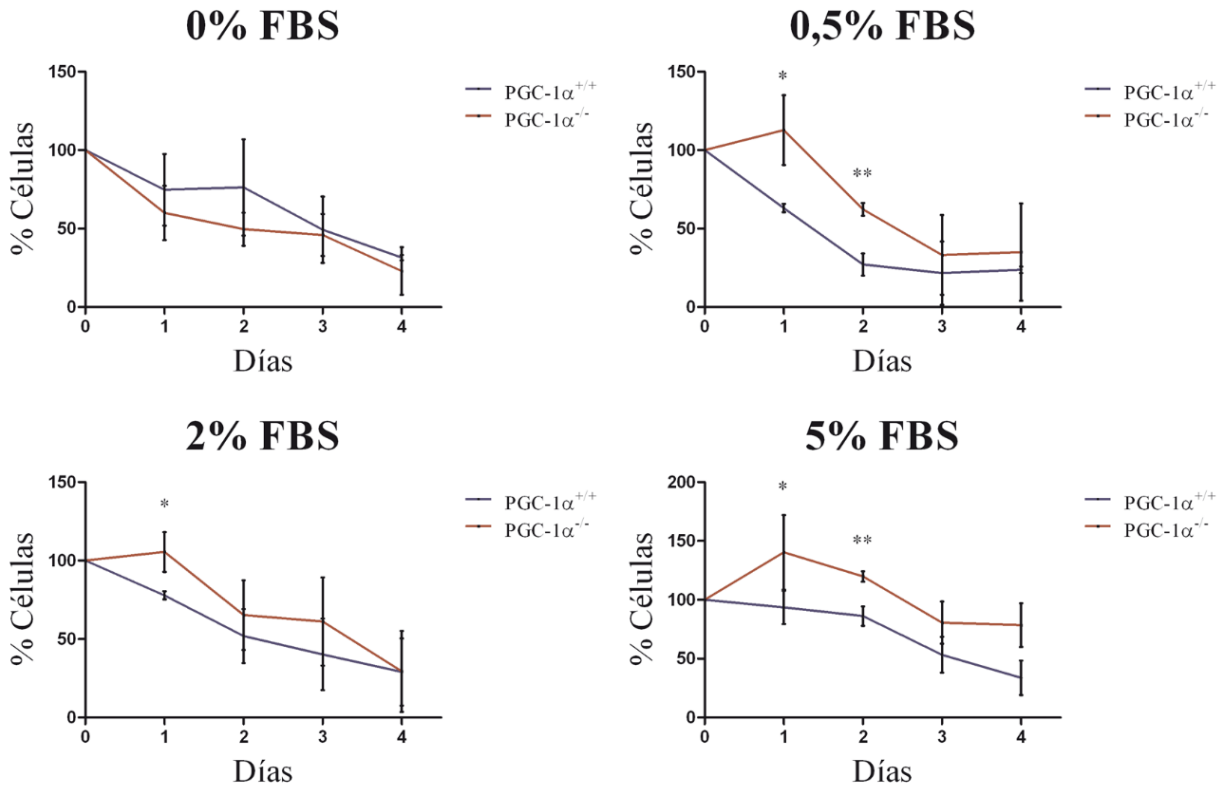

Figura 20. Supervivencia de MEF inmortalizados silvestres y deficientes en PGC-1α, en diferentes concentraciones de FBS en el medio de cultivo, a 1, 2, 3 y 4 días. Los datos están representados como la media ± desviación típica. N=3. *, $p < 0.05$; **, $p \leq 0.01$; ***, $p \leq 0.005$.

Los MEF inmortalizados silvestres que fueron cultivadas en medio con 5 % de FBS durante los siguientes dos días se mantuvieron quiescentes y al tercer día empezó a ser evidente la pérdida de viabilidad. En contraposición, en ausencia de PGC-1α, los MEF inmortalizados fueron capaces, no solo de no iniciar la muerte celular, sino de seguir creciendo durante los días siguientes (Fig. 20).

Respecto a los cultivos incubados con 2 % y 0,5 % de FBS en el medio de cultivo, la reducción en la concentración de suero redujo la viabilidad en ambos genotipos, manteniéndose las diferencias entre ellos. En los cultivos de MEF inmortalizados silvestres comenzó a descender el número de células desde las primeras 24 h, entre un 25 % y un 35 %, mientras que los MEF inmortalizados sin PGC-1α lograron retrasar el inicio de la muerte celular hasta el segundo día en que se produjo una disminución del 35 % de la viabilidad celular, cuando en presencia de PGC-1α, la pérdida de viabilidad celular se situó por debajo del 50 % (Fig. 20).

En ausencia de FBS, la viabilidad disminuyó desde el primer día y no se observaron diferencias significativas entre los MEF inmortalizados de ambos genotipos (Fig. 20).

Concluimos, por tanto, que la ausencia de PGC-1α aumentaba la resistencia a la inducción de muerte celular en condiciones limitantes de factores de crecimiento.

Seguidamente, para evaluar la capacidad de escapar a las señales supresoras del crecimiento de los cultivos, realizamos un experimento de inhibición por contacto. Las células confluentes deben de parar su crecimiento y mantenerse en monocapa adheridas a la placa de cultivo con la excepción de las células tumorales que pierden la inhibición por contacto y forman estructuras de crecimiento en 3 dimensiones.

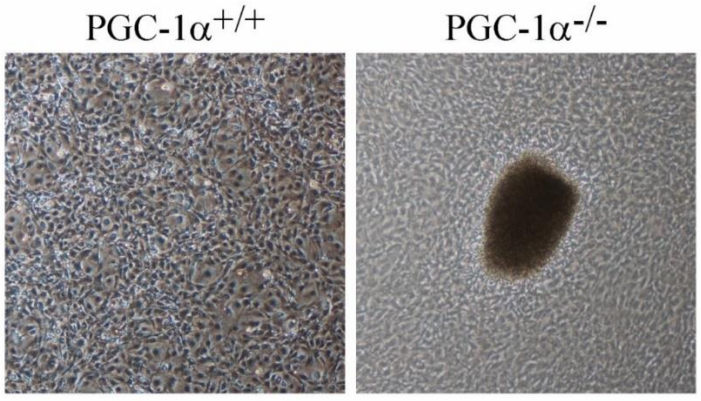

Figura 21. Imágenes representativas de la formación de estructuras en tres dimensiones por la pérdida de inhibición por contacto en MEF inmortalizados silvestres y deficientes en PGC-1α.

Para ello, dejamos crecer los MEF inmortalizados hasta que llegaron a confluencia y los mantuvimos 15 días más en cultivo. En presencia de PGC-1α, los cultivos detuvieron su crecimiento una vez alcanzada la confluencia de la placa de cultivo. Sin embargo, en ausencia de PGC-1α, se formaron colonias visibles, lo que sugería una relativa pérdida del control de la inhibición por contacto (Fig. 21).

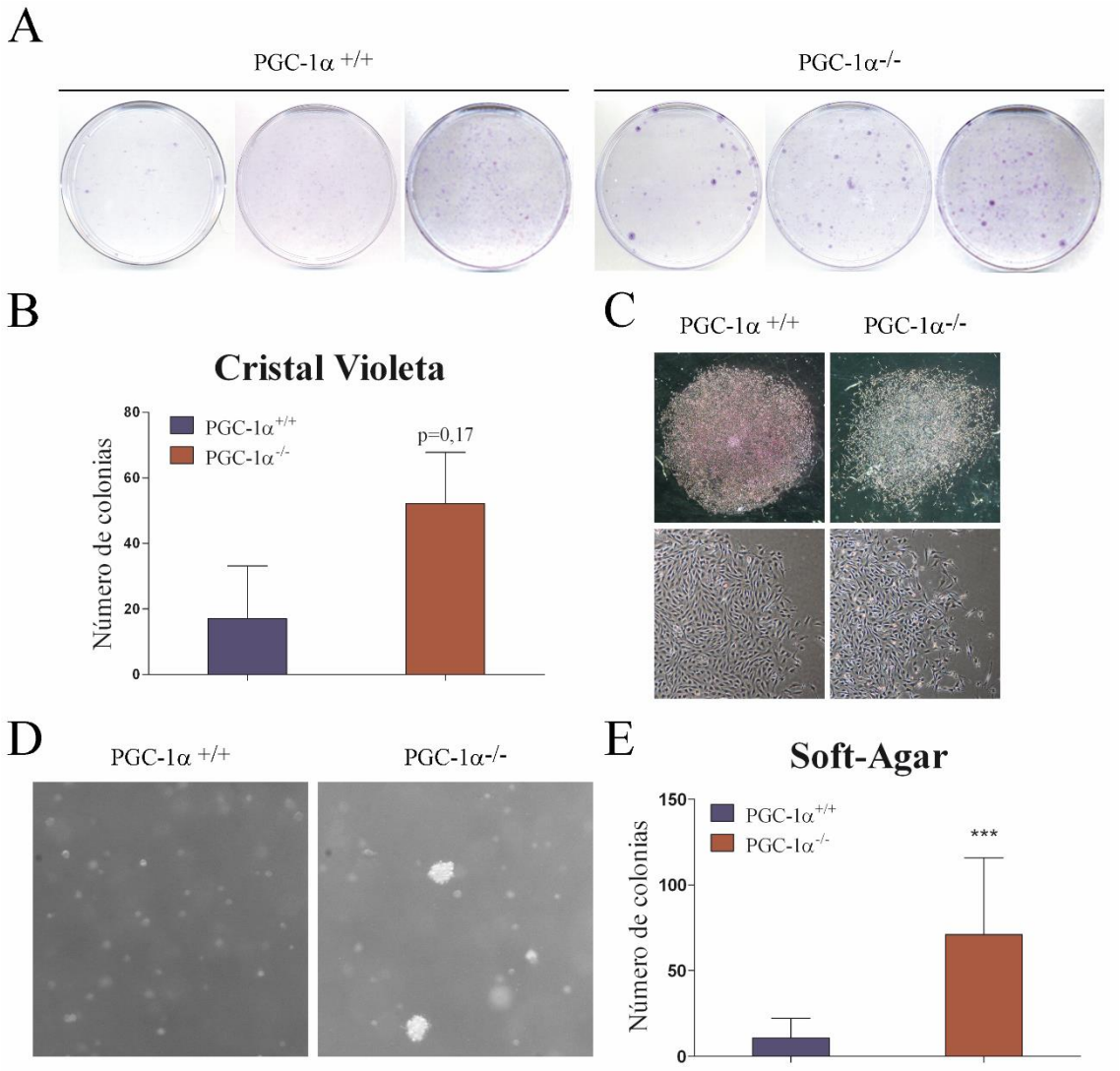

Figura 22. A) Imágenes de las placas de cultivo de MEF inmortalizados silvestres y deficientes en PGC-1α teñidas con cristal violeta. **B)** Cuantificación del número de colonias formadas tras la siembra a baja densidad de MEF inmortalizados silvestres y deficientes en PGC-1α. N=3. **C)** Imágenes representativas de las colonias formadas (arriba) y del borde de la colonia (abajo) en MEF inmortalizados silvestres y deficientes en PGC-1α. **D)** Imágenes representativas de las colonias formadas en ausencia de anclaje. **E)** Cuantificación de las colonias formadas en ausencia de anclaje en MEF inmortalizados silvestres y deficientes en PGC-1α. N=3. Los datos están representados como la media ± desviación típica. *, $p < 0.05$; **, $p \leq 0.01$; ***, $p \leq 0.005$.

Con el fin de valorar si, en ausencia de PGC-1α, existe una mayor proliferación sostenida decidimos evaluar la capacidad de formación de colonias en placas de cultivo sembradas a baja densidad celular. Las células normales requieren de la presencia de factores generados de manera paracrina por otras células para promover su proliferación y la independencia de esta señalización es una marca de malignidad. Para ello, se sembraron 2000 células en placas de 10 cm de diámetro y se evaluó el número y el tipo de colonias formadas por los MEF inmortalizados. Tanto los MEF inmortalizados silvestres como los deficientes en PGC-1α fueron capaces de formar un número similar de colonias (Fig. 22A-B), lo que indicaba que la dependencia de señales paracrinas para la proliferación era similar en ambos genotipos. Sin

embargo, la observación detallada de las colonias mostró diferencias relevantes. En presencia de PGC-1α, las colonias formadas por los MEF inmortalizados tenían bordes regulares, mientras que en ausencia de PGC-1α mostraron bordes altamente irregulares (Fig. 22C). Este tipo de fenotipo presentado por los MEF inmortalizados deficientes en PGC-1α se asocia con la pérdida del fenotipo epitelial propia de la TEM.

La TEM suele estar asociada a una menor dependencia, para el crecimiento celular, de la presencia de un sustrato. Además, habíamos observado la formación de colonias en el estudio de inhibición por contacto, lo que sugería también una posible menor dependencia de sustrato. Para valorar directamente la capacidad de crecimiento independiente de anclaje, realizamos un estudio de formación de colonias en una matriz de *soft-agar*. Se sembraron $3*10^5$ células por placa y se valoró la aparición de colonias visibles durante cuatro semanas. Se observó que los MEF inmortalizados sin PGC-1α dieron lugar a un número significativamente mayor de colonias que en presencia de PGC-1α (Fig. 22D-E), mientras que el número de colonias formadas partir de MEF inmortalizados silvestres se situó en 11 por placa, aproximadamente, los MEF inmortalizados deficientes en PGC-1α formaron 71 colonias por placa; un resultado consistente con un fenotipo más mesenquimal en ausencia de PGC-1α.

La principal característica de la TEM es la adquisición de motilidad celular que permite la migración e invasión de otros órganos y tejidos. Para estudiar la capacidad de migración de los MEF inmortalizados, se realizaron dos tipos de experimentos, uno de cierre de herida *in vitro* y otro de migración en cámara de Boyden.

En el experimento de cierre de herida *in vitro*, se tomaron fotos cada 30 minutos en un equipo *Cell Observer* de los surcos realizados en la monocapa celular. De esta manera, fue posible realizar una evaluación cuantitativa de las diferencias en la migración de los MEF inmortalizados entre ambos genotipos. Los MEF inmortalizados deficientes en PGC-1α mostraron una mayor velocidad en el cierre de la herida que los MEF inmortalizados silvestres. Mientras que en ausencia de PGC-1α consiguieron ocupar el 50 % del espacio libre en aproximadamente 10 horas y el 100 % del surco creado aproximadamente en 18 horas, en presencia de PGC-1α, el cierre del 50 % del espacio formado se alcanzó en aproximadamente 16 horas y el 100 % a las 28 horas tras la formación del surco en la monocapa celular (Fig. 23A-B).

Otra diferencia evidente entre los genotipos fue la falta de direccionalidad en la migración de los MEF inmortalizados sin PGC-1α. Mientras que los MEF inmortalizados que si tienen PGC-1α identificaron la zona sin células y migraron ordenadamente, el movimiento de los MEF inmortalizados deficientes en PGC-1α fue desordenado y aleatorio.

Además, el grado de confluencia final alcanzada en el área de la herida también resultó diferente entre los dos genotipos. Los MEF inmortalizados con presencia de PGC-1α generaron un cierre de herida más compacto, mientras que los MEF inmortalizados deficientes en PGC-1α quedaron más dispersos (Fig. 23C). Esta observación, junto con la mayor independencia de sustrato y la reducida inhibición por

contacto, sugiere que el establecimiento de interacciones celulares está más reducido en ausencia de PGC-1α, un importante factor de progresión tumoral, como ya se ha indicado anteriormente.

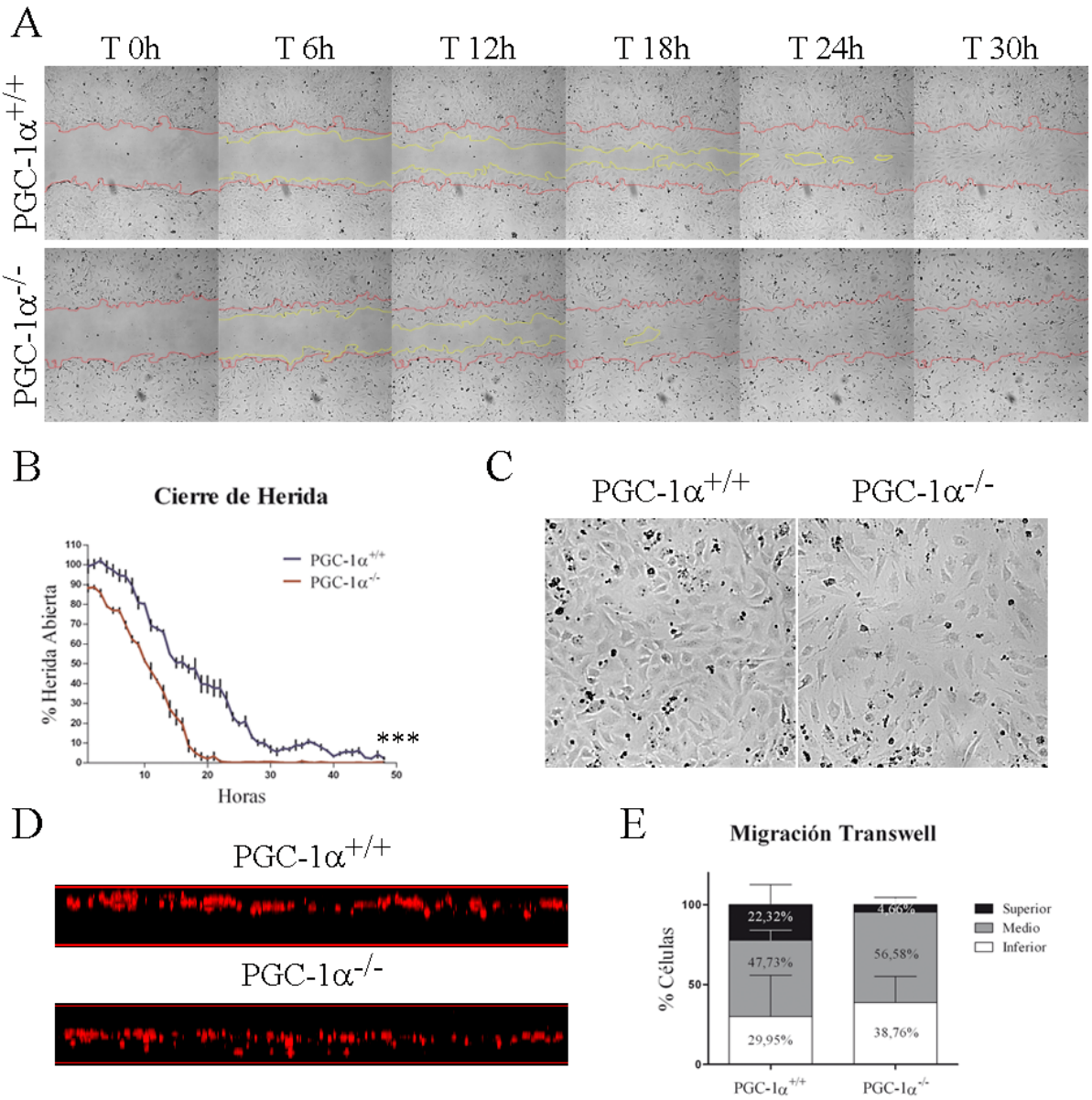

Figura 23. A) Imágenes de la migración para el cierre de herida de MEF inmortalizados silvestres y deficientes en PGC-1α. La línea roja marca el borde del surco inicial y la línea amarilla el borde del surco en el tiempo especificado para cada imagen. **B)** Cuantificación del porcentaje de herida abierta a medida que pasa el tiempo en MEF inmortalizados silvestres y deficientes en PGC-1α. N=3. **C)** Imágenes representativas de la confluencia final en las zonas de migración en MEF inmortalizados silvestres y deficientes en PGC-1α. **D)** Imágenes ortogonales de la membrana porosa por la que han migrado MEF inmortalizados silvestres y deficientes en PGC-1α tomada con un microscopio confocal. **E)** Distribución de los MEF inmortalizados silvestres y deficientes en PGC-1α en la parte superior, media o inferior de la membrana porosa del experimento de migración en cámara de Boyden. N=3. Los datos están representados como la media ± desviación típica. *, $p < 0.05$; **, $p \leq 0.01$; ***, $p \leq 0.005$.

Para cuantificar la velocidad de migración de los MEF inmortalizados deficientes en PGC-1α, se realizó un ensayo de migración en cámara de Boyden. Se sembraron $1,5*10^4$ células sobre una membrana con poros de 8 μm. Tras 18 horas, las células se fijaron, se tiñeron y se montaron las membranas en portas para su observación en microscopio confocal, tomando fotos en todo el grosor de la membrana. Se hizo un montaje transversal de las imágenes para visualizar el eje Z y valorar la distancia migrada por las células. Se observó que, en ausencia de PGC-1α, los MEF inmortalizados migraban más distancia a través de la membrana porosa de la cámara, alojándose en su mayoría en la parte inferior de dicha membrana, mientras que los MEF inmortalizados silvestres llegaron a ocupar solamente el tercio superior y el medio de la membrana (Fig. 23D-E). Por tanto, este resultado confirmaba que los MEF inmortalizados deficientes en PGC-1α migran más rápidamente que los silvestres.

La pérdida de dependencia a otras células y de anclaje al sustrato, y la mayor capacidad migratoria son características de mala prognosis en la progresión tumoral por alto riesgo de metástasis. Como hemos mencionado, estas características suelen venir asociadas con la llamada TEM, que a nivel molecular implica, entre otros eventos, la pérdida de uniones adherentes mediadas por cadherinas y la translocación de la membrana al núcleo de la proteína β-catenina donde actúa como factor de transcripción prooncogénico, regulando la expresión de proteínas con diferentes funciones como proliferación, desdiferenciación, supervivencia, angiogénesis y migración (Korinek et al. 1997). Por tanto, la localización nuclear de β-catenina es un biomarcador diagnóstico tumoral de mal pronóstico.

Por todo ello, decidimos evaluar mediante inmunofluorescencia la localización subcelular de β-catenina en los MEF inmortalizados con y sin PGC-1α. El análisis de las imágenes de microscopía confocal, permitió determinar que los MEF inmortalizados sin PGC-1α presentaban mayor nivel de β-catenina nuclear; mientras que en los MEF inmortalizados con PGC-1α la localización de β-catenina resulto ser fundamentalmente en la membrana citoplasmática (Fig. 24).

Cabe reseñar que entre los genes regulados por β-catenina se encuentra c-myc, un factor de transcripción con un papel clave en transformación tumoral y proliferación celular que, como hemos visto, está inducido en los cultivos de MEF inmortalizados deficientes en PGC-1α respecto a los MEF inmortalizados silvestres.

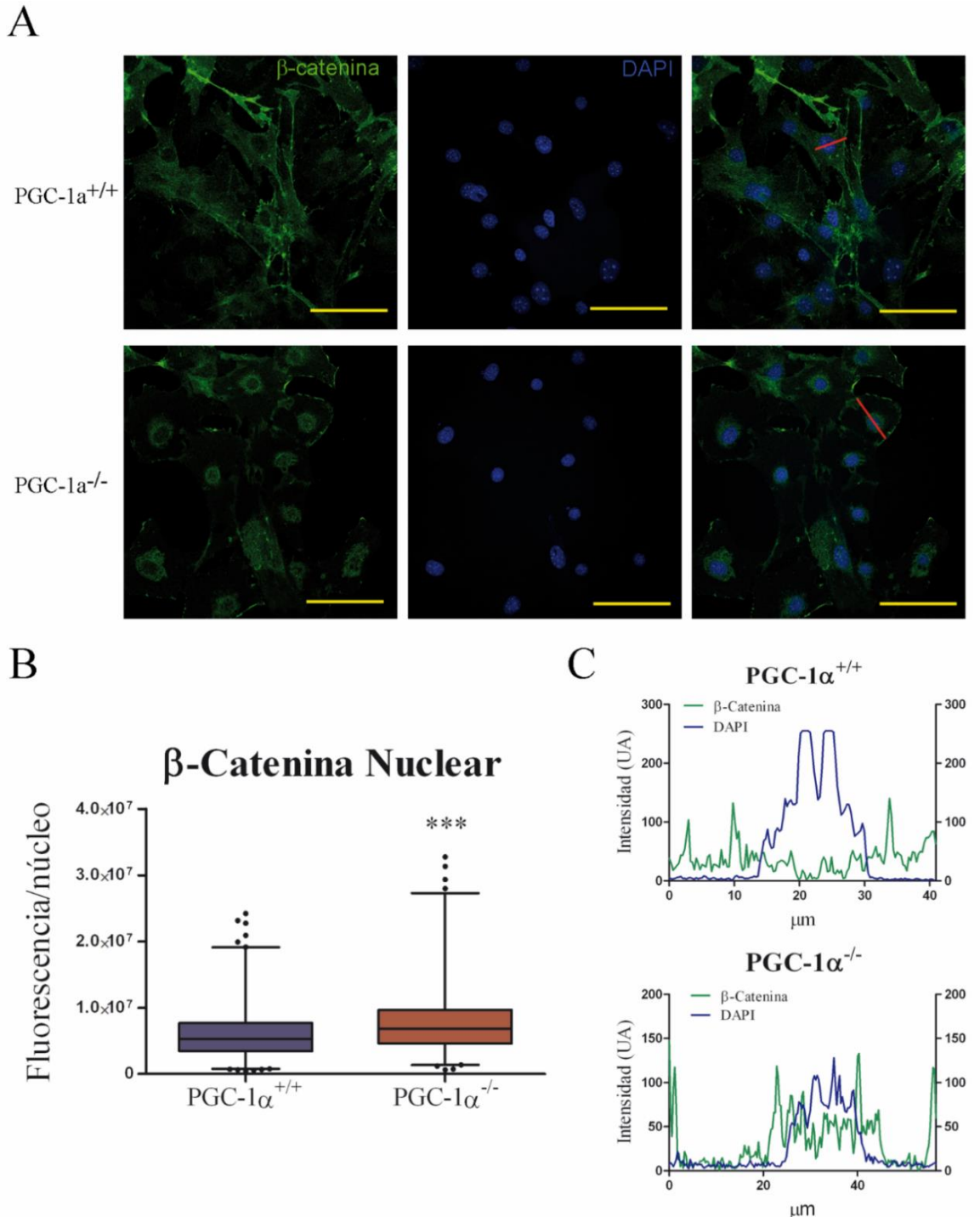

Figura 24. A) Imágenes representativas de la localización subcelular de β-catenina en MEF inmortalizados silvestres y deficientes en PGC-1α. Escala 100 μm. **B)** Cuantificación de la fluorescencia emitida en la zona nuclear por el anticuerpo para β-catenina. N=3. **C)** Intensidad de las señales de fluorescencia a lo largo de la línea roja presente en las imágenes de la izquierda en **A)**. Los datos están representados como la media ± desviación típica. *, $p < 0.05$; **, $p \leq 0.01$; ***, $p \leq 0.005$.

Capítulo III: La ausencia de PGC-1α incrementa el crecimiento tumoral y la capacidad de formación de metástasis *in vivo*.

Los resultados obtenidos *in vitro*, tanto el perfil bioquímico como el fenotípico, resultaron consistentes con un perfil de peor pronóstico tumoral en ausencia de PGC-1α. Para determinar si la ausencia de PGC-1α podría ser realmente responsable de la formación de tumores más agresivos, el siguiente paso fue trasladar dichos resultados a modelos animales. Para ello, se realizaron varios experimentos en los que se evaluó la supervivencia de las células en un organismo vivo, la proliferación, la capacidad de formación de un tumor primario tumoral y la capacidad de favorecer el desarrollo de metástasis.

Los MEF inmortalizados deficientes en PGC-1α muestran un mayor crecimiento tumoral *in vivo* que los silvestres.

Se comenzó evaluando la capacidad de supervivencia y proliferación de los MEF inmortalizados *in vivo*. Para ello se inyectaron, en el dorso de ratones C57BL/6 de genotipo silvestre, $2*10^6$ MEF inmortalizados junto a una matriz (Matrigel) portadora de factores de crecimiento y factores proangiogénicos, para que la proliferación no estuviera limitada por la ausencia de matriz, de factores de crecimiento o de irrigación vascular con el fin de maximizar su supervivencia dentro de un organismo vivo. Tras dos meses postinyección, se diseccionó la matriz que contenía las células y se valoró histológicamente. El contaje de células presentes en la matriz resultó ser superior en las matrices que contenían MEF inmortalizados deficientes en PGC-1α, lo que sugería que en ausencia de PGC-1α los MEF inmortalizados tenían mayor capacidad de supervivencia y/o proliferación *in vivo* (Fig. 25A-B).

Sin embargo, dado que la matriz puede ser también invadida por células del ratón hospedador, en particular por células del sistema inmunitario, células vasculares y fibroblastos, se decidió realizar una aproximación complementaria que permitiera el seguimiento de las células inyectadas. Para ello, se utilizaron retrovirus para la generación de líneas modificadas que expresaban de forma constitutiva GFP, y estas se inyectaron en presencia de Matrigel mediante inyección subcutánea, de $2*10^6$ MEF inmortalizados, en el dorso de ratones C57BL/6.

Nuevamente, tras dos meses, se diseccionaron las matrices inyectadas y se valoraron histológicamente, valorándose tanto el número de células con GFP (GFP^+) como el número de células en proliferación activa ($Ki67^+$), mediante un ensayo de inmunofluorescencia dirigido contra Ki67, un marcador de proliferación celular. El contaje de células GFP^+ confirmó que las células sin PGC-1α sobreviven y/o proliferan más que las silvestres (Fig. 25A-C), confirmando el resultado obtenido anteriormente. El 5 % de las células observadas en las matrices con MEF inmortalizados silvestres

diseccionadas fueron GFP+ mientras que en las matrices con MEF inmortalizados deficientes en PGC-1α el 39 % de las células observadas fueron GFP+. Además, el contaje de las células Ki67+, mostró un mayor número de células proliferativas en las matrices que contenían MEF inmortalizados deficientes para PGC-1α, un 12,7 % de las células observadas por un 2,3 % en el caso de los MEF inmortalizados silvestres, lo que sugería que estas proliferan más *in vivo* (Fig. 25A-D).

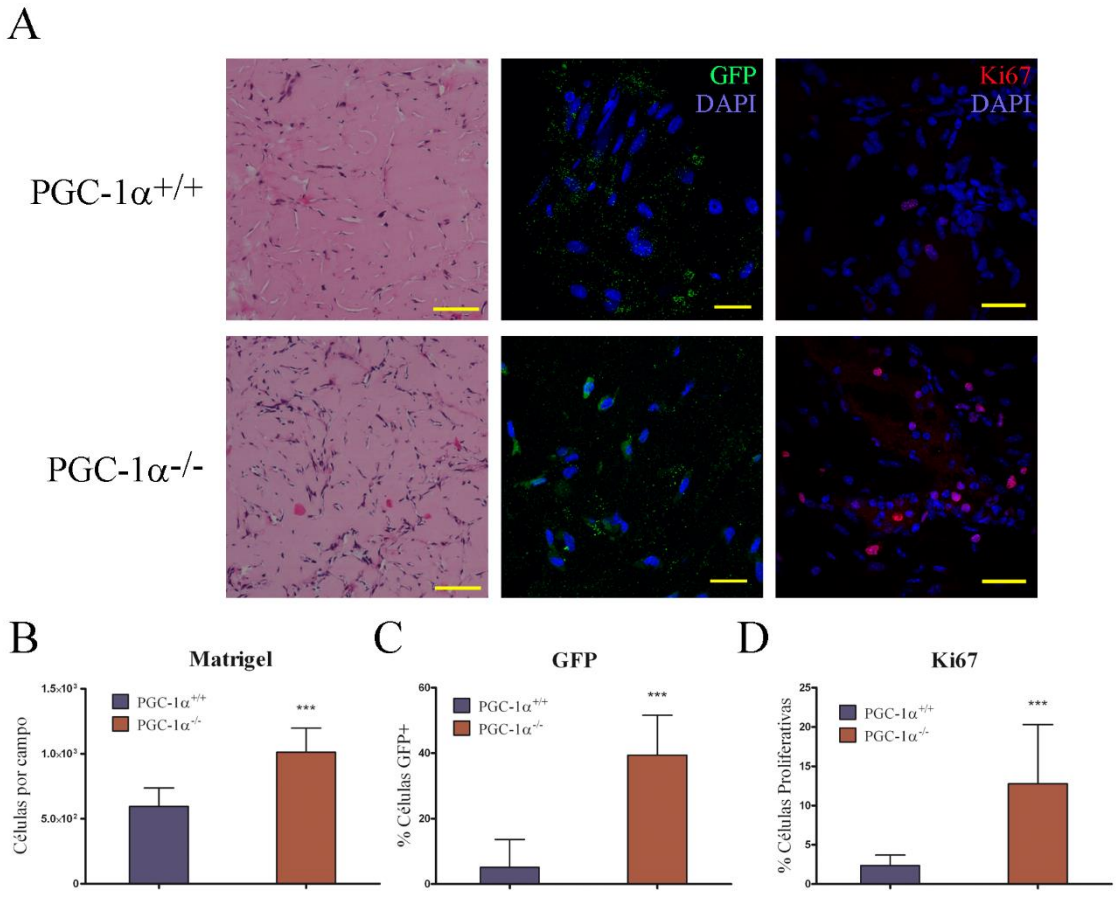

Figura 25. A) Panel Izquierdo: Imágenes representativas de las matrices tras dos meses inyectadas en el dorso de ratones C57BL6 con MEF inmortalizados silvestres y deficientes en PGC-1α. Panel medio: Imágenes representativas de células con presencia de GFP. Panel derecho: Imágenes representativas de células proliferativas en matrices inyectadas en el dorso de ratones C57BL6. **B)** Cuantificación de las células por campo en las fotos de matrices inyectadas en el dorso de ratones C57BL6. **C)** Cuantificación de células con presencia de GFP en las matrices inyectadas en el dorso de ratones C57BL6. **D)** Cuantificación de núcleos positivos para Ki67, marcador de proliferación. Los datos están representados como la media ± desviación típica. *, $p < 0.05$; **, $p \leq 0.01$; ***, $p \leq 0.005$.

Para valorar si la capacidad de supervivencia y proliferación *in vivo* era suficiente para la formación de tumores primarios se realizó un estudio del crecimiento tumoral *in vivo* mediante la inyección subcutánea de 10^7 células sin matriz en ratones inmunodeprimidos NOD-SCID. Tras 14 días, los tumores primarios se diseccionaron para su valoración histológica. El tamaño de los tumores se valoró en el momento de su disección, observándose que los tumores formados por MEF inmortalizados deficientes

en PGC-1α midieron 15,4 mm^3 de media y eran significativamente mayores que los formados por los silvestres que midieron 5,6 mm^3 de media (Fig. 26A-B).

Histológicamente, los tumores formados por MEF inmortalizados sin PGC-1α mostraron una mayor densidad celular, con un núcleo central con una gran concentración de células, mientras que los obtenido de los ratones que habían sido inyectados con MEF inmortalizados silvestres presentaban menor densidad celular total. En ambos genotipos se observó presencia de vascularización y hemorragias (Fig. 26C).

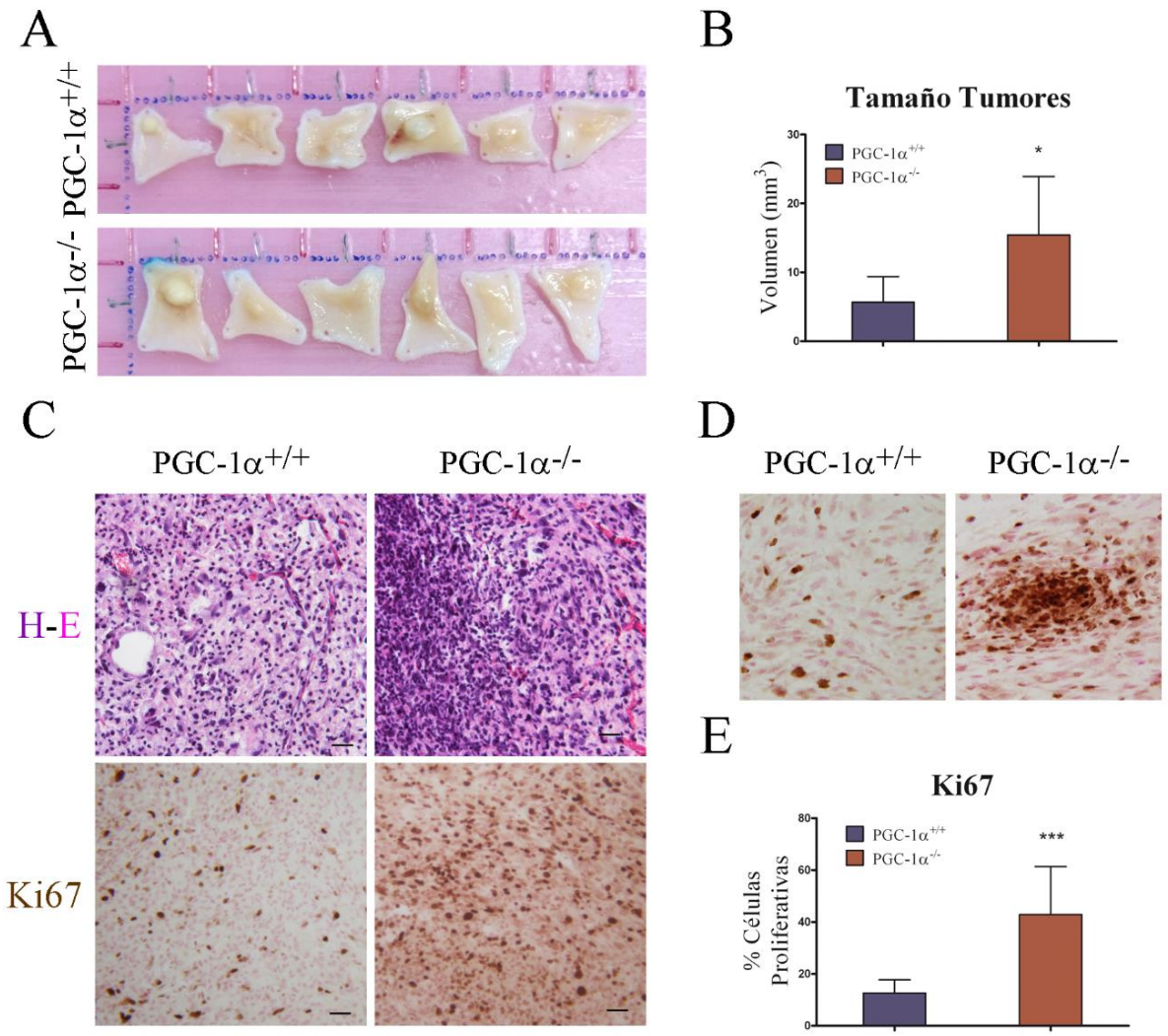

Figura 26. A) Tumores extraidos del dorso de ratones NOD-SCID. Arriba, formados a partir de MEF inmortalizados silvestres. Abajo, formados a partir de MEF inmortalizados deficientes en PGC-1α. **B)** Medida del volumen tumoral en el momento de la disección tras la inyección de MEF inmortalizados silvestres y deficientes en PGC-1α en el dorso de ratones NOD-SCID. N=6. **C)** Imágenes representativas de Hematoxilina-Eosina e inmunohistiquimica para Ki67, marcador de proliferación. **D)** Imágenes de focos de proliferación en los tumores formados tras inyectar MEF inmortalizados silvestres y deficientes en PGC-1α en el dorso de ratones NOD-SCID. **E)** Cuantificación de núcleos positivos para Ki67. N=6. Los datos están representados como la media ± desviación típica. *, $p < 0.05$; **, $p \leq 0.01$; ***, $p \leq 0.005$.

Además, se realizó una valoración del número de células proliferativas mediante inmunohistoquímica dirigida contra Ki67. El 43 % de las células observadas presentaron marcaje de Ki67 en ausencia de PGC-1α mientras que en MEF inmortalizados silvestres el número de células proliferativas se situó en torno al 13 % (Fig. 26C-E). En ausencia de PGC-1α se observaron, también, zonas donde estas células proliferativas se concentraban en nódulos hiperproliferativos, mientras que estas zonas no se observaron en los tumores formados con MEF inmortalizados con PGC-1α (Fig. 26D), lo que sugería un proceso tumoral más agresivo en ausencia de PGC-1α.

La ausencia de PGC-1α en MEF inmortalizados favorece la formación de metástasis *in vivo*.

Teniendo en cuenta los resultados obtenidos en los estudios *in vitro*, donde se había observado una migración más rápida y desordenada en ausencia de PGC-1α; los resultados de localización subcelular de β-catenina, que mostraba una translocación hacia el núcleo y una activación de la TEM en MEF inmortalizados deficientes para PGC-1α; y los resultados de crecimiento *in vivo*, donde se vio que la supervivencia y la proliferación de los MEF inmortalizados deficientes en PGC-1α era mayor, se consideró valorar la hipótesis de que la ausencia de PGC-1α favoreciera la formación de metástasis *in vivo*.

Para ello, se realizó un experimento de metástasis experimental *in vivo*, que consistió en la inoculación, por la vena lateral de la cola de ratones NOD-SCID, de $5*10^5$ de las células objeto de estudio. Al inocular las células tumorales por esta vía, está descrito que el órgano principal en el que estas células pueden anidar, formando nódulos metastáticos, es en el pulmón.

Para poder realizar un seguimiento de las células inoculadas, se generaron líneas modificadas que expresaban constitutivamente luciferasa y GFP, mediante infección con partículas lentivirales recombinantes. La expresión de la luciferasa permite la detección *in vivo* por bioluminiscencia tras la inyección del sustrato de la luciferasa.

La inoculación de MEF inmortalizados en ratones NOD-SCID no generó nódulos metastáticos trazables mediante la detección de bioluminiscencia ni tras la disección de los pulmones. Con el fin de potenciar la capacidad de formación de tumores de los MEF inmortalizados, estas se inocularon junto con células de melanoma murino B16-V5 ($5*10^5$ con una relación 1:1), que tienen un gran potencial metastático, también modificadas con lentivirus recombinantes para que expresaran luciferasa y GFP.

A las dos semanas postinoculación, se detectó por bioluminiscencia la formación de nódulos metastáticos en los ratones inoculados con MEF inmortalizados deficientes en PGC-1α, mientras que no se observaron nódulos metastáticos en ratones inoculados con MEF inmortalizados silvestres hasta la segunda evaluación por bioluminiscencia a las cuatro semanas postinoculación (Fig. 27A). Seguidamente,

los animales fueron sacrificados. 8 ratones de 15 inoculados con MEF inmortalizados sin PGC-1α mostraron señal bioluminiscente mientras que solo 2 de los 15 ratones inoculados con MEF inmortalizados con PGC-1α mostró señal bioluminiscente.

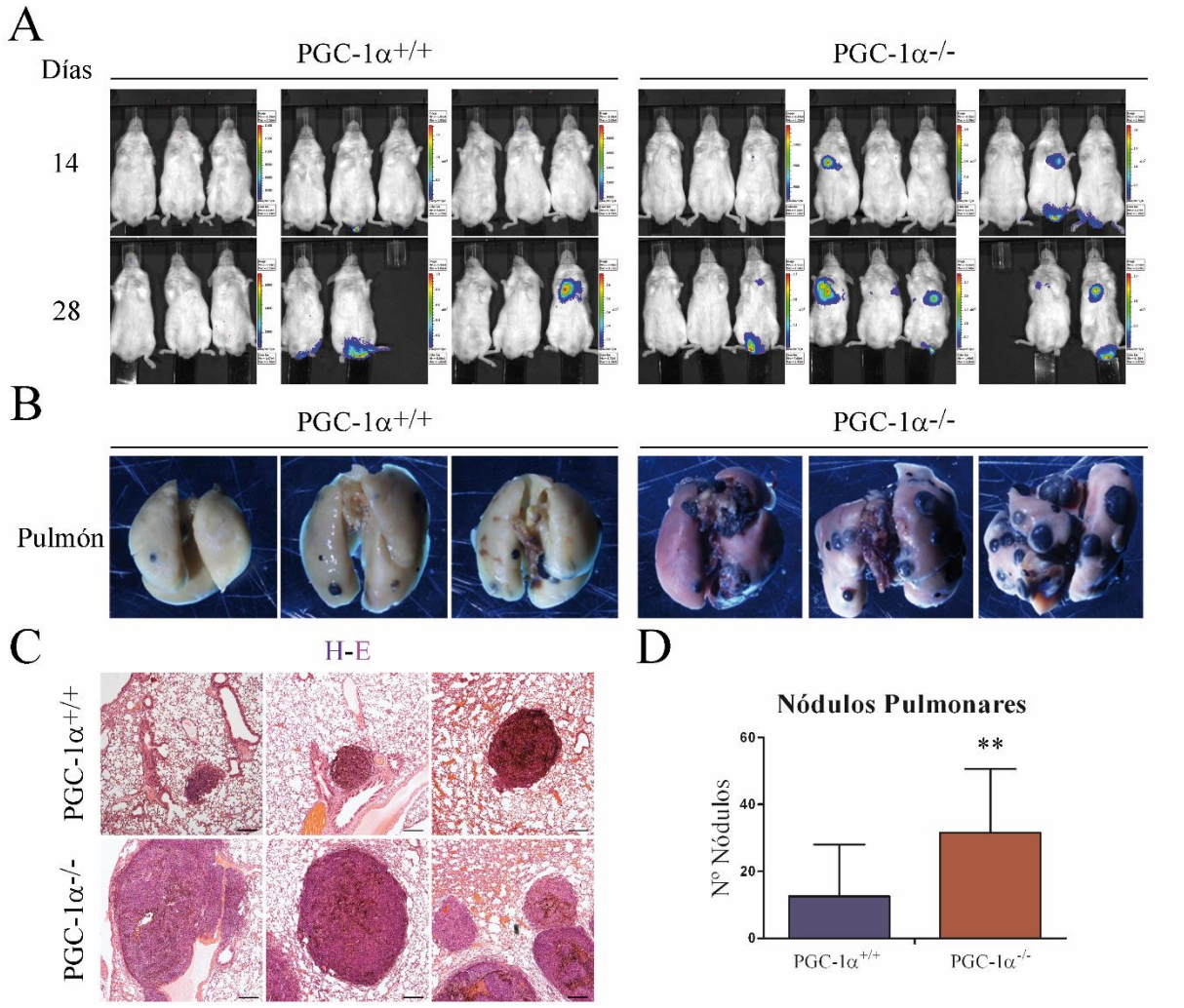

Figura 27. A) Imágenes obtenidas mediante la detección de bioluminiscencia en ratones NOD-SCID co-inoculados con MEF inmortalizados, silvestres o deficientes en PGC-1α; y células B16-V5, que expresan luciferasa. **B)** Imágenes tomadas con una lupa de los pulmones diseccionados a los ratones NOD-SCID co-inoculados con MEF inmortalizados y células B16-V5 que expresan luciferasa. **C)** Hematoxilina-Eosina de los pulmones diseccionados a los ratones NOD-SCID co-inoculados con MEF inmortalizados y células B16-V5 que expresan luciferasa. **D)** Cuantificación del número de nódulos metastáticos presentes en los pulmones diseccionados. N=15. Los datos están representados como la media ± desviación típica. *, $p < 0.05$; **, $p \leq 0.01$; ***, $p \leq 0.005$.

Tras ser diseccionados los pulmones de los ratones inoculados, se contaron, con la ayuda de una lupa los nódulos macroscópicos que se habían formado en los pulmones tras su tinción con *Bouin's Solution*. Pese a no haber sido detectados por el sistema de detección de bioluminiscencia, probablemente debido a ser de pequeño tamaño, la prácticamente totalidad de los pulmones estudiados presentaron nódulos metastáticos a excepción de uno de cada grupo (Fig. 27B-C). La cuantificación del número de nódulos indicó que el número de estos era significativamente mayor en ratones inoculados con MEF

inmortalizados deficientes en PGC-1α que en los inoculados con MEF inmortalizados silvestres (Fig. 27D). La coinoculación de células de melanoma murino con MEF inmortalizados silvestres formó 12,5 nódulos pulmonares de media por ratón mientras que en ausencia de PGC-1α este número aumentó hasta 31,5 nódulos pulmonares por ratón. Este resultado apoya, por tanto, la idea de que la ausencia de PGC-1α puede favorecer la formación de metástasis.

DISCUSIÓN

El estudio del papel de los ROS en el desarrollo tumoral sigue estando en el foco de continuas revisiones y estudios debido al papel dual de estas moléculas en la fisiología celular. En un principio se conocía la naturaleza altamente reactiva de los ROS, que son capaces de oxidar todo tipo de macromoléculas. Esto convierte a los ROS en el principal agente mutagénico para las células en un contexto de estrés oxidativo. Como ya se ha mencionado, esta cualidad promueve la aparición de rutas de señalización alteradas, por mutaciones en distintas proteínas, que inducen la formación de tumores. Sin embargo, cuando algunos tipos de tumores se tratan con antioxidantes también se observa un aumento o aceleración en la formación de tumores, lo que indica que los ROS, además de agentes mutagénicos, y promotores de la entrada en ciclo, cuando se producen en exceso pueden limitar el crecimiento de la célula tumoral (Chio and Tuveson 2017).

De la misma manera, cuando se ha estudiado el nivel de expresión de PGC-1α, por ser regulador clave del control de la función mitocondrial, en diferentes tipos de tumores se ha encontrado que, generalmente, aparece inactivado o con una baja expresión, pero que su inducción en células tumorales confiere a estas de una plasticidad metabólica clave en la aparición de resistencia a diversas terapias contra el cáncer (C. Luo et al. 2016a).

Con el fin de evaluar de manera comprensiva el riesgo que confiere a un organismo el tener disminuida la actividad de PGC-1α se ha realizado el presente estudio en el que se ha hecho un seguimiento completo del proceso tumoral utilizando un modelo *in vitro* de inmortalización espontánea de células MEF en ausencia de PGC-1α aportando nuevos datos sobre la implicación de este coactivador transcripcional en oncogénesis y que apoyan su papel fundamental como supresor tumoral al ser regulador clave del control redox celular y del metabolismo oxidativo.

En las primeras etapas de la progresión tumoral se producen respuestas para frenar la proliferación descontrolada de las células tumorales, entre las que se encuentra la inducción de la senescencia celular. Este proceso es considerado como una respuesta preventiva contra la progresión tumoral de una célula que ha alcanzado su límite funcional. De hecho, la inducción de este proceso celular está siendo investigada como una prometedora terapia en pacientes con cáncer (Calcinotto and Alimonti 2017). La inducción del estado senescente puede darse en respuesta a una gran variedad de estímulos, como pueden ser el acortamiento telomérico, la expresión de oncogenes, el daño en el ADN y el estrés oxidativo entre otros. Este último, el estrés oxidativo, se caracteriza por la acumulación de ROS y sus conocidos efectos fisiológicos. Además, independientemente del estímulo que provoque la entrada en senescencia, está descrito que las células senescentes producen más ROS que las células no senescentes (Correia-Melo and Passos 2015).

Desde que Hayflick y Moorhead describieran la senescencia replicativa a mitad del siglo XX (Hayflick and Moorhead 1961), muchos estudios les han sucedido describiendo las alteraciones que se producen en las células senescentes. Las células senescentes sufren cambios morfológicos, acumulación de daño en el ADN, reordenación de la cromatina, inducción de inhibidores del ciclo celular y liberación de

un conjunto de factores de crecimiento, citoquinas y proteasas al exterior celular conocido como *Senescence-associated Secretory Phenotype* (SASP) (Bernardes de Jesus and Blasco 2012).

Cabe resaltar que el SASP promueve el reclutamiento de macrófagos y células del sistema inmunitario para la eliminación de las células senescentes. Este efecto se ve reforzado por la acumulación y difusión de ROS al medio extracelular, actuando de forma paracrina sobre las células del sistema inmunitario que infiltran el tejido. La inducción de la inflamación junto a la inestabilidad genómica son consideradas características habilitantes en la progresión tumoral, permitiendo adquirir el resto de las características que definen a una célula tumoral explicadas en la introducción (Hanahan and Weinberg 2011). Por ello, el papel de la senescencia celular durante la progresión tumoral sigue en un intenso debate. No está claro aún si la inducción de la senescencia protege de un crecimiento aberrante o forma parte del proceso de progresión tumoral. Además, el SASP también es responsable de la aparición de señales inmunosupresoras, que evitan el reconocimiento de las células tumorales por parte de células del sistema inmunitario; de la remodelación de la matriz celular, un proceso importante en migración e invasión celular; y de la proliferación por la liberación de factores de crecimiento (S. G. Rao and Jackson 2016).

En nuestro estudio hemos observado que la ausencia de PGC-1α acelera la aparición de marcadores clásicos de senescencia celular, pero, además, también hemos observado una acelerada inmortalización de los MEF deficientes en PGC-1α. Estos resultados son consistentes con el modelo que propone que la inducción de la senescencia celular es una etapa del proceso de oncogénesis y que los ROS son un efector clave en dicho proceso.

Así, el estudio ha servido para determinar que los MEF primarios deficientes en PGC-1α acumulan más ROS que los MEF silvestres y esto se asocia a un mayor nivel de oxidación y daño en el ADN. Los experimentos diseñados para el estudio del control de los ROS mostraron, como ya está descrito (Davalli et al. 2016), que a medida que las células se acercan al estado senescente acumulan más ROS. Consistentemente, en nuestro experimento de entrada en senescencia observamos que la cantidad de proteína de MnSOD, que cataliza la reacción de generación de H_2O_2 a partir del ion superóxido, fue menor en ausencia de PGC-1α y se relaciona con la mayor cantidad de ion superóxido presente en MEF deficientes en PGC-1α estudiado mediante la adición de MitoSOX. Además, el nivel de expresión de cit C, que forma parte de la ETC, también fue menor en MEF deficientes en PGC-1α que en MEF silvestres.

Tanto MnSOD como cit C son dianas de expresión de PGC-1α (Olmos et al. 2009; Sanchez-Ramos et al. 2011; Valle et al. 2005) y la pérdida de expresión de ambas proteínas dependiente de la ausencia de PGC-1α explica la aparición de estrés oxidativo. MnSOD es una enzima detoxificante y en su ausencia se acumulan más ROS al no poder ser eliminados mientras que cit C forma parte de la ETC y su disminución puede ser indicador de presencia de disfunción mitocondrial, condición que se relaciona con una mayor producción de ROS en la mitocondria.

Nuestros resultados muestran, también, un mayor daño oxidativo en MEF deficientes en PGC-1α tanto en ácidos nucleicos como en lípidos y un mayor nivel de roturas de ADN, probablemente asociadas a oxidación del ADN. Hemos estudiado los efectos de los ROS en el ADN mediante una inmunofluorescencia con un anticuerpo frente al principal producto de la oxidación del ADN, la base nitrogenada 8-OH-dG, y lo relacionamos con roturas en el ADN mediante la adición de nucleótidos biotilinados en las zonas de rotura y la inmunofluorescencia de proteínas que se reclutan en zonas de rotura con función en la reparación de las mismas, como TP53BP1 y γH2AX. Los resultados indican una mayor oxidación de ADN asociada a la formación de más dobles roturas en el ADN y más focos de reparación en MEF deficientes en PGC-1α.

Las roturas en el ADN pueden dar lugar a mutaciones puntuales y reordenamientos cromosómicos, provocando inestabilidad genómica. Esta situación hace que la aparición de mutaciones de ganancia de función o silenciamiento génico de genes implicados en proliferación, supervivencia, migración o algunas de las características tumorales restantes sea posible. Por tanto, a raíz de los resultados obtenidos, concluimos que los MEF deficientes en PGC-1α deben ser más propensos a portar mutaciones que, potencialmente, pueden promover la progresión tumoral.

Además, observamos que los MEF deficientes en PGC-1α presentan una disminución significativa en la capacidad de reparar roturas de ADN. En el experimento diseñado para ver la dinámica de reparación observamos que ésta presenta un retraso en los MEF deficientes en PGC-1α si los comparamos con los de genotipo silvestre. La relación de PGC-1α con la reparación del ADN necesita ser investigada con mayor profundidad, pero está descrita una interacción de PGC-1α con TLS para la expresión de los genes de respuesta frente a estrés oxidativo (Sanchez-Ramos et al. 2011). TLS forma parte de una familia que se asocia a sitios de rotura en el ADN, está regulada por factores de respuesta a daño en el ADN y se ha descrito que participa en la reparación de roturas de ADN de doble cadena por recombinación homóloga (Schwartz et al. 2015). Por tanto, es posible especular que la interacción de PGC-1α con TLS puede ser al menos en parte responsable de la menor capacidad reparativa en ausencia de PGC-1α, pero debería ser estudiado con mayor detenimiento.

Respecto al daño oxidativo provocado en lípidos, se realizó un perfil de lípidos que nos permitió establecer niveles de peroxidación en base a la acumulación y síntesis de ácidos grasos concretos. La mayor susceptibilidad a la peroxidación de lípidos, calculada como el índice de peroxibilidad, que muestran los MEF deficientes en PGC-1α son un resultado más que apoya la mayor acumulación de ROS que se produce en ausencia de PGC-1α.

Cabe reseñar que el análisis de lípidos mostró, también, que en los MEF deficientes en PGC-1α tienen mayor nivel de AA y menor de ácido oleico (OA). La relación inversamente proporcional del AA y el OA está descrita previamente asociada a diversas patologías en las que el AA está aumentado, entre las que destaca el cáncer (Hostmark and Haug 2013a, 2013b). El AA es precursor de moléculas

proinflamatorias como prostaglandinas, leucotrienos y tromboxanos; y la liberación aumentada de prostaglandinas está descrita en cáncer como el principal responsable de la inmunosupresión tumoral (Sinha et al. 2007; D. Wang and DuBois 2015) y de la angiogénesis (Chang et al. 2004), favoreciendo la progresión tumoral. Este resultado es consistente con la observación de que la inhibición o silenciamiento de PGC-1α hace que aumente la actividad de ciclooxigenasas, que son las enzimas responsables de la síntesis de estos mediadores inflamatorios a partir del AA (Lu et al. 2015).

Recientemente, el estudio del ambiente tumoral se ha intensificado y hay muchas evidencias del importante papel que tienen diferentes tipos celulares que se encuentran en el ambiente tumoral, como son células del sistema inmunitario, fibroblastos y células endoteliales. Las células del ambiente tumoral son responsables de la secreción de citoquinas proinflamatorias, factores de crecimiento, factores proangiogénesis y enzimas responsables de la remodelación de la matriz extracelular. Por ello, pese a que no son células tumorales propiamente dichas, son células esenciales en la progresión tumoral. De la misma manera, la entrada transitoria en senescencia por parte de las células tumorales promueve un ambiente tumoral que favorece el crecimiento tumoral por la generación de ROS y la liberación de moléculas proinflamatorias como las prostaglandinas.

Estas observaciones sugieren que en ausencia de PGC-1α se podría favorecer un estado protumoral también desde el punto de vista del sistema inmunitario, aunque en nuestro estudio, al ser *in vitro*, no permite evaluar directamente este componente.

No obstante, cabe resaltar que la composición de las membranas es un factor clave en la señalización celular y la inhibición de enzimas importantes en la síntesis de ácidos grasos provoca alteraciones en la ruta de señalización, por ejemplo, de Rho, una GTPasa pequeña que regula proliferación, adhesión y migración (X. Wei et al. 2016). Además, la peroxidación de lípidos produce moléculas que se ha visto que tienen un papel importante en la señalización celular como el 4-hidroxinonenal (4-HNE), que se forma a partir del AA y otros PUFA. Este producto de la peroxidación de lípidos puede alterar rutas implicadas en la progresión tumoral como la de Akt, por oxidación e inactivación de PTEN; o la ruta de las MAPK. Además, se ha descrito que puede inducir senescencia celular, siendo un regulador del ciclo celular, aunque hay evidencias tanto de la inducción como de la represión del ciclo celular (A. Ayala et al. 2014). Sería conveniente realizar experimentos sobre la formación de este compuesto en ausencia de PGC-1α en el contexto de la progresión tumoral, estudiando su incidencia en las principales rutas de señalización.

La acumulación de ROS y los efectos en las células observados en nuestro estudio son estímulos bien establecidos como responsables de la inducción de la entrada en senescencia. Por ello, debido a las diferencias encontradas entre los MEF de ambos genotipos en acumulación de ROS y su daño asociado, en especial en el ADN, esperábamos una diferencia en la tasa de proliferación entre ambos genotipos que no encontramos en nuestro estudio. La tasa de proliferación de los MEF deficientes en PGC-1α fue ligeramente menor, pero sin alcanzar significación estadística, a pesar de que los MEF deficientes en PGC-

1α mostraron una aparición más temprana de marcadores de senescencia como puede ser la actividad de la β-galactosidasa asociada a senescencia o la inducción de inhibidores del ciclo celular, como p16, p19 y p21.

Sin embargo, el tiempo de inmortalización entre ambos genotipos si mostró diferencias significativas, los MEF deficientes en PGC-1α inmortalizan antes que los MEF de genotipo silvestre. El hecho de que inmortalicen antes en ausencia de PGC-1α sugiere una menor capacidad de inducir muerte celular en estos cultivos ya que cuando los cultivos están saliendo del estado de arresto del ciclo celular se generan señales antagónicas, tanto proliferativas como apoptóticas o senescentes. En este contexto, el que los cultivos deficientes en PGC-1α comiencen a proliferar antes puede ser debido a una menor capacidad de responder ante las señales antiproliferativas o apoptóticas. Este resultado contrasta aparentemente con estudios anteriores en los que se mostraba que PGC-1α protege de la apoptosis inducida por estrés oxidativo al inducir la expresión de antioxidantes y sugiere que, por encima de un cierto umbral de ROS, PGC-1α es proapoptótico, sin embargo, esta hipótesis requeriría otros estudios para su validación.

La inmortalización prematura en MEF deficientes en PGC-1α podría también indicar, que la selección clonal es más rápida en ausencia de PGC-1α, bien sea por tener estos una mayor tasa de acumulación de mutaciones bien sea por contribuir a un estado protumoral o bien sea por una señalización alterada debido al estrés oxidativo, pero siempre debido a la acumulación de ROS y sus efectos en la fisiología celular.

En conjunto, los resultados obtenidos en esta primera parte del estudio apoyan la idea de que la entrada en senescencia es parte de la progresión tumoral, y este proceso se acelera en ausencia de PGC-1α, sin que esto contradiga su bien conocida función fisiológica. Muchos mecanismos descritos en cáncer, como puede ser la TEM o la activación de algunos factores de transcripción, tienen también una función importante en el desarrollo embrionario, caracterizado, como el cáncer, por la proliferación y migración celular. Hay evidencias del papel que juega la senescencia durante el desarrollo embrionario en el cierre del tubo neural y la formación de varias estructuras embrionarias (Munoz-Espin et al. 2013; Storer et al. 2013). Por ello, la senescencia puede formar parte de los mecanismos y procesos del desarrollo embrionario que en organismos adultos se activan durante la progresión tumoral.

Además de las posibles rutas alteradas por el 4-HNE, un regulador clave en la inducción de la senescencia es p53. La interacción de p53 y PGC-1α está descrita y, además, un mutante descrito para el primer sitio de transactivación de p53 muestra un fenotipo similar al observado en asuencia de PGC-1α, es decir, disminuye su capacidad de inducir varias dianas de expresión de p53, no es capaz de inducir apoptosis, pero mantiene la capacidad de inducir senescencia (Brady et al. 2011). Sin embargo, si es capaz de inducir el metabolismo oxidativo (D. Jiang et al. 2015), lo que indica que esta regulación mediada por PGC-1α no depende de su interacción con p53. Nuevamente, es necesario realizar más experimentos para explorar la interacción de p53 con PGC-1α durante la entrada en senescencia celular porque si bien es cierto que en nuestro experimento no observamos diferencias en la cantidad de proteína total ni de su

forma activada, si pueden existir diferencias en los procesos que regulan conjuntamente. De hecho, el análisis de la expresión de dianas de p53 mostró unos niveles disminuidos en genes reguladores de parada de ciclo y apoptosis en las células deficientes en PGC-1α.

Tras la inmortalización prematura en ausencia de PGC-1α, estos MEF inmortalizados mostraron un fenotipo más glucolítico y menos oxidativo que los MEF inmortalizados silvestres, como está descrito por el Efecto Warburg. Se realizaron varios experimentos para dilucidar como era el metabolismo de nuestros cultivos inmortalizados y ver las similitudes que se muestran en trabajos anteriores sobre metabolismo tumoral y Efecto Warburg.

La primera observación realizada fue el incremento del flujo glucolítico hacia la formación de lactato y, por tanto, una disminución del consumo de oxígeno en ausencia de PGC-1α. En nuestro estudio, observamos esta producción de lactato, tanto indirectamente, por el descenso del pH del medio de cultivo de los MEF inmortalizados deficientes en PGC-1α; como directamente, tras realizar el experimento de trazabilidad de sustratos en el que observamos una mayor secreción de lactato al medio de los MEF inmortalizados sin PGC-1α respecto a los de genotipo silvestre. La relación de PGC-1α con la formación de lactato está bien descrita en tejidos con una alta demanda energética, como el músculo esquelético en situaciones de ejercicio, donde PGC-1α induce la expresión de LDHB, que transforma el lactato en piruvato; al mismo tiempo que reduce la expresión de LDHA, responsable de formación de lactato, reduciendo la síntesis de lactato y favoreciendo su oxidación (Summermatter et al. 2013). En algunos trabajos en cáncer también se relaciona inversamente la expresión de PGC-1α con la formación de lactato (Haq et al. 2013; Sancho et al. 2015).

En nuestro estudio del metabolismo de los MEF inmortalizados vimos que la expresión de PDK3 estaba aumentada en ausencia de PGC-1α. Las PDK son inhibidores de una de las enzimas importantes en el metabolismo mitocondrial y que en células tumorales se ve fuertemente inhibida para que se favorezca la producción de lactato, la PDH, que es responsable de la conversión del piruvato en Ac-CoA. En trabajos realizados en musculo esquelético, los niveles de PGC-1α y PDH muestran una relación directa, aunque el efecto de PGC-1α en su actividad y regulación aún está por demostrarse (Kiilerich et al. 2010). Otros trabajos, también en músculo esquelético, sugieren que PGC-1α activa la expresión de PDK4 (Wende et al. 2005), resultado que se contradice con el nuestro, e incluso que la ausencia de PGC-1α disminuye el nivel de las PDK y las PDP, fosfatasas que antagonizan la función de las PDK (Gudiksen and Pilegaard 2017). En todo caso, este resultado sugiere una regulación negativa de la entrada de piruvato en el ciclo TCA por medio de la PDH en ausencia de PGC-1α y explica porque en nuestros cultivos sin PGC-1α se produce más lactato y un menor consumo de O_2 aun en condiciones aerobias.

Al ser la glucolisis seguida de la formación de lactato menos eficiente en la producción de ATP que la fosforilación oxidativa, cabía esperar que el flujo de glucosa estuviera aumentado, pero pese a la mayor producción de lactato en ausencia de PGC-1α en nuestro estudio no observamos diferencias claras

en este sentido. El análisis del nivel de PFKFB3 mediante *western blot* confirma una mayor inducción de la glucolisis en ausencia de PGC-1α. La acción de PFKFB3 provoca la activación de la PFK, lo que aumenta el flujo glucolítico, pero, además, está descrito que activa a CDK1 promoviendo la progresión del ciclo celular (Yalcin et al. 2014), por lo que nuestros resultados parecen indicar un catabolismo de la glucosa aumentado en las células sin PGC-1α. Sin embargo, en los experimentos de trazabilidad de sustratos marcados con ^{13}C no se observó un aumento del consumo de glucosa en los MEF inmortalizados deficientes en PGC-1α respecto al control de genotipo silvestre. La relación de PGC-1α con la expresión de los transportadores GLUT está descrita en trabajos previos que establecen que la ausencia de PGC-1α provoca la disminución de la expresión de estos transportadores (Cao et al. 2014; Higashida et al. 2009). Así, el hecho de no observar diferencias en la entrada de glucosa puede estar explicada por el efecto de la ausencia de PGC-1α pese a estar descrito que, en células tumorales, la expresión de los transportadores de glucosa está aumentada, aunque para tratar de esclarecer este interrogante podría estudiarse el nivel de expresión, y la regulación, de los transportadores de glucosa o de otras enzimas importantes en la entrada de glucosa como la enzima HK. Aun así, independientemente de si se está produciendo una mayor entrada de glucosa en las células en cultivo deficientes en PGC-1α, los resultados son consistentes con un aumento de las reacciones que forman parte de la glucolisis en MEF inmortalizados sin PGC-1α, lo que podría indicar una mayor actividad de la ruta de las pentosas fosfato en las células silvestres.

La glucolisis y el ciclo TCA son responsables de la generación de precursores de las vías de síntesis de macromoléculas, esenciales en el metabolismo tumoral. En nuestro estudio hemos observado un aumento en la ruta de síntesis de ácidos grasos. Los MEF inmortalizados deficientes en PGC-1α mostraron mayor producción de ácidos grasos. En el ciclo TCA, el citrato producido en la mitocondria puede ser transportado hasta el citosol para promover la síntesis de ácidos grasos. Este es un proceso muy importante en células tumorales por sostener la tasa de proliferación, contribuyendo fundamentalmente en la síntesis de membranas biológicas además de regular la señalización celular. Ya hemos visto las diferencias en la síntesis de ácidos grasos en los MEF primarios, en los que la ausencia de PGC-1α hace que se sintetice más AA, y sus posibles implicaciones protumorales. Estas diferencias se mantienen en los MEF inmortalizados por lo que posiblemente, tras la inmortalización, la ausencia de PGC-1α puede promover cambios metabólicos, para mantener una mayor síntesis de ácidos grasos, como la formación y posterior salida del citrato mitocondrial.

Otra diferencia metabólica observada en ausencia de PGC-1α respecto a los MEF inmortalizados silvestres es la inducción de rutas anapleróticas del ciclo TCA. En concreto, hemos visto inducida la carboxilación del piruvato a OAA por medio de la PCx y la glutaminolisis. La salida de citrato de la mitocondria tiene consecuencias en la regeneración de OAA en el ciclo TCA al no completarse el ciclo, por lo que es necesaria la entrada de otros metabolitos en el ciclo TCA para regenerar el OAA. En nuestro estudio, el posible aumento en la generación de citrato para la síntesis de ácidos grasos, por parte de los MEF inmortalizados deficientes en PGC-1α, está apoyada por la observación de que los MEF

inmortalizados deficientes en PGC-1α presentan una actividad aumentada de la enzima PCx, como sugiere el experimento de trazabilidad de sustratos. Además, este resultado está apoyado por los mayores niveles de expresión observados para el ARNm de la enzima PCx en los cultivos de MEF inmortalizados sin PGC-1α.

Así mismo, hemos valorado la dependencia de los MEF inmortalizados hacia la glutamina y hemos observado que los MEF inmortalizados deficientes en PGC-1α sobreviven peor en ausencia de glutamina y comienzan a morir antes que los de genotipo silvestre, lo que sugiere una mayor dependencia hacia la glutamina. Además, el análisis de aminoácidos intracelulares apoya la mayor utilización de glutamina, y su mayor entrada en el ciclo TCA al observarse mayor cantidad de glutamato y mayor formación de aminoácidos relacionados con las reacciones de transaminación en las que participa la glutamina, como el aspartato y la alanina. Además de la glucosa, las células tumorales son especialmente dependientes de la presencia de glutamina. El papel protagonista que adquiere la glutamina como sustrato metabólico en células tumorales parece deberse a su utilización como fuente de carbono y de nitrógeno y se asocia con un mayor grado de disfunción mitocondrial. Mediante la glutaminolisis, la glutamina se convierte en glutamato y posteriormente en α-KG, intermediario del ciclo TCA y que permite la entrada de carbono proveniente de la glutamina en el metabolismo mitocondrial. Por otra parte, la glutamina es, también, responsable de una gran cantidad de reacciones importantes en el metabolismo intermediario de aminoácidos y bases nitrogenadas.

Estos resultados sugieren que la síntesis de ácidos grasos es clave en la progresión tumoral y que provoca cambios más profundos en el metabolismo celular. De hecho, en nuestro estudio hemos encontrado evidencias de que la glutamina que entra en el ciclo TCA posiblemente pueda seguir el ciclo en reverso para formar citrato en ausencia de PGC-1α y este resultado se apoya en la inducción de la enzima IDH1, clave en la ruta reversa del ciclo TCA.

Además, se ha observado una inducción de rutas que generan poder reductor en MEF inmortalizados deficientes en PGC-1α. Esto es debido a otro de los efectos que tiene sobre la célula el incremento de la síntesis de ácidos grasos, que es la necesidad de generar poder reductor en forma de NADPH. Parte de este poder reductor se genera en rutas biosintéticas como la ruta PPP, durante la glutaminolisis o durante la conversión de malato en piruvato por acción de la ME.

Estas tres rutas metabólicas posiblemente están aumentadas en los MEF inmortalizados deficientes en PGC-1α. El aumento de la glutaminolisis ya ha sido discutido. La ruta PPP podría estar aumentada por el mayor tráfico a través de la glucolisis, además, teniendo en cuenta que se producen precursores de la síntesis de nucleótidos, poder reductor y que algunos de los intermediarios pueden retornar a la glucolisis en diferentes puntos es muy probable su inducción en los cultivos deficientes en PGC-1α, pero un estudio de la actividad de las principales enzimas implicadas es necesario para valorar su implicación en la generación de NADPH en los MEF inmortalizados utilizados. Por último, el

experimento de trazabilidad de sustratos muestra un aumento de la actividad de la ME en los MEF inmortalizados deficientes en PGC-1α, y dicho resultado se ve apoyado por los niveles de expresión, analizados tanto a nivel de ARNm como de proteína, de la ME, que ve su expresión aumentada en ausencia de PGC-1α.

Por tanto, los MEF inmortalizados deficientes en PGC-1α presentan, en comparación con los de genotipo silvestre, un aumento del flujo glucolítico que unido a una deficiencia en la actividad de la PDH hace que generen y secreten más lactato al exterior celular. Para suplir el déficit en la entrada de piruvato en el TCA, en ausencia de PGC-1α se aumenta la entrada de glutamina en el ciclo transformándola en α-KG. Esta mayor entrada de glutamina está acompañada de la utilización de la carboxilación reductiva, inducida por la mayor salida de citrato al citosol como precursor de ácidos grasos. Para mantener los requerimientos de poder reductor de la síntesis de ácidos grasos aumenta, no solo la glutaminolisis, sino también la actividad de la ME. Para finalizar, para reestablecer los niveles de OAA y que el ciclo continúe funcionando, se produce una mayor entrada de piruvato mediante carboxilación a OAA.

Los resultados obtenidos relativos al metabolismo son coherentes, por una parte, con lo que se conoce sobre la función de PGC-1α como regulador del metabolismo oxidativo, y por otra, sugieren que el perfil metabólico de las células sin PGC-1α es coherente con un perfil tumoral más agresivo, generalmente asociado a la actividad de c-myc. Sin embargo, estos cambios metabólicos observados asociados a la ausencia de PGC-1α, que se incluyen entre los descritos durante la oncogénesis, son compartidos con la mayoría de las células en proliferación. Si tenemos en cuenta que las células utilizadas como objeto de estudio están inmortalizadas y tienen la habilidad de proliferar ilimitadamente, es necesario valorar si este perfil, aparentemente más agresivo desde el punto de vista metabólico, se corresponde realmente con unas características tumorales más agresivas y, por ello, se realizó la siguiente fase del estudio.

Se buscó correlacionar las diferencias metabólicas encontradas en MEF inmortalizados deficientes en PGC-1α con un comportamiento más tumoral, es decir, con células con mayor capacidad de supervivencia, más proliferativas y con mayor motilidad celular. Se realizaron ensayos *in vitro* para estudiar estas características antes de confirmarlas mediante experimentos *in vivo* de crecimiento tumoral y metástasis.

En nuestro estudio encontramos que los MEF inmortalizados deficientes en PGC-1α sobreviven mejor ante situaciones de deprivación de factores de crecimiento y tienen mayor capacidad migratoria.

En ausencia de PGC-1α, observamos una mayor capacidad de supervivencia *in vitro* al exponer a los MEF inmortalizados, tanto de genotipo silvestre como deficientes en PGC-1α, a la privación, total o parcial, de factores de crecimiento en el medio de cultivo y observar la supervivencia cada 24 h. Las células tumorales tienen que ser capaces de sobrevivir y proliferar con cantidades reducidas de factores de crecimiento, así como a la falta de oxígeno, a niveles elevados de ROS o a condiciones de inestabilidad

genómica. Ante estos estímulos, muestran una gran plasticidad que se caracteriza por la evasión de la muerte celular o apoptosis. Como hemos visto en la primera parte del estudio los MEF inmortalizados deficientes en PGC-1α parece que son más resistentes a apoptosis ya que escapan antes del estado senescente e inmortalizan. Por ello, estos resultados sugieren, de nuevo, que en ausencia de PGC-1α los MEF inmortalizados pueden ser capaces de evadir la muerte celular.

El déficit de PGC-1α muestra que los cultivos de MEF inmortalizados no detienen su proliferación *in vitro* pese a ocupar toda la placa de cultivo, como ocurre con cultivos tumorales *in vitro*, lo que sugiere una mayor capacidad de evitar las señales antiproliferativas de contacto en cultivos deficientes en PGC-1α. Además, con los experimentos de formación de colonias se observó que los MEF inmortalizados deficientes en PGC-1α son capaces de formar más colonias en ausencia de matriz extracelular y una menor dependencia de señales proliferativas en los cultivos deficientes en PGC-1α. En general, los datos acerca de la proliferación *in vitro* indican una mayor capacidad proliferativa de los MEF inmortalizados PGC-1α$^{-/-}$ en contextos desfavorables. Estas observaciones son consistentes con los datos *in vivo* cuando posteriormente se comprobaron en ensayos de xenotransplante.

En estos ensayos, los MEF inmortalizados sobreviven mejor al ser inyectados en el dorso de ratones C57BL6 y NOD-SCID ya que observamos mayor cantidad de células tras la disección de las matrices en las que habían sido inyectados los MEF inmortalizados sin PGC-1α y este resultado quedó comprobado cuando se inyectaron MEF inmortalizados con expresión constitutiva de GFP y podían ser distinguidas. Respecto a la proliferación, tanto los tumores diseccionados provenientes de ratones C57BL/6 como de ratones NOD-SCID mostraron un mayor número de células positivas para el marcador de proliferación Ki67. Es poco probable que las diferencias observadas en los estudios *in vivo* se deban a una proliferación más rápida dado que el análisis *in vitro* muestra que en condiciones no limitantes, ni los MEF primarios ni los inmortalizados, muestran diferencias significativas en este sentido entre los dos genotipos, pero sí son capaces de proliferar en situaciones restrictivas en ausencia de PGC-1α.

Los MEF inmortalizados deficientes en PGC-1α también presentan una mayor capacidad migratoria. Lo primero que se observó fue que las colonias formadas en el experimento de crecimiento a baja densidad celular muestran, en su mayoría, un fenotipo más invasivo en ausencia de PGC-1α, con un borde de la colonia más difuso con células más separadas entre ellas y alejándose de la colonia, en contraposición con las colonias formadas a partir de MEF inmortalizados silvestres, que tienen el borde de la colonia continuo y las células están más unidas unas con otras. Para estudiar con mayor profundidad este proceso se realizaron ensayos *in vitro* de migración, por cierre de herida y migración en cámara de Boyden. En ambos ensayos se observa una mayor velocidad migración en ausencia de PGC-1α y, además, el experimento de cierre de herida muestra que los MEF inmortalizados deficientes en PGC-1α presentan una migración menos coordinada, que puede ser señal de mayor invasividad y es consistente con una pérdida de interacciones celulares. Un componente importante de las uniones entre células es la β-catenina, que en nuestro estudio aparece localizada en el núcleo de los MEF inmortalizados sin PGC-1α

mientras que se encuentra en la membrana en MEF inmortalizados silvestres. La localización nuclear de la β-catenina parece indicar que está ejerciendo una función de regulación de la expresión génica, descrita en tumores y asociada a la TEM. Es importante reseñar que la mayor capacidad migratoria de las células deficientes en PGC-1α se debe a la mayor producción de ROS y se suprime con antioxidantes (Borniquel et al. 2010).

Estas características en principio más proinvasivas observadas *in vitro*, de los MEF inmortalizados deficientes en PGC-1α, resultaron consistentes con los estudios *in vivo*, en los que se observó una mayor capacidad de formación de nódulos tumorales en el pulmón al coinocular los MEF inmortalizados con células de melanoma en ratones NOD-SCID, confirmando la mayor invasividad en ausencia de PGC-1α.

Para resumir este apartado, la ausencia de PGC-1α en MEF inmortalizados está asociada a un metabolismo más glucolítico y menos oxidativo, como cabría esperar, pero que, además, presenta otras diferencias con los cultivos silvestres como el aumento de las rutas anapleróticas del ciclo TCA y una mayor síntesis de ácidos grasos que se correlacionan con una mayor supervivencia, proliferación y migración celular.

En células no proliferativas, el catabolismo celular está predominantemente asociado a los requerimientos energéticos y se observa un uso preferencial de la oxidación de macromoléculas mediante la fosforilación oxidativa mitocondrial para obtener ATP. En contraste, tejidos con altas tasas de proliferación, utilizan los recursos bioenergéticos para permitir la progresión del ciclo celular y, para ello, se aumenta el flujo glucolítico, la producción de lactato y la biosíntesis de macromoléculas. Por ello, el control del metabolismo comparte rutas de regulación con el control de la proliferación y la migración (Fritz and Fajas 2010).

Akt es el principal regulador que comparten proliferación y metabolismo, al ser parte de la ruta de señalización de los RTK para mantener la proliferación y su sobreactivación está asociada a la aparición de tumores (Mundi et al. 2016), y también provoca la inducción de la glucolisis (Hers et al. 2011). Akt actúa como un represor de PGC-1α, mediante fosforilación, inhibiendo el metabolismo oxidativo (X. Li et al. 2007). Además, PGC-1α regula la actividad de los factores FOXO (Olmos et al. 2009; Puigserver et al. 2003), principal diana de expresión de Akt para la inducción de apoptosis en respuesta a estés (X. Zhang et al. 2011). En nuestro estudio, la alteración de la señalización dependiente de Akt puede tener relevancia por la resistencia a inducir apoptosis en ausencia de PGC-1α y la rápida inmortalización tras la entrada en senescencia y sería interesante estudiar la ruta de señalización con más detalle.

Otro nodo importante de conexión entre el metabolismo y el control del ciclo celular es la familia de factores de transcripción E2F, reguladores directos de la expresión de genes metabólicos, que juegan un papel esencial en la coordinación ente el ciclo celular y el metabolismo (Ambrus et al. 2013; Blanchet et al. 2011; Cam et al. 2004). E2F reprime la función mitocondrial por medio de la represión de PGC-1α (Blanchet et al. 2011). Además, la familia de este factor de transcripción está fuertemente regulado por la

familia del supresor tumoral Rb. Cabe destacar que p16 y p21 son inhibidores de las CDK, principales reguladores de la actividad de Rb y los hemos encontrado inducidos en MEF primarios deficientes en PGC-1α durante la inducción de la senescencia celular y está descrito que se inducen en un contexto celular de estrés oxidativo (Bieging-Rolett et al. 2016; Jenkins et al. 2011). Por tanto, en nuestro estudio, en el contexto de senescencia celular, E2F podría estar reprimido y no inducir proliferación celular ni reprimir el metabolismo oxidativo, pero una vez inmortalizados los MEF posiblemente no sea reprimido por Rb e induzca ciclo celular y reprima el metabolismo oxidativo. Como esta represión del metabolismo oxidativo parece que la realiza a través de PGC-1α, esta ruta puede ser muy relevante para entender como las diferencias metabólicas encontradas entre ambos genotipos de MEF inmortalizados se asocian a oncogenes.

Reseñar además el papel del supresor tumoral p53, que además de inducir parada de ciclo, muerte celular y senescencia en respuesta a la presencia de estrés oxidativo, también regula la expresión de genes antioxidantes de forma más directa, como por ejemplo mediante la regulación de SCO2, que induce el metabolismo oxidativo (Matoba et al. 2006); y reguladores del metabolismo como TIGAR, que inhibe la glucolisis (Bensaad et al. 2006). PGC-1α también ve inducida su expresión por p53 (Aquilano et al. 2013), y actúa, como coactivador de p53 precisamente en la regulación de genes del ciclo celular, la homeostasis de ROS y del metabolismo oxidativo (Sen et al. 2011). La transactivación de p53 por parte de PGC-1α promueve la supervivencia celular ante situaciones de estrés metabólico (Aquilano et al. 2013; Sen et al. 2011). En el contexto de nuestro estudio p53 debería inducirse en respuesta al daño en el ADN, aunque nosotros no lo hemos observado, probablemente por la alta cantidad de proteína que observamos desde los primeros pases y que puede ser debido a que el proceso de congelación y descongelación de las células active respuestas a estrés en los MEF utilizados. Tras la inmortalización, p53 es posible que se reprima permitiendo, en parte, el cambio metabólico asociado a sus dianas de expresión

Finalmente, otro factor de transcripción, el oncogén c-myc, tiene un papel esencial en carcinogénesis como regulador positivo del ciclo celular, supresor del metabolismo oxidativo y, también, controla el uso de la glutamina promoviendo la progresión tumoral. En cáncer, la expresión de c-myc está aumentada y es inversamente proporcional a la de PGC-1α (Sancho et al. 2015), y esta observación es consistente con lo observado en nuestros cultivos de MEF inmortalizados en los que la ausencia de PGC-1α se relaciona con la inducción de la expresión de c-myc. c-myc ve su expresión inducida tras la traslocación de la β-catenina al núcleo (S. Zhang et al. 2012), tal y como muestran nuestros resultados, en los que tanto β-catenina se localiza en el núcleo como c-myc está inducido, en ausencia de PGC-1α. Esta inducción puede tener relevancia tanto en el metabolismo más glucolítico observado y el uso de glutamina en el ciclo TCA como en la regulación de la capacidad de proliferación y la migración celular.

En resumen, la asociación de PGC-1α con parte de los reguladores clave en progresión tumoral regulando el cambio metabólico descrito en el Efecto Warburg está en consonancia con los resultados presentados en el presente estudio y pone de manifiesto su relevancia en dicho proceso, apoyando su

papel como supresor tumoral mediado, al menos en parte, por su regulación del metabolismo oxidativo y de la homeostasis de lo ROS.

CONCLUSIONES

1. En MEF primarios, la ausencia de PGC-1α produce una mayor acumulación de ROS que en MEF primarios silvestres, acentuándose las diferencias a medida que los cultivos se acercan al estado de senescencia celular. Este efecto se asocia a una mayor oxidación del ADN y un mayor número de roturas en el ADN.

2. El mayor nivel de daño observado en MEF primarios deficientes en PGC-1α va acompañado de la inducción temprana de inhibidores del ciclo celular y otros marcadores de senescencia celular.

3. La inducción temprana, en ausencia de PGC-1α, de inhibidores del ciclo celular, no da lugar a una disminución significativa en la velocidad de proliferación, siendo esta similar en MEF primarios de ambos genotipos. Además, el tiempo de inmortalización es más corto en ausencia de PGC-1α.

4. Los MEF inmortalizados deficientes en PGC-1α presentan un mayor flujo glucolítico que se corresponde con una mayor formación de lactato no acompañado de un mayor consumo de oxígeno.

5. En ausencia de PGC-1α, la glucolisis y el ciclo TCA de MEF inmortalizados son utilizados para la generación de precursores biosintéticos en mayor medida que en MEF inmortalizados silvestres, siendo detectable la formación de citrato, que presumiblemente se dirija a la síntesis de ácidos grasos.

6. Los MEF inmortalizados deficientes en PGC-1α muestran una mayor utilización de vías anapleróticas, presumiblemente activadas para compensar las deficiencias del ciclo TCA. En particular destacan: la entrada de glutamina en el ciclo TCA por glutaminolisis, la utilización de la enzima málica para obtener poder reductor y la utilización de la enzima Piruvato Carboxilasa para la regeneración del OAA.

7. Las diferencias metabólicas observadas entre MEF inmortalizados correlacionan con unas características fenotípicas tumorales más agresivas *in vitro*. En ausencia de PGC-1α, los MEF inmortalizados sobreviven más ante situaciones de deprivación de factores de crecimiento, proliferan aun en presencia de estímulos antiproliferativos o en ausencia de sustrato y migran más rápido.

8. *In vivo*, la ausencia de PGC-1α se asocia a una mayor tasa de supervivencia y proliferación celular al ser inyectadas los MEF inmortalizados en el dorso de ratones C57BL6 y ratones inmunodeprimidos NOD-SCID.

9. La coinoculación intravenosa de células de melanoma con MEF inmortalizados deficientes en PGC-1α genera más nódulos pulmonares que al inocularlas junto a MEF inmortalizados silvestres, lo que indica que la ausencia de PGC-1α podría favorecer la formación de metástasis.

10. Los resultados obtenidos apoyan la hipótesis de que PGC-1α funciona fundamentalmente como supresor tumoral.

BIBLIOGRAFÍA

Ambrus, A. M., et al. (2013), 'Loss of dE2F compromises mitochondrial function', *Dev Cell,* 27 (4), 438-51.
Anastasiou, D., et al. (2011), 'Inhibition of pyruvate kinase M2 by reactive oxygen species contributes to cellular antioxidant responses', *Science,* 334 (6060), 1278-83.
Andersson, U. and Scarpulla, R. C. (2001), 'Pgc-1-related coactivator, a novel, serum-inducible coactivator of nuclear respiratory factor 1-dependent transcription in mammalian cells', *Mol Cell Biol,* 21 (11), 3738-49.
Aquilano, K., et al. (2013), 'p53 orchestrates the PGC-1alpha-mediated antioxidant response upon mild redox and metabolic imbalance', *Antioxid Redox Signal,* 18 (4), 386-99.
Arany, Z., et al. (2005), 'Transcriptional coactivator PGC-1 alpha controls the energy state and contractile function of cardiac muscle', *Cell Metab,* 1 (4), 259-71.
Ayala, A., Munoz, M. F., and Arguelles, S. (2014), 'Lipid peroxidation: production, metabolism, and signaling mechanisms of malondialdehyde and 4-hydroxy-2-nonenal', *Oxid Med Cell Longev,* 2014, 360438.
Ayala, F. R., et al. (2010), 'GLUT1 and GLUT3 as potential prognostic markers for Oral Squamous Cell Carcinoma', *Molecules,* 15 (4), 2374-87.
Baar, K., et al. (2002), 'Adaptations of skeletal muscle to exercise: rapid increase in the transcriptional coactivator PGC-1', *FASEB J,* 16 (14), 1879-86.
Bando, H., et al. (2005), 'Phosphorylation of the 6-phosphofructo-2-kinase/fructose 2,6-bisphosphatase/PFKFB3 family of glycolytic regulators in human cancer', *Clin Cancer Res,* 11 (16), 5784-92.
Bardella, C., Pollard, P. J., and Tomlinson, I. (2011), 'SDH mutations in cancer', *Biochim Biophys Acta,* 1807 (11), 1432-43.
Basu, S., Broxmeyer, H. E., and Hangoc, G. (2013), 'Peroxisome proliferator-activated-gamma coactivator-1alpha-mediated mitochondrial biogenesis is important for hematopoietic recovery in response to stress', *Stem Cells Dev,* 22 (11), 1678-92.
Baysal, B. E., et al. (2002), 'Prevalence of SDHB, SDHC, and SDHD germline mutations in clinic patients with head and neck paragangliomas', *J Med Genet,* 39 (3), 178-83.
Bell, R. J., et al. (2015), 'Cancer. The transcription factor GABP selectively binds and activates the mutant TERT promoter in cancer', *Science,* 348 (6238), 1036-9.
Bensaad, K., et al. (2006), 'TIGAR, a p53-inducible regulator of glycolysis and apoptosis', *Cell,* 126 (1), 107-20.
Bernardes de Jesus, B. and Blasco, M. A. (2012), 'Assessing cell and organ senescence biomarkers', *Circ Res,* 111 (1), 97-109.
Berthet, C., et al. (2006), 'Combined loss of Cdk2 and Cdk4 results in embryonic lethality and Rb hypophosphorylation', *Dev Cell,* 10 (5), 563-73.
Bhalla, K., et al. (2011), 'PGC1alpha promotes tumor growth by inducing gene expression programs supporting lipogenesis', *Cancer Res,* 71 (21), 6888-98.
Bieging-Rolett, K. T., et al. (2016), 'p19(Arf) is required for the cellular response to chronic DNA damage', *Oncogene,* 35 (33), 4414-21.
Blanco, R. and Gerhardt, H. (2013), 'VEGF and Notch in tip and stalk cell selection', *Cold Spring Harb Perspect Med,* 3 (1), a006569.
Blanchet, E., et al. (2011), 'E2F transcription factor-1 regulates oxidative metabolism', *Nat Cell Biol,* 13 (9), 1146-52.
Bodnar, A. G., et al. (1998), 'Extension of life-span by introduction of telomerase into normal human cells', *Science,* 279 (5349), 349-52.
Bonde, A. K., et al. (2012), 'Intratumoral macrophages contribute to epithelial-mesenchymal transition in solid tumors', *BMC Cancer,* 12, 35.
Borniquel, S., et al. (2010), 'Inactivation of Foxo3a and subsequent downregulation of PGC-1 alpha mediate nitric oxide-induced endothelial cell migration', *Mol Cell Biol,* 30 (16), 4035-44.
Brady, C. A., et al. (2011), 'Distinct p53 transcriptional programs dictate acute DNA-damage responses and tumor suppression', *Cell,* 145 (4), 571-83.

Brunelle, J. K., et al. (2005), 'Oxygen sensing requires mitochondrial ROS but not oxidative phosphorylation', *Cell Metab,* 1 (6), 409-14.
Buller, C. L., et al. (2008), 'A GSK-3/TSC2/mTOR pathway regulates glucose uptake and GLUT1 glucose transporter expression', *Am J Physiol Cell Physiol,* 295 (3), C836-43.
Bunting, S. F., et al. (2010), '53BP1 inhibits homologous recombination in Brca1-deficient cells by blocking resection of DNA breaks', *Cell,* 141 (2), 243-54.
Burma, S., et al. (2001), 'ATM phosphorylates histone H2AX in response to DNA double-strand breaks', *J Biol Chem,* 276 (45), 42462-7.
Burns, P. A. and Wilson, D. J. (2003), 'Angiogenesis mediated by metabolites is dependent on vascular endothelial growth factor (VEGF)', *Angiogenesis,* 6 (1), 73-7.
Cai, L., et al. (2011), 'Acetyl-CoA induces cell growth and proliferation by promoting the acetylation of histones at growth genes', *Mol Cell,* 42 (4), 426-37.
Calcinotto, A. and Alimonti, A. (2017), 'Aging tumour cells to cure cancer: "pro-senescence" therapy for cancer', *Swiss Med Wkly,* 147, w14367.
Callen, E., et al. (2013), '53BP1 mediates productive and mutagenic DNA repair through distinct phosphoprotein interactions', *Cell,* 153 (6), 1266-80.
Cam, H., et al. (2004), 'A common set of gene regulatory networks links metabolism and growth inhibition', *Mol Cell,* 16 (3), 399-411.
Cano, A., et al. (2000), 'The transcription factor snail controls epithelial-mesenchymal transitions by repressing E-cadherin expression', *Nat Cell Biol,* 2 (2), 76-83.
Cao, D., et al. (2014), 'PGC-1alpha integrates glucose metabolism and angiogenesis in multiple myeloma cells by regulating VEGF and GLUT-4', *Oncol Rep,* 31 (3), 1205-10.
Cardaci, S., et al. (2015), 'Pyruvate carboxylation enables growth of SDH-deficient cells by supporting aspartate biosynthesis', *Nat Cell Biol,* 17 (10), 1317-26.
Carvalho, K. C., et al. (2011), 'GLUT1 expression in malignant tumors and its use as an immunodiagnostic marker', *Clinics (Sao Paulo),* 66 (6), 965-72.
Casneuf, V. F., et al. (2008), 'Expression of SGLT1, Bcl-2 and p53 in primary pancreatic cancer related to survival', *Cancer Invest,* 26 (8), 852-9.
Castro-Vega, L. J., et al. (2014), 'Germline mutations in FH confer predisposition to malignant pheochromocytomas and paragangliomas', *Hum Mol Genet,* 23 (9), 2440-6.
Colegio, O. R., et al. (2014), 'Functional polarization of tumour-associated macrophages by tumour-derived lactic acid', *Nature,* 513 (7519), 559-63.
Collaborators, G. B. D. Risk Factors (2016), 'Global, regional, and national comparative risk assessment of 79 behavioural, environmental and occupational, and metabolic risks or clusters of risks, 1990-2015: a systematic analysis for the Global Burden of Disease Study 2015', *Lancet,* 388 (10053), 1659-724.
Comijn, J., et al. (2001), 'The two-handed E box binding zinc finger protein SIP1 downregulates E-cadherin and induces invasion', *Mol Cell,* 7 (6), 1267-78.
Commisso, C., et al. (2013), 'Macropinocytosis of protein is an amino acid supply route in Ras-transformed cells', *Nature,* 497 (7451), 633-7.
Cormio, A., et al. (2009), 'The PGC-1alpha-dependent pathway of mitochondrial biogenesis is upregulated in type I endometrial cancer', *Biochem Biophys Res Commun,* 390 (4), 1182-5.
Correia-Melo, C. and Passos, J. F. (2015), 'Mitochondria: Are they causal players in cellular senescence?', *Biochim Biophys Acta,* 1847 (11), 1373-9.
Cui, X. P., et al. (2014), 'HOXA10 promotes cell invasion and MMP-3 expression via TGFbeta2-mediated activation of the p38 MAPK pathway in pancreatic cancer cells', *Dig Dis Sci,* 59 (7), 1442-51.
Cunningham, J. T., et al. (2014), 'Protein and nucleotide biosynthesis are coupled by a single rate-limiting enzyme, PRPS2, to drive cancer', *Cell,* 157 (5), 1088-103.
Chajes, V., et al. (2006), 'Acetyl-CoA carboxylase alpha is essential to breast cancer cell survival', *Cancer Res,* 66 (10), 5287-94.

Chandler, J. D., et al. (2003), 'Expression and localization of GLUT1 and GLUT12 in prostate carcinoma', *Cancer,* 97 (8), 2035-42.
Chaneton, B., et al. (2012), 'Serine is a natural ligand and allosteric activator of pyruvate kinase M2', *Nature,* 491 (7424), 458-62.
Chang, S. H., et al. (2004), 'Role of prostaglandin E2-dependent angiogenic switch in cyclooxygenase 2-induced breast cancer progression', *Proc Natl Acad Sci U S A,* 101 (2), 591-6.
Chatterjee, S., et al. (2013), 'Tumor VEGF:VEGFR2 autocrine feed-forward loop triggers angiogenesis in lung cancer', *J Clin Invest,* 123 (4), 1732-40.
Chen, P. L., et al. (2013), 'Mitochondrial genome instability resulting from SUV3 haploinsufficiency leads to tumorigenesis and shortened lifespan', *Oncogene,* 32 (9), 1193-201.
Cheng, D., et al. (2015), 'K-Ras promotes the non-small lung cancer cells survival by cooperating with sirtuin 1 and p27 under ROS stimulation', *Tumour Biol,* 36 (9), 7221-32.
Cheng, T., et al. (2011), 'Pyruvate carboxylase is required for glutamine-independent growth of tumor cells', *Proc Natl Acad Sci U S A,* 108 (21), 8674-9.
Chio, I. I. C. and Tuveson, D. A. (2017), 'ROS in Cancer: The Burning Question', *Trends Mol Med,* 23 (5), 411-29.
Chipuk, J. E., et al. (2004), 'Direct activation of Bax by p53 mediates mitochondrial membrane permeabilization and apoptosis', *Science,* 303 (5660), 1010-4.
Christofk, H. R., et al. (2008), 'The M2 splice isoform of pyruvate kinase is important for cancer metabolism and tumour growth', *Nature,* 452 (7184), 230-3.
Dal Bello, B., et al. (2010), 'Glutamine synthetase immunostaining correlates with pathologic features of hepatocellular carcinoma and better survival after radiofrequency thermal ablation', *Clin Cancer Res,* 16 (7), 2157-66.
Dang, L., Yen, K., and Attar, E. C. (2016), 'IDH mutations in cancer and progress toward development of targeted therapeutics', *Ann Oncol,* 27 (4), 599-608.
Darlington, Y., et al. (2012), 'Absence of Wip1 partially rescues Atm deficiency phenotypes in mice', *Oncogene,* 31 (9), 1155-65.
Davalli, P., et al. (2016), 'ROS, Cell Senescence, and Novel Molecular Mechanisms in Aging and Age-Related Diseases', *Oxid Med Cell Longev,* 2016, 3565127.
DeBerardinis, R. J., et al. (2007), 'Beyond aerobic glycolysis: transformed cells can engage in glutamine metabolism that exceeds the requirement for protein and nucleotide synthesis', *Proc Natl Acad Sci U S A,* 104 (49), 19345-50.
Deblois, G., St-Pierre, J., and Giguere, V. (2013), 'The PGC-1/ERR signaling axis in cancer', *Oncogene,* 32 (30), 3483-90.
Dey, P., et al. (2017), 'Genomic deletion of malic enzyme 2 confers collateral lethality in pancreatic cancer', *Nature,* 542 (7639), 119-23.
Ding, L., et al. (2008), 'Somatic mutations affect key pathways in lung adenocarcinoma', *Nature,* 455 (7216), 1069-75.
Dombrauckas, J. D., Santarsiero, B. D., and Mesecar, A. D. (2005), 'Structural basis for tumor pyruvate kinase M2 allosteric regulation and catalysis', *Biochemistry,* 44 (27), 9417-29.
Dunham, M. A., et al. (2000), 'Telomere maintenance by recombination in human cells', *Nat Genet,* 26 (4), 447-50.
DuPage, M., et al. (2012), 'Expression of tumour-specific antigens underlies cancer immunoediting', *Nature,* 482 (7385), 405-9.
Duvel, K., et al. (2010), 'Activation of a metabolic gene regulatory network downstream of mTOR complex 1', *Mol Cell,* 39 (2), 171-83.
Eger, A., et al. (2005), 'DeltaEF1 is a transcriptional repressor of E-cadherin and regulates epithelial plasticity in breast cancer cells', *Oncogene,* 24 (14), 2375-85.
El Hallani, S., et al. (2010), 'A new alternative mechanism in glioblastoma vascularization: tubular vasculogenic mimicry', *Brain,* 133 (Pt 4), 973-82.

Ellenrieder, V., et al. (2001), 'Transforming growth factor beta1 treatment leads to an epithelial-mesenchymal transdifferentiation of pancreatic cancer cells requiring extracellular signal-regulated kinase 2 activation', *Cancer Res,* 61 (10), 4222-8.

Escribano-Diaz, C., et al. (2013), 'A cell cycle-dependent regulatory circuit composed of 53BP1-RIF1 and BRCA1-CtIP controls DNA repair pathway choice', *Mol Cell,* 49 (5), 872-83.

Estrella, V., et al. (2013), 'Acidity generated by the tumor microenvironment drives local invasion', *Cancer Res,* 73 (5), 1524-35.

Falkenberg, M., et al. (2002), 'Mitochondrial transcription factors B1 and B2 activate transcription of human mtDNA', *Nat Genet,* 31 (3), 289-94.

Fan, J., et al. (2013), 'Glutamine-driven oxidative phosphorylation is a major ATP source in transformed mammalian cells in both normoxia and hypoxia', *Mol Syst Biol,* 9, 712.

Feilchenfeldt, J., et al. (2004), 'Peroxisome proliferator-activated receptors (PPARs) and associated transcription factors in colon cancer: reduced expression of PPARgamma-coactivator 1 (PGC-1)', *Cancer Lett,* 203 (1), 25-33.

Ferrer, C. M., et al. (2014), 'O-GlcNAcylation regulates cancer metabolism and survival stress signaling via regulation of the HIF-1 pathway', *Mol Cell,* 54 (5), 820-31.

Figueroa, M. E., et al. (2010), 'Leukemic IDH1 and IDH2 mutations result in a hypermethylation phenotype, disrupt TET2 function, and impair hematopoietic differentiation', *Cancer Cell,* 18 (6), 553-67.

Finkel, T. (2006), 'Cell biology: a clean energy programme', *Nature,* 444 (7116), 151-2.

Fischer, K., et al. (2007), 'Inhibitory effect of tumor cell-derived lactic acid on human T cells', *Blood,* 109 (9), 3812-9.

Flores, J. F., et al. (1996), 'Loss of the p16INK4a and p15INK4b genes, as well as neighboring 9p21 markers, in sporadic melanoma', *Cancer Res,* 56 (21), 5023-32.

Formentini, L., et al. (2012), 'The mitochondrial ATPase inhibitory factor 1 triggers a ROS-mediated retrograde prosurvival and proliferative response', *Mol Cell,* 45 (6), 731-42.

Fraga, M. F., et al. (2005), 'Loss of acetylation at Lys16 and trimethylation at Lys20 of histone H4 is a common hallmark of human cancer', *Nat Genet,* 37 (4), 391-400.

Frezza, C., et al. (2011), 'Haem oxygenase is synthetically lethal with the tumour suppressor fumarate hydratase', *Nature,* 477 (7363), 225-8.

Fritz, V. and Fajas, L. (2010), 'Metabolism and proliferation share common regulatory pathways in cancer cells', *Oncogene,* 29 (31), 4369-77.

Fukagawa, A., et al. (2015), 'deltaEF1 associates with DNMT1 and maintains DNA methylation of the E-cadherin promoter in breast cancer cells', *Cancer Med,* 4 (1), 125-35.

Gama, V., et al. (2014), 'The E3 ligase PARC mediates the degradation of cytosolic cytochrome c to promote survival in neurons and cancer cells', *Sci Signal,* 7 (334), ra67.

Garaulet, G., et al. (2013), 'IL10 released by a new inflammation-regulated lentiviral system efficiently attenuates zymosan-induced arthritis', *Mol Ther,* 21 (1), 119-30.

Garcia-Hernandez, M. L., et al. (2002), 'Interleukin-10 promotes B16-melanoma growth by inhibition of macrophage functions and induction of tumour and vascular cell proliferation', *Immunology,* 105 (2), 231-43.

Garcia-Quintans, N., et al. (2016), 'Oxidative stress induces loss of pericyte coverage and vascular instability in PGC-1alpha-deficient mice', *Angiogenesis,* 19 (2), 217-28.

Gerhardt, H., et al. (2003), 'VEGF guides angiogenic sprouting utilizing endothelial tip cell filopodia', *J Cell Biol,* 161 (6), 1163-77.

Giampazolias, E. and Tait, S. W. (2016), 'Mitochondria and the hallmarks of cancer', *FEBS J,* 283 (5), 803-14.

Giorgio, M., et al. (2005), 'Electron transfer between cytochrome c and p66Shc generates reactive oxygen species that trigger mitochondrial apoptosis', *Cell,* 122 (2), 221-33.

Glasauer, A. and Chandel, N. S. (2014), 'Targeting antioxidants for cancer therapy', *Biochem Pharmacol,* 92 (1), 90-101.

Goetze, K., et al. (2011), 'Lactate enhances motility of tumor cells and inhibits monocyte migration and cytokine release', *Int J Oncol,* 39 (2), 453-63.
Gottfried, E., et al. (2006), 'Tumor-derived lactic acid modulates dendritic cell activation and antigen expression', *Blood,* 107 (5), 2013-21.
Gowans, G. J., et al. (2013), 'AMP is a true physiological regulator of AMP-activated protein kinase by both allosteric activation and enhancing net phosphorylation', *Cell Metab,* 18 (4), 556-66.
Greten, F. R., et al. (2004), 'IKKbeta links inflammation and tumorigenesis in a mouse model of colitis-associated cancer', *Cell,* 118 (3), 285-96.
Guaita, S., et al. (2002), 'Snail induction of epithelial to mesenchymal transition in tumor cells is accompanied by MUC1 repression and ZEB1 expression', *J Biol Chem,* 277 (42), 39209-16.
Gudiksen, A. and Pilegaard, H. (2017), 'PGC-1alpha and fasting-induced PDH regulation in mouse skeletal muscle', *Physiol Rep,* 5 (7).
Guo, J., et al. (2011), 'Frequent truncating mutation of TFAM induces mitochondrial DNA depletion and apoptotic resistance in microsatellite-unstable colorectal cancer', *Cancer Res,* 71 (8), 2978-87.
Guo, J. Y., et al. (2013), 'Autophagy suppresses progression of K-ras-induced lung tumors to oncocytomas and maintains lipid homeostasis', *Genes Dev,* 27 (13), 1447-61.
Guzy, R. D., et al. (2005), 'Mitochondrial complex III is required for hypoxia-induced ROS production and cellular oxygen sensing', *Cell Metab,* 1 (6), 401-8.
Haidar, M. A., et al. (1995), 'p16INK4A and p15INK4B gene deletions in primary leukemias', *Blood,* 86 (1), 311-5.
Han, B., et al. (2011), 'Human mitochondrial transcription factor A functions in both nuclei and mitochondria and regulates cancer cell growth', *Biochem Biophys Res Commun,* 408 (1), 45-51.
Hanahan, D. and Weinberg, R. A. (2011), 'Hallmarks of cancer: the next generation', *Cell,* 144 (5), 646-74.
Hangaishi, A., et al. (1996), 'Inactivation of multiple tumor-suppressor genes involved in negative regulation of the cell cycle, MTS1/p16INK4A/CDKN2, MTS2/p15INK4B, p53, and Rb genes in primary lymphoid malignancies', *Blood,* 87 (12), 4949-58.
Haq, R., et al. (2013), 'Oncogenic BRAF regulates oxidative metabolism via PGC1alpha and MITF', *Cancer Cell,* 23 (3), 302-15.
Harley, C. B., Futcher, A. B., and Greider, C. W. (1990), 'Telomeres shorten during ageing of human fibroblasts', *Nature,* 345 (6274), 458-60.
Hata, K., et al. (2011), 'Expression of the vascular endothelial growth factor (VEGF) gene in epithelial ovarian cancer: an approach to anti-VEGF therapy', *Anticancer Res,* 31 (2), 731-7.
Hayashi, K., et al. (2012), 'c-Myc is crucial for the expression of LAT1 in MIA Paca-2 human pancreatic cancer cells', *Oncol Rep,* 28 (3), 862-6.
Hayflick, L. and Moorhead, P. S. (1961), 'The serial cultivation of human diploid cell strains', *Exp Cell Res,* 25, 585-621.
He, D., et al. (2012), 'IL-17 mediated inflammation promotes tumor growth and progression in the skin', *PLoS One,* 7 (2), e32126.
Heaphy, C. M., et al. (2011a), 'Altered telomeres in tumors with ATRX and DAXX mutations', *Science,* 333 (6041), 425.
Heaphy, C. M., et al. (2011b), 'Prevalence of the alternative lengthening of telomeres telomere maintenance mechanism in human cancer subtypes', *Am J Pathol,* 179 (4), 1608-15.
Helmke, B. M., et al. (2004), 'Expression of SGLT-1 in preneoplastic and neoplastic lesions of the head and neck', *Oral Oncol,* 40 (1), 28-35.
Herbig, U., et al. (2004), 'Telomere shortening triggers senescence of human cells through a pathway involving ATM, p53, and p21(CIP1), but not p16(INK4a)', *Mol Cell,* 14 (4), 501-13.
Hers, I., Vincent, E. E., and Tavare, J. M. (2011), 'Akt signalling in health and disease', *Cell Signal,* 23 (10), 1515-27.

Higashida, K., Higuchi, M., and Terada, S. (2009), 'Dissociation between PGC-1alpha and GLUT-4 expression in skeletal muscle of rats fed a high-fat diet', *J Nutr Sci Vitaminol (Tokyo),* 55 (6), 486-91.

Hitosugi, T., et al. (2009), 'Tyrosine phosphorylation inhibits PKM2 to promote the Warburg effect and tumor growth', *Sci Signal,* 2 (97), ra73.

Hitosugi, T., et al. (2012), 'Phosphoglycerate mutase 1 coordinates glycolysis and biosynthesis to promote tumor growth', *Cancer Cell,* 22 (5), 585-600.

Hlubek, F., et al. (2007), 'Heterogeneous expression of Wnt/beta-catenin target genes within colorectal cancer', *Int J Cancer,* 121 (9), 1941-8.

Hobbs, G. A., Der, C. J., and Rossman, K. L. (2016), 'RAS isoforms and mutations in cancer at a glance', *J Cell Sci,* 129 (7), 1287-92.

Hobo, W., et al. (2012), 'B and T lymphocyte attenuator mediates inhibition of tumor-reactive CD8+ T cells in patients after allogeneic stem cell transplantation', *J Immunol,* 189 (1), 39-49.

Honda, R. and Yasuda, H. (1999), 'Association of p19(ARF) with Mdm2 inhibits ubiquitin ligase activity of Mdm2 for tumor suppressor p53', *EMBO J,* 18 (1), 22-7.

Honda, R., Tanaka, H., and Yasuda, H. (1997), 'Oncoprotein MDM2 is a ubiquitin ligase E3 for tumor suppressor p53', *FEBS Lett,* 420 (1), 25-7.

Hostmark, A. T. and Haug, A. (2013a), 'Percentage oleic acid is inversely related to percentage arachidonic acid in total lipids of rat serum', *Lipids Health Dis,* 12, 40.

--- (2013b), 'Percentages of oleic acid and arachidonic acid are inversely related in phospholipids of human sera', *Lipids Health Dis,* 12, 106.

Howe, L. R., et al. (2003), 'Twist is up-regulated in response to Wnt1 and inhibits mouse mammary cell differentiation', *Cancer Res,* 63 (8), 1906-13.

Hsu, C. P., et al. (2015), 'Epidermal growth factor activates telomerase activity by direct binding of Ets-2 to hTERT promoter in lung cancer cells', *Tumour Biol,* 36 (7), 5389-98.

Hu, T. H., et al. (2003), 'Expression of hepatoma-derived growth factor in hepatocellular carcinoma', *Cancer,* 98 (7), 1444-56.

Huang, F. W., et al. (2013), 'Highly recurrent TERT promoter mutations in human melanoma', *Science,* 339 (6122), 957-9.

Huang, S. P., et al. (2004), 'Interleukin-6 increases vascular endothelial growth factor and angiogenesis in gastric carcinoma', *J Biomed Sci,* 11 (4), 517-27.

Hulit, J., et al. (2007), 'N-cadherin signaling potentiates mammary tumor metastasis via enhanced extracellular signal-regulated kinase activation', *Cancer Res,* 67 (7), 3106-16.

Hunt, T. K., et al. (2007), 'Aerobically derived lactate stimulates revascularization and tissue repair via redox mechanisms', *Antioxid Redox Signal,* 9 (8), 1115-24.

Huss, J. M., Kopp, R. P., and Kelly, D. P. (2002), 'Peroxisome proliferator-activated receptor coactivator-1alpha (PGC-1alpha) coactivates the cardiac-enriched nuclear receptors estrogen-related receptor-alpha and -gamma. Identification of novel leucine-rich interaction motif within PGC-1alpha', *J Biol Chem,* 277 (43), 40265-74.

Hutter, E., et al. (2004), 'Senescence-associated changes in respiration and oxidative phosphorylation in primary human fibroblasts', *Biochem J,* 380 (Pt 3), 919-28.

Iqbal, M. A., et al. (2014), 'Missense mutations in pyruvate kinase M2 promote cancer metabolism, oxidative endurance, anchorage independence, and tumor growth in a dominant negative manner', *J Biol Chem,* 289 (12), 8098-105.

Irrcher, I., Ljubicic, V., and Hood, D. A. (2009), 'Interactions between ROS and AMP kinase activity in the regulation of PGC-1alpha transcription in skeletal muscle cells', *Am J Physiol Cell Physiol,* 296 (1), C116-23.

Ishikawa, K., et al. (2008), 'ROS-generating mitochondrial DNA mutations can regulate tumor cell metastasis', *Science,* 320 (5876), 661-4.

Ishikawa, N., et al. (2001), 'SGLT gene expression in primary lung cancers and their metastatic lesions', *Jpn J Cancer Res,* 92 (8), 874-9.

Itkonen, H. M., et al. (2013), 'O-GlcNAc transferase integrates metabolic pathways to regulate the stability of c-MYC in human prostate cancer cells', *Cancer Res,* 73 (16), 5277-87.
Jackson, R. J., et al. (2002), 'Loss of the cell cycle inhibitors p21(Cip1) and p27(Kip1) enhances tumorigenesis in knockout mouse models', *Oncogene,* 21 (55), 8486-97.
Jenkins, N. C., et al. (2011), 'The p16(INK4A) tumor suppressor regulates cellular oxidative stress', *Oncogene,* 30 (3), 265-74.
Jiang, D., et al. (2015), 'Analysis of p53 transactivation domain mutants reveals Acad11 as a metabolic target important for p53 pro-survival function', *Cell Rep,* 10 (7), 1096-109.
Jiang, W. G., Douglas-Jones, A., and Mansel, R. E. (2003), 'Expression of peroxisome-proliferator activated receptor-gamma (PPARgamma) and the PPARgamma co-activator, PGC-1, in human breast cancer correlates with clinical outcomes', *Int J Cancer,* 106 (5), 752-7.
Jin, D., et al. (2010), 'CD73 on tumor cells impairs antitumor T-cell responses: a novel mechanism of tumor-induced immune suppression', *Cancer Res,* 70 (6), 2245-55.
Kamphorst, J. J., et al. (2015), 'Human pancreatic cancer tumors are nutrient poor and tumor cells actively scavenge extracellular protein', *Cancer Res,* 75 (3), 544-53.
Karsli-Uzunbas, G., et al. (2014), 'Autophagy is required for glucose homeostasis and lung tumor maintenance', *Cancer Discov,* 4 (8), 914-27.
Kessler, R., et al. (2008), '6-Phosphofructo-2-kinase/fructose-2,6-bisphosphatase (PFKFB3) is up-regulated in high-grade astrocytomas', *J Neurooncol,* 86 (3), 257-64.
Kiilerich, K., et al. (2010), 'PGC-1alpha increases PDH content but does not change acute PDH regulation in mouse skeletal muscle', *Am J Physiol Regul Integr Comp Physiol,* 299 (5), R1350-9.
Killela, P. J., et al. (2013), 'TERT promoter mutations occur frequently in gliomas and a subset of tumors derived from cells with low rates of self-renewal', *Proc Natl Acad Sci U S A,* 110 (15), 6021-6.
Killian, J. K., et al. (2013), 'Succinate dehydrogenase mutation underlies global epigenomic divergence in gastrointestinal stromal tumor', *Cancer Discov,* 3 (6), 648-57.
Kim, J. W., et al. (2006), 'HIF-1-mediated expression of pyruvate dehydrogenase kinase: a metabolic switch required for cellular adaptation to hypoxia', *Cell Metab,* 3 (3), 177-85.
Kim, J. W., et al. (2007), 'Hypoxia-inducible factor 1 and dysregulated c-Myc cooperatively induce vascular endothelial growth factor and metabolic switches hexokinase 2 and pyruvate dehydrogenase kinase 1', *Mol Cell Biol,* 27 (21), 7381-93.
Kim, N. W., et al. (1994), 'Specific association of human telomerase activity with immortal cells and cancer', *Science,* 266 (5193), 2011-5.
Kinoshita, H., et al. (2013), 'Interleukin-6 mediates epithelial-stromal interactions and promotes gastric tumorigenesis', *PLoS One,* 8 (4), e60914.
Klomp, J. A., et al. (2010), 'Birt-Hogg-Dube renal tumors are genetically distinct from other renal neoplasias and are associated with up-regulation of mitochondrial gene expression', *BMC Med Genomics,* 3, 59.
Kodama, M., et al. (2010), 'Requirement of ATM for rapid p53 phosphorylation at Ser46 without Ser/Thr-Gln sequences', *Mol Cell Biol,* 30 (7), 1620-33.
Kollareddy, M., et al. (2015), 'Regulation of nucleotide metabolism by mutant p53 contributes to its gain-of-function activities', *Nat Commun,* 6, 7389.
Korinek, V., et al. (1997), 'Constitutive transcriptional activation by a beta-catenin-Tcf complex in APC-/- colon carcinoma', *Science,* 275 (5307), 1784-7.
Krajcovic, M., et al. (2013), 'mTOR regulates phagosome and entotic vacuole fission', *Mol Biol Cell,* 24 (23), 3736-45.
Ku, M. J., et al. (2015), 'Maclurin suppresses migration and invasion of human non-small-cell lung cancer cells via anti-oxidative activity and inhibition of the Src/FAK-ERK-beta-catenin pathway', *Mol Cell Biochem,* 402 (1-2), 243-52.

Kulbe, H., et al. (2007), 'The inflammatory cytokine tumor necrosis factor-alpha generates an autocrine tumor-promoting network in epithelial ovarian cancer cells', *Cancer Res,* 67 (2), 585-92.

Kung, H. N., Marks, J. R., and Chi, J. T. (2011), 'Glutamine synthetase is a genetic determinant of cell type-specific glutamine independence in breast epithelia', *PLoS Genet,* 7 (8), e1002229.

Labelle, M., Begum, S., and Hynes, R. O. (2011), 'Direct signaling between platelets and cancer cells induces an epithelial-mesenchymal-like transition and promotes metastasis', *Cancer Cell,* 20 (5), 576-90.

LaGory, E. L., et al. (2015), 'Suppression of PGC-1alpha Is Critical for Reprogramming Oxidative Metabolism in Renal Cell Carcinoma', *Cell Rep,* 12 (1), 116-27.

Landry, W. D. and Cotter, T. G. (2014), 'ROS signalling, NADPH oxidases and cancer', *Biochem Soc Trans,* 42 (4), 934-8.

Lane, D. P. (1992), 'Cancer. p53, guardian of the genome', *Nature,* 358 (6381), 15-6.

LeBleu, V. S., et al. (2014), 'PGC-1alpha mediates mitochondrial biogenesis and oxidative phosphorylation in cancer cells to promote metastasis', *Nat Cell Biol,* 16 (10), 992-1003, 1-15.

Lee, H. J., et al. (2009), 'PPAR(gamma)/PGC-1(alpha) pathway in E-cadherin expression and motility of HepG2 cells', *Anticancer Res,* 29 (12), 5057-63.

Lehman, J. J., et al. (2000), 'Peroxisome proliferator-activated receptor gamma coactivator-1 promotes cardiac mitochondrial biogenesis', *J Clin Invest,* 106 (7), 847-56.

Letouze, E., et al. (2013), 'SDH mutations establish a hypermethylator phenotype in paraganglioma', *Cancer Cell,* 23 (6), 739-52.

Li, D., et al. (2015), 'Inhibition of glutamine metabolism counteracts pancreatic cancer stem cell features and sensitizes cells to radiotherapy', *Oncotarget,* 6 (31), 31151-63.

Li, H. Y., et al. (2014), 'Pyk2 and Src mediate signaling to CCL18-induced breast cancer metastasis', *J Cell Biochem,* 115 (3), 596-603.

Li, X., et al. (2007), 'Akt/PKB regulates hepatic metabolism by directly inhibiting PGC-1alpha transcription coactivator', *Nature,* 447 (7147), 1012-6.

Li, Y., et al. (2016), 'SIRT1 facilitates hepatocellular carcinoma metastasis by promoting PGC-1alpha-mediated mitochondrial biogenesis', *Oncotarget,* 7 (20), 29255-74.

Lim, J. H., et al. (2014), 'Targeting mitochondrial oxidative metabolism in melanoma causes metabolic compensation through glucose and glutamine utilization', *Cancer Res,* 74 (13), 3535-45.

Lim, S. K., et al. (2012), 'BTG2 suppresses cancer cell migration through inhibition of Src-FAK signaling by downregulation of reactive oxygen species generation in mitochondria', *Clin Exp Metastasis,* 29 (8), 901-13.

Lin, C. Y., et al. (2013a), 'Enhanced expression of glucose transporter-1 in vascular smooth muscle cells via the Akt/tuberous sclerosis complex subunit 2 (TSC2)/mammalian target of rapamycin (mTOR)/ribosomal S6 protein kinase (S6K) pathway in experimental renal failure', *J Vasc Surg,* 57 (2), 475-85.

Lin, J., et al. (2002a), 'Peroxisome proliferator-activated receptor gamma coactivator 1beta (PGC-1beta), a novel PGC-1-related transcription coactivator associated with host cell factor', *J Biol Chem,* 277 (3), 1645-8.

Lin, J., et al. (2002b), 'Transcriptional co-activator PGC-1 alpha drives the formation of slow-twitch muscle fibres', *Nature,* 418 (6899), 797-801.

Lin, X., et al. (2013b), 'Oxidative stress in malignant melanoma enhances tumor necrosis factor-alpha secretion of tumor-associated macrophages that promote cancer cell invasion', *Antioxid Redox Signal,* 19 (12), 1337-55.

Litonin, D., et al. (2010), 'Human mitochondrial transcription revisited: only TFAM and TFB2M are required for transcription of the mitochondrial genes in vitro', *J Biol Chem,* 285 (24), 18129-33.

Liu, B., et al. (2014), 'CtIP is required for DNA damage-dependent induction of P21', *Cell Cycle,* 13 (1), 90-5.

Liu, C. Y., et al. (2015), 'Vimentin contributes to epithelial-mesenchymal transition cancer cell mechanics by mediating cytoskeletal organization and focal adhesion maturation', *Oncotarget,* 6 (18), 15966-83.
Livak, K. J. and Schmittgen, T. D. (2001), 'Analysis of relative gene expression data using real-time quantitative PCR and the 2(-Delta Delta C(T)) Method', *Methods,* 25 (4), 402-8.
Locasale, J. W., et al. (2011), 'Phosphoglycerate dehydrogenase diverts glycolytic flux and contributes to oncogenesis', *Nat Genet,* 43 (9), 869-74.
Lou, C., et al. (2016), 'MiR-485-3p and miR-485-5p suppress breast cancer cell metastasis by inhibiting PGC-1alpha expression', *Cell Death Dis,* 7, e2159.
Lovejoy, C. A., et al. (2012), 'Loss of ATRX, genome instability, and an altered DNA damage response are hallmarks of the alternative lengthening of telomeres pathway', *PLoS Genet,* 8 (7), e1002772.
Lu, H., et al. (2015), 'PGC-1alpha regulates the expression and activity of IRF-1', *IUBMB Life,* 67 (4), 300-5.
Luo, C., Widlund, H. R., and Puigserver, P. (2016a), 'PGC-1 Coactivators: Shepherding the Mitochondrial Biogenesis of Tumors', *Trends Cancer,* 2 (10), 619-31.
Luo, C., et al. (2016b), 'A PGC1alpha-mediated transcriptional axis suppresses melanoma metastasis', *Nature,* 537 (7620), 422-26.
Luo, W., et al. (2011), 'Pyruvate kinase M2 is a PHD3-stimulated coactivator for hypoxia-inducible factor 1', *Cell,* 145 (5), 732-44.
Lv, L., et al. (2013), 'Mitogenic and oncogenic stimulation of K433 acetylation promotes PKM2 protein kinase activity and nuclear localization', *Mol Cell,* 52 (3), 340-52.
Lv, L., et al. (2011), 'Acetylation targets the M2 isoform of pyruvate kinase for degradation through chaperone-mediated autophagy and promotes tumor growth', *Mol Cell,* 42 (6), 719-30.
Macip, S., et al. (2003), 'Influence of induced reactive oxygen species in p53-mediated cell fate decisions', *Mol Cell Biol,* 23 (23), 8576-85.
Mahale, A. M., et al. (2008), 'Clonal selection in malignant transformation of human fibroblasts transduced with defined cellular oncogenes', *Cancer Res,* 68 (5), 1417-26.
Mandriota, S. J., et al. (2015), 'Ataxia-telangiectasia mutated (ATM) silencing promotes neuroblastoma progression through a MYCN independent mechanism', *Oncotarget,* 6 (21), 18558-76.
Manis, J. P., et al. (2004), '53BP1 links DNA damage-response pathways to immunoglobulin heavy chain class-switch recombination', *Nat Immunol,* 5 (5), 481-7.
Mannava, S., et al. (2008), 'Direct role of nucleotide metabolism in C-MYC-dependent proliferation of melanoma cells', *Cell Cycle,* 7 (15), 2392-400.
Marin-Valencia, I., et al. (2012), 'Analysis of tumor metabolism reveals mitochondrial glucose oxidation in genetically diverse human glioblastomas in the mouse brain in vivo', *Cell Metab,* 15 (6), 827-37.
Martini, M., et al. (2014), 'PI3K/AKT signaling pathway and cancer: an updated review', *Ann Med,* 46 (6), 372-83.
Matoba, S., et al. (2006), 'p53 regulates mitochondrial respiration', *Science,* 312 (5780), 1650-3.
Matsushita, H., et al. (2012), 'Cancer exome analysis reveals a T-cell-dependent mechanism of cancer immunoediting', *Nature,* 482 (7385), 400-4.
Mazurek, S., et al. (2005), 'Pyruvate kinase type M2 and its role in tumor growth and spreading', *Semin Cancer Biol,* 15 (4), 300-8.
McDonnell, T. J. and Korsmeyer, S. J. (1991), 'Progression from lymphoid hyperplasia to high-grade malignant lymphoma in mice transgenic for the t(14; 18)', *Nature,* 349 (6306), 254-6.
McGuire, S. (2016), 'World Cancer Report 2014. Geneva, Switzerland: World Health Organization, International Agency for Research on Cancer, WHO Press, 2015', *Adv Nutr,* 7 (2), 418-9.
Meng, F., et al. (2006), 'Over-expression of interleukin-6 enhances cell survival and transformed cell growth in human malignant cholangiocytes', *J Hepatol,* 44 (6), 1055-65.

Metallo, C. M., et al. (2011), 'Reductive glutamine metabolism by IDH1 mediates lipogenesis under hypoxia', *Nature,* 481 (7381), 380-4.
Migita, T., et al. (2013), 'Inhibition of ATP citrate lyase induces an anticancer effect via reactive oxygen species: AMPK as a predictive biomarker for therapeutic impact', *Am J Pathol,* 182 (5), 1800-10.
Miniaci, M. C., et al. (2015), 'Glucose deprivation promotes activation of mTOR signaling pathway and protein synthesis in rat skeletal muscle cells', *Pflugers Arch,* 467 (6), 1357-66.
Mittal, D., et al. (2014), 'New insights into cancer immunoediting and its three component phases--elimination, equilibrium and escape', *Curr Opin Immunol,* 27, 16-25.
Moiseeva, O., et al. (2009), 'Mitochondrial dysfunction contributes to oncogene-induced senescence', *Mol Cell Biol,* 29 (16), 4495-507.
Mootha, V. K., et al. (2004), 'Erralpha and Gabpa/b specify PGC-1alpha-dependent oxidative phosphorylation gene expression that is altered in diabetic muscle', *Proc Natl Acad Sci U S A,* 101 (17), 6570-5.
Mullen, A. R., et al. (2011), 'Reductive carboxylation supports growth in tumour cells with defective mitochondria', *Nature,* 481 (7381), 385-8.
Mullen, A. R., et al. (2014), 'Oxidation of alpha-ketoglutarate is required for reductive carboxylation in cancer cells with mitochondrial defects', *Cell Rep,* 7 (5), 1679-90.
Mundi, P. S., et al. (2016), 'AKT in cancer: new molecular insights and advances in drug development', *Br J Clin Pharmacol,* 82 (4), 943-56.
Muniz Lino, M. A., et al. (2014), 'Comparative proteomic profiling of triple-negative breast cancer reveals that up-regulation of RhoGDI-2 is associated to the inhibition of caspase 3 and caspase 9', *J Proteomics,* 111, 198-211.
Munoz-Espin, D., et al. (2013), 'Programmed cell senescence during mammalian embryonic development', *Cell,* 155 (5), 1104-18.
Murai, S., et al. (2017), 'Inhibition of malic enzyme 1 disrupts cellular metabolism and leads to vulnerability in cancer cells in glucose-restricted conditions', *Oncogenesis,* 6 (5), e329.
Muteliefu, G., et al. (2012), 'Indoxyl sulfate promotes vascular smooth muscle cell senescence with upregulation of p53, p21, and prelamin A through oxidative stress', *Am J Physiol Cell Physiol,* 303 (2), C126-34.
Nakano, K. and Vousden, K. H. (2001), 'PUMA, a novel proapoptotic gene, is induced by p53', *Mol Cell,* 7 (3), 683-94.
Nakase, I., et al. (2015), 'Active macropinocytosis induction by stimulation of epidermal growth factor receptor and oncogenic Ras expression potentiates cellular uptake efficacy of exosomes', *Sci Rep,* 5, 10300.
Nickerson, N. K., et al. (2013), 'Autocrine-derived epidermal growth factor receptor ligands contribute to recruitment of tumor-associated macrophage and growth of basal breast cancer cells in vivo', *Oncol Res,* 20 (7), 303-17.
Nilsson, R., et al. (2014), 'Metabolic enzyme expression highlights a key role for MTHFD2 and the mitochondrial folate pathway in cancer', *Nat Commun,* 5, 3128.
Nishimura, K., et al. (2012), 'Mesenchymal stem cells provide an advantageous tumor microenvironment for the restoration of cancer stem cells', *Pathobiology,* 79 (6), 290-306.
O'Neal, J., et al. (2016), 'Inhibition of 6-phosphofructo-2-kinase (PFKFB3) suppresses glucose metabolism and the growth of HER2+ breast cancer', *Breast Cancer Res Treat,* 160 (1), 29-40.
Oda, Y., et al. (2005), 'Frequent alteration of p16(INK4a)/p14(ARF) and p53 pathways in the round cell component of myxoid/round cell liposarcoma: p53 gene alterations and reduced p14(ARF) expression both correlate with poor prognosis', *J Pathol,* 207 (4), 410-21.
Oliveira de Oliveira, L. B., et al. (2014), 'Morphological characterization of sprouting and intussusceptive angiogenesis by SEM in oral squamous cell carcinoma', *Scanning,* 36 (3), 293-300.
Olmos, Y., et al. (2009), 'Mutual dependence of Foxo3a and PGC-1alpha in the induction of oxidative stress genes', *J Biol Chem,* 284 (21), 14476-84.

Omori, M., et al. (2015), 'Dysregulation of CDK inhibitors and p53 in HPV-negative endocervical adenocarcinoma', *Int J Gynecol Pathol,* 34 (2), 196-203.
Palm, W., et al. (2015), 'The Utilization of Extracellular Proteins as Nutrients Is Suppressed by mTORC1', *Cell,* 162 (2), 259-70.
Papandreou, I., et al. (2006), 'HIF-1 mediates adaptation to hypoxia by actively downregulating mitochondrial oxygen consumption', *Cell Metab,* 3 (3), 187-97.
Park, M. J., et al. (2014), 'Thioredoxin-interacting protein mediates hepatic lipogenesis and inflammation via PRMT1 and PGC-1alpha regulation in vitro and in vivo', *J Hepatol,* 61 (5), 1151-7.
Parrella, P., et al. (2001), 'Detection of mitochondrial DNA mutations in primary breast cancer and fine-needle aspirates', *Cancer Res,* 61 (20), 7623-6.
Passalidou, E., et al. (2003), 'Vascular patterns in reactive lymphoid tissue and in non-Hodgkin's lymphoma', *Br J Cancer,* 88 (4), 553-9.
Passos, J. F., et al. (2010), 'Feedback between p21 and reactive oxygen production is necessary for cell senescence', *Mol Syst Biol,* 6, 347.
Pate, K. T., et al. (2014), 'Wnt signaling directs a metabolic program of glycolysis and angiogenesis in colon cancer', *EMBO J,* 33 (13), 1454-73.
Patel, D., et al. (2016), 'Aspartate Rescues S-phase Arrest Caused by Suppression of Glutamine Utilization in KRas-driven Cancer Cells', *J Biol Chem,* 291 (17), 9322-9.
Pavlova, N. N. and Thompson, C. B. (2016), 'The Emerging Hallmarks of Cancer Metabolism', *Cell Metab,* 23 (1), 27-47.
Paz, M. F., et al. (2002), 'Germ-line variants in methyl-group metabolism genes and susceptibility to DNA methylation in normal tissues and human primary tumors', *Cancer Res,* 62 (15), 4519-24.
Pellegata, N. S., et al. (2006), 'Germ-line mutations in p27Kip1 cause a multiple endocrine neoplasia syndrome in rats and humans', *Proc Natl Acad Sci U S A,* 103 (42), 15558-63.
Pikarsky, E., et al. (2004), 'NF-kappaB functions as a tumour promoter in inflammation-associated cancer', *Nature,* 431 (7007), 461-6.
Populo, H., Lopes, J. M., and Soares, P. (2012), 'The mTOR signalling pathway in human cancer', *Int J Mol Sci,* 13 (2), 1886-918.
Possemato, R., et al. (2011), 'Functional genomics reveal that the serine synthesis pathway is essential in breast cancer', *Nature,* 476 (7360), 346-50.
Puigserver, P., et al. (1998), 'A cold-inducible coactivator of nuclear receptors linked to adaptive thermogenesis', *Cell,* 92 (6), 829-39.
Puigserver, P., et al. (2003), 'Insulin-regulated hepatic gluconeogenesis through FOXO1-PGC-1alpha interaction', *Nature,* 423 (6939), 550-5.
Qian, Y., et al. (2016), 'Extracellular ATP a New Player in Cancer Metabolism: NSCLC Cells Internalize ATP In Vitro and In Vivo Using Multiple Endocytic Mechanisms', *Mol Cancer Res,* 14 (11), 1087-96.
Qian, Y., et al. (2014), 'Extracellular ATP is internalized by macropinocytosis and induces intracellular ATP increase and drug resistance in cancer cells', *Cancer Lett,* 351 (2), 242-51.
Rangarajan, A., et al. (2004), 'Species- and cell type-specific requirements for cellular transformation', *Cancer Cell,* 6 (2), 171-83.
Rangwala, S. M., et al. (2007), 'Estrogen-related receptor alpha is essential for the expression of antioxidant protection genes and mitochondrial function', *Biochem Biophys Res Commun,* 357 (1), 231-6.
Rao, S. G. and Jackson, J. G. (2016), 'SASP: Tumor Suppressor or Promoter? Yes!', *Trends Cancer,* 2 (11), 676-87.
Rao, X., et al. (2015), 'O-GlcNAcylation of G6PD promotes the pentose phosphate pathway and tumor growth', *Nat Commun,* 6, 8468.
Rashid, K., Sinha, K., and Sil, P. C. (2013), 'An update on oxidative stress-mediated organ pathophysiology', *Food Chem Toxicol,* 62, 584-600.

Rattigan, Y. I., et al. (2012), 'Lactate is a mediator of metabolic cooperation between stromal carcinoma associated fibroblasts and glycolytic tumor cells in the tumor microenvironment', *Exp Cell Res,* 318 (4), 326-35.

Regad, T. (2015), 'Targeting RTK Signaling Pathways in Cancer', *Cancers (Basel),* 7 (3), 1758-84.

Reynolds, M. R., et al. (2014), 'Control of glutamine metabolism by the tumor suppressor Rb', *Oncogene,* 33 (5), 556-66.

Ricketts, C. J., et al. (2012), 'Succinate dehydrogenase kidney cancer: an aggressive example of the Warburg effect in cancer', *J Urol,* 188 (6), 2063-71.

Robinson, B. H., et al. (1992), 'Nonviability of cells with oxidative defects in galactose medium: a screening test for affected patient fibroblasts', *Biochem Med Metab Biol,* 48 (2), 122-6.

Rohas, L. M., et al. (2007), 'A fundamental system of cellular energy homeostasis regulated by PGC-1alpha', *Proc Natl Acad Sci U S A,* 104 (19), 7933-8.

Rohrig, F. and Schulze, A. (2016), 'The multifaceted roles of fatty acid synthesis in cancer', *Nat Rev Cancer,* 16 (11), 732-49.

Saab, J., et al. (2017), 'Fatty Acid Synthase and Acetyl-CoA Carboxylase Are Expressed in Nodal Metastatic Melanoma But Not in Benign Intracapsular Nodal Nevi', *Am J Dermatopathol*.

Sahin, E., et al. (2011), 'Telomere dysfunction induces metabolic and mitochondrial compromise', *Nature,* 470 (7334), 359-65.

Samper, E., Nicholls, D. G., and Melov, S. (2003), 'Mitochondrial oxidative stress causes chromosomal instability of mouse embryonic fibroblasts', *Aging Cell,* 2 (5), 277-85.

Sanchez-Cenizo, L., et al. (2010), 'Up-regulation of the ATPase inhibitory factor 1 (IF1) of the mitochondrial H+-ATP synthase in human tumors mediates the metabolic shift of cancer cells to a Warburg phenotype', *J Biol Chem,* 285 (33), 25308-13.

Sanchez-Ramos, C., et al. (2011), 'PGC-1alpha regulates translocated in liposarcoma activity: role in oxidative stress gene expression', *Antioxid Redox Signal,* 15 (2), 325-37.

Sancho, P., et al. (2015), 'MYC/PGC-1alpha Balance Determines the Metabolic Phenotype and Plasticity of Pancreatic Cancer Stem Cells', *Cell Metab,* 22 (4), 590-605.

Santacatterina, F., et al. (2016), 'Down-regulation of oxidative phosphorylation in the liver by expression of the ATPase inhibitory factor 1 induces a tumor-promoter metabolic state', *Oncotarget,* 7 (1), 490-508.

Sardari Nia, P., et al. (2007), 'Distinct angiogenic and non-angiogenic growth patterns of lung metastases from renal cell carcinoma', *Histopathology,* 51 (3), 354-61.

Sasaki, H., et al. (2012), 'Overexpression of GLUT1 correlates with Kras mutations in lung carcinomas', *Mol Med Rep,* 5 (3), 599-602.

Sasaki, M., et al. (2014), 'Reactive oxygen species promotes cellular senescence in normal human epidermal keratinocytes through epigenetic regulation of p16(INK4a.)', *Biochem Biophys Res Commun,* 452 (3), 622-8.

Savagner, P., Yamada, K. M., and Thiery, J. P. (1997), 'The zinc-finger protein slug causes desmosome dissociation, an initial and necessary step for growth factor-induced epithelial-mesenchymal transition', *J Cell Biol,* 137 (6), 1403-19.

Schreiber, S. N., et al. (2004), 'The estrogen-related receptor alpha (ERRalpha) functions in PPARgamma coactivator 1alpha (PGC-1alpha)-induced mitochondrial biogenesis', *Proc Natl Acad Sci U S A,* 101 (17), 6472-7.

Schwartz, J. C., Cech, T. R., and Parker, R. R. (2015), 'Biochemical Properties and Biological Functions of FET Proteins', *Annu Rev Biochem,* 84, 355-79.

Sellers, K., et al. (2015), 'Pyruvate carboxylase is critical for non-small-cell lung cancer proliferation', *J Clin Invest,* 125 (2), 687-98.

Semaan, A., et al. (2011), 'Expression of GLUT-1 in epithelial ovarian carcinoma: correlation with tumor cell proliferation, angiogenesis, survival and ability to predict optimal cytoreduction', *Gynecol Oncol,* 121 (1), 181-6.

Sen, N., Satija, Y. K., and Das, S. (2011), 'PGC-1alpha, a key modulator of p53, promotes cell survival upon metabolic stress', *Mol Cell,* 44 (4), 621-34.

Serrano, M., Hannon, G. J., and Beach, D. (1993), 'A new regulatory motif in cell-cycle control causing specific inhibition of cyclin D/CDK4', *Nature,* 366 (6456), 704-7.
Shankaran, V., et al. (2001), 'IFNgamma and lymphocytes prevent primary tumour development and shape tumour immunogenicity', *Nature,* 410 (6832), 1107-11.
Shi, Y., et al. (2012), 'Mammalian transcription factor A is a core component of the mitochondrial transcription machinery', *Proc Natl Acad Sci U S A,* 109 (41), 16510-5.
Shibue, T., et al. (2003), 'Integral role of Noxa in p53-mediated apoptotic response', *Genes Dev,* 17 (18), 2233-8.
Shibutani, S., Takeshita, M., and Grollman, A. P. (1991), 'Insertion of specific bases during DNA synthesis past the oxidation-damaged base 8-oxodG', *Nature,* 349 (6308), 431-4.
Shirakihara, T., Saitoh, M., and Miyazono, K. (2007), 'Differential regulation of epithelial and mesenchymal markers by deltaEF1 proteins in epithelial mesenchymal transition induced by TGF-beta', *Mol Biol Cell,* 18 (9), 3533-44.
Shyh-Chang, N., et al. (2013), 'Influence of threonine metabolism on S-adenosylmethionine and histone methylation', *Science,* 339 (6116), 222-6.
Sinha, P., et al. (2007), 'Prostaglandin E2 promotes tumor progression by inducing myeloid-derived suppressor cells', *Cancer Res,* 67 (9), 4507-13.
St-Pierre, J., et al. (2003), 'Bioenergetic analysis of peroxisome proliferator-activated receptor gamma coactivators 1alpha and 1beta (PGC-1alpha and PGC-1beta) in muscle cells', *J Biol Chem,* 278 (29), 26597-603.
St-Pierre, J., et al. (2006), 'Suppression of reactive oxygen species and neurodegeneration by the PGC-1 transcriptional coactivators', *Cell,* 127 (2), 397-408.
Stein, R. A., et al. (2008), 'Estrogen-related receptor alpha is critical for the growth of estrogen receptor-negative breast cancer', *Cancer Res,* 68 (21), 8805-12.
Stiff, T., et al. (2004), 'ATM and DNA-PK function redundantly to phosphorylate H2AX after exposure to ionizing radiation', *Cancer Res,* 64 (7), 2390-6.
Storer, M., et al. (2013), 'Senescence is a developmental mechanism that contributes to embryonic growth and patterning', *Cell,* 155 (5), 1119-30.
Strasser, A., et al. (1990), 'Novel primitive lymphoid tumours induced in transgenic mice by cooperation between myc and bcl-2', *Nature,* 348 (6299), 331-3.
Strohecker, A. M., et al. (2013), 'Autophagy sustains mitochondrial glutamine metabolism and growth of BrafV600E-driven lung tumors', *Cancer Discov,* 3 (11), 1272-85.
Summermatter, S., et al. (2013), 'Skeletal muscle PGC-1alpha controls whole-body lactate homeostasis through estrogen-related receptor alpha-dependent activation of LDH B and repression of LDH A', *Proc Natl Acad Sci U S A,* 110 (21), 8738-43.
Summermatter, S., et al. (2010), 'Peroxisome proliferator-activated receptor {gamma} coactivator 1{alpha} (PGC-1{alpha}) promotes skeletal muscle lipid refueling in vivo by activating de novo lipogenesis and the pentose phosphate pathway', *J Biol Chem,* 285 (43), 32793-800.
Sun, L., et al. (2008), 'Transforming growth factor-beta 1 promotes matrix metalloproteinase-9-mediated oral cancer invasion through snail expression', *Mol Cancer Res,* 6 (1), 10-20.
Sun, Q., et al. (2014), 'Competition between human cells by entosis', *Cell Res,* 24 (11), 1299-310.
Sun, W., et al. (2012), 'Overexpression of HIF-1alpha in primary gallbladder carcinoma and its relation to vasculogenic mimicry and unfavourable prognosis', *Oncol Rep,* 27 (6), 1990-2002.
Svensson, R. U., et al. (2016), 'Inhibition of acetyl-CoA carboxylase suppresses fatty acid synthesis and tumor growth of non-small-cell lung cancer in preclinical models', *Nat Med,* 22 (10), 1108-19.
Tai, P. and Ascoli, M. (2011), 'Reactive oxygen species (ROS) play a critical role in the cAMP-induced activation of Ras and the phosphorylation of ERK1/2 in Leydig cells', *Mol Endocrinol,* 25 (5), 885-93.
Takahashi, A., et al. (2006), 'Mitogenic signalling and the p16INK4a-Rb pathway cooperate to enforce irreversible cellular senescence', *Nat Cell Biol,* 8 (11), 1291-7.
Tardito, S., et al. (2015), 'Glutamine synthetase activity fuels nucleotide biosynthesis and supports growth of glutamine-restricted glioblastoma', *Nat Cell Biol,* 17 (12), 1556-68.

Tedeschi, P. M., et al. (2015), 'Mitochondrial Methylenetetrahydrofolate Dehydrogenase (MTHFD2) Overexpression Is Associated with Tumor Cell Proliferation and Is a Novel Target for Drug Development', *Mol Cancer Res,* 13 (10), 1361-6.

Thomas, A. G., et al. (2015), 'High-Throughput Assay Development for Cystine-Glutamate Antiporter (xc-) Highlights Faster Cystine Uptake than Glutamate Release in Glioma Cells', *PLoS One,* 10 (8), e0127785.

Todaro, G. J. and Green, H. (1963), 'Quantitative studies of the growth of mouse embryo cells in culture and their development into established lines', *J Cell Biol,* 17, 299-313.

Tomlinson, I. P., et al. (2002), 'Germline mutations in FH predispose to dominantly inherited uterine fibroids, skin leiomyomata and papillary renal cell cancer', *Nat Genet,* 30 (4), 406-10.

Torrano, V., et al. (2016), 'The metabolic co-regulator PGC1alpha suppresses prostate cancer metastasis', *Nat Cell Biol,* 18 (6), 645-56.

Tung, E. W. and Winn, L. M. (2011), 'Valproic acid-induced DNA damage increases embryonic p27(KIP1) and caspase-3 expression: a mechanism for valproic-acid induced neural tube defects', *Reprod Toxicol,* 32 (3), 255-60.

Turcan, S., et al. (2012), 'IDH1 mutation is sufficient to establish the glioma hypermethylator phenotype', *Nature,* 483 (7390), 479-83.

Valle, I., et al. (2005), 'PGC-1alpha regulates the mitochondrial antioxidant defense system in vascular endothelial cells', *Cardiovasc Res,* 66 (3), 562-73.

Vazquez, F., et al. (2013), 'PGC1alpha expression defines a subset of human melanoma tumors with increased mitochondrial capacity and resistance to oxidative stress', *Cancer Cell,* 23 (3), 287-301.

Velarde, M. C., et al. (2012), 'Mitochondrial oxidative stress caused by Sod2 deficiency promotes cellular senescence and aging phenotypes in the skin', *Aging (Albany NY),* 4 (1), 3-12.

Vervoort, S. J., et al. (2013), 'SOX4 mediates TGF-beta-induced expression of mesenchymal markers during mammary cell epithelial to mesenchymal transition', *PLoS One,* 8 (1), e53238.

Villena, J. A. (2015), 'New insights into PGC-1 coactivators: redefining their role in the regulation of mitochondrial function and beyond', *FEBS J,* 282 (4), 647-72.

Wang, D. and DuBois, R. N. (2015), 'Immunosuppression associated with chronic inflammation in the tumor microenvironment', *Carcinogenesis,* 36 (10), 1085-93.

Wang, P., et al. (2015a), 'Structural insight into mechanisms for dynamic regulation of PKM2', *Protein Cell,* 6 (4), 275-87.

Wang, Y., Sharpless, N., and Chang, S. (2013), 'p16(INK4a) protects against dysfunctional telomere-induced ATR-dependent DNA damage responses', *J Clin Invest,* 123 (10), 4489-501.

Wang, Y., et al. (2015b), 'Mitochondrial biogenesis is impaired in osteoarthritis chondrocytes but reversible via peroxisome proliferator-activated receptor gamma coactivator 1alpha', *Arthritis Rheumatol,* 67 (8), 2141-53.

Warburg, O. (1956a), 'On respiratory impairment in cancer cells', *Science,* 124 (3215), 269-70.

--- (1956b), 'On the origin of cancer cells', *Science,* 123 (3191), 309-14.

Ward, I. M., et al. (2003a), 'p53 Binding protein 53BP1 is required for DNA damage responses and tumor suppression in mice', *Mol Cell Biol,* 23 (7), 2556-63.

Ward, I. M., et al. (2003b), 'Accumulation of checkpoint protein 53BP1 at DNA breaks involves its binding to phosphorylated histone H2AX', *J Biol Chem,* 278 (22), 19579-82.

Watkins, G., et al. (2004), 'The localisation and reduction of nuclear staining of PPARgamma and PGC-1 in human breast cancer', *Oncol Rep,* 12 (2), 483-8.

Wei, L., et al. (2015a), 'Lactate promotes PGE2 synthesis and gluconeogenesis in monocytes to benefit the growth of inflammation-associated colorectal tumor', *Oncotarget,* 6 (18), 16198-214.

Wei, X., et al. (2016), 'Fatty acid synthesis configures the plasma membrane for inflammation in diabetes', *Nature,* 539 (7628), 294-98.

Wei, Z., et al. (2015b), 'Elevated expression of secreted autocrine growth factor progranulin increases cervical cancer growth', *Cell Biochem Biophys,* 71 (1), 189-93.

Wellen, K. E., et al. (2009), 'ATP-citrate lyase links cellular metabolism to histone acetylation', *Science,* 324 (5930), 1076-80.
Wende, A. R., et al. (2005), 'PGC-1alpha coactivates PDK4 gene expression via the orphan nuclear receptor ERRalpha: a mechanism for transcriptional control of muscle glucose metabolism', *Mol Cell Biol,* 25 (24), 10684-94.
Wieman, H. L., Wofford, J. A., and Rathmell, J. C. (2007), 'Cytokine stimulation promotes glucose uptake via phosphatidylinositol-3 kinase/Akt regulation of Glut1 activity and trafficking', *Mol Biol Cell,* 18 (4), 1437-46.
Wise, D. R., et al. (2008), 'Myc regulates a transcriptional program that stimulates mitochondrial glutaminolysis and leads to glutamine addiction', *Proc Natl Acad Sci U S A,* 105 (48), 18782-7.
Wu, C. C. and Bratton, S. B. (2013), 'Regulation of the intrinsic apoptosis pathway by reactive oxygen species', *Antioxid Redox Signal,* 19 (6), 546-58.
Wu, Z., et al. (1999), 'Mechanisms controlling mitochondrial biogenesis and respiration through the thermogenic coactivator PGC-1', *Cell,* 98 (1), 115-24.
Xiao, D., et al. (2015), 'Myc promotes glutaminolysis in human neuroblastoma through direct activation of glutaminase 2', *Oncotarget,* 6 (38), 40655-66.
Xiao, M., et al. (2012), 'Inhibition of alpha-KG-dependent histone and DNA demethylases by fumarate and succinate that are accumulated in mutations of FH and SDH tumor suppressors', *Genes Dev,* 26 (12), 1326-38.
Xu, W., et al. (2011), 'Oncometabolite 2-hydroxyglutarate is a competitive inhibitor of alpha-ketoglutarate-dependent dioxygenases', *Cancer Cell,* 19 (1), 17-30.
Xu, X., et al. (2015), 'Tumor suppressor NDRG2 inhibits glycolysis and glutaminolysis in colorectal cancer cells by repressing c-Myc expression', *Oncotarget,* 6 (28), 26161-76.
Xu, Y., et al. (1996), 'Targeted disruption of ATM leads to growth retardation, chromosomal fragmentation during meiosis, immune defects, and thymic lymphoma', *Genes Dev,* 10 (19), 2411-22.
Yalcin, A., et al. (2014), '6-Phosphofructo-2-kinase (PFKFB3) promotes cell cycle progression and suppresses apoptosis via Cdk1-mediated phosphorylation of p27', *Cell Death Dis,* 5, e1337.
Yang, C., et al. (2014), 'Glutamine oxidation maintains the TCA cycle and cell survival during impaired mitochondrial pyruvate transport', *Mol Cell,* 56 (3), 414-24.
Yang, J., et al. (2004), 'Twist, a master regulator of morphogenesis, plays an essential role in tumor metastasis', *Cell,* 117 (7), 927-39.
Yang, Y., et al. (2013), 'HIFs, angiogenesis, and cancer', *J Cell Biochem,* 114 (5), 967-74.
Yi, W., et al. (2012), 'Phosphofructokinase 1 glycosylation regulates cell growth and metabolism', *Science,* 337 (6097), 975-80.
Ying, H., et al. (2012), 'Oncogenic Kras maintains pancreatic tumors through regulation of anabolic glucose metabolism', *Cell,* 149 (3), 656-70.
Yoo, H., et al. (2008), 'Quantifying reductive carboxylation flux of glutamine to lipid in a brown adipocyte cell line', *J Biol Chem,* 283 (30), 20621-7.
Yoon, J. C., et al. (2001), 'Control of hepatic gluconeogenesis through the transcriptional coactivator PGC-1', *Nature,* 413 (6852), 131-8.
Yun, M. H. and Hiom, K. (2009), 'CtIP-BRCA1 modulates the choice of DNA double-strand-break repair pathway throughout the cell cycle', *Nature,* 459 (7245), 460-3.
Zaidi, N., et al. (2012), 'ATP citrate lyase knockdown induces growth arrest and apoptosis through different cell- and environment-dependent mechanisms', *Mol Cancer Ther,* 11 (9), 1925-35.
Zambrano, A., et al. (2014), 'The thyroid hormone receptor beta induces DNA damage and premature senescence', *J Cell Biol,* 204 (1), 129-46.
Zeng, L., et al. (2010), 'IL-10 promotes resistance to apoptosis and metastatic potential in lung tumor cell lines', *Cytokine,* 49 (3), 294-302.
Zergoun, A. A., et al. (2016), 'IL-6/NOS2 inflammatory signals regulate MMP-9 and MMP-2 activity and disease outcome in nasopharyngeal carcinoma patients', *Tumour Biol,* 37 (3), 3505-14.

Zhang, S., et al. (2012), 'Wnt/beta-catenin signaling pathway upregulates c-Myc expression to promote cell proliferation of P19 teratocarcinoma cells', *Anat Rec (Hoboken),* 295 (12), 2104-13.

Zhang, X., et al. (2011), 'Akt, FoxO and regulation of apoptosis', *Biochim Biophys Acta,* 1813 (11), 1978-86.

Zhang, Y., et al. (2007), 'PGC-1alpha induces apoptosis in human epithelial ovarian cancer cells through a PPARgamma-dependent pathway', *Cell Res,* 17 (4), 363-73.

Zhao, X., et al. (2014), 'Peroxisome proliferator-activated receptor gamma coactivator 1alpha and FoxO3A mediate chondroprotection by AMP-activated protein kinase', *Arthritis Rheumatol,* 66 (11), 3073-82.

Zhao, Z., et al. (2010), 'p53 loss promotes acute myeloid leukemia by enabling aberrant self-renewal', *Genes Dev,* 24 (13), 1389-402.

Zheng, F. J., et al. (2012), 'Repressing malic enzyme 1 redirects glucose metabolism, unbalances the redox state, and attenuates migratory and invasive abilities in nasopharyngeal carcinoma cell lines', *Chin J Cancer,* 31 (11), 519-31.

Zhu, G., et al. (2014), 'TNF-alpha promotes gallbladder cancer cell growth and invasion through autocrine mechanisms', *Int J Mol Med,* 33 (6), 1431-40.

Zhuo, B., et al. (2015), 'PI3K/Akt signaling mediated Hexokinase-2 expression inhibits cell apoptosis and promotes tumor growth in pediatric osteosarcoma', *Biochem Biophys Res Commun,* 464 (2), 401-6.

ANEXO

Los siguientes artículos científicos han sido publicados durante la realización de esta tesis con la participación de IGNACIO PRIETO ARROYO no siendo recogidos en los resultados de esta tesis.

Free Radical Biology and Medicine 93 (2016) 41–51

Contents lists available at ScienceDirect

Free Radical Biology and Medicine

journal homepage: www.elsevier.com/locate/freeradbiomed

Original Contribution

Regulation of endothelial dynamics by PGC-1α relies on ROS control of VEGF-A signaling

Nieves García-Quintans [a,1], Ignacio Prieto [a,5], Cristina Sánchez-Ramos [a,2,5], Alfonso Luque [b,3], Elvira Arza [b], Yolanda Olmos [b,4], María Monsalve [a,*]

[a] Instituto de Investigaciones Biomédicas "Alberto Sols" (CSIC-UAM), Arturo Duperier 4, 28029 Madrid, Spain
[b] Fundación Centro Nacional de Investigaciones Cardiovasculares Carlos III, Melchor Fernández Almagro 3, 28029 Madrid, Spain

ARTICLE INFO

Article history:
Received 19 June 2015
Received in revised form
15 January 2016
Accepted 26 January 2016
Available online 29 January 2016

Keywords:
Vascular endothelium
VEGF-A
PGC-1α
Oxidative stress
Mitochondria

ABSTRACT

Peroxisome proliferator activated receptor γ co-activator 1α (PGC-1α) is a regulator of mitochondrial metabolism and reactive oxygen species (ROS) that is known to play a relevant role in angiogenesis.
Aims: This study aims to investigate the role of ROS on the regulation by PGC-1α of angiogenesis.
Methods and results: We found that endothelial cells (ECs) from mice deleted for PGC-1α display attenuated adhesion to the extracellular matrix, together with slower and reversible spreading. Structural analysis demonstrates unstable formation of focal adhesions, defective cytoskeleton reorganization in response to cellular matrix adhesion, cell migration and cell–cell adhesion. Confluent cultures showed also a reduction of membrane bound VE-cadherin, suggesting defective inter-cellular junction formation. Functional consequences included impaired directional migration, and enhanced tip phenotype in aortic explants sprouting assays. At the molecular level, PGC-1α-deleted ECs exhibit a constitutive activation of the vascular endothelial growth factor-A (VEGF-A) signaling pathway and a defective response to VEGF-A. All these alterations are partially reversed by administration of the antioxidant EUK-189. The contribution of mitochondrial ROS and NOX activation was confirmed using a mitochondrial targeted antioxidant (MitoTEMPO) and a NOX inhibitor (VAS-2870). These results indicate that elevated production of ROS in the absence of PGC-1α is a key factor in the alteration of the VEGF-A signaling pathway and the capacity of endothelial cells to form stable interactions with other endothelial cells and with the extracellular matrix. Our findings show that PGC-1α control of ROS homeostasis plays an important role in the control of endothelial response to VEGF-A.

1. Introduction

While caloric restriction boost in the organism the use of mitochondria as a source of ATP, overfeeding tends to decrease the use of mitochondria as a source of ATP and leads to a preponderance of anaerobic glycolysis in a variety of tissues [1,2]. This decrease in mitochondrial function is mediated by the down-regulation and functional inactivation of key metabolic regulators like the transcriptional coactivator Peroxisome proliferator-activated receptor gamma coactivator-1-alpha (PGC-1α) [3,4], a master regulator of genes involved in oxidative metabolism. Loss of PGC-1α activity results in an increase of mitochondrial-derived reactive oxygen species (ROS) [5], and elevated ROS levels (oxidative stress) have been found in the majority of vascular complications associated with metabolic disorders.

The importance of protecting the body from the most common metabolic disorders, including obesity and type 2 diabetes cannot be overstated, and their prevalence continues to increase yearly and World-wide. Dysfunctions of the human vascular tree are the major source of morbidity and mortality. Generally, the damaging effects can be separated into macrovascular (coronary artery disease, peripheral arterial disease, and stroke) and microvascular (nephropathy, neuropathy, and retinopathy) injury [6]. Diabetic retinopathy is one of the most common microvascular complications of diabetes, and is a leading cause of ~10,000 new cases of blindness every year in the United States alone [7].

* Correspondence to: Instituto de Investigaciones Biomédicas "Alberto Sols" (CSIC-UAM), Arturo Duperier 4, Room 1.3.2., 28029 Madrid, Spain.
E-mail address: mpmonsalve@iib.uam.es (M. Monsalve).
[1] Present address: Centro de Biología Molecular Severo Ochoa (CSIC-UAM), Nicolas Cabrera 1, 28049 Madrid, Spain.
[2] Present address: Fundación Centro Nacional de Investigaciones Cardiovasculares Carlos III, Melchor Fernández Almagro 3, 28029 Madrid, Spain.
[3] Present address: Instituto de Investigación de Enfermedades Raras, Instituto de Salud Carlos III, Carretera Majadahonda-Pozuelo km, 2, Majadahonda, 28220 Madrid, Spain.
[4] Present address: Department of Cancer Cell Biology and Imaging, Division of Cancer Studies, School of Medicine, Kings College, SE1 1UL London, UK.
[5] These authors contributed equally to this work.

http://dx.doi.org/10.1016/j.freeradbiomed.2016.01.021
0891-5849/

Reduced mitochondrial activity has been amply reported as a hallmark of type 2 diabetes [8,9] and reduced activity of PGC-1α in diabetic subjects has been show in several tissues including the skeletal muscle [2]. However, elevated mRNA levels of PGC-1α have been found in the liver of type 2 diabetic subjects and it has been proposed that elevated PGC-1α in diabetic subjects increases gluconeogenesis pointing to a putative detrimental role of PGC-1α in type 2 diabetes. More recently, it has also been proposed that PGC-1α activation in the retina may be involved in type 2 diabetic retinopathy, through the induction of VEGF-A levels [10,11].

Previous results from our group showed that PGC-1α was present in vascular endothelial cells (ECs), and its levels were reduced by hyperglycemia. Furthermore, PGC-1α could coordinate ECs oxidative metabolism and antioxidant capacity [12], suggesting that PGC-1α could play a key role in the physiology of the vascular endothelium. ROS (i.e. hydrogen peroxide) are acknowledged as important signaling mediators regulating cell proliferation and migration [13]. Additional studies from our laboratory showed that, at least *in vitro*, PGC-1α was a negative regulator of EC migration indicating that PGC-1α activity could be important for the control of vascular stability and angiogenesis. Accordingly, in response to angiogenesis mediators, PI3K-AKT activation resulted in the down-regulation of PGC-1α leading to increased mitochondrial ROS levels (oxygen superoxide and hydrogen peroxide) and enhanced EC migration [14]. More recently, it has been shown that PGC-1α deficient mice show defective induction of VEGF-A in response to ischemia and impaired angiogenesis [15,16]. However, the molecular mechanisms involved, other than altered endothelial cell migration were largely unknown. Importantly, hydrogen peroxide is increasingly recognized as a regulator of VEGF-A signaling [17,18]. Since VEGF-A activity is a crucial factor in the regulation of endothelial motility and interaction with other cells and with the basal membrane. In this study we aimed to characterize the role of PGC-1α as a regulator of ROS homeostasis in the control of endothelial adhesion dynamics and VEGF-A signaling.

We found that ECs deleted for PGC-1α had a reduced capacity to interact with each other and with the extracellular matrix, and were unable to form angiotubes *in vitro*. Furthermore, PGC-1α deleted ECs moved faster but in a non-coordinated manner, and displayed a tip-like phenotype. Importantly, their response to VEGF-A was impaired. These characteristics would be consistent with a reduced capacity to form a stable vasculature. Crucially, this phenotype could be partially rescued by antioxidant treatment, suggesting that excessive hydrogen peroxide production is likely to play an important role in vascular stability.

2. Material and methods

2.1. Animal handling

C57BL6 PGC-1α$^{+/+}$ and PGC-1α$^{-/-}$ were used. C57BL/6 PGC-1α$^{-/-}$ mice were originally provided by Dr. Bruce Spiegelman (Dana-Farber Cancer Institute, Harvard Medical School) and following embryo transfer, a colony was established at the CNIC and IIB SPF animal facilities. Animal experimental protocols were approved by the Institutional Animal Care and Use Committee of the CNIC (No. PI 19/09) and the CSIC (SAF2012-37693). All procedures conformed to the Declaration of Helsinki and the NIH guidelines for animal care and use (NIH publication No. 85-23). Animals were maintained at a constant temperature of 21 ± 1 °C and on a 12-h light–dark cycle. Animal experimental protocols were approved by the Institutional Animal Care and Use Committee of the CNIC and the CSIC. All procedures conformed to the Declaration of Helsinki and the NIH guidelines for animal care and use (NIH publication No. 85-23). Mice were euthanized by carbon dioxide inhalation or cervical dislocation.

2.2. Cell culture

Bovine Aortic Endothelial Cells (BAECs) and Mouse Lung Endothelial Cells (MLECs) were obtained and cultured as described [14]. Bovine Aortas were obtained from an authorized slaughterhouse (El Matadero S.C.M., Colmenar Viejo, Madrid, Spain). Adenovirus overexpression and infection protocols have been described [19].

2.3. Cell-attachment and cell spreading assays

Experiments were performed in triplicate in 96-well plates. Wells were coated with fibronectin (1 μg/ml, Sigma) or collagen I (30 μg/ml, INAMEN Biomaterials) and then blocked for 90 min with 1% heat-denatured BSA in PBS. MLECs were plated at 9×10^4 cells/well for up to 1 hour, washed, fixed with 3% PFA for 1 min, permeabilized with 2% methanol for 3 min, stained with 0.5% crystal violet in 20% methanol for 2 min, washed with water and examined by brightfield microscopy (Nikon Eclipse 90Ti with objectives: Plan Fluor 4 × /0.13 Ph1 DL, Plan Fluor 10 × /0.30 Ph1 DLL, Plan Fluor ELWD 40 × /0.60 Ph2 DH). Cells were classified as spread if the nucleus and cytoplasmic extensions were distinguishable.

2.4. Time lapse video imaging of scratch assays

Scratch assays were performed as previously described [14], and images were taken every 20 min for up to 30 h with a Nikon Eclipse Ti microscope (objective 4 ×).

2.5. Sprouting angiogenesis on aortic explants

Assays were performed as described [20].

2.6. Immunofluorescence and phalloidin staining

MLECs grown on coverslips were fixed with 3.6% PFA, permeabilized with 0.1% Triton X-100, blocked with 2% BSA and then incubated consecutively with primary antibody (α-p-paxillin or α-VE-cadherin) and a secondary antibody (αIgG rabbit ALEXA-488 conjugate), or stained with FITC-phalloidin (Molecular Probes) in PBS for 1 h. Cells were then counterstained with DAPI, mounted and examined with a confocal microscope (Nikon A1R, objective 40 ×) for VE-cadherin or a TIRF microscope (Leica, objective HCX Pl Apo 100 × 1.46 Oil) for p-paxilin.

2.7. In vitro endothelial cell tube formation

Assays were performed essentially as described [21]. 96-well plates were coated with 40 μl of growth factor reduced (GFR) BD Matrigel per well. MLECs (17,000 cells) resuspended in 100 μl of tissue culture media with 2% Horse Serum (HS) and containing, as indicated, 50 ng/ml of VEGF-A, were seeded per well. Images were taken every 20 min for up to 48 h with a Nikon EclipseTi microscope.

2.8. Vascular endothelial growth factor-A (VEGF-A) treatment

MLECs were grown to confluence in DMEM-F12 medium with 20% FBS. Following overnight serum starvation o/n (0.5% FBS) the cells were first pre-incubated with 10 μM EUK-189 or 20 μM VAS-2870 for 2 h, or 10 μM MitoTEMPO for 3 h as indicated and then incubated with 12.5 ng/ml of VEGF for up to 4 h and harvested.

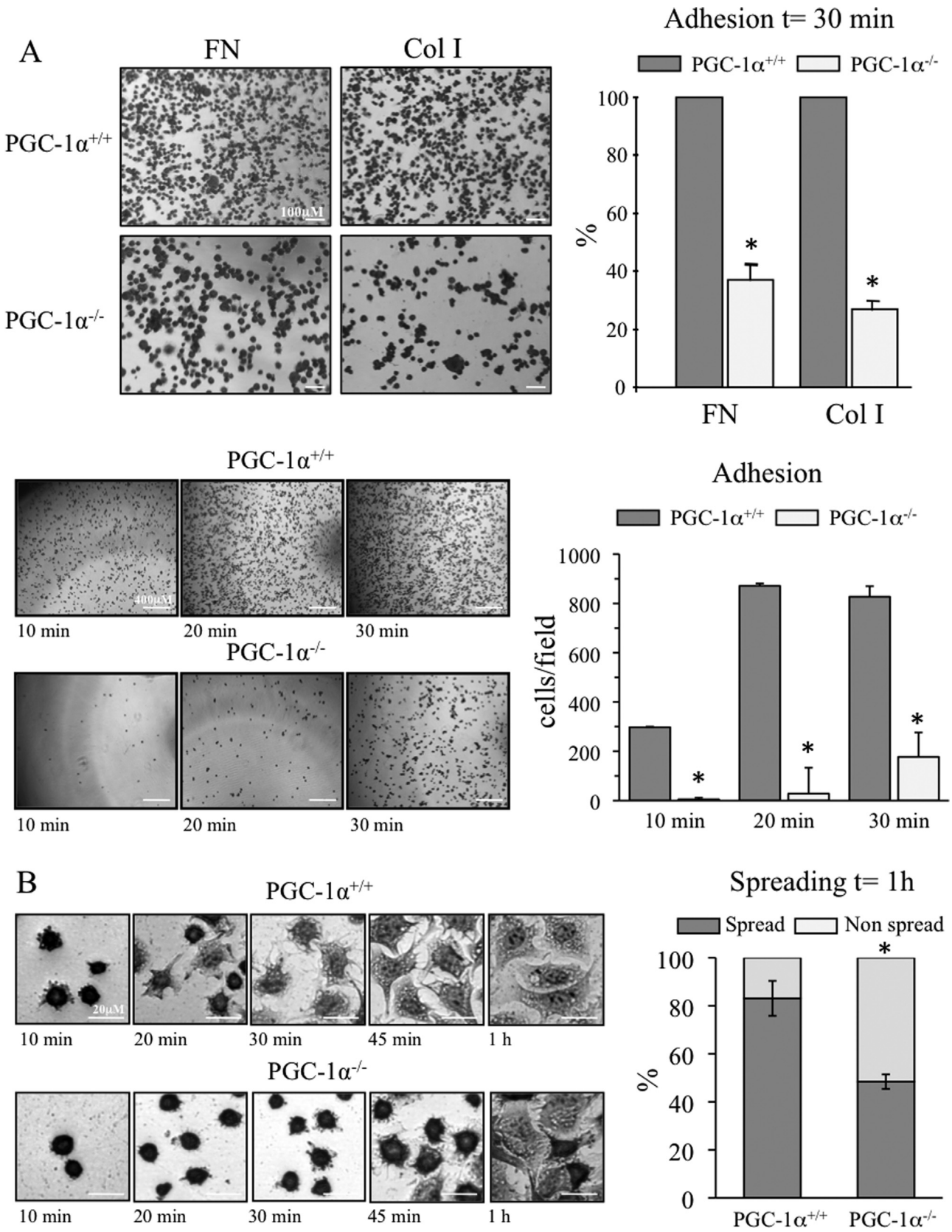

Fig. 1. Endothelial cell adhesion and spreading dynamics are regulated by PGC-1α. Wild-type and PGC-1α$^{-/-}$ MLECs were seeded on plates coated with fibronectin or collagen I and allowed to adhere for up to 30 min (A) or to spread for up to 2 h (B). Cells were washed, fixed, bright field visualized on a microscope and counted. Left panels show images from representative experiments. Right panels show the quantifications. Data are means+SD. (*) $p \leq 0.05$ vs. control. A (top panel) $n=9$. A (bottom panel) $n=8$ and (B) $n=6$.

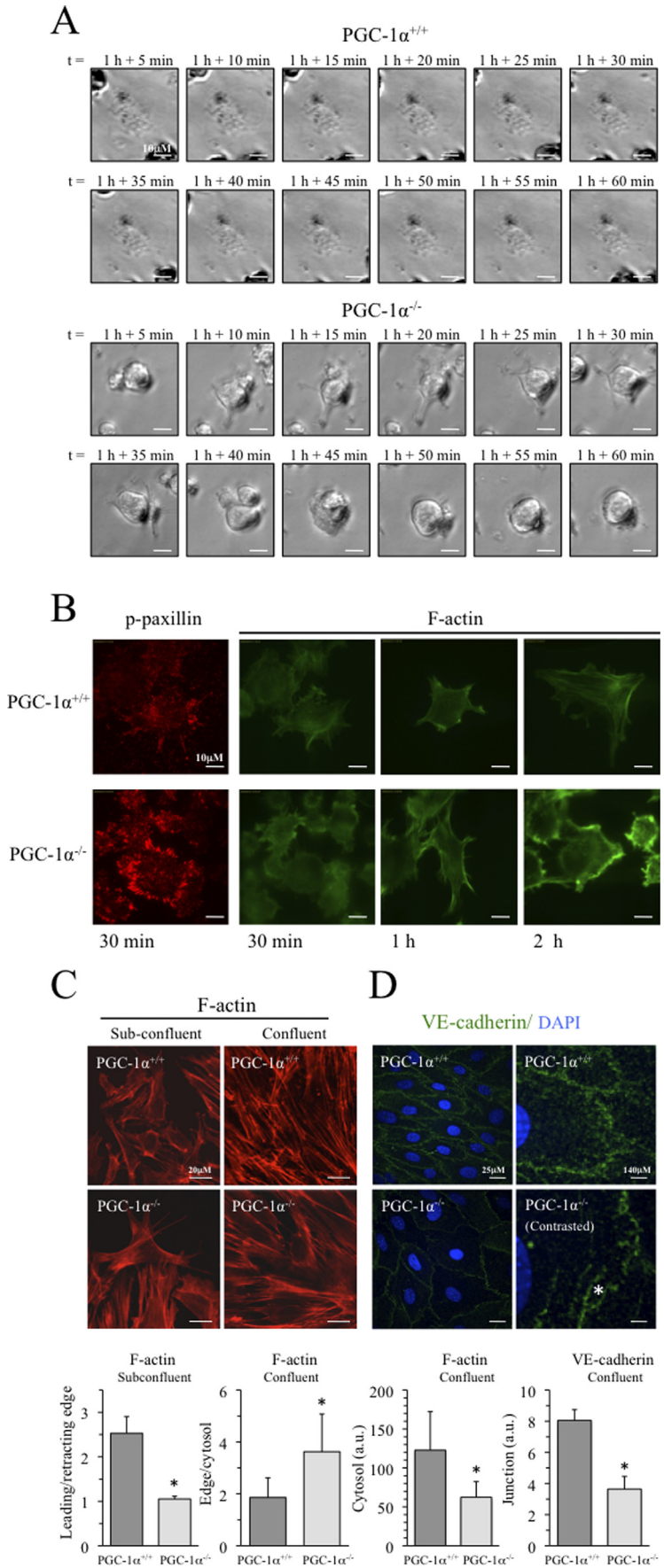

Fig. 2. PGC-1α$^{-/-}$ MLEC form unstable cell–matrix and cell–cell contacts. (A) Time-lapse bright field video images of live cells that have been allowed to adhere for 1 h. Images show the dynamics of representative cells at 5 min intervals for 1 h ($n=3$). (B) Focal adhesion dynamics was analyzed by IF staining of cells with a p-paxillin antibody and polymerized actin filaments with phalloidin. Focal adhesions were visualized using a TIRF microscope ($n=3$). (C) Wild-type and PGC-1α$^{-/-}$ MLECs actin filaments stained with phalloidin in sub-confluent and confluent MLECs and visualized with a fluorescence microscope ($n=3$). (D) IF of VE-cadherin of confluent wild-type and PGC-1α$^{-/-}$ MLECs on a fibronectin-coated plate. Nuclei were stained with DAPI ($n=3$). Data are means+SD. (*) $p \leq 0.05$ vs. control.

2.9. Protein extraction and Western blotting

Protein extraction was as previously described [19]. Protein extracts 20–25 μg of were resolved by electrophoresis in 6–12% SDS-PAGE gels, followed by transfer to PVDF Hybond-P membranes (Amersham Biosciences) and incubated with specific antibodies against HIF-1α (#610958, BD Transduction Laboratories), VEGF-A, (VG-1, Santa Cruz), VEGF-R2 (#55B11, 1:1000), P-VEGFR2 (#2471, 1:1000), NICD (#4147, 1:1000), AKT (#2920) and phosphorylated AKT-Ser^{473} (#4060) (1:2000), all from Cell Signaling Technology®, and β-actin (A 5441, Sigma). β-actin was used as a loading control.

2.10. Image analysis

ImageJ software was used to analyze western blots, for global determination of areas in inmunofluorescent images, and membrane/cytosol ratios of VE-cadherin. *In vitro* angiogenesis images were analyzed using the Angiogenesis Analyzer tool for Image J developed by Gilles Carpertier.

2.11. Statistics

Data are expressed as means ± SD. Statistical significance was evaluated by analysis of variance or a nonparametric test, as appropriate. Values were considered statistically significant at $p < 0.05$. $n \geq 3$ in all experiments. The number of independent experiments, for each particular experiment, is indicated in the corresponding figure legends.

3. Results

3.1. PGC-1α enhances endothelial adhesion to the extracellular matrix

To evaluate the role of PGC-1α during ECs interaction with the extracellular matrix (ECM), MLECs obtained from PGC-1α$^{-/-}$ and PGC-1α$^{+/+}$ mice were allowed to adhere to collagen I or fibronectin-coated slides for 30 min and were subsequently counted. These substrates where selected because they are the most commonly used substrates for endothelial cells grown *in vitro*. Compared with wild type MLECs, significantly fewer PGC-1α$^{-/-}$ MLECs adhered to both fibronectin and collagen I (Fig. 1A, top panel); although adherence of both was greater to fibronectin than to collagen matrix. To determine whether PGC-1α$^{-/-}$ MLECs adhered more slowly to ECM or with less stability, a time course analysis using fibronectin was performed, and attached cells were counted. At 20 min, the number of wild-type MLECs attached reached a maximum while PGC-1α$^{-/-}$ MLECs continued to adhere after 30 min (Fig. 1A, bottom panel), suggesting that matrix attachment might be less efficient in PGC-1α$^{-/-}$ MLECs.

To determine whether the absence of PGC-1α reduced the initial contacts only, or also had an effect on the formation of stable interactions with the matrix, we evaluated the cell spreading process by determining the number of attached cells that had spread 1 h after plating. Results showed that whereas greater than 80% of wild-type MLECs had spread onto the matrix, approximately 45% of PGC-1α$^{-/-}$ MLEC had done so (Fig. 1B), suggesting that PGC-1α deficiency reduced the formation of stable adhesions.

3.2. Absence of PGC-1α results in unstable adhesion and spreading

To corroborate these results, we monitored the cell adhesion–spreading process using time-lapse video imaging of cell movements for 1 h after attachment to collagen I matrix. In contrast to wild-type MLECs, which displayed very limited motility after initial spreading, PGC-1α$^{-/-}$ MLECs not only moved faster once attached, as has been previously described [14], but also showed incomplete and fully reversible spreading and detachment (Fig. 2A). Collectively, these results suggest that both the initial interaction with the matrix and also the formation of stable focal adhesions may be impaired in PGC-1α$^{-/-}$ ECs.

To assess whether PGC-1α regulated the formation of focal adhesions, we next analyzed the focal adhesion complex-component paxillin. Paxillin is activated and phosphorylated by focal adhesion kinase (FAK) in response to integrin signaling, resulting in the formation of a focal adhesion complex. However, it must be dephosphorylated to allow the stabilization of the focal adhesion, and therefore can be used to monitor the turnover rate of newly formed focal adhesions. Analysis of phospo (p)-paxillin in MLECs that had been allowed to attach for 30 min, revealed that p-paxillin was localized to the tips of spreading filopoidia in wild-type MLECs (Fig. 2B). In contrast, PGC-1α$^{-/-}$ MLECs displayed intense p-paxillin staining throughout the cell periphery, suggesting a random and highly active turnover of focal adhesions. These findings imply that the reduced adhesion capacity of PGC-1α$^{-/-}$ MLECs is not due to an inability to form focal adhesion complexes but rather might be the consequence of an excessive FAK activity and high turnover rate [22].

3.3. Defective cytoskeleton dynamics in absence of PGC-1α

Cellular interactions with matrix components triggers stress fiber-formation of the polymerized actin cytoskeleton. In wild-type MLECs, F-actin was found concentrated in the extending filopodia of spreading cells 1 h after plating, and stress fibers were fully formed 2 h following plating (Fig. 2B). In contrast, MLECs from PGC-1α$^{-/-}$ mice exhibited dispersed F-actin foci throughout the cell periphery, and no stress fibers were detected even after 2 h (Fig. 2B). To determine if this disorganization was a consequence of a deficient cell adhesion process, or could also be conspicuous in other situations, we analyzed the actin cytoskeleton of migrating and confluent cell cultures. Interestingly, while actin filaments reorganized in wild-type cells, and were about 2.5 × more concentrated in the leading edge than in the retracting edge, this was barely detectable in PGC-1α$^{-/-}$ MLECs (Fig. 2C). In confluent cultures, actin filaments are normally more concentrated in the cellular periphery than in the cytosol. Remarkably, this difference was more marked in PGC-1α$^{-/-}$ MLEC, while mean cytosolic phalloiding stain was lower PGC-1α$^{-/-}$ MLEC (Fig. 2C). These two characteristics could be related to the higher mobility of these cells. Moreover, PGC-1α$^{-/-}$ MLECs were, on average, approximately 50% larger than wild-type counterparts, possibly a consequence of actin disorganization (Fig. 2D).

3.4. Endothelial cells show reduced formation of adherens junctions in absence of PGC-1α

To test whether intercellular junctions were also affected by the absence of PGC-1α, we analyzed VE-cadherin staining in confluent cultures. VE-cadherin plays a major role in the organization of intercellular adherens junctions in ECs. PGC-1α$^{-/-}$ MLECs exhibited a reduction in VE-cadherin levels relative to wild-type cells; also, staining was not continuous and gaps could be detected together in zones where the membranes were not in direct contact despite the confluence of the culture (Fig. 2D, Supplementary Fig. 1).

3.5. PGC-1α regulates endothelial cell coordination during migration

To assess how these deficiencies could impact on cell migration processes, we monitored cell motility using *in vitro* scratch assays and time-lapse video imaging. Whereas wild-type cells appeared to stream together as they migrated, we noted that the absence of PGC-1α resulted not only in an accelerated cell movement as

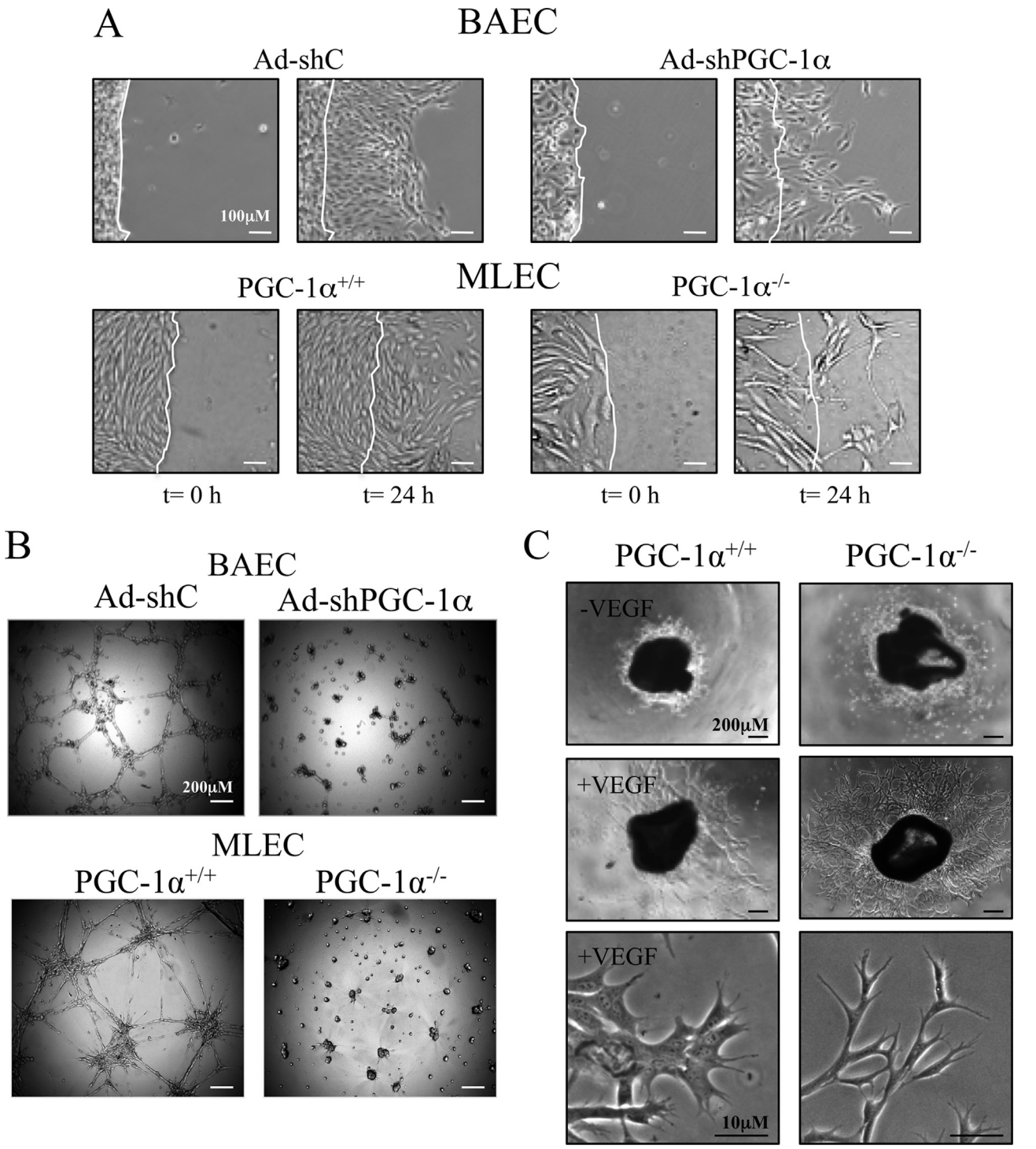

Fig. 3. Lack of PGC-1α results in reduced intercellular junction/coordination during migration, and failure to form angiotubes *in vitro*. (A) Scratch assays of BAECs infected with the indicated adenovirus to knock-down PGC-1α, and wild-type or PGC-1α$^{-/-}$ MLECs. The migratory front is highlighted with a white line ($n=6$). (B) *In vitro* angiotube assay on Matrigel using BAECs silenced for PGC-1α (upper panel), and wild-type and PGC-1α$^{-/-}$ MLECs (lower panel) ($n=5$). (C) Endothelial cells sprouting from aorta explants from wild-type and PGC-1α$^{-/-}$ mice. Bright field images were taken after 5 days, the lower panels show higher magnification images of tip cells from the migratory edge ($n=6$). Data are means+SD. (*) $p \leq 0.05$ vs. control.

already described [14], but also on a pronounced tendency to disperse over a larger area (Fig. 3A, lower panel; Supplmentary Information Video Files). A similar effect was observed in BAECs upon PGC-1α silencing (Fig. 3A, lower panel; Supplmentary Information Video Files). Fig. 3A shows only one side of the scratch in order to increase the magnification of the image and therefore be able to visualize how the cells spread out into the gap. In the images can be appreciated that cell density is lower when PGC-1α is absent or reduced. This is not due to differences in confluency, all cultures were 100% confluent, but is mainly attributable to the bigger size (about 50%) of PGC-1α deficient cells (Fig. 2D). Nevertheless, PGC-1α$^{-/-}$ fully-confluent cultures always show small gaps between cells (Fig. 2D), these could be attribute to problems in the formation of cell–cell contacts.

Supplementary material related to this article can be found online at http://dx.doi.org/10.1016/j.freeradbiomed.2016.01.021.

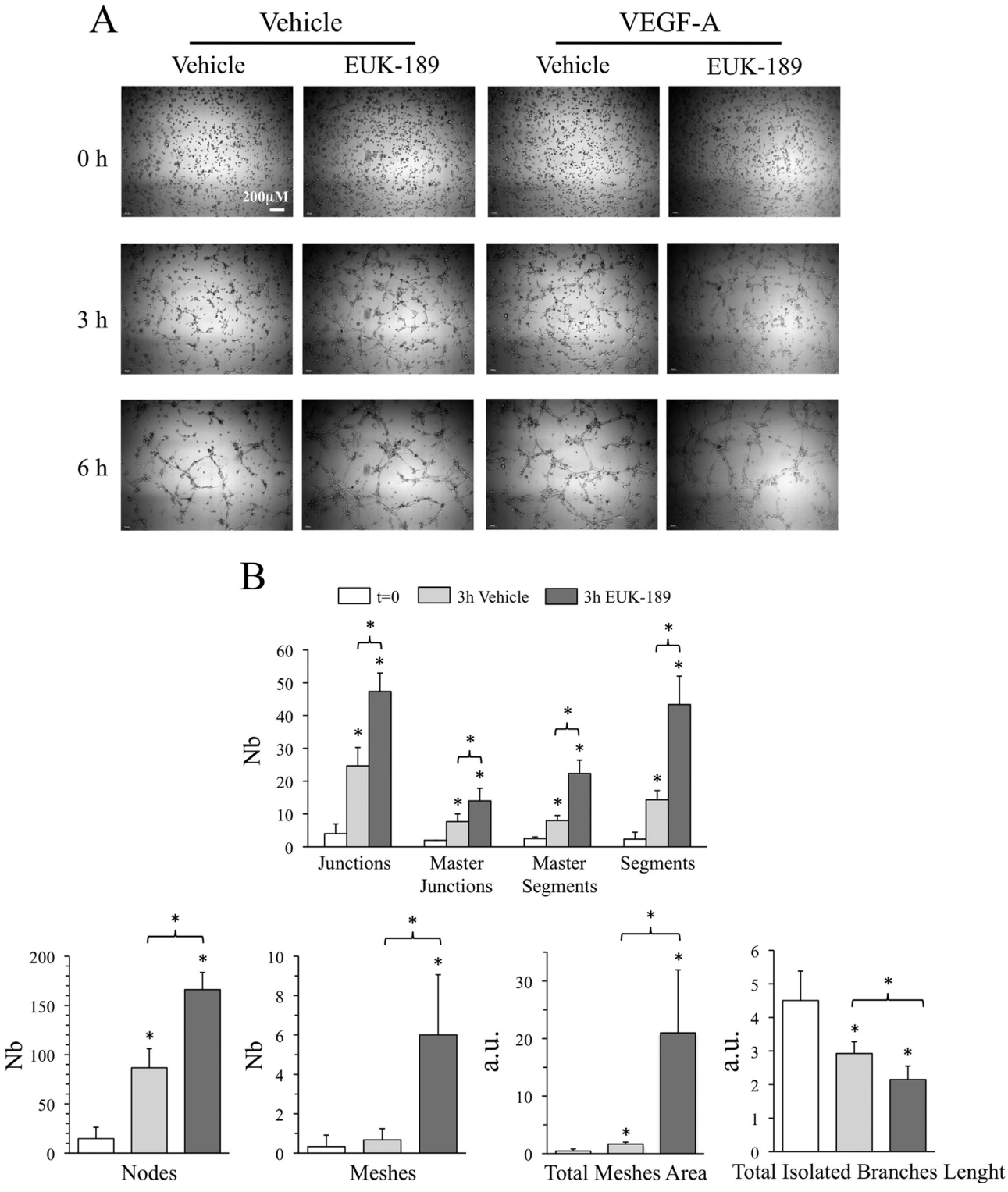

Fig. 4. Antioxidant treatment improves *in vitro* angiotube formation in PGC-1α$^{-/-}$ MLECs. (A) *In vitro* angiotube assay on Matrigel using PGC-1α$^{-/-}$ MLECs, treated with VEGF-A and/or EUK-189 ($n=3$). (B) Analysis of structures formed in the angiotube assay. Data are means+SD. (*) $p \leq 0.05$ vs. control.

3.6. Absence of PGC-1α results in impaired angiotube formation

The ability to form stable cell-to-cell contacts is not only important to ensure organized cell migration, it is also critical for the formation and stabilization of the newly formed vessel. Thus, we next tested vessel formation using an *in vitro* angiotube formation assay. Interestingly, results from silencing of PGC-1α expression in BAECs (Fig. 3B upper panel) and the absence of PGC-1α in MLECs (Fig. 3B lower panel), showed that both approaches led to an almost complete inability of ECs to form angiotubes *in vitro*, even though cells migrated and aggregated. This result suggested that deficient interactions of intercellular junctions provoked by the absence of PGC-1α are likely to be crucial for *in vivo* formation of blood vessels.

3.7. PGC-1α$^{-/-}$ endothelial cells display an enhanced tip phenotype

In a complementary approach to test EC migration and intercellular junction interactions in combination, we utilized an *ex vivo* angiogenesis assay using Matrigel-embedded aortic ring explants. We found that even in the absence of VEGF-A, PGC-1α$^{-/-}$ ECs had the capacity to migrate, while wild-type ECs could not migrate unless VEGF-A was added to the medium, and then did so in an individual manner, in the absence of interacting cells (Fig. 3C, upper panel). Moreover, we observed that, in the presence of VEGF-A, the cellular "chords" of sprouting cells exiting the aortic rings from PGC-1α$^{-/-}$ mice appeared thinner than those sprouting from wild-type aortic rings. Upon closer inspection of migratory edges, we observed that while wild-type ECs where closely packed, in several cell-wide chords, with filopodia only in the outermost migratory edge, PGC-1α$^{-/-}$ cells formed single-cell chords, and were highly elongated with extensive filopodia (Fig. 3C, lower panel). These observations suggested that in the absence of PGC-1α endothelial cells can migrate even in the absence of VEGF and they do not respond normally to VEGF-A, possibly inducing an enhanced tip-like phenotype.

3.8. PGC-1α$^{-/-}$ endothelial cells respond to antioxidant treatment enhancing VEGF-A signaling

Our previous *in vitro* results indicated that PGC-1α$^{-/-}$ MLECs exhibited a greater migration capacity compared with wild-type cells due to an overproduction of hydrogen peroxide [14]. Indeed, hydrogen peroxide is acknowledged as an important player in angiogenesis [18] and mediate EC migration and proliferation [23]. Thus, we evaluated whether the angiogenesis defects found in PGC-1α$^{-/-}$ mice could be attributed to an excess production of hydrogen peroxide. To this end, we treated PGC-1α$^{-/-}$ MLECs with an antioxidant and measured their ability to form angiotubes *in vitro*. Pre-incubation of PGC-1α$^{-/-}$ MLECs with EUK-189, a synthetic superoxide dismutase/catalase mimetic, enhanced the formation of angiotubes (Fig. 4, Supplementary Fig. 2), pointing to a participation of hydrogen peroxide in capillary formation. To elucidate the molecular mechanisms that could link elevated hydrogen peroxide levels with the vascular instability observed in PGC-1α$^{-/-}$ mice, we next analyzed the response of wild-type and PGC-1α$^{-/-}$ MLECs to VEGF-A. This signaling pathway has been suggested previously to be highly sensitive to hydrogen peroxide [17,18]. Consistently, PGC-1α$^{-/-}$ MLEC showed increased levels of phosphorylated VEGFR2, phosphorylated AKT and greater levels of NICD, compared with wild-type cells in the absence of VEGF-A (Fig. 5). Furthermore, relative to wild-type cells, the response to VEGF-A treatment was very poor in PGC-1α$^{-/-}$ MLECs in terms of VEGFR2 induced phosphorylation, supporting the notion that PGC-1α-deleted ECs are largely insensitive to VEGF-A activation. Importantly, when PGC-1α$^{-/-}$ MLECs were pre-incubated with EUK-189, the response to VEGF-A was partially recovered, while the basal levels of phosphorylated VEGFR2, phosphorylated AKT and

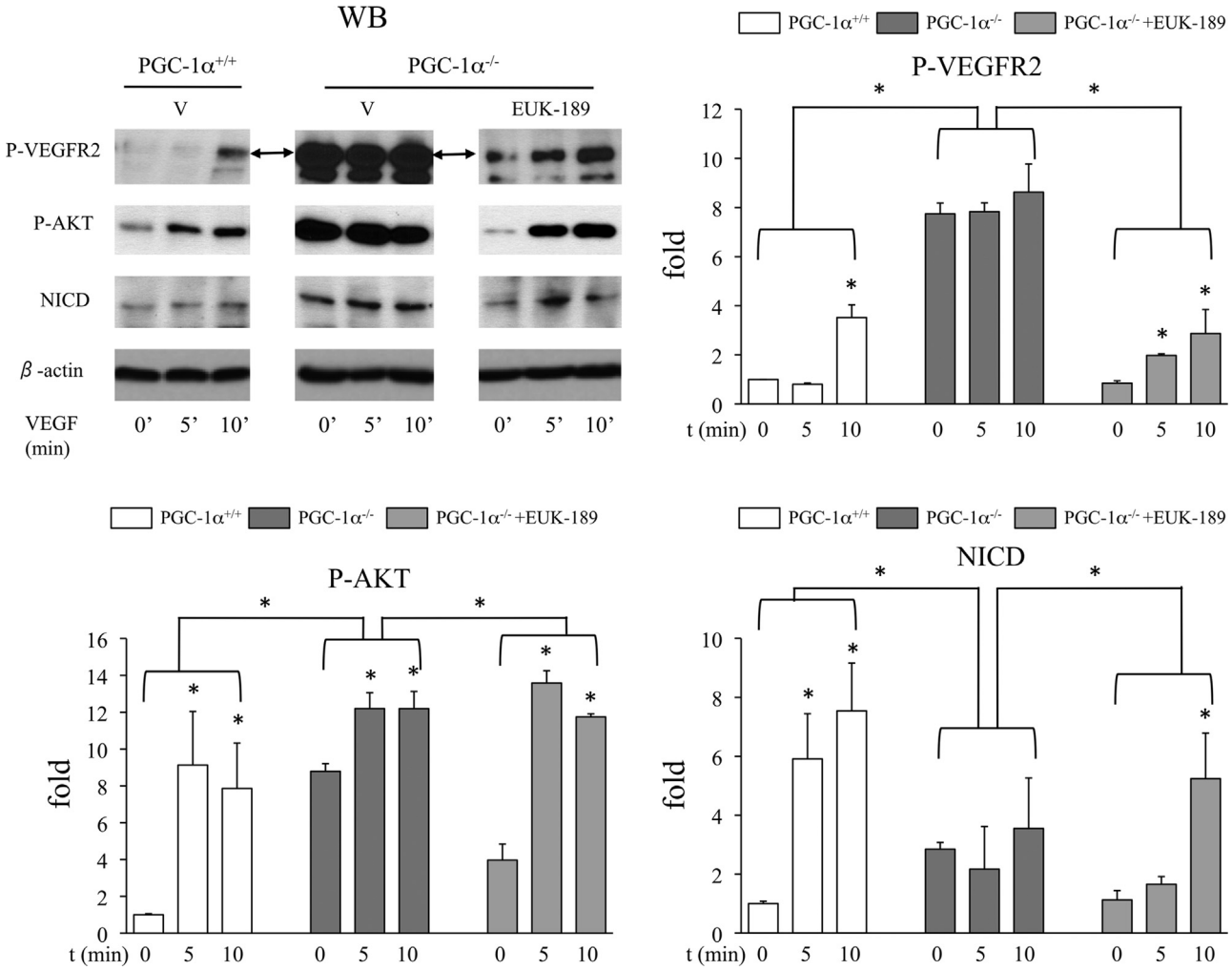

Fig. 5. Antioxidant treatment restores VEGF-A signaling in PGC-1α$^{-/-}$ MLECs. PGC-1α$^{-/-}$ MLECs were treated with VEGF-A and/or EUK-189 for the indicated time periods. Western blot analysis of whole cell extracts of relevant proteins in VEGF-A signaling: VEGFR2, NICD and AKT ($n=3$). Data are means ± SD. (*) $p \leq 0.05$ vs. control.

NICD, were reduced (Fig. 5). This observation is consistent with previous reports demonstrating the sensitivity of VEGFR2 and its phosphatases to hydrogen peroxide [17,18]. Moreover, these findings indicate that the response of VEGFR2 to VEGF-A requires the tight control of intracellular hydrogen peroxide levels. This control may be lost when important metabolic regulators such as PGC-1α are largely inactive [3]. mRNA levels were not significantly affected by EU-189 (Supplementary Fig. 3).

PGC-1α has been shown to induce the expression of several mitochondrial antioxidant proteins, and its absence results in enhanced mitochondrial superoxide levels. Concomitantly, PGC-1α also regulates the expression of important extra-mitochondrial antioxidants, like catalase. In order to validate the contribution of mitochondrial ROS to the observed alteration in VEGF signaling, we treated PGC-1α$^{-/-}$ MLEC with a mitochondria-targeted SOD mimetic, MitoTEMPO and evaluated the effect on VEGF-A signaling. We found a significant reduction in the basal levels of phosphorylation of VEGFR2 and AKT, as well as a reduction in the basal levels of NICD (Fig. 6A, central panel). VEGF-A treatment also resulted in an enhanced fold induction of VEGFR2 and AKT

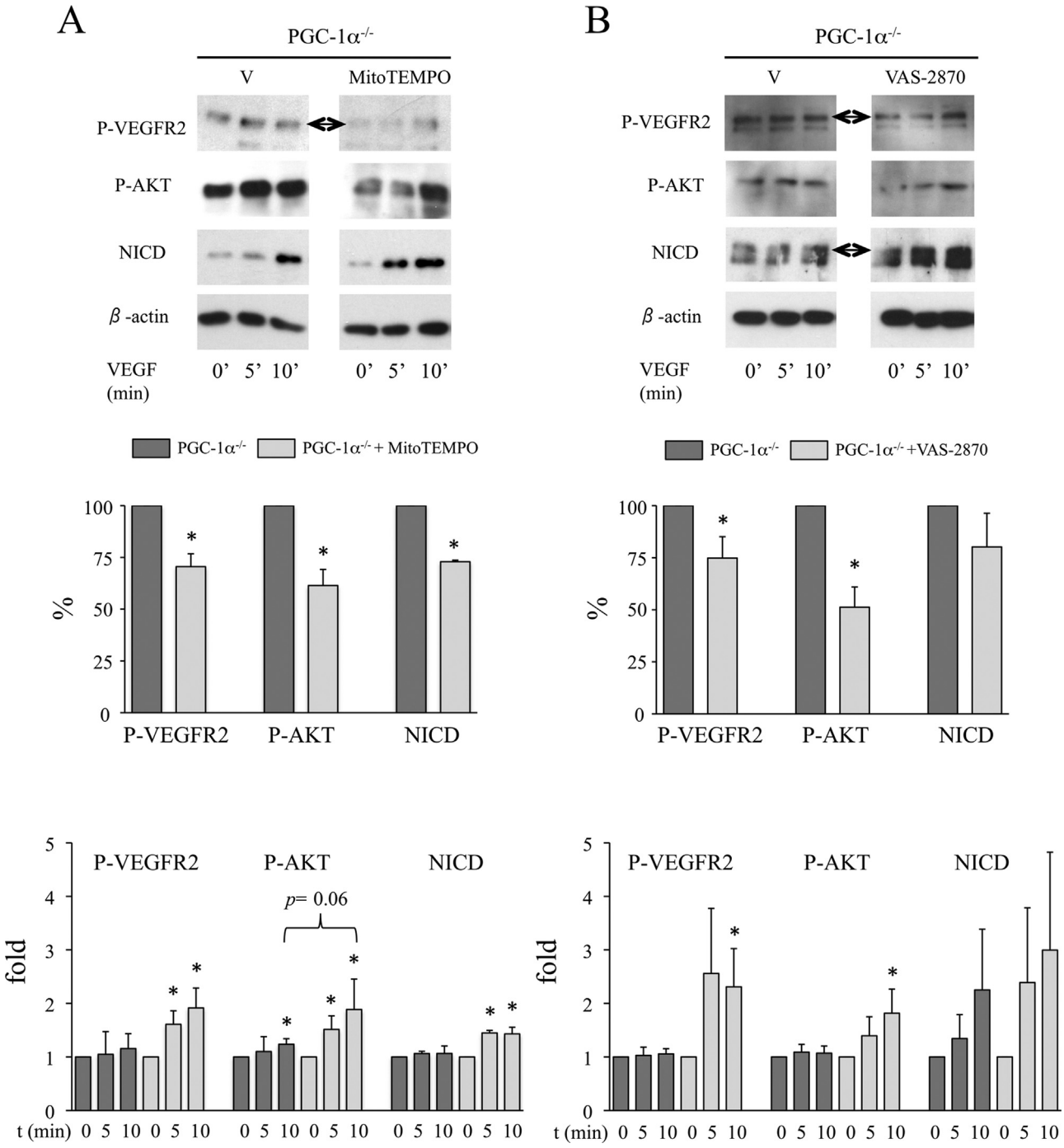

Fig. 6. Both detoxification of mitochondrial ROS and NOX inhibition restores VEGF signaling in PGC-1α$^{-/-}$ MLECs. PGC-1α$^{-/-}$ MLECs were pre-treated with the mitochondria-targeted SOD mimetic MitoTEMPO (10 μM) for 3 h (A, $n=5$) or with a general NOX inhibitor (VAS-2870, 20 μM) for 2h (B, $n=3$), then VEGF-A was added and downstream signaling (VEGFR2, NICD and AKT) was analyzed by western blot ($n=5$). Top panels show representative western blots. Central panels show the quantitative analysis of data at time 0, prior to VEGF-A addition. The bottom panels show the fold induction upon VEGF-A addition, values are normalized for those at time 0, that have been assigned the arbitrary value of 1. Data are means ± SD. (*) $p \leq 0.05$ vs. control.

phosphorylation, as well as in the levels of NICD upon stimulation (Fig. 6A, bottom panel). These results suggest that there is a relevant contribution of mitochondrial ROS production to the observed phenotype.

Finally, since hydrogen peroxide dependent inactivation of VEGF signaling pathway has been proposed to be mediated by NOX activity, we tested whether NOX inhibition would be able to restore VEGF-A signaling in PGC-1α$^{-/-}$ cells, and we found that pretreatment with the general NOX inhibitor VAS-2870 also resulted in significant reduction in the basal levels of phosphorylation of VEGFR2 and AKT and an enhanced sensitivity (fold induction) of the VEGFR2 receptor to VEGF-A dependent phosphorylation, that correlated with and enhanced AKT phosphorylation, supporting the involvement of NOX activity (Fig. 6B).

4. Discussion

The results of this study show that regulation of ROS homeostasis by PGC-1α plays an important role in the control of endothelial function, in particular in the regulation by VEGF-A of the stability of the cellular and cellular-matrix contacts. We demonstrate that, in the absence of PGC-1α, the vascular endothelial cells appears to be constitutively activated, characterized by faster migrating ECs which adhere slowly to the substrate. Also, ECs spread slowly and can reverse this process and detach again. These alterations are likely due to the low stability and high turnover of the focal adhesions, an inability to form a structured f-actin cytoskeleton, and a reduced formation of VE-cadherin adherens junctions. Succinctly, ECs interact poorly with the substrate and with other cells. Clearly, these alterations are likely to be relevant in metabolic disorders where PGC-1α activity is generally found to be low, and in particular might be related to the development of diabetic retinopathy.

Reduced intercellular contacts in PGC-1α-deficient ECs resulted in the loss of coordinated cell movement in scratch assays, and a failure to form angiotubes *in vitro*. Analysis of the endothelial sprouting process from aortic rings further suggested that PGC-1α-deficient cells actively migrate even in the absence of VEGF-A, and form tip cells independently of their location, indicating a defective response to VEGF-A. Treatment of MLECs with VEGF-A *in vitro,* together with analysis of the VEGF-A pathway, confirmed that the absence of PGC-1α resulted in the constitutive activation of the VEGF-A signaling pathway, plus a poor response to exogenous VEGF-A. This defective response to VEGF-A may explain the constitutively-activated phenotype of PGC-1α deficient ECs.

PGC-1α deficient ECs have elevated levels of oxygen superoxide and hydrogen peroxide [5]. Given that the VEGF-A signaling pathway has been shown to be sensitive to hydrogen peroxide, and that oxidative modifications of VEGFR2 [18,24] and its main phosphatases have been described [17], we hypothesized that elevated ROS levels found in PGC-1α-deficient ECs would be responsible for the poor VEGF-A response. Consistent with this idea, we found that antioxidant treatment largely restored normal VEGF-A response in PGC-1α deficient ECs. Furthermore, EUK-189 treatment also restored the capacity of those cells to form angiotubes *in vitro*, indicating a normalization of the inter-cellular interactions.

Long regarded as by-products of oxidative metabolism, ROS are now recognized as signaling mediators in their own right. The prototypic redox-regulated targets are the protein tyrosine phosphatases that are inactivated by hydrogen peroxide; however, identification of redox-sensitive kinases such as Src has led to the slow emergence of a role for redox regulation of tyrosine kinases by concurrent oxidative activation of tyrosine kinases. Thus, ROS fine-tune the duration and amplification of the phosphorylation signal. Importantly, the activity of VEGFR2 and two of its phosphatases, DEP1 and PTP1B, have been shown to be regulated by hydrogen peroxide [17,24,18]. Demonstration of the physiological relevance of these regulations has been hampered by the lack of relevant disease models, since the majority of experimental evidence derives from *in vitro* assays with artificially generated or exogenously added ROS; this is the case for VEGFR2 signaling pathways.

PGC-1α is known to regulate the levels of mitochondrial ROS [5]. However, most recent studies stress the role played by NADPH oxidases (NOXs) in the ROS-dependent control of growth factor signaling processes [25] and less attention has been paid to the role of mitochondrial ROS. Nevertheless, although a largely neglected area of research, a body of evidence shows that elevated mitochondrial production of ROS is commonly found in cells with elevated NOX activity, and it has been shown that mitochondria can regulate NOX function and *viceversa* [26]. Additionally, most, if not all, physiological settings where ROS appear to play an important role, including angiogenesis, describe both enhanced NOX and elevated mitochondrial ROS levels [27,28]. Furthermore, mitochondria-targeted antioxidants have been proposed to have potential therapeutic value in retinopathy [29]. Nonetheless, it remains to be determined whether PGC-1α could also directly regulate the expression or activity of NOX or alternatively of PrxII, the peroxiredoxin antioxidant that appears to modulate VEGFR2 oxidation [18].

In conclusion, our study strongly supports the idea that PGC-1α control of hydrogen peroxide levels in endothelial cells plays a major role in the formation of stable interactions of endothelial cells with other cells and with the matrix, a process likely to be relevant in metabolic disorders where microvascular complications are prevalent, like diabetic retinopathy. Since antioxidant therapies have shown significant caveats, alternative therapies that aim to re-wire normal ROS homeostasis, boosting PGC-1α activity might represent a therapeutic approach for retinopathy patients.

Conflict of Interest

None declared.

Acknowledgments

This work was supported by grants from the Spanish “Ministerio de Economía y Competitividad” [Grant no. SAF2009-07599 & SAF2012-37693 to M.M and CSD 2007-00020 to M.M.]; and the “Comunidad Autónoma de Madrid” [Grant no. S2010/BMD-2361 to M.M.].

We thank Dr. Enrique Samper for providing EUK-189 and technical advice on its handling and use in experimental models. We thank Dr. Manuela García for providing VAS-2870 and Dr. Alberto Ortíz-Arduán for providing MitoTEMPO and technical advice on its handling and use in experimental models. We thank Dr. Santiago Lamas and Dr. María Ángeles Higueras for careful reading of the manuscript. Editorial support was provided by Dr. Kenneth McCreath.

Appendix A. Supplementary material

Supplementary data associated with this article can be found in the online version at http://dx.doi.org/10.1016/j.freeradbiomed.2016.01.021.

References

[1] M.M. Rogge, The role of impaired mitochondrial lipid oxidation in obesity, Biol. Res. Nurs. 10 (2009) 356–373.

[2] A.M. Joseph, D.R. Joanisse, R.G. Baillot, D.A. Hood, Mitochondrial dysregulation in the pathogenesis of diabetes: potential for mitochondrial biogenesis-mediated interventions, Exp. Diabetes Res. (2012) 642038.

[3] V.K. Mootha, C.M. Lindgren, K.F. Eriksson, A. Subramanian, S. Sihag, J. Lehar, P. Puigserver, E. Carlsson, M. Ridderstrale, E. Laurila, N. Houstis, M.J. Daly, N. Patterson, J.P. Mesirov, T.R. Golub, P. Tamayo, B. Spiegelman, E.S. Lander, J. N. Hirschhorn, D. Altshuler, L.C. Groop, PGC-1alpha-responsive genes involved in oxidative phosphorylation are coordinately downregulated in human diabetes, Nat. Genet. 34 (2003) 267–273.

[4] G.P. Holloway, C.G. Perry, A.B. Thrush, G.J. Heigenhauser, D.J. Dyck, A. Bonen, L. L. Spriet, PGC-1alpha's relationship with skeletal muscle palmitate oxidation is not present with obesity despite maintained PGC-1alpha and PGC-1beta protein, Am. J. Physiol. Endocrinol. Metab. 294 (2008) E1060–E1069.

[5] Y. Olmos, I. Valle, S. Borniquel, A. Tierrez, E. Soria, S. Lamas, M. Monsalve, Mutual dependence of Foxo3a and PGC-1alpha in the induction of oxidative stress genes, J. Biol. Chem. 284 (2009) 14476–14484.

[6] P. Theuma, V.A. Fonseca, Novel cardiovascular risk factors and macrovascular and microvascular complications of diabetes, Curr. Drug Targets 4 (2003) 477–486.

[7] D.A. Antonetti, R. Klein, T.W. Gardner, Diabetic retinopathy, N. Engl. J. Med. 366 (2012) 1227–1239.

[8] X. Chen, S. Wei, F. Yang, Mitochondria in the pathogenesis of diabetes: a proteomic view, Protein Cell 3 (2012) 648–660.

[9] J. Szendroedi, E. Phielix, M. Roden, The role of mitochondria in insulin resistance and type 2 diabetes mellitus, Nat. Rev. Endocrinol. 8 (2012) 92–103.

[10] N. Sawada, A. Jiang, F. Takizawa, A. Safdar, A. Manika, Y. Tesmenitsky, K.T. Kang, J. Bischoff, H. Kalwa, J.L. Sartoretto, Y. Kamei, L.E. Benjamin, H. Watada, Y. Ogawa, Y. Higashikuni, C.W. Kessinger, F.A. Jaffer, T. Michel, M. Sata, K. Croce, R. Tanaka, Z. Arany, Endothelial PGC-1alpha mediates vascular dysfunction in diabetes, Cell Metab. 19 (2014) 246–258.

[11] A. Besseiche, J.P. Riveline, J.F. Gautier, B. Breant, B. Blondeau, Metabolic roles of PGC-1alpha and its implications for type 2 diabetes, Diabetes Metab. (2015).

[12] I. Valle, A. Alvarez-Barrientos, E. Arza, S. Lamas, M. Monsalve, PGC-1alpha regulates the mitochondrial antioxidant defense system in vascular endothelial cells, Cardiovasc. Res. 66 (2005) 562–573.

[13] X.Z. West, N.L. Malinin, A.A. Merkulova, M. Tischenko, B.A. Kerr, E.C. Borden, E. A. Podrez, R.G. Salomon, T.V. Byzova, Oxidative stress induces angiogenesis by activating TLR2 with novel endogenous ligands, Nature 467 (2010) 972–976.

[14] S. Borniquel, N. Garcia-Quintans, I. Valle, Y. Olmos, B. Wild, F. Martinez-Granero, E. Soria, S. Lamas, M. Monsalve, Inactivation of Foxo3a and subsequent downregulation of PGC-1 alpha mediate nitric oxide-induced endothelial cell migration, Mol. Cell. Biol. 30 (2010) 4035–4044.

[15] Z. Arany, S.Y. Foo, Y. Ma, J.L. Ruas, A. Bommi-Reddy, G. Girnun, M. Cooper, D. Laznik, J. Chinsomboon, S.M. Rangwala, K.H. Baek, A. Rosenzweig, B. M. Spiegelman, HIF-independent regulation of VEGF and angiogenesis by the transcriptional coactivator PGC-1alpha, Nature 451 (2008) 1008–1012.

[16] M. Saint-Geniez, A. Jiang, S. Abend, L. Liu, H. Sweigard, K.M. Connor, Z. Arany, PGC-1alpha regulates normal and pathological angiogenesis in the retina, Am. J . Pathol. 182 (2013) 255–265.

[17] J. Oshikawa, N. Urao, H.W. Kim, N. Kaplan, M. Razvi, R. McKinney, L.B. Poole, T. Fukai, M. Ushio-Fukai, Extracellular SOD-derived H_2O_2 promotes VEGF signaling in caveolae/lipid rafts and post-ischemic angiogenesis in mice, PLoS One 5 (2010) e10189.

[18] D.H. Kang, D.J. Lee, K.W. Lee, Y.S. Park, J.Y. Lee, S.H. Lee, G.Y. Koh, C. Choi, D. Y. Yu, J. Kim, S.W. Kang, Peroxiredoxin II is an essential antioxidant enzyme that prevents the oxidative inactivation of VEGF receptor-2 in vascular endothelial cells, Mol. Cell 44 (2011) 545–558.

[19] Y. Olmos, F.J. Sanchez-Gomez, B. Wild, N. Garcia-Quintans, S. Cabezudo, S. Lamas, M. Monsalve, SirT1 regulation of antioxidant genes is dependent on the formation of a FoxO3a/PGC-1alpha complex, Antioxid. Redox Signal. 19 (13) (2013) 1507–1521.

[20] I. Arnaoutova, J. George, H.K. Kleinman, G. Benton, The endothelial cell tube formation assay on basement membrane turns 20: state of the science and the art, Angiogenesis 12 (2009) 267–274.

[21] P. Rodriguez, M.A. Higueras, A. Gonzalez-Rajal, A. Alfranca, M. Fierro-Fernandez, R.A. Garcia-Fernandez, M.J. Ruiz-Hidalgo, M. Monsalve, F. Rodriguez-Pascual, J.M. Redondo, J.L. de la Pompa, J. Laborda, S. Lamas, The non-canonical NOTCH ligand DLK1 exhibits a novel vascular role as a strong inhibitor of angiogenesis, Cardiovasc. Res. 93 (2012) 232–241.

[22] B. Wehrle-Haller, Assembly and disassembly of cell matrix adhesions, Curr. Opin. Cell Biol. 24 (2012) 569–581.

[23] M. Ushio-Fukai, Redox signaling in angiogenesis: role of NADPH oxidase, Cardiovasc. Res. 71 (2006) 226–235.

[24] M. Lee, W.C. Choy, M.R. Abid, Direct sensing of endothelial oxidants by vascular endothelial growth factor receptor-2 and c-Src, PLoS One 6 (2011) e28454.

[25] A. Corcoran, T.G. Cotter, Redox regulation of protein kinases, FEBS J. 280 (2013) 1944–1965.

[26] S. Dikalov, Cross talk between mitochondria and NADPH oxidases, Free Radic. Biol. Med. 51 (2011) 1289–1301.

[27] S. Coso, I. Harrison, C.B. Harrison, A. Vinh, C.G. Sobey, G.R. Drummond, E. D. Williams, S. Selemidis, NADPH oxidases as regulators of tumor angiogenesis: current and emerging concepts, Antioxid. Redox Signal. 16 (2012) 1229–1247.

[28] S. Dai, Y. He, H. Zhang, L. Yu, T. Wan, Z. Xu, D. Jones, H. Chen, W. Min, Endothelial-specific expression of mitochondrial thioredoxin promotes ischemia-mediated arteriogenesis and angiogenesis, Arterioscler. Thromb. Vasc. Biol. 29 (2009) 495–502.

[29] A.M. Markovets, A.Z. Fursova, N.G. Kolosova, Therapeutic action of the mitochondria-targeted antioxidant SkQ1 on retinopathy in OXYS rats linked with improvement of VEGF and PEDF gene expression, PLoS One 6 (2011) e21682.

Angiogenesis
DOI 10.1007/s10456-016-9502-0

ORIGINAL PAPER

Oxidative stress induces loss of pericyte coverage and vascular instability in PGC-1α-deficient mice

Nieves García-Quintans[1,3] · Cristina Sánchez-Ramos[1,5] · Ignacio Prieto[1] · Alberto Tierrez[2] · Elvira Arza[2] · Arantzazu Alfranca[2,4] · Juan Miguel Redondo[2] · María Monsalve[1]

Received: 23 September 2015 / Accepted: 19 February 2016

Abstract Peroxisome proliferator-activated receptor γ coactivator 1α (PGC-1α) is a regulator of mitochondrial oxidative metabolism and reactive oxygen species (ROS) homeostasis that is known to be inactivated in diabetic subjects. This study aimed to investigate the contribution of PGC-1α inactivation to the development of oxygen-induced retinopathy. We analyzed retinal vascular development in PGC-1α$^{-/-}$ mice. Retinal vasculature of PGC-1α$^{-/-}$ mice showed reduced pericyte coverage, a de-structured vascular plexus, and low perfusion. Exposure of PGC-1α$^{-/-}$ mice to hyperoxia during retinal vascular development exacerbated these vascular abnormalities, with extensive retinal hemorrhaging and highly unstructured areas as compared with wild-type mice. Structural analysis demonstrated a reduction in membrane-bound VE-cadherin, which was suggestive of defective intercellular junctions. Interestingly, PGC-1α$^{-/-}$ retinas showed a constitutive activation of the VEGF-A signaling pathway. This phenotype could be partially reversed by antioxidant administration, indicating that elevated production of ROS in the absence of PGC-1α could be a relevant factor in the alteration of the VEGF-A signaling pathway. Collectively, our findings suggest that PGC-1α control of ROS homeostasis plays an important role in the regulation of *de novo* angiogenesis and is required for vascular stability.

Keywords PGC-1α · Retinopathy · Vascular stability · Angiogenesis · ROS

Abbreviations

AKT	Protein kinase B
cdh-5	Cadherin 5
DAPI	4′,6-diamino-2-fenilindol
dll1	Delta-like-1
dll4	Delta-like-4
EUK-189	Eukarion-189
hes1	Hairy and enhancer of split-1
hey1	Hairy/enhancer of split related with YRPW motif protein 1
HNE	4-Hydroxynonenal
HIF-1α	Hypoxia inducible factor-1α
IF	Immunofluorescence
IsoB4	Isolectin B4
NG2	Neuron-glial antigen 2
NICD	NOTCH intracellular domain
P	Phosphorylated
PGC-1α	Peroxisome proliferator-activated receptor γ-coactivator 1α
(P17)	Postnatal day 17
ROS	Reactive oxygen species

Electronic supplementary material The online version of this article (doi:10.1007/s10456-016-9502-0) contains supplementary material, which is available to authorized users.

✉ María Monsalve
mpmonsalve@iib.uam.es

[1] Instituto de Investigaciones Biomédicas "Alberto Sols" (CSIC-UAM), Arturo Duperier 4, Room 1.3.2, 28029- Madrid, Spain

[2] Fundación Centro Nacional de Investigaciones Cardiovasculares Carlos III, Melchor Fernández Almagro 3, 28029- Madrid, Spain

[3] Present Address: Centro de Biología Molecular Severo Ochoa (CSIC-UAM), Nicolas Cabrera 1, 28049- Madrid, Spain

[4] Present Address: Fundación para la Investigación Biomédida del Hospital Universitario La Princesa, Diego de León 62, 28006- Madrid, Spain

[5] Present Address: Fundación Centro Nacional de Investigaciones Cardiovasculares Carlos III, Melchor Fernández Almagro 3, 28029- Madrid, Spain

Published online: 07 March 2016

Smooth muscle actin	SMA
VEGF-A	Vascular endothelial growth factor-A
VE-Cadherin	Vascular endothelial cadherin
flk1 (gene), VEGFR2 (protein)	Vascular endothelial growth factor receptor 2

Introduction

The importance of protecting the body from the most common metabolic disorders including obesity and type 1 and type 2 diabetes cannot be overstated, and their prevalence continues to increase yearly and worldwide. Dysfunctions of the human vascular tree are the major sources of morbidity and mortality. Generally, the damaging effects can be separated into macrovascular (coronary artery disease, peripheral arterial disease, and stroke) and microvascular (nephropathy, neuropathy, and retinopathy) injury [1]. Diabetic retinopathy is one of the most common microvascular complications of diabetes and is a leading cause of $\sim$10,000 new cases of blindness every year in the USA alone [2].

Metabolic disorders are characterized fundamentally by a poor use of mitochondria as a source of ATP and a preponderance of anaerobic glycolysis [3, 4]. This decrease in mitochondrial function is mediated principally by the down-regulation and functional inactivation of the transcriptional coactivator peroxisome proliferator-activated receptor gamma coactivator-1-α (PGC-1α) [5, 6], a master regulator of genes involved in oxidative metabolism. Loss of PGC-1α activity results in an increase in mitochondrial-derived reactive oxygen species (ROS) [7], and elevated ROS levels (oxidative stress) have been found in the majority of vascular complications associated with metabolic disorders.

Our previous results showed that PGC-1α was present in vascular endothelial cells (ECs), and its levels were reduced by hyperglycemia. Furthermore, PGC-1α could coordinate EC oxidative metabolism and antioxidant capacity [8], suggesting that PGC-1α could play a key role in the physiology of the vascular endothelium. Additional studies from our laboratory showed that, at least in vitro, PGC-1α was a negative regulator of EC migration indicating that PGC-1α activity could be important for the control of vascular stability and angiogenesis. Accordingly, activation of PI3K-AKT signaling in response to angiogenesis mediators resulted in the down-regulation of PGC-1α, leading to increased mitochondrial ROS levels and enhanced EC migration [9]. ROS are acknowledged as important signaling mediators regulating cell proliferation and migration [10].

In this study we aimed to characterize the role of PGC-1α as a regulator of mitochondrial function and ROS in the control of angiogenesis and to evaluate its possible contribution to vascular diseases, particularly diabetic retinopathy.

We found that the retinal vasculature in PGC-1$\alpha^{-/-}$ animals exhibited characteristics of an unstable phenotype that was exacerbated upon exposure to an oxygen-induced retinopathy (OIR) protocol. Crucially, this phenotype could be partially rescued by antioxidant treatment, suggesting that excessive ROS production likely plays a role in microvascular instability.

Materials and methods

Animal handling

C57BL/6 PGC-1$\alpha^{+/+}$ and PGC-1$\alpha^{-/-}$ were used. All animal experiments were performed in accordance with the ARVO Statement for the Use of Animals in Ophthalmic and Vision Research. Animal protocols were approved by the Institutional Animal Care and Use Committee of the CNIC and the CSIC. All procedures conformed to the Declaration of Helsinki and the NIH guidelines for animal care and use (NIH publication No. 85–23).

Oxygen-induced retinopathy (OIR)

Ischemic retinopathy was generated according to an established OIR protocol [11]. In brief, p7 pups were transferred with their mothers to a hyperoxia chamber set at 70 % O_2 where they stayed for 5 days and then returned to normoxic conditions. P17 pups were killed. EUK-189 (30 mg/kg in PBS) was administered daily by intraperitoneal injection from day 4 to day 7 and from day 12 to day 17. EUK-189 is a salen–manganese complex and superoxide dismutase/catalase mimetic that has been shown to be effective as antioxidant in vivo and in the inactivation of mitochondrial ROS [12].

Retina isolation

Postnatal day 17 (P17) pups were euthanized in a CO_2 chamber. Eyes were enucleated and fixed in 4 % paraformaldehyde (PFA) in PBS at 4 °C for 48 h.

Whole-mount staining

Retinas were postfixed for 1 h in fixative solution, blocked, and permeabilized in PBS containing 1 % bovine serum albumin (BSA) and 0.5 % Triton X-100, for 2.5 h at RT. The staining solution was PBS pH 6.8 with 0.1 mM $CaCl_2$, 0.1 mM $MgCl_2$ and 0.1 mM $MnCl_2$ and the antibodies

used were: FITC-conjugated anti-*Griffonia simplicifolia* Isolectin B_4 from Sigma-Aldrich (L2895), anti-NG2 from Millipore (#AB5320), and Cy3-conjugated anti-smooth muscle α-actin from Sigma-Aldrich (C6198). Staining was performed for 48 h at 4 °C. For VE-cadherin staining (#550548, anti-CD144, BD PharMingen), the retinas were first blocked and permeabilized with PBS containing 5 % FBS and 0.3 % Triton X-100 and then washed for 1.5 h in PBS. Incubations with fluorescent-tagged secondary antibodies were performed for 2 h at RT and included Alexa-fluor 647 chicken anti-rabbit (Invitrogen) and Alexa-fluor 488 chicken anti-rat (Invitrogen). DAPI (1:1000) (Invitrogen) was used for nuclear visualization. Retinal images were acquired with a Zeiss LSM 700 or LSM 710. Unless otherwise indicated, images shown are maximal projections of z-stacks covering the whole retinal section.

Eye cross sections

Eyes were enucleated, fixed (70 % ethanol, 10 % formalin and 5 % acetic acid) for 48 h, and embedded in paraffin. Sections of 4 µm were stained with hematoxylin and eosin (H&E). Images were acquired with a Nikon 90i microscope.

Vascular perfusion and leakage

Mice were injected via tail vein or retro-orbitally with 100 µl FITC–dextran (FD2000S; Sigma-Aldrich) at a concentration of 40 mg/ml in PBS. The animals were killed 5 min later. Images of retinal flat mounts were obtained by confocal microscopy. Retinal segments were merged to generate a whole retinal image using Nikon A1R software.

Matrigel angiogenesis assay

Matrigel and growth factor-reduced (GFR) Matrigel (10 mg/ml) were mixed with 25 U/ml heparin (Sigma-Aldrich). VEGF-A (8 µg/ml) was added to GFR Matrigel as indicated. Three hundred microliters of the mixture was injected subcutaneously. Implants were harvested after 2 weeks and fixed in formalin for 12 h. Half of the sample was embedded in OCT and frozen. The other half was embedded in paraffin. Samples were analyzed by immunofluorescence using the previously indicated antibodies and an anti-CD31 antibody to assess blood vessel formation and vascular patterns (#557355, BD PharMingen).

Cell culture

Mouse lung endothelial cells (MLECs) were obtained and cultured as described [9]. Wild-type and PGC-$1^{-/-}$ MLEC were cultured in round glass coverslips, fixed with PFA 4 %, permeabilized, and blocked with 10 % FBS, 0.3 % Triton X-100 in PBS and were incubated with an antibody against Tomm22 (HPA003037, Sigma-Aldrich). Cells were counterstained with DAPI (Molecular Probes) and mounted with ProLong (Molecular Probes). Photographs were taken with a spectral confocal microscope LSM710 (Zeiss) and analyzed using ImageJ software. Whole-cell extracts were analyzed by western blotting using antibodies directed against PGC-1α (#ST1202, Millipore) and 4-hydroxynonenal (HNE) (#HNE11, Alpha Diagnostic Int.).

Protein extraction and western blotting was performed as previously described [13]. Specific antibodies used were: HIF-1α (#610958, BD Transduction Laboratories), VEGF-A, (VG-1, Santa Cruz), VEGF-R2 (#55B11, 1:1000), P-VEGFR2 (# 2471, 1:1000), NICD (#4147, 1:1000), AKT (#2920), and phosphorylated AKT-Ser^{473} (#4060) (1:2000), all from Cell Signaling Technology, and *β*-actin (A 5441, Sigma).

RNA isolation and qRT-PCR were performed as previously described [13].

Specific oligonucleotides were:

vegf-a
Forward: 5′-GAAGTCCCATGAAGTGATCAAGT-3′
Reverse: 5′-CTTTGGTCTGCATTCACATCT-3′
flk1
Forward: 5′-CTCTCCACCTTCAAAGTCTCAT-3′
Reverse: 5′-GGCTTTGTGTGAACTCGGACAA-3′
dll 4
Forward: 5′-ACCAACTCCTTCGTCGTCAG-3′
Reverse: 5′-AGGGTGTCATTTTGCTCGTCT-3′
notch 1
Forward: 5′-GGTGTCTTCCAGATCCTGCT-3′
Reverse: 5′-AGTCTCCTCCTTGTTGTTCTG-3′
dll 1
Forward: 5′-CAATGGAGGACGATGTTCAG-3′
Reverse: 5′-CAGGTAAGAGTTGCCGAGGT-3′
hes 1
Forward: 5′-CTGCTACCCCAGCCAGTGT-3′
Reverse: 5′-CGGAGGTGCTTCACAGTCATT-3′
hey 1
Forward: 5′-GAAAAGACGGAGAGGCATCAT-3′
Reverse: 5′-GTGCGCGTCAAAATAACCTT-3′
jagged 1
Forward: 5′-CAGTGCCTCTGTGAGACCAA-3′
Reverse: 5′-GTTATGGCAGGGGTCAGAGA-3′
cdh 5 (VE-cadherin)
Forward: 5′-CCAAATCGTGAAAGGAAATGA-3′
Reverse: 5′-CAGGCACCGAAAATGTGTATG-3′

Image analysis

ImageJ software was used to analyze western blots signals and for global determination of areas in immunofluorescent

images, vascular shape analysis of Matrigel plugs, and membrane/cytosol ratios of VE-cadherin. AngioTool was used for analysis of retinal vascular plexus. H&E images were reviewed manually.

Statistics

Data are expressed as mean ± SD. Statistical significance was evaluated by analysis of variance or a nonparametric test, as appropriate. Values were considered statistically significant at $p < 0.05$; $n = 3$ independent experiments, where $n = 3$–5 animals per group in each independent experiment.

Results

To assess the functional consequences of PGC-1α deficiency, we analyzed the retinal vasculature of PGC-1$\alpha^{-/-}$ pups. The retinal vasculature develops postnatally in the mouse and at P17 angiogenesis initiating at the center of the retina is expected to have reached the retinal edge. No gross structural differences could be detected in the vascular network of retinas from P17 PGC-1$\alpha^{-/-}$ mice compared with wild-type littermates as visualized by FITC-isolectin B4 immunohistochemistry, indicating a lack of major developmental problems (Fig. 1a, top panel). Furthermore, no reduction in the density of the vascular plexus was detected (Fig. 1a, top panel). We analyzed pericyte coverage in the retina by immunohistochemistry using an anti-NG2 antibody that labels pericytes in the micro- and macrovasculature and an anti-SMA antibody that labels smooth muscle cells of large blood vessels. No differences were detected in SMA staining between retinas from PGC-1$\alpha^{-/-}$ and PGC-1$\alpha^{+/+}$ mice (Fig. 1a, top panel). However, pericyte coverage was markedly reduced in PGC-1$\alpha^{-/-}$ retinas stained with NG2, and this reduction was more dramatic in the center of the retina than on the retinal edge where active angiogenesis was still ongoing (Fig. 1a, top panel). This interesting finding suggested that pericytes were initially recruited during the angiogenesis process and then lost. To discern the functional consequences of reduced pericyte coverage, we examined the microvascular structure. Retinas of PGC-1$\alpha^{-/-}$ mice had substantial disorganization of the microvasculature, with many ghost-like blood vessels unlikely to be perfused (Fig. 1a, mid-panel). Consistently, average lacunarity in the primary plexus, but not in the inner plexus, was significantly reduced in PGC-1$\alpha^{-/-}$ retinas. Moreover, junction density was increased whereas average vessel length was not significantly altered (Fig. 1a, mid-panel, and Online Supp. Figure 1).

As the in vitro characterization of PGC-1$\alpha^{-/-}$ ECs suggested a greater propensity to form tip cells, we examined retinal tip cell formation in PGC-1$\alpha^{-/-}$ retinas. As expected, tip cells were found only in the retinal edge in wild-type mice indicating active angiogenesis, with filopodia decorating only the tips of elongated cells (Fig. 1a, bottom panel). In contrast, PGC-1$\alpha^{-/-}$ retinas contained tip cells in the middle regions of the retina and on phalanx cells in the middle of a vessel, and with large numbers of filopodia close to the cell body (Fig. 1a, bottom panel). This phenotype, which is characteristic of excessive tip activity, is typically associated with dense vascular plexus and within this context, could be related to the low stability of the blood vessels.

Because poor formation of intercellular junctions can result in an unstable microvasculature, we examined endothelial intercellular junction interactions by immunostaining for VE-cadherin. Nevertheless, VE-cadherin staining showed that its normal membrane distribution was preserved in PGC-1$\alpha^{-/-}$ animals (Fig. 1b, top panel).

Examination of retinal cross sections stained with H&E revealed a normal retinal structure in PGC-1$\alpha^{-/-}$ mice, although a slight disorganization of the ganglion cell layer could be observed with loss of epithelial-like structure that could be related to poor visual function (Fig. 1b, bottom panel). The origin of these differences was not investigated further.

To determine the impact of the reduced vascular stability on general vascular perfusion, we analyzed retinal perfusion using retro-orbitally injected FITC–dextran. As expected, a marked and general reduction in the perfusion in PGC-1$\alpha^{-/-}$ mice was detected, with a significant reduction in both the mean fluorescence intensity and the detectable area covered by vascular structures (Fig. 1c).

To determine whether the low vascular stability of PGC-1$\alpha^{-/-}$ retinas might be due to an alteration in VEGF-A levels or activity of its downstream effectors, we monitored the expression of VEGF-A together with the activity/phosphorylation of its main angiogenesis receptor, VEGFR2, and its main effectors, AKT and NICD. Levels of VEGF-A in PGC-1$\alpha^{-/-}$ retinas were comparable with retinas from control animals. In contrast, increased levels of total and phosphorylated VEGFR2, phosphorylated AKT, and the active form of NOTCH1, NICD, were detected (Fig. 1d). This result was unexpected, since PGC-1α is known to induce the expression of VEGF-A [14]. We therefore measured *vegf-a* mRNA levels. Consistent with previous reports [15, 16], we detected lower levels in PGC-1$\alpha^{-/-}$ mice (Online Supp. Figure 2). We also analyzed *flk1* (VEGFR2) and *cdh5* (VE-cadherin) mRNA levels. Although *cdh5* levels were on average somewhat lower in PGC-1$\alpha^{-/-}$ mice, no significant differences were detected relative to wild-type mice. These findings suggested that posttranscriptional regulation could be responsible for the observed differences in protein levels and were consistent

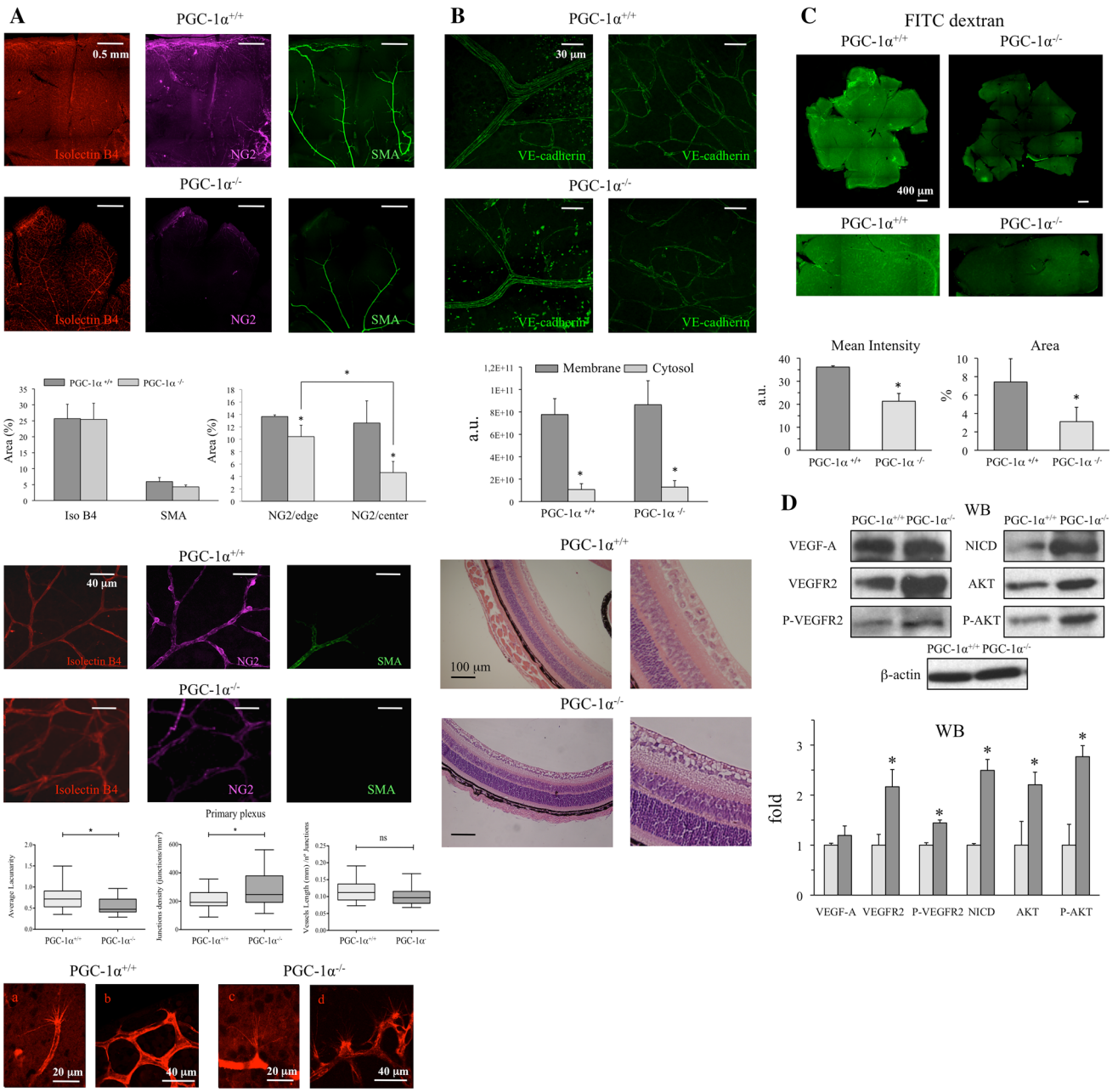

Fig. 1 Reduced pericyte coverage, structural disorganization, and impaired perfusion in retinas from PGC-1α$^{-/-}$ mice despite normal VEGF-A levels. **a** Flat-mount retinas from wild-type and PGC-1α$^{-/-}$ mice were immunostained with Isolectin B4 (ECs), NG2 (pericytes), SMA (smooth muscle), and VE-cadherin (EC tight junctions). **a** *top* Center to edge sections show general vascular system (×10 objective). **a** *Mid* Arterioles and microvasculature (×40 objective). **a** *bottom* Tip cells (×60 objective). **b** *Top* VE-cadherin staining in the microvasculature (×40 objective). **b** *Bottom* H&E staining of retina cross sections from wild-type and PGC-1α$^{-/-}$ mice. **c** Flat-mount retinas from wild-type and PGC-1α$^{-/-}$ mice perfused with FITC dextran; the lower panel shows higher magnification images. **d** Western blot analysis of retinal extracts of relevant proteins in the control of angiogenesis: VEGF-A, VEGFR2, NICD, and AKT. Data are from three independent experiments, $n = 3$–5 animals per group in each independent experiment. Data are mean ± SD. *$p \leq 0.05$ versus control

with an enhanced constitutive activity of VEGFR2 (Fig. 1g, Online Supp. Figure 2).

It was possible that these findings could result from increased levels of NOTCH1 ligands or elevated *Notch1* expression. This second scenario, however, was unlikely since the expression levels of *notch1* and its ligands *jagg1, dll1*, *and dll4* were not increased in PGC-1α$^{-/-}$ retinas; indeed, *dll4* expression was decreased. Furthermore, the elevated level of NICD was not associated with an increased expression of the NICD target genes *hes1* and

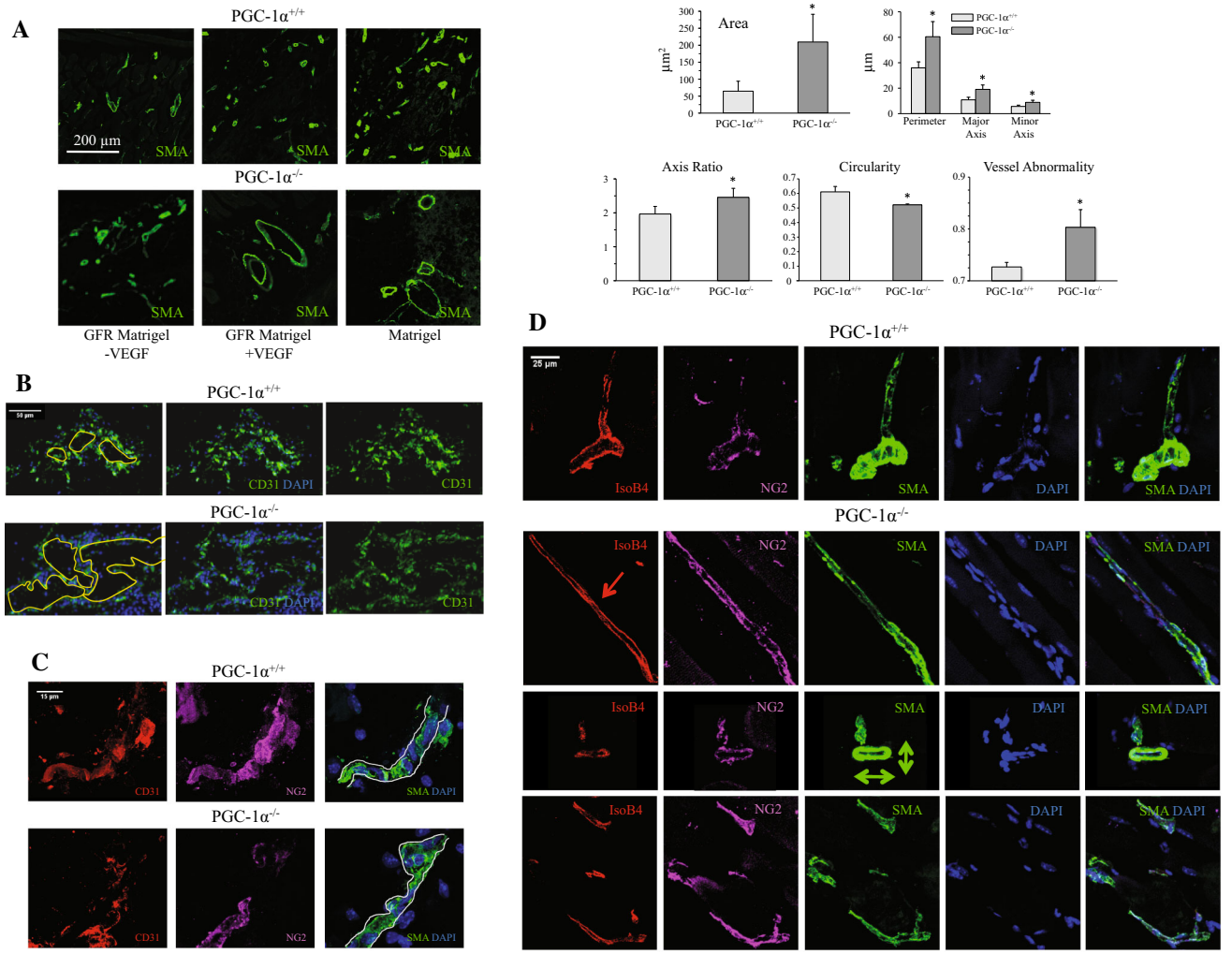

Fig. 2 Absence of PGC-1α results in the formation of enlarged and irregular blood vessels in Matrigel implants. **a–d** Immunofluorescence stain of Matrigel implants from wild-type and PGC-1α$^{-/-}$ mice. **a** SMA stain of Matrigel implants and GFR Matrigel implants with or without VEGF-A (×25 objective). **b** CD31 and DAPI (×40 objective **c** CD31, NG2, DAPI (×60 objective). **d** IsoB4, NG2, SMA, DAPI (×40 objective). Data are from three independent experiments, *n*= 3–5 animals per group in each independent experiment. Data are mean ± SD. *$p \leq 0.05$ versus control

hey1, which were comparable between wild-type and PGC-1α$^{-/-}$ mice, possibly suggesting a reduced transcriptional activity of NICD in PGC-1α$^{-/-}$ mice (Fig. 1g, Online Supp. Figure 2). Taken together, these observations suggested that the reduced vascular density observed in PGC-1α$^{-/-}$ mice did not result from changes in VEGF-A or NICD.

To evaluate the role of PGC-1α in the control of angiogenesis in vivo, in a system where VEGF-A could be provided in a controlled manner, we used a Matrigel plug assay of neovessel formation and injected this matrix subcutaneously into wild-type and PGC-1α$^{-/-}$ mice. Three conditions were tested: Matrigel rich in growth factors, including VEGF, and GFR Matrigel with or without added VEGF. Angiogenesis was allowed to proceed for 2 weeks and plugs were extracted and analyzed to evaluate the number, size, and shape of neovessels. No differences were detected in the number of neovessels between wild-type and PGC-1α$^{-/-}$ mice (SMA staining; data not shown). In contrast, significantly larger blood vessels were detected in PGC-1α$^{-/-}$ mice under all conditions tested (Fig. 2a and Online Supp. Figure 3). Furthermore, the shape of the vessels was more irregular in PGC-1α$^{-/-}$ animals, with larger differences in the axis ratio, and reduced circularity and larger vessel abnormality values (Fig. 2a). The nature of the vessels was confirmed by staining with the endothelial markers CD31 and IsoB4 (Fig. 2b–d). Pericyte coverage, determined by NG2 staining, was also more irregular in PGC-1α$^{-/-}$ mice (Fig. 2c). Figure 2d contrasts a typical branching wild-type vessel on the top panel, with

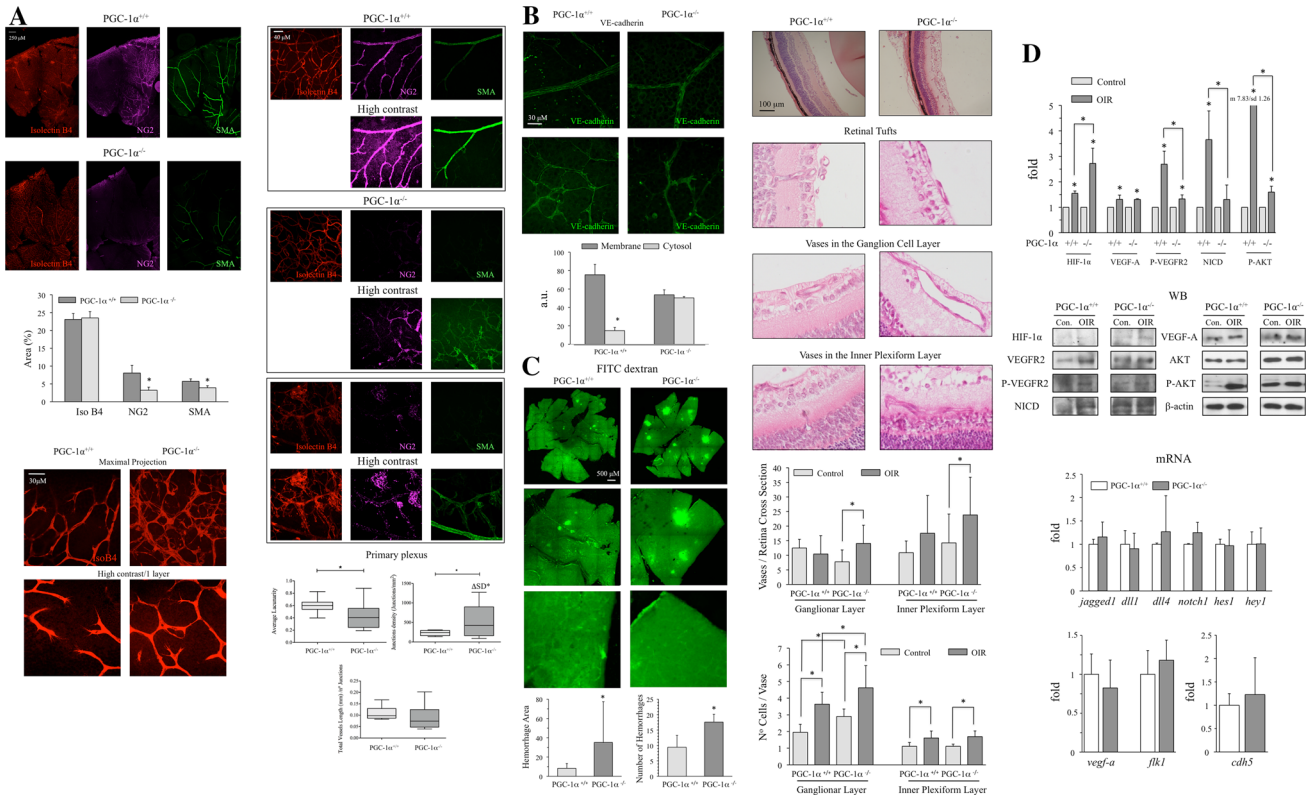

Fig. 3 OIR in PGC-1α$^{-/-}$ mice severely disrupts the retinal vascular structure, but does not induce VEGF-A levels or activity. Abnormally large blood vessels in the ganglionar layer, loss of endothelial junctions, highly irregular vascular plexus with poor pericyte coverage, and large hemorrhagic areas are observed in PGC-1α$^{-/-}$ mice. **a** Flat-mount retinas from wild-type and PGC-1α$^{-/-}$ mice where immunostained with Isolectin B4, NG2, SMA, and VE-cadherin. **a** *top* Center to edge sections show general vascular system (×10 objective). **a** *Mid* Arterioles and microvasculature (×40 objective). **a** *Bottom* Tip cells (×60 objective). **b** *Left* VE-cadherin stain in the microvasculature (×40 objective). **b** *right* H&E stain of retina cross sections from wild-type and PGC-1α$^{-/-}$ mice. **c** Flat-mount retinas from wild-type and PGC-1α$^{-/-}$ mice perfused with FITC dextran; lower panels show higher magnification images. **d** *Top* Western blot analysis of retinal extracts of relevant proteins in the control of angiogenesis: VEGF-A, VEGFR2, NICD, and AKT. **d** *bottom* qRT-PCR analysis of mRNA levels of relevant genes in the control of angiogenesis. Data are from three independent experiments, *n*= 3–5 animals per group in each independent experiment. Data are mean ± SD. *$p \leq 0.05$ versus control

examples of the anomalies that we could find in PGC-1α$^{-/-}$ mice, from top to bottom we can see, the irregularity of the lumen in a lengthwise section of a vessel, with a constriction point, a cross section of a collapsed vessel, and a dilated irregular vessel in cross section.

To further evaluate the role played by PGC-1α in the control of vascular stability and the response to VEGF-A, we used the oxygen-induced retinopathy model (OIR) where one-week-old mice and their mothers are first exposed to hyperoxia (70 % O_2) for 5 days and then returned to normoxic conditions for a further 5 days. This generates a hypoxia inducible factor-1α (HIF-1α)-dependent overproduction of VEGF-A in the developing retinal vasculature, which promotes neovascularization in the retinal periphery. As such, this model recapitulates the vascular anomalies found in proliferative diabetic retinopathy [17].

Flat-mount retinas from 17-day-old OIR wild-type and PGC-1α$^{-/-}$ mice were immunostained with isolectin B4, NG2, and SMA antibodies and examined by confocal microscopy. OIR decreased the general vascular density both in wild-type and PGC-1α$^{-/-}$ mice (Fig. 3a, top panel, Online Supp. Figure 4). OIR resulted in the loss of pericyte coverage and this reduction was more dramatic in PGC-1α$^{-/-}$ retinas (Fig. 3a). SMA staining was also more reduced by OIR in PGC-1α$^{-/-}$ than in wild-type retinas, suggesting that vascular instability induced by the loss of PGC-1α extended also to the macrovasculature (Fig. 3a, top panel). Closer examination of isolectin B4-stained vascular structures revealed that, compared with wild-type, PGC-1α$^{-/-}$ retinas contained highly-disorganized areas (Fig. 3a, mid-panel). High-contrast imaging indicated that pericyte coverage in OIR wild-type animals was low but structurally organized (Fig. 3a, mid-panel). In contrast,

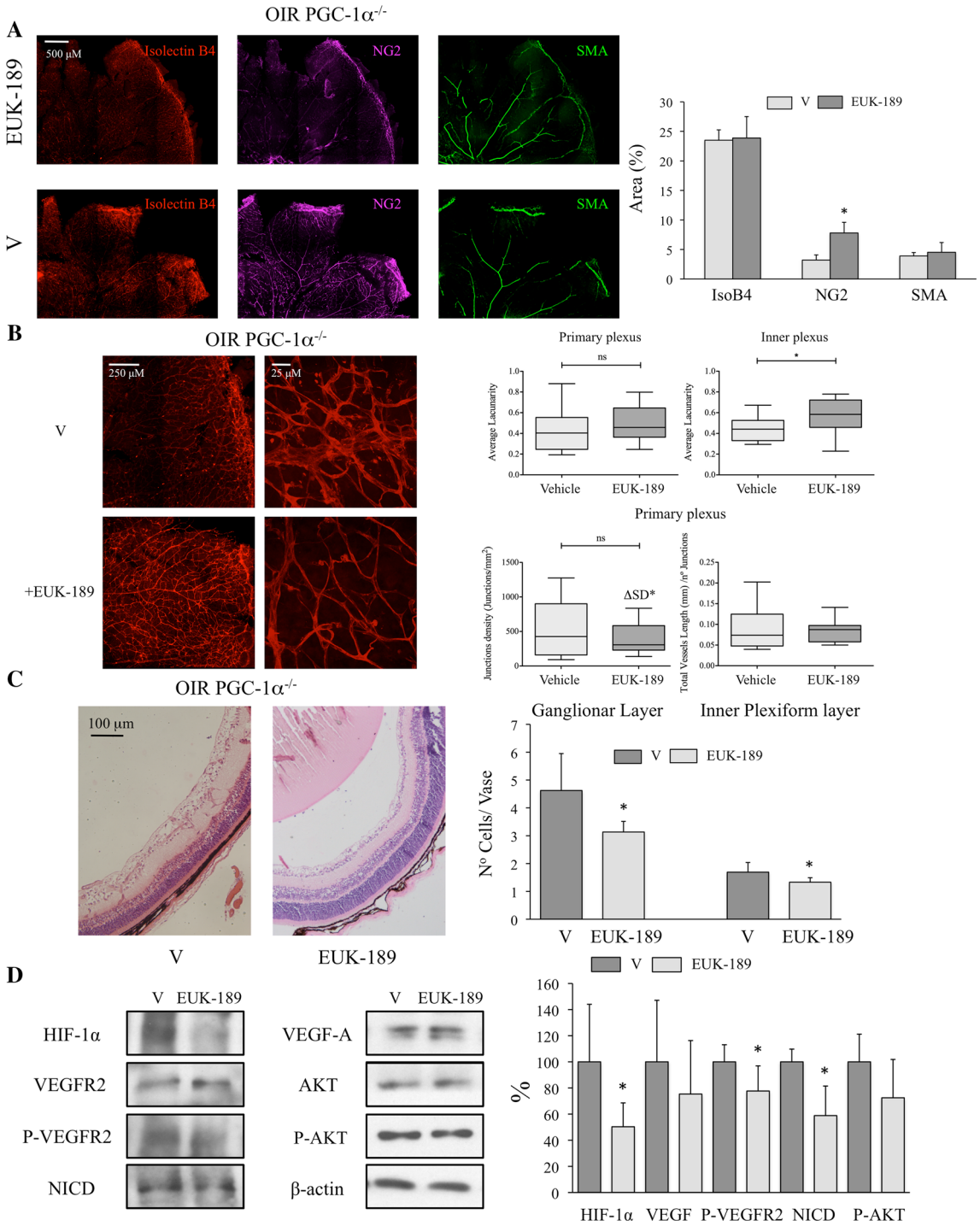

Fig. 4 Severity of OIR in PGC-1α$^{-/-}$ mice is prevented by EUK-189 treatment. **a–c** Flat-mount retinas from wild-type and PGC-1α$^{-/-}$ mice were immunostained with Isolectin B4 (endothelial cells), NG2 (pericytes), SMA (smooth muscle cells), and VE-cadherin (tight junctions of ECs). **a** Center to edge sections of the vascular system (×10 objective). **b** Arterioles and microvasculature (×40 objective). **c** H&E stain of retina cross sections from wild-type and PGC-1α$^{-/-}$ mice. **d** Western blot analysis of retinal extracts of relevant proteins in the control of angiogenesis. Data are from three independent experiments, n= 3–5 animals per group in each independent experiment. Data are mean ± SD. *$p \leq 0.05$ versus control. *ns* not significant

OIR PGC-1α$^{-/-}$ mice exhibited an aberrant distribution of pericytes with large neovascular structures showing NG2 and SMA staining. Quantitative analysis showed reduced lacunarity in the primary plexus and increased junction density, in the absence of significant changes in the average vessel length, in OIR PGC-1α$^{-/-}$ retinas, (Fig. 3a, mid-

panel). Additionally, a significant increase in the standard deviation (SD) of the junction density was detected in OIR PGC-1$\alpha^{-/-}$ mice, indicating a more marked disorganization of the retinal plexus. Analysis of z-stack layers of high-resolution images allowed the identification of tip cells. In wild-type retinas tip cells were typically found in pairs, with filopodia pointing toward each other, and with both cells located in the same vascular plexus, whereas tip cells showed no apparent directionality in PGC-1$\alpha^{-/-}$ retinas (Fig. 3a, bottom panel).

Endothelial intercellular junctions were evaluated by VE-cadherin staining. In wild-type retinas normal, membrane-bound, staining was preserved, while PGC-1$\alpha^{-/-}$ mice exhibited diffuse (cytosolic) VE-cadherin staining in both capillaries and larger blood vessels (Fig. 5b, left panel, Online Supp. Figure 5). This finding suggested a predominantly intracellular location of VE-cadherin in PGC-1$\alpha^{-/-}$ mice, with massive loss of intercellular junctions and vascular instability.

As previously reported, OIR in wild-type mice induces the formation of penetrating capillaries across the plexiform layer and ECs tufts on the inner limiting membrane of the retina extending into the vitreous, which together contribute to the neovascularization process [11]. Using H&E staining to survey the vascular architecture after OIR, anomalous blood vessel formation was also detected in PGC-1$\alpha^{-/-}$ mice (Fig. 3b, right panel). Indeed, no substantial differences were found between wild-type and knockout mice in the number of tufts (Online Supp. Figure 6). However, notable differences were found in the ganglionar and inner plexiform layers. PGC-1$\alpha^{-/-}$ mice responded to the OIR protocol with a more dramatic increase in the number of anomalous blood vessels than wild-type mice (Fig. 3b, right panel). Moreover, the vessels in the ganglionar layer were larger in PGC-1$\alpha^{-/-}$ mice (Fig. 3b, right panel), and, on occasion, hemorrhagic (Online Supp. Figure 7). All these observations are consistent with the results shown in Fig. 2 indicating that the loss of PGC-1α has a particular high impact on the structure of the newly formed vessels, rather than on the vessel number.

To evaluate the functional relevance of these findings, we analyzed vascular perfusion and permeability by tail vein injection of FITC–dextran. A reduced vascular perfusion together with the appearance of hemorrhagic lesions was observed in wild-type mice (Fig. 3c), as previously described for OIR. PGC-1$\alpha^{-/-}$ mice exhibited a more severe phenotype with extended non-perfused areas together with a greater number of larger hemorrhages (Fig. 3c). The three images of Fig. 3c show from top to bottom the whole retina, where we can appreciate the elevated number of hemorrhages in PGC-1$\alpha^{-/-}$ mice, a higher amplification image, focused on the size comparison between hemorrhagic lesion in wild-type and PGC-1$\alpha^{-/-}$ mice and a further zoom in image to visualize the absence of perfused vessels in extensive areas of PGC-1$\alpha^{-/-}$ mouse retinas. The graph at the bottom shows the quantification of the number and the size of the hemorrhages.

To investigate whether these anomalies might be related to alterations in the induction of angiogenesis mediators, we measured HIF-1α, VEGF-A, and its downstream effectors in retinas. As expected, OIR increased the levels of HIF-1α and VEGF-A protein, increased the phosphorylation of VEGFR2 and AKT, and also increased the levels of NICD in wild-type mice (Fig. 3d, top panel). In PGC-1$\alpha^{-/-}$ mice, OIR resulted in a more marked induction of HIF-1α and a significantly attenuated increase in phosphorylated VEGFR2, phosphorylated AKT and NICD (Fig. 3d, top panel), while VEGF-A was induced to the same extent in wild-type and PGC-1$\alpha^{-/-}$ retinas. These results suggested that HIF-α induction is boosted in PGC-1$\alpha^{-/-}$ mice, possibly indicating that PGC-1α is working as a negative regulator of HIF-α protein levels. In fact, HIF-1α is positively regulated by ROS and ROS are elevated in the absence of PGC-1α. They also indicate that HIF-1α can induce VEGF-A levels both in the presence and in the absence of PGC-1α. However, while the wild-type mice respond to elevated levels of VEGF-A induced by OIR with an corresponding activation of the VEGFR2 and its downstream effectors, this activation is significantly blunted in PGC-1α mice, suggesting a poorer response to VEGF-A. Retinal mRNA expression levels of the NOTCH1 ligands *jagged1*, *dll4*, and *dll1*, of *notch1* itself, its target genes *hes1* and *hey1, vegf-a, flk1*, and *cdh5* were also evaluated. No significant differences were found between wild-type and PGC-1$\alpha^{-/-}$ mice, suggesting that the phenotype observed was not likely to be attributable to differences in NOTCH1 activity (Fig. 3d, bottom panel). Collectively, these results suggest that PGC-1α-deficient mice are more sensitive to OIR, likely due to an inability to form stable/mature blood vessels.

PGC-1$\alpha^{-/-}$ MLECs migrate faster than wild-type cells due to an overproduction of ROS [9]. Indeed, ROS are important players in EC migration and proliferation [18, 19]. Thus, we evaluated whether the vascular instability in PGC-1$\alpha^{-/-}$ mice could be attributed to an excess of ROS. To test this idea, the antioxidant EUK-189 was administered to OIR PGC-1$\alpha^{-/-}$ mice daily by intraperitoneal injection from day 4 to day 7, when the pups entered the hyperoxia chamber, and from day 12 to day 17 when they were returned to normoxia. Flat-mount retinas from 17-day-old OIR-treated PGC-1$\alpha^{-/-}$ mice were immunostained with isolectin B4, NG2, and SMA antibodies. Endothelial staining with isolectin showed that EUK-189 did not alter the vascular density of OIR-treated PGC-1$\alpha^{-/-}$ mice but improved the structural organization of the

vascular plexus (Fig. 4a). NG2 staining indicated an improvement in coverage in EUK-189-treated mice (Fig. 4a). SMA staining was marginally enhanced by EUK-189, although differences were not significant (Fig. 4a). Structural analysis revealed that EUK-189 treatment increased the average lacunarity in the inner plexus and decreased the junction density, as well as its variability, in the primary plexus without significantly changing the total vessel length (Fig. 4b). Nevertheless, EUK-189 failed to fully restore the microvascular structure in OIR-treated PGC-1$\alpha^{-/-}$ mice, and a significant number of abnormally twisted capillaries were apparent (Fig. 4b). The number of tip cells was reduced in EUK-189-treated mice, and the tip cells showed a reduced number of filopodia but did not show the polarity normally found in tip cells where filopodia can be found only on one side of the cell, while the other is firmly associated with a stalk cell (Online Supp. Figure 8). The effect of EUK-189 on the vascular anomalies induced by OIR was further analyzed by H&E staining of retinal cross sections. The size of the abnormal blood vessels in the ganglion cell layer and the inner plexiform layer was reduced by EUK-189 treatment (Fig. 4c). These observations suggested that the reduced vascular stability provoked by the absence of PGC-1α was partially restored by antioxidant treatment.

Finally, to test whether this structural recovery was associated with a restoration of a normal VEGF-A-dependent response, we measured protein (Fig. 4d) and mRNA levels (Online Supp. Figure 9) of VEGF-responsive factors. EUK-189 treatment significantly reduced the levels of HIF-1α, phosphorylated VEGFR2, and NICD, but had no effect on VEGF-A protein levels, suggesting that in vivo treatment with EUK-189 improved VEGF-A signaling in PGC-1$\alpha^{-/-}$ mice. EUK-189 treatment did not produce significant changes in the mRNA levels of *notch1*, its ligands *dll1*, *dll4*, its targets *hes1*, *hey1*, or *flk1* and *cdh5*, indicating that EUK-189 did not modulate NOTCH1 activity.

Discussion

The present study shows that PGC-1α plays an important role in the control of angiogenesis and in the stability of the mature vasculature. In the absence of PGC-1α, the vascular endothelium appears to be constitutively activated, probably due to elevated ROS levels that cause constitutive activation of the VEGF-A signaling pathway. These alterations are likely to be relevant in diabetic retinopathy where PGC-1α activity is generally found to be low.

The physiological consequences of PGC-1α deficiency in angiogenesis were analyzed in the retinas of PGC-1$\alpha^{-/-}$ mice. The retinal vasculature showed clear signs of instability, including a reduction in endothelial intercellular junctions and a significant loss of pericyte coverage. Furthermore, tip cells could be found in what should be quiescent vessels and displayed a lack of polarity. Reduced pericyte coverage is unlikely to be the result of defective recruitment but rather to their ulterior loss since pericytes were found in regions of active angiogenic activity. These alterations closely resemble those observed in diabetic retinopathy; however, VEGF-A protein levels were comparable in retinas from both groups of mice suggesting that differences in VEGF-A levels were not responsible for the observed phenotype.

Since elevated VEGF-A levels are generally regarded to be the main driver of the formation of anomalous blood vessels in diabetic retinopathy [20], we used the OIR protocol that recapitulates most if not all features of human diabetic retinopathy to question how PGC-1α-deficient mice respond to VEGF-A. OIR exacerbated the vascular instability observed under basal conditions in PGC-1$\alpha^{-/-}$ mice. The number of anomalous blood vessels was unaffected by the loss of PGC-1α, but these vessels were larger, fully collapsed and/or largely irregular in diameter. Analysis of the VEGF-A signaling pathway suggested that in wild-type animals OIR induces an activation of the pathway, while in PGC-1$\alpha^{-/-}$ animals the pathway is constitutively active and is non-responsive to elevated VEGF-A levels. Importantly, HIF-1α levels are more strongly induced in PGC-1$\alpha^{-/-}$-deficient mice and could account for the exacerbation of the phenotype.

PGC-1α-deficient ECs have elevated levels of ROS [7], and antioxidant treatment re-establishes the normal motility of PGC-1α-deficient ECs [9]. Given that the VEGF-A signaling pathway has been shown to be ROS sensitive [18, 21, 22], we hypothesized that elevated ROS could be responsible for the observed phenotype. Consistent with this hypothesis, antioxidant treatment partially restored vascular structure and VEGF-A signaling in PGC-1α-deficient mice.

It is generally acknowledged that pericyte coverage is essential for vessel stabilization, and there are several pathways involved in the intimate cross talk between the vascular endothelial cell and the pericyte. As a result, endothelial dysfunction generally results in pericyte loss and vice versa. Among the pathways involved, the TGF-β and the angiotensin system have been extensively characterized [23]. Importantly, the VEGFR2 has also been shown to be involved in this regulatory process [24]. In light of the previous evidence showing that loss of PGC-1α results in enhanced cell migration and of the present results suggesting that loss of PGC-1α alters the VEGFR2 signaling pathway, it is possible that this alteration may be responsible for the observed loss in pericyte coverage, although alternative scenarios are also possible.

Importantly, recent reports suggest a connection between the TGF-β pathway and PGC-1α [25].

That antioxidant treatment was not sufficient for a complete functional recovery in OIR-treated PGC-1α$^{-/-}$ retina raises several questions. It could be considered that since ROS are part of the normal signaling processes, complete detoxification of ROS cannot be expected to be fully beneficial [26]. Another reasonable possibility is that part of this phenotype cannot be attributed to ROS alone and might involve other PGC-1α target genes.

An attractive hypothesis is that PGC-1α might be necessary to recover the endothelial oxidative capacity following the "ischemic" period. In the OIR model, hyperoxia produces vasoconstriction that results in tissue hypoxia, activation of HIF-1α, and HIF-1α-dependent induction of VEGF-A [27]. HIF-1α activates glycolytic metabolism to prevent cell death during hypoxia [28]; however, excessive HIF-1α activity prevents the re-activation of oxidative metabolism and stabilization of the newly formed vasculature by an unknown mechanism. This inability to perfuse results in organ damage, e.g., cardiac hypertrophy [29]. Therefore, it is possible that the exacerbation of the vascular anomalies observed in OIR-treated animals and the partial effect of antioxidants can be attributed to the inability of ECs to reinitiate oxidative metabolism following HIF-1α activation, in the absence of PGC-1α.

In conclusion, our study supports the idea that PGC-1α plays a major role in the control of angiogenesis and is likely to be relevant in diabetic retinopathy. Furthermore, it suggests that constitutive activation of the VEGF-A signaling pathway can limit the therapeutic potential of VEGF-A-based therapies in the absence of a good redox balance. Future studies should be directed to investigate this re-wiring of normal ROS homeostasis.

Acknowledgments We thank Enrique Samper (NIMGenetics, Madrid, Spain) for providing EUK-189 and technical advice on its handling and use in experimental models. We thank Santiago Lamas and Maria Angeles Higueras (CBMSO, Madrid, Spain) for careful reading of the manuscript. We thank Kenneth McCreath for editorial support. This work was supported by grants from the Spanish ''Ministerio de Economía y Competitividad'' (Grant number SAF2009-07599 & SAF2012-37693 to M.M and CSD 2007-00020 to M.M.) and the ''Comunidad de Madrid'' (Grant Number S2010/BMD-2361 to M.M.).

Compliance with ethical standards

Conflict of interest The authors declare that they have no conflict of interest.

Human and animal rights This article does not contain any studies with human participants performed by any of the authors. All applicable international, national, and/or institutional guidelines for the care and use of animals were followed. All procedures performed in studies involving animals were in accordance with the ethical standards of the institution or practice at which the studies were conducted.

References

1. Theuma P, Fonseca VA (2003) Novel cardiovascular risk factors and macrovascular and microvascular complications of diabetes. Curr Drug Targets 4(6):477–486
2. Antonetti DA, Klein R, Gardner TW (2012) Diabetic retinopathy. N Engl J Med 366(13):1227–1239. doi:10.1056/NEJMra1005073
3. Rogge MM (2009) The role of impaired mitochondrial lipid oxidation in obesity. Biol Res Nurs 10(4):356–373. doi:10.1177/1099800408329408
4. Joseph AM, Joanisse DR, Baillot RG, Hood DA (2012) Mitochondrial dysregulation in the pathogenesis of diabetes: potential for mitochondrial biogenesis-mediated interventions. Exp Diabetes Res. doi:10.1155/2012/642038
5. Mootha VK, Lindgren CM, Eriksson KF, Subramanian A, Sihag S, Lehar J, Puigserver P, Carlsson E, Ridderstrale M, Laurila E, Houstis N, Daly MJ, Patterson N, Mesirov JP, Golub TR, Tamayo P, Spiegelman B, Lander ES, Hirschhorn JN, Altshuler D, Groop LC (2003) PGC-1α-responsive genes involved in oxidative phosphorylation are coordinately downregulated in human diabetes. Nat Genet 34(3):267–273. doi:10.1038/ng1180
6. Holloway GP, Perry CG, Thrush AB, Heigenhauser GJ, Dyck DJ, Bonen A, Spriet LL (2008) PGC-1α's relationship with skeletal muscle palmitate oxidation is not present with obesity despite maintained PGC-1α and PGC-1β protein. Am J Physiol Endocrinol Metab 294(6):E1060–1069. doi:10.1152/ajpendo.00726.2007
7. Olmos Y, Valle I, Borniquel S, Tierrez A, Soria E, Lamas S, Monsalve M (2009) Mutual dependence of Foxo3a and PGC-1α in the induction of oxidative stress genes. J Biol Chem 284(21):14476–14484. doi:10.1074/jbc.M807397200
8. Valle I, Alvarez-Barrientos A, Arza E, Lamas S, Monsalve M (2005) PGC-1α regulates the mitochondrial antioxidant defense system in vascular endothelial cells. Cardiovasc Res 66(3):562–573
9. Borniquel S, Garcia-Quintans N, Valle I, Olmos Y, Wild B, Martinez-Granero F, Soria E, Lamas S, Monsalve M (2010) Inactivation of Foxo3a and subsequent downregulation of PGC-1α mediate nitric oxide-induced endothelial cell migration. Mol Cell Biol 30(16):4035–4044. doi:10.1128/MCB.00175-10
10. West XZ, Malinin NL, Merkulova AA, Tischenko M, Kerr BA, Borden EC, Podrez EA, Salomon RG, Byzova TV (2010) Oxidative stress induces angiogenesis by activating TLR2 with novel endogenous ligands. Nature 467(7318):972–976. doi:10.1038/nature09421
11. Smith LE, Wesolowski E, McLellan A, Kostyk SK, D'Amato R, Sullivan R, D'Amore PA (1994) Oxygen-induced retinopathy in the mouse. Investig Ophthalmol Vis Sci 35(1):101–111
12. Hinerfeld D, Traini MD, Weinberger RP, Cochran B, Doctrow SR, Harry J, Melov S (2004) Endogenous mitochondrial oxidative stress: neurodegeneration, proteomic analysis, specific respiratory chain defects, and efficacious antioxidant therapy in superoxide dismutase 2 null mice. J Neurochem 88(3):657–667
13. Olmos Y, Sanchez-Gomez FJ, Wild B, Garcia-Quintans N, Cabezudo S, Lamas S, Monsalve M (2013) SirT1 regulation of antioxidant genes is dependent on the formation of a FoxO3a/PGC-1α complex. Antioxid Redox Signal 19:1507–1521. doi:10.1089/ars.2012.4713
14. Arany Z, Foo SY, Ma Y, Ruas JL, Bommi-Reddy A, Girnun G, Cooper M, Laznik D, Chinsomboon J, Rangwala SM, Baek KH,

Rosenzweig A, Spiegelman BM (2008) HIF-independent regulation of VEGF and angiogenesis by the transcriptional coactivator PGC-1α. Nature 451(7181):1008–1012
15. Saint-Geniez M, Jiang A, Abend S, Liu L, Sweigard H, Connor KM, Arany Z (2013) PGC-1α regulates normal and pathological angiogenesis in the retina. Am J Pathol 182(1):255–265. doi:10.1016/j.ajpath.2012.09.003
16. Sawada N, Jiang A, Takizawa F, Safdar A, Manika A, Tesmenitsky Y, Kang KT, Bischoff J, Kalwa H, Sartoretto JL, Kamei Y, Benjamin LE, Watada H, Ogawa Y, Higashikuni Y, Kessinger CW, Jaffer FA, Michel T, Sata M, Croce K, Tanaka R, Arany Z (2014) Endothelial PGC-1α mediates vascular dysfunction in diabetes. Cell Metab 19(2):246–258. doi:10.1016/j.cmet.2013.12.014
17. Lange C, Ehlken C, Stahl A, Martin G, Hansen L, Agostini HT (2009) Kinetics of retinal vaso-obliteration and neovascularisation in the oxygen-induced retinopathy (OIR) mouse model. Graefes Arch Clin Exp Ophthalmol 247(9):1205–1211. doi:10.1007/s00417-009-1116-4
18. Kang DH, Lee DJ, Lee KW, Park YS, Lee JY, Lee SH, Koh YJ, Koh GY, Choi C, Yu DY, Kim J, Kang SW (2011) Peroxiredoxin II is an essential antioxidant enzyme that prevents the oxidative inactivation of VEGF receptor-2 in vascular endothelial cells. Mol Cell 44(4):545–558. doi:10.1016/j.molcel.2011.08.040
19. Ushio-Fukai M (2006) Redox signaling in angiogenesis: role of NADPH oxidase. Cardiovasc Res 71(2):226–235
20. Gupta N, Mansoor S, Sharma A, Sapkal A, Sheth J, Falatoonzadeh P, Kuppermann B, Kenney M (2013) Diabetic retinopathy and VEGF. Open Ophthalmol J 7:4–10. doi:10.2174/1874364101307010004
21. Lee M, Choy WC, Abid MR (2011) Direct sensing of endothelial oxidants by vascular endothelial growth factor receptor-2 and c-Src. PLoS One 6(12):e28454. doi:10.1371/journal.pone.0028454
22. Oshikawa J, Urao N, Kim HW, Kaplan N, Razvi M, McKinney R, Poole LB, Fukai T, Ushio-Fukai M (2010) Extracellular SOD-derived H_2O_2 promotes VEGF signaling in caveolae/lipid rafts and post-ischemic angiogenesis in mice. PLoS One 5(4):e10189. doi:10.1371/journal.pone.0010189
23. Armulik A, Abramsson A, Betsholtz C (2005) Endothelial/pericyte interactions. Circ Res 97(6):512–523. doi:10.1161/01.RES.0000182903.16652.d7
24. Lin SL, Chang FC, Schrimpf C, Chen YT, Wu CF, Wu VC, Chiang WC, Kuhnert F, Kuo CJ, Chen YM, Wu KD, Tsai TJ, Duffield JS (2011) Targeting endothelium-pericyte cross talk by inhibiting VEGF receptor signaling attenuates kidney microvascular rarefaction and fibrosis. Am J Pathol 178(2):911–923. doi:10.1016/j.ajpath.2010.10.012
25. Tiano JP, Springer DA, Rane SG (2015) SMAD3 negatively regulates serum irisin and skeletal muscle FNDC5 and peroxisome proliferator-activated receptor gamma coactivator 1-α (PGC-1α) during exercise. J Biol Chem 290(18):11431. doi:10.1074/jbc.A114.617399
26. Oshikawa J, Kim SJ, Furuta E, Caliceti C, Chen GF, McKinney RD, Kuhr F, Levitan I, Fukai T, Ushio-Fukai M (2012) Novel role of p66Shc in ROS-dependent VEGF signaling and angiogenesis in endothelial cells. Am J Physiol Heart Circ Physiol 302(3):H724–732. doi:10.1152/ajpheart.00739.2011
27. Weidemann A, Johnson RS (2008) Biology of HIF-1α. Cell Death Differ 15(4):621–627
28. Rajabi M, Kassiotis C, Razeghi P, Taegtmeyer H (2007) Return to the fetal gene program protects the stressed heart: a strong hypothesis. Heart Fail Rev 12(3–4):331–343. doi:10.1007/s10741-007-9034-1
29. Shiojima I, Walsh K (2006) Regulation of cardiac growth and coronary angiogenesis by the Akt/PKB signaling pathway. Genes Dev 20(24):3347–3365

ANTIOXIDANTS & REDOX SIGNALING
Volume 00, Number 00, 2016

DOI: 10.1089/ars.2016.6698

ORIGINAL RESEARCH COMMUNICATION

Heme-Oxygenase I and PCG-1α Regulate Mitochondrial Biogenesis *via* Microglial Activation of Alpha7 Nicotinic Acetylcholine Receptors Using PNU282987

Elisa Navarro,[1,2] Laura Gonzalez-Lafuente,[1] Irene Pérez-Liébana,[1] Izaskun Buendia,[1,2] Elia López-Bernardo,[2,3] Cristina Sánchez-Ramos,[4] Ignacio Prieto,[4] Antonio Cuadrado,[4] Jorgina Satrustegui,[3] Susana Cadenas,[2,3] Maria Monsalve,[4] and Manuela G. López[1,2]

Abstract

Aims: A loss in brain acetylcholine and cholinergic markers, subchronic inflammation, and impaired mitochondrial function, which lead to low-energy production and high oxidative stress, are common pathological factors in several neurodegenerative diseases (NDDs). Glial cells are important for brain homeostasis, and microglia controls the central immune response, where α7 acetylcholine nicotinic receptors (nAChR) seem to play a pivotal role; however, little is known about the effects of this receptor in metabolism. Therefore, the aim of this study was to evaluate if glial mitochondrial energetics could be regulated through α7 nAChR. ***Results:*** Primary glial cultures treated with the α7 nicotinic agonist PNU282987 increased their mitochondrial mass and their mitochondrial oxygen consumption without increasing oxidative stress; these changes were abolished when nuclear erythroid 2-related factor 2 (Nrf2) was absent, heme oxygenase-1 (HO-1) was inhibited, or peroxisome proliferator-activated receptor gamma coactivator 1α (PGC-1α) was silenced. More specifically, microglia of animals treated intraperitoneally with the α7 nAChR agonist PNU282987 (10 mg/kg) showed a significant increase in mitochondrial mass. Interestingly, $LysM^{cre}$-$Hmox1^{\Delta/\Delta}$ and PGC-$1\alpha^{-/-}$ animals showed lower microglial mitochondrial levels and treatment with PNU282987 did not produce effects on mitochondrial levels. ***Innovation:*** Increases in microglial mitochondrial mass and metabolism can be achieved *via* α7 nAChR by a mechanism that implicates Nrf2, HO-1, and PGC-1α. This signaling pathway could open a new strategy for the treatment of NDDs, such as Alzheimer's, characterized by a reduction of cholinergic markers. ***Conclusion:*** α7 nAChR signaling increases glial mitochondrial mass, both *in vitro* and *in vivo, via* HO-1 and PCG-1α. These effects could be of potential benefit in the context of NDDs. *Antioxid. Redox Signal*. 00, 000–000.

Introduction

AGING AND NEURODEGENERATION share common factors such as low-grade chronic inflammation and impaired mitochondrial function, which lead to low energy production and high oxidative stress (8). Furthermore, inherited mitochondrial defects have also been related to neurodegeneration. Indeed, dysfunctional mitochondria are the main source of reactive oxygen species (ROS) production.

Mitochondria are the main producers of adenosine triphosphate (ATP), and therefore, a reduction in their number or functionality is translated into a reduction in brain energetic metabolism, which alters brain function. Beyond energy production, mitochondria serve for multiple functions, such as controlling the levels of metabolites, amino acids, or cofactors of regulating enzymes, synthesis of heme and Fe-S clusters, and calcium homeostasis (25). Therefore, strategies based on increasing mitochondrial number could be of potential interest to provide neuroprotection.

[1]Instituto Teófilo Hernando, Departamento Farmacología, Facultad de Medicina, Universidad Autónoma de Madrid, Madrid, Spain.
[2]Instituto de Investigación Sanitaria Princesa (IIS-IP), Madrid, Spain.
[3]Centro de Biología Molecular ''Severo Ochoa'' (CSIC-UAM), Departamento de Biología Molecular, Universidad Autónoma de Madrid, Madrid, Spain.
[4]Instituto de Investigaciones Biomédicas Alberto Sols, Madrid, Spain.

Innovation

Increases in microglial mitochondrial mass and metabolism can be achieved *via* the α7 nicotinic acetylcholine receptor (nAChR) by a mechanism that implicates nuclear erythroid 2-related factor 2 (Nrf2) heme-oxygenase-1 (HO-1) and peroxisome proliferator-activated receptor gamma coactivator 1α (PGC-1α). By improving microglial mitochondrial function through activation of this new pathway, the brain could, in principle, better resolve inflammation and contribute to reduce pathology.

Mitochondria have a limited half-life and cells can respond to different situations by controlling their mitochondrial content by different pathways, among others through mitochondrial biogenesis. Mitochondrial biogenesis is a highly controlled and coordinated mechanism that implicates the transcription of both, nuclear and mitochondrial genes. There are a large number of physiological and pathological situations that demand an increase in mitochondrial number, such as nutrient deficits, temperature changes, exercise, hormones or growth factors (40), and inflammatory resolution (34). Different transcription factors are implicated in mitochondrial biogenesis, such as the nuclear respiratory factors (NRF-1 and NRF-2), members of the nuclear receptor (NR), the peroxisome proliferator-activated receptors (PPARs), the estrogen-related receptors (ERRs) (13), or additional transcription factors, including YY1, MEF2, and c-myc (41). Regardless of the transcription factor implicated, these signals converge in the activation of transcriptional coactivator peroxisome proliferator-activated receptor gamma coactivator-1α (PGC-1α) which acts as the master regulator of mitochondrial biogenesis.

PGC-1α integrates the activity of a variety of transcription factors such as NRF1-2, PPARα, and mitochondrial transcription factor A (mtTFA), regulating the generation of new mitochondria and the cellular energetic status (6, 10, 13). Several studies have demonstrated that PGC-1α is involved in the activation of the mitochondrial respiratory chain and fatty acid oxidation genes, and also in increasing mitochondrial number and respiratory capacity (41). PGC-1α also plays a pivotal role in controlling the cellular antioxidant responses since it controls the expression of many antioxidant genes such as glutathione peroxidase, catalase, or superoxide dismutase-1 (43). In this way, PGC-1α controls the generation of new mitochondria without increasing cellular oxidative stress. Moreover, deficiency in PGC-1α relates to early neurodegeneration (17) and alterations in this transcription factor have been related to the progression of different neurodegenerative diseases (NDDs) (4a).

Nicotinic acetylcholine receptors (nAChRs) are a family of ion-gated channels, which are expressed both in the periphery and in the central nervous system (CNS). Within the brain, the α7 nAChR subtype is expressed both in neurons, where it controls neurotransmission or neurite outgrowth, and in microglia, where it is known to control the cholinergic anti-inflammatory pathway. Furthermore, its activation has been reported to exert neuroprotection against a variety of pathological situations (12, 36); the intracellular signaling pathway to afford neuroprotection includes activation of the transcription factor nuclear erythroid 2-related factor 2 (Nrf2) (12, 22, 30), considered as the master regulator of redox homeostasis. When Nrf2 is activated it promotes the expression of phase II antioxidant enzymes to protect against oxidative damage. Among these phase II antioxidant enzymes, the role of heme-oxygenase-1 (HO-1) must be highlighted.

HO-1 catalyzes the rate-limiting step of the degradation of heme group generating carbon monoxide (CO); biliverdin, which is rapidly converted to bilirubin by biliverdin reductase; and ferrous iron. Both HO-1 and its three by-products have antioxidant and cytoprotective effects (2, 27), and HO-1 also has an anti-inflammatory effect as its activity is accompanied by the expression of IL-10 and IL-1βRa (34). Interestingly, the HO-1/CO axis has been reported to control mitochondrial biogenesis in a way that implies superoxide dismutase 2 (SOD2) expression and mitochondrial H_2O_2 production, which leads to the induction of Nrf2 *via* Akt/PKB and binding to the NRF-1 promoter (47). As a result, this transcriptional mechanism links the mitochondrial expansion to the antioxidant and counterinflammatory defenses.

Microglia are considered the resident macrophages of the CNS and are responsible for the brain's innate immune system. During aging, microglia lose their homeostastic functional role and could contribute to neurodegeneration (45, 46). By improving glial mitochondrial function, the brain could, in principle, better resolve inflammation and contribute to reduce pathology. Based on the participation of HO-1 in mitochondrial biogenesis (33, 34), in this study we have focused on the participation of the glial α7 nAChR in the generation of new mitochondria. Our results show that activation of α7 nAChR in glial cells increases mitochondrial mass and improves cellular mitochondrial respiration, both processes dependent on HO-1 and PGC-1α activity.

Results

The α7 nAChR agonist PNU282987 increased mitochondrial mass in glial cells

Our group and others have previously described the anti-inflammatory and antioxidant properties mediated by α7 nAChRs (12, 22). Due to the close relationship between those processes and mitochondrial biogenesis (34, 43), we thought of interest to study if α7 nAChR signaling could be increasing the mitochondrial content. To address this question, we used primary glial cultures treated with the specific α7 nAChR agonist, PNU282987, at a concentration of 10 μM during 48 h; thereafter, different methodological approaches were used to evaluate if changes in mitochondrial mass were taking place. Using the fluorescent stain MitoTracker-Green (Mtg), which is characterized for being independent of mitochondrial potential, we measured the mitochondrial content by flow cytometry. With this protocol, we obtained that cells treated with PNU282987 presented a higher mitochondrial content, comparable to the results obtained with the positive control resveratrol (Fig. 1A). We also labeled glial cells with Mtg and took images in a confocal microscope, observing higher fluorescent levels in cells treated with PNU282987 (Fig. 1B).

To ensure the results above, the expression of mitochondrial proteins, such as cytochrome *c* and manganese SOD (MnSOD), was also measured by Western blot. As shown in Figure 1C and D, PNU282987-treated glial cells increased by two- and threefold the expression of cytochrome *c* and MnSOD, respectively. Taken together, we can conclude that

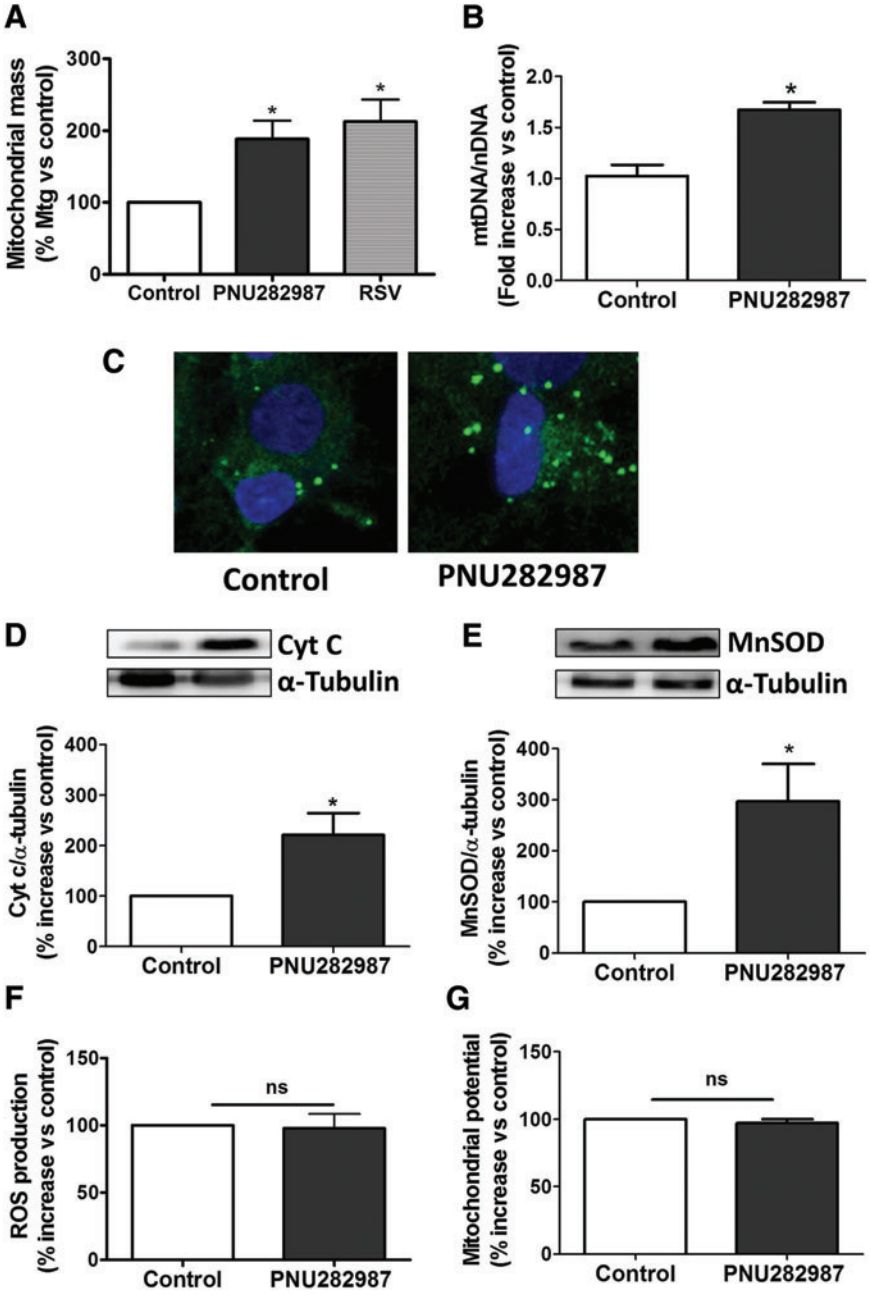

FIG. 1. Treatment with PNU282987 10 μM during 48 h increases mitochondrial mass in primary glial culture. (A) Mitochondrial mass was measured using Mtg fluorescent stain by flow cytometry. PNU282987, as well as the positive control resveratrol 10 μM, significantly increased Mtg fluorescence. Values are expressed as mean ± SEM ($n = 5$ different experiments). Analysis was performed using one-way ANOVA test. $^*p < 0.05$ compared to control. **(B)** The copy number of mtDNA and nDNA was assessed by PCR. PNU282987 increased the ratio mtDNA/nDNA. Values are expressed as mean ± SEM of five to six measures of two independent cultures. **(C)** Representative images taken by confocal microscopy of cells stained with Mtg. **(D, E)** PNU282987 increased the expression of the mitochondrial proteins cytochrome *c* and MnSOD as shown in the representative immunoblots and quantification plots. Data correspond to mean ± SEM ($n = 9$ different experiments). Analysis was performed using paired *t*-test. $^*p < 0.05$ *versus* control. **(F)** PNU282987 treatment did not increase ROS production or **(G)** modify mitochondrial membrane potential measured by flow cytometry using H_2DCFDA or TMRE stains, respectively. Graphs represent mean ± SEM ($n = 3$–4 different experiments). Analysis was performed using paired *t*-test. ANOVA, analysis of variance; H_2DCFDA, 2′,7′,-dichlorofluorescein diacetate; MnSOD, manganese superoxide dismutase; mtDNA, mitochondrial DNA; Mtg, MitoTracker-Green; nDNA, nuclear DNA; PCR, polymerase chain reaction; ROS, reactive oxygen species; SEM, standard error of the mean; TMRE, tetramethylrhodamine, ethyl ester, perchlorate. To see this illustration in color, the reader is referred to the web version of this article at www.liebertpub.com/ars

the treatment of glial cells with the α7 nAChR agonist increased mitochondrial mass.

The increase in mitochondrial mass was not associated with increased ROS production or mitochondrial membrane potential alterations

The main source of oxidative stress within the cell is the mitochondria and excessive ROS production can be deleterious to the cells. Therefore, we analyzed if the increase in mitochondrial content elicited by PNU282987 was accompanied by an increase in ROS production or alterations in mitochondrial membrane potential. For that purpose, we labeled the cells with the fluorescent dyes 2′,7′-dichlorofluorescein diacetate (H_2DCFDA; to measure ROS) and tetramethylrhodamine, ethyl ester, perchlorate (TMRE; to assess changes in mitochondrial potential) and analyzed them by flow cytometry. We obtained that the increase in mitochondrial mass elicited by PNU282987 was not associated to changes in cellular redox status as we did not observe changes in H_2DCFDA fluorescence (Fig. 1E). Furthermore, no mitochondrial membrane potential changes were detected using the ratio TMRE/Mtg (Fig. 1F).

Glial cells exhibit a higher mitochondrial respiratory efficiency after PNU282987 treatment

Changes in the cellular mitochondrial content are not always accompanied by alterations in respiratory parameters. To assess if PNU282987 treatment had any effect on mitochondrial bioenergetics, we used the XF24 Extracellular Flux Analyzer (Seahorse Bioscience, North Billerica, MA) to determine the oxygen consumption rate (OCR) in cultured

cells (Fig. 2A). OCR was measured in control conditions, after the addition of oligomycin to determine the oxygen consumption linked to ATP synthesis, and after the addition of the uncoupling agent 2,4-dinitrophenol (DNP) to obtain the maximal respiratory capacity. At the end of each measurement, rotenone plus antimycin A were added to completely block mitochondrial respiration and to determine the nonmitochondrial respiration. This value was subtracted to all conditions.

Our results show that PNU282987 increased OCR levels under basal conditions (Control 3.7 ± 0.28 nmol/min·mg protein; PNU282987: 4.65 ± 0.29 nmol/min·mg protein; Fig. 2B). Moreover, PNU282987 also increased the OCR due to ATP turnover (Control: 1.14 ± 0.18 nmol/min·mg protein; PNU282987: 1.65 ± 0.15 nmol/min·mg protein; Fig. 2C), whereas it had no effect on the proton leak (Fig. 2D). The α7 nAChR agonist also improved the maximal respiratory capacity of glial cells (Control: 3.81 ± 0.24 nmol/min·mg protein; PNU282987: 4.69 ± 0.26 nmol/min·mg protein; Fig. 2E). Taken together, these results indicate that the increase in mitochondrial mass elicited by PNU282987 treatment is accompanied by an increase in mitochondrial oxygen consumption and ATP synthesis.

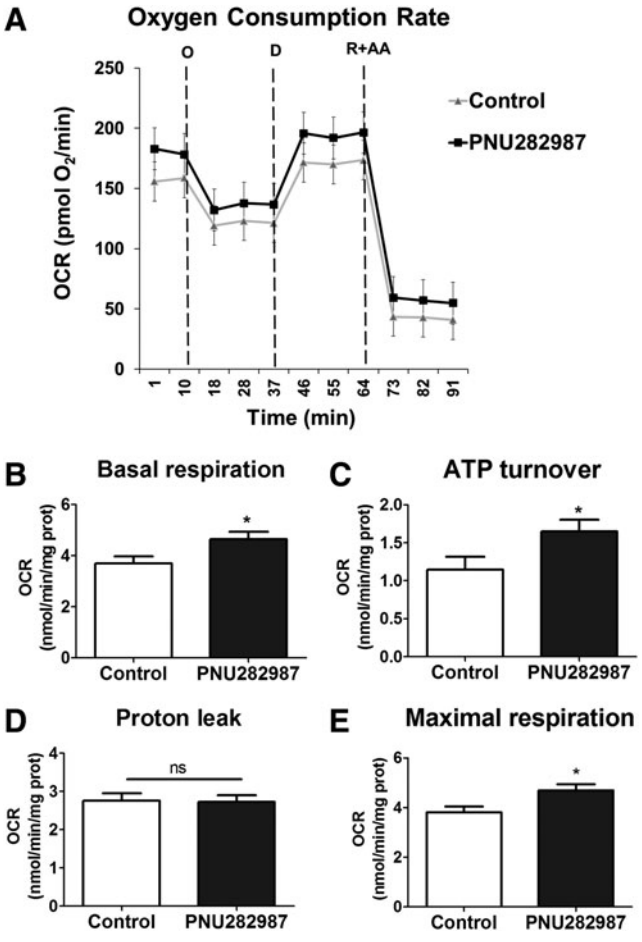

FIG. 2. PNU282987 treatment increased mitochondrial respiratory parameters in glial cultures. **(A)** Representative plot of the OCR measured in control cells and cells treated with PNU282987 10 μM during 48 h. The sequential additions are indicated by *arrows*: 5 μg/ml oligomycin (O), 500 μM DNP (D), and 1 μM rotenone +1 μM antimycin A (R+AA). Plots of OCR quantification corrected using total mg of protein. **(B)** basal: OCR under basal situation, **(C)** ATP turnover: basal minus oligomycin, **(D)** proton leak: OCR after the addition of oligomycin, **(E)** maximal respiration: OCR after the addition of DNP. Nonmitochondrial respiration (rotenone plus antimycin A) was subtracted for each condition. Graphs represent mean ± SEM of six independent experiments. Analysis was performed using paired *t*-test. $^*p < 0.05$ *versus* control situation. ATP, adenosine triphosphate; DNP, 2,4,-dinitrophenol; OCR, oxygen consumption rate.

Changes observed in mitochondrial mass were α7 nAChR specific and dependent on Nrf2/HO-1

It has been previously described how signaling mediated by α7 nAChR leads to an induction in HO-1 enzyme *via* Nrf2 transcription factor (22, 31). Since HO-1 has been reported to participate in mitochondrial biogenesis (33, 38), we decided to evaluate the implication of Nrf2/HO-1 in the effects elicited by PNU282987.

First of all, we performed glial cultures from wild-type (WT) and $Nrf2^{-/-}$ mice and observed that the increase in mitochondrial population elicited by PNU282987 was lost when Nrf2 was absent (Fig. 3A). To study the implication of HO-1, we first confirmed that treatment with the α7 nAChR agonist produced an induction of the enzyme; indeed, PNU282987 almost doubled the basal expression of HO-1 (Fig. 3B). Then, by inhibiting HO-1 with 3 μM tin protoporphyrin-IX dichloride (SnPP), the increase in mitochondrial mass induced by the α7 nAChR agonist was lost (Fig. 3B). Furthermore, we used 100 nM α-bungarotoxin (α-Bgtx) as an α7 nAChR blocker to determine that the effects observed with PNU282987 were receptor specific. Glial cultures were treated with PNU282987, in the absence or presence of the HO-1 and α7 nAChR inhibitors, and thereafter, mitochondrial mass and respiratory parameters were assessed. When cells were treated during 48 h with PNU282987 (10 μM) in the presence of α-Bgtx, changes observed in mitochondrial mass (Fig. 3C) and respiratory parameters (basal and maximal respiration, and ATP turnover) were abolished (Fig. 3D, E), indicating that the effects elicited by PNU282987 were specific of α7 nAChR activation. Moreover, the increase in mitochondrial mass (Fig. 3C) and mitochondrial respiration (basal and maximal respiration and ATP turnover) observed with the α7 nAChR agonist was lost when HO-1 was inhibited (Fig. 3D, E). Changes in proton leak were not observed among the different treatments.

These results provide a clear indication that induction of HO-1 *via* Nrf2 is necessary for mitochondrial biogenesis within the signaling pathway activated by α7 nAChR.

The increase in mitochondrial mass elicited by PNU282987 was dependent on PGC-1α activity

PGC-1α has been widely described as the master regulator of mitochondrial biogenesis but little is known about its relationship with α7 nAChR signaling. In this study, we demonstrate that activation of α7 nAChR produces an increase in the expression of PGC-1α measured by Western blot (Fig. 4A). We also observed activation of pAMPK and pCREB; two proteins associated with the activation of PGC-1α (Fig. 4B, C).

Moreover, mouse embryonic fibroblast (MEF) cells were transfected with the PGC-1α promoter linked to a luciferase reporter gene and they showed increased luciferase activity after Nrf2 transfection or sulforaphane (Sfn) treatment

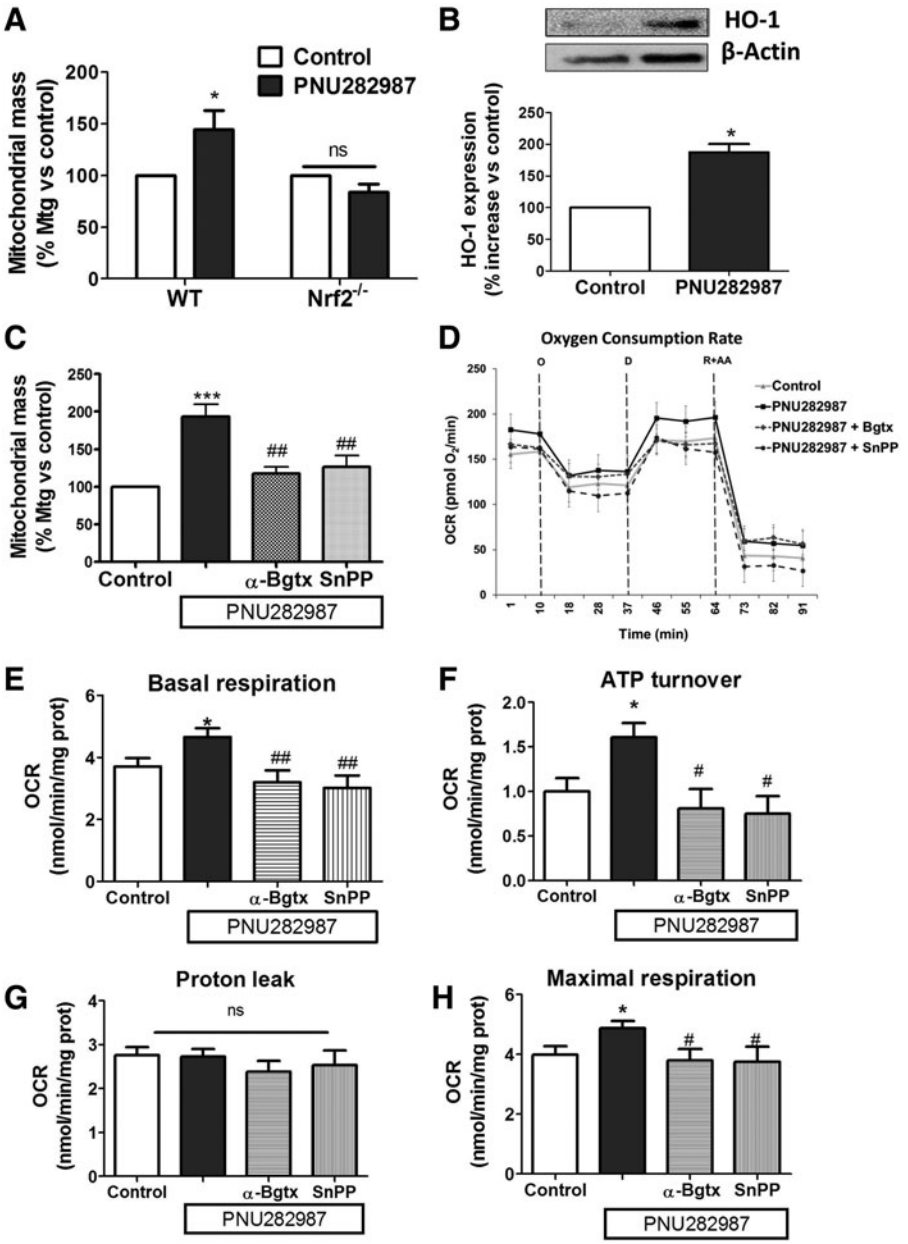

FIG. 3. The effect of PNU282987 on mitochondrial biogenesis depends on the α7 nAChR/Nrf2/HO-1 axis. (A) Mitochondrial mass was assessed as Mtg fluorescence by FACS in WT and $Nrf2^{-/-}$ mice. PNU282987 increased the number of mitochondria in WT cultures but not in $Nrf2^{-/-}$. Values represent mean ± SEM of eight to nine independent experiments. Analysis was performed using two-way ANOVA. $*p < 0.05$ *versus* control situation. **(B)** The treatment with PNU282987 increased the expression of HO-1 measured by Western blot. Data correspond to mean ± SEM of three independent experiments. Analysis was performed using paired *t*-test. $*p < 0.05$ *versus* control situation. **(C)** The effects of PNU282987 on mitochondrial mass, measured as Mtg fluorescence by flow cytometry in the presence of 100 n*M* of α-Bgtx and 3 *μM* of SnPP, were abolished. Values represented are mean ± SEM ($n = 4$ independent experiments). Analysis was performed using one-way ANOVA test. $***p < 0.001$ *versus* control, $^{\#\#}p < 0.01$ *versus* PNU282987. **(D)** Representative plot of the OCR measured in control cells and in cells exposed to PNU282987 10 *μM* during 48 h, in the presence or absence of 100 n*M* α-Bgtx or 3 *μM* SnPP. The sequential additions are indicated by *arrows*: 5 μg/ml oligomycin (O), 500 *μM* DNP (D), and 1 *μM* rotenone +1 *μM* antimycin A (R+AA). Plots of OCR quantification corrected using total mg of protein: **(E)** basal conditions, **(F)** ATP turnover: basal minus oligomycin, **(G)** proton leak: OCR after the addition of oligomycin, **(H)** maximal respiration: OCR after the addition of DNP. Nonmitochondrial respiration (rotenone plus antimycin A) was subtracted for each condition. Graphs represent mean ± SEM of four independent experiments. Analysis was performed using one-way ANOVA. $*p < 0.05$ *versus* control, $^{\#}p < 0.05$ *versus* PNU282987, $^{\#\#}p < 0.01$ *versus* PNU282987. α7 nAChr, alpha7 nicotinic acetylcholine receptor; α-Bgtx, alpha-bungarotoxin; HO-1, heme-oxygenase-1; Nrf2, nuclear erythroid 2-related factor 2; SnPP, tin protoporphyrin-IX dichloride; WT, wild type.

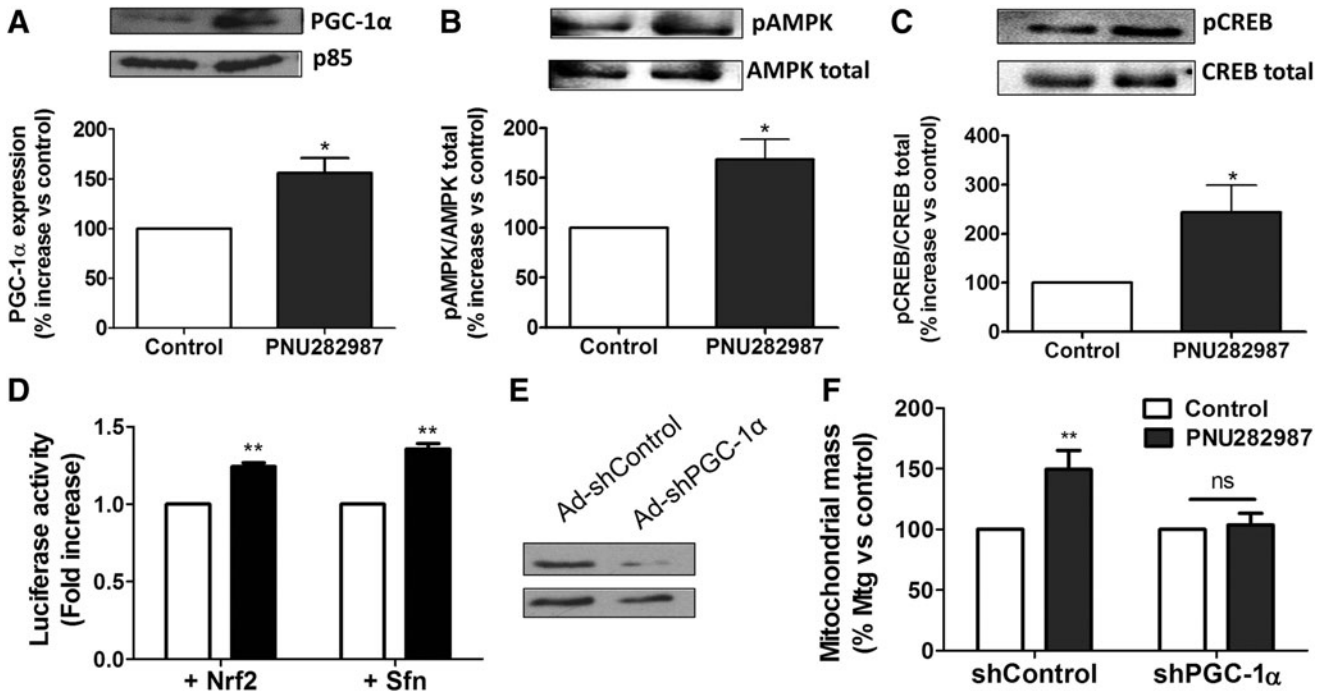

FIG. 4. PGC-1α participates in the effect of PNU282987 on mitochondrial mass. **(A)** PNU282987 increased the expression of PGC-1α measured by Western blot. Data correspond to mean ± SEM of four independent experiments. Analysis was performed using paired *t*-test. $*p < 0.05$ *versus* control situation. **(B)** PNU282987 increased the phosphorylation of AMPK protein and **(C)** CREB transcription factor. Data correspond to mean and SEM ($n = 4$–6 independent experiments). Analysis was performed using paired *t*-test. $*p < 0.05$ *versus* control. **(D)** MEFs were transfected with the PGC-1α promoter linked to luciferase reporter gene and they were either cotransfected with Nrf2 plasmid of treated with 10 *μM* Sfn. Both Nrf2 and Sfn produced an increase in luciferase activity. Data represent mean and SEM of three independent experiments performed in duplicate. $**p < 0.01$ *versus* control condition. **(E)** Efficacy of silencing PGC-1α was assessed by Western blot in control glial cells silenced using adeno-associated viral vectors. **(F)** Quantification plot of Mtg fluorescence after treatment with PNU282987 in cells infected with adeno-associated virus with scrambled RNA (shControl) or shPGC-1α. Data are mean ± SEM ($n = 5$ independent experiments). Analysis was performed using two-way ANOVA test. $**p < 0.01$ *versus* control. MEFs, mouse embryonic fibroblasts; PGC-1α, peroxisome proliferator-activated receptor gamma coactivator 1α; Sfn, sulforaphane; sh, small hairpin.

(potent inductor of Nrf2). These results provide evidence on the possible regulation of the expression of PGC-1α *via* Nrf2 transcription factor.

To assess the implication of PGC-1α in mitochondrial biogenesis activated by α7 nAChR, we used adeno-associated viral infection to silence the expression of PGC-1α and then studied the effect of PNU282987 treatment. Cells were infected for 8 h with the adeno-associated vectors expressing (i) scrambled small hairpin RNA (shRNA; shControl) and (ii) shRNA targeting PGC-1α (shPGC-1α), followed by overnight cell recovery. As shown by Western blot, PGC-1α was silenced in glial cells treated with shPG-1α and not in those treated with scrambled shRNA (Fig. 4E). Afterward, PNU282987 was added during 48 h and mitochondrial mass was assessed as Mtg fluorescence by flow cytometry. As it can be observed in Figure 4F, PGC-1α silencing prevented the changes in mitochondrial mass elicited by PNU282987, highlighting the implication of PGC-1α in the effect that PNU282987 had on this process.

Repeated intraperitoneal injection of PNU282987 increased mitochondrial content specifically in microglia only when HO-1 and PGC-1α were present

To further confirm our results, we decided to assess if the increase in mitochondrial mass mediated *via* α7 nAChR could be reproduced *in vivo*. For that purpose, we performed repeated intraperitoneal (i.p.) injections (twice per day) of 10 mg/kg of PNU282987 during 2 days (Fig. 5A). Body weight was monitored throughout the experiment, but no changes were observed (data not shown). Forty-eight hours after the first injection, animals were sacrificed; the microglial population was isolated by Percoll gradient and cells were stained with CD45-FITC, CD11b-PE, and GLAST-APC to confirm the purity of the microglial enrichment protocol. As shown in Figure 5B, the isolated population was positive for CD11b (microglial marker), expressed low levels of CD45 (macrophage marker), and was negative for GLAST (astrocytic marker), indicating that the population isolated was indeed microglia (purity: 82.1% ± 3.4%).

Once the purity of the population was established, cells were stained with CD11b and Mtg to evaluate changes in mitochondrial content in $CD11b^+$ cells after PNU282987 injection. As represented in Figure 5C and D, PNU282987 treatment elicited a significant increase in mitochondrial content in the microglial population of WT animals (Saline: 1.0 ± 0.09 *vs.* PNU282987: 1.3 ± 0.08).

To establish conclusively the involvement of HO-1 in the effects of α7 nAChR stimulation on mitochondrial biogenesis, we performed the same experiment using $LysM^{cre}$-$Hmox1^{\Delta/\Delta}$ animals, in which HO-1 expression is absent specifically in myeloid cells. The results were normalized

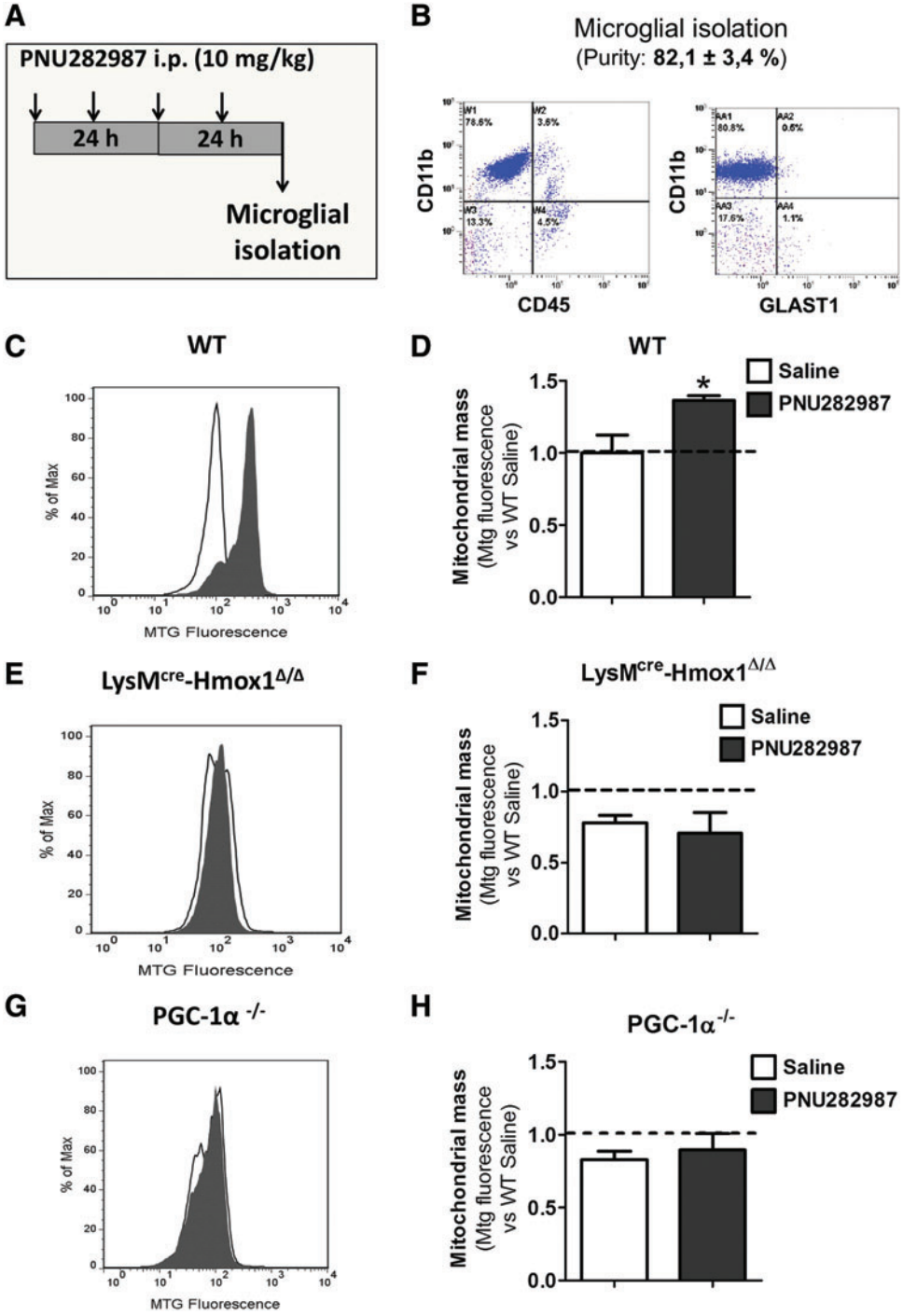

FIG. 5. Repeated i.p. injection of PNU282987 increases mitochondrial mass *in vivo* specifically in microglial population: HO-1 and PGC-1α dependency. **(A)** Experimental protocol. PNU282987 was administered i.p. 10 mg/kg twice per day during 2 days. **(B)** Microglial population purity. Microglia were isolated using Percoll gradient, and purity was measured by flow cytometry using the markers CD11b, CD45, and GLAST. **(C, D)** PNU282987 treatment increased mitochondrial content in microglial population in WT animals. Mitochondrial content was assessed in CD11b-positive cells using Mtg fluorescent staining. **(C)** Representative flow cytometry plot and **(D)** quantification plot. Data correspond to mean and SEM ($n=8$ animals treated with saline and $n=6$ animals treated with PNU282987). $*p<0.05$ *versus* saline. **(E, F)** Animals that did not express HO-1 in myeloid lineage (LysMcre-Hmox1$^{\Delta/\Delta}$) showed decreased number of mitochondria in microglia compared to their controls and PNU282987 did not produce any increase. Representative flow cytometry plot **(E)** and quantification plot **(F).** Data correspond to mean and SEM ($n=6$ animals/group). **(G, H)** Animals PGC-1$\alpha^{-/-}$ also showed decreased levels of microglial mitochondria and no changes were observed after the treatment with PNU282987. **(G)** Representative flow cytometry plot and **(H)** quantification plot. Data correspond to mean and SEM ($n=4$ animals/group). In all cases, analysis was performed using paired *t*-test. i.p., intraperitoneal. To see this illustration in color, the reader is referred to the web version of this article at www.liebertpub.com/ars

against their age control littermates, named as WT. Noteworthy was the finding that LysM^{cre}-Hmox1$^{\Delta/\Delta}$ mice injected with saline presented lower mitochondrial content in comparison with their age control littermates (WT Saline: 1.0 ± 0.08 *vs.* LysM^{cre}-Hmox1$^{\Delta/\Delta}$ Saline: 0.78 ± 0.057; Fig. 5D, F). Moreover, LysM^{cre}-Hmox1$^{\Delta/\Delta}$ animals injected with PNU282987 did not show an increase in mitochondrial content (LysM^{cre}-Hmox1$^{\Delta/\Delta}$ Saline: 0.78 ± 0.056 *vs.* PNU282987: 0.71 ± 0.16; Fig. 5E, F), corroborating the previous results obtained *in vitro* (Fig. 3).

We also aimed to further demonstrate the implication of PGC-1α in the effect of PNU282987 on mitochondrial biogenesis; for this issue we used PGC-1α$^{-/-}$ mice. The absence of PGC-1α produced similar effects to those found in LysM^{cre}-Hmox1$^{\Delta/\Delta}$ mice. When we analyzed the mitochondrial content in the microglial population, we also observed a decrease in mitochondrial mass in these animals when normalized against PGC-1α$^{+/+}$ (named as WT; WT Saline: 1.0 ± 0.04 *vs.* PGC-1α$^{-/-}$ Saline: 0.83 ± 0.063; Fig. 5D, H). Moreover, when PGC-1α$^{-/-}$ animals were injected with PNU282987, no changes were observed in mitochondrial content (PGC-1α$^{-/-}$ Saline: 0.83 ± 0.063 *vs.* PGC-1α$^{-/-}$ PNU282987: 0.89 ± 0.13; Fig. 5G, H). These observations are in concordance with the results obtained *in vitro* (Fig. 4).

Taken together, these results highlight the implication of α7 nAChR in promoting mitochondrial biogenesis not only *in vitro* but also *in vivo*. Moreover, we provide clear evidence that HO-1 and PGC-1α are necessary to induce the increase in the number of mitochondria elicited by α7 nAChR activation.

Discussion

In this study we show as far as we know, for the first time, that α7 nAChR activation increases the mitochondrial content and respiratory capacity in microglia by a mechanism that implicates Nrf2, HO-1, and PGC-1α.

Mitochondria are crucial organelles for cellular homeostasis, which govern pivotal functions such as ATP production, calcium homeostasis, and apoptosis; therefore, it is known that processes which alter mitochondrial activity can lead to disease. During neurodegeneration, besides mitochondrial dysfunction, a decrease in cholinergic markers such as nAChRs has been recognized (35). Among nAChRs, the α7 subtype is emerging as an interesting target for neuroprotection as it is implicated in a variety of processes. In the CNS, α7 nAChRs are expressed not only in neuronal cells, where they participate in neurotransmission and neurite outgrowth, but also in non-neuronal cells where they participate in several functions such as the control of inflammation (12).

In this study, we provide data for a new effect of the α7 nAChR, such as mitochondrial energetics. Indeed, we have described that α7 nAChR activation (using PNU282987 as agonist) activates glial mitochondrial biogenesis *in vitro* and *in vivo*, as evidenced by the following results: (i) treatment of glial cells with PNU282987 increased cellular mitochondrial mass (Fig. 1A–D); (ii) PNU282987 improved mitochondrial respiration (increasing basal oxygen consumption, ATP-linked respiration, and maximal respiration; Fig. 2); and (iii) i.p. administration of PNU282987 (10 mg/kg) increased mitochondrial mass in the microglial population *in vivo* (Fig. 5C, D).

As a decrease in the number and function of mitochondria seems to play a pivotal role in the development of a wide variety of pathologies such as Alzheimer's disease (AD) or Parkinson's disease (PD), these results position α7 nAChRs as target for neuroprotection. For instance, AD brains are also characterized by a decreased expression of mitochondrial complexes, decreased blood flow, and metabolic failure (16, 21, 37). Moreover, amyloid-beta (Aβ) and tau, both proteins associated to AD, have been reported to inhibit the activity of mitochondrial complexes of the electron transport chain, which derives in decreased synthesis of ATP (39).

Similarly, there are also bioenergetic defects associated to PD. For instance, mutations in parkin, which is a leading cause of PD development, alter mitochondrial biogenesis causing a loss in dopaminergic neurons (44). Moreover, decreases of ATP levels have been related to the widely reported decreased activity in complex I (14, 32, 42). Furthermore, the mitochondrial dysfunction associated to both diseases and other NDDs produces increased ROS levels which, in turn, trigger mitochondrial DNA (mtDNA) mutations, inhibit mitochondrial proliferation, and increase apoptosis, which finally lead to neurodegeneration (4a).

To understand the pathway by which α7 nAChR activates mitochondrial biogenesis, we have focused on the Nrf2/HO-1 axis. Our group has previously described that the neuroprotective properties mediated by α7 nAChR depend on the activation of the Jak2/PI3K/Akt cascade, which finally leads to an overexpression of HO-1 *via* Nrf2 transcription factor (9, 31).

In this study, we have shown that Nrf2 and HO-1 are necessary for the effects of PNU282987 on mitochondrial mass and function as indicated by the following evidences: (i) PNU282987 did not increase mitochondrial mass in Nrf2$^{-/-}$ animals (Fig. 3A), (ii) the specific inhibitor of HO-1 (SnPP) prevented the increase in mitochondrial mass produced by PNU282987 (Fig. 3C), (iii) α7 nAChR did not produce an increase in mitochondrial respiratory parameters when HO-1 was inhibited (Fig. 3D), and (iv) LysM^{cre}-Hmox1$^{\Delta/\Delta}$ animals injected with PNU282987 did not show an increase in microglial mitochondrial mass (Fig. 5E, F).

Several authors have previously described that HO-1 could be involved in mitochondrial biogenesis, although the mechanism has not been completely elucidated. This idea was raised by Suliman *et al.* who reported in 2007 that CO, a by-product of HO-1, increased cardiac mitochondrial biogenesis (47). These results have been corroborated also in hepatoma cells, where mitochondrial biogenesis was activated using a CO-releasing molecule and cobalt protoporphyrin (a HO-1 inducing agent) (15).

These authors demonstrated that this process was abolished when using a CO scavenger, indicating the implication of this by-product. Piantadosi *et al.* proposed that CO produced by HO-1 would cause the release of H_2O_2 from mitochondria, which could be activating the Nrf2 transcription factor that binds to the antioxidant response elements (ARE) activating the expression of a wide variety of genes, among them NRF-1, and thus activating mitochondrial biogenesis (33). Although the exact mechanism should be further investigated, our results corroborate the implication of Nrf2/HO-1 in the generation of new mitochondria.

As stated in the Introduction section, PGC-1α is considered the master regulator of mitochondrial biogenesis. In this study, we show that activation of α7 nAChR increases the expression of this transcriptional factor (Fig. 4A), which participates in the changes in mitochondrial mass elicited by PNU282987 (Fig. 4F). There are evidences in the literature that would link the expression of PGC-1α to Nrf2. Indeed,

both transcription factors have overlapping functions in regulating the antioxidant system, having been described to increase the expression of SODs or glutathione peroxidase 1 (3), among other antioxidant enzymes. These notions raise the possibility that the expression of one gene could be regulated by the expression of the other.

In this line, PGC-1α has been described to increase the expression of Nrf2 in a model of metabolic imbalance (1), although the direct interaction between them has not been demonstrated. Nevertheless, no changes in Nrf2 mRNA levels were observed when comparing WT and PGC-1$\alpha^{-/-}$ MEF cells (26). On the contrary, the PGC-1α promoter has two ARE core sequences (3, 43) even though they have not been demonstrated to be active. To assess this last regulation, we used PGC-1α promoter linked to luciferase reporter gene and we observed that Nrf2 increased the luciferase activity, indicating that Nrf2 could be controlling the expression of PGC-1α. In addition, pAMPK and pCREB could also be implicated in the activation of PGC-1α since these proteins were also upregulated in cells treated with the α7 nAChR agonist (Fig. 4B, C).

Taking into account that a decrease in PGC-1α or alterations in its signaling have been described in NDDs (4a) and PGC-1α knockout mice show neuropathology at earlier stages (17), these results are interesting from a pharmacological point of view. For that reason, compounds that could restore energy production and antioxidant capacity would be useful for the treatment of these pathologies and this is why PGC-1α is emerging as a new therapeutic target for neurodegenerative disorders (4a). Our results describe that the changes in mitochondrial mass elicited by α7 nAChR depend on the activation of PGC-1α as we did not observe mitochondrial biogenesis when we silenced PGC-1α in glial cultures (Fig. 4E) or when we used PGC-1α knockout mice (Fig. 5E, F). In conclusion, we describe a new pathway for increasing PGC-1α, which in turn increases mitochondrial content.

Interestingly, we have observed that the increase in mitochondrial number and activity derived from PNU282987 treatment was not accompanied by alteration in the mitochondrial membrane potential or an increase in the production of ROS (Fig. 1E, F). These results could be explained by the fact that the mechanism by which PNU282987 increased mitochondrial mass implicates PGC-1α and HO-1. PGC-1α has been reported to not only trigger the generation of new mitochondria but to also improve the antioxidant capacity and suppress ROS (43). Regarding HO-1, it is considered that both the enzyme itself and also its by-products have antioxidant properties, which could contribute to the maintenance of oxidative stress levels.

Although the aerobic respiration and generation of ATP have been considered the principal function of mitochondria, recent studies indicate the implication of mitochondria in controlling the inflammatory response (34, 48). Since α7 nAChRs have anti-inflammatory properties in macrophages (19, 49) and microglia (11, 30), we hypothesize that a potential link between the anti-inflammatory response and the increase in the cellular energetic capacity may coexist, although further studies need to be done to confirm this.

In conclusion, with this study we have progressed in the knowledge of α7 nAChR signaling. We describe for the first time how α7 nAChR activation, specifically in glia, increases not only mitochondrial mass but also mitochondrial function, showing a new mechanism that could complement the protective and anti-inflammatory properties of α7 nAChR signaling. We also provide mechanistic evidences showing the implication of HO-1 and PGC-1α, both controlled under Nrf2.

It should be noted that, apart from mitochondrial biogenesis, there are other processes necessary for the quality control of these organelles, such as mitochondrial fusion, mitochondrial mobility, or mitophagy. Whether α7 nAChR has the ability to control these processes remains unexplored and should be studied to better understand the implication of α7 nAChR in the mitochondrial network. Nevertheless, so far we can firmly conclude that microglial α7 nAChR improves mitochondrial functioning and this effect can be complementary to its anti-neuroinflammatory and neuroprotective properties for the treatment of NDDs.

Materials and Methods

Materials

Dulbecco's modified Eagle's medium: nutrient mixture F-12 (DMEM-F12) and fetal bovine serum (FBS) were obtained from Invitrogen (Madrid, Spain). Penicillin/Streptomycin purchased from Sigma (Madrid, Spain). TMRE, H_2DCFDA, Mtg-FM, and Hoechst were purchased from Molecular Probes (Invitrogen). PNU282987 and α-Bgtx were purchased from Tocris Scientific/Biogen (Madrid, Spain), SnPP from Frontier Scientific Europe (Lancashire, United Kingdom), CD45-FITC, CD11b-PE, and GLAST-APC were purchased from Miltenyi Biotec (Madrid, Spain).

Animals

All animal assays were carried out following the Guide for the Care and Use of Laboratory Animals and were previously approved by the Institutional Ethics Committee of Universidad Autónoma de Madrid, Spain, according to the European Guidelines for the use and care of animals for research in accordance with the European Union Directive of September 22, 2010 (2010/63/UE), and with the Spanish Royal Decree of February 1, 2013 (53/2013). All efforts were made to minimize the number of animals used and their suffering.

Mixed glial culture

Glial culture was performed using neonatal Sprague-Dawley rats (2–4 days old) as described before (29). Briefly, brain cortex was removed, mechanically homogenized, and passed through a 70-μm nylon filter. Cells were centrifuged at 1000 rpm for 5 min and plated at a density of 300,000 cells/ml in DMEM/F12 supplemented with 20% FBS. After 5 days *in vitro* (DIV), the medium was replaced by DMEM/F12 10% FBS. The medium was changed twice a week and experiments were performed after 7/10 DIV. The same protocol was used for mice glial cultures (WT and Nrf2$^{-/-}$) In all treatments, PNU282987 was used at a concentration of 10 μM during 48 h.

Flow cytometry

Samples were analyzed using Cytomics FC500 (Beckman Coulter, Madrid, Spain). Briefly, after the treatments, cells were collected and after centrifugation they were resuspended in 100 μl 1 × binding buffer (BD Biosciences, Madrid, Spain) containing the appropriate concentration of fluorescent dye

(MitoTracker Green-FM 100 n*M*, H_2DCFDA 1 μM, TMRE 100 n*M*, CD45-FITC, CD11b-PE, and GLAST-APC 1:100). After a 15-min incubation in the dark, 200 μl of phosphate buffered saline (PBS) 1 × was added. Cells were then subjected to FACS analysis with a total of 10,000 events per assay.

Mitochondrial copy number

Once the experiment was finished, cells were washed with PBS and DNA was isolated as follows. Cells were lysed in 500 μl of buffer containing 1 M Tris-HCl (pH 8), 5 M NaCl, 0.5 M EDTA, 10% sodium dodecyl sulfate (SDS), and 0.5 mg/ml proteinase K. After 2 h at 55°C, 500 μl of phenol/chloroform/isoamyl alcohol was added and mixed by vortex. Samples were centrifuged at 13,000 rpm for 10 min and the aqueous phase was transferred to a solution containing 0.7 (v/v) isopropanol and 0.3 sodium acetate 2 *M* at 50%. Samples were centrifuged 15 min at 13,000 rpm, and pellets were washed with 70% ethanol. After 5 min at 13,000 rpm centrifugation, pellets were dried and resuspended in water. DNA was amplified by quantitative polymerase chain reaction using the following primers: COII (subunit II cytochrome oxidase): F-CATTATTCCTAGAACCAGGCAGAC and R-GAATTA ATTCTAGGACGATGGGC; β-actin: F-CACCTTCCAGCA GATGTGGA and R-AGCATTTGCGGTGGACGATGG. The ratio COII/β-actin represents mtDNA/nuclear DNA (nDNA).

Immunofluorescence

Once the experiment was finished, cells were washed three times with PBS (NaCl 9 g/L, 10 m*M* NaH_2PO_4, 10 m*M* K_2HPO_4) and stained with the mitochondrial fluorescent stain MitoTracker Green FM (100 n*M*) for 20 min. Then, cells were washed three times with PBS and the nuclear marker Hoechst (1 μg/ml) was added in the second wash. Finally, images were taken with a confocal microscope (TCS SPE; Leica, Wetzlar, Germany) with a magnification of 63 ×.

Western blot

After treatment, cells were lysed in ice-cold lysis buffer (1% Nonidet P-40, 10% glycerol, 137 m*M* NaCl, 20 m*M* Tris–HCl, pH 7.5, 1 μg/ml leupeptin, 1 m*M* phenylmethylsulfonyl fluoride, 20 m*M* NaF, 1 m*M* sodium pyrophosphate, and 1 m*M* Na_3VO_4) supplemented with one tablet of protease inhibitor cocktail (Complete Mini; Roche, Mannhein, Germany). Thirty micrograms of protein lysates was resolved by polyacrylamide gel electrophoresis-SDS and transferred to immobilon-P membranes (Millipore Iberica, SA, Madrid, Spain). Membranes were incubated with anti-AMPKα [pT^{172}] (1:1000; Invitrogen), anti-AMPKα (1:500; Invitrogen), anti-p-CREB [Ser133] (1:1000; Cell Signaling), anti-CREB (1:1000; Cell Signaling), anti-HO-1 (1:1000; Santa Cruz), anti-PGC-1α (1:1000; Cayman Chemical), anti-MnSOD (1:1000; Stressgen), anti-cytochrome c (1:1000; BD PharMingen), anti-p-85-PI3K (1:50,000; Merck Millipore), anti-tubulin (1:10,000; Calbiochem), and anti-β-actin (1:100,000; Sigma).

Measurement of OCR in cultured cells

Oxygen consumption was measured using the XF24 Extracellular Flux Analyzer (Seahorse Bioscience). To obtain a homogeneous monolayer of cells, 150,000 cells per well were plated in XF24 cell culture microplates (Seahorse Bioscience) 7–10 days before the experiment.

To study the effect of PNU282987 on cell respiration, glial cells were exposed to 10 μM PNU282987 for 48 h and then incubated in unbuffered DMEM supplemented with 25 m*M* glucose, 1 m*M* pyruvate, and 2 m*M* glutamine at 37°C in a CO_2-free incubator for 1 h for equilibration before the experiment, period in which PNU282987 treatment was maintained in the unbuffered DMEM. A calibration cartridge (Seahorse Bioscience) was equilibrated overnight and then loaded with unbuffered DMEM (port A), 5 μg/ml oligomycin (port B), 500 μM DNP (port C), and 1 μM rotenone plus 1 μM antimycin A (port D), all obtained from Sigma-Aldrich. This allowed the determination of basal respiration, the amount of oxygen consumption linked to ATP production, the proton leak, the maximal respiration capacity, the reserve capacity, and the nonmitochondrial oxygen consumption. In all experiments, the protein concentration in each well was determined at the end of the measurements, using the Pierce BCA protein assay kit (Thermo Scientific) after cell lysis in RIPA buffer (Sigma-Aldrich) supplemented with protease inhibitor cocktail (Complete Mini; Roche), and was used to calibrate the oxygen consumption data.

Luciferase assay

For this assay, we used immortalized MEF cells derived from WT C57BL/6 mice. They were transfected using Lipofectamine 2000™ with 100 ng of a plasmid containing 2 kb of PGC-1α promoter linked to luciferase reporter gene (4). In addition, cells were transfected with 200 ng of either empty vector (pcDNA3.1) as control or with an expression factor of V5-tagged Nrf2 [pcDNA3.1-Nrf2-V5, kind gift of John Huyes (20)]. Twenty-four hours later, cells were treated with Sfn 10 μM or vehicle for 48 h. Forty-eight hours post-transfection, luciferase activity was determined with the Dual-Luciferase Reporter Assay System (Promega).

Adenoviral vectors and infections

Silencing Ad-shPGC-1α was constructed using the pSilencerTM Adeno 1.0 Cytomegalo-virus Promoter System from Ambion (Carlsbad, CA), as previously described (26). Primary glial cultures were infected during 8 h with adenoviral vectors. After infection, the medium was changed for cell recovery overnight, and then cells were treated for 48 h with PNU282987 10 μM.

Animal treatments

In vivo experiments were performed using C57BL/6 mice as WT at the age of 8–10 weeks. PNU282987 was administered at a concentration of 10 mg/kg by i.p. injection twice per day during 2 days.

$LysM^{Cre}Hmox1^{\Delta/\Delta}$ were generated in the Universidad Autónoma de Madrid from C57BL/6 $Hmox1^{LoxP}$ x $LysM^{Cre}$ mice (29). $Hmox1^{LoxP}$ mice were generated by the laboratory of Dr. Masayuki Yamamoto (Tohoku University Graduate School of Medicine) (18). They were obtained through RIKEN BioResource Center (B6J.129P2 Hmox1). C57BL/6 $LysM^{Cre}$ mice were generated by the laboratory of Dr. Forster (5) and obtained through the Jackson Laboratory [B6.129P2-Lyz2tm1(cre)Ifo/J Stock No. 004781].

Mice were used at 8–10 weeks of age and littermates were used as controls.

PGC-1$\alpha^{+/+}$ and PGC-1$\alpha^{-/-}$ mice were originally provided by Dr. Bruce Spiegelman (Dana-Farber Cancer Institute, Harvard Medical School) and following embryo transfer, a colony was established at the Instituto de Investigaciones Biomédicas (Madrid, Spain). Mice were used at 8–10 weeks of age and littermates as controls.

Microglial isolation

Microglia were isolated from whole-brain homogenates using Percoll gradient as previously described (23, 24). Briefly, animals were killed and brains were homogenized by passing through a 70-μM cell strainer using PBS 1 × (pH 7.4). Homogenates were centrifuged at 600 × *g* during 6 min at 10°C. Thereafter, brains were resuspended in isotonic Percoll of 70% and a discontinuous Percoll gradient was layered (70%, 50%, 35%, and 0%). The gradient was centrifuged at 2000 × *g* during 20 min at 10°C. Microglia were collected from the interface between 50% and 70% layers and cells were washed with PBS and ready for flow cytometry analysis.

Statistical analysis

Results are expressed as mean ± standard error of the mean. Statistical analysis was performed using GraphPad Prism 5.0 program. Every independent experiment was normalized with respect to control situation and the remaining variables were referred to that value. Analysis was performed using the following tests: paired *t*-test, one-way analysis of variance (ANOVA) followed by Newman–Keuls *post-hoc* test or two-way ANOVA followed by Bonferroni *post-hoc* test. Statistical significance was considered when $p \leq 0.05$.

Acknowledgments

This work was supported by the Spanish Ministry of Economy and Competence Ref. SAF2012-23332 and SAF2015-63935-R to M.G.L.; Ref. SAF2012-37693 to M.M. Comunidad Autónoma de Madrid grant number S2010/BMD-2361 to M.M. E.N. a predoctoral fellowship from Universidad Autónoma de Madrid. The work in SC laboratory is supported by grants from the Instituto de Salud Carlos III FIS (PI12/00933 and PI15/00448) and by Comunidad de Madrid (S2011/BMD-2402). We thank Laura Molero and Ana I. de las Heras for technical assistance in flow cytometry experiments and Javier Fernández-López for supervising statistical analyses. We also thank the Fundación Teófilo Hernando, the Network of Excellence Nrf2-net of MINECO, and the European Cooperation and Technology (COST Action BM1203/EU-ROS).

Author Disclosure Statement

No competing financial interests exist.

References

1. Aquilano K, Baldelli S, Pagliei B, Cannata SM, Rotilio G, and Ciriolo MR. p53 Orchestrates the PGC-1alpha-mediated antioxidant response upon mild redox and metabolic imbalance. *Antioxid Redox Signal* 18: 386–399, 2013.
2. Bach FH. Heme oxygenase-1: A therapeutic amplification funnel. *FASEB J* 19: 1216–1219, 2005.
3. Baldelli S, Aquilano K, and Ciriolo MR. Punctum on two different transcription factors regulated by PGC-1alpha: Nuclear factor erythroid-derived 2-like 2 and nuclear respiratory factor 2. *Biochim Biophys Acta* 1830: 4137–4146, 2013.
4. Borniquel S, Garcia-Quintans N, Valle I, Olmos Y, Wild B, Martinez-Granero F, Soria E, Lamas S, and Monsalve M. Inactivation of Foxo3a and subsequent down-regulation of PGC-1 alpha mediate nitric oxide-induced endothelial cell migration. *Mol Cell Biol* 30: 4035–4044, 2010.

4a. Chaturvedi RK and Flint Beal M. Mitochondrial diseases of the brain. *Free Radic Biol Med* 63: 1–29, 2013.

5. Clausen BE, Burkhardt C, Reith W, Renkawitz R, and Forster I. Conditional gene targeting in macrophages and granulocytes using LysMcre mice. *Transgenic Res* 8: 265–277, 1999.
6. Corona JC and Duchen MR. Impaired mitochondrial homeostasis and neurodegeneration: Towards new therapeutic targets? *J Bioenerg Biomembr* 47: 89–99, 2015.
7. This reference has been deleted.
8. De la Fuente M and Miquel J. An update of the oxidation-inflammation theory of aging: The involvement of the immune system in oxi-inflamm-aging. *Curr Pharm Des* 15: 3003–3026, 2009.
9. Del Barrio L, Martin-de-Saavedra MD, Romero A, Parada E, Egea J, Avila J, McIntosh JM, Wonnacott S, and Lopez MG. Neurotoxicity induced by okadaic acid in the human neuroblastoma SH-SY5Y line can be differentially prevented by alpha7 and beta2* nicotinic stimulation. *Toxicol Sci* 123: 193–205, 2011.
10. Dominy JE and Puigserver P. Mitochondrial biogenesis through activation of nuclear signaling proteins. *Cold Spring Harb Perspect Biol* 5: 1–16, 2013.
11. Egea J, Buendia I, Parada E, Navarro E, Leon R, and Lopez MG. Anti-inflammatory role of microglial alpha7 nAChRs and its role in neuroprotection. *Biochem Pharmacol* 97: 463–472, 2015.
12. Egea J, Buendia I, Parada E, Navarro E, Leon R, and Lopez MG. Anti-inflammatory role of microglial alpha7 nAChRs and its role in neuroprotection. *Biochem Pharmacol* 97: 463–472, 2015.
13. Friedman JR and Nunnari J. Mitochondrial form and function. *Nature* 505: 335–343, 2014.
14. Janetzky B, Hauck S, Youdim MB, Riederer P, Jellinger K, Pantucek F, Zochling R, Boissl KW, and Reichmann H. Unaltered aconitase activity, but decreased complex I activity in substantia nigra pars compacta of patients with Parkinson's disease. *Neurosci Lett* 169: 126–128, 1994.
15. Kim SK, Joe Y, Zheng M, Kim HJ, Yu JK, Cho GJ, Chang KC, Kim HK, Han J, Ryter SW, and Chung HT. Resveratrol induces hepatic mitochondrial biogenesis through the sequential activation of nitric oxide and carbon monoxide production. *Antioxid Redox Signal* 20: 2589–2605, 2014.
16. Liang WS, Reiman EM, Valla J, Dunckley T, Beach TG, Grover A, Niedzielko TL, Schneider LE, Mastroeni D, Caselli R, Kukull W, Morris JC, Hulette CM, Schmechel D, Rogers J, and Stephan DA. Alzheimer's disease is associated with reduced expression of energy metabolism genes in posterior cingulate neurons. *Proc Natl Acad Sci U S A* 105: 4441–4446, 2008.

17. Lin J, Wu PH, Tarr PT, Lindenberg KS, St-Pierre J, Zhang CY, Mootha VK, Jager S, Vianna CR, Reznick RM, Cui L, Manieri M, Donovan MX, Wu Z, Cooper MP, Fan MC, Rohas LM, Zavacki AM, Cinti S, Shulman GI, Lowell BB, Krainc D, and Spiegelman BM. Defects in adaptive energy metabolism with CNS-linked hyperactivity in PGC-1alpha null mice. *Cell* 119: 121–135, 2004.
18. Mamiya T, Katsuoka F, Hirayama A, Nakajima O, Kobayashi A, Maher JM, Matsui H, Hyodo I, Yamamoto M, and Hosoya T. Hepatocyte-specific deletion of heme oxygenase-1 disrupts redox homeostasis in basal and oxidative environments. *Tohoku J Exp Med* 216: 331–339, 2008.
19. Martelli D, McKinley MJ, and McAllen RM. The cholinergic anti-inflammatory pathway: A critical review. *Auton Neurosci* 182: 65–69, 2014.
20. McMahon M, Itoh K, Yamamoto M, and Hayes JD. Keap1-dependent proteasomal degradation of transcription factor Nrf2 contributes to the negative regulation of antioxidant response element-driven gene expression. *J Biol Chem* 278: 21592–21600, 2003.
21. Mosconi L, Tsui WH, De Santi S, Li J, Rusinek H, Convit A, Li Y, Boppana M, and de Leon MJ. Reduced hippocampal metabolism in MCI and AD: Automated FDG-PET image analysis. *Neurology* 64: 1860–1867, 2005.
22. Navarro E, Buendia I, Parada E, Leon R, Jansen-Duerr P, Pircher H, Egea J, and Lopez MG. Alpha7 nicotinic receptor activation protects against oxidative stress via heme-oxygenase I induction. *Biochem Pharmacol* 97: 473–481, 2015.
23. Norden DM, Fenn AM, Dugan A, and Godbout JP. TGFbeta produced by IL-10 redirected astrocytes attenuates microglial activation. *Glia* 62: 881–895, 2014.
24. Norden DM, Trojanowski PJ, Villanueva E, Navarro E, and Godbout JP. Sequential activation of microglia and astrocyte cytokine expression precedes increased iba-1 or GFAP immunoreactivity following systemic immune challenge. *Glia* 64: 300–316, 2015.
25. Nunnari J and Suomalainen A. Mitochondria: In sickness and in health. *Cell* 148: 1145–1159, 2012.
26. Olmos Y, Sanchez-Gomez FJ, Wild B, Garcia-Quintans N, Cabezudo S, Lamas S, and Monsalve M. SirT1 regulation of antioxidant genes is dependent on the formation of a FoxO3a/PGC-1alpha complex. *Antioxid Redox Signal* 19: 1507–1521, 2013.
27. Otterbein LE, Soares MP, Yamashita K, and Bach FH. Heme oxygenase-1: Unleashing the protective properties of heme. *Trends Immunol* 24: 449–455, 2003.
28. This reference has been deleted.
29. Parada E, Buendia I, Navarro E, Avendano C, Egea J, and Lopez MG. Microglial HO-1 induction by curcumin provides antioxidant, antineuroinflammatory, and glioprotective effects. *Mol Nutr Food Res* 59: 1690–1700, 2015.
30. Parada E, Egea J, Buendia I, Negredo P, Cunha AC, Cardoso S, Soares MP, and Lopez MG. The microglial alpha7-acetylcholine nicotinic receptor is a key element in promoting neuroprotection by inducing heme oxygenase-1 via nuclear factor erythroid-2-related factor 2. *Antioxid Redox Signal* 19: 1135–1148, 2013.
31. Parada E, Egea J, Romero A, del Barrio L, Garcia AG, and Lopez MG. Poststress treatment with PNU282987 can rescue SH-SY5Y cells undergoing apoptosis via alpha7 nicotinic receptors linked to a Jak2/Akt/HO-1 signaling pathway. *Free Radic Biol Med* 49: 1815–1821, 2010.
32. Parker WD, Jr., Parks JK, and Swerdlow RH. Complex I deficiency in Parkinson's disease frontal cortex. *Brain Res* 1189: 215–218, 2008.
33. Piantadosi CA, Carraway MS, Babiker A, and Suliman HB. Heme oxygenase-1 regulates cardiac mitochondrial biogenesis via Nrf2-mediated transcriptional control of nuclear respiratory factor-1. *Circ Res* 103: 1232–1240, 2008.
34. Piantadosi CA, Withers CM, Bartz RR, MacGarvey NC, Fu P, Sweeney TE, Welty-Wolf KE, and Suliman HB. Heme oxygenase-1 couples activation of mitochondrial biogenesis to anti-inflammatory cytokine expression. *J Biol Chem* 286: 16374–16385, 2011.
35. Picciotto MR and Zoli M. Nicotinic receptors in aging and dementia. *J Neurobiol* 53: 641–655, 2002.
36. Quik M, Zhang D, McGregor M, and Bordia T. Alpha7 nicotinic receptors as therapeutic targets for Parkinson's disease. *Biochem Pharmacol* 97: 399–407, 2015.
37. Rapoport SI. In vivo PET imaging and postmortem studies suggest potentially reversible and irreversible stages of brain metabolic failure in Alzheimer's disease. *Eur Arch Psychiatry Clin Neurosci* 249 Suppl 3: 46–55, 1999.
38. Rayamajhi N, Kim SK, Go H, Joe Y, Callaway Z, Kang JG, Ryter SW, and Chung HT. Quercetin induces mitochondrial biogenesis through activation of HO-1 in HepG2 cells. *Oxid Med Cell Longev* 2013: 154279, 2013.
39. Rhein V, Song X, Wiesner A, Ittner LM, Baysang G, Meier F, Ozmen L, Bluethmann H, Drose S, Brandt U, Savaskan E, Czech C, Gotz J, and Eckert A. Amyloid-beta and tau synergistically impair the oxidative phosphorylation system in triple transgenic Alzheimer's disease mice. *Proc Natl Acad Sci U S A* 106: 20057–20062, 2009.
40. Scarpulla RC. Transcriptional paradigms in mammalian mitochondrial biogenesis and function. *Physiol Rev* 88: 611–638, 2008.
41. Scarpulla RC, Vega RB, and Kelly DP. Transcriptional integration of mitochondrial biogenesis. *Trends Endocrinol Metab* 23: 459–466, 2012.
42. Schapira AH, Cooper JM, Dexter D, Clark JB, Jenner P, and Marsden CD. Mitochondrial complex I deficiency in Parkinson's disease. *J Neurochem* 54: 823–827, 1990.
43. St-Pierre J, Drori S, Uldry M, Silvaggi JM, Rhee J, Jager S, Handschin C, Zheng K, Lin J, Yang W, Simon DK, Bachoo R, and Spiegelman BM. Suppression of reactive oxygen species and neurodegeneration by the PGC-1 transcriptional coactivators. *Cell* 127: 397–408, 2006.
44. Stevens DA, Lee Y, Kang HC, Lee BD, Lee YI, Bower A, Jiang H, Kang SU, Andrabi SA, Dawson VL, Shin JH, and Dawson TM. Parkin loss leads to PARIS-dependent declines in mitochondrial mass and respiration. *Proc Natl Acad Sci U S A* 112: 11696–11701, 2015.
45. Streit WJ. Microglial senescence: does the brain's immune system have an expiration date? *Trends Neurosci* 29: 506–510, 2006.
46. Streit WJ and Xue QS. Life and death of microglia. *J Neuroimmune Pharmacol* 4: 371–379, 2009.
47. Suliman HB, Carraway MS, Tatro LG, and Piantadosi CA. A new activating role for CO in cardiac mitochondrial biogenesis. *J Cell Sci* 120: 299–308, 2007.
48. Suliman HB, Sweeney TE, Withers CM, and Piantadosi CA. Co-regulation of nuclear respiratory factor-1 by

NFkappaB and CREB links LPS-induced inflammation to mitochondrial biogenesis. *J Cell Sci* 123: 2565–2575, 2010.
49. Wang H, Yu M, Ochani M, Amella CA, Tanovic M, Susarla S, Li JH, Yang H, Ulloa L, Al-Abed Y, Czura CJ, and Tracey KJ. Nicotinic acetylcholine receptor alpha7 subunit is an essential regulator of inflammation. *Nature* 421: 384–388, 2003.

Address correspondence to:
Prof. Manuela G. Lopez
Departamento de Farmacología
Instituto Teófilo Hernando
Facultad de Medicina
Universidad Autónoma de Madrid
C/Arzobispo Morcillo 4
28029 Madrid
Spain

E-mail: manuela.garcia@uam.es

Date of first submission to ARS Central, March 16, 2016; date of final revised submission, August 23, 2016; date of acceptance, August 23, 2016.

Abbreviations Used

α7 nAChR = alpha7 nicotinic acetylcholine receptor
α-Bgtx = alpha-bungarotoxin
AD = Alzheimer's disease
ANOVA = analysis of variance
ARE = antioxidant response elements
ATP = adenosine triphosphate
CNS = central nervous system
CO = carbon monoxide
DIV = days *in vitro*
DNP = 2,4,-dinitrophenol
FBS = fetal bovine serum
H_2DCFDA = 2′,7′-dichlorofluorescein diacetate
HO-1 = heme-oxygenase-1
i.p. = intraperitoneal
MnSOD = manganese superoxide dismutase
mtDNA = mitochondrial DNA
Mtg = MitoTracker-Green
NDDs = neurodegenerative diseases
Nrf2 = nuclear erythroid 2-related factor 2
NRFs = nuclear respiratory factors
OCR = oxygen consumption rate
PBS = phosphate buffered saline
PD = Parkinson's disease
PGC-1α = peroxisome proliferator-activated receptor gamma coactivator 1α
PPARs = peroxisome proliferator-activated receptors
ROS = reactive oxygen species
SDS = sodium dodecyl sulfate
SEM = standard error of the mean
Sfn = sulforaphane
sh = small hairpin
SnPP = tin protoporphyrin-IX dichloride
SOD = superoxide dismutase
TMRE = tetramethylrhodamine, ethyl ester, perchlorate
WT = wild type

ANTIOXIDANTS & REDOX SIGNALING
Volume 00, Number 00, 2017

DOI: 10.1089/ars.2016.6836

ORIGINAL RESEARCH COMMUNICATION

PGC-1α Downregulation in Steatotic Liver Enhances Ischemia-Reperfusion Injury and Impairs Ischemic Preconditioning

Cristina Sánchez-Ramos,[1,#]; Ignacio Prieto,[1] Alberto Tierrez,[2] Javier Laso,[2,*] M. Pilar Valdecantos,[3] Ramon Bartrons,[4] Joan Roselló-Catafau,[5] and María Monsalve[1]

Abstract

Aims: Liver steatosis is associated with mitochondrial dysfunction and elevated reactive oxygen species (ROS) levels together with enhanced sensitivity to ischemia-reperfusion (IR) injury and limited response to preconditioning protocols. Here, we sought to determine whether the downregulation in the steatotic liver of peroxisome proliferator-activated receptor γ co-activator 1α (PGC-1α), a master regulator of mitochondrial metabolism and ROS that is known to play a role in liver metabolic control, could be responsible for the sensitivity of the steatotic liver to ischemic damage.

Results: PGC-1α was induced in normal liver after exposure to an IR protocol, which was concomitant with an increase in the levels of antioxidant proteins. By contrast, its induction was severely blunted in the steatotic liver, resulting in a modest induction of antioxidant proteins. Livers of PGC-$1\alpha^{-/-}$ mice on a chow diet were normal, but they exhibited an enhanced sensitivity to IR injury and also a lack of response to ischemic preconditioning (IPC), a phenotype that recapitulated the features of the steatotic liver in terms of liver damage, although the inflammatory response differed between both models. Utilizing an *in vitro* model of IPC, we found that PGC-1α expression was downregulated in hepatic cells cultured at 1% O_2; whereas it was induced after reoxygenation (3% O_2), and it was responsible for the recovery of antioxidant gene expression after the ischemic period.

Innovation & Conclusion: PGC-1α plays an important role in the protection against IR injury in the liver, which is likely associated with its capacity to induce antioxidant gene expression. *Antioxid. Redox Signal*. 00, 000–000.

Keywords: mitochondria, oxidative metabolism, antioxidants, oxidative stress, reactive oxygen species

Introduction

LIVER AND KIDNEY are the most frequently and successfully transplanted organs; however, the number of donor livers is insufficient to meet the rising demand for transplants (37). Moreover, a maximum of 40% of livers for transplant present macrovascular steatosis, a characteristic associated with a poor tolerance of the transplanted organ to ischemia-reperfusion (IR) injury (21, 27). Consequently, there is a pressing need to limit the primary non-function or liver failure of such transplants.

This challenge has guided the development of strategies to improve IR tolerance of steatotic livers and several preconditioning techniques have been tested, including ischemic preconditioning (IPC), by which prior application of brief IR confer a state of protection against subsequent IR injury.

[1]Instituto de Investigaciones Biomédicas ''Alberto Sols'' (CSIC-UAM), Madrid, Spain.
[2]Fundación Centro Nacional de Investigaciones Cardiovasculares Carlos III (CNIC), Madrid, Spain.
[3]Centro de Investigación Biomédica en Red de Diabetes y Enfermedades Metabólicas Asociadas (CIBERdem), ISCIII, Madrid, Spain.
[4]Unitat de Bioquímica i Biologia Molecular, Departament de Ciències Fisiològiques, Campus de Bellvitge, IDIBELL-Universitat de Barcelona, Hospitalet, Spain.
[5]Experimental Hepatic Ischemia–Reperfusion Unit, Institut d'Investigacions Biomèdiques de Barcelona (CSIC), Barcelona, Spain.
[#]*Current affiliation:* Fundación Centro Nacional de Investigaciones Cardiovasculares Carlos (CNIC), Madrid, Spain.
[*]*Current affiliation:* Laboratori de Referència de Catalunya, Barcelona, Spain.

Innovation

The contribution of oxidative stress to the enhanced sensitivity of the steatotic liver to IR injury and the poor response to preconditioning protocols are well established. However, the molecular basis remains a matter of controversy. This study identifies peroxisome proliferator-activated receptor γ co-activator 1α (PGC-1α) as a key mediator of this effect and elucidates the molecular mechanism involved. This result has clinical significance, as it suggests that evaluation of PGC-1α levels can have predictive value in liver transplantation.

Unfortunately, the limited success of IPC has prevented its widespread use in the clinical setting (30, 44).

The poor tolerance of the steatotic liver to IR has been attributed, at least in part, to the generation of high levels of reactive oxygen species (ROS) (9, 11, 13). ROS are well-characterized mediators of hepatocyte cell death after reperfusion (18), and it has been hypothesized that because the steatotic liver is under basal oxidative stress, the further increase of ROS during reperfusion drives the massive induction of hepatocyte death in this setting (16, 41).

This hypothesis has led to the evaluation of different antioxidants that are expected to limit IR injury in the steatotic liver. Although results have been partially encouraging, at least for acute liver damage (35, 49), they have not proved to be efficacious in humans, possibly because ROS are long-term preconditioning mediators and their signaling activity is also required for the successful engraftment of the transplant (2, 36). More promising are the results on new experimental approaches that aim at controlling ROS levels, but are not based on antioxidant therapy (5, 31).

Peroxisome proliferator-activated receptor γ co-activator 1α (PGC-1α) is a transcriptional coactivator that controls the expression of most, if not all, of the metabolic pathways that allow the cellular adaptation to limited nutrient availability or to increased metabolic demand (i.e., cold, exercise) (43). Importantly, PGC-1α boosts the catabolic and oxidative capacity of the cell, and it coordinately induces the expression of a suite of antioxidant enzymes that prevents oxidative damage under these conditions (48). As a result of PGC-1α induction, cells present an enhanced antioxidant capacity and a net reduction in ROS levels.

Obesity and the metabolic syndrome are usually associated with a decrease in PGC-1α activity in all the tissues and cell types where it has been investigated, including the liver (1, 4, 32, 39, 50). Previous results from our group have shown that PGC-1α regulates antioxidant gene expression and ROS levels in hepatocytes (38), pointing to a role for PGC-1α in IR tolerance. This notion is supported by several reports suggesting that PGC-1α may play a protective role against ischemic injury in heart, kidney, and the central nervous system (15, 20, 26).

In the present study, we aimed at elucidating the role of PGC-1α in the poor tolerance of the steatotic liver to IR injury and IPC. We found that IR induces PGC-1α expression in the normal liver and its induction drives the increased expression of antioxidant enzymes; however, this response is absent in the steatotic liver. Furthermore, we demonstrate that the absence of PGC-1α prevents effective IPC. Our findings lead us to conclude that the poor response of the steatotic liver to IR and IPC is, at least in part, attributable to the failure of PGC-1α to induce antioxidant systems in response to IR.

Results

Liver steatosis downregulates PGC-1α expression and leads to a reduction in the levels of antioxidant proteins

To assess the role of PGC-1α in the response of the steatotic liver to IR, we first evaluated the impact of hepatic steatosis for PGC-1α expression and activity. To do this, C57BL/6 wild-type (PGC-1$\alpha^{+/+}$) mice were fed either a standard chow diet (control) or a high-fat diet (HFD) for 7 weeks. Although HFD had only a marginal effect on the whole body (Fig. 1A) and liver weight (Fig. 1B), after this time, it led to a substantial level of hepatic steatosis as evidenced by the marked paler color of the liver (Fig. 1B). The presence of macrovesicular steatosis in the liver of HFD-fed mice was confirmed by Oil Red O staining of frozen liver sections (Fig. 1C and Supplementary Fig. S1; Supplementary Data are available online at www.liebertpub.com/ars).

Analysis of liver histology by hematoxylin and eosin (H&E) staining showed a vacuolated pattern that is generally associated with liver steatosis in HFD-fed mice that was absent in the liver of chow-fed mice, and a preservation of the general structure of the parenchyma (Fig. 1D).

We next measured PGC-1α protein expression in the liver of mice on the two diets by Western blotting to assess the impact of HFD on PGC-1α. In agreement with a previous report (1), PGC-1α expression in the liver was significantly lower in HFD-fed mice than in mice on a chow diet (Fig. 2A and Supplementary Fig. S2A), indicating that steatosis downregulates its expression.

To confirm this finding, we evaluated the impact of liver PGC-1α downregulation on the expression of well-characterized PGC-1α-regulated proteins, including antioxidants. Thus, we compared the impact of liver steatosis in wild-type mice with that of mice with whole-body genetic deletion of PGC-1α. PGC-1$\alpha^{-/-}$ mice are slightly leaner than PGC-1$\alpha^{+/+}$ mice and do not present liver steatosis under a standard chow diet (Fig. 1A, B). However, quantification of triglyceride (TG) liver content showed that both HFD-fed mice and chow-fed PGC-1$\alpha^{-/-}$ mice had significantly higher levels than PGC-1$\alpha^{+/+}$ mice on a chow diet (Supplementary Fig. S3).

When wild-type mice on a chow diet were compared with HFD-fed mice and PGC-1$\alpha^{-/-}$ mice, the expression of several antioxidant proteins, including MnSOD, Prx3, Prx5, Trx2, and TR2 together with other PGC-1α-regulated proteins (Cyt c and VEGF-A), was downregulated both in PGC-1$\alpha^{+/+}$ steatotic liver provoked by HFD and in PGC-1$\alpha^{-/-}$ liver. By contrast, the expression of UCP-2 and catalase was induced in PGC-1$\alpha^{+/+}$ steatotic liver (Fig. 2B and Supplementary Fig. S3). UCP-2 has been previously reported to be induced in the steatotic liver by ROS and free lipids (14, 22, 46), and catalase is elevated in patients with non-alcoholic fatty liver disease and enhanced oxidative stress (34).

Collectively, these data suggest that the general decrease of antioxidant protein expression in the steatotic liver results from the downregulation of PGC-1α expression and are consistent with a possible role for PGC-1α in maintaining ROS homeostasis in the liver.

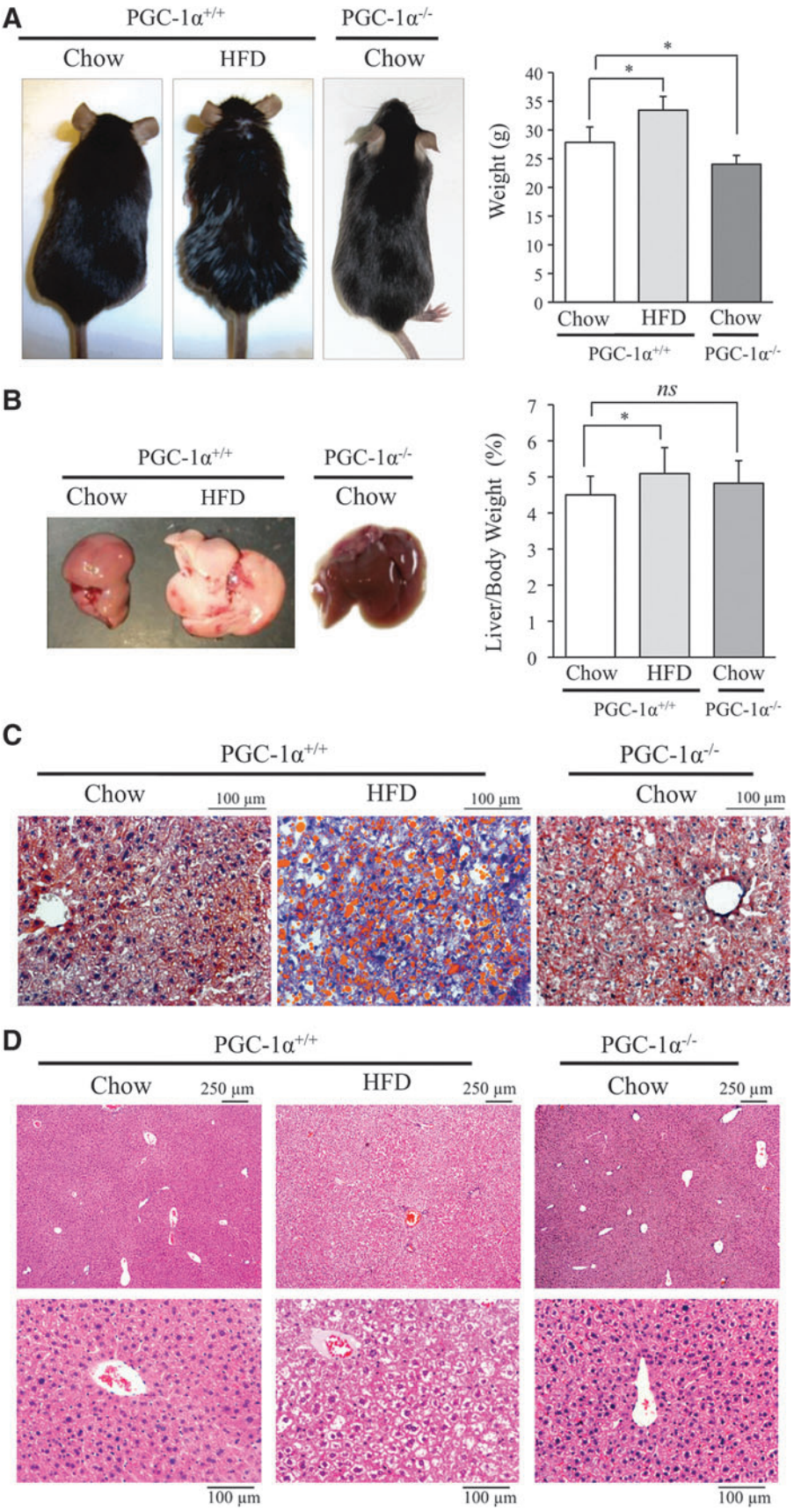

FIG. 1. PGC-1α$^{+/+}$ mice fed with HFD for 7 weeks develop hepatic steatosis, whereas PGC-1α$^{-/-}$ mice fed a standard chow diet do not present hepatic steatosis. (A) *Left panel*: representative images of mice in the study groups: PGC-1α$^{+/+}$ mice fed with a standard chow diet or HFD for 7 weeks and PGC-1α$^{-/-}$ mice fed with a standard chow diet. *Right panel*: average body weight at the time the animals were sacrificed. **(B)** *Left panel*: whole liver representative images. *Right panel*: relative liver/body weight. **(C)** Oil Red O staining of liver cryosections. Scale bars are 100 μm. **(D)** Liver sections stained with H&E. Scale bars are 100 and 250 μm. Data are means ± SD. *$p < 0.05$; *ns*, non-significant. H&E, hematoxylin and eosin; HFD, high-fat diet; PGC-1α, peroxisome proliferator-activated receptor γ co-activator 1α.

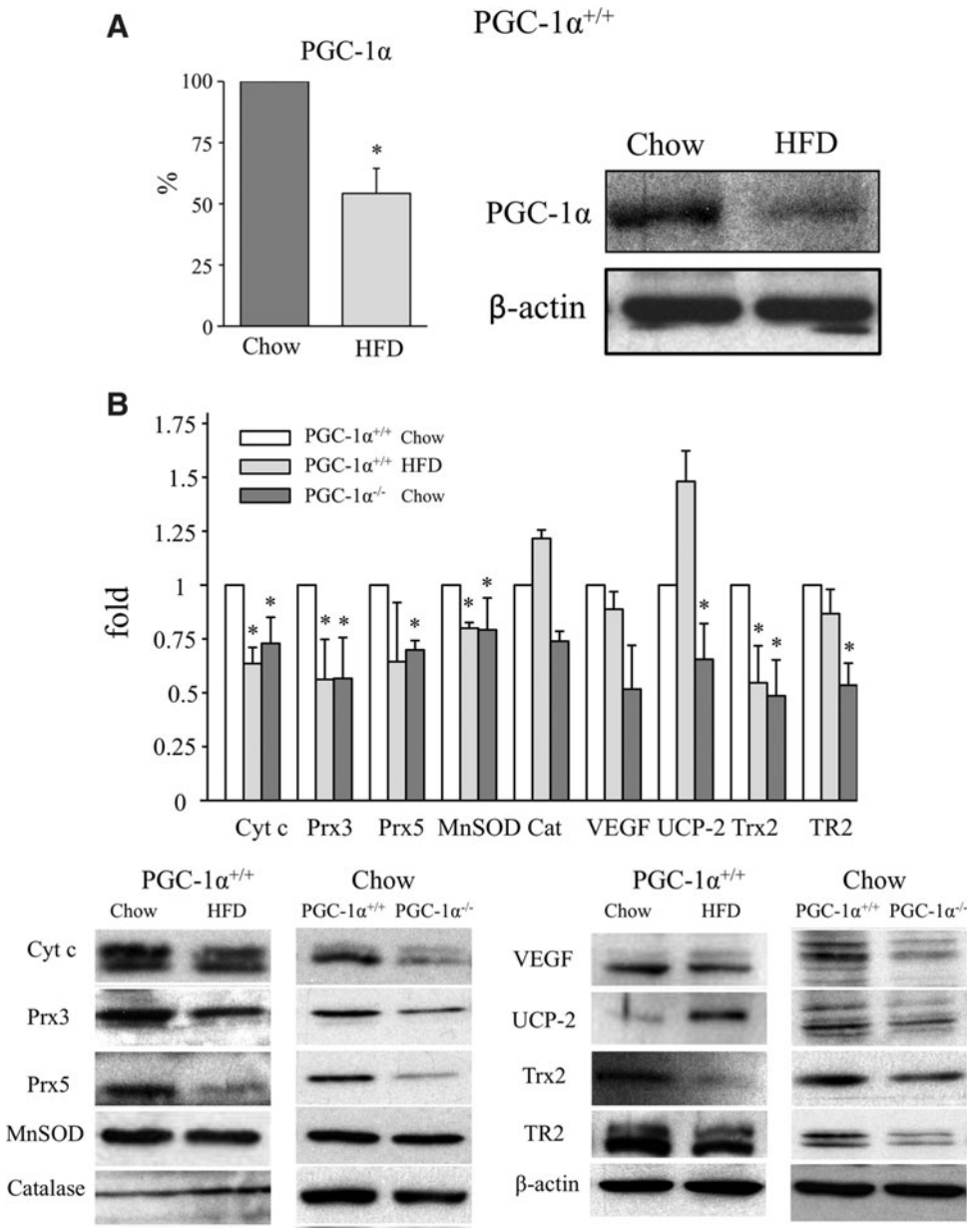

FIG. 2. Liver steatosis downregulates PGC-1α expression and reduces antioxidant protein levels. PGC-1$\alpha^{+/+}$ mice were fed with a chow diet or HFD for 7 weeks, and PGC-1$\alpha^{-/-}$ mice were fed with a chow diet. **(A)** PGC-1α levels were analyzed by WB. **(B)** WB analysis of proteins regulated by PGC-1α. β-actin was used as a loading control. Data are means ± SD. $*p < 0.05$. WB, Western blotting.

PGC-1α is induced in the liver after IR

Elevated generation of ROS after reperfusion has been demonstrated to play an important role in tissue damage by IR (12, 23, 40, 51–53), and to be a key mediator of the adaptive changes that are associated with IPC (24, 25). It has also been proposed that the elevated levels of ROS produced by the steatotic liver are responsible for its enhanced vulnerability to IR damage (9). Because PGC-1α has been shown to be induced by ROS and hypoxia (3, 29, 42, 48), we next analyzed PGC-1α expression in the liver of wild-type mice on a chow diet and HFD after exposure to IR and IPC protocols.

We found that both PGC-1α mRNA and protein levels were increased by IR and even more so by IPC 6 h after reperfusion in chow-fed mice (Fig. 3A and Supplementary Fig. S4A). By contrast, PGC-1α expression was only marginally increased in the steatotic liver of HFD-fed mice (Fig. 3A and Supplementary Fig. S4A). At 4 h post-IR, PGC-1α levels did not show significant differences among the groups (Supplementary Fig. S5).

Since PGC-1α regulates antioxidant gene expression in the liver, we next evaluated whether PGC-1α induction was associated with an induction of antioxidant enzymes and other PGC-1α target genes after IR. Among the genes tested in wild-type mice on a chow diet, we detected a significant increase in the mRNA levels of UCP-2 and Trx2 at 24 h after IR, whereas IPC resulted in a significant increase in Cyt c, Prx3, MnSOD, VEGF, UCP-2, Trx2 mRNA, Cyt c, Prx3, Prx5, catalase, VEGF, UCP-2, and TrxR2 protein (Fig. 3B, C and Supplementary Figs. S4B and S6).

The enhanced vulnerability of the steatotic liver to IR damage has been proposed to be the consequence of elevated ROS levels. When we repeated the analysis in HFD-fed mice, the absence of PGC-1α induction in response to IR or IPC was associated with a significantly reduced induction of antioxidant

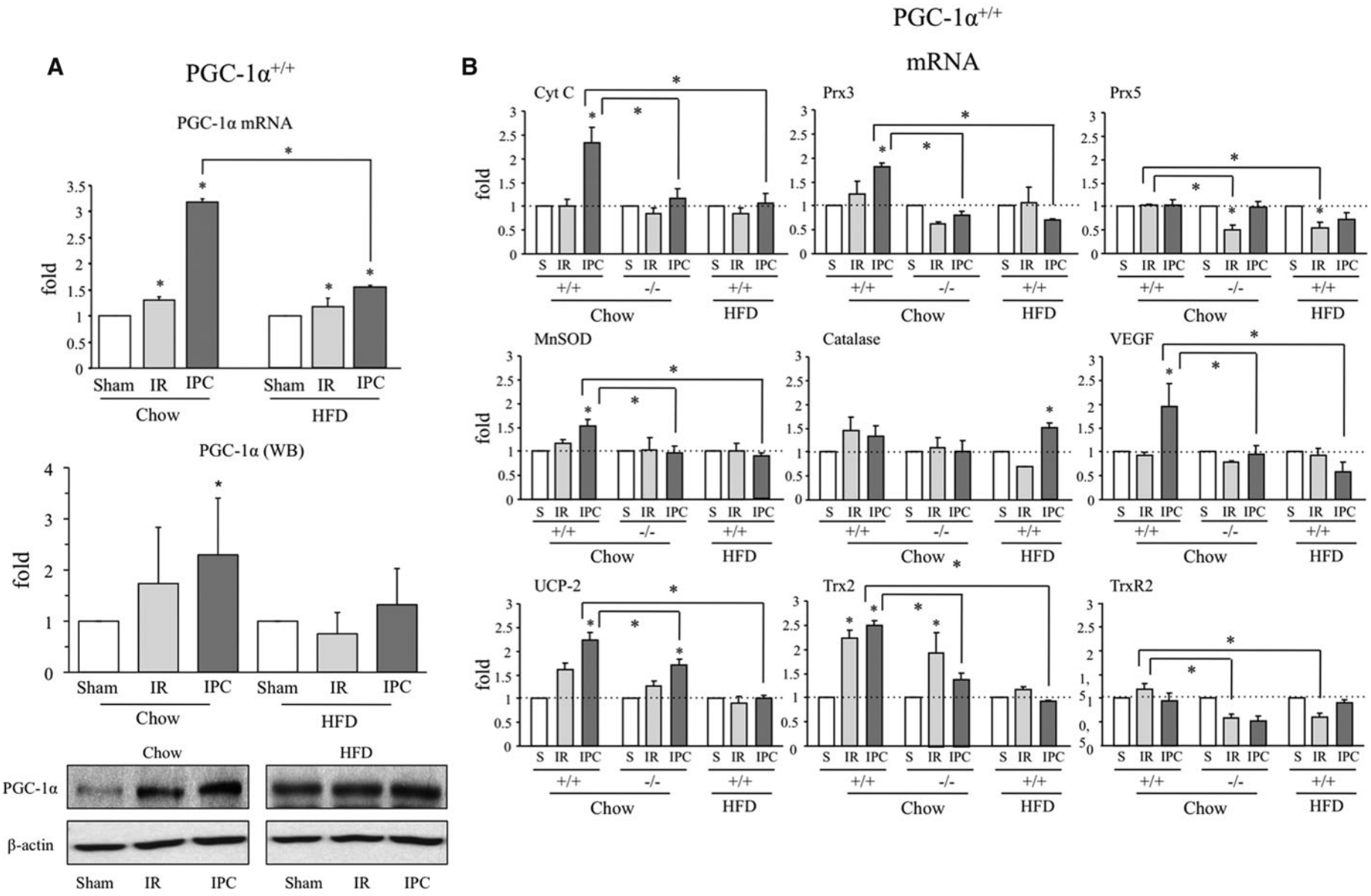

FIG. 3. Liver steatosis blocks PGC-1α induction in response to IPC. PGC-1$\alpha^{+/+}$ mice were fed with a chow diet or HFD for 7 weeks, and PGC-1$\alpha^{-/-}$ mice were fed with a chow diet. Mice were subjected to a total liver IR protocol with or without prior preconditioning (IPC). Animals were sacrificed, and liver samples were collected at 6 h and 24 h post-IR. **(A)** mRNA and protein levels of PGC-1α. Control samples were assigned the value of 1. **(B)** mRNA levels of PGC-1α target genes. **(C)** WB analysis of PGC-1α targets. β-actin was used as a loading control. Data are means ± SD. *$p < 0.05$. IPC, ischemic preconditioning; IR, ischemia-reperfusion.

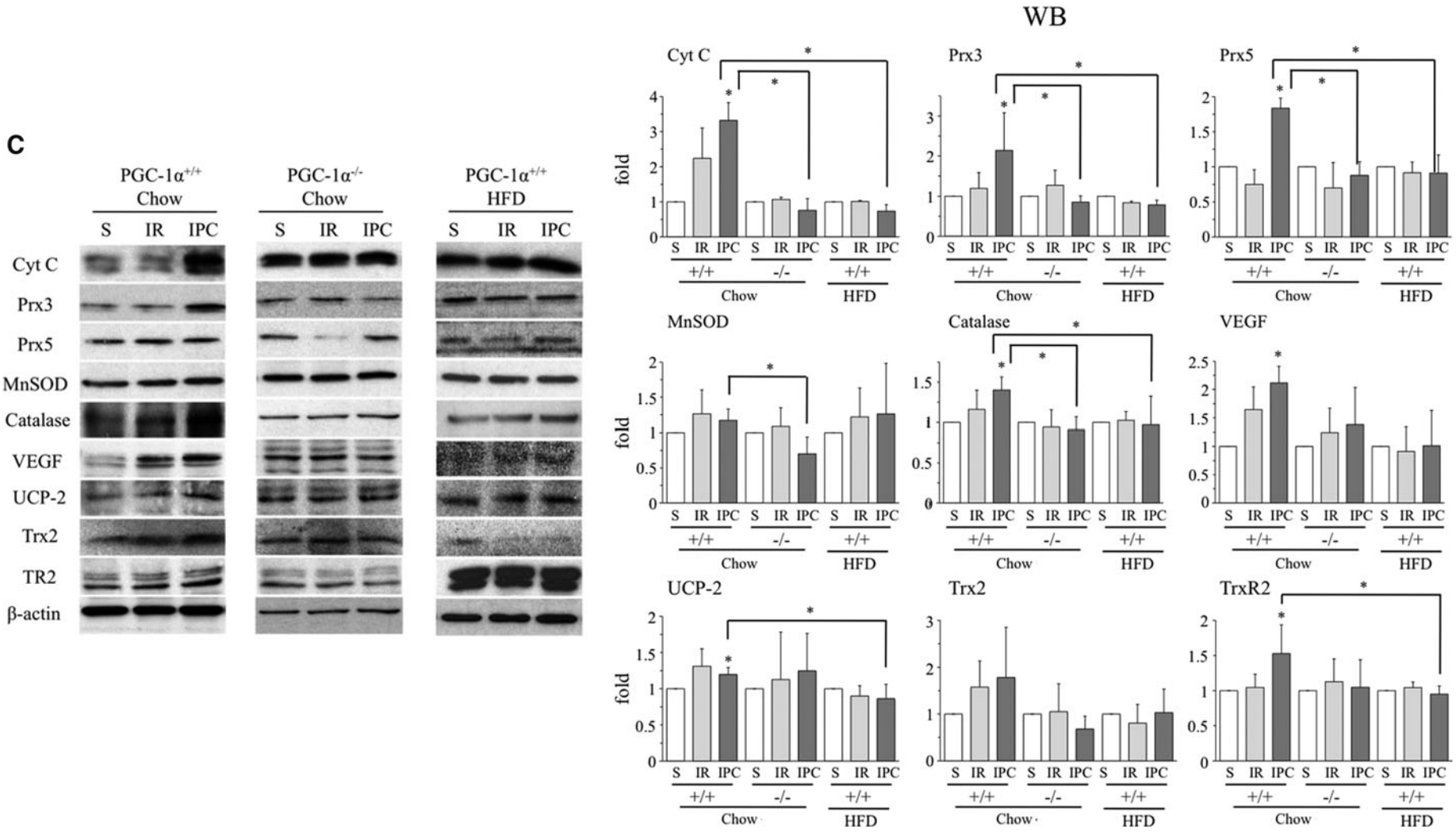

FIG. 3. (Continued)

enzymes in the steatotic liver (Fig. 3B, C and Supplementary Fig. S4D), pointing to a role for PGC-1α in this process.

To test this hypothesis, we analyzed antioxidant enzyme induction after IR and IPC in the liver of PGC-1$\alpha^{-/-}$mice. As anticipated, antioxidant induction was significantly reduced in PGC-1$\alpha^{-/-}$ mice (Fig. 3B, C and Supplementary Fig. S4C). These results strongly suggest that PGC-1α mediates the induction of antioxidant enzymes in response to IR. Importantly, oxidative stress markers such as 4-HNE protein modification and oxidative DNA damage (8-OH-dG) were higher in the liver of PGC-1$\alpha^{-/-}$ mice than in lean PGC-1$\alpha^{+/+}$ mice (Supplementary Fig. S7).

PGC-1α mediates IPC

Despite significant efforts, IPC has failed to show efficacy in improving the poor tolerance of the fatty liver to IR damage. Given that the enhanced susceptibility of the fatty liver to IR damage has been attributed to its high levels of ROS, we speculated that failure to induce PGC-1α and the consequent reduction in antioxidant defense could be related to the poor tolerance of the steatotic liver to IR and IPC protocols. To test this idea, we compared the liver damage induced by IR with or without prior IPC between PGC-1$\alpha^{-/-}$ and PGC-1$\alpha^{+/+}$ mice with a normal or steatotic liver. Sham-treated animals were used to determine basal parameters.

Severity of IR injury was first assessed by determining plasma levels of the liver transaminases alanine aminotransferase (ALT/GPT) and aspartate aminotransferase (AST/GOT) 24 h after reperfusion. We found that prior IPC reduced the plasma concentration of the IR liver damage markers ALT/AST in PGC-1$\alpha^{+/+}$ mice with a normal liver, whereas it increased their concentration both in PGC-1$\alpha^{+/+}$ mice with a steatotic liver and in PGC-1$\alpha^{-/-}$ mice (Fig. 4A). These results pointed to a requirement of PGC-1α for preconditioning of the liver and suggested that reduced PGC-1α expression in the steatotic liver may be responsible for the failure to induce tolerance to ischemic insult after an IPC protocol.

We next evaluated the extent of damage in liver parenchyma in the same groups of mice by histology 24 h and 1 week after IR. At 24 h, we expected to find evidence for hepatocyte cell death, collapsed microvessels, and inflammation, and at 1 week we expected to find evidence for ongoing remodeling, resolution of the inflammatory phase, and regenerative activity, including angiogenesis. H&E-stained sections from 24 h samples of liver from PGC-1$\alpha^{+/+}$ mice on a chow diet showed that the relatively large lesions (areas of disrupted parenchymal structure) detected after IR were significantly decreased by the IPC protocol. By contrast, in PGC-1$\alpha^{+/+}$ mice with a steatotic liver and in PGC-1$\alpha^{-/-}$ mice, the IPC protocol increased the lesion size and perivascular inflammatory infiltrates could be identified (Fig. 4B).

However, a marked difference was noted between PGC-1$\alpha^{+/+}$ steatotic livers and PGC-1$\alpha^{-/-}$ livers regarding the extent of inflammatory infiltration: PGC-1$\alpha^{+/+}$ steatotic livers had extensive parenchymal infiltrates after IR and IPC protocols, whereas infiltrates were more restricted to perivascular areas in PGC-1$\alpha^{-/-}$ livers (Fig. 4B). Anti-F4/80 IHQ analysis of the number of macrophages present in the liver did not evidence any clear differences among the groups, but showed a statistically significant difference in the response to IR/IPC that could relate to a higher basal level of macrophages in PGC-1$\alpha^{-/-}$ mice and a poorer inflammatory response to IR/IPC (Supplementary Fig. S8A, B).

Quantitative PCR of retro-transcribed cDNA (qRT-PCR) analysis of the main inflammatory mediators showed higher levels of IL-1β and iNOS and lower levels of IL-4 in PGC-1$\alpha^{-/-}$ mice, which could suggest a shift in the M1/M2 ratio in PGC-1$\alpha^{-/-}$ mice (Supplementary Fig. S8C).

Apoptotic cell death at 24 h was evaluated by terminal transferase dUTP nick end-labeling (TUNEL) staining of histological sections. Consistent with the earlier results, the extent of apoptotic cell death (measured as the number of TUNEL-positive cells) after IR in PGC-1$\alpha^{+/+}$ mice with a normal liver was significantly reduced by the IPC protocol, whereas in both PGC-1$\alpha^{+/+}$ mice with steatotic livers and in PGC-1$\alpha^{-/-}$ mice, the IPC protocol did not reduce but rather increased the number of TUNEL-positive cells (Fig. 4C).

Moreover, the number of TUNEL-positive cells was higher in PGC-1$\alpha^{+/+}$ steatotic livers than in PGC-1$\alpha^{-/-}$ livers, a result in accord with the findings of liver damage by plasma transaminase activity (Fig. 4C). Intriguingly, this difference did not seem to correlate with the size of the lesions, as determined by H&E staining (Fig. 4B). Altogether, these findings suggest that PGC-1α induction of antioxidant genes protects the liver from IR damage and is an important mediator of IPC.

Histological analysis of the liver at 1-week post-IR in PGC-1$\alpha^{+/+}$ mice on a chow diet revealed what appeared to be small fibrotic areas, which were essentially absent in the same group treated with an IPC protocol (Fig. 5A). Consistent with the results from 24 h post-IR, the IPC protocol did not reduce but rather increased the size of the remodeling area both in PGC-1$\alpha^{+/+}$ mice with a steatotic liver and in PGC-1$\alpha^{-/-}$ mice (Fig. 5A), supporting the presumably protective role of PGC-1α in both acute and long-term IR injury in the liver.

Nevertheless, closer inspection of the liver structure after the IPC protocol revealed a more marked disruption in PGC-1$\alpha^{-/-}$ liver than in PGC-1$\alpha^{+/+}$ steatotic liver. Two structural differences were evident: Inflammatory cells showed a more dispersed pattern in PGC-1$\alpha^{-/-}$ liver, with the majority of inflammatory foci presenting a perivascular location (Fig. 5B); in addition, the liver of PGC-1$\alpha^{-/-}$ mice had larger blood vessels, which were frequently occluded, whereas vessels were generally smaller in PGC-1$\alpha^{+/+}$ mice with a steatotic liver and were loaded with erythrocytes (Fig. 5B). These observations likely relate to the low survival rate noted in the group of PGC-1$\alpha^{+/+}$ mice with a steatotic liver (70% died at day 5 post-IR), whereas all PGC-1$\alpha^{-/-}$ mice survived the entire week despite extensive liver damage.

The extent of leukocyte infiltration 1-week post-IR was quantified in histological sections using the pan leukocyte marker CD45. In sham animals, the number of CD45$^+$ cells was significantly higher in PGC-1$\alpha^{-/-}$ and PGC-1$\alpha^{+/+}$ mice with a steatotic liver than in normal PGC-1$\alpha^{+/+}$ mice, suggesting that the low-grade chronic inflammation associated with steatosis is also present in PGC-1$\alpha^{-/-}$ mice (Fig. 5C).

The IR protocol resulted in a significant increase in the number of CD45$^+$ cells in both wild-type and steatotic PGC-1$\alpha^{+/+}$ mice, but it failed to induce a corresponding increase in PGC-1$\alpha^{-/-}$ mice, suggesting a poor response to normal inflammatory stimuli in these animals that is consistent with the restricted perivascular distribution observed in histology (Fig. 5C). No significant differences were found in the number of CD45$^+$ cells between the IR and IPC protocols in any animal group.

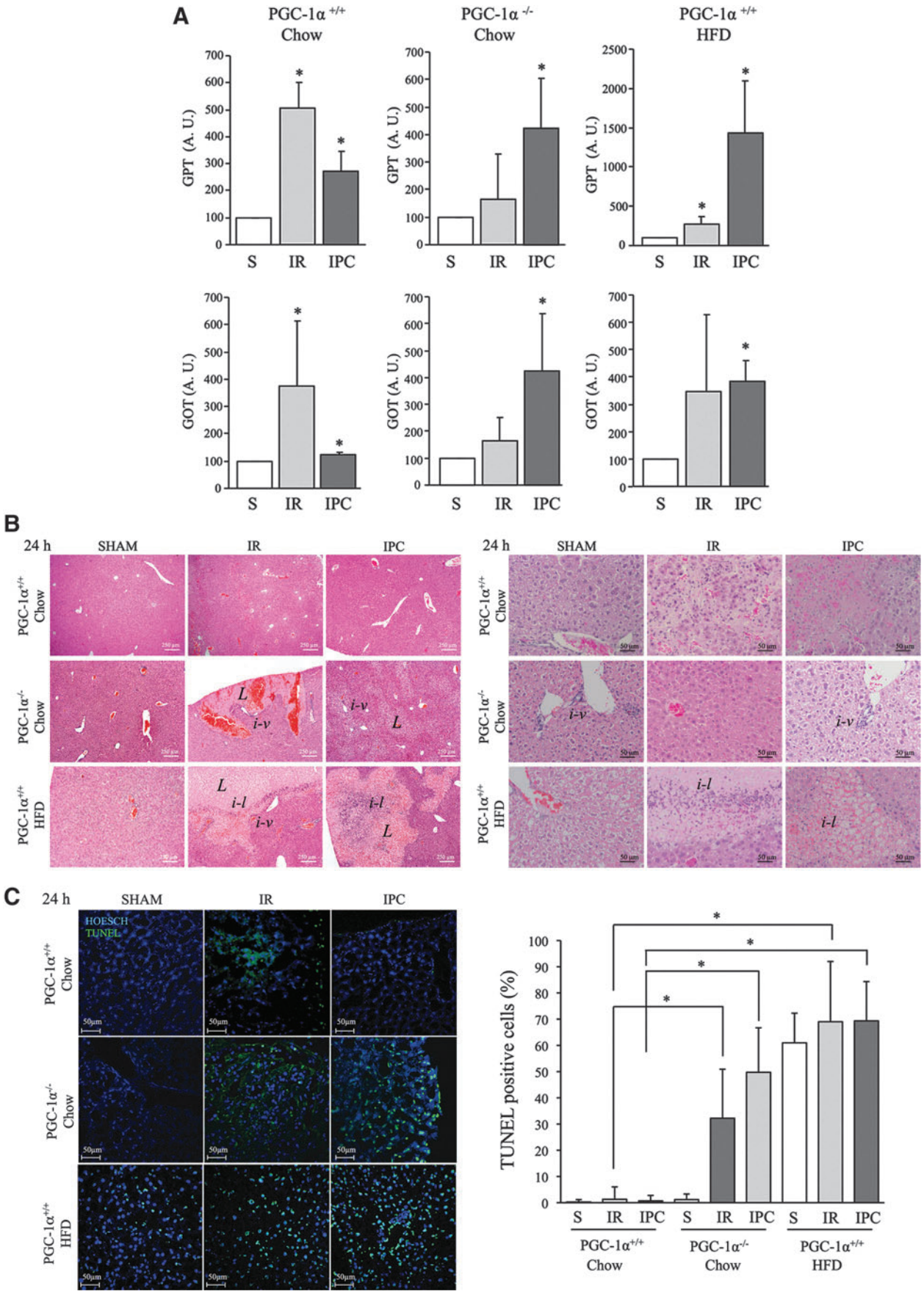

FIG. 4. Liver of PGC-1α$^{-/-}$ mice does not respond to IPC. PGC-1α$^{+/+}$ mice were fed with a chow diet or HFD for 7 weeks, and PGC-1α$^{-/-}$ mice were fed with a chow diet. Mice were subjected to a total liver IR protocol with or without prior preconditioning (IPC). **(A)** Plasma levels of transaminases GPT and GOT 24 h post-IR. **(B)** H&E -stained histological sections 24 h post-IR. Scale bars are 250 μm (*left panel*) and 50 μm (*right panel*). L/l, lesion; i, infiltrate; v, vascular. **(C)** *Left panel*: TUNEL staining of histological sections 24 h post-IR. Scale bars are 50 μm. *Right panel*: the percentage of TUNEL-positive cells relative to the number of nuclei stained with Hoechst 33258. Data are means ± SD. $*p < 0.05$. TUNEL, terminal transferase dUTP nick end-labeling.

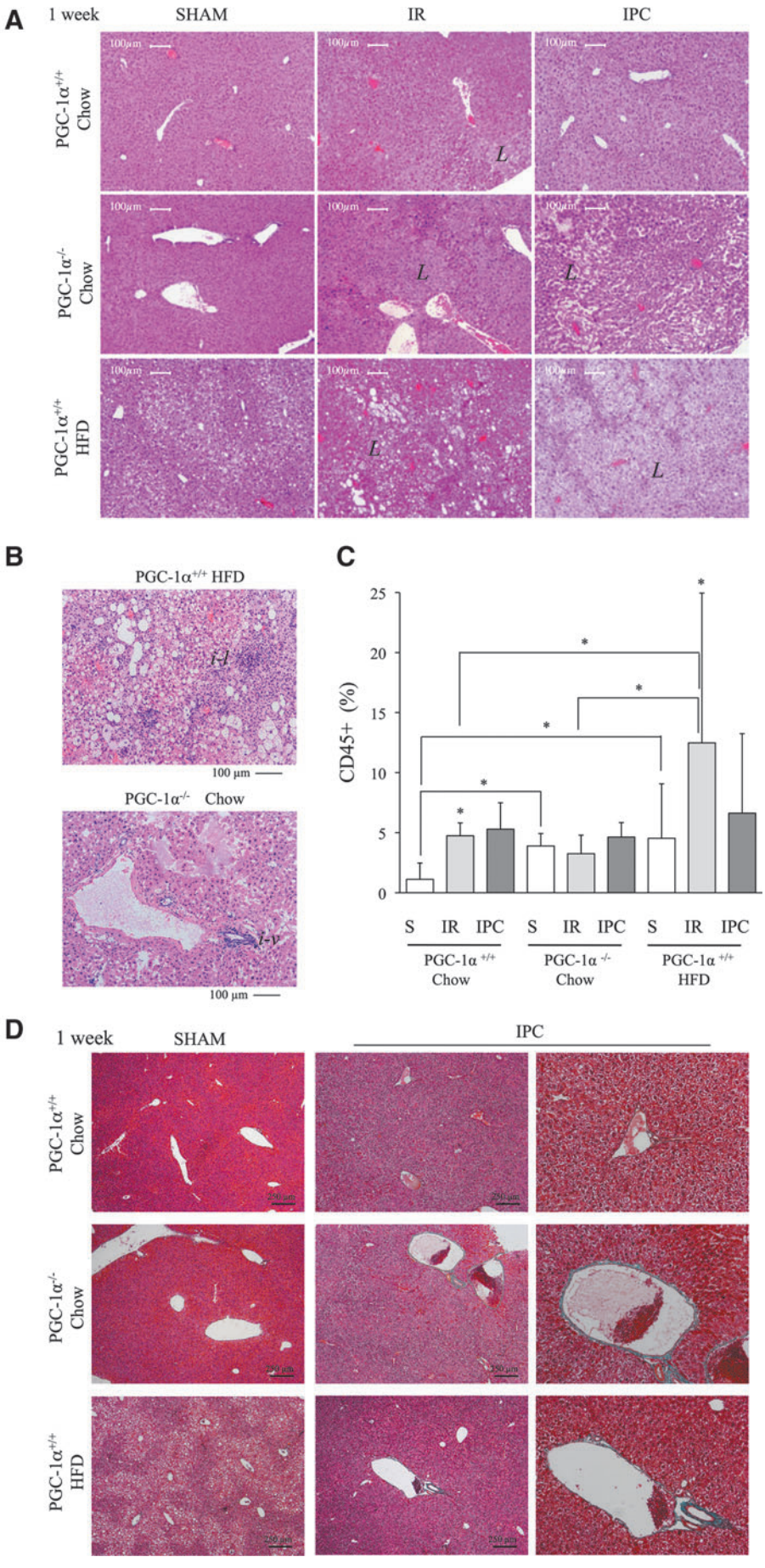

FIG. 5. Resolution of liver IR damage 1-week post-IR differs between PGC-1α$^{-/-}$ mice and PGC-1α$^{+/+}$ mice with a steatotic liver. PGC-1α$^{+/+}$ mice were fed with a chow diet or HFD for 7 weeks, and PGC-1α$^{-/-}$ mice were fed with a chow diet. Mice were subjected to a total liver IR protocol with or without prior preconditioning (IPC). **(A, B)** H&E-stained liver histological sections 1 week post-IR. L/l, lesion; i, infiltrate; v, vascular. Scale bars are 100 μm. **(C)** Quantitative analysis of CD45^{+} cells present in histological sections 1-week post-IR. Data are means ± SD. *$p < 0.05$. **(D)** Masson's trichrome-stained liver histological sections 1-week post-IR. Scale bars are 250 μm. *Right panels* show zooms in sections of the IPC images on the *left*.

We next evaluated the extent of fibrosis by staining liver sections with Masson's trichrome. Vascular fibrosis was evident in large vessels in IPC-treated steatotic PGC-1$\alpha^{+/+}$ mice and in PGC-1$\alpha^{-/-}$ mice, but not in the liver from wild-type mice. This was particularly prominent in PGC-1$\alpha^{-/-}$ liver (Fig. 5D).

These results were confirmed by Sirius Red staining, which allowed the quantification of the total fibrotic area and the vascular media thickness and the qRT-PCR quantification of αSMA mRNA levels (Supplementary Fig. S9). These observations could be relevant in terms of IR injury since it has been suggested that IPC protects from IR injury, at least in part through the preservation of microcirculation (17). Taken together, these results confirm that PGC-1α plays a protective role against IR injury in the liver, likely due to its regulation of antioxidant gene expression, and it is also a mediator of IPC.

To test the capacity of PGC-1α to provide protection against IR injury, recombinant adenovirus that drives the expression of PGC-1α or a control adenovirus was administered by iv tail vein injection to steatotic PGC-1$\alpha^{+/+}$ mice and 72 h later, these animals were subjected to IR/IPC protocols. H&E analysis of histological sections at 1 week showed a reduced disruption of the parenchymal structure in Ad-PGC-1α mice than in control Ad-Shuttle mice. Moreover, the survival rate till 7 days post-IR was significantly higher in the control Ad-Shuttle group than in the PGC-1α overexpressing mice (Supplementary Fig. S10).

Reoxygenation drives PGC-1α-mediated induction of antioxidant genes

The results thus far indicate that PGC-1α is induced in response to IR in the liver. Since PGC-1α is induced by hypoxia and ROS in other systems, we next aimed at assessing whether PGC-1α regulation of antioxidant gene expression was associated with the hypoxic induction of PGC-1α or with the burst of ROS after reoxygenation. To do this, we established an *in vitro* protocol to analyze the response of primary mouse hepatocytes to hypoxia and reoxygenation. Considering that normal O_2 tension in liver parenchyma is ~3% (10), freshly isolated hepatocytes were maintained in a cell incubator at this tension and cells were serum starved overnight before the initiation of the experimental protocol.

To evaluate the effect of hypoxia only, hepatocytes were transferred to a hypoxic chamber at 1% O_2 for 12 h. To evaluate the effect of reoxygenation, cells were first placed at 1% O_2 and then incubated at 3% O_2 for a further 6 h. After incubation, cells were collected and processed for mRNA and protein analysis. Results showed that the level of PGC-1α mRNA and protein expression was lower in cells incubated at 1% O_2 than at 3% O_2, but recovered after reoxygenation (Fig. 6A and Supplementary Fig. S11A). These results contrast with previous findings where the reference O_2 tension was 21%. This apparent incongruity may relate to the well-established observation that cells at 21% O_2 have a reduced respiratory capacity relative to those at lower oxygen tensions, presumably because the electron flux in the mitochondrial electron transport chain produces massive amounts of ROS (45).

We then analyzed the response to hypoxia and the reoxygenation of PGC-1α target genes. Hypoxia downregulated mRNA (Fig. 6B) and protein levels (Fig. 6C and Supplementary Fig. S11) of antioxidant proteins and Cyt c in both PGC-1$\alpha^{+/+}$ and PGC-1$\alpha^{-/-}$ hepatocytes, suggesting that antioxidant gene expression was modulated by hypoxia in a PGC-1α-independent manner (Fig. 6B). However, reoxygenation led to an induction in the mRNA and protein levels of antioxidants and Cyt c in PGC-1$\alpha^{+/+}$ hepatocytes, but this recovery was blunted in PGC-1$\alpha^{-/-}$ hepatocytes (Fig. 6B, C and Supplementary Fig. S11). This result strongly suggests that PGC-1α is necessary for the recovery of antioxidant gene expression after reoxygenation.

Discussion

The mechanisms that mediate IR injury are complex and have been investigated for decades. It is well established that ROS are required for IPC and are also important mediators of IR-induced cell death in various organs, including the liver. The elevated level of oxidative stress in the steatotic liver is considered a key element in its enhanced sensitivity to IR damage. However, the inability of the steatotic liver to respond to IPC has so far puzzled researchers. In this study, we show that PGC-1α is an important mediator of IPC. In the context of liver steatosis, PGC-1α expression is downregulated and the resulting failure to restore antioxidant gene expression after reperfusion may underlie both the hypersensitivity of the steatotic liver to IR injury and its inability to respond adequately to IPC.

We found that IR induces PGC-1α expression in the normal liver, which is enhanced by IPC. This observation is consistent with a previous study showing that IR and IPC protocols induce PGC-1α levels in the heart (20). However, in the steatotic liver, PGC-1α basal levels are low and fail to be induced by IR and/or by preconditioning. Accordingly, IR induced PGC-1α-regulated antioxidant enzyme expression, and this induction was generally boosted by IPC in the normal liver but not in the steatotic liver. We used PGC-1$\alpha^{-/-}$ mice to evaluate how its absence and the resultant reduction in antioxidant defense could impact liver IR injury. We found that in the extent of liver damage by IR, PGC-1$\alpha^{-/-}$ mice behaved similarly to PGC-1$\alpha^{+/+}$ steatotic mice, with an enhanced sensitivity to IR damage and a loss of response to IPC.

These results demonstrate the protective role of PGC-1α activity in IR injury and suggest that this activity may be related to the induction of antioxidant systems. Furthermore, our findings suggest that the lack of induction of PGC-1α target genes in the steatotic liver could explain its poor response to IPC and its enhanced sensitivity to IR damage.

Finally, we aimed at elucidating the mechanism involved in the induction of PGC-1α and downstream antioxidant genes in response to changing oxygen tensions. Using a hypoxia-reoxygenation protocol in primary hepatocytes, we found that PGC-1α was downregulated by hypoxia and upregulated by subsequent reoxygenation, possibly suggesting that PGC-1α could be activated *in vivo* during the reperfusion phase.

Importantly, when we examined antioxidant gene expression in PGC-1$\alpha^{+/+}$ and PGC-1$\alpha^{-/-}$ hepatocytes, we noted that although hypoxia resulted in a general reduction in the expression of antioxidant genes in both groups, their induction by reoxygenation was generally blunted in PGC-1$\alpha^{-/-}$ hepatocytes, indicating that PGC-1α does not mediate the hypoxic downregulation of those genes but is rather involved in their reactivation during the reoxygenation phase. Thus,

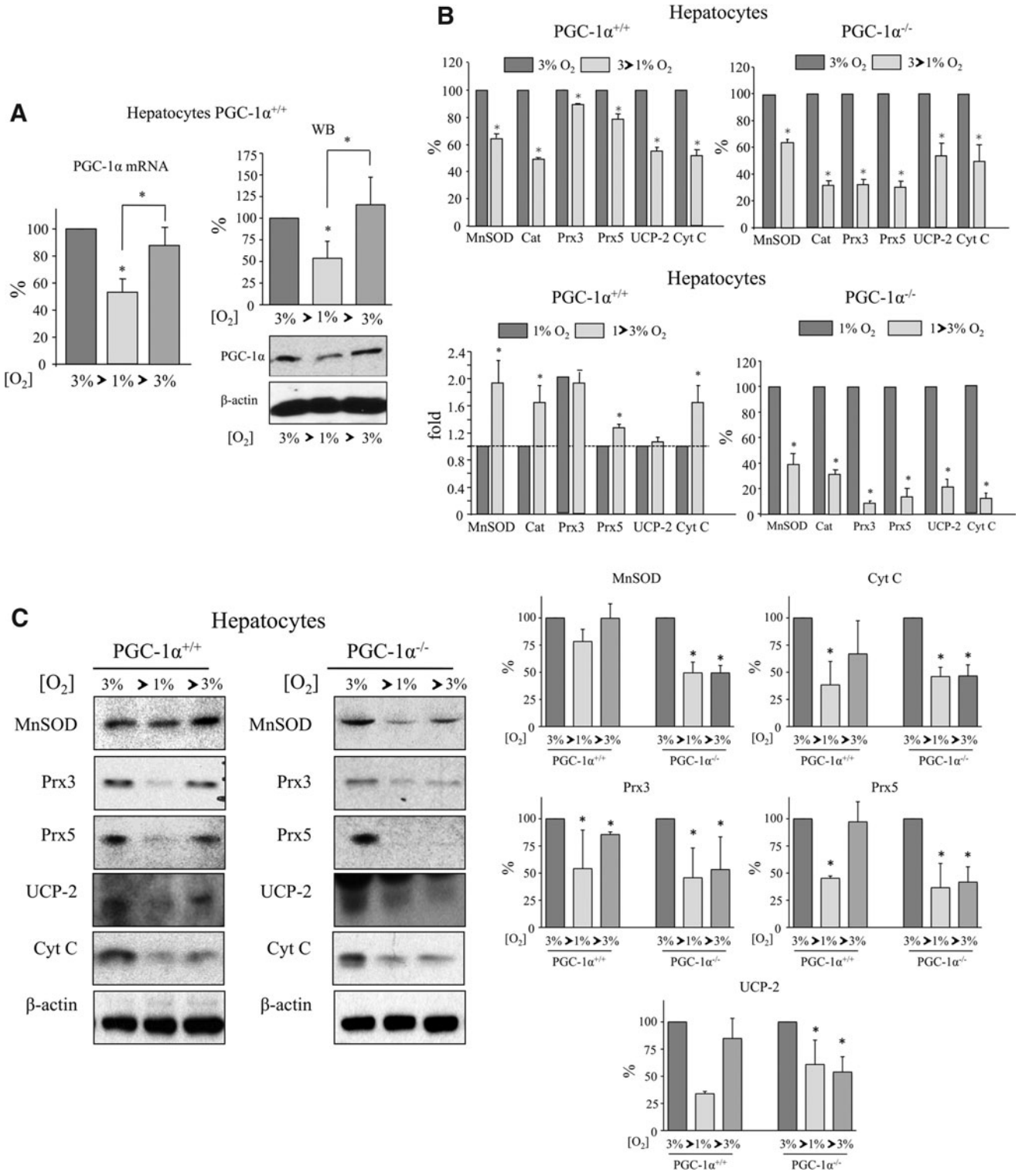

FIG. 6. Hypoxia downregulates antioxidant gene expression in a PGC-1α independent manner, whereas induction in the reoxygenation phase requires PGC-1α. Primary hepatocytes were isolated from PGC-1$\alpha^{+/+}$ and PGC-1$\alpha^{-/-}$ mice and maintained at 3% O_2. As indicated, they remained at 3%, were exposed to 1% O_2 for 12 h, or re-exposed to 3% O_2 for 6 h. **(A)** qRT-PCR analysis and WB of PGC-1α in response to the IPC protocol. Control samples were assigned the value of 1. **(B)** qRT-PCR analysis of PGC-1α target genes in response to the IPC protocol. **(C)** WB of proteins regulated by PGC-1α in response to the IPC protocol. β-actin was used as loading control. Data are means ± SD. *$p < 0.05$. qRT-PCR, quantitative PCR of retro-transcribed cDNA.

PGC-1α activity could be particularly relevant *in vivo* to sustain antioxidant gene expression after organ reperfusion.

Interestingly, metformin administration has been shown to have protective effects against IR injury in the heart (19), an effect that is dependent on the activation of AMPK and correlates with the induction of PGC-1α. This observation is particularly relevant while taking into account that regulation of PGC-1α by AMPK and metformin administration has been amply demonstrated to be functionally relevant in the liver (8).

In conclusion, we show that PGC-1α is a mediator of IPC that is downregulated in the steatotic liver, blunting the induction of protective antioxidant enzymes. In light of the general failure of classical antioxidant treatments to translate into clinical settings, targeting PGC-1α activity and/or expression might be a therapeutic option to improve the acute failure of steatotic liver transplants.

Materials and Methods

Animals

Male C57BL/6 and C57BL/6 PGC-1$\alpha^{-/-}$ mice were used in this study. Mice at 8–10 weeks of age were placed on a standard chow diet or an HFD (Harlan TD88137) for 7 weeks. Animal experimental protocols were approved by the Institutional Animal Care and Use Committee of the CNIC and the CSIC. All procedures conformed to the Declaration of Helsinki. All animals received humane care according to the criteria outlined in the ''Guide for the Care and Use of Laboratoriy Animals'' prepared by the National Academy of Sciences and published by the National Institutes of Health (No. 86-23 revised 1985).

Cell culture

Primary hepatocytes from 12- to 16 week-old female C57BL/6 wild-type and PGC-1$\alpha^{-/-}$ mice were isolated and cultured as described (38). Dispersed cells were seeded onto collagen-coated plates (0.2% gelatin, 1% collagen) and cultured in Williams E Medium containing 10% fetal bovine serum, 2 m*M* L-glutamine, 100 n*M* dexamethasone, 100 n*M* insulin, and antibiotics. Fresh medium was added 4 h after plating. In some experiments, hepatocytes were cultured in a humidified hypoxia incubator at 37°C with 3% O_2 and 5% CO_2 for 24 h and serum starved overnight. Hepatocytes were then transferred to a hypoxia chamber set at 3% or 1% O_2 for 12 h. To test the effect of reoxygenation, hepatocyte cultures were re-exposed to 3% O_2 for 6 h.

Liver IR and IPC

An established protocol of total warm hepatic IR and IPC was used (33), with minor modifications. For the IR protocol, an atraumatic clip was applied to interrupt the blood flow to the liver lobes. The clip was removed after 30 min to restore blood flow. The IPC protocol involved 5 min of ischemia followed by 10 min of reperfusion before 30 min of ischemia. Mice were anesthetized with 2% isofluorane inhalation. Buprenorphine (0.1 mg/kg) was administered subcutaneously 6 h before surgery and every 24 h for 3 days after surgery for analgesia. Experimental groups: (1) Sham operated, PGC-1$\alpha^{+/+}$ Chow, $n=13$; PGC-1$\alpha^{+/+}$ HFD, $n=8$; PGC-1$\alpha^{-/-}$ Chow, $n=11$. (2) IR, PGC-1$\alpha^{+/+}$ Chow, $n=13$; PGC-1$\alpha^{+/+}$ HFD, $n=8$; PGC-1$\alpha^{-/-}$ Chow, $n=11$. (3) IPC, PGC-1$\alpha^{+/+}$ Chow, $n=13$; PGC-1$\alpha^{+/+}$ HFD, $n=8$; PGC-1$\alpha^{-/-}$ Chow, $n=11$.

Adenoviral infection

Ad-Shuttle and Ad-PGC-1α have been previously described (48); 10^{10} pfu in PBS was injected through the tail vein. Seventy-two hours after the infection, the mice were subjected to laparotomy and total warm hepatic IR and IPC procedures or were sham operated.

Histological analysis

Liver sections were fixed in 10% buffered formalin and embedded in paraffin or in OCT™ (optimal cutting temperature). For histology, 4-μm sections were stained with H&E. To assess the presence of liver infiltrating macrophages and neutrophils, 6-μm sections were immunostained with an anti-CD45 antibody (30-F11, No. 553081; BD Biosciences), followed by incubation with a fluorescent tagged secondary antibody. Positive cells were counted from a random selection of ×10 images that were acquired with a Nikon fluorescence microscope by using ImageJ software (NIH). Nuclei were stained with TO-PRO-3 or Hoechst 33258.

Fibrosis analysis

Four-micrometer sections were stained with Masson's trichrome and Sirius Red. For Sirius Red staining, 4 μm paraffin-included slides were de-waxed in xylol, hydrated with serial washes of ethanol (100%, 96%, and 70%), and stained with Sirius Red Solution for 1 h. Then, they were washed in acidified water and dehydrated with ethanol. Photographs were taken with a Nikon 90i microscope (Nikon) and analyzed with ImageJ (NIH).

Hepatic TG content was determined as described (47). In brief, hepatic lipids were extracted as described (6). After purification, lipids were re-suspended in isopropyl alcohol and TG were analyzed with a colorimetric kit (Biosystems). Hepatic TG content was also evaluated by Oil Red O staining of liver cryosections.

TUNEL assay

The In Situ Cell Death Detection Kit Fluorescein (Roche) was used to label apoptotic cells in frozen histological sections by following the manufacturer's instructions. Images were acquired with a fluorescence microscope. The presence of nicks in the DNA was identified by the addition of fluorescein-labeled dUTPs by the enzyme terminal deoxynucleotidyl transferase (TdT). Apoptotic nuclei were counted in a random selection of ×10 images that were acquired with a Nikon fluorescence microscope by using ImageJ software.

Immunohistochemistry

Four-micrometer paraffin-included slides were de-waxed in xylol and hydrated with serial washes of ethanol (100%, 96%, and 70%). Antigen retrieval was made with citrate buffer in a microwave for 5 min, and endogenous peroxidase activity inhibition was done with 0.3% H_2O_2 in methanol for 30 min. The slides were blocked by following the manufacturer's instructions of the ABC Kit (Vector) and incubated

with the primary antibody O/N: 8-OH-deoxyguanosine (1:100, NB600-1508; Novus Biologicals) or F4/80 (1:150, MCA497; AbD Serotec). For secondary antibody and DAB incubation, ABC Kit and DAB Kit (Vector) were used, respectively. Photographs were taken with a Nikon 90i microscope (Nikon) and analyzed with ImageJ (NIH).

Determination of plasma transaminase

Blood samples were collected by puncture of the caudal cava vein, and enzymatic determinations of alanine aminotransferase (GPT) and aspartate aminotransferase (GOT) in plasma were performed by using diagnostic kits (GN 41125, GN 40125 RAL) following the manufacturer's instructions.

RNA isolation and qRT-PCR

Total mRNA was isolated from frozen samples of liver tissue that were homogenized in 1 ml of TRIZOL (Thermo Fisher Scientific). The protocol for qRT-PCR and several primers used have been previously described (7, 29, 38, 48).

Non-previously described qPCR oligonucleotides:
αSMA: Forward 5′-GCTGAAGTATCCGATAGAAC ACG-3′
Reverse 5′-GGTCTCAAACATAATCTGGGTCA-3′
IL-4: Forward 5′-CGAAGAACACCACAGAGAGTGA GCT-3′
Reverse 5′-GACTCATTCATGGTGCAGCTTATCG-3′
iNOS: Forward 5′-GAGCTGGGCTGTACAAACCTT-3′
Reverse 5′-CATTGGAAGTGAAGCGTTTCG-3′
TNFα: Forward 5′-ATGAGAAGTTCCAAATGGCC-3′
Reverse 5′-TGGTTTGCTACGACGTGGG-3′
IL-1β: Forward 5′-GCTGAAAGCTCTCCACCTCA-3′
Reverse 5′-AGGCCACAGGTATTTTGTCG-3
Arg-1: Forward 5′-CTCCAAGCCAAAGTCCTTAGAG-3′
Reverse 5′-AGGAGCTGTCATTAGGGACATC-3′

Protein extraction and Western blotting

Whole liver extracts were prepared from frozen samples of liver tissue that were homogenized in 1 ml of lysis solution and analyzed by Western blotting as previously described (28).

Antibodies used for Western blot

HNE (1:1000, HNE11-S; Alpha Diagnostic). All other antibodies used have been previously described (7, 29, 38, 48).

Image analysis

ImageJ software was used to analyze Western blots and to determine the number of nuclei in histological section fields.

Statistics

Data are expressed as means ± SD. Statistical significance was evaluated by one-way analysis of variance or by the two-tailed unpaired *t*-test. ANOVA was used to evaluate whether the effect of IR/IPC was affected by the PGC-1α genotype and/or diet. *t*-test was used for simple direct comparisons (*e.g.*, PGC-1$\alpha^{+/+}$ *vs.* PGC-1$\alpha^{-/-}$). Values were considered statistically significant at $p < 0.05$; $n \geq 3$ for all experimental conditions.

Acknowledgments

The authors thank Dr. Santiago Lamas (CBMSO, Madrid, Spain) for a careful reading of the article and Dr. Mercedes Ricote (CNIC, Madrid, Spain) for qPCR primers to quantitate Arg-1 and IL-1β mRNA levels. Editorial support was provided by Dr. Kenneth McCreath. This work was supported by grants from the Spanish ''Ministerio de Economía y Competitividad'' (MINECO) and FEDER funds (Grant Nos. SAF2012-37693, SAF2015-63904-R [MINECO/FEDER], CSD 2007-00020 & SAF2015-71521-REDC, SAF2015-65267-R), the ''Comunidad Autónoma de Madrid'' (grant No. S2010/BMD-2361), and CIBER (ISCIII).

Author Disclosure Statement

No competing financial interests exist.

References

1. Aharoni-Simon M, Hann-Obercyger M, Pen S, Madar Z, and Tirosh O. Fatty liver is associated with impaired activity of PPARgamma-coactivator 1alpha (PGC1alpha) and mitochondrial biogenesis in mice. *Lab Invest* 91: 1018–1028, 2011.
2. Akhtar MZ, Henderson T, Sutherland A, Vogel T, and Friend PJ. Novel approaches to preventing ischemia-reperfusion injury during liver transplantation. *Transplant Proc* 45: 2083–2092, 2013.
3. Arany Z, Foo SY, Ma Y, Ruas JL, Bommi-Reddy A, Girnun G, Cooper M, Laznik D, Chinsomboon J, Rangwala SM, Baek KH, Rosenzweig A, and Spiegelman BM. HIF-independent regulation of VEGF and angiogenesis by the transcriptional coactivator PGC-1alpha. *Nature* 451: 1008–1012, 2008.
4. Barroso E, Rodriguez-Calvo R, Serrano-Marco L, Astudillo AM, Balsinde J, Palomer X, and Vazquez-Carrera M. The PPARbeta/delta activator GW501516 prevents the down-regulation of AMPK caused by a high-fat diet in liver and amplifies the PGC-1alpha-Lipin 1-PPARalpha pathway leading to increased fatty acid oxidation. *Endocrinology* 152: 1848–1859, 2011.
5. Bejaoui M, Pantazi E, Folch-Puy E, Baptista PM, Garcia-Gil A, Adam R, and Rosello-Catafau J. Emerging concepts in liver graft preservation. *World J Gastroenterol* 21: 396–407, 2015.
6. Bligh EG and Dyer WJ. A rapid method of total lipid extraction and purification. *Can J Biochem Physiol* 37: 911–917, 1959.
7. Borniquel S, Valle I, Cadenas S, Lamas S, and Monsalve M. Nitric oxide regulates mitochondrial oxidative stress protection via the transcriptional coactivator PGC-1alpha. *FASEB J* 20: 1889–1891, 2006.
8. Canto C and Auwerx J. PGC-1alpha, SIRT1 and AMPK, an energy sensing network that controls energy expenditure. *Curr Opin Lipidol* 20: 98–105, 2009.
9. Caraceni P, Domenicali M, Vendemiale G, Grattagliano I, Pertosa A, Nardo B, Morselli-Labate AM, Trevisani F, Palasciano G, Altomare E, and Bernardi M. The reduced tolerance of rat fatty liver to ischemia reperfusion is associated with mitochondrial oxidative injury. *J Surg Res* 124: 160–168, 2005.
10. Carreau A, El Hafny-Rahbi B, Matejuk A, Grillon C, and Kieda C. Why is the partial oxygen pressure of human

tissues a crucial parameter? Small molecules and hypoxia. *J Cell Mol Med* 15: 1239–1253, 2011.
11. Charlton M. Evolving aspects of liver transplantation for nonalcoholic steatohepatitis. *Curr Opin Organ Transplant* 18: 251–258, 2013.
12. Chen Q, Moghaddas S, Hoppel CL, and Lesnefsky EJ. Reversible blockade of electron transport during ischemia protects mitochondria and decreases myocardial injury following reperfusion. *J Pharmacol Exp Ther* 319: 1405–1412, 2006.
13. Feldstein AE and Bailey SM. Emerging role of redox dysregulation in alcoholic and nonalcoholic fatty liver disease. *Antioxid Redox Signal* 15: 421–424, 2011.
14. Fulop P, Derdak Z, Sheets A, Sabo E, Berthiaume EP, Resnick MB, Wands JR, Paragh G, and Baffy G. Lack of UCP2 reduces Fas-mediated liver injury in ob/ob mice and reveals importance of cell-specific UCP2 expression. *Hepatology* 44: 592–601, 2006.
15. Funk JA and Schnellmann RG. Accelerated recovery of renal mitochondrial and tubule homeostasis with SIRT1/PGC-1alpha activation following ischemia-reperfusion injury. *Toxicol Appl Pharmacol* 273: 345–354, 2013.
16. Gehrau RC, Mas VR, Dumur CI, Suh JL, Sharma AK, Cathro HP, and Maluf DG. Donor hepatic steatosis induce exacerbated ischemia-reperfusion injury through activation of innate immune response molecular pathways. *Transplantation* 99: 2523–2533, 2015.
17. Glanemann M, Vollmar B, Nussler AK, Schaefer T, Neuhaus P, and Menger MD. Ischemic preconditioning protects from hepatic ischemia/reperfusion-injury by preservation of microcirculation and mitochondrial redox-state. *J Hepatol* 38: 59–66, 2003.
18. Granger DN and Kvietys PR. Reperfusion injury and reactive oxygen species: the evolution of a concept. *Redox Biol* 6: 524–551, 2015.
19. Gundewar S, Calvert JW, Jha S, Toedt-Pingel I, Ji SY, Nunez D, Ramachandran A, Anaya-Cisneros M, Tian R, and Lefer DJ. Activation of AMP-activated protein kinase by metformin improves left ventricular function and survival in heart failure. *Circ Res* 104: 403–411, 2009.
20. Han JS, Wang HS, Yan DM, Wang ZW, Han HG, Zhu HY, and Li XM. Myocardial ischaemic and diazoxide preconditioning both increase PGC-1alpha and reduce mitochondrial damage. *Acta Cardiol* 65: 639–644, 2010.
21. Harring TR, O'Mahony CA, and Goss JA. Extended donors in liver transplantation. *Clin Liver Dis* 15: 879–900, 2011.
22. Jiang Y, Zhang H, Dong LY, Wang D, and An W. Increased hepatic UCP2 expression in rats with nonalcoholic steatohepatitis is associated with upregulation of Sp1 binding to its motif within the proximal promoter region. *J Cell Biochem* 105: 277–289, 2008.
23. Kevin LG, Camara AK, Riess ML, Novalija E, and Stowe DF. Ischemic preconditioning alters real-time measure of O2 radicals in intact hearts with ischemia and reperfusion. *Am J Physiol Heart Circ Physiol* 284: H566–H574, 2003.
24. Kim J, Jang HS, and Park KM. Reactive oxygen species generated by renal ischemia and reperfusion trigger protection against subsequent renal ischemia and reperfusion injury in mice. *Am J Physiol Renal Physiol* 298: F158–F166, 2010.
25. Lebuffe G, Schumacker PT, Shao ZH, Anderson T, Iwase H, and Vanden Hoek TL. ROS and NO trigger early preconditioning: relationship to mitochondrial KATP channel. *Am J Physiol Heart Circ Physiol* 284: H299–H308, 2003.
26. Luo Y, Zhu W, Jia J, Zhang C, and Xu Y. NMDA receptor dependent PGC-1alpha up-regulation protects the cortical neuron against oxygen-glucose deprivation/reperfusion injury. *J Mol Neurosci* 39: 262–268, 2009.
27. McCormack L, Dutkowski P, El-Badry AM, and Clavien PA. Liver transplantation using fatty livers: always feasible? *J Hepatol* 54: 1055–1062, 2011.
28. Monsalve M, Wu Z, Adelmant G, Puigserver P, Fan M, and Spiegelman BM. Direct coupling of transcription and mRNA processing through the thermogenic coactivator PGC-1. *Mol Cell* 6: 307–316, 2000.
29. Olmos Y, Valle I, Borniquel S, Tierrez A, Soria E, Lamas S, and Monsalve M. Mutual dependence of Foxo3a and PGC-1alpha in the induction of oxidative stress genes. *J Biol Chem* 284: 14476–14484, 2009.
30. Pantazi E, Bejaoui M, Folch-Puy E, Adam R, and Rosello-Catafau J. Advances in treatment strategies for ischemia reperfusion injury. *Expert Opin Pharmacother* 17: 169–179, 2016.
31. Pantazi E, Folch-Puy E, Bejaoui M, Panisello A, Varela AT, Rolo AP, Palmeira CM, and Rosello-Catafau J. PPARalpha agonist WY-14643 induces SIRT1 activity in rat fatty liver ischemia-reperfusion injury. *Biomed Res Int* 2015: 894679, 2015.
32. Patti ME, Butte AJ, Crunkhorn S, Cusi K, Berria R, Kashyap S, Miyazaki Y, Kohane I, Costello M, Saccone R, Landaker EJ, Goldfine AB, Mun E, DeFronzo R, Finlayson J, Kahn CR, and Mandarino LJ. Coordinated reduction of genes of oxidative metabolism in humans with insulin resistance and diabetes: potential role of PGC1 and NRF1. *Proc Natl Acad Sci U S A* 100: 8466–8471, 2003.
33. Peralta C, Perales JC, Bartrons R, Mitchell C, Gilgenkrantz H, Xaus C, Prats N, Fernandez L, Gelpi E, Panes J, and Rosello-Catafau J. The combination of ischemic preconditioning and liver Bcl-2 overexpression is a suitable strategy to prevent liver and lung damage after hepatic ischemia-reperfusion. *Am J Pathol* 160: 2111–2122, 2002.
34. Perlemuter G, Davit-Spraul A, Cosson C, Conti M, Bigorgne A, Paradis V, Corre MP, Prat L, Kuoch V, Basdevant A, Pelletier G, Oppert JM, and Buffet C. Increase in liver antioxidant enzyme activities in non-alcoholic fatty liver disease. *Liver Int* 25: 946–953, 2005.
35. Pratschke S, Angele MK, Grutzner U, Tufman A, Bilzer M, Loehe F, Jauch KW, and Schauer RJ. GSH attenuates organ injury and improves function after transplantation of fatty livers. *Eur Surg Res* 45: 13–19, 2010.
36. Reiniers MJ, van Golen RF, van Gulik TM, and Heger M. Reactive oxygen and nitrogen species in steatotic hepatocytes: a molecular perspective on the pathophysiology of ischemia-reperfusion injury in the fatty liver. *Antioxid Redox Signal* 21: 1119–1142, 2014.
37. Routh D, Naidu S, Sharma S, Ranjan P, and Godara R. Changing pattern of donor selection criteria in deceased donor liver transplant: a review of literature. *J Clin Exp Hepatol* 3: 337–346, 2013.
38. Sanchez-Ramos C, Tierrez A, Fabregat-Andres O, Wild B, Sanchez-Cabo F, Arduini A, Dopazo A, and Monsalve M. PGC-1alpha regulates translocated in liposarcoma activity: role in oxidative stress gene expression. *Antioxid Redox Signal* 15: 325–337, 2011.
39. Semple RK, Crowley VC, Sewter CP, Laudes M, Christodoulides C, Considine RV, Vidal-Puig A, and O'Rahilly S. Expression of the thermogenic nuclear hormone receptor coactivator PGC-1alpha is reduced in the adipose tissue of

morbidly obese subjects. *Int J Obes Relat Metab Disord* 28: 176–179, 2004.
40. Solaini G and Harris DA. Biochemical dysfunction in heart mitochondria exposed to ischaemia and reperfusion. *Biochem J* 390: 377–394, 2005.
41. Song X, Xu H, Feng Y, Li X, Lin M, and Cao L. Protective effect of grape seed proanthocyanidins against liver ischemic reperfusion injury: particularly in diet-induced obese mice. *Int J Biol Sci* 8: 1345–1362, 2012.
42. St-Pierre J, Drori S, Uldry M, Silvaggi JM, Rhee J, Jager S, Handschin C, Zheng K, Lin J, Yang W, Simon DK, Bachoo R, and Spiegelman BM. Suppression of reactive oxygen species and neurodegeneration by the PGC-1 transcriptional coactivators. *Cell* 127: 397–408, 2006.
43. Summermatter S and Handschin C. PGC-1alpha and exercise in the control of body weight. *Int J Obes (Lond)* 36: 1428–1435, 2012.
44. Tashiro H, Kuroda S, Mikuriya Y, and Ohdan H. Ischemia-reperfusion injury in patients with fatty liver and the clinical impact of steatotic liver on hepatic surgery. *Surg Today* 44: 1611–1625, 2014.
45. Tiede LM, Cook EA, Morsey B, and Fox HS. Oxygen matters: tissue culture oxygen levels affect mitochondrial function and structure as well as responses to HIV viroproteins. *Cell Death Dis* 2: e246, 2011.
46. Uchino S, Yamaguchi Y, Furuhashi T, Wang FS, Zhang JL, Okabe K, Kihara S, Yamada S, Mori K, and Ogawa M. Steatotic liver allografts up-regulate UCP-2 expression and suffer necrosis in rats. *J Surg Res* 120: 73–82, 2004.
47. Valdecantos MP, Pardo V, Ruiz L, Castro-Sanchez L, Lanzon B, Fernandez-Millan E, Garcia-Monzon C, Arroba AI, Gonzalez-Rodriguez A, Escriva F, Carmen A, Ruperez FJ, Barbas C, Konkar A, Naylor J, Hornigold D, Dos Santos A, Bednarek M, Grimsby J, Rondinone CM, and Valverde AM. A novel glucagon-like peptide 1/glucagon receptor dual agonist improves steatohepatitis and liver regeneration in mice. *Hepatology* 65: 950–968, 2016.
48. Valle I, Alvarez-Barrientos A, Arza E, Lamas S, and Monsalve M. PGC-1alpha regulates the mitochondrial antioxidant defense system in vascular endothelial cells. *Cardiovasc Res* 66: 562–573, 2005.
49. Yang HJ, Tang LM, Zhou XJ, Qian J, Zhu J, Lu L, and Wang XH. Ankaflavin ameliorates steatotic liver ischemia-reperfusion injury in mice. *Hepatobiliary Pancreat Dis Int* 14: 619–625, 2015.
50. Yang X, Enerback S, and Smith U. Reduced expression of FOXC2 and brown adipogenic genes in human subjects with insulin resistance. *Obes Res* 11: 1182–1191, 2003.
51. Zhou W, Zhang Y, Hosch MS, Lang A, Zwacka RM, and Engelhardt JF. Subcellular site of superoxide dismutase expression differentially controls AP-1 activity and injury in mouse liver following ischemia/reperfusion. *Hepatology* 33: 902–914, 2001.
52. Zwacka RM, Zhang Y, Zhou W, Halldorson J, and Engelhardt JF. Ischemia/reperfusion injury in the liver of BALB/c mice activates AP-1 and nuclear factor kappaB independently of IkappaB degradation. *Hepatology* 28: 1022–1030, 1998.
53. Zweier JL and Talukder MA. The role of oxidants and free radicals in reperfusion injury. *Cardiovasc Res* 70: 181–190, 2006.

Address correspondence to:
Dr. María Monsalve
Instituto de Investigaciones Biomédicas
''Alberto Sols'' (CSIC-UAM)
Arturo Duperier 4, Room 1.3.2
Madrid 28029
Spain

E-mail: mpmonsalve@iib.uam.es

Date of first submission to ARS Central, July 18, 2016; date of final revised submission, March 3, 2017; date of acceptance, March 4, 2017.

Abbreviations Used

CNS = central nervous system
GOT = aspartate aminotransferase
GPT = alanine aminotransferase
H&E = hematoxylin and eosin
HFD = high-fat diet
IPC = ischemic preconditioning
IR = ischemia-reperfusion
PGC-1α = peroxisome proliferator activated receptor γ co-activator 1α
qRT-PCR = quantitative PCR of retro-transcribed cDNA
ROS = reactive oxygen species
TAG = triacylglicerols
TdT = terminal deoxynucleotidyl transferase
TG = triglyceride
TUNEL = terminal transferase dUTP nick end-labeling assay
WB = Western blotting

Redox Biology 6 (2015) 51–72

Contents lists available at ScienceDirect

Redox Biology

journal homepage: www.elsevier.com/locate/redox

Review Article

Redox regulation of FoxO transcription factors

Lars-Oliver Klotz [a,*], Cristina Sánchez-Ramos [b], Ignacio Prieto-Arroyo [b], Pavel Urbánek [a], Holger Steinbrenner [a], Maria Monsalve [b,*]

[a] Institute of Nutrition, Department of Nutrigenomics, Friedrich-Schiller-Universität Jena, Dornburger Straße 29, 07743 Jena, Germany
[b] Instituto de Investigaciones Biomédicas "Alberto Sols" (CSIC-UAM), Arturo Duperier, 4, 28029 Madrid, Spain

ARTICLE INFO

Article history:
Received 28 May 2015
Received in revised form
25 June 2015
Accepted 30 June 2015
Available online 3 July 2015

Keywords:
Forkhead box proteins
Oxidative stress
Stress signaling
Antioxidant proteins
DAF-16
C. elegans
Insulin signaling
Akt

ABSTRACT

Transcription factors of the forkhead box, class O (FoxO) family are important regulators of the cellular stress response and promote the cellular antioxidant defense. On one hand, FoxOs stimulate the transcription of genes coding for antioxidant proteins located in different subcellular compartments, such as in mitochondria (i.e. superoxide dismutase-2, peroxiredoxins 3 and 5) and peroxisomes (catalase), as well as for antioxidant proteins found extracellularly in plasma (*e.g.*, selenoprotein P and ceruloplasmin). On the other hand, reactive oxygen species (ROS) as well as other stressful stimuli that elicit the formation of ROS, may modulate FoxO activity at multiple levels, including posttranslational modifications of FoxOs (such as phosphorylation and acetylation), interaction with coregulators, alterations in FoxO subcellular localization, protein synthesis and stability. Moreover, transcriptional and posttranscriptional control of the expression of genes coding for FoxOs is sensitive to ROS. Here, we review these aspects of FoxO biology focusing on redox regulation of FoxO signaling, and with emphasis on the interplay between ROS and FoxOs under various physiological and pathophysiological conditions. Of particular interest are the dual role played by FoxOs in cancer development and their key role in whole body nutrient homeostasis, modulating metabolic adaptations and/or disturbances in response to low *vs.* high nutrient intake. Examples discussed here include calorie restriction and starvation as well as adipogenesis, obesity and type 2 diabetes.

Contents

* Corresponding authors.
E-mail addresses: lars-oliver.klotz@uni-jena.de (L.-O. Klotz), mpmonsalve@iib.uam.es (M. Monsalve).

http://dx.doi.org/10.1016/j.redox.2015.06.019
2213-2317/

1. Introduction

"Fork head" was first identified in *Drosophila* as a potential transcriptional regulator [1], and demonstrated to harbor a so-called winged-helix DNA binding domain that was then recognized to be present in other transcriptional regulators, including the mammalian hepatocyte-enriched nuclear factor (HNF)-3A (now FoxA1) [2]. This domain was christened the fork head domain [2], and later the dozens of proteins with such a winged helix/fork head domain identified by then were categorized into different classes of forkhead box (Fox) proteins [3]. Fox proteins – specifically, the forkhead box, class O, proteins (FoxO) – were first linked to stress resistance when long-lived mutants of *Caenorhabditis elegans* were analyzed with respect to genetic traits contributing to their longevity. It was found that insulin-like signaling along the cascade orthologous to the mammalian insulin receptor/phosphoinositide 3′-kinase/Akt (InsR/PI3K/Akt) cascade was involved in that mutants with impaired signaling along this cascade had extended life spans [4] (Fig. 1). It was then demonstrated that the *daf-16* gene conferred this life span extension [5] and that DAF-16 (DAF, dauer formation) is a transcription factor of the Fox family (specifically, a FoxO orthologue) essential to this process [6,7].

Mutants with deficient *daf-2*, coding for a *C. elegans* InsR orthologue [8], were then shown to not only display a long-lived phenotype but also a phenotype ("Oxr") characterized by oxidative stress resistance: A *daf-2*-inactive mutant had an enhanced resistance towards redox cycling compounds such as paraquat or menadione [9]. Like the longevity phenotype, this Oxr phenotype was prevented by mutations in *daf-16*, suggesting that transcriptional targets of DAF-16 might be involved in conferring stress resistance. In fact, the expression of *sod-3*, the gene for one of the two manganese-containing superoxide dismutases of *C. elegans* (but neither *sod-1* nor *sod-2*, coding for Cu, Zn-dependent SOD and a second Mn-dependent SOD, respectively [10]), was upregulated in long-lived *daf-2* mutants, which was prevented by an additional *daf-16* mutation [9].

These findings suggested that the expression of genes coding for antioxidant enzymes such as superoxide dismutases might be under the control of forkhead-type transcription factors. In fact, expression of the human Mn-SOD (mitochondrial SOD-2 in humans) was demonstrated to be transcriptionally controlled by the human DAF-16 orthologue, the forkhead box transcription factor, FoxO3a [11]. Despite the fact that it was later demonstrated that SOD-3 is not essential to the longevity phenotype in *daf-2* mutants [12], a link was established between forkhead box transcription factors and cellular antioxidant defense.

The purpose of this review is to provide an overview on the role of FoxO transcription factors in the cellular response to (oxidative) stress – including antioxidant defense – and on the

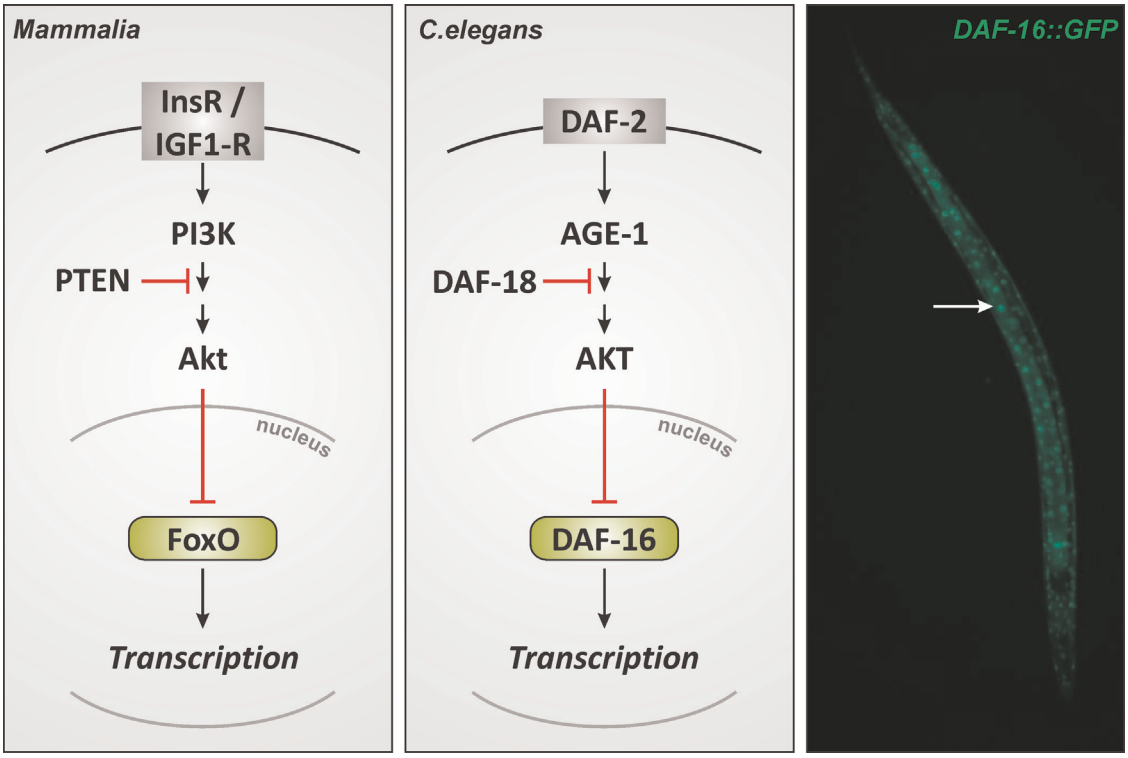

Fig. 1. Insulin signaling in mammalian cells and in *C. elegans*. See text for further details. Right panel: *C. elegans* transgenic strain TJ356 stably expresses a DAF-16::GFP fusion protein. DAF-16::GFP accumulates in nuclei upon exposure of worms to an oxidative stress (induced by diamide, a thiol oxidizing agent). Speckles (arrow) represent nuclei with DAF-16::GFP.

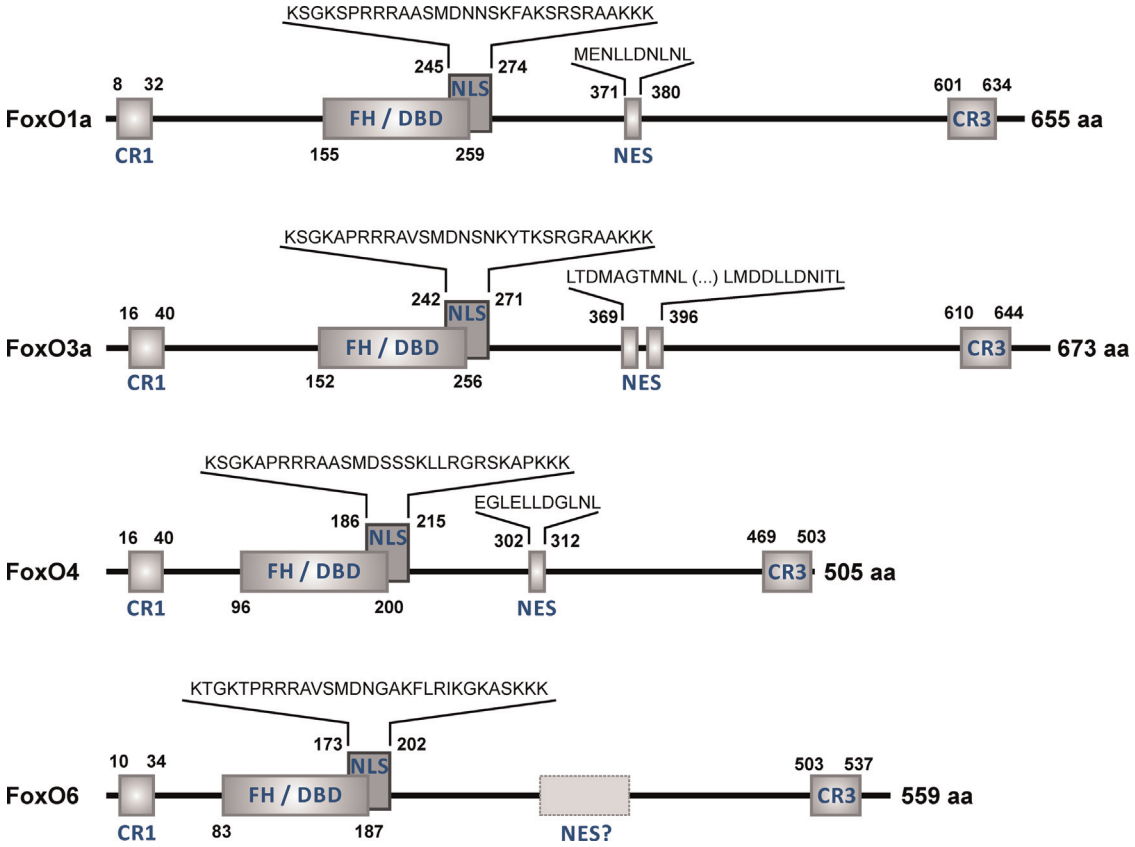

Fig. 2. Domain organization of human FoxO proteins. Positions of the most conserved domains and of some functionally characterized sequence motifs in human FoxO proteins are depicted. The numbers next to the domain or motif indicate its beginning and end within the sequence. Total length (in aa, amino acids) of each FOXO protein is indicated to the right of its schematic depiction. CR1 and CR3, conserved regions 1 and 3; CR3 represents a conserved C-terminal transactivation domain [326,327]. FH/DBD, forkhead box/DNA-binding domain [129,309,328]; NLS, nuclear localization signal; NES, nuclear export sequence. The amino acid sequence range of FoxO4 NLS is according to Obsilova et al. [329]. The corresponding homologous regions are depicted for FoxO1a, FoxO3a, and FoxO6 NLS. Whereas NES regions were defined for FoxO1a, 3a and 4 [330–332], the presence of a NES in FoxO6 is being debated [312,313]. The scheme and numbers depicted are based on the following NCBI RefSeq (National Center for Biotechnology Information Reference Sequence Database; [333]) entries: FoxO1a – NP_002006.2 (GI:9257222); FoxO3a – NP_001446.1 (GI:4503739); FoxO4 – NP_005929.2 (GI:103472003); FoxO6 – NP_001278210.2 (GI:849540648).

contribution of redox signaling to the biological activity of FoxOs.

Four FoxO proteins are present in humans (Fig. 2), FoxO1a, FoxO3a, FoxO4 and FoxO6 (for an overview on FoxO nomenclature, see [13]). All are widely expressed in diverse tissues [14] – including FoxO6, which has frequently been said to be primarily found in brain, but has now been shown to be ubiquitously expressed as well [15]. In terms of a functional classification of FoxO target genes, three major categories are “stress response and antioxidative defense”, “metabolism”, and “cell death and proliferation” [16].

2. FoxO target genes: antioxidant defense

FoxO targets include genes coding for both intra- and extracellular antioxidant proteins interfering with all levels of oxygen reduction that would otherwise generate diverse ROS and cause oxidative damage to biomolecules. In humans, these FoxO-regulated antioxidants include Mn-SOD (SOD-2) [11], catalyzing disproportionation (dismutation) of the first oxygen reduction product, superoxide, to generate oxygen and hydrogen peroxide (H_2O_2). Moreover, there are indications of a regulation of cytoplasmic Cu,Zn-SOD (SOD-1) in murine erythroblasts by FoxOs, further supporting a role of these transcription factors in the cellular defense against superoxide [17]. H_2O_2 is further dismutated to water and oxygen in a reaction catalyzed by catalase, a peroxisomal heme peroxidase whose generation was found to be regulated by FoxO3a [18]. Alternatively, H_2O_2 may be reduced to water at the expense of reducing equivalents provided by NADPH *via* thioredoxin or glutathione (GSH), and the formation of two enzymes catalyzing this reduction was demonstrated to be regulated by FoxOs (peroxiredoxin-3, Prx3, and Prx5) [19,20] or to be likely regulated by FoxOs (glutathione peroxidase-1, GPx-1) [17], respectively. The interesting aspect here is that in addition to peroxisomal catalase, the mitochondrial Prx3 and Prx5, and the cytoplasmic GPx-1 appear to establish a FoxO-regulated battery of enzymes ascertaining that H_2O_2 may be reduced in multiple cellular compartments in parallel. Moreover, the expression of mitochondrial thioredoxin (Trx2) and mitochondrial thioredoxin reductase (TrxR2) were demonstrated to be regulated by FoxO3a in bovine aortic endothelial cells [20] and can be anticipated to contribute to the reduction of mitochondrial Prx3.

In the presence of redox-active metal ions, *e.g.* Fe^{2+} or Cu^{+}, H_2O_2 may be reduced in a Fenton-type reaction to generate the hydroxyl radical $^{\bullet}OH$, a most aggressive oxidant. Chelating such metal ions would prevent hydroxyl radical formation and its initiating lipid peroxidation and oxidation of other biomolecules. In cells, chelation of copper ions is achieved by metallothioneins (MT), and one cellular iron sink is ferritin. Expression of *C. elegans* metallothionein-1 and a resulting resistance of the worms towards copper stress appears to be supported by DAF-16 [21], and expression of a ferritin ortholog, *ftn-1*, is regulated by DAF-16 [22]. Similarly, metallothionein mRNA levels were shown in mammalian cells to be increased upon stimulation of FoxO3a, particularly

so following FoxO3a phosphorylation by AMP-activated kinase (AMPK) [23]. Interestingly, hepatic expression of the major plasma copper protein in mammals, ceruloplasmin (Cp), is controlled by FoxOs [24,25]. Cp harbors several copper ions per molecule and has antioxidant activity in that it acts as ferroxidase to oxidize Fe^{2+} released from cells to Fe^{3+}. Not only does this prevent Fenton-type reactions but it also allows for transport of iron as Fe^{3+} by transferrin [26,27].

Another aspect of FoxO proteins regulating antioxidant networks was established when expression of the *SEPP1* gene, coding for the major plasma selenoprotein, selenoprotein P (SelP), was found to be regulated by FoxO1a [28,29]. SelP has some hydroperoxidase activity *per se* [30,31], protecting LDL against oxidation [32]. However, its major physiological function is the transport of selenium from the liver to extrahepatic tissues *via* blood [33], providing selenium for the synthesis of cellular antioxidant selenoenzymes, such as glutathione peroxidases, including GPx-1 and GPx-4 [34], or thioredoxin reductases, and thus rendering cells more resistant against oxidative stress [35,36].

In summary, FoxO transcription factors regulate the expression of genes coding for intra- and extracellular antioxidant proteins, with different intracellular compartments as well as the major required steps in antioxidant defense covered (Fig. 3).

Activity of FoxO transcriptional regulators is modulated at several levels, including (i) posttranslational modifications, (ii) subcellular localization, (iii) interaction with coregulators and (iv) *FOXO* gene expression and FoxO formation and stability. Subcellular localization and interaction with coregulators are governed by posttranslational modifications (PTM), some of which will be discussed in the following section.

3. Redox regulation of FoxO activity

FoxO PTMs that respond to changes in ROS levels and/or regulate FoxO antioxidant activity include phosphorylation, acetylation and ubiquitination. These modifications affect FoxO subcellular localization, activity as a transcriptional regulator, and stability. More recently, methylation and O-glycosylation were added to the list of FoxO modifications. For a compilation of FoxO posttranslational modifications and the respective FoxO sites of modification, see [16,37].

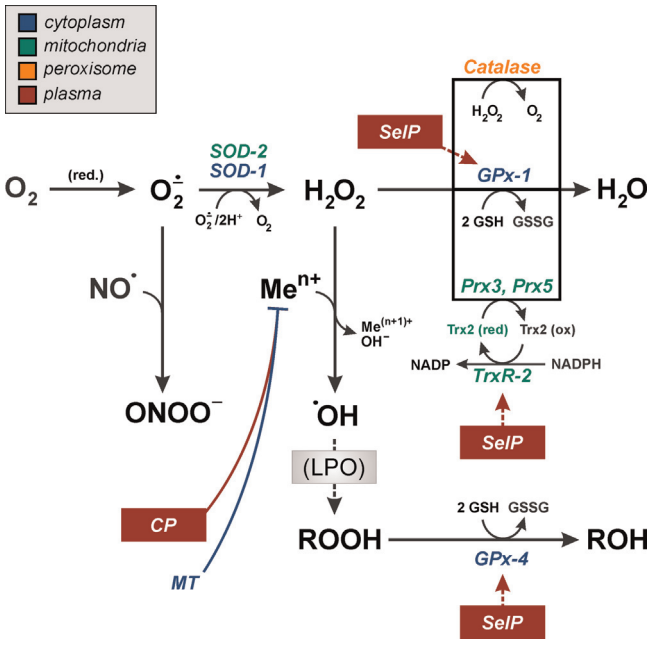

Fig. 3. FoxO target genes coding for antioxidant proteins: subcellular localization and functional significance of gene products. See text for further details. Abbreviations: CP, ceruloplasmin; GPx, glutathione peroxidase; GSH, glutathione; GSSG, glutathione disulfide; LPO, lipid peroxidation; MT, metallothionein; Prx, peroxiredoxin; SelP, selenoprotein P; SOD, superoxide dismutase; Trx, thioredoxin; TrxR, thioredoxin reductase. Inset: color code to indicate subcellular localization of proteins. (For interpretation of the references to color in this figure legend, the reader is referred to the web version of this article.)

3.1. Endogenous and exogenous sources of ROS and their effect on FoxO phosphorylation

Stimulation of receptor tyrosine kinases (RTK) by their natural ligands frequently comes with a transient generation of ROS – this is true for stimulation of the insulin receptor with insulin [38], the epidermal growth factor (EGF) receptor with EGF [39,40] or the platelet-derived growth factor (PDGF) receptor with PDGF [41]. NADPH oxidases are the source of these ROS, whose formation results in modulation of downstream signaling. These signaling events occur through transient oxidative inhibition of protein tyrosine phosphatases (PTP) that are associated with the respective RTK. This appears to be required for a significant ligand-induced increase in RTK phosphorylation and therefore a significant intracellular signal to be initiated. For example, NOX4 generates H_2O_2, which was shown to attenuate dephosphorylation of EGFR [42]. Similarly, insulin-dependent signaling is modulated by NOX-derived reactive oxygen species. Not only does insulin stimulation of cells cause the generation of H_2O_2, but this peroxide formation is also essential to insulin signaling: by reversible oxidation of a redox-sensitive cysteine residue, H_2O_2 transiently inhibits PTP1B, a PTP that controls insulin receptor tyrosine phosphorylation [43–45]. A major H_2O_2 source in insulin-exposed adipocytes was then identified as NOX4, whose activity controls PTP1B activity and insulin receptor-dependent signaling [46].

NADPH oxidase complexes were originally identified as membrane-bound flavoenzymes responsible for the generation of superoxide in phagocytes upon stimulation. Five different isoforms of the catalytic subunit, NOX 1 through 5, have been identified, and NADPH oxidases are now known to be present in many non-phagocytes, to be activated by numerous stimuli, and to be crucial mediators in cellular signaling processes [47,48].

The exact mode of coupling the insulin receptor to NOX4 for an acute increase in ROS generation is unclear at present, particularly considering the current view of NOX4 as largely constitutively active (in contrast to NOX1 or 2) and regulated mainly at the level of expression [49]. However, a link between insulin exposure and a prolonged increase in generation of NOX4-derived ROS was established in 3T3-L1 fibroblasts [50]; insulin-induced signaling results in an enhanced expression of NOX4. Interestingly, insulin-induced NOX4 expression entailed the enhanced formation of MAPK-phosphatase-1 (MKP1) in that study, a dual-specificity phosphatase regulating MAPK phosphorylation that is also known as an immediate-early gene expressed under stress [51].

Stimulation of RTK-dependent signaling, including insulin signaling, may result in modulation of cascades that ultimately affect FoxO transcription factors. Two classical RTK-dependent signaling cascades result in activation of the Ser/Thr kinases Akt (protein kinase B) and the extracellular signal-regulated kinases (ERK) -1 and -2. Both are stimulated in cells exposed to various stressful stimuli, including ROS such as hydrogen peroxide, singlet oxygen or peroxynitrite [52–56]. Moreover, both modulate FoxO activities (see below). Further stress-responsive kinases include the other major mitogen-activated protein kinase (MAPK) family members in addition to ERK-1/ERK-2, $p38^{MAPK}$ isoforms and c-Jun-N-terminal kinases (JNKs). Again, $p38^{MAPK}$ and JNKs are stimulated by ROS and stimuli acting *via* the formation of ROS, such as ultraviolet radiation [57–59], singlet oxygen [60,61], peroxynitrite [55] or

Table 1
Phosphorylation sites in FoxO proteins[a].

Kinases[b]		Sites phosphorylated				Comment
Group [304,305]		***FoxO1a***	***FoxO3a***	***FoxO4***	***FoxO6***	
AGC [306]	**Akt**	T24, S256, S319 [307,308]	T32, S253, S315 [309]	T28, S193, S258 [310,311][c]	T26, S184 [312,313]	Interaction with 14-3-3 ↑; FoxO1a/3a/4: inactivation, nuclear exclusion; FoxO6: inactivation
	SGK		T32, (S253), S315 [314]			See Akt
	PKA	T24, S256, S319 [315]				See Akt
CMGC [316]	**JNK**		Not defined, but likely phosphorylated [317]; (*in vitro* only: S294, S425 [78])	T447, T451 [93][c]		FoxO3a: inactivation, nuclear exclusion [317] FoxO4: activation, nuclear accumulation [93]
	ERK	S246, S284, S295, S326 (analogous to human S329), S413, S415, S429, S467, S475 (numbers for murine FoxO1) [66]	S294, S344, S425 [65]			FoxO1a: enhanced interaction with other transcription factors suggested [66] FoxO3a: inactivation, nuclear exclusion, Mdm2-mediated degradation↑ [65]
	p38^{MAPK}	S284, S295, S326, S467, S475 (numbers for murine FoxO1) [66]	S7 [78]; (*in vitro* only: S12, S294, S344, S425 [78])			FoxO1a: enhanced interaction with other transcription factors hypothesized (in analogy to ERK) [66] FoxO3a: nuclear accumulation [78]
	CDK1	S249 [318]				FoxO1a: Interaction with 14-3-3↓; activation, nuclear accumulation [318]
	CDK2	S249, (S298) [94]				FoxO1a: inactivation, nuclear exclusion [94]; S249 phosphorylation verified, but no nuclear exclusion in some cells [318].
	DYRK1	S329 [98]				FoxO1a: inactivation, nuclear exclusion [98]
	GSK3	S325 (only *in vitro*) [319]				
	NLK	S329 (plus up to 7 other *Ser*-Pro) [320]				FoxO1a: inactivation, nuclear exclusion [320]
CK1 [321]	**CK1**	S322, S325 [319]				FoxO1a: phospho-S319 (Akt/SGK) generates recognition motif for CK1 to phosphorylate S322; thereafter, S325 is phosphorylated [319]. Inactivation, nuclear exclusion.
CAMK	**AMPK**		T179, S399, S413, S555, S588, S626 [23]			FoxO3a: activation; no effect on subcellular localization [23]
	MK5	S215 (murine FoxO1a; analogous to S218 in hFoxO1a) [322]	S215 (S253, S551, S555) [323]			FoxO1a: activation [322] FoxO3a: nuclear accumulation and activation [323]
STE	**MST1**	S212 [324]	S207 (S213, S229/230, S241) [324][d]			FoxO3a: interaction with 14-3-3↓; nuclear accumulation and activation [324]
Other	**IKKβ**		S644 [325]			FoxO3a: inactivation, nuclear exclusion, degradation↑ [325]
	PERK	S298, (S301, S303) [244]	Not defined, but likely phosphorylated [244]			FoxO1a: nuclear accumulation and activation [244]

[a] Numbers refer to human FoxO proteins, unless noted otherwise (*e.g.*, ERK, MK5).

[b] Abbreviations: AGC – kinase group incorporating, among others, the protein kinase A, protein kinase G, protein kinase C families; AMPK – AMP-activated kinase; CAMK – kinase group incorporating calcium and calmodulin-regulated kinases and related families; CDK – cyclin-dependent kinase; CK – casein kinase; CMGC – kinase group named after some of its members, such as the CDK, MAPK, GSK3, CDK-like kinase families; DYRK – dual specificity, tyrosine phosphorylation-regulated kinase; ERK – extracellular signal-regulated kinase; GSK – glycogen synthase kinase; IKK – inhibitor of κB kinase; JNK – cJun N-terminal kinase; MAPK – mitogen-activated protein kinase; MK5 – MAPK-activated protein kinase (MAPKAPK) 5; MST – mammalian sterile 20-like; NLK – nemo-like kinase; PERK – protein kinase R-like endoplasmic reticulum kinase; PKA – protein kinase A; SGK – serum/glucocorticoid-regulated kinase; STE – kinase group incorporating several yeast sterile kinase-like kinases.

[c] FoxO4 phosphorylation sites: the corresponding positions in the current version of the human FoxO4 sequence are T32, S197, S262, T451, and T455 [NCBI RefSeq accession number NP_005929.2 (GI:103472003)].

[d] FoxO3a phosphorylatiuon sites listed in Ref. [324]: the corresponding positions in the current version of the human FoxO3a amino acid sequence are S209, S215, S231/232, and S243 [NCBI RefSeq accession number of the sequence: NP_001446.1 (GI:4503739)].

hydrogen peroxide [62]. Akt-induced FoxO phosphorylation (at three sites in FoxO1a, 3a and 4, at two in FoxO6), as elicited upon stimulation of cells with insulin, usually results in FoxO inactivation and nuclear exclusion, resulting in an attenuation of FoxO-dependent expression of genes like those coding for glucose 6-phosphatase or phosphoenolpyruvate carboxykinase [63, 64]. Similarly, FoxO phosphorylation by ERK-1/-2 causes modulation of its activity: ERK-dependent phosphorylation of FoxO3a triggers its poly-ubiquitination by murine double minute (MDM)-2, followed by FoxO3a degradation [65]. Moreover, Asada et al. identified phosphorylation of (murine) Foxo1a by ERK (and by $p38^{MAPK}$) as regulating its transcriptional coregulator activity of Ets-1 transcription factor [66].

Mitochondria are another important endogenous source of ROS. Mitochondrial dysfunction can be the result of a metabolic imbalance, such as in the case of hyperglycemia, which is also linked to glycation of proteins and the formation of advanced glycation end products (AGEs), and fosters other oxidative processes causing elevated ROS formation, including NOX activation and uncoupling of eNOS [67]. Human aortic endothelial cells held under hyperglycemic conditions had elevated iNOS levels and activities, enhancing oxidation of LDL coincubated with the cells; FoxO1a was identified as the mediator, being upregulated by hyperglycemia, inducing iNOS and causing LDL oxidation [68]. High levels of H_2O_2 are also generated in peroxisomal fatty acid oxidation – *e.g.* by fatty acyl-CoA oxidase, the first enzyme of the classical peroxisomal fatty acid β-oxidation system – and in cytochrome *P*450-dependent xenobiotic metabolism [69–71].

Certain xenobiotics generate reactive oxygen species in cells by undergoing redox cycles, i.e. they are reduced by cellular enzymes at the expense of reducing equivalents such as NADH or NADPH, followed by reoxidation of the product by physically dissolved molecular oxygen, generating superoxide and reaction products thereof [72,73]. Certain quinones are examples of such redox cyclers and stimulate RTK signaling [74], in part through the generation of ROS [75], and can thus be expected to affect FoxO-dependent processes by modulating kinases known to phosphorylate FoxO proteins.

Doxorubicin is an anthraquinone derivative, DNA intercalating agent and topoisomerase inhibitor known to generate ROS (although probably not through redox cycling of the quinone moiety) in cells [76]. It is a known stimulator of ERK activation [77] and also causes p38 activation as well as p38-dependent FoxO3a phosphorylation (at Ser7), resulting in its nuclear accumulation and activation in MCF-7 breast cancer cells [78]. Doxorubicin treatment also appears to affect *Foxo* expression as it leads to an upregulation of *Foxo1a and 3a* mRNA levels in rat cardiac and skeletal muscle, but it is not known whether ROS formation is involved in this effect [79].

Redox-active metal ions can undergo redox cycling as well, and exposure to copper or iron ions will cause the generation of ROS in cells. Exposure of human hepatoma cells to copper ions strongly stimulated PI3K/Akt signaling [80] and FoxO phosphorylation and inactivation [81], which – despite formation of ROS – was independent of the generation of reactive oxygen species [82]. This explains why redox-inert metal ions like Zn^{2+} and Cd^{2+} also stimulate PI3K/Akt/FoxO signaling in a similar fashion, albeit less strongly so [82]. Different from these ions, Ni^{2+} did not stimulate a significant Akt-dependent FoxO phosphorylation [83]. Cu, Zn and Cd ions share an affinity for thiols, and a direct interaction with PTPase-type phosphatases such as PTEN was hypothesized as a potential mechanism of signaling initiation – which was indeed demonstrated to be the case for Zn [84].

Exposure of cells to arsenite – another molecule with high affinity towards thiols – results in oxidative damage to biomolecules [85,86], suggesting the generation of ROS. Exposure of rat pheochromocytoma cells to arsenite led to an induction of apoptosis *via* p38-dependent Foxo3a activation, followed by Foxo-dependent Bim-EL expression [87]. In human cells – HaCaT keratinocytes [88] and HepG2 hepatoma cells [89] – a stimulation of insulin-like signaling was observed, leading to an Akt-dependent phosphorylation of FoxOs and the inactivation of FoxO signaling.

Interestingly, even certain flavonoids, commonly categorized as antioxidants, may generate hydrogen peroxide through autoxidation in cell culture [90,91], which may cause stimulation of the PI3K/Akt cascade and phosphorylation of FoxO proteins, resulting in their inactivation and nuclear exclusion [92].

MAPK are proline (Pro)-directed kinases, and FoxO proteins contain several potential phosphorylation sites, i.e. a Ser or Thr, followed by a Pro residue. Therefore, it comes as no surprise that not only ERK, but also $p38^{MAPK}$ and JNK were shown to phosphorylate FoxO proteins. For example, (murine) Foxo1a – with 15 potential phosphorylation sites (14 of which are conserved in human FOXO1a) – is phosphorylated by ERK and $p38^{MAPK}$, but not by JNK [66], whereas FoxO4 is phosphorylated by JNK under conditions of oxidative stress, stimulating FoxO4 nuclear accumulation [93].

Other Pro-directed kinases may be expected to phosphorylate FoxOs – such as cyclin-dependent kinases (CDKs), glycogen synthase kinase-3 (GSK3) or dual specificity tyrosine-regulated kinase (DYRK)-1a. In fact, CDK2 was shown to phosphorylate FoxO1a in response to DNA damage, inducing its nuclear exclusion and inactivation [94]. In line with a potential direct interaction with FoxO proteins, GSK-3 stimulates FoxO transcriptional activity to result in enhanced IGF1-receptor formation [95]. Nevertheless, no GSK-3-dependent FoxO phosphorylation in vivo has yet been reported. DYRK-1a is a Pro-directed kinase [96,97] that phosphorylates Ser329 in FoxO1a, which appears to slightly support nuclear exclusion and to moderately affect FoxO activity [98]. The flavonoid, epigallocatechin gallate (EGCG), while generating H_2O_2 in cell culture at high concentrations, is a potent inhibitor of DYRK-1a [99]. This explains why very low EGCG concentrations under conditions that do not generate any detectable H_2O_2 in the experimental setup stimulate nuclear accumulation of FoxO1a rather than a H_2O_2-induced nuclear exclusion [92]. Similar effects were seen with *C. elegans*: EGCG induced the nuclear accumulation of DAF-16 and enhanced expression of SOD-3 [92].

In summary, several kinases phosphorylate FoxO proteins in response to elevated levels of ROS and upon exposure of cells to stressful stimuli. Table 1 provides a summary of known FoxO phosphorylation events. Akt, ERK, $p38^{MAPK}$ and JNK are among the stress-responsive kinases known to target FoxOs, and to contribute to the modulation of FoxO activity and subcellular localization: while Akt usually inactivates FoxOs and causes their nuclear exclusion, JNK may phosphorylate and activate FoxO4, stimulating its nuclear accumulation (see Fig. 4 for an overview on FoxO phosphorylation events and their consequences). However, other PTMs may fine-tune the consequences of FoxO phosphorylation. Thus, the following section will focus on FoxO acetylation and ubiquitination in the cellular response to oxidative stimuli.

3.2. ROS control of FoxO activity by lysine modification: acetylation and ubiquitination

The ε-amino group of lysine (Lys, K) residues in proteins can be modified post-translationally through acetylation and mono- or poly-ubiquitination. Calnan and Brunet [16] listed six known acetylation sites each in human FoxO1a (K245, K248, K262, K274, K294, K559) and in human FoxO3a (K242, K245, K259, K271, K290, K569) as well as five acetylation sites each in human FoxO4 (K186, K189, K215, K237, K407) and in human FoxO6 (K173, K176, K190, K202, K229). Another previous compilation specified FoxO1a

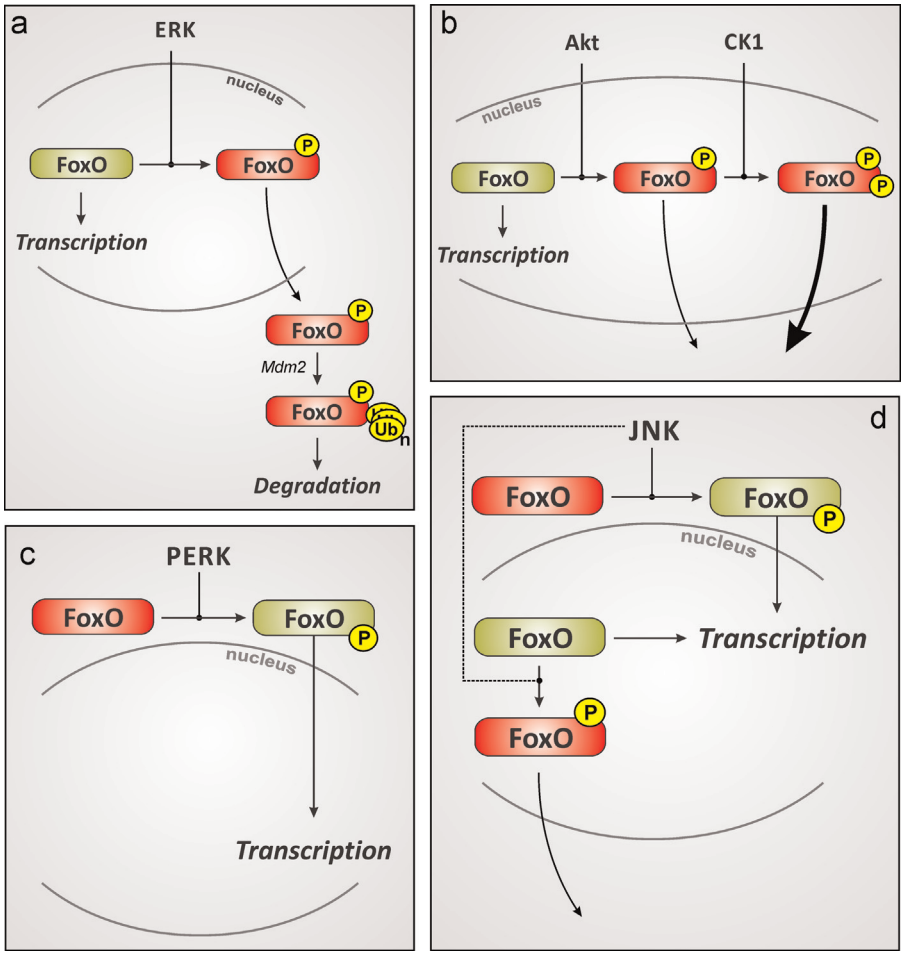

Fig. 4. FoxO phosphorylation and its biological consequences. Schematic representation of FoxO phosphorylation by different kinases and the consequences with respect to activity and subcellular localization. (A) ERK-catalyzed phosphorylation of FoxOs may cause nuclear exclusion and murine double-minute (Mdm)-2-dependent proteasomal degradation [65]. Similarly, Akt (B) catalyzed FoxO phosphorylation will cause FoxO inactivation, nuclear exclusion and may trigger FoxO degradation (not shown). Interestingly, FoxO1a phosphorylation at S319 was shown to prime for a consecutive phosphorylation by casein kinase 1 (CK1), which further enhances nuclear exclusion [319]. FoxO phosphorylation may also result in nuclear accumulation and activation: (C) ER-stress may cause PERK-dependent FoxO phosphorylation and activation [244]. (D) c-Jun-N-terminal kinase (JNK)-dependent FoxO phosphorylation was described as activating (FoxO4 [93]) or inactivating (FoxO3a; dashed lines [317]). Phosphorylation is indicated by a black "P" on yellow background and stands for phosphorylations at multiple different sites (*e.g.* Akt: T24, S256, S319 for human FoxO1a). See Table 1 for further explanations. (For interpretation of the references to color in this figure legend, the reader is referred to the web version of this article.)

(K265) and FoxO3a (K203) as additional acetylation sites [100]. Reversible lysine acetylation is accomplished by the action of histone acetyltransferases and deacetylases: CBP (CREB-binding protein), p300 and p300/CBP-associated factor (PCAF) acetylate FoxOs, using acetyl-CoA as co-substrate, whereas enzymes of the sirtuin (Sirt, orthologues of silent information regulator) family catalyze NAD^+-dependent deacetylation of FoxOs [101–107]. Most of the acetylation sites in human FoxO proteins surround a consensus site for Akt-induced serine phosphorylation (S256 in the case of human FoxO1a) within the nuclear localization signal (NLS) motif, a region that is highly conserved among the FoxO isoforms [100] (Fig. 2). This conserved localization of major acetylation sites in the FoxO proteins implies functional links between their acetylation state and metabolic regulation of reversible phosphorylation, cytoplasmic/nuclear shuttling and transcriptional activity of FoxOs, which indeed have been identified and turned out to be very complex and in part controversial. Acetylation has been shown to result in both stimulation and inhibition of the transcriptional activity of FoxOs, depending on the examined FoxO isoforms and their binding partners such as other transcription factors and transcriptional co-activators, the FoxO target genes and the cell types used in the studies [103,104,106,108,109]. The molecular mechanisms underlying those discrepancies are still not completely understood. The enzymes in charge of FoxO acetylation and deacetylation also alter the acetylation state of histones and of the FoxO coactivator PGC-1α (peroxisome proliferator-activated receptor γ-coactivator-1α) [110], which may modify the effect of a stimulus on FoxO-induced gene transcription.

The histone acetyltransferase (HAT) and transcriptional coactivator p300 was initially identified as a coactivator of FoxO proteins [111]. Early reports stressed the fact that p300-dependent acetylation of FoxO proteins resulted in enhanced FoxO transcriptional activity [105,112], and the interaction between the two proteins facilitated the recruitment of p300 to the promoter regions of target genes, where p300 further enhanced gene transcription by recruiting the basal transcriptional machinery and by facilitating chromatin remodeling through its intrinsic HAT activity [113]. It was also proposed that p300-mediated acetylation of FoxOs increase their transcriptional activity. However, it was soon noted that, at least in some contexts, p300-induced acetylation could also suppress their transcriptional activity [114]. This observation was quickly followed by the identification of the histone deacetylase Sirt as a positive regulator of FoxO activity [102].

In addition to acetylation, the above-mentioned lysine residues in FoxO proteins can also become ubiquitinated. Mono-ubiquitination has been shown to result in nuclear translocation and

increased transcriptional activity of FoxO4 [115]. As the same lysine residues are shared for acetylation and ubiquitination, deacetylation may facilitate FoxO ubiquitination: deacetylation by Sirt1 or Sirt2 promoted FoxO3a poly-ubiquitination mediated by increased binding of the E3 ubiquitin ligase subunit Skp2 and subsequent FoxO3a proteasomal degradation [116]. As mentioned above for FoxO3a [65], the phosphorylation state of FoxOs may also affect their susceptibility to poly-ubiquitination and degradation: FoxO1a has been shown to be ubiquitinated by Skp2, and prior Akt-mediated phosphorylation at serine residue S256 facilitated FoxO1a poly-ubiquitination [117].

Oxidative stress mediated by increases in intracellular levels of ROS, specifically H_2O_2, has been identified as a key mediator of the acetylation and ubiquitination state of FoxOs [101,104,109,115,118]. Besides H_2O_2, the redox-cycling oxidant menadione induced transient FoxO3a acetylation, whereas UV and γ-irradiation had no effect [101]. Importantly, though, application of moderately high doses of exogenous H_2O_2, typically 25–500 μM, was required to trigger interaction of acetyl transferases with FoxOs [101,109]. These doses are considerably higher than the (physiological) levels of 0.1–7 μM H_2O_2 that stimulate cellular proliferation and mimic insulin-induced phosphorylation of FoxOs [119]. In contrast, application of exogenous H_2O_2 in higher micromolar concentrations initially induces growth arrest and possibly a subsequent cellular adaptation to oxidative stress [119]. The molecular mechanism of H_2O_2-mediated FoxO acetylation has been elucidated for FoxO4: Exogenously added H_2O_2 at a minimum concentration of 25 μM triggered the formation of heterodimers between p300/CBP acetylases and FoxO4 through intermolecular disulfide bridges, linking redox-sensitive cysteine residues [109]. Moreover, an increase in endogenous cellular ROS production resulting from glucose deprivation of the culture medium was also sufficient to induce hetero-dimerization of p300/CBP and FoxO4, whereas the antioxidant N-acetyl cysteine (NAC) counteracted this redox-sensitive interaction between the proteins [109]. Turnover of the p300/CBP-FoxO4 complex was regulated by the disulfide-reducing activity of thioredoxin-1 [109], a small antioxidant protein localized both in cytosol and nucleus [120]. The p300/CBP-FoxO4 interaction is primarily mediated through cysteine residue C477 in human FoxO4, and intriguingly, this cysteine residue is conserved among all human and murine FoxO isoforms [109]. This suggests the possibility that redox-sensitive hetero-dimerization with acetylases might represent the general mechanism of H_2O_2-induced FoxO acetylation. However, a recent screening study identified several proteins including peroxiredoxins and glyceraldehyde-3-phosphate dehydrogenase (GAPDH) that bound after H_2O_2 treatment to the homologous cysteine residue in human FoxO3a (C622), but acetylases were not included in the provided list. Also, the other redox-sensitive cysteine residues in human FoxO3a did not interact with acetyltransferases [121].

Under conditions of oxidative stress, acetylated FoxO3a has been shown to translocate from the cytosol into the nucleus, where it may interact with the nuclear sirtuin Sirt1 to become deacetylated [101]. Sirt1 activity is regulated by the NAD^+/NADH ratio and acts as a sensor of the cellular redox status that becomes activated when reducing equivalents are limiting [122]. Likewise, FoxO1a and FoxO4 are deacetylated by Sirt1, causing their nuclear trapping and modifying their transcriptional activity [102–104]. In most cases, transcriptional activity of FoxOs is elevated upon deacetylation. As net result of the successive acetylation and deacetylation events, deacetylated FoxOs become enriched in the nucleus and increase transcription of cell cycle arrest genes such as *CDKN1B* (coding for cyclin-dependent kinase inhibitor $p27^{Kip1}$), DNA repair genes such as *GADD45* (growth arrest and DNA damage-inducible protein 45) and genes coding for antioxidant enzymes such as SOD-2, whereas transcription of apoptotic genes is decreased [101, 107, 118]. This switch may allow cells to survive oxidative and metabolic stresses, as it has been demonstrated for FoxO3a in the landmark study by Brunet et al. [101]. This model has since been confirmed for FoxO1a and FoxO4: both successive acetylation/deacetylation of FoxO1a and FoxO4 induced the expression of *CDKN1B* and *SOD2* [102,123]. The physiological relevance of this regulation was later demonstrated in mouse models of oxidative stress-induced heart failure [124,125]. The report by Alcendor et al. [125] also showed that Sirt1-mediated FoxO deacetylation regulates the catalase gene. A later study demonstrated regulation of catalase production by the FoxO/Sirt1 complex in renal tubular cells [126]. Recently, it was found that Sirt1-mediated FoxO deacetylation regulates FoxO-dependent expression of genes coding for additional ROS detoxification enzymes, peroxiredoxins 3 and 5 (Prx3, Prx5), thioredoxin 2 (Trx2), thioredoxin reductase 2 (TrxR2), and also uncoupling protein 2 (UCP-2), a protein that protects mitochondria from excessive superoxide generation in the electron transport chain (ETC) [20]. Importantly, FoxOs are indispensable for Sirt1-dependent cell survival under oxidative stress [127]. In another study, successive acetylation/deacetylation of FoxO1a protected against acute β-cell failure induced by H_2O_2, preserving insulin biosynthesis and secretion through induction of the transcription factors NeuroD and MafA [128]. As deacetylated FoxOs are then again more sensitive to poly-ubiquitination and proteasomal degradation [116,128], the (de)acetylation-mediated switch in gene expression of FoxO target genes is expected to protect cells from acute but not from chronic stress.

Several studies have analyzed the mechanistic details that underlie FoxO regulation by successive acetylation/deacetylation. It has been reported that acetylation by p300 reduces the DNA binding affinity of FoxO only marginally [129], while it significantly destabilizes FoxO binding to nucleosome-bound DNA [130]. Stable nucleosome binding is essential for efficient FoxO-dependent chromatin remodeling, because FoxOs work as pioneer transcription factors capable of binding compacted hypoacetylated chromatin [131]. Daitoku et al. proposed a model by which formation of the p300–FoxO complex causes histone acetylation and the recruitment of a preinitiation complex containing RNA polymerase II (RNAPII) to the target promoter and the induced transcription could be attenuated by the subsequent FoxO1a acetylation by CBP [132]. Olmos et al. [20] analyzed Sirt1 binding and histone acetylation in the promoter regions of Sirt1/FoxO target antioxidant genes. Their study found that Sirt1 binding to these promoters was associated with decreased nucleosome acetylation and decreased RNAPII binding. Importantly, decreased RNAPII binding was compensated by enhanced formation of elongation RNAPII complexes, resulting in a net induction of gene expression. These results may suggest that in those promoters where transcription elongation is not a kinetically limiting factor, Sirt1-dependent lowering of RNAPII binding would lead to transcriptional down-regulation, while in those where transcriptional elongation is the kinetically limiting step, Sirt1 activity would result in transcriptional activation. The higher transcriptional activity of deacetylated FoxOs has also been explained by a better binding capability to target DNA sequences due to the presence of positively charged lysine residues; conversely, lysine acetylation weakened the FoxO1a-DNA interaction and made FoxO1a more prone to Akt-induced S256 phosphorylation and in turn nuclear exclusion [108]. It should be noted, too, that the higher DNA binding capability of deacetylated FoxOs can result in trans-repression of target genes of other transcription factors. As an example, iron-induced deacetylation of FoxO1a in adipocytes has been found to decrease transcription of the PPAR-γ target gene adiponectin due to enhanced binding of FoxO1a at the PPAR-γ response element in the adiponectin promoter [133].

In addition to Sirt1, other sirtuins have been proposed to regulate FoxO activity. It has been shown that the cytosolic isoform Sirt2 is capable of deacetylating FoxO1a and FoxO3a, thereby promoting their re-localization from the cytoplasm to the nucleus and increasing FoxO-dependent transcription of antioxidant enzymes [134,135].

Sirt3 is the only sirtuin whose expression has been linked to human longevity [136,137]. Initially described as a mitochondria-specific deacetylase [138], it is in fact a nuclear protein that is translocated to the mitochondria upon oxidative stress [138,139]. It has been described that FoxO3a and Sirt3 directly interact in the mitochondria and that Sirt3 activates FoxO3a-dependent gene expression, probably by increasing the binding of FoxO3a to the promoters of its target genes [140]. In cardiomyocytes, a Sirt3-mediated increase in FoxO3a activity prevented cardiac hypertrophy through induction of SOD-2 and catalase [141] and by suppressing the calcium/calcineurin-dependent activation of NFAT [142]. Therefore, NFAT inhibition might be indirect and mediated by a reduction in ROS levels.

Also, the role of Sirt6 is increasingly appreciated. In *C. elegans*, it has been shown that the Sirt6 orthologue SIR-2.4 promotes nuclear localization of the FoxO orthologue DAF-16 in response to stress [143]. In mammals, studies demonstrating a functional interaction of Sirt6 with FoxO3a relate to cholesterol homeostasis in the liver. Sirt6 was shown to affect FoxO3a-dependent transcription of SREBP2 (sterol-regulatory element binding protein 2), a major transcriptional regulator of cholesterol biosynthesis, and PCSK9 (proprotein convertase subtilisin/kexin type 9), a crucial enzyme for the control of LDL receptor degradation: FoxO3a recruits Sirt6 to the promoters, where Sirt6 histone deacetylation promotes a repressive chromatin state [144, 145].

4. Redox regulation of FOXO expression

Compared to the well-studied regulation of FoxO activity by posttranslational modifications and protein-protein interactions, mechanisms regulating FoxO gene transcription and mRNA stability are much less known. Here, we provide examples of studies that describe up- or downregulation of FoxO gene expression, often in response to stressful stimuli, including DNA damage, hypoxia/reoxygenation, or oxidative stress.

4.1. Transcriptional regulation of FoxO gene expression

The first transcription factor identified as regulating FoxO genes was E2F-1 [146]. E2F-1 controls cell cycle progression and apoptosis in various cell types [147–150]. Nowak et al. [146] found several putative E2F binding sites in the promoters of the human FoxO1a and FoxO3a genes. Using a human neuroblastoma cell line stably expressing an E2F-1-ER (estrogen receptor) fusion protein, they showed that both FoxO1a and FoxO3a are direct target genes of E2F-1 and are strongly upregulated by this factor [146]. Moreover, using chromatin immunoprecipitation, the direct binding of endogenous E2F-1, as well as of E2F-2 and E2F-3, to the FoxO1a promoter was demonstrated. Of note, upregulation of FoxO by E2F-1-ER was cell type- and species-specific [146], pointing to a possible involvement of additional transcription factors/co-factors or chromatin modifications.

A role of the E2F-1/FoxO axis in regulating the apoptotic response of cardiomyocytes to ischemia/reperfusion (I/R) injury was identified in mice [151,152]. Using E2F-1 knockout mice, Angelis et al. [151] showed that both E2F-1 and FoxO1a are upregulated in the wild-type mice after I/R injury, while in E2F-1-null animals FoxO1a mRNA was not increased. In agreement with that, several pro-apoptotic FoxO1a target genes were also upregulated in the wild-type but not in the E2F-1 knockout mice, and extent of I/R injury (infarct area) was attenuated in the mutant animals. The role of FoxO1a as a critical regulator of cardiomyocyte apoptosis in response to hypoxia followed by reoxygenation was further confirmed *in vitro*, using primary adult mouse cardiomyocytes and neonatal rat ventricular myocytes [151].

In an apparent discrepancy to the above results, Sengupta et al. [152] showed that FoxO1a and FoxO3a are necessary and sufficient to promote cardiomyocyte cell survival upon induction of oxidative stress by acute I/R or myocardial infarction (MI). The mice with conditional, cardiomyocyte-specific, combined deletion of FoxO1a and FoxO3a exhibited significant increase in infarct area and decreased expression of anti-apoptotic molecules, antioxidant enzymes and autophagy-related proteins following I/R, as compared to controls. The same conditional FoxO knockout mice subjected to MI had increased apoptotic cell death relative to controls, among other cardiac defects [152]. The seemingly opposing results of the two reports could be explained by (i) the dual role of FoxO in combating oxidative stress – pro-survival and pro-apoptotic, where both pathways might be activated following the initial stress signals, and the final outcome would depend on the severity of the cardiomyocyte injury, and (ii) the fact that the absence of the pro-apoptotic FoxO function in FoxO knockout cardiomyocytes might be compensated for by some other apoptotic pathway. Consequently, such cells and cardiac regions would display a higher degree of injury compared to the wild-type controls, as well as to the imaginary E2F-$1^{-/-}$ $FoxO^{+/+}$ "control", where FoxO pro-apoptotic function could be impaired, while its pro-survival role would remain operative.

The link between E2F-1 and FoxO may be more intricate than outlined above. Shats et al. [153] found that FoxO1a and FoxO3a, with their genes being E2F-1 targets, can act in a feed-forward regulatory loop by forming a complex with E2F-1 to reinforce gene induction of multiple apoptotic genes. However, as the experiments were done in U2OS human osteosarcoma cells stably expressing an E2F-1-ER fusion, it is not clear whether the same type of regulation can take place also in cardiomyocytes and/or under conditions of severe hypoxia/reoxygenation. Indeed, at least some target genes are regulated differently, as the E2F-1/FoxO complex in U2OS cells upregulates, for example, the classic apoptotic gene APAF1 [153], whereas APAF1 is not upregulated in the myocardium after I/R injury [151]. This may reflect cell context or species-specific (human *vs.* mouse) differences.

In human fibroblasts, E2F-1 enhances cellular senescence, whereas FoxOs antagonize senescence by upregulating the formation of ROS scavenging proteins [154,155]. Xie et al. [156] showed that E2F-1 attenuates FoxO3a-mediated expression of MnSOD and catalase. They mapped interaction between E2F-1 and FoxO3a to a region including the DNA binding domain of E2F-1 and the C-terminal transcription activation domain of FoxO3a. They propose that E2F-1 inhibits FoxO3a function by directly binding FoxO3a in the nucleus and preventing the activation of its target genes [156]. Depending on the cellular and promoter context (and possibly also on the redox conditions in the cell), the two proteins can therefore act synergistically, or one can antagonize the activity of the other.

The real promoter scenarios are likely to be even more complicated. In their impressive study, Zheng et al. [157] uncovered the mechanism that underlies and dictates two mutually exclusive biological outcomes of E2F-1 activity. They describe the site-specific methylation of E2F-1 by the asymmetrically dimethylating protein arginine methyltransferase 1 (PRMT1) and symmetrically dimethylating PRMT5. Methylation by PRMT1 blocks methylation by PRMT5, which strengthens E2F-1-driven apoptosis in cells harboring damaged DNA. Conversely, PRMT5-catalysed methylation and cyclin A binding to E2F-1 block PRMT1 methylation and

promote proliferation [157]. It will be interesting to see how the PRMT1 asymmetric methylation mark on E2F-1 is read on the promoters of its apoptotic target genes.

E2F-1 is not the only transcription factor known so far to directly regulate FoxO genes. Two recent reports reveal roles for p53 tumor suppressor protein as an upstream regulator of FoxO3a [158,159]. Kurinna et al. [158] report FoxO3a as a new p53/p73 target gene. They demonstrate that in the quiescent liver of the adult mouse, p53 and the transactivating isoform of its homolog p73 (TA-p73) reside on the FoxO3a promoter and maintain its transcription active. TA-p73 can bind the same consensus site as p53, and the authors detected binding of both proteins to a predicted p53 response element located -3.7 kb upstream of the FoxO3a transcription start site. In marked contrast to the quiescent state, transcription of the FoxO3a gene is strongly downregulated during the proliferative stage of liver regeneration following partial hepatectomy. This is apparently caused by the disruption of p53, TA-p73, and acetyltransferase p300 binding to, and loss of active chromatin structure within the FoxO3a promoter region. The factors maintaining FoxO3a expression are reestablished and FoxO3a transcription upregulated with the growth completion and recovery of liver mass [158].

Loss of both p53 function and FoxO3-mediated regulation of transcription have been linked to increased proliferation and tumorigenesis [65,160,161]. In summary, the authors [158] suggest a regulatory axis between the p53 family members and FoxO tumor suppressors that functions in the surveillance of normal hepatocytes and is temporarily turned off in the course of liver regeneration. In this context, it would be interesting to survey the FoxO3a promoter status in various liver cancers.

In the second report, Renault et al. [159] point out a number of similarities in function between FoxO3a and p53, *e.g.* in induction of cell cycle arrest, apoptosis and DNA repair, and to both direct and indirect interactions between the two proteins (see [159] and references therein). This raised a question as to whether one of the proteins could regulate transcription of the other. Indeed, it was found that p53 specifically upregulates the transcription of the mouse FoxO3a gene in embryonic fibroblasts (MEF) and in thymocytes in response to DNA damage [159]. Furthermore, using *in silico* searches, the authors found four putative p53 binding sites, three of them in the promoter and one in the second intron of the FoxO3a gene. The subsequent chromatin immunoprecipitation assays with extracts from MEFs identified p53 binding to the site in the second intron, but not to those in the promoter region. Although p53 was bound to the intronic site even in the absence of DNA damage, its recruitment to the site was slightly increased following doxorubicin treatment. Moreover, the intronic p53 binding site was proven to be necessary and sufficient for p53-specific transactivation of a luciferase reporter. Further experiments showed that FoxO3a is not required for p53-dependent cell cycle arrest, but it has a role in p53-directed apoptosis [159].

The above two reports describe p53 binding to two sites within the mouse FoxO3a gene; one located in the promoter region and the other in the second intron. Notably, the site occupancy by the p53 protein differs between the adult liver and MEFs, in agreement with different modes of transcriptional regulation in the two tissues. In quiescent liver, the p53/p73 proteins seem to maintain FoxO3a expression at a constant level, in order to prevent hepatocyte proliferation, whereas in MEFs the role of p53 is to upregulate FoxO3a following DNA damage. Possibly, different locations of the binding sites reflect involvement of different cooperating factors/cofactors in order to ensure the proper regulatory mode.

A positive feedback loop in the regulation of FoxO genes transcription has been characterized within the FoxO family itself [162]. Essaghir et al. [162] showed in human fibroblasts that FoxO3a can upregulate FoxO1a and FoxO4 genes expression. At least with the FoxO1a gene, this is achieved by direct binding of FoxO3a to the FoxO binding site, identified in the FoxO1a promoter and characterized in this study. Conversely, all three genes are repressed by growth factors, *e.g.* PDGF and FGF, and in case of FoxO1a and FoxO4 this may be achieved by inactivation of FoxO3a protein by phosphorylation. Understanding the downregulation of the FoxO3a gene itself by growth factors such as FGF requires further studies. The authors conclude that this new mechanism operating at the transcriptional level modulates fibroblast proliferation [162].

By contrast, Zhu et al. [163] report that FoxO3a negatively regulates autophagy by inhibiting FoxO1a transcription in prostate cancer PC3 cells. It is possible that the transactivating effect of FoxO3a on the FoxO1a promoter is reversed to a repressive one in the tumor cell line context, however, this issue requires further experiments.

Bakker et al. [164] showed that FoxO3a transcription is upregulated during hypoxia in a hypoxia-inducible factor-1α (HIF-1α)-dependent manner in MEFs and NIH3T3 fibroblasts. Under these conditions, FoxO3a in turn induces transcription of CITED2, which inhibits HIF-1α-induced apoptosis in a negative feedback loop. Thus, FoxO3a plays a pro-survival role in response to hypoxic stress [164]. The authors found nine HIF-responsive elements conserved in human and mouse FoxO3a promoters. Whether FoxO3a is a direct target of HIF-1α has yet to be documented. HIF-1α -dependent increase of FoxO3a mRNA and protein levels under hypoxic conditions or following hypoxia-mimetic dimethyloxalyl glycine treatment has more recently been confirmed by Samarin et al. for mouse glomerular microvascular endothelial cell line glEND.2 [165].

Two recent reports analyze regulation of FoxO transcription during fasting and metabolic stress. Wondisford et al. [166] report increases of FoxO1a transcript and protein levels both in the liver of mice fasted for 16 h, as well as in hepatocytes treated with dibutyryl cAMP. The authors identified and functionally characterized tandem cAMP-response elements in the FoxO1a promoter and showed that co-activator p300 regulates FoxO1a gene expression in complex with the cAMP-response element-binding protein (CREB). Lützner et al. [167] identified two functional glucocorticoid-responsive elements (GREs) in the promoter of the FoxO3a gene. FoxO3 transcription was induced by glucocorticoid receptor (GR)-binding steroids and further augmented by activation of AMP-activated protein kinase (AMPK). Moreover, FoxO3a protein upregulated its own promoter, thus acting in a positive autoregulatory feedback loop. The study shows how, under conditions of metabolic stress, GR and high levels of intracellular AMP cooperate to induce FoxO3 gene transcription and post-translationally activate FoxO3a protein [167]. Multiple functional GREs were recently detected also in the murine FoxO1 promoter [168]. These experiments, performed in the C2C12 myoblasts, suggested an additional mechanism by which GR stimulates muscle atrophy [168].

Finally, the FoxO1a gene has been shown to be a direct transcriptional target of FoxC1 in cultured human trabecular meshwork (TM) cells (cells originating from the eye) and in the zebrafish developing eye [169]. FoxC1 binding to an evolutionarily conserved element in the FoxO1a promoter was demonstrated *in vivo*. Furthermore, siRNA-based downregulation of FoxC1 increased cell death in response to oxidative stress in TM cells (imposed by H_2O_2 treatment), and in the developing zebrafish eye, indicating the role of the FoxC1–FoxO1a axis in cellular homeostasis and stress protection [169].

While the above data raise an intriguing possibility that E2F-1, p53, FoxO3a, Hif1, p300, GR, and FoxC1 interact in regulating the transcription of FoxO genes, there are further reports describing the up- or downregulation of FoxO gene expression, *e.g.* during differentiation processes and/or as a cellular response to certain physiological cues, with the regulating transcription factor unknown. For example, an upregulation of *FoxO1a and -3a* but not *-4* mRNAs as well as FoxO1a protein by oxidative stress was observed

in murine follicular granulosa cells, followed by FoxO nuclear accumulation and apoptosis [170].

As detailed in a later paragraph, FoxO1a is involved in the regulation of adipocyte differentiation [171,172]. FoxO levels increase during the differentiation of preadipocytes to mature adipocytes, and it has been proposed that FoxO1a-mediated upregulation of antioxidant enzymes may limit the risk of oxidative damage provoked by the generation of intracellular ROS during adipogenesis [173].

FoxO1a is also upregulated during differentiation of human endometrial stromal cells into decidual cells (endometrial decidualization), a process induced by cAMP and progesterone signaling and accompanied by elevated ROS levels and oxidative stress [174–177]. In parallel to the FoxO1a gene induction in the course of the differentiation, FoxO3a expression is downregulated. It is thought that while FoxO1a enhances resistance to oxidative damage during this process, FoxO3a downregulation prevents induction of apoptosis in differentiated, decidualized cells [176].

Expression of FoxO genes has also been shown to change in response to nutritional and hormonal factors [178], aging and caloric restriction [179], and as a result of B cell receptor signaling [180,181].

In conclusion, the transcription of FoxO genes is regulated in response to a number of physiological cues and pathological stress stimuli that are frequently associated with increased oxidative stress. The altered FoxO protein levels impact pro-survival or pro-apoptotic pathways within the cells.

4.2. Posttranscriptional regulation of FoxO levels

Posttranscriptional regulation of FoxO expression emerges as a new level of complexity in controlling FoxO functions in both normal and cancer cells. Four distinct mechanisms have been identified so far: (i) the RNA-binding protein, HuR, stabilizes FoxO-mRNA, (ii) the RNA-binding protein Quaking decreases FoxO mRNA stability, (iii) the FoxO1a 3′UTR may function as a competing endogenous RNA (ceRNA), and (iv) numerous microRNAs have been described that target FoxO transcripts.

The RNA binding protein HuR responds to stressful stimuli that cause its cytosolic accumulation. These stimuli include hydrogen peroxide [182,183], or conditions that generate ROS – including UV radiation [182,184], exposure to arsenite [185], or *tert*-butylhydroquinone [186]. All these stimuli activate $p38^{MAPK}$, which directly or indirectly (*e.g.*, *via* MAPK-activated kinase-2, MK2) stimulates phosphorylation of HuR, which in turn mediates stress-induced cytoplasmic accumulation of HuR and enhances its mRNA stabilizing activity [187–189].

Additionally, it was proposed that HuR itself could act as a redox sensor. A cysteine residue in the first of the three HuR RNA recognition motifs was identified as crucial for homodimerization. Homodimerization is required for full HuR activity, and the authors of the study suggest that this cysteine may respond to oxidative stress and affect HuR homodimer formation and activity [190].

Li et al. [191] identified HuR as interacting with the 3′-untranslated region (3′UTR) of human FoxO1a mRNA, which leads to transcript stabilization and positive regulation of FoxO1a expression. Furthermore, 5-fluorouracil (5-FU) treatment induced FoxO1a expression in a HuR-dependent manner, and that enhanced 5-FU-induced apoptosis in breast cancer cells [191].

Conversely, Yu et al. [192] showed negative regulation of FoxO1 mRNA at the posttranscriptional level by the RNA-binding protein Quaking (QKI). QKI binding to three QKI-response elements (QREs), found in the FoxO1 3′UTR, destabilizes and downregulates FoxO1 mRNA in breast cancer cell lines [192].

Yang et al. found that miR-9 binds both FoxO1a and E-cadherin 3′ UTR, indicating a competition for this miRNA between the two transcripts. The results suggest that FoxO1a 3′UTR can function as a ceRNA, promoting E-cadherin expression and inhibiting epithelial-to-mesenchymal transition and metastasis of breast cancer cells [193].

Numerous reports show that upregulation of specific microRNAs leads to downregulation of FoxO1a (*e.g.*, miR-137, miR-223, miR-370) or FoxO3a (*e.g.*, miR-96, miR-155) transcripts in various cancer cells, thus promoting their proliferation [194–199].

4.3. FoxO transcriptional coregulators in redox regulation of FoxO activity

The transcriptional coactivator PGC-1α is an upstream regulator of carbohydrate and lipid metabolism as well as mitochondrial biogenesis and function that associates with different transcription factors to regulate target gene expression; and it has been shown to regulate FoxO activity in different systems [14]. PGC-1α is a positive regulator of fasting-induced hepatic gluconeogenesis and this is mediated through its interaction with FoxO1a [200]. Similarly, the FoxO1a-mediated stimulation of selenoprotein P (SelP) expression in hepatocytes is enhanced by interaction of PGC-1α with FoxO1a [29]. PGC-1α has also been shown to interact with FoxO3a to regulate antioxidant gene expression in endothelial cells and in the skeletal muscle where PGC-1α overexpression is sufficient to attenuate muscle atrophy induced by expression of a constitutively active FoxO transgene [201]. Importantly, the role of PGC-1α inhibition of FoxO3a to increase muscle resistance to catabolic wasting does not compromise the capacity of PGC-1α to reduce oxidative stress in cardiac muscle [202].

In the kidney, high fat diet-induced renal lipotoxicity is associated with insulin resistance and dyslipidemia, possibly due to the downregulation of FoxO3a and PGC-1α and associated with increased oxidative stress. Administration of TEMPOL, a radical scavenger [203] that was recently shown to prevent renal injury by modulating PI3K-Akt-FoxO signaling [204], ameliorated high fat diet-induced renal damage, probably due to the upregulation of FoxO3a and PGC-1α which resulted in protection against oxidative stress and lipoapoptosis [205].

Coordinated upregulation of FoxO and PGC-1α in response to manganese-induced neurotoxicity has been observed, suggesting a coordinated regulation of antioxidant gene expression [206]. Such a co-regulation of genes involved in the protection against oxidative stress has been previously described in endothelial cells [207].

The transcriptional cofactor and lysine demethylase KDM has recently been shown to induce the expression of genes involved in antioxidant defense through its interaction with FoxO. The results show that the principal role for the complex is to maintain the basal expression of oxidative stress resistance genes rather than their induction in response to exogenous oxidative stress [208]. The results further suggest that FoxO access to different chromatin contexts and nuclear microenvironments may rely on different cofactors.

In human cell lines, Ataxin-3/ATXN3 has been shown to interact with FoxO4 and to increase FoxO-dependent transcription of the gene coding for SOD-2. Upon stimulation of oxidative stress, ATXN3 and FoxO4 translocate to the nucleus and coordinately induce the expression of *SOD2*. Cell lines from patients with spinocerebellar ataxia type 3, deficient in ATXN3, when exposed to oxidative stress, show reduced binding of FoxO4 to the *SOD2* promoter, impaired upregulation of SOD-2, and a significantly increased formation of ROS that correlates with the increase in cytotoxicity [209].

5. Physiological and pathophysiological consequences of redox (dys)regulation of FoxOs: selected examples

5.1. Metabolic adaptation to low nutrient intake

The acetylation state of FoxOs affects FoxO-controlled gene regulation in metabolic adaptation to fasting, caloric restriction

and starvation. In response to fasting signals, Sirt1 deacetylates both FoxO1a and PGC-1α in hepatocytes, resulting in increased transcription of gluconeogenic genes and elevated glucose release from the liver [104,110]. Nutrient deprivation has been shown to trigger intracellular formation of H_2O_2 that serves as signaling molecule for the induction of autophagy [210]. Autophagy is an adaptation mechanism to support cellular survival during starvation through delivering cytoplasmic constituents to lysosomes for degradation and recycling [211]. Protein levels of both FoxO1a and Sirt1 were elevated in cultured cardiac myocytes after 2 h of glucose deprivation; Sirt1-catalyzed deacetylation of FoxO1a caused an increase in the autophagic flux through stimulating the expression of Rab7, a GTP-binding protein that mediates the fusion of autophagosomes and lysosomes [212]. *In vivo*, deacetylation of FoxO1a by Sirt1 has also been shown to be required for induction of autophagy and for resistance against oxidative stress in the heart [125,212]. Sirt1 expression became elevated in response to pressure overload and oxidative stress in the heart of wild-type mice, while moderate Sirt1 overexpression protected the heart of transgenic mice against paraquat-induced oxidative stress through up-regulation of the FoxO-dependent antioxidant enzyme catalase [125]. Apparently, it depends on the cell type whether autophagy is stimulated by deacetylated or by acetylated FoxO proteins: FoxO3a controls fasting-induced autophagy during muscle atrophy [213]. But in contrast to liver and heart, protein levels of Sirt1 have been reported to decrease in type II skeletal muscle of starved mice; transgenic overexpression of Sirt1 resulting in FoxO3a deacetylation prevented the up-regulation of atrophy-related genes in skeletal muscle during fasting [214]. An unexpected molecular mechanism of autophagy induction, which does not depend on the activity of FoxOs as transcription factors, has been delineated for acetylated FoxO1a located in the cytosol of human cancer cell lines: in response to oxidative stress or serum starvation, cytosolic FoxO1a became acetylated following its dissociation from Sirt2. Acetylated FoxO1a then induced the autophagic process through interaction with Atg7 (ubiquitin-like modifier-activating enzyme 7), a key regulator in the formation of the autophagosome [215].

Activity of FoxO3a under conditions of nutrient restriction has also been assessed with respect to metabolism and gene regulation in mitochondria [216]. In myotubes, glucose restriction induces the formation of a FoxO3a/Sirt3 complex that recruited mitochondrial RNA polymerase at mitochondrial DNA-regulatory regions (mtDNA-RR) to activate mitochondrial transcription, resulting in increased mitochondrial respiration capacity. The relevance of Sirt3 regulation of FoxO3a to control mitochondrial function is further supported by recent studies showing that, in response to oxidative stress, Sirt3-mediated deacetylation of FoxO3a upregulates a set of nuclear genes involved in mitochondrial homeostasis including biogenesis, fusion/fission, mitophagy and ROS control [217–219]. Accordingly, it has been reported that chronic dietary restriction increases FoxO3a and FoxO4 levels in skeletal muscle, and these changes correlate with increased expression of genes associated with stress resistance, antioxidants, DNA repair, protein turnover and cell death [220].

5.2. Adipocyte differentiation

Sirt2 is the major sirtuin in adipocytes, and deacetylation of FoxO1a by Sirt2 has been implicated in the regulation of adipogenesis [106]. Adipogenesis takes place in adipose tissue, where mesenchymal stem cells are first committed to preadipocytes, which subsequently undergo clonal expansion, growth arrest and terminal differentiation into mature fat-accumulating adipocytes [221]. Hormonal induction of adipocyte differentiation *in vitro* is accompanied by a transient increase in intracellular superoxide and H_2O_2, as described for human adipose tissue-derived stem cells [173] as well as for murine 3T3-L1 preadipocytes [222], the most widely used model cell line for the study of adipogenesis. H_2O_2 is thought to serve as signaling molecule to increase the stimulating action of insulin on adipogenesis and lipogenesis; exogenous application of H_2O_2 may both induce and augment adipocyte differentiation of preadipocytes [173,223]. On the other hand, excessive ROS generation would be detrimental and is thus counteracted through staggered induction of antioxidant enzymes such as isoforms of the glutathione peroxidase and thioredoxin reductase selenoenzymes and the FoxO target genes SOD-2 and catalase [173,222,224]. Gene expression and protein synthesis, intracellular localization and posttranslational modifications (phosphorylation, acetylation) of FoxO proteins are tightly and timely regulated in the course of adipocyte differentiation: FoxO1a, FoxO3a and FoxO4 mRNA and protein levels are very low in preadipocytes and increase during adipogenesis, with FoxO1a being the major FoxO isoform in mature adipocytes and in adipose tissue [171,173]. While the levels of FoxO1a begin to rise already in the early stage of adipogenesis, it does not become transcriptionally active before the end of the clonal expansion phase [171]. The delay in FoxO1a activation is accomplished through posttranslational modifications (phosphorylation at S253 of murine Foxo1a, and acetylation), resulting in FoxO1a exclusion from the nucleus during the clonal expansion phase [106,171]. Reversible acetylation of FoxO1a during adipogenesis is controlled through strict regulation of Sirt2 levels: Sirt2 is highly expressed in preadipocytes, strongly down-regulated immediately after the initiation of adipocyte differentiation and partly restored after the clonal expansion phase [106,135]. Both overexpression of Sirt2 and overexpression of a constitutively active FoxO1a mutant, which cannot be excluded from the nucleus, suppressed adipocyte differentiation of preadipocytes [106,135,171]. Conceivably, a strict control of FoxO expression and activity is crucial for the regulation of the intracellular redox state during adipogenesis; switching off FoxOs in early stages ensures more oxidized conditions that favor adipocyte differentiation, while switching on FoxOs in later stages counter-acts oxidative damage through induction of FoxO-dependent antioxidant enzymes (Fig. 5).

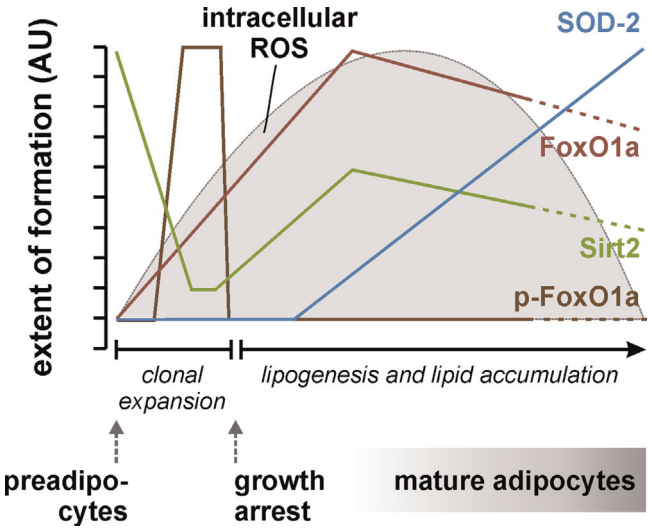

Fig. 5. Schematic representation of the time course of Sirt2, FoxO1a, SOD-2 formation as well as of intracellular ROS levels during adipocyte differentiation in 3T3-L1 murine preadipocytes. The transient increase in intracellular ROS levels is shut down through induction of FoxO1a target genes such as SOD-2. Following a brief period of Akt-dependent phosphorylation of FoxO1a (p-FoxO1a, referring to FoxO phosphorylated at Ser253 – the equivalent of human FoxO1a Ser256), it is upregulated during adipogenesis, and it becomes transcriptionally active after the clonal expansion phase due to its deacetylation through interaction with Sirt2 [106,135,171,222].

5.3. Obesity and diabetes

Carbohydrate and lipid homeostasis is not controlled properly in patients suffering from diabetes mellitus. The metabolic disturbances in diabetes are either caused by lack of insulin due to autoimmune destruction of pancreatic β-cells (type 1 diabetes mellitus, T1DM) or by insulin resistance combined with progressive β-cell failure (type 2 diabetes mellitus, T2DM). Overweight and obesity increase the risk to develop T2DM. By 2030, 573 million adults world-wide are projected to be obese and 366 million individuals may have diabetes [225,226]. The steadily increasing prevalence of overweight, obesity and T2DM gave rise to the concept of a global epidemic of diabetes and to considerable scientific efforts to decipher molecular mechanisms underlying the pathogenesis of T2DM. Oxidative stress is considered a key factor in the development and progression of diabetes and its complications. Excess of glucose and saturated fatty acids elicits overproduction of superoxide and H_2O_2 through activation of NOX, elevated oxidative phosphorylation in the mitochondrial respiratory chain and uncoupled NO synthase (NOS) [227]. Other potentially harmful ROS in obesity and T2DM derive from ER stress and from chronic low-grade inflammation [228]. Oxidative stress is linked to insulin resistance of liver, skeletal muscle and adipose tissue [227,228]. The insulin-producing pancreatic β-cells are particularly susceptible to oxidative stress-induced damage due to their low expression of antioxidant enzymes [229]. In addition, the vascular endothelium is impaired in diabetes, because excessive superoxide lowers the bioavailability of nitric oxide (NO) through formation of peroxynitrite. This may result in endothelial dysfunction, a major diabetic complication [230]. Increased flux of glucose and sorbitol through the polyol pathway may contribute to cellular redox imbalance under hyperglycemic conditions and is also thought to be involved in the pathogenesis of diabetic complications such as retinopathy, neuropathy, nephropathy and cardiovascular disease [227].

FoxO proteins, in particular FoxO1, are highly expressed in the major insulin target tissues as well as in the insulin-producing β-cells. Hyper-activation of FoxOs has been reported to be associated with hallmarks of overt diabetes such as hyperglycemia, hypertriglyceridemia, insulin resistance and an impaired compensatory increase in β-cell mass as well as with diabetic complications [231–234]. Overexpression of constitutively active Foxo1a in liver and pancreatic β-cells was sufficient to induce diabetes in transgenic mice, due to increased hepatic glucose production combined with decreased β-cell compensation [231]. Conversely, haploinsufficiency of the *Foxo1* gene rescued the diabetic phenotype of insulin-resistant mice through lowering hepatic expression of gluconeogenic enzymes and increasing adipocyte expression of insulin-sensitizing genes [231]. In other studies with transgenic mice, both overexpression of constitutively active Foxo1a as well as knockdown of Foxo1a and Foxo3a likewise resulted in hypertriglyceridemia [232,235]. Diabetic complications such as retinopathy and impaired fracture healing have been linked to elevated FoxO1a transcriptional activity under hyperglycemic conditions [234,236,237]. However, FoxOs also have beneficial effects with respect to diabetes, as FoxO-dependent transcription of antioxidant enzymes may counteract oxidative stress-induced cellular damage [233]. FoxO1-mediated induction of NeuroD and MafA has been shown to protect pancreatic β-cells against glucose toxicity [128]. Mice with a triple knockdown of Foxos (*Foxo1a*, *Foxo3a* and *Foxo4*) in pancreatic β-cells developed a maturity-onset diabetes of the young (MODY)-like phenotype characterized by an insulin secretory defect due to impaired ATP generation after glucose stimulation and preferential use of lipids as nutrient source instead of glucose [238].

Dys-regulated hepatic glucose production and release contributes to the fasting and postprandial hyperglycemia that is characteristic of overt diabetes. High glucose stimulates transcription of the FoxO target gene glucose-6-phosphatase in the diabetic liver [239], resulting in a vicious cycle of further increased hepatic glucose release despite high blood glucose levels in diabetes (Fig. 6). Activation of hepatic FoxO1a at high glucose concentrations occurs through its coactivator PGC-1α: expression of PGC-1α is increased in the diabetic liver [240]. In response to high glucose, PGC-1α binds to the enzyme O-GlcNAc transferase and targets it to FoxOs, resulting in increased FoxO GlcNAcylation and increased FoxO-dependent transcription of gluconeogenic enzymes [241]. Moreover, hepatic gene expression and secretion of the FoxO1a target gene SelP is elevated at high glucose concentrations [242,243], and this may result in higher plasma SelP and selenium levels and promote the development of insulin resistance in liver and skeletal muscle [243] (Fig. 6).

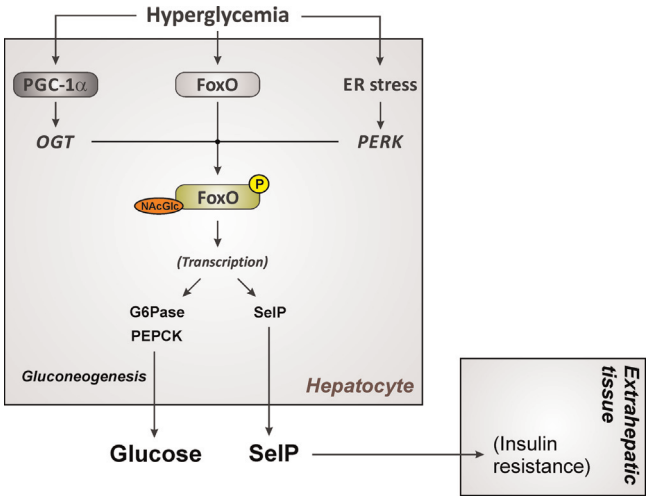

Fig. 6. Hyperactivation of FoxO1a induced by hyperglycemia and ER stress in the diabetic liver results in permanent upregulation of FoxO1a target genes. Elevated hepatic glucose and selenoprotein P (SelP) release may further augment insulin resistance in type 2 diabetes mellitus. G6Pase, glucose 6-phosphatase; OGT, O-linked N-acetylglucosamine transferase; PEPCK, phosphoenolpyruvate carboxykinase; PERK – protein kinase R-like endoplasmic reticulum kinase.

FoxO transcriptional activity is also promoted by the protein kinase PERK (Fig. 4c): PERK has been reported to phosphorylate FoxOs in response to ER stress, thus overriding the inhibitory effect of FoxO phosphorylation *via* the insulin/Akt signaling pathway [244]. In addition to FoxO activation through posttranslational modifications under diabetic conditions, FoxO1a gene expression has been found to be elevated in the liver of animal models for T1DM and T2DM [232]. It is still not understood completely how the actions of FoxOs on hepatic glucose and lipid metabolism are integrated under conditions of insulin sensitivity and insulin resistance or deficiency. A recently published study proposed a model that distinguishes between early and late stages in the course of pathogenesis of T2DM [245]: in early insulin resistance, the reactive increase in β-cell mass and insulin secretion results initially in hyperinsulinemia and suppression of hepatic FoxO activity, thereby switching off gluconeogenesis and redirecting glycolysis-derived pyruvate to *de novo* lipogenesis. In contrast, FoxOs are strongly activated in overt T2DM, resulting in elevated gluconeogenesis, while hepatic lipogenesis is predicted to be stimulated through the transcription factors sterol regulatory element-binding protein 1c (SREBP-1c) and carbohydrate-responsive element-binding protein (ChREBP) [245].

5.4. Cancer

The role of FoxOs in tumor development and progression has been widely investigated. Initially believed to be oncogenes, based on

elevated FoxO levels in tumor samples, later evidence showed that tumor development was strongly associated with constitutive activation of Akt and loss of FoxO activity. It has also been well documented that loss of FoxO activity is a poor prognosis factor [246–248]. However, the identification of tumor stem cells has further complicated that picture, since it was recognized that FoxO activity, even in the presence of constitutively active Akt, was a prevalent factor linked to drug resistance and invasiveness [234]. FoxOs have a role in chemotherapy resistance due to their regulation of the synthesis of enzymes essential for detoxification. FoxO1a is involved in drug resistance in ovarian cancer exposed to paclitaxel, and is overexpressed in paclitaxel-resistant cancer, attenuating the cytotoxic effect [249]. Importantly, controlling the levels of ROS seems to play a major role in these two aspects of FoxO activity in cancer.

Due to the high degree of homology among FoxO1a, FoxO3a and FoxO4, there is some functional redundancy, and single or double FoxO knockout mice frequently do not show clear phenotypes. Single and double FoxO knockout mice did not show increased rates of tumorigenesis, but the triple deletion of *Foxo1a*, *Foxo3a* and *Foxo4* resulted in accelerated tumor progression in adult mice, together with increased intracellular ROS levels [250]. In contrast, a single knockout of the less related FoxO6 resulted in increased cellular proliferation and promoted the development of gastric cancer [251].

Cancer cells tend to have elevated intracellular ROS levels [252]. ROS can induce cell proliferation and damage DNA, thereby increasing mutation rates and promoting DNA instability. Elevated ROS and a low antioxidant capacity render cancer cells generally more sensitive towards drugs that induce the formation of intracellular ROS, and this sensitivity has been exploited in chemotherapy [253]. FoxO activity is both crucial to control ROS levels and promote cell quiescence, and to induce apoptotic cell death in response to chemotherapeutic drugs.

Inactivation of FoxOs in tumors occurs through several mechanisms; many tumors show enhanced activation of the PI3K/Akt pathway. Inactivation of the phosphatase PTEN is most frequently observed, resulting in increased FoxO phosphorylation by Akt, their nuclear exclusion and degradation (see also Fig. 1). Other growth factor signaling pathways also converge at the inactivation of FoxO. Importantly, it has been recently described that ROS-dependent oxidation of PTPN12 in breast cancer cells inhibits FoxO activity by enhancing SGK1-mediated FoxO phosphorylation [254].

As mentioned above, microRNAs modulate FoxO levels. Several miRNAs have been demonstrated to be involved in the regulation of FoxO activity in tumor cells. Decreased FoxO levels due to microRNA-induced downregulation may result in higher proliferation and tumor growth in gastric cancer [255] and in bladder cancer [256]. Inactivation of FoxO1a is related to an increase of microvascular area in cancer *via* a ROS dependent HIF-1α stabilization and activation of the VEGF pathway [257].

Regarding the role of PTMs, some studies have suggested a role of p300 acetylation of FoxO factors in inducing apoptotic cell death in response to a chemotherapeutic agent, particularly those whose mechanism of action depends on increased cellular oxidative stress [258].

Cancer cells make limited use of mitochondria for production of ATP, but they use mitochondria as a source of ROS to stimulate proliferative signaling and as a source of intermediary metabolites to fuel cell growth [259]. Importantly, two recent studies have shown that, in addition to controlling antioxidant gene expression in cancer cells, FoxO3a inhibits c-Myc through several mechanisms: inhibition of c-Myc resulted in downregulation of a large number of nuclear genes encoding mitochondrial proteins, in suppression of mitochondrial ROS production and in prevention of ROS-dependent stabilization of the hypoxia inducible factor HIF-1α, a key player in tumor development [260]. This pathway is likely to be relevant for normal cellular adaptation to hypoxia, preventing the excessive production of mitochondrial ROS in response to low oxygen tensions [261].

6. FoxOs and ROS in different organs

6.1. Liver

The liver as the central metabolic organ has an active metabolism that generates high levels of ROS. In fact, oxidative stress is implicated in many liver diseases [262–265]. Hepatocytes express high levels of antioxidant enzymes, but excessive damage or failure of control mechanisms are common under pathological conditions and generally result in cell death. FoxO3a has recently been shown to have a pro-apoptotic function in hepatocytes exposed to excessive oxidative stress. Importantly, knockdown of β-catenin in hepatocytes rendered mice more sensitive to hepatotoxin-induced liver injury and resulted in elevated expression of FoxO3a target genes such as the pro-apoptotic proteins Bim and p27. Conversely, β-catenin prevented oxidative stress-induced apoptosis through inhibition of FoxO3a [266]. The Wnt/β-catenin pathway had been previously implicated in hepatocyte survival and shown to contribute to the activation of cellular antioxidant defense systems, activating survival pathways and suppressing apoptotic cell death [267,268]. The functional relevance of this regulatory pathway is supported by studies carried out in the context of colon cancer [269–271].

Calorie restriction has been found to result in elevated levels of FoxO1a and FoxO1a-dependent genes coding for proteins involved in antioxidant protection, cell cycle arrest, DNA repair and apoptosis in the liver; thus, the authors suggested that FoxO1a might contribute to the anti-neoplastic effect of calorie restriction [272]. The close interplay between metabolic and oxidative control is highlighted by a recent report that identified a novel mechanism of negative regulation of FoxO activity, involving class IIa HDACs (HDAC4, 5, and 7) in glioblastoma cells. In response to stimulation, mTORC2 promotes inactivation of class IIa histone deacetylases, which leads to increased acetylation of FoxO factors, release of c-Myc inhibition and induction of glycolysis [273]. In contrast, in response to fasting, glucagon in liver induces the dephosphorylation and nuclear translocation of class IIa HDACs, where they recruit HDAC3, which in turn deacetylates FoxOs and boosts gluconeogenesis [274].

6.2. Skeletal muscle

The best characterized specific function of FoxOs in skeletal muscle is the promotion of muscle atrophy in cachexia and denervation. Studies on the role of acetylation in the control of FoxO activity in the muscle have evidenced a differential effect of acetylation on FoxO3a and FoxO1. While increased p300 activity induces FoxO3a degradation and prevented its nuclear localization, it increased FoxO1a nuclear localization [275,276]. Importantly, it has been recently shown that the deacetylation of FoxO3a by HDAC1 is the main driver of muscle atrophy [277] while Sirt1-mediated deacetylation of FoxO1a and 3a inhibits muscle atrophy [214]. In this scenario, it has been an extremely controversial issue whether or not control of ROS levels by FOXOs is relevant in aging sarcopenia, and if so, which are the relevant mechanisms involved. A recent study has now conclusively demonstrated that FoxOs do not significantly contribute to sarcopenia in aging [278]. Furthermore, another recent study strongly argues that FoxO control of ROS in muscle plays a crucial role in lifespan and healthy aging [279].

6.3. Bone

FoxOs have been shown to play an important role in bone metabolism by influencing osteoblast generation and survival *via* ROS-dependent and -independent mechanisms. FoxO1a inactivation in osteoblasts decreases osteoblast numbers, bone formation rate, and bone volume by 50%. Importantly, it has been shown that FoxO-mediated defense against oxidative stress in osteoblasts regulates skeletal homeostasis. In fact, the bone formation phenotype of FoxO1a osteoblast deficient mice can be attributed to decreased antioxidant defense mechanisms in the absence of FoxO1. Elevated ROS activated the p53 signaling cascade, inducing cell cycle arrest and limiting osteoblast proliferation. The antioxidant N-acetyl cysteine (NAC) normalized redox levels and restored osteoblast proliferation and bone formation [280,281].

Osteoclasts are highly specialized myeloid cells capable of dissolving and digesting the organic bone matrix. *In vitro*, osteoclast formation induced by parathyroid hormone and interleukin-1 was accompanied by increased superoxide levels, and superoxide dismutase inhibited osteoclastic resorption, indicating that ROS are required for osteoclast differentiation and bone resorption [282]. Both RANKL and M-CSF increase the levels of ROS in osteoclast progenitors and potentiate osteoclast formation and activation [283,284]. Oxidative stress has been also implicated in the pathologic bone resorption associated with estrogen deficiency [285]. However, the link between ROS generation and osteoclast formation was circumstantial. A recent study using murine conditional loss or gain of function FoxO mutants, or mitochondria-targeted catalase in osteoclasts has shown that FoxOs inhibit osteoclast differentiation, at least in part, by stimulating catalase production and thus downregulating H_2O_2 levels [286].

In cartilage, the expression of FoxO1a and FoxO3a and their nuclear localization has been found to be reduced both in mice and humans in the marginal zone of cartilage exposed to maximal weight – possibly as a consequence of increased levels of pro-inflammatory cytokines [287]. A recent study has shown that knockdown of FoxO1a and FoxO3a in human articular chondrocytes resulted in significantly decreased levels of glutathione peroxidase 1 (GPx-1), catalase, light chain 3 (LC3), beclin1, and Sirt1; following treatment with *tert.*-butyl hydroperoxide (*t*BHP), susceptibility to ROS-induced apoptotic cell death was increased [288]. This study is particularly relevant in view of the previously noted observation that aging chondrocytes show reduced levels of antioxidants and increased vulnerability to ROS-induced cell death of [289].

6.4. Central nervous system

Brain-specific ablation of FoxO3a or combined inactivation of FoxO1a/3a/4 in mice resulted in a phenotype that resembled age-dependent depletion of the neural stem cell (NSC) population [290,291]. Furthermore, an *ex-vivo* assay demonstrated decreased self-renewal capacity of FoxO knockout cells in an age-dependent fashion. Decreased self-renewal of FoxO-deficient NSC can be partially attributable to enhanced intracellular ROS, which leads to decreased NSC reserve and neurogenesis. Analyses of gene expression profiles showed that FoxO3a regulates genes involved in cellular quiescence, differentiation, oxygen metabolism and antioxidants [290]. FoxO3a maintains NSC quiescence preventing premature differentiation under hypoxic conditions by regulating their entry into the cell cycle and ROS levels [291,292]. These studies parallel earlier observations on the role of FoxOs in the control of long-term proliferative capacity of hematopoietic stem cells [293]. In both studies, administration of the antioxidant NAC rescued the aberrant proliferation and loss of self-renewal capacity, supporting the major role of ROS in FoxO deficient stem cell phenotypes.

The amyloid precursor protein (APP) is a transmembrane protein that has been involved in the pathogenesis of Alzheimer's disease (AD). APP can be cleaved at multiple sites to generate a series of fragments, including the amyloid β (Aβ) peptides and APP intracellular domain (AICD). A recent study has shown that FoxO is a crucial mediator of APP-induced AICD-dependent cell death. AICD functions as a transcriptional co-activator of FoxO that, together with FoxO, translocates into the nucleus upon oxidative stress, and promotes FoxO-induced transcription of the gene encoding the pro-apoptotic protein Bim [294].

Astrocytes, in collaborating with neurons in terms of antioxidant defense, contribute to the prevention of oxidative stress-induced neuronal damage and neurodegeneration [295]. Environmental exposure to manganese and other transition metals increases cellular oxidative stress and has been associated with an increased risk of neurodegeneration. A recent report shows that FoxO levels and activity were induced in astrocytes following Mn exposure [206].

6.5. Blood

FoxOs have been identified as mediators of hematopoietic stem cell resistance to physiologic oxidative stress. Ablation of the three major FoxO isoforms in *hematopoietic stem cells* (HSC) results in excessive proliferation and early exhaustion of the HSC pool, due to excessive ROS levels in mice [293]. A later study using hematopoietic progenitors from *Drosophila* further demonstrated that ROS control by FoxOs prevents unprimed differentiation. These results are in line with a number of studies showing that differentiation factors induce a transient increase in ROS levels in the target cells [296].

Oxidative stress has also been shown to regulate erythropoiesis; in the absence of FoxO3a, excessive ROS levels induce cell cycle arrest in precursor cells, preventing maturation, and shorten the viability of mature erythrocytes [17]. In contrast, myeloid-specific triple FoxO knockout mice showed increased proliferation of granulocyte–monocyte progenitors, resulting in neutrophilia with monocytosis, increased inducible nitric oxide synthase (iNOS) expression and oxidative stress in macrophages. As a result, these mice developed larger atherosclerotic lesions than wild-type controls, with an increased number of intralesional macrophages, but a decreased percentage of apoptotic macrophages [297].

Finally, accumulated evidence suggests that downregulation of Sirt1 and FoxO factors in endothelial cells contributes to oxidative stress, accelerates senescence [298] and induces apoptosis in response to hypoxia [299]. Vascular endothelial senescence has been proposed as a relevant factor in atherogenesis and diabetic retinopathy.

6.6. Kidney

Diabetic nephropathy and glycogen storage disease type Ia (GSD-Ia)-linked nephropathy have been associated with reduced FoxO activity suppression of antioxidant enzymes and activation of NADPH oxidases contributing to disease progression [300,301].

6.7. Skin

FoxO1a also functions in keratinocytes to reduce oxidative stress and prevent cell death as well as to regulate TGF-β signaling. Importantly, ROS are key mediators of cell migration and TGF-β signaling. As a result, the role of FoxO in wound healing is dramatically different in normal and diabetic mice. FoxO1a plays a positive role in wound healing in normal mice [302]. It coordinates the response of keratinocytes to wound healing through upregulation of TGF-β1 and its downstream targets, which are needed for

keratinocyte migration. However, in the diabetic wounds, when oxidative stress is more extreme FoxO1a has been linked to impaired wound healing. FoxO1a activity is driven by TNF-α and associated with higher levels of apoptosis and reduced proliferation of fibroblasts [303].

7. Conclusions

While oxidative stress may contribute to the pathogenesis of many diseases, low physiological concentrations of ROS, particularly of hydrogen peroxide, have emerged as indispensable signaling molecules in the hormone- and growth factor-mediated control of cellular metabolism. Apparently, this is not by chance reminiscent of the partially opposite roles of FoxO transcription factors in metabolism and stress response under physiological and pathophysiological conditions. The activity of FoxOs and the cellular redox state are intrinsically linked to each other: FoxOs act as cellular redox sensors that become modified post-translationally through phosphorylation, acetylation and ubiquitination in response to oxidative stress, affecting FoxO cytoplasmic/nuclear shuttling, FoxO stability, and eventually transcription of FoxO-controlled target genes. Moreover, FoxOs may interact with other proteins including co-regulators and antioxidant peroxiredoxins in a redox-sensitive manner, and there is some evidence for redox-sensitive regulation of FoxO gene expression itself. On the other hand, some of the FoxO target genes are antioxidant enzymes that affect the intra- and extracellular redox state by catalyzing dismutation and reduction of superoxide and hydrogen peroxide, respectively. The net result of FoxO-mediated gene expression influences the cell fate upon oxidative damage, inducing either apoptotic cell death or cell cycle arrest and subsequent repair processes. Under physiological conditions, FoxOs are involved in the regulation of cellular differentiation, energy metabolism and nutrient homeostasis. In contrast, FoxO hyper-activation under some pathological conditions associated with oxidative stress may augment metabolic disturbances in type 2 diabetes mellitus or cause muscle atrophy. Such adverse effects emphasize the need for a strict and timely control of FoxO expression and activity.

Acknowledgments

Several authors of this review were supported by the European Cooperation in Science and Technology (COST) Action BM1203/EU-ROS. We thank Dr. N. Urban for the *C. elegans* photograph in Fig. 1.

References

[1] D. Weigel, G. Jürgens, F. Küttner, E. Seifert, H. Jäckle, The homeotic gene fork head encodes a nuclear protein and is expressed in the terminal regions of the Drosophila embryo, Cell 57 (1989) 645–658.
[2] D. Weigel, H. Jäckle, The fork head domain: a novel DNA binding motif of eukaryotic transcription factors? Cell 63 (1990) 455–456.
[3] K.H. Kaestner, W. Knochel, D.E. Martinez, Unified nomenclature for the winged helix/forkhead transcription factors, Genes Dev. 14 (2000) 142–146.
[4] C. Kenyon, The first long-lived mutants: discovery of the insulin/IGF-1 pathway for ageing, Philos. Trans. R. Soc. Lond. B: Biol. Sci. 366 (2011) 9–16.
[5] C. Kenyon, J. Chang, E. Gensch, A. Rudner, R.A. Tabtiang, *C. elegans* mutant that lives twice as long as wild type, Nature 366 (1993) 461–464.
[6] S. Ogg, S. Paradis, S. Gottlieb, G.I. Patterson, L. Lee, H.A. Tissenbaum, G. Ruvkun, The Fork head transcription factor DAF-16 transduces insulin-like metabolic and longevity signals in *C. elegans*, Nature 389 (1997) 994–999.
[7] K. Lin, J.B. Dorman, A. Rodan, C. Kenyon, daf-16: An HNF-3/forkhead family member that can function to double the life-span of *Caenorhabditis elegans*, Science 278 (1997) 1319–1322.
[8] K.D. Kimura, H.A. Tissenbaum, Y. Liu, G. Ruvkun, daf-2, An insulin receptor-like gene that regulates longevity and diapause in *Caenorhabditis elegans*, Science 277 (1997) 942–946.
[9] Y. Honda, S. Honda, The daf-2 gene network for longevity regulates oxidative stress resistance and Mn-superoxide dismutase gene expression in *Caenorhabditis elegans*, FASEB J. 13 (1999) 1385–1393.
[10] Y. Honda, S. Honda, Oxidative stress and life span determination in the nematode *Caenorhabditis elegans*, Ann. N.Y. Acad. Sci. 959 (2002) 466–474.
[11] G.J. Kops, T.B. Dansen, P.E. Polderman, I. Saarloos, K.W. Wirtz, P.J. Coffer, T. T. Huang, J.L. Bos, R.H. Medema, B.M. Burgering, Forkhead transcription factor FOXO3a protects quiescent cells from oxidative stress, Nature 419 (2002) 316–321.
[12] R. Doonan, J.J. McElwee, F. Matthijssens, G.A. Walker, K. Houthoofd, P. Back, A. Matscheski, J.R. Vanfleteren, D. Gems, Against the oxidative damage theory of aging: superoxide dismutases protect against oxidative stress but have little or no effect on life span in *Caenorhabditis elegans*, Genes Dev. 22 (2008) 3236–3241.
[13] E.L. Greer, A. Brunet, FOXO transcription factors at the interface between longevity and tumor suppression, Oncogene 24 (2005) 7410–7425.
[14] M. Monsalve, Y. Olmos, The complex biology of FOXO, Curr. Drug Targets 12 (2011) 1322–1350.
[15] D.H. Kim, G. Perdomo, T. Zhang, S. Slusher, S. Lee, B.E. Phillips, Y. Fan, N. Giannoukakis, R. Gramignoli, S. Strom, S. Ringquist, H.H. Dong, FoxO6 integrates insulin signaling with gluconeogenesis in the liver, Diabetes 60 (2011) 2763–2774.
[16] D.R. Calnan, A. Brunet, The FoxO code, Oncogene 27 (2008) 2276–2288.
[17] D. Marinkovic, X. Zhang, S. Yalcin, J.P. Luciano, C. Brugnara, T. Huber, S. Ghaffari, Foxo3 is required for the regulation of oxidative stress in erythropoiesis, J. Clin. Investig. 117 (2007) 2133–2144.
[18] S. Nemoto, T. Finkel, Redox regulation of forkhead proteins through a p66shc-dependent signaling pathway, Science 295 (2002) 2450–2452.
[19] C.B. Chiribau, L. Cheng, I.C. Cucoranu, Y.S. Yu, R.E. Clempus, D. Sorescu, FOXO3A regulates peroxiredoxin III expression in human cardiac fibroblasts, J. Biol. Chem. 283 (2008) 8211–8217.
[20] Y. Olmos, F.J. Sanchez-Gomez, B. Wild, N. Garcia-Quintans, S. Cabezudo, S. Lamas, M. Monsalve, SirT1 regulation of antioxidant genes is dependent on the formation of a FoxO3a/PGC-1alpha complex, Antioxid. Redox Signal. 19 (2013) 1507–1521.
[21] D. Barsyte, D.A. Lovejoy, G.J. Lithgow, Longevity and heavy metal resistance in daf-2 and age-1 long-lived mutants of *Caenorhabditis elegans*, FASEB J. 15 (2001) 627–634.
[22] C.P. Anderson, E.A. Leibold, Mechanisms of iron metabolism in *Caenorhabditis elegans*, Front. Pharmacol. 5 (2014) 113.
[23] E.L. Greer, P.R. Oskoui, M.R. Banko, J.M. Maniar, M.P. Gygi, S.P. Gygi, A. Brunet, The energy sensor AMP-activated protein kinase directly regulates the mammalian FOXO3 transcription factor, J. Biol. Chem. 282 (2007) 30107–30119.
[24] M. Leyendecker, P. Korsten, R. Reinehr, B. Speckmann, D. Schmoll, W. A. Scherbaum, S.R. Bornstein, A. Barthel, L.O. Klotz, Ceruloplasmin expression in rat liver cells is attenuated by insulin: role of FoxO transcription factors, Horm. Metab. Res. 43 (2011) 268–274.
[25] A. Sidhu, P.J. Miller, A.D. Hollenbach, FOXO1 stimulates ceruloplasmin promoter activity in human hepatoma cells treated with IL-6, Biochem. Biophys. Res. Commun. 404 (2011) 963–967.
[26] N.E. Hellman, J.D. Gitlin, Ceruloplasmin metabolism and function, Annu. Rev. Nutr. 22 (2002) 439–458.
[27] K.N. White, C. Conesa, L. Sanchez, M. Amini, S. Farnaud, C. Lorvoralak, R. W. Evans, The transfer of iron between ceruloplasmin and transferrins, Biochim. Biophys. Acta 1820 (2012) 411–416.
[28] P.L. Walter, H. Steinbrenner, A. Barthel, L.O. Klotz, Stimulation of selenoprotein P promoter activity in hepatoma cells by FoxO1a transcription factor, Biochem. Biophys. Res. Commun. 365 (2008) 316–321.
[29] B. Speckmann, P.L. Walter, L. Alili, R. Reinehr, H. Sies, L.O. Klotz, H. Steinbrenner, Selenoprotein P expression is controlled through interaction of the coactivator PGC-1alpha with FoxO1a and hepatocyte nuclear factor 4alpha transcription factors, Hepatology 48 (2008) 1998–2006.
[30] Y. Saito, T. Hayashi, A. Tanaka, Y. Watanabe, M. Suzuki, E. Saito, K. Takahashi, Selenoprotein P in human plasma as an extracellular phospholipid hydroperoxide glutathione peroxidase. Isolation and enzymatic characterization of human selenoprotein p, J. Biol. Chem. 274 (1999) 2866–2871.
[31] G. Takebe, J. Yarimizu, Y. Saito, T. Hayashi, H. Nakamura, J. Yodoi, S. Nagasawa, K. Takahashi, A comparative study on the hydroperoxide and thiol specificity of the glutathione peroxidase family and selenoprotein P, J. Biol. Chem. 277 (2002) 41254–41258.
[32] H. Traulsen, H. Steinbrenner, D.P. Buchczyk, L.O. Klotz, H. Sies, Selenoprotein P protects low-density lipoprotein against oxidation, Free Radic. Res. 38 (2004) 123–128.
[33] R.F. Burk, K.E. Hill, P. Selenoprotein, An extracellular protein with unique physical characteristics and a role in selenium homeostasis, Annu. Rev. Nutr. 25 (2005) 215–235.
[34] P.R. Hoffmann, S.C. Hoge, P.A. Li, F.W. Hoffmann, A.C. Hashimoto, M.J. Berry, The selenoproteome exhibits widely varying, tissue-specific dependence on selenoprotein P for selenium supply, Nucleic Acids Res. 35 (2007) 3963–3973.
[35] H. Steinbrenner, L. Alili, E. Bilgic, H. Sies, P. Brenneisen, Involvement of selenoprotein P in protection of human astrocytes from oxidative damage, Free Radic. Biol. Med. 40 (2006) 1513–1523.
[36] H. Steinbrenner, E. Bilgic, L. Alili, H. Sies, P. Brenneisen, Selenoprotein P protects endothelial cells from oxidative damage by stimulation of

glutathione peroxidase expression and activity, Free Radic. Res. 40 (2006) 936–943.
[37] Y. Zhao, Y. Wang, W.G. Zhu, Applications of post-translational modifications of FoxO family proteins in biological functions, J. Mol. Cell. Biol. 3 (2011) 276–282.
[38] J.M. May, C. de Haen, Insulin-stimulated intracellular hydrogen peroxide production in rat epididymal fat cells, J. Biol. Chem. 254 (1979) 2214–2220.
[39] Y.S. Bae, S.W. Kang, M.S. Seo, I.C. Baines, E. Tekle, P.B. Chock, S.G. Rhee, Epidermal growth factor (EGF)-induced generation of hydrogen peroxide. Role in EGF receptor-mediated tyrosine phosphorylation, J. Biol. Chem. 272 (1997) 217–221.
[40] G.J. DeYulia Jr., J.M. Carcamo, EGF receptor–ligand interaction generates extracellular hydrogen peroxide that inhibits EGFR-associated protein tyrosine phosphatases, Biochem. Biophys. Res. Commun. 334 (2005) 38–42.
[41] M. Sundaresan, Z.X. Yu, V.J. Ferrans, K. Irani, T. Finkel, Requirement for generation of H_2O_2 for platelet-derived growth factor signal transduction, Science 270 (1995) 296–299.
[42] K. Chen, M.T. Kirber, H. Xiao, Y. Yang, J.F. Keaney Jr., Regulation of ROS signal transduction by NADPH oxidase 4 localization, J. Cell Biol. 181 (2008) 1129–1139.
[43] K. Mahadev, X. Wu, A. Zilbering, L. Zhu, J.T. Lawrence, B.J. Goldstein, Hydrogen peroxide generated during cellular insulin stimulation is integral to activation of the distal insulin signaling cascade in 3T3-L1 adipocytes, J. Biol. Chem. 276 (2001) 48662–48669.
[44] K. Mahadev, A. Zilbering, L. Zhu, B.J. Goldstein, Insulin-stimulated hydrogen peroxide reversibly inhibits protein-tyrosine phosphatase 1b in vivo and enhances the early insulin action cascade, J. Biol. Chem. 276 (2001) 21938–21942.
[45] T.C. Meng, D.A. Buckley, S. Galic, T. Tiganis, N.K. Tonks, Regulation of insulin signaling through reversible oxidation of the protein-tyrosine phosphatases TC45 and PTP1B, J. Biol. Chem. 279 (2004) 37716–37725.
[46] K. Mahadev, H. Motoshima, X. Wu, J.M. Ruddy, R.S. Arnold, G. Cheng, J. D. Lambeth, B.J. Goldstein, The NAD(P)H oxidase homolog Nox4 modulates insulin-stimulated generation of H_2O_2 and plays an integral role in insulin signal transduction, Mol. Cell. Biol. 24 (2004) 1844–1854.
[47] M. Katsuyama, K. Matsuno, C. Yabe-Nishimura, Physiological roles of NOX/NADPH oxidase, the superoxide-generating enzyme, J. Clin. Biochem. Nutr. 50 (2012) 9–22.
[48] E. Schulz, P. Wenzel, T. Munzel, A. Daiber, Mitochondrial redox signaling: interaction of mitochondrial reactive oxygen species with other sources of oxidative stress, Antioxid. Redox Signal. 20 (2014) 308–324.
[49] B. Lassegue, A. San Martin, K.K. Griendling, Biochemistry, physiology, and pathophysiology of NADPH oxidases in the cardiovascular system, Circ. Res. 110 (2012) 1364–1390.
[50] K. Schröder, K. Wandzioch, I. Helmcke, R.P. Brandes, Nox4 acts as a switch between differentiation and proliferation in preadipocytes, Arterioscler. Thromb. Vasc. Biol. 29 (2009) 239–245.
[51] L.M. Wancket, W.J. Frazier, Y. Liu, Mitogen-activated protein kinase phosphatase (MKP)-1 in immunology, physiology, and disease, Life Sci. 90 (2012) 237–248.
[52] K.Z. Guyton, Y. Liu, M. Gorospe, Q. Xu, N.J. Holbrook, Activation of mitogen-activated protein kinase by H_2O_2. Role in cell survival following oxidant injury, J. Biol. Chem. 271 (1996) 4138–4142.
[53] X. Wang, K.D. McCullough, T.F. Franke, N.J. Holbrook, Epidermal growth factor receptor-dependent Akt activation by oxidative stress enhances cell survival, J. Biol. Chem. 275 (2000) 14624–14631.
[54] S.M. Schieke, C. von Montfort, D.P. Buchczyk, A. Timmer, S. Grether-Beck, J. Krutmann, N.J. Holbrook, L.O. Klotz, Singlet oxygen-induced attenuation of growth factor signaling: possible role of ceramides, Free Radic. Res. 38 (2004) 729–737.
[55] S.M. Schieke, K. Briviba, L.O. Klotz, H. Sies, Activation pattern of mitogen-activated protein kinases elicited by peroxynitrite: attenuation by selenite supplementation, FEBS Lett. 448 (1999) 301–303.
[56] L.O. Klotz, S.M. Schieke, H. Sies, N.J. Holbrook, Peroxynitrite activates the phosphoinositide 3-kinase/Akt pathway in human skin primary fibroblasts, Biochem. J. 352 (Pt 1) (2000) 219–225.
[57] B. Derijard, M. Hibi, I.H. Wu, T. Barrett, B. Su, T. Deng, M. Karin, R.J. Davis, JNK1: a protein kinase stimulated by UV light and Ha-Ras that binds and phosphorylates the c-Jun activation domain, Cell 76 (1994) 1025–1037.
[58] C. Sachsenmaier, A. Radler-Pohl, R. Zinck, A. Nordheim, P. Herrlich, H. J. Rahmsdorf, Involvement of growth factor receptors in the mammalian UVC response, Cell 78 (1994) 963–972.
[59] L.O. Klotz, N.J. Holbrook, H. Sies, UVA and singlet oxygen as inducers of cutaneous signaling events, Curr. Probl. Dermatol. 29 (2001) 95–113.
[60] L.O. Klotz, K. Briviba, H. Sies, Singlet oxygen mediates the activation of JNK by UVA radiation in human skin fibroblasts, FEBS Lett. 408 (1997) 289–291.
[61] L.O. Klotz, C. Pellieux, K. Briviba, C. Pierlot, J.M. Aubry, H. Sies, Mitogen-activated protein kinase (p38-, JNK-, ERK-) activation pattern induced by extracellular and intracellular singlet oxygen and UVA, Eur. J. Biochem. 260 (1999) 917–922.
[62] X. Wang, J.L. Martindale, Y. Liu, N.J. Holbrook, The cellular response to oxidative stress: influences of mitogen-activated protein kinase signalling pathways on cell survival, Biochem. J. 333 (1998) 291–300.
[63] D. Schmoll, K.S. Walker, D.R. Alessi, R. Grempler, A. Burchell, S. Guo, R. Walther, T.G. Unterman, Regulation of glucose-6-phosphatase gene expression by protein kinase Balpha and the forkhead transcription factor FKHR. Evidence for insulin response unit-dependent and -independent effects of insulin on promoter activity, J. Biol. Chem. 275 (2000) 36324–36333.
[64] A. Barthel, D. Schmoll, T.G. Unterman, FoxO proteins in insulin action and metabolism, Trends Endocrinol. Metab. 16 (2005) 183–189.
[65] J.Y. Yang, C.S. Zong, W. Xia, H. Yamaguchi, Q. Ding, X. Xie, J.Y. Lang, C.C. Lai, C. J. Chang, W.C. Huang, H. Huang, H.P. Kuo, D.F. Lee, L.Y. Li, H.C. Lien, X. Cheng, K.J. Chang, C.D. Hsiao, F.J. Tsai, C.H. Tsai, A.A. Sahin, W.J. Muller, G.B. Mills, D. Yu, G.N. Hortobagyi, M.C. Hung, ERK promotes tumorigenesis by inhibiting FOXO3a via MDM2-mediated degradation, Nat. Cell Biol. 10 (2008) 138–148.
[66] S. Asada, H. Daitoku, H. Matsuzaki, T. Saito, T. Sudo, H. Mukai, S. Iwashita, K. Kako, T. Kishi, Y. Kasuya, A. Fukamizu, Mitogen-activated protein kinases, Erk and p38, phosphorylate and regulate Foxo1, Cell Signal. 19 (2007) 519–527.
[67] C. Ott, K. Jacobs, E. Haucke, A. Navarrete Santos, T. Grune, A. Simm, Role of advanced glycation end products in cellular signaling, Redox Biol. 2 (2014) 411–429.
[68] J. Tanaka, L. Qiang, A.S. Banks, C.L. Welch, M. Matsumoto, T. Kitamura, Y. Ido-Kitamura, R.A. DePinho, D. Accili, Foxo1 links hyperglycemia to LDL oxidation and endothelial nitric oxide synthase dysfunction in vascular endothelial cells, Diabetes 58 (2009) 2344–2354.
[69] A.V. Yeldandi, M.S. Rao, J.K. Reddy, Hydrogen peroxide generation in peroxisome proliferator-induced oncogenesis, Mutat. Res. 448 (2000) 159–177.
[70] I.J. Lodhi, C.F. Semenkovich, Peroxisomes: a nexus for lipid metabolism and cellular signaling, Cell Metab. 19 (2014) 380–392.
[71] M. Nordgren, M. Fransen, Peroxisomal metabolism and oxidative stress, Biochimie 98 (2014) 56–62.
[72] L.O. Klotz, Oxidative stress, antioxidants, and chemoprevention: on the role of oxidant-induced signaling in cellular adaptation, in: C. Jacob, G. Kirsch, A. J. Slusarenko, P.G. Winyard, T. Burkholz (Eds.), Recent Advances in Redox Active Plant and Microbial Products, Springer, Dordrecht, 2014, pp. 119–146.
[73] L.O. Klotz, X. Hou, C. Jacob, 1,4-Naphthoquinones: from oxidative damage to cellular and inter-cellular signaling, Molecules 19 (2014) 14902–14918.
[74] J.I. Beier, C. von Montfort, H. Sies, L.O. Klotz, Activation of ErbB2 by 2-methyl-1,4-naphthoquinone (menadione) in human keratinocytes: role of EGFR and protein tyrosine phosphatases, FEBS Lett. 580 (2006) 1859–1864.
[75] V. Klaus, T. Hartmann, J. Gambini, P. Graf, W. Stahl, A. Hartwig, L.O. Klotz, 1,4-Naphthoquinones as inducers of oxidative damage and stress signaling in HaCaT human keratinocytes, Arch. Biochem. Biophys. 496 (2010) 93–100.
[76] S. Zhang, X. Liu, T. Bawa-Khalfe, L.S. Lu, Y.L. Lyu, L.F. Liu, E.T. Yeh, Identification of the molecular basis of doxorubicin-induced cardiotoxicity, Nat. Med. 18 (2012) 1639–1642.
[77] K. Abdelmohsen, C. von Montfort, D. Stuhlmann, P.A. Gerber, U.K. Decking, H. Sies, L.O. Klotz, Doxorubicin induces EGF receptor-dependent down-regulation of gap junctional intercellular communication in rat liver epithelial cells, Biol. Chem. 386 (2005) 217–223.
[78] K.K. Ho, V.A. McGuire, C.Y. Koo, K.W. Muir, N. de Olano, E. Maifoshie, D. J. Kelly, U.B. McGovern, L.J. Monteiro, A.R. Gomes, A.R. Nebreda, D. G. Campbell, J.S. Arthur, E.W. Lam, Phosphorylation of FOXO3a on Ser-7 by p38 promotes its nuclear localization in response to doxorubicin, J. Biol. Chem. 287 (2012) 1545–1555.
[79] A.N. Kavazis, A.J. Smuder, S.K. Powers, Effects of short-term endurance exercise training on acute doxorubicin-induced FoxO transcription in cardiac and skeletal muscle, J. Appl. Physiol. 117 (2014) 223–230.
[80] E.A. Ostrakhovitch, M.R. Lordnejad, F. Schliess, H. Sies, L.O. Klotz, Copper ions strongly activate the phosphoinositide-3-kinase/Akt pathway independent of the generation of reactive oxygen species, Arch. Biochem. Biophys. 397 (2002) 232–239.
[81] P.L. Walter, A. Kampkötter, A. Eckers, A. Barthel, D. Schmoll, H. Sies, L. O. Klotz, Modulation of FoxO signaling in human hepatoma cells by exposure to copper or zinc ions, Arch. Biochem. Biophys. 454 (2006) 107–113.
[82] A. Barthel, E.A. Ostrakhovitch, P.L. Walter, A. Kampkötter, L.O. Klotz, Stimulation of phosphoinositide 3-kinase/Akt signaling by copper and zinc ions: mechanisms and consequences, Arch. Biochem. Biophys. 463 (2007) 175–182.
[83] A. Eckers, K. Reimann, L.O. Klotz, Nickel and copper ion-induced stress signaling in human hepatoma cells: analysis of phosphoinositide 3'-kinase/Akt signaling, Biometals 22 (2009) 307–316.
[84] L.M. Plum, A. Brieger, G. Engelhardt, S. Hebel, A. Nessel, M. Arlt, J. Kaltenberg, U. Schwaneberg, M. Huber, L. Rink, H. Haase, PTEN-inhibition by zinc ions augments interleukin-2-mediated Akt phosphorylation, Metallomics (2014).
[85] K. Jomova, M. Valko, Advances in metal-induced oxidative stress and human disease, Toxicology 283 (2011) 65–87.
[86] T. Schwerdtle, I. Walter, I. Mackiw, A. Hartwig, Induction of oxidative DNA damage by arsenite and its trivalent and pentavalent methylated metabolites in cultured human cells and isolated DNA, Carcinogenesis 24 (2003) 967–974.
[87] B. Cai, Z. Xia, p38 MAP kinase mediates arsenite-induced apoptosis through FOXO3a activation and induction of Bim transcription, Apoptosis 13 (2008) 803–810.
[88] I. Hamann, L.O. Klotz, Arsenite-induced stress signaling: Modulation of the phosphoinositide 3'-kinase/Akt/FoxO signaling cascade, Redox Biol. 1 (2013) 104–109.
[89] I. Hamann, K. Petroll, X. Hou, A. Anwar-Mohamed, A.O. El-Kadi, L.O. Klotz, Acute and long-term effects of arsenite in HepG2 cells: modulation of insulin signaling, Biometals 27 (2014) 317–332.
[90] L.H. Long, A.N. Lan, F.T. Hsuan, B. Halliwell, Generation of hydrogen peroxide

by “antioxidant” beverages and the effect of milk addition. Is cocoa the best beverage? Free Radic. Res. 31 (1999) 67–71.
[91] L.H. Long, M.V. Clement, B. Halliwell, Artifacts in cell culture: rapid generation of hydrogen peroxide on addition of (−)-epigallocatechin, (−)-epigallocatechin gallate, (+)-catechin, and quercetin to commonly used cell culture media, Biochem. Biophys. Res. Commun. 273 (2000) 50–53.
[92] A. Bartholome, A. Kampkötter, S. Tanner, H. Sies, L.O. Klotz, Epigallocatechin gallate-induced modulation of FoxO signaling in mammalian cells and *C. elegans*: FoxO stimulation is masked via PI3K/Akt activation by hydrogen peroxide formed in cell culture, Arch. Biochem. Biophys. 501 (2010) 58–64.
[93] M.A. Essers, S. Weijzen, A.M. de Vries-Smits, I. Saarloos, N.D. de Ruiter, J. L. Bos, B.M. Burgering, FOXO transcription factor activation by oxidative stress mediated by the small GTPase Ral and JNK, EMBO J. 23 (2004) 4802–4812.
[94] H. Huang, K.M. Regan, Z. Lou, J. Chen, D.J. Tindall, CDK2-dependent phosphorylation of FOXO1 as an apoptotic response to DNA damage, Science 314 (2006) 294–297.
[95] X. Huo, S. Liu, T. Shao, H. Hua, Q. Kong, J. Wang, T. Luo, Y. Jiang, GSK3 protein positively regulates type I insulin-like growth factor receptor through forkhead transcription factors FOXO1/3/4, J. Biol. Chem. 289 (2014) 24759–24770.
[96] S. Himpel, W. Tegge, R. Frank, S. Leder, H.G. Joost, W. Becker, Specificity determinants of substrate recognition by the protein kinase DYRK1A, J. Biol. Chem. 275 (2000) 2431–2438.
[97] S. Aranda, A. Laguna, S. de la Luna, DYRK family of protein kinases: evolutionary relationships, biochemical properties, and functional roles, FASEB J. 25 (2011) 449–462.
[98] Y.L. Woods, G. Rena, N. Morrice, A. Barthel, W. Becker, S. Guo, T.G. Unterman, P. Cohen, The kinase DYRK1A phosphorylates the transcription factor FKHR at Ser329 in vitro, a novel in vivo phosphorylation site, Biochem. J. 355 (2001) 597–607.
[99] J. Bain, H. McLauchlan, M. Elliott, P. Cohen, The specificities of protein kinase inhibitors: an update, Biochem. J. 371 (2003) 199–204.
[100] T. Obsil, V. Obsilova, Structure/function relationships underlying regulation of FOXO transcription factors, Oncogene 27 (2008) 2263–2275.
[101] A. Brunet, L.B. Sweeney, J.F. Sturgill, K.F. Chua, P.L. Greer, Y. Lin, H. Tran, S. E. Ross, R. Mostoslavsky, H.Y. Cohen, L.S. Hu, H.L. Cheng, M.P. Jedrychowski, S. P. Gygi, D.A. Sinclair, F.W. Alt, M.E. Greenberg, Stress-dependent regulation of FOXO transcription factors by the SIRT1 deacetylase, Science 303 (2004) 2011–2015.
[102] H. Daitoku, M. Hatta, H. Matsuzaki, S. Aratani, T. Ohshima, M. Miyagishi, T. Nakajima, A. Fukamizu, Silent information regulator 2 potentiates Foxo1-mediated transcription through its deacetylase activity, Proc. Natl. Acad. Sci. U.S.A. 101 (2004) 10042–10047.
[103] M.C. Motta, N. Divecha, M. Lemieux, C. Kamel, D. Chen, W. Gu, Y. Bultsma, M. McBurney, L. Guarente, Mammalian SIRT1 represses forkhead transcription factors, Cell 116 (2004) 551–563.
[104] D. Frescas, L. Valenti, D. Accili, Nuclear trapping of the forkhead transcription factor FoxO1 via Sirt-dependent deacetylation promotes expression of glucogenetic genes, J. Biol. Chem. 280 (2005) 20589–20595.
[105] V. Perrot, M.M. Rechler, The coactivator p300 directly acetylates the forkhead transcription factor Foxo1 and stimulates Foxo1-induced transcription, Mol. Endocrinol. 19 (2005) 2283–2298.
[106] E. Jing, S. Gesta, C.R. Kahn, SIRT2 regulates adipocyte differentiation through FoxO1 acetylation/deacetylation, Cell Metab. 6 (2007) 105–114.
[107] J. Nakae, M. Oki, Y. Cao, The FoxO transcription factors and metabolic regulation, FEBS Lett. 582 (2008) 54–67.
[108] H. Matsuzaki, H. Daitoku, M. Hatta, H. Aoyama, K. Yoshimochi, A. Fukamizu, Acetylation of Foxo1 alters its DNA-binding ability and sensitivity to phosphorylation, Proc. Natl. Acad. Sci. U.S.A. 102 (2005) 11278–11283.
[109] T.B. Dansen, L.M. Smits, M.H. van Triest, P.L. de Keizer, D. van Leenen, M. G. Koerkamp, A. Szypowska, A. Meppelink, A.B. Brenkman, J. Yodoi, F. C. Holstege, B.M. Burgering, Redox-sensitive cysteines bridge p300/CBP-mediated acetylation and FoxO4 activity, Nat. Chem. Biol. 5 (2009) 664–672.
[110] J.T. Rodgers, C. Lerin, W. Haas, S.P. Gygi, B.M. Spiegelman, P. Puigserver, Nutrient control of glucose homeostasis through a complex of PGC-1alpha and SIRT1, Nature 434 (2005) 113–118.
[111] N. Nasrin, S. Ogg, C.M. Cahill, W. Biggs, S. Nui, J. Dore, D. Calvo, Y. Shi, G. Ruvkun, M.C. Alexander-Bridges, DAF-16 recruits the CREB-binding protein coactivator complex to the insulin-like growth factor binding protein 1 promoter in HepG2 cells, Proc. Natl. Acad. Sci. U.S.A. 97 (2000) 10412–10417.
[112] D.L. Mahmud, M.G.A. Deb, D.K. Platanias, L.C. Uddin, S. Wickrema, Phosphorylation of forkhead transcription factors by erythropoietin and stem cell factor prevents acetylation and their interaction with coactivator p300 in erythroid progenitor cells, Oncogene 21 (2002) 1556–1562.
[113] B.M. Spiegelman, R. Heinrich, Biological control through regulated transcriptional coactivators, Cell 119 (2004) 157–167.
[114] M. Fukuoka, H. Daitoku, M. Hatta, H. Matsuzaki, S. Umemura, A. Fukamizu, Negative regulation of forkhead transcription factor AFX (Foxo4) by CBP-induced acetylation, Int. J. Mol. Med. 12 (2003) 503–508.
[115] A. van der Horst, A.M. de Vries-Smits, A.B. Brenkman, M.H. van Triest, N. van den Broek, F. Colland, M.M. Maurice, B.M. Burgering, FOXO4 transcriptional activity is regulated by monoubiquitination and USP7/HAUSP, Nat. Cell Biol. 8 (2006) 1064–1073.
[116] F. Wang, C.H. Chan, K. Chen, X. Guan, H.K. Lin, Q. Tong, Deacetylation of FOXO3 by SIRT1 or SIRT2 leads to Skp2-mediated FOXO3 ubiquitination and degradation, Oncogene 31 (2012) 1546–1557.
[117] H. Huang, K.M. Regan, F. Wang, D. Wang, D.I. Smith, J.M. van Deursen, D. J. Tindall, Skp2 inhibits FOXO1 in tumor suppression through ubiquitin-mediated degradation, Proc. Natl. Acad. Sci. U.S.A. 102 (2005) 1649–1654.
[118] P. Storz, Forkhead homeobox type O transcription factors in the responses to oxidative stress, Antioxid. Redox Signal. 14 (2011) 593–605.
[119] J.R. Stone, S. Yang, Hydrogen peroxide: a signaling messenger, Antioxid. Redox Signal. 8 (2006) 243–270.
[120] T.C. Zschauer, S. Matsushima, J. Altschmied, D. Shao, J. Sadoshima, J. Haendeler, Interacting with thioredoxin-1 – disease or no disease? Antioxid. Redox Signal. 18 (2013) 1053–1062.
[121] M. Putker, H.R. Vos, K. van Dorenmalen, H. de Ruiter, A.G. Duran, B. Snel, B. M. Burgering, M. Vermeulen, T.B. Dansen, Evolutionary acquisition of cysteines determines FOXO paralog-specific redox signaling, Antioxid. Redox Signal. 22 (2015) 15–28.
[122] S. Imai, L. Guarente, NAD+ and sirtuins in aging and disease, Trends Cell. Biol. 24 (2014) 464–471.
[123] A. van der Horst, L.G. Tertoolen, L.M. de Vries-Smits, R.A. Frye, R.H. Medema, B.M. Burgering, FOXO4 is acetylated upon peroxide stress and deacetylated by the longevity protein hSir2(SIRT1), J. Biol. Chem. 279 (2004) 28873–28879.
[124] M. Tanno, A. Kuno, T. Yano, T. Miura, S. Hisahara, S. Ishikawa, K. Shimamoto, Y. Horio, Induction of manganese superoxide dismutase by nuclear translocation and activation of SIRT1 promotes cell survival in chronic heart failure, J. Biol. Chem. 285 (2010) 8375–8382.
[125] R.R. Alcendor, S. Gao, P. Zhai, D. Zablocki, E. Holle, X. Yu, B. Tian, T. Wagner, S. F. Vatner, J. Sadoshima, Sirt1 regulates aging and resistance to oxidative stress in the heart, Circ. Res. 100 (2007) 1512–1521.
[126] K. Hasegawa, S. Wakino, K. Yoshioka, S. Tatematsu, Y. Hara, H. Minakuchi, N. Washida, H. Tokuyama, K. Hayashi, H. Itoh, Sirt1 protects against oxidative stress-induced renal tubular cell apoptosis by the bidirectional regulation of catalase expression, Biochem. Biophys. Res. Commun. 372 (2008) 51–56.
[127] Y.S. Hori, A. Kuno, R. Hosoda, Y. Horio, Regulation of FOXOs and p53 by SIRT1 modulators under oxidative stress, PLoS One 8 (2013) e73875.
[128] Y.I. Kitamura, T. Kitamura, J.P. Kruse, J.C. Raum, R. Stein, W. Gu, D. Accili, FoxO1 protects against pancreatic beta cell failure through NeuroD and MafA induction, Cell Metab. 2 (2005) 153–163.
[129] M.M. Brent, R. Anand, R. Marmorstein, Structural basis for DNA recognition by FoxO1 and its regulation by posttranslational modification, Structure 16 (2008) 1407–1416.
[130] Y. Yang, H. Hou, E.M. Haller, Nicosia SV, Bai W. Suppression of FOXO1 activity by FHL2 through SIRT1-mediated deacetylation, EMBO J. 24 (2005) 1021–1032.
[131] M. Hatta, L.A. Cirillo, Chromatin opening and stable perturbation of core histone:DNA contacts by FoxO1, J. Biol. Chem. 282 (2007) 35583–35593.
[132] H. Daitoku, J. Sakamaki, A. Fukamizu, Regulation of FoxO transcription factors by acetylation and protein–protein interactions, Biochim. Biophys. Acta 1813 (2011) 1954–1960.
[133] J.S. Gabrielsen, Y. Gao, J.A. Simcox, J. Huang, D. Thorup, D. Jones, R.C. Cooksey, D. Gabrielsen, T.D. Adams, S.C. Hunt, P.N. Hopkins, W.T. Cefalu, D.A. McClain, Adipocyte iron regulates adiponectin and insulin sensitivity, J. Clin. Investig. 122 (2012) 3529–3540.
[134] F. Wang, M. Nguyen, F.X. Qin, Q. Tong, SIRT2 deacetylates FOXO3a in response to oxidative stress and caloric restriction, Aging Cell 6 (2007) 505–514.
[135] F. Wang, Q. Tong, SIRT2 suppresses adipocyte differentiation by deacetylating FOXO1 and enhancing FOXO1's repressive interaction with PPARgamma, Mol. Biol. Cell 20 (2009) 801–808.
[136] G. Rose, S. Dato, K. Altomare, D. Bellizzi, S. Garasto, V. Greco, G. Passarino, E. Feraco, V. Mari, C. Barbi, M. BonaFe, C. Franceschi, Q. Tan, S. Boiko, A. I. Yashin, G. De Benedictis, Variability of the SIRT3 gene, human silent information regulator Sir2 homologue, and survivorship in the elderly, Exp. Gerontol. 38 (2003) 1065–1070.
[137] D. Bellizzi, G. Rose, P. Cavalcante, G. Covello, S. Dato, F. De Rango, V. Greco, M. Maggiolini, E. Feraco, V. Mari, C. Franceschi, G. Passarino, G. De Benedictis, A novel VNTR enhancer within the SIRT3 gene, a human homologue of SIR2, is associated with survival at oldest ages, Genomics 85 (2005) 258–263.
[138] B. Schwer, B.J. North, R.A. Frye, M. Ott, E. Verdin, The human silent information regulator (Sir)2 homologue hSIRT3 is a mitochondrial nicotinamide adenine dinucleotide-dependent deacetylase, J. Cell Biol. 158 (2002) 647–657.
[139] M.B. Scher, A. Vaquero, D. Reinberg, SirT3 is a nuclear NAD+-dependent histone deacetylase that translocates to the mitochondria upon cellular stress, Genes Dev. 21 (2007) 920–928.
[140] K.M. Jacobs, J.D. Pennington, K.S. Bisht, N. Aykin-Burns, H.S. Kim, M. Mishra, L. Sun, P. Nguyen, B.H. Ahn, J. Leclerc, C.X. Deng, D.R. Spitz, D. Gius, SIRT3 interacts with the daf-16 homolog FOXO3a in the mitochondria, as well as increases FOXO3a dependent gene expression, Int. J. Biol. Sci. 4 (2008) 291–299.
[141] N.R. Sundaresan, M. Gupta, G. Kim, S.B. Rajamohan, A. Isbatan, M.P. Gupta, Sirt3 blocks the cardiac hypertrophic response by augmenting Foxo3a-dependent antioxidant defense mechanisms in mice, J. Clin. Investig. 119 (2009) 2758–2771.
[142] Y.G. Ni, K. Berenji, N. Wang, M. Oh, N. Sachan, A. Dey, J. Cheng, G. Lu, D. J. Morris, D.H. Castrillon, R.D. Gerard, B.A. Rothermel, J.A. Hill, Foxo transcription factors blunt cardiac hypertrophy by inhibiting calcineurin signaling, Circulation 114 (2006) 1159–1168.

[143] W.C. Chiang, D.X. Tishkoff, B. Yang, J. Wilson-Grady, X. Yu, T. Mazer, M. Eckersdorff, S.P. Gygi, D.B. Lombard, A.L. Hsu, *C. elegans* SIRT6/7 homolog SIR-2.4 promotes DAF-16 relocalization and function during stress, PLoS Genet. 8 (2012) e1002948.
[144] R. Tao, X. Xiong, R.A. DePinho, C.X. Deng, X.C. Dong, FoxO3 transcription factor and Sirt6 deacetylase regulate low density lipoprotein (LDL)-cholesterol homeostasis via control of the proprotein convertase subtilisin/kexin type 9 (Pcsk9) gene expression, J. Biol. Chem. 288 (2013) 29252–29259.
[145] R. Tao, X. Xiong, R.A. DePinho, C.X. Deng, X.C. Dong, Hepatic SREBP-2 and cholesterol biosynthesis are regulated by FoxO3 and Sirt6, J. Lipid Res. 54 (2013) 2745–2753.
[146] K. Nowak, K. Killmer, C. Gessner, W. Lutz, E2F-1 regulates expression of FOXO1 and FOXO3a, Biochim. Biophys. Acta 1769 (2007) 244–252.
[147] J.M. Trimarchi, J.A. Lees, Sibling rivalry in the E2F family, Nat. Rev. Mol. Cell. Biol. 3 (2002) 11–20.
[148] B. Shan, W.H. Lee, Deregulated expression of E2F-1 induces S-phase entry and leads to apoptosis, Mol. Cell. Biol. 14 (1994) 8166–8173.
[149] J. DeGregori, G. Leone, A. Miron, L. Jakoi, J.R. Nevins, Distinct roles for E2F proteins in cell growth control and apoptosis, Proc. Natl. Acad. Sci. U.S.A. 94 (1997) 7245–7250.
[150] X.Q. Qin, D.M. Livingston, W.G. Kaelin Jr., P.D. Adams, Deregulated transcription factor E2F-1 expression leads to S-phase entry and p53-mediated apoptosis, Proc. Natl. Acad. Sci. U.S.A. 91 (1994) 10918–10922.
[151] E. Angelis, P. Zhao, R. Zhang, J.I. Goldhaber, W.R. Maclellan, The role of E2F-1 and downstream target genes in mediating ischemia/reperfusion injury in vivo, J. Mol. Cell. Cardiol. 51 (2011) 919–926.
[152] A. Sengupta, J.D. Molkentin, J.H. Paik, R.A. DePinho, K.E. Yutzey, FoxO transcription factors promote cardiomyocyte survival upon induction of oxidative stress, J. Biol. Chem. 286 (2011) 7468–7478.
[153] I. Shats, M.L. Gatza, B. Liu, S.P. Angus, L. You, J.R. Nevins, FOXO transcription factors control E2F1 transcriptional specificity and apoptotic function, Cancer Res. 73 (2013) 6056–6067.
[154] G.P. Dimri, K. Itahana, M. Acosta, J. Campisi, Regulation of a senescence checkpoint response by the E2F1 transcription factor and p14(ARF) tumor suppressor, Mol. Cell. Biol. 20 (2000) 273–285.
[155] V. Nogueira, Y. Park, C.C. Chen, P.Z. Xu, M.L. Chen, I. Tonic, T. Unterman, N. Hay, Akt determines replicative senescence and oxidative or oncogenic premature senescence and sensitizes cells to oxidative apoptosis, Cancer Cell 14 (2008) 458–470.
[156] Q. Xie, S. Peng, L. Tao, H. Ruan, Y. Yang, T.M. Li, U. Adams, S. Meng, X. Bi, M. Q. Dong, Z. Yuan, E2F transcription factor 1 regulates cellular and organismal senescence by inhibiting Forkhead box O transcription factors, J. Biol. Chem. 289 (2014) 34205–34213.
[157] S. Zheng, J. Moehlenbrink, Y.C. Lu, L.P. Zalmas, C.A. Sagum, S. Carr, J. F. McGouran, L. Alexander, O. Fedorov, S. Munro, B. Kessler, M.T. Bedford, Q. Yu, N.B. La Thanque, Arginine methylation-dependent reader–writer interplay governs growth control by E2F-1, Mol. Cell 52 (2013) 37–51.
[158] S. Kurinna, S.A. Stratton, W.W. Tsai, K.C. Akdemir, W. Gu, P. Singh, T. Goode, G. J. Darlington, M.C. Barton, Direct activation of forkhead box O3 by tumor suppressors p53 and p73 is disrupted during liver regeneration in mice, Hepatology 52 (2010) 1023–1032.
[159] V.M. Renault, P.U. Thekkat, K.L. Hoang, J.L. White, C.A. Brady, D. Kenzelmann Broz, O.S. Venturelli, T.M. Johnson, P.R. Oskoui, Z. Xuan, E.E. Santo, M. Q. Zhang, H. Vogel, L.D. Attardi, A. Brunet, The pro-longevity gene FoxO3 is a direct target of the p53 tumor suppressor, Oncogene 30 (2011) 3207–3221.
[160] B. Vogelstein, D. Lane, A.J. Levine, Surfing the p53 network, Nature 408 (2000) 307–310.
[161] L.C. Trotman, A. Alimonti, P.P. Scaglioni, J.A. Koutcher, C. Cordon-Cardo, P. P. Pandolfi, Identification of a tumour suppressor network opposing nuclear Akt function, Nature 441 (2006) 523–527.
[162] A. Essaghir, N. Dif, C.Y. Marbehant, P.J. Coffer, J.B. Demoulin, The transcription of FOXO genes is stimulated by FOXO3 and repressed by growth factors, J. Biol. Chem. 284 (2009) 10334–10342.
[163] W.L. Zhu, H. Tong, J.T. Teh, M. Wang, Forkhead box protein O3 transcription factor negatively regulates autophagy in human cancer cells by inhibiting forkhead box protein O1 expression and cytosolic accumulation, PLoS One 9 (2014) e115087.
[164] W.J. Bakker, I.S. Harris, T.W. Mak, FOXO3a is activated in response to hypoxic stress and inhibits HIF1-induced apoptosis via regulation of CITED2, Mol. Cell 28 (2007) 941–953.
[165] J. Samarin, J. Wessel, I. Cicha, S. Kroening, C. Warnecke, M. Goppelt-Struebe, FoxO proteins mediate hypoxic induction of connective tissue growth factor in endothelial cells, J. Biol. Chem. 285 (2010) 4328–4336.
[166] A.R. Wondisford, L. Xiong, E. Chang, S. Meng, D.J. Meyers, M. Li, P.A. Cole, L. He, Control of Foxo1 gene expression by co-activator P300, J. Biol. Chem. 289 (2014) 4326–4333.
[167] N. Lützner, H. Kalbacher, A. Krones-Herzig, F. Rösl, FOXO3 is a glucocorticoid receptor target and regulates LKB1 and its own expression based on cellular AMP levels via a positive autoregulatory loop, PLoS One 7 (2012) e42166.
[168] W. Qin, J. Pan, Y. Qin, D.N. Lee, W.A. Bauman, C. Cardozo, Identification of functional glucocorticoid response elements in the mouse FoxO1 promoter, Biochem. Biophys. Res. Commun. 450 (2014) 979–983.
[169] F.B. Berry, J.M. Skarie, F. Mirzayans, Y. Fortin, T.J. Hudson, V. Raymond, B. A. Link, M.A. Walter, FOXC1 is required for cell viability and resistance to oxidative stress in the eye through the transcriptional regulation of FOXO1A, Hum. Mol. Genet. 17 (2008) 490–505.
[170] M. Shen, F. Lin, J. Zhang, Y. Tang, W.K. Chen, H. Liu, Involvement of the up-regulated FoxO1 expression in follicular granulosa cell apoptosis induced by oxidative stress, J. Biol. Chem. 287 (2012) 25727–25740.
[171] J. Nakae, T. Kitamura, Y. Kitamura, W.H. Biggs 3rd, K.C. Arden, D. Accili, The forkhead transcription factor Foxo1 regulates adipocyte differentiation, Dev. Cell 4 (2003) 119–129.
[172] G.S. Liu, E.C. Chan, M. Higuchi, G.J. Dusting, F. Jiang, Redox mechanisms in regulation of adipocyte differentiation: beyond a general stress response, Cells 1 (2012) 976–993.
[173] M. Higuchi, G.J. Dusting, H. Peshavariya, F. Jiang, S.T. Hsiao, E.C. Chan, G.S. Liu, Differentiation of human adipose-derived stem cells into fat involves reactive oxygen species and Forkhead box O1 mediated upregulation of antioxidant enzymes, Stem Cells Dev. 22 (2013) 878–888.
[174] M. Christian, X. Zhang, T. Schneider-Merck, T.G. Unterman, B. Gellersen, J. O. White, J.J. Brosens, Cyclic AMP-induced forkhead transcription factor, FKHR, cooperates with CCAAT/enhancer-binding protein beta in differentiating human endometrial stromal cells, J. Biol. Chem. 277 (2002) 20825–20832.
[175] S. Labied, T. Kajihara, P.A. Madureira, L. Fusi, M.C. Jones, J.M. Higham, R. Varshochi, J.M. Francis, G. Zoumpoulidou, A. Essafi, S. Fernandez de Mattos, E.W. Lam, J.J. Brosens, Progestins regulate the expression and activity of the forkhead transcription factor FOXO1 in differentiating human endometrium, Mol. Endocrinol. 20 (2006) 35–44.
[176] T. Kajihara, M. Jones, L. Fusi, M. Takano, F. Feroze-Zaidi, G. Pirianov, H. Mehmet, O. Ishihara, J.M. Higham, E.W. Lam, J.J. Brosens, Differential expression of FOXO1 and FOXO3a confers resistance to oxidative cell death upon endometrial decidualization, Mol. Endocrinol. 20 (2006) 2444–2455.
[177] M. Takano, Z. Lu, T. Goto, L. Fusi, J. Higham, J. Francis, A. Withey, J. Hardt, B. Cloke, A.V. Stavropoulou, O. Ishihara, E.W. Lam, T.G. Unterman, J.J. Brosens, J.J. Kim, Transcriptional cross talk between the forkhead transcription factor forkhead box O1A and the progesterone receptor coordinates cell cycle regulation and differentiation in human endometrial stromal cells, Mol. Endocrinol. 21 (2007) 2334–2349.
[178] M. Imae, Z. Fu, A. Yoshida, T. Noguchi, H. Kato, Nutritional and hormonal factors control the gene expression of FoxOs, the mammalian homologues of DAF-16, J. Mol. Endocrinol. 30 (2003) 253–262.
[179] T. Furuyama, H. Yamashita, K. Kitayama, Y. Higami, I. Shimokawa, N. Mori, Effects of aging and caloric restriction on the gene expression of Foxo1, 3, and 4 (FKHR, FKHRL1, and AFX) in the rat skeletal muscles, Microsc. Res. Tech. 59 (2002) 331–334.
[180] X. Zhu, R. Hart, M.S. Chang, J.W. Kim, S.Y. Lee, Y.A. Cao, D. Mock, E. Ke, B. Saunders, A. Alexander, J. Grossoehme, K.M. Lin, Z. Yan, R. Hsueh, J. Lee, R. H. Scheuermann, D.A. Fruman, W. Seaman, S. Subramaniam, P. Sternweis, M. I. Simon, S. Choi, Analysis of the major patterns of B cell gene expression changes in response to short-term stimulation with 33 single ligands, J. Immunol. 173 (2004) 7141–7149.
[181] R.M. Hinman, J.N. Bushanam, W.A. Nichols, A.B. Satterthwaite, B cell receptor signaling down-regulates forkhead box transcription factor class O 1 mRNA expression via phosphatidylinositol 3-kinase and Bruton's tyrosine kinase, J. Immunol. 178 (2007) 740–747.
[182] W. Wang, H. Furneaux, H. Cheng, M.C. Caldwell, D. Hutter, Y. Liu, N. Holbrook, M. Gorospe, HuR regulates p21 mRNA stabilization by UV light, Mol. Cell. Biol. 20 (2000) 760–769.
[183] H. Tran, F. Maurer, Y. Nagamine, Stabilization of urokinase and urokinase receptor mRNAs by HuR is linked to its cytoplasmic accumulation induced by activated mitogen-activated protein kinase-activated protein kinase 2, Mol. Cell. Biol. 23 (2003) 7177–7188.
[184] N.S. Fernau, D. Fugmann, M. Leyendecker, K. Reimann, S. Grether-Beck, S. Galban, N. Ale-Agha, J. Krutmann, L.O. Klotz, Role of HuR and p38MAPK in ultraviolet B-induced post-transcriptional regulation of COX-2 expression in the human keratinocyte cell line HaCaT, J. Biol. Chem. 285 (2010) 3896–3904.
[185] S.N. Bhattacharyya, R. Habermacher, U. Martine, E.I. Closs, W. Filipowicz, Relief of microRNA-mediated translational repression in human cells subjected to stress, Cell 125 (2006) 1111–1124.
[186] I.S. Song, S. Tatebe, W. Dai, M.T. Kuo, Delayed mechanism for induction of gamma-glutamylcysteine synthetase heavy subunit mRNA stability by oxidative stress involving p38 mitogen-activated protein kinase signaling, J. Biol. Chem. 280 (2005) 28230–28240.
[187] K. Abdelmohsen, Y. Kuwano, H.H. Kim, M. Gorospe, Posttranscriptional gene regulation by RNA-binding proteins during oxidative stress: implications for cellular senescence, Biol. Chem. 389 (2008) 243–255.
[188] K. Subbaramaiah, T.P. Marmo, D.A. Dixon, A.J. Dannenberg, Regulation of cyclooxgenase-2 mRNA stability by taxanes: evidence for involvement of p38, MAPKAPK-2, and HuR, J. Biol. Chem. 278 (2003) 37637–37647.
[189] V. Lafarga, A. Cuadrado, I. Lopez de Silanes, R. Bengoechea, O. Fernandez-Capetillo, A.R. Nebreda, p38 Mitogen-activated protein kinase- and HuR-dependent stabilization of p21(Cip1) mRNA mediates the G(1)/S checkpoint, Mol. Cell. Biol. 29 (2009) 4341–4351.
[190] R.M. Benoit, N.C. Meisner, J. Kallen, P. Graff, R. Hemmig, R. Cebe, C. Ostermeier, H. Widmer, M. Auer, The x-ray crystal structure of the first RNA recognition motif and site-directed mutagenesis suggest a possible HuR redox sensing mechanism, J. Mol. Biol. 397 (2010) 1231–1244.
[191] Y. Li, J. Yu, D. Du, S. Fu, Y. Chen, F. Yu, P. Gao, Involvement of post-transcriptional regulation of FOXO1 by HuR in 5-FU-induced apoptosis in breast cancer cells, Oncol. Lett. 6 (2013) 156–160.
[192] F. Yu, L. Jin, G. Yang, L. Ji, F. Wang, Z. Lu, Post-transcriptional repression of

FOXO1 by QKI results in low levels of FOXO1 expression in breast cancer cells, Oncol. Rep. 31 (2014) 1459–1465.
[193] J. Yang, T. Li, C. Gao, X. Lv, K. Liu, H. Song, Y. Xing, T. Xi, FOXO1 3′UTR functions as a ceRNA in repressing the metastases of breast cancer cells via regulating miRNA activity, FEBS Lett. 588 (2014) 3218–3224.
[194] H. Lin, T. Dai, H. Xiong, X. Zhao, X. Chen, C. Yu, J. Li, X. Wang, L. Song, Unregulated miR-96 induces cell proliferation in human breast cancer by downregulating transcriptional factor FOXO3a, PLoS One 5 (2010) e15797.
[195] Z. Wu, H. Sun, W. Zeng, J. He, X. Mao, Upregulation of MircoRNA-370 induces proliferation in human prostate cancer cells by downregulating the transcription factor FOXO1, PLoS One 7 (2012) e45825.
[196] L. Wu, H. Li, C.Y. Jia, W. Cheng, M. Yu, M. Peng, Y. Zhu, Q. Zhao, Y.W. Dong, K. Shao, A. Wu, X.Z. Wu, MicroRNA-223 regulates FOXO1 expression and cell proliferation, FEBS Lett. 586 (2012) 1038–1043.
[197] C. Fan, S. Liu, Y. Zhao, Y. Han, L. Yang, G. Tao, Q. Li, L. Zhang, Upregulation of miR-370 contributes to the progression of gastric carcinoma via suppression of FOXO1, Biomed. Pharmacother. 67 (2013) 521–526.
[198] N. Ling, J. Gu, Z. Lei, M. Li, J. Zhao, H.T. Zhang, X. Li, microRNA-155 regulates cell proliferation and invasion by targeting FOXO3a in glioma, Oncol. Rep. 30 (2013) 2111–2118.
[199] C. Tan, S. Liu, S. Tan, X. Zeng, H. Yu, A. Li, C. Bei, X. Qiu, Polymorphisms in microRNA target sites of forkhead box O genes are associated with hepatocellular carcinoma, PLoS One 10 (2015) e0119210.
[200] P. Puigserver, J. Rhee, J. Donovan, C.J. Walkey, J.C. Yoon, F. Oriente, Y. Kitamura, J. Altomonte, H. Dong, D. Accili, B.M. Spiegelman, Insulin-regulated hepatic gluconeogenesis through FOXO1-PGC-1alpha interaction, Nature 423 (2003) 550–555.
[201] M. Sandri, J. Lin, C. Handschin, W. Yang, Z.P. Arany, S.H. Lecker, A.L. Goldberg, B.M. Spiegelman, PGC-1alpha protects skeletal muscle from atrophy by suppressing FoxO3 action and atrophy-specific gene transcription, Proc. Natl. Acad. Sci. U.S.A. 103 (2006) 16260–16265.
[202] T. Geng, P. Li, X. Yin, Z. Yan, PGC-1alpha promotes nitric oxide antioxidant defenses and inhibits FOXO signaling against cardiac cachexia in mice, Am. J. Pathol. 178 (2011) 1738–1748.
[203] C.S. Wilcox, A. Pearlman, Chemistry and antihypertensive effects of tempol and other nitroxides, Pharmacol. Rev. 60 (2008) 418–469.
[204] H.E. Yoon, S.J. Kim, S.J. Kim, S. Chung, S.J. Shin, Tempol attenuates renal fibrosis in mice with unilateral ureteral obstruction: the role of PI3K-Akt-FoxO3a signaling, J. Korean Med. Sci. 29 (2014) 230–237.
[205] H.W. Chung, J.H. Lim, M.Y. Kim, S.J. Shin, S. Chung, B.S. Choi, H.W. Kim, Y. S. Kim, C.W. Park, Y.S. Chang, High-fat diet-induced renal cell apoptosis and oxidative stress in spontaneously hypertensive rat are ameliorated by fenofibrate through the PPARalpha-FoxO3a-PGC-1alpha pathway, Nephrol. Dial. Transplant. 27 (2012) 2213–2225.
[206] V. Exil, L. Ping, Y. Yu, S. Chakraborty, S.W. Caito, K.S. Wells, P. Karki, E. Lee, M. Aschner, Activation of MAPK and FoxO by manganese (Mn) in rat neonatal primary astrocyte cultures, PLoS One 9 (2014) e94753.
[207] Y. Olmos, I. Valle, S. Borniquel, A. Tierrez, E. Soria, S. Lamas, M. Monsalve, Mutual dependence of Foxo3a and PGC-1alpha in the induction of oxidative stress genes, J. Biol. Chem. 284 (2009) 14476–14484.
[208] X. Liu, C. Greer, J. Secombe, KDM5 interacts with Foxo to modulate cellular levels of oxidative stress, PLoS Genet. 10 (2014) e1004676.
[209] J. Araujo, P. Breuer, S. Dieringer, S. Krauss, S. Dorn, K. Zimmermann, A. Pfeifer, T. Klockgether, U. Wuellner, B.O. Evert, FOXO4-dependent upregulation of superoxide dismutase-2 in response to oxidative stress is impaired in spinocerebellar ataxia type 3, Hum. Mol. Genet. 20 (2011) 2928–2941.
[210] R. Scherz-Shouval, E. Shvets, E. Fass, H. Shorer, L. Gil, Z. Elazar, Reactive oxygen species are essential for autophagy and specifically regulate the activity of Atg4, EMBO J. 26 (2007) 1749–1760.
[211] N. Mizushima, Autophagy: process and function, Genes Dev. 21 (2007) 2861–2873.
[212] N. Hariharan, Y. Maejima, J. Nakae, J. Paik, R.A. Depinho, J. Sadoshima, Deacetylation of FoxO by Sirt1 plays an essential role in mediating starvation-induced autophagy in cardiac myocytes, Circ. Res. 107 (2010) 1470–1482.
[213] C. Mammucari, G. Milan, V. Romanello, E. Masiero, R. Rudolf, P. Del Piccolo, S. J. Burden, R. Di Lisi, C. Sandri, J. Zhao, A.L. Goldberg, S. Schiaffino, M. Sandri, FoxO3 controls autophagy in skeletal muscle in vivo, Cell Metab. 6 (2007) 458–471.
[214] D. Lee, A.L. Goldberg, SIRT1 protein, by blocking the activities of transcription factors FoxO1 and FoxO3, inhibits muscle atrophy and promotes muscle growth, J. Biol. Chem. 288 (2013) 30515–30526.
[215] Y. Zhao, J. Yang, W. Liao, X. Liu, H. Zhang, S. Wang, D. Wang, J. Feng, L. Yu, W. G. Zhu, Cytosolic FoxO1 is essential for the induction of autophagy and tumour suppressor activity, Nat. Cell Biol. 12 (2010) 665–675.
[216] A. Peserico, F. Chiacchiera, V. Grossi, A. Matrone, D. Latorre, M. Simonatto, A. Fusella, J.G. Ryall, L.W. Finley, M.C. Haigis, G. Villani, P.L. Puri, V. Sartorelli, C. Simone, A novel AMPK-dependent FoxO3A-SIRT3 intramitochondrial complex sensing glucose levels, Cell. Mol. Life Sci. 70 (2013) 2015–2029.
[217] I.C. Chen, W.F. Chiang, P.F. Chen, H.C. Chiang, STRESS-responsive deacetylase SIRT3 is up-regulated by areca nut extract-induced oxidative stress in human oral keratinocytes, J. Cell. Biochem. 115 (2014) 328–339.
[218] A.H. Tseng, S.S. Shieh, D.L. Wang, SIRT3 deacetylates FOXO3 to protect mitochondria against oxidative damage, Free Radic. Biol. Med. 63 (2013) 222–234.
[219] A.H. Tseng, L.H. Wu, S.S. Shieh, D.L. Wang, SIRT3 interactions with FOXO3 acetylation, phosphorylation and ubiquitinylation mediate endothelial cell responses to hypoxia, Biochem. J. 464 (2014) 157–168.
[220] E.M. Mercken, S.D. Crosby, D.W. Lamming, L. JeBailey, S. Krzysik-Walker, D. T. Villareal, M. Capri, C. Franceschi, Y. Zhang, K. Becker, D.M. Sabatini, R. de Cabo, L. Fontana, Calorie restriction in humans inhibits the PI3K/AKT pathway and induces a younger transcription profile, Aging Cell 12 (2013) 645–651.
[221] A.G. Cristancho, M.A. Lazar, Forming functional fat: a growing understanding of adipocyte differentiation, Nat. Rev. Mol. Cell. Biol. 12 (2011) 722–734.
[222] P.H. Ducluzeau, M. Priou, M. Weitheimer, M. Flamment, L. Duluc, F. Iacobazi, R. Soleti, G. Simard, A. Durand, J. Rieusset, R. Andriantsitohaina, Y. Malthiery, Dynamic regulation of mitochondrial network and oxidative functions during 3T3-L1 fat cell differentiation, J. Physiol. Biochem. 67 (2011) 285–296.
[223] H. Lee, Y.J. Lee, H. Choi, E.H. Ko, J.W. Kim, Reactive oxygen species facilitate adipocyte differentiation by accelerating mitotic clonal expansion, J. Biol. Chem. 284 (2009) 10601–10609.
[224] A.M. Rajalin, M. Micoogullari, H. Sies, H. Steinbrenner, Upregulation of the thioredoxin-dependent redox system during differentiation of 3T3-L1 cells to adipocytes, Biol. Chem. 395 (2014) 667–677.
[225] T. Kelly, W. Yang, C.S. Chen, K. Reynolds, J. He, Global burden of obesity in 2005 and projections to 2030, Int. J. Obes. (Lond.) 32 (2008) 1431–1437.
[226] S. Wild, G. Roglic, A. Green, R. Sicree, H. King, Global prevalence of diabetes: estimates for the year 2000 and projections for 2030, Diabetes Care 27 (2004) 1047–1053.
[227] L. Rochette, M. Zeller, Y. Cottin, C. Vergely, Diabetes, oxidative stress and therapeutic strategies, Biochim. Biophys. Acta 1840 (2014) 2709–2729.
[228] T. Tiganis, Reactive oxygen species and insulin resistance: the good, the bad and the ugly, Trends Pharmacol. Sci. 32 (2011) 82–89.
[229] M. Tiedge, S. Lortz, J. Drinkgern, S. Lenzen, Relation between antioxidant enzyme gene expression and antioxidative defense status of insulin-producing cells, Diabetes 46 (1997) 1733–1742.
[230] C.M. Sena, A.M. Pereira, R. Seica, Endothelial dysfunction – a major mediator of diabetic vascular disease, Biochim. Biophys. Acta 1832 (2013) 2216–2231.
[231] J. Nakae, W.H. Biggs 3rd, T. Kitamura, W.K. Cavenee, C.V. Wright, K.C. Arden, D. Accili, Regulation of insulin action and pancreatic beta-cell function by mutated alleles of the gene encoding forkhead transcription factor Foxo1, Nat. Genet. 32 (2002) 245–253.
[232] J. Altomonte, L. Cong, S. Harbaran, A. Richter, J. Xu, M. Meseck, H.H. Dong, Foxo1 mediates insulin action on apoC-III and triglyceride metabolism, J. Clin. Investig. 114 (2004) 1493–1503.
[233] D.N. Gross, A.P. van den Heuvel, M.J. Birnbaum, The role of FoxO in the regulation of metabolism, Oncogene 27 (2008) 2320–2336.
[234] Y. Wang, Y. Zhou, D.T. Graves, FOXO transcription factors: their clinical significance and regulation, Biomed. Res. Int. (2014) 925350 2014.
[235] K. Zhang, L. Li, Y. Qi, X. Zhu, B. Gan, R.A. DePinho, T. Averitt, S. Guo, Hepatic suppression of Foxo1 and Foxo3 causes hypoglycemia and hyperlipidemia in mice, Endocrinology 153 (2012) 631–646.
[236] Y. Behl, P. Krothapalli, T. Desta, S. Roy, D.T. Graves, FOXO1 plays an important role in enhanced microvascular cell apoptosis and microvascular cell loss in type 1 and type 2 diabetic rats, Diabetes 58 (2009) 917–925.
[237] J. Alblowi, R.A. Kayal, M. Siqueira, E. McKenzie, N. Krothapalli, J. McLean, J. Conn, B. Nikolajczyk, T.A. Einhorn, L. Gerstenfeld, D.T. Graves, High levels of tumor necrosis factor-alpha contribute to accelerated loss of cartilage in diabetic fracture healing, Am. J. Pathol. 175 (2009) 1574–1585.
[238] J.Y. Kim-Muller, S. Zhao, S. Srivastava, Y. Mugabo, H.L. Noh, Y.R. Kim, S. R. Madiraju, A.W. Ferrante, E.Y. Skolnik, M. Prentki, D. Accili, Metabolic inflexibility impairs insulin secretion and results in MODY-like diabetes in triple FoxO-deficient mice, Cell Metab. 20 (2014) 593–602.
[239] D. Massillon, N. Barzilai, W. Chen, M. Hu, L. Rossetti, Glucose regulates in vivo glucose-6-phosphatase gene expression in the liver of diabetic rats, J Biol Chem 271 (1996) 9871–9874.
[240] J.C. Yoon, P. Puigserver, G. Chen, J. Donovan, Z. Wu, J. Rhee, G. Adelmant, J. Stafford, C.R. Kahn, D.K. Granner, C.B. Newgard, B.M. Spiegelman, Control of hepatic gluconeogenesis through the transcriptional coactivator PGC-1, Nature 413 (2001) 131–138.
[241] M.P. Housley, N.D. Udeshi, J.T. Rodgers, J. Shabanowitz, P. Puigserver, D. F. Hunt, G.W. Hart, A PGC-1alpha-O-GlcNAc transferase complex regulates FoxO transcription factor activity in response to glucose, J. Biol. Chem. 284 (2009) 5148–5157.
[242] B. Speckmann, H. Sies, H. Steinbrenner, Attenuation of hepatic expression and secretion of selenoprotein P by metformin, Biochem. Biophys. Res. Commun. 387 (2009) 158–163.
[243] H. Misu, T. Takamura, H. Takayama, H. Hayashi, N. Matsuzawa-Nagata, S. Kurita, K. Ishikura, H. Ando, Y. Takeshita, T. Ota, M. Sakurai, T. Yamashita, E. Mizukoshi, T. Yamashita, M. Honda, K. Miyamoto, T. Kubota, N. Kubota, T. Kadowaki, H.J. Kim, I.K. Lee, Y. Minokoshi, Y. Saito, K. Takahashi, Y. Yamada, N. Takakura, S. Kaneko, A liver-derived secretory protein, selenoprotein P, causes insulin resistance, Cell Metab. 12 (2010) 483–495.
[244] W. Zhang, V. Hietakangas, S. Wee, S.C. Lim, J. Gunaratne, S.M. Cohen, ER stress potentiates insulin resistance through PERK-mediated FOXO phosphorylation, Genes Dev. 27 (2013) 441–449.
[245] R.A. Haeusler, K. Hartil, B. Vaitheesvaran, I. Arrieta-Cruz, C.M. Knight, J. R. Cook, H.L. Kammoun, M.A. Febbraio, R. Gutierrez-Juarez, I.J. Kurland, D. Accili, Integrated control of hepatic lipogenesis versus glucose production requires FoxO transcription factors, Nat. Commun. 5 (2014) 5190.
[246] S. Sugita, Y. Arai, A. Tonooka, N. Hama, Y. Totoki, T. Fujii, T. Aoyama, H. Asanuma, T. Tsukahara, M. Kaya, T. Shibata, T. Hasegawa, A novel ClC-

FOXO4 gene fusion in undifferentiated small round cell sarcoma: a genetically distinct variant of Ewing-like sarcoma, Am. J. Surg. Pathol. 38 (2014) 1571–1576.
[247] L. Xie, A. Ushmorov, F. Leithauser, H. Guan, C. Steidl, J. Farbinger, C. Pelzer, M. J. Vogel, H.J. Maier, R.D. Gascoyne, P. Moller, T. Wirth, FOXO1 is a tumor suppressor in classical Hodgkin lymphoma, Blood 119 (2012) 3503–3511.
[248] M. Korani, S. Fallah, A. Tehranian, M. Nourbakhsh, A. Samadikuchaksaraei, M. S. Pour, J. Maleki, The evaluation of the FOXO1, KLF9 and YT521 genes expression in human endometrial cancer, Clin. Lab. 59 (2013) 483–489.
[249] T. Goto, M. Takano, J. Hirata, H. Tsuda, The involvement of FOXO1 in cytotoxic stress and drug-resistance induced by paclitaxel in ovarian cancers, Br. J. Cancer 98 (2008) 1068–1075.
[250] J.H. Paik, R. Kollipara, G. Chu, H. Ji, Y. Xiao, Z. Ding, L. Miao, Z. Tothova, J. W. Horner, D.R. Carrasco, S. Jiang, D.G. Gilliland, L. Chin, W.H. Wong, D. H. Castrillon, R.A. DePinho, FoxOs are lineage-restricted redundant tumor suppressors and regulate endothelial cell homeostasis, Cell 128 (2007) 309–323.
[251] L. Qinyu, C. Long, D. Zhen-dong, S. Min-min, W. Wei-ze, Y. Wei-ping, P. Cheng-hong, FOXO6 promotes gastric cancer cell tumorigenicity via up-regulation of C-myc, FEBS Lett. 587 (2013) 2105–2111.
[252] N. Aykin-Burns, I.M. Ahmad, Y. Zhu, L.W. Oberley, D.R. Spitz, Increased levels of superoxide and H_2O_2 mediate the differential susceptibility of cancer cells versus normal cells to glucose deprivation, Biochem. J. 418 (2009) 29–37.
[253] W. Sun, A.L. Kalen, B.J. Smith, J.J. Cullen, L.W. Oberley, Enhancing the anti-tumor activity of adriamycin and ionizing radiation, Cancer Res. 69 (2009) 4294–4300.
[254] I.S. Harris, H. Blaser, J. Moreno, A.E. Treloar, C. Gorrini, M. Sasaki, J.M. Mason, C.B. Knobbe, A. Rufini, M. Halle, A.J. Elia, A. Wakeham, M.L. Tremblay, G. Melino, S. Done, T.W. Mak, PTPN12 promotes resistance to oxidative stress and supports tumorigenesis by regulating FOXO signaling, Oncogene 33 (2014) 1047–1054.
[255] G.J. Wang, G.H. Liu, Y.W. Ye, Y. Fu, X.F. Zhang, The role of microRNA-1274a in the tumorigenesis of gastric cancer: accelerating cancer cell proliferation and migration via directly targeting FOXO4, Biochem. Biophys. Res. Commun. 459 (2015) 629–635.
[256] X.P. Mao, L.S. Zhang, B. Huang, S.Y. Zhou, J. Liao, L.W. Chen, S.P. Qiu, J.X. Chen, Mir-135a enhances cellular proliferation through post-transcriptionally regulating PHLPP2 and FOXO1 in human bladder cancer, J. Transl. Med. 13 (2015) 86.
[257] S.Y. Kim, J. Yoon, Y.S. Ko, M.S. Chang, J.W. Park, H.E. Lee, M.A. Kim, J.H. Kim, W. H. Kim, B.L. Lee, Constitutive phosphorylation of the FOXO1 transcription factor in gastric cancer cells correlates with microvessel area and the expressions of angiogenesis-related molecules, BMC Cancer 11 (2011) 264.
[258] K.C. Pramanik, N.M. Fofaria, P. Gupta, S.K. Srivastava, CBP-mediated FOXO-1 acetylation inhibits pancreatic tumor growth by targeting SirT, Mol. Cancer Ther. 13 (2014) 687–698.
[259] B. Peck, E.C. Ferber, A. Schulze, Antagonism between FOXO and MYC regulates cellular powerhouse, Front. Oncol. 3 (2013) 96.
[260] E.C. Ferber, B. Peck, O. Delpuech, G.P. Bell, P. East, A. Schulze, FOXO3a regulates reactive oxygen metabolism by inhibiting mitochondrial gene expression, Cell Death Differ. 19 (2012) 968–979.
[261] K.S. Jensen, T. Binderup, K.T. Jensen, I. Therkelsen, R. Borup, E. Nilsson, H. Multhaupt, C. Bouchard, B. Quistorff, A. Kjaer, G. Landberg, P. Staller, FoxO3A promotes metabolic adaptation to hypoxia by antagonizing Myc function, EMBO J. 30 (2011) 4554–4570.
[262] C. Loguercio, A. Federico, Oxidative stress in viral and alcoholic hepatitis, Free Radic. Biol. Med. 34 (2003) 1–10.
[263] D.L. Diesen, P.C. Kuo, Nitric oxide and redox regulation in the liver: Part I. General considerations and redox biology in hepatitis, J. Surg. Res. 162 (2010) 95–109.
[264] A. Dey, A.I. Cederbaum, Alcohol and oxidative liver injury, Hepatology 43 (2006) S63–S74.
[265] P. Muriel, Role of free radicals in liver diseases, Hepatol. Int. 3 (2009) 526–536.
[266] G.Z. Tao, N. Lehwald, K.Y. Jang, J. Baek, B. Xu, M.B. Omary, K.G. Sylvester, Wnt/beta-catenin signaling protects mouse liver against oxidative stress-induced apoptosis through the inhibition of forkhead transcription factor FoxO3, J. Biol. Chem. 288 (2013) 17214–17224.
[267] P.J. Kim, J. Plescia, H. Clevers, E.R. Fearon, D.C. Altieri, Survivin and molecular pathogenesis of colorectal cancer, Lancet 362 (2003) 205–209.
[268] J.C. Tapia, V.A. Torres, D.A. Rodriguez, L. Leyton, A.F. Quest, Casein kinase 2 (CK2) increases survivin expression via enhanced beta-catenin-T cell factor/lymphoid enhancer binding factor-dependent transcription, Proc. Natl. Acad. Sci. U.S.A. 103 (2006) 15079–15084.
[269] M. Dehner, M. Hadjihannas, J. Weiske, O. Huber, J. Behrens, Wnt signaling inhibits Forkhead box O3a-induced transcription and apoptosis through up-regulation of serum- and glucocorticoid-inducible kinase 1, J. Biol. Chem. 283 (2008) 19201–19210.
[270] S.P. Tenbaum, P. Ordonez-Moran, I. Puig, I. Chicote, O. Arques, S. Landolfi, Y. Fernandez, J.R. Herance, J.D. Gispert, L. Mendizabal, S. Aguilar, S. Ramon y Cajal, S. Schwartz Jr., A. Vivancos, E. Espin, S. Rojas, J. Baselga, J. Tabernero, A. Munoz, H.G. Palmer, beta-catenin confers resistance to PI3K and AKT inhibitors and subverts FOXO3a to promote metastasis in colon cancer, Nat. Med. 18 (2012) 892–901.
[271] Y. Yan, M.R. Lackner, FOXO3a and beta-catenin co-localization: double trouble in colon cancer? Nat. Med. 18 (2012) 854–856.
[272] H. Yamaza, T. Komatsu, S. Wakita, C. Kijogi, S. Park, H. Hayashi, T. Chiba, R. Mori, T. Furuyama, N. Mori, I. Shimokawa, FoxO1 is involved in the anti-neoplastic effect of calorie restriction, Aging Cell 9 (2010) 372–382.
[273] K. Masui, K. Tanaka, D. Akhavan, I. Babic, B. Gini, T. Matsutani, A. Iwanami, F. Liu, G.R. Villa, Y. Gu, C. Campos, S. Zhu, H. Yang, W.H. Yong, T.F. Cloughesy, I. K. Mellinghoff, W.K. Cavenee, R.J. Shaw, P.S. Mischel, mTOR complex 2 controls glycolytic metabolism in glioblastoma through FoxO acetylation and upregulation of c-Myc, Cell Metab. 18 (2013) 726–739.
[274] M.M. Mihaylova, D.S. Vasquez, K. Ravnskjaer, P.D. Denechaud, R.T. Yu, J. G. Alvarez, M. Downes, R.M. Evans, M. Montminy, R.J. Shaw, Class IIa histone deacetylases are hormone-activated regulators of FOXO and mammalian glucose homeostasis, Cell 145 (2011) 607–621.
[275] S.M. Senf, P.B. Sandesara, S.A. Reed, A.R. Judge, p300 Acetyltransferase activity differentially regulates the localization and activity of the FOXO homologues in skeletal muscle, Am. J. Physiol. Cell Physiol. 300 (2011) C1490–C1501.
[276] E. Bertaggia, L. Coletto, M. Sandri, Posttranslational modifications control FoxO3 activity during denervation, Am. J. Physiol. Cell Physiol. 302 (2012) C587–C596.
[277] A.W. Beharry, P.B. Sandesara, B.M. Roberts, L.F. Ferreira, S.M. Senf, A.R. Judge, HDAC1 activates FoxO and is both sufficient and required for skeletal muscle atrophy, J. Cell Sci. 127 (2014) 1441–1453.
[278] M. Sandri, L. Barberi, A.Y. Bijlsma, B. Blaauw, K.A. Dyar, G. Milan, C. Mammucari, C.G. Meskers, G. Pallafacchina, A. Paoli, D. Pion, M. Roceri, V. Romanello, A.L. Serrano, L. Toniolo, L. Larsson, A.B. Maier, P. Munoz-Canoves, A. Musaro, M. Pende, C. Reggiani, R. Rizzuto, S. Schiaffino, Signalling pathways regulating muscle mass in ageing skeletal muscle: the role of the IGF1-Akt-mTOR-FoxO pathway, Biogerontology 14 (2013) 303–323.
[279] E. Owusu-Ansah, W. Song, N. Perrimon, Muscle mitohormesis promotes longevity via systemic repression of insulin signaling, Cell 155 (2013) 699–712.
[280] E. Ambrogini, M. Almeida, M. Martin-Millan, J.H. Paik, R.A. Depinho, L. Han, J. Goellner, R.S. Weinstein, R.L. Jilka, C.A. O'Brien, S.C. Manolagas, FoxO-mediated defense against oxidative stress in osteoblasts is indispensable for skeletal homeostasis in mice, Cell Metab. 11 (2010) 136–146.
[281] M.T. Rached, A. Kode, L. Xu, Y. Yoshikawa, J.H. Paik, R.A. Depinho, S. Kousteni, FoxO1 is a positive regulator of bone formation by favoring protein synthesis and resistance to oxidative stress in osteoblasts, Cell Metab. 11 (2010) 147–160.
[282] I.R. Garrett, B.F. Boyce, R.O. Oreffo, L. Bonewald, J. Poser, G.R. Mundy, Oxygen-derived free radicals stimulate osteoclastic bone resorption in rodent bone in vitro and in vivo, J. Clin. Investig. 85 (1990) 632–639.
[283] N.K. Lee, Y.G. Choi, J.Y. Baik, S.Y. Han, D.W. Jeong, Y.S. Bae, N. Kim, S.Y. Lee, A crucial role for reactive oxygen species in RANKL-induced osteoclast differentiation, Blood 106 (2005) 852–859.
[284] N.Y. Bhatt, T.W. Kelley, V.V. Khramtsov, Y. Wang, G.K. Lam, T.L. Clanton, C. B. Marsh, Macrophage-colony-stimulating factor-induced activation of extracellular-regulated kinase involves phosphatidylinositol 3-kinase and reactive oxygen species in human monocytes, J. Immunol. 169 (2002) 6427–6434.
[285] S.C. Manolagas, From estrogen-centric to aging and oxidative stress: a revised perspective of the pathogenesis of osteoporosis, Endocr. Rev. 31 (2010) 266–300.
[286] S.M. Bartell, H.N. Kim, E. Ambrogini, L. Han, S. Iyer, S. Serra Ucer, P. Rabinovitch, R.L. Jilka, R.S. Weinstein, H. Zhao, C.A. O'Brien, S.C. Manolagas, M. Almeida, FoxO proteins restrain osteoclastogenesis and bone resorption by attenuating H_2O_2 accumulation, Nat. Commun. 5 (2014) 3773.
[287] Y. Akasaki, A. Hasegawa, M. Saito, H. Asahara, Y. Iwamoto, M.K. Lotz, Dysregulated FOXO transcription factors in articular cartilage in aging and osteoarthritis, Osteoarthr. Cartil. 22 (2014) 162–170.
[288] Y. Akasaki, O. Alvarez-Garcia, M. Saito, B. Carames, Y. Iwamoto, M.K. Lotz, FoxO transcription factors support oxidative stress resistance in human chondrocytes, Arthritis Rheumatol. 66 (2014) 3349–3358.
[289] N. Jallali, H. Ridha, C. Thrasivoulou, C. Underwood, P.E. Butler, T. Cowen, Vulnerability to ROS-induced cell death in ageing articular cartilage: the role of antioxidant enzyme activity, Osteoarthrit. Cartil. 13 (2005) 614–622.
[290] V.M. Renault, V.A. Rafalski, A.A. Morgan, D.A. Salih, J.O. Brett, A.E. Webb, S. A. Villeda, P.U. Thekkat, C. Guillerey, N.C. Denko, T.D. Palmer, A.J. Butte, A. Brunet, FoxO3 regulates neural stem cell homeostasis, Cell Stem Cell 5 (2009) 527–539.
[291] J.H. Paik, Z. Ding, R. Narurkar, S. Ramkissoon, F. Muller, W.S. Kamoun, S. S. Chae, H. Zheng, H. Ying, J. Mahoney, D. Hiller, S. Jiang, A. Protopopov, W. H. Wong, L. Chin, K.L. Ligon, R.A. DePinho, FoxOs cooperatively regulate diverse pathways governing neural stem cell homeostasis, Cell Stem Cell 5 (2009) 540–553.
[292] C. Neri, Role and therapeutic potential of the pro-longevity factor FOXO and its regulators in neurodegenerative disease, Front. Pharmacol. 3 (2012) 15.
[293] Z. Tothova, R. Kollipara, B.J. Huntly, B.H. Lee, D.H. Castrillon, D.E. Cullen, E. P. McDowell, S. Lazo-Kallanian, I.R. Williams, C. Sears, S.A. Armstrong, E. Passegue, R.A. DePinho, D.G. Gilliland, FoxOs are critical mediators of hematopoietic stem cell resistance to physiologic oxidative stress, Cell 128 (2007) 325–339.
[294] X. Wang, Z. Wang, Y. Chen, X. Huang, Y. Hu, R. Zhang, M.S. Ho, L. Xue, FoxO mediates APP-induced AICD-dependent cell death, Cell Death Dis. 5 (2014) e1233.
[295] M. Belanger, P.J. Magistretti, The role of astroglia in neuroprotection,

Dialogues Clin. Neurosci. 11 (2009) 281–295.
[296] E. Owusu-Ansah, U. Banerjee, Reactive oxygen species prime Drosophila haematopoietic progenitors for differentiation, Nature 461 (2009) 537–541.
[297] K. Tsuchiya, M. Westerterp, A.J. Murphy, V. Subramanian, A.W. Ferrante Jr., A. R. Tall, D. Accili, Expanded granulocyte/monocyte compartment in myeloid-specific triple FoxO knockout increases oxidative stress and accelerates atherosclerosis in mice, Circ. Res. 112 (2013) 992–1003.
[298] R. Mortuza, S. Chen, B. Feng, S. Sen, S. Chakrabarti, High glucose induced alteration of SIRTs in endothelial cells causes rapid aging in a p300 and FOXO regulated pathway, PLoS One 8 (2013) e54514.
[299] S. Zhang, Y. Zhao, M. Xu, L. Yu, Y. Zhao, J. Chen, Y. Yuan, Q. Zheng, X. Niu, FoxO3a modulates hypoxia stress induced oxidative stress and apoptosis in cardiac microvascular endothelial cells, PLoS One 8 (2013) e80342.
[300] W.H. Yiu, P.A. Mead, H.S. Jun, B.C. Mansfield, J.Y. Chou, Oxidative stress mediates nephropathy in type Ia glycogen storage disease, Lab. Investig. 90 (2010) 620–629.
[301] Q. Lu, Y. Zhai, Q. Cheng, Y. Liu, X. Gao, T. Zhang, Y. Wei, F. Zhang, X. Yin, The Akt-FoxO3a-manganese superoxide dismutase pathway is involved in the regulation of oxidative stress in diabetic nephropathy, Exp. Physiol. 98 (2013) 934–945.
[302] B. Ponugoti, F. Xu, C. Zhang, C. Tian, S. Pacios, D.T. Graves, FOXO1 promotes wound healing through the up-regulation of TGF-beta1 and prevention of oxidative stress, J. Cell Biol. 203 (2013) 327–343.
[303] B. Ponugoti, G. Dong, D.T. Graves, Role of forkhead transcription factors in diabetes-induced oxidative stress, Exp. Diabetes Res. (2012) 939751.
[304] S.K. Hanks, T. Hunter, Protein kinases 6. The eukaryotic protein kinase superfamily: kinase (catalytic) domain structure and classification, FASEB J. 9 (1995) 576–596.
[305] G. Manning, D.B. Whyte, R. Martinez, T. Hunter, S. Sudarsanam, The protein kinase complement of the human genome, Science 298 (2002) 1912–1934.
[306] L.R. Pearce, D. Komander, D.R. Alessi, The nuts and bolts of AGC protein kinases, Nat. Rev. Mol. Cell. Biol. 11 (2010) 9–22.
[307] G. Rena, S. Guo, S.C. Cichy, T.G. Unterman, P. Cohen, Phosphorylation of the transcription factor forkhead family member FKHR by protein kinase B, J. Biol. Chem. 274 (1999) 17179–17183.
[308] S. Guo, G. Rena, S. Cichy, X. He, P. Cohen, T. Unterman, Phosphorylation of serine 256 by protein kinase B disrupts transactivation by FKHR and mediates effects of insulin on insulin-like growth factor-binding protein-1 promoter activity through a conserved insulin response sequence, J. Biol. Chem. 274 (1999) 17184–17192.
[309] A. Brunet, A. Bonni, M.J. Zigmond, M.Z. Lin, P. Juo, L.S. Hu, M.J. Anderson, K. C. Arden, J. Blenis, M.E. Greenberg, Akt promotes cell survival by phosphorylating and inhibiting a Forkhead transcription factor, Cell 96 (1999) 857–868.
[310] G.J. Kops, N.D. de Ruiter, A.M. De Vries-Smits, D.R. Powell, J.L. Bos, B. M. Burgering, Direct control of the Forkhead transcription factor AFX by protein kinase B, Nature 398 (1999) 630–634.
[311] H. Takaishi, H. Konishi, H. Matsuzaki, Y. Ono, Y. Shirai, N. Saito, T. Kitamura, W. Ogawa, M. Kasuga, U. Kikkawa, Y. Nishizuka, Regulation of nuclear translocation of forkhead transcription factor AFX by protein kinase B, Proc. Natl. Acad. Sci. U.S.A. 96 (1999) 11836–11841.
[312] F.M. Jacobs, L.P. van der Heide, P.J. Wijchers, J.P. Burbach, M.F. Hoekman, M. P. Smidt, FoxO6, a novel member of the FoxO class of transcription factors with distinct shuttling dynamics, J. Biol. Chem. 278 (2003) 35959–35967.
[313] L.P. van der Heide, F.M. Jacobs, J.P. Burbach, M.F. Hoekman, M.P. Smidt, FoxO6 transcriptional activity is regulated by Thr26 and Ser184, independent of nucleo-cytoplasmic shuttling, Biochem. J. 391 (2005) 623–629.
[314] A. Brunet, J. Park, H. Tran, L.S. Hu, B.A. Hemmings, M.E. Greenberg, Protein kinase SGK mediates survival signals by phosphorylating the forkhead transcription factor FKHRL1 (FOXO3a), Mol. Cell. Biol. 21 (2001) 952–965.
[315] J.W. Lee, H. Chen, P. Pullikotil, M.J. Quon, Protein kinase A-alpha directly phosphorylates FoxO1 in vascular endothelial cells to regulate expression of vascular cellular adhesion molecule-1 mRNA, J. Biol. Chem. 286 (2011) 6423–6432.
[316] N. Kannan, A.F. Neuwald, Evolutionary constraints associated with functional specificity of the CMGC protein kinases MAPK, CDK, GSK, SRPK, DYRK, and CK2alpha, Protein Sci. 13 (2004) 2059–2077.
[317] S. Clavel, S. Siffroi-Fernandez, A.S. Coldefy, K. Boulukos, D.F. Pisani, B. Derijard, Regulation of the intracellular localization of Foxo3a by stress-activated protein kinase signaling pathways in skeletal muscle cells, Mol. Cell. Biol. 30 (2010) 470–480.
[318] Z. Yuan, E.B. Becker, P. Merlo, T. Yamada, S. DiBacco, Y. Konishi, E.M. Schaefer, A. Bonni, Activation of FOXO1 by Cdk1 in cycling cells and postmitotic neurons, Science 319 (2008) 1665–1668.
[319] G. Rena, Y.L. Woods, A.R. Prescott, M. Peggie, T.G. Unterman, M.R. Williams, P. Cohen, Two novel phosphorylation sites on FKHR that are critical for its nuclear exclusion, EMBO J. 21 (2002) 2263–2271.
[320] S. Kim, Y. Kim, J. Lee, J. Chung, Regulation of FOXO1 by TAK1-Nemo-like kinase pathway, J. Biol. Chem. 285 (2010) 8122–8129.
[321] E. Vielhaber, D.M. Virshup, Casein kinase I: from obscurity to center stage, IUBMB Life 51 (2001) 73–78.
[322] K.T. Chow, G.A. Timblin, S.M. McWhirter, M.S. Schlissel, MK5 activates Rag transcription via Foxo1 in developing B cells, J. Exp. Med. 210 (2013) 1621–1634.
[323] T.R. Kress, I.G. Cannell, A.B. Brenkman, B. Samans, M. Gaestel, P. Roepman, B. M. Burgering, M. Bushell, A. Rosenwald, M. Eilers, The MK5/PRAK kinase and Myc form a negative feedback loop that is disrupted during colorectal tumorigenesis, Mol. Cell 41 (2011) 445–457.
[324] M.K. Lehtinen, Z. Yuan, P.R. Boag, Y. Yang, J. Villen, E.B. Becker, S. DiBacco, N. de la Iglesia, S. Gygi, T.K. Blackwell, A. Bonni, A conserved MST-FOXO signaling pathway mediates oxidative-stress responses and extends life span, Cell 125 (2006) 987–1001.
[325] M.C. Hu, D.F. Lee, W. Xia, L.S. Golfman, F. Ou-Yang, J.Y. Yang, Y. Zou, S. Bao, N. Hanada, H. Saso, R. Kobayashi, M.C. Hung, IkappaB kinase promotes tumorigenesis through inhibition of forkhead FOXO3a, Cell 117 (2004) 225–237.
[326] C.W. So, M.L. Cleary, MLL-AFX requires the transcriptional effector domains of AFX to transform myeloid progenitors and transdominantly interfere with forkhead protein function, Mol. Cell. Biol. 22 (2002) 6542–6552.
[327] F. Wang, C.B. Marshall, K. Yamamoto, G.Y. Li, M.J. Plevin, H. You, T.W. Mak, M. Ikura, Biochemical and structural characterization of an intramolecular interaction in FOXO3a and its binding with p53, J. Mol. Biol. 384 (2008) 590–603.
[328] E. Boura, J. Silhan, P. Herman, J. Vecer, M. Sulc, J. Teisinger, V. Obsilova, T. Obsil, Both the N-terminal loop and wing W2 of the forkhead domain of transcription factor Foxo4 are important for DNA binding, J. Biol. Chem. 282 (2007) 8265–8275.
[329] V. Obsilova, J. Vecer, P. Herman, A. Pabianova, M. Sulc, J. Teisinger, E. Boura, T. Obsil, 14-3-3 Protein interacts with nuclear localization sequence of forkhead transcription factor FoxO4, Biochemistry 44 (2005) 11608–11617.
[330] W.H. Biggs 3rd, J. Meisenhelder, T. Hunter, W.K. Cavenee, K.C. Arden, Protein kinase B/Akt-mediated phosphorylation promotes nuclear exclusion of the winged helix transcription factor FKHR1, Proc. Natl. Acad. Sci. U.S.A. 96 (1999) 7421–7426.
[331] A. Brunet, F. Kanai, J. Stehn, J. Xu, D. Sarbassova, J.V. Frangioni, S.N. Dalal, J. A. DeCaprio, M.E. Greenberg, M.B. Yaffe, 14-3-3 Transits to the nucleus and participates in dynamic nucleocytoplasmic transport, J. Cell Biol. 156 (2002) 817–828.
[332] A.M. Brownawell, G.J. Kops, I.G. Macara, B.M. Burgering, Inhibition of nuclear import by protein kinase B (Akt) regulates the subcellular distribution and activity of the forkhead transcription factor AFX, Mol. Cell. Biol. 21 (2001) 3534–3546.
[333] K.D. Pruitt, G.R. Brown, S.M. Hiatt, F. Thibaud-Nissen, A. Astashyn, O. Ermolaeva, C.M. Farrell, J. Hart, M.J. Landrum, K.M. McGarvey, M. R. Murphy, N.A. O'Leary, S. Pujar, B. Rajput, S.H. Rangwala, L.D. Riddick, A. Shkeda, H. Sun, P. Tamez, R.E. Tully, C. Wallin, D. Webb, J. Weber, W. Wu, M. DiCuccio, P. Kitts, D.R. Maglott, T.D. Murphy, J.M. Ostell, RefSeq: an update on mammalian reference sequences, Nucleic Acids Res. 42 (2014) D756–D763.

Redox Biology 12 (2017) 1020–1025

Contents lists available at ScienceDirect

Redox Biology

journal homepage: www.elsevier.com/locate/redox

ROS homeostasis, a key determinant in liver ischemic-preconditioning

Ignacio Prieto, María Monsalve*

Instituto de Investigaciones Biomédicas "Alberto Sols" (CSIC-UAM), Arturo Duperier 4, 28029 Madrid, Spain

ARTICLE INFO

Keywords:
ROS
Liver
Ischemia-reperfusion
Ischemic preconditioning
Steatosis

ABSTRACT

Reactive Oxygen Species (ROS) are key mediators of ischemia-reperfusion injury but also required for the induction of the stress response that limits tissue injury and underlies the protection provided by ischemic-preconditioning protocols. Liver steatosis is an important risk factor for liver transplant failure. Liver steatosis is associated with mitochondrial dysfunction and excessive mitochondrial ROS production. Studies aiming at decreasing the sensibility of the steatotic liver to ischemia-reperfusion injury using pre-conditioning protocols, have shown that the steatotic liver has a reduced capacity to respond to these protocols. Recent studies indicate that these effects are related to a reduced capacity of the steatotic liver to respond to elevated ROS levels following reperfusion by inducing a compensatory response. This failure to respond to ROS is associated with reduced levels of antioxidants, mitochondrial damage, hepatocyte cell death, activation of the immune system and induction of pro-fibrotic mediators.

1. Liver transplants

The prevalence of the steatotic liver is rapidly increasing worldwide reaching almost 30% of the total population in some countries [1,2], with incidences rapidly rising in the pediatric population [3]. Hepatic steatosis is largely considered the hepatic manifestation of the metabolic syndrome [4], although, in fact, recent studies have shown that it actually precedes the development of metabolic syndrome [5] and its prevalence is expected to rise along with the number of overweight and obese people [6]. Traditionally considered a benign condition, a plethora of studies have more than clearly demonstrated that the steatotic liver is more sensitive than the lean liver to a vast array of pathological insults, and the most prevalent and significant risk factor for the development of NAFLD [7–9].

The particular sensitivity of the steatotic liver has been dramatically attested in the transplant field [10]. Liver and kidney are the most commonly transplanted organs. Liver transplantation is the only treatment option for end-stage liver disease, acute hepatic failure, hepatocellular carcinoma (HCC), hilar cholangiocarcinoma and several other disorders. While the number of patients requiring a liver transplant increases, the number of livers donated following cardiac death (DCD) or brain death (DBD) donated in Europe has not increased at the same pace. Furthermore, the number of livers coming from healthy young people, deceased in fatal car accidents has decreased. Organ shortage has been compensated in Asian countries with increasing numbers of living-donor liver transplantation (LDLT). In western countries the limitation has fostered the need to extend donor's criteria, in particular the degree of steatosis considered acceptable has been increased [11].

Steatosis is an important risk factor in liver surgery due to the special sensitivity of the steatotic liver to ischemia reperfusion injury (IRI), [12], which impairs liver regeneration and is a major cause of liver damage [13]. The exact mechanism responsible for the increased susceptibility is not fully understood, but clearly involves mitochondrial dysfunction. The steatotic liver produces higher levels of mitochondrial ROS [14], both baseline and in response to ischemia reperfusion (IR), reduced levels of antioxidants [15] and has a reduced capacity to recover normal ATP levels following reperfusion, leading to enhanced cell death [16]. A recent study further showed that the steatotic liver has reduced electron transport chain (ETC) complex I (CI) activity both baseline and in response to IR, and more importantly, CI activity did not recover even following long reperfusion times [13]. The CI complex is a major site of generation of superoxide in the mitochondria [17].

Despite improved allograft preservation techniques many livers continue to go unused and many studies have attempted to develop protocols that improve the safety of steatotic liver transplants with limited success. A particular focus of attention has been the ischemic preconditioning protocol (IPC) first described in the heart [18]. The liver is conditioned with a brief ischemic period followed by reperfusion, prior to sustained ischemia. IPC boost the resistance of the liver to a longer ischemic insult. It has been used and tested in many experimental and some clinical contexts but so far it has not shown general clinical benefit and its use is not clinically implemented [19]. The molecular pathways involved in IPC have been extensively

* Corresponding author. Mailing address: Instituto de Investigaciones Biomédicas "Alberto Sols" (CSIC-UAM), Arturo Duperier 4, Room 1.3.2, 28029 Madrid, Spain.
E-mail address: mpmonsalve@iib.uam.es (M. Monsalve).

http://dx.doi.org/10.1016/j.redox.2017.04.036
Received 31 March 2017; Received in revised form 26 April 2017; Accepted 29 April 2017
Available online 04 May 2017

characterized. IPC suppresses neutrophil infiltration, decreases the production of oxygen free radicals and increases antioxidant activity in the hepatocyte, prevents the activation of the apoptotic cascade and the occlusion of microvessels [20]. Importantly, it has been suggested that all these effects are mediated through the protection of mitochondrial function [21].

2. Ischemic-preconditioning

Among the many possible strategies to rescue steatotic livers before transplantation in clinical and experimental studies [22], important efforts have focused on the applicability of IPC protocols to the steatotic liver that would allow their use in transplants [23]. However, despite some limited improvement in some liver damage biomarkers (ie ATL), the lack of significant positive effect in clinical outcome have so far prevented its translation to the clinical setting, possibly related to the failure to recover the mitochondrial CI activity noted for the steatotic liver following IR [13] and the associated loss in ROS homeostasis.

Evidence for oxidative stress might seem an almost irrelevant or non-specific finding, since there is a plethora of pathological conditions associated with oxidative stress, in fact all that involve inflammation, that the correlation may seem of little clinical relevance. However, accumulated data indicate otherwise. Increased ROS levels following the reperfusion phase have been shown to be the main triggering factor responsible for the induction of hepatocyte cell death following IR, and are therefore, the key mediators of acute liver failure following liver transplant [24,25]. Furthermore, sustained low-grade oxidative stress has been proposed to promote pathological progression to liver fibrosis and could be associated to an increased risk of mid-term graft failure [26].

During the ischemic phase, ATP depletion is compensated through the increase in the anaerobic catabolism of glucose, producing an increase in lactate levels and a drop in the intracellular pH. This drop activates the Na^+/H^+ anti-porter, and the ensuing increase in intracellular Na^+ levels cannot be compensated due to the limiting ATP concentrations, leading to an increase in the intracellular levels of Ca^{2+}, and facilitates the activation of pro-apoptotic pathways. Once perfusion is restored the sudden increase in O_2 levels produces a mitochondrial burst of ROS, that together with the elevated Ca^{2+} and the low pH can induce the opening of the MTP and result in cell apoptosis [27].

Following reperfusion, ROS induce inflammation in two phases, an initial or acute phase, and a late or sub-acute phase [28]. The acute phase corresponds to the first 6 h following reperfusion, in this stage mitochondrial ROS seem essential for the activation of the Kuppfer cells, that will later mediate the release of proinflammatory cytokines [29].

The sub-acute phase is the inflammatory stage, characterized by a massive infiltration of neutrophils, release of cytotoxic and proinflammatory mediators, and activation of the mesenchymal stem cells, that can contribute to the development offibrosis. During this stage, the main source of ROS are the NOX enzymes and work as amplifiers of the inflammatory reaction [26].

At the molecular level, elevated ROS levels boost the inflammatory cascade, at least partially through the direct activation of the transcription factor NF-κB [30], although there are other indirect mechanisms through which ROS can also promote a pro-inflammatory status increasing the levels/activity of TGF-β, TNFα and IL-1ß among others [31].

3. ROS, preconditionong mediators

However, ROS do not only have deleterious effects, ROS dependent signaling is a crucial mediator of ischemic preconditioning. Therefore, increased ROS production following IR is a necessary step during liver preconditioning [32]. ROS trigger many cellular responses that could potentially contribute to ischemic preconditioning. In particular, ROS facilitates the activation of AMPK and stabilization of the transcription factor HIF-1α, resulting in a shift in the cellular metabolism, that makes the liver more glycolytic and less dependent on O_2. This compensatory effect facilitates survival immediately following reperfusion, since during reperfusion not all the tissue recovers immediately a normal oxygen tension and capillaries tend to collapse [33]. Recovery of normal tissue perfusion depends on the formation of new microvessels, a process that can take about two weeks to be successfully completed and that largely depends on the HIF-1α dependent activation of the angiogenesis mediator VEGF-A [34,35].

The picture that emerges is that ROS play a double edged role in IR, on one hand promotes apoptotic cell death and induces inflammatory mediators, on the other hand, facilitates cell survival in hypoxic conditions and induces antioxidant defenses.

ROS dependent IRI is to a large extent dependent on the tissue levels of antioxidants. In fact, reduced levels of the antioxidant proteins MnSOD, catalase and GPx have been associated with larger lesions while forced increase of antioxidants has the opposite effect [36,37]. Conversely, ROS exposure can result in the induction/activation of antioxidant systems through the activation of the transcription factors nuclear factor erythroid 2-related factor 2 (Nrf2) [38,39] and the transcriptional coactivator PGC-1α have been shown to be activated/induced in response to oxidative stress and drive the increased expression of antioxidant systems in hepatocytes [40–42].

Nrf2 is considered a master regulator of cellular redox homeostasis [39]. Under normal conditions Keap1 binds to Nrf2 in the cytoplasm, and promotes its degradation by the proteasome. Exposure to ROS leads to Keap1, Nrf2 stabilization and nuclear translocation where it binds to the anti-oxidant response element (ARE) to induce the expression a set of antioxidant genes [43]. Is has been proposed that following IR induction of Nrf2 plays a key role in the control of the inflammatory response, reducing apoptotic cell death [44].

PGC-1α is a master regulator of mitochondrial biogenesis and activity [45]. Oxidative catabolism is associated with increased mitochondrial production of superoxide. To prevent oxidative stress in conditions of high mitochondrial oxidative activity PGC-1α also controls the expression of several antioxidant proteins [41]. PGC-1α is highly expressed in the liver where it controls both oxidative catabolism and gluconeogenesis in response to reduced nutrient availability [46]. PGC-1α levels are highly sensitive to the nutritional status being induced by starvation and inhibited by feeding [47]. Importantly, in the steatotic liver PGC-1α levels are reduced [48] and this downregulation results in a reduction of antioxidant systems in the liver [49]. This fact, together with the observation of a protective role of PGC-1α in IR tolerance in the liver [49] and several other tissues (ie heart, kidney, the central nervous system (CNS)) [50–52] suggest that PGC-1α regulation of antioxidant systems can be relevant in the enhanced sensitivity of the steatotic liver to IR. This concept is supported by the observation that in terms of liver damage following IR, PGC-1α KO mice behave similarly to WT mice with steatotic livers [49].

4. ROS homeostasis

In order to elucidate the reason why the steatotic liver, that produces more ROS than the normal liver, cannot precondition, some studies have focused on the evaluation of the activity of antioxidant enzymes and found conflicting results, with some enzymes being overexpressed in the steatotic liver and some others with reduced levels in steatosis [15]. Importantly, several studies have shown the positive effects of antioxidants against IR injury [53] suggesting that the steatotic liver has lost its capacity to modulate the production of ROS and hence of using ROS as signaling mediators. The study by Sanchez Ramos et al. [49] showed that while the normal liver responds to IR inducing PGC-1α and antioxidant gene expression, and this induction is further enhanced by preconditioning, the steatotic liver shows a

significant reduction in its capacity to induce antioxidant gene expression in response to IR and IPC protocols. Furthermore, the study supports the notion that this induction depends on PGC-1α, since PGC-1α KO mice also fail to induce PGC-1α and antioxidant gene expression in response to IR.

The work by C. Sanchez et al. has demonstrated that the down-regulation of the transcriptional co-activator PGC-1α in the steatotic liver limits its capacity to control antioxidant enzyme levels and to modulate them in response to IR. In the healthy liver, in response to IR, PGC-1α levels are induced and this induction results in the augmentation of the cellular antioxidant defenses. In steatosis, not only PGC-1α levels are reduced but the steatotic liver fails to induce PGC-1α and its target antioxidant genes in response to IR, resulting in enhanced liver damage. Aiming to understand why PGC-1α levels are regulated in response to IR, the same study analyzed why the steatotic liver fail to induce them in response to IR.

5. ROS control following hypoxia

It is not at all clear how ROS work in preconditioning to protect the mitochondria from depolarization following IR and how do they work to attenuate the inflammatory response. Recent identification of NDUFA4L2 (NADH dehydrogenase [ubiquinone] 1 alpha subcomplex, 4-like 2) as an hypoxia sensitive inhibitor of complex I has served to demonstrate the relevance of a pathway that controls mitochondrial ROS production in response to ischemia [54]. Taking into account that NDUFA4L2 is a HIF-1α induced protein, HIF-1α stabilization is ROS sensitive [55] and HIF-1α is induced following IR in the liver [56], it is tempting to speculate that its induction must also be ROS sensitive, what would provide a mechanism that could explain ROS dependent mitochondrial protection. An important open question is what happens in the fatty liver, where ROS are produced but do not seem to exert their protective effects while they do exert their damaging effects. Activation of HIF-1α does not seem to be impaired in the steatotic liver, in fact HIF-1α activity is higher in the fatty liver than in the normal liver [57,58].

PGC-1α levels are also regulated by oxygen tension [59]. This regulation could seem a paradoxical effect, since oxidative metabolism requires oxygen and limiting oxygen availability may result in mitochondrial dysfunction. The physiological relevance of this regulation seems related to the PGC-1α dependent induction of VEGF-A levels that promote angiogenesis to increase tissue perfusion and allow oxidative metabolism [60]. However, C. Sanchez and col. [49] showed that severe hypoxic conditions actually down-regulate PGC-1α levels at least in cell culture conditions while restoration of normal oxygen tension results in the induction of PGC-1α levels, indicating that induction of PGC-1α following IR in vivo, is likely to occur during the reperfusion phase.

Taking into account that reperfusion is associated with a burst in mitochondrial ROS, and that is has been previously demonstrated that ROS induce PGC-1α expression, is likely that ROS are key mediators in PGC-1α induction following IR, and the lack of an adaptive response in the steatotic liver also relate to the inability in this context of ROS to induce PGC-1α (Fig. 1).

The association of liver steatosis with oxidative stress results in a low-grade chronic inflammatory profile, that is generally associated with poor inflammatory resolution profiles, with a limited M2 macrophage activation [61,62]. In contrast, acute exposure to ROS promotes concomitant activation of M1 and M2 macrophages and expression of resolution cytokines [63,64]. Although the mechanisms are only partially elucidated, these effects could be also relevant in ROS dependent preconditioning effects and its failure in the steatotic liver. Importantly, M2 activation has been shown to be strongly dependent on the activation of oxidative phosphorylation and mitochondrial function [65], feasibly via PGC-1α.

6. Translation into the clinical setting

The challenge now is to translate this knowledge into clinical applications. There are some clinical studies in human patients focused in the role of oxidative stress in IRI and postoperative complications in patients after an orthotopic liver transplant (OLT). Since we are not able to measure the levels of ROS in humans due to their short lifetime, others strategies are followed in these clinical studies, as measure oxidative markers, such as lipid peroxidation; the levels of glutathione or enzymatic antioxidants, such as superoxide dismutase (SOD), catalase or peroxiredoxins in blood samples or liver biopsies [66].

Recent clinical researches show that also in humans during ischemia the amounts of ROS increase resulting in oxidative stress imbalance as evidenced by an increase in oxidative stress markers and antioxidant response [67–69] and this oxidative imbalance persist in late post-operative stage (1 year after liver transplant) [70]. Additionally, as noted above, steatotic livers have poor prognosis in liver transplant that is associated to evidence of mitochondrial dysfunction and enhanced production of ROS [71].

The gene expression profile of transplanted liver versus normal liver shows an induction of stress response genes in transplanted livers, as well as an increase of liver metabolism and inflammatory response. When transplanted livers subjects were analyzed for the correlation of transaminase levels, as hepatic injury marker and the expression of oxidative stress genes, it was found that oxidative stress response significantly correlated with liver injury [72] most probably due to the generation of higher amounts of ROS in these livers. Related to this study, it has also been described that the levels of lipid peroxidation increase at 1 h post-operation and are maintained over basal levels up to 5 days following liver transplant. Lipid peroxidation in turn correlates with the upregulation of enzymatic antioxidants such as superoxide dismutase (SOD), catalase, glutathione peroxidase (GPx) and glutathione reductase (GR) [69]. Furthermore, the level of lipid peroxidation also correlates with pre-operative hepatic injury markers such as bilirubin, AST, ALT, model of end-stage liver disease score (MELD score), International Normalized Ratio (INR) and with expression of pro-inflammatory cytokines [73].

From this perspective, several strategies have been devised to decrease hepatic transplant failure due to oxidative stress trying to avoid the generation of ROS during ischemia and reperfusion. These strategies include ischemic preconditioning (IPC), antioxidant therapy and graft preservation in external perfusion machines. Even though the protective effect of IPC in IRI has been amply demonstrated in pre-clinical studies, clinical studies have shown conflicting results in normal and steatotic livers [23,74]. Some studies support the protective effect of IPC in human liver ischemia [75–77] even in steatotic livers, while other studies indicate that IPC do not have clinical relevance in liver transplantation [78,79] suggesting that new approaches are needed to facilitate the use of IPC protocols in the clinical setting.

Early evidence on the role of ROS in IR injury led to the evaluation of antioxidant administration as a possible therapeutical approach. Glutathione is the major antioxidant system and some precursors of glutathione have been evaluated as IRI treatment, such as N-Acetylcysteine (NAC) or L-Alanyl-Glutamine with conflicting results. NAC was described as a possible antioxidant treatment against IRI [80] but failed when is administrated during graft cold preservation [81,82], moreover, other studies do not support the protective role of NAC in IRI [83]. In a meta analysis of several clinical studies on NAC treatment the authors concluded that NAC administration improved transaminase levels but without patient or graft survival correlation [84]. L-Alanyl-Glutamine has promising results decreasing lipid peroxidation after liver transplantation [85] but more clinical results are required. Another antioxidant tested for IRI is melatonin, an antioxidant produced in the pineal gland that showed a protective effect against IRI, supraphysiological doses of melatonin improve the general outcome after liver resection [86,87]. Finally, there is a study on Propofol, an

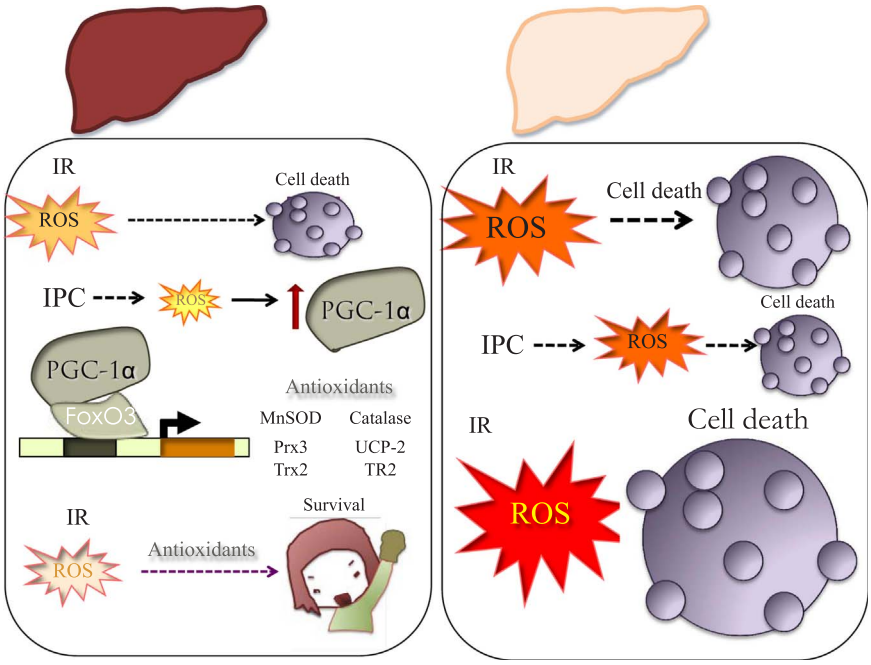

Fig. 1. *Response to IR in normal vs steatotic liver.* Induction of antioxidant systems in the normal liver facilitates survival in response to preconditioning protocols. Reduced PGC-1α activity in the steatotic liver limits antioxidant induction and results in extensive hepatocyte cell death. IR, Ischemia-Reperfusion; IPC, Ischemic Preconditioning; and ROS, Reactive Oxygen Species.

anesthetic compound with antioxidant features, in IRI of liver transplant recipients. The authors showed an improvement on lipids peroxidation in the recipients anesthetized with Propofol [88]. Probably, antioxidant therapy could improve their efficacy with a synergistic approach, using antioxidants both in recipients and grafts without forgetting the important role of ROS in cell signaling.

Graft preservation during ischemia is a critical step in liver transplant, since high amounts of ROS are produced at this stage [89]. Storage solutions are a good way to treat ROS production during graft ischemia. A review of different preservation solutions correlates poor prognosis with those livers preserved in solutions with less antioxidants [90]. In other studies, the authors attribute the protection effect of Institut Georges Lopez preservation solution (IGL-1) on their antioxidant effect, decreasing ROS levels and mitochondrial damage [91]. In addition, storage solution supplemented with a recombinant Manganese Superoxide Dismutase (rMnSOD) showed efficiency reducing O_2^- levels in human liver biopsies from donors of hepatic transplantation [92].

In the last decade a novel technology, a hypothermic preservation machine, was developed and implemented to avoid the deleterious effects of ischemia in organs transplantation. First studied in kidney grafts, some liver studies with hypothermic machine preservation (HMP) were realized. HMP showed an improvement of graft function after transplantation, with less hepatic injury markers [93] and later were described the increase of several antioxidants markers, as upregulation of SOD or HIFα [94]. Regarding the temperature storage in the preservation machine, an improvement of mitochondrial function of excluded livers for transplantation was described [95].

7. Conclusions

In sum, oxidative stress has a harmful effect in hepatic IRI in humans as seen in animal models. Limiting ROS production with different approaches or with a synergistic approach may improve the graft function and recipient survival. However, antioxidant treatments aiming at reducing liver injury have not reached the clinical stage. This failure could be related to the fact that ROS are signaling mediators, whose absence can be as detrimental as their excess. In fact, antioxidant treatment prevents ischemic preconditioning, which can also result from the "dual" nature of many antioxidants. They are in fact molecules that can also work as pro-oxidants depending on the redox status of the environment, being strongly modulated by the levels of reducing equivalents, oxygen, pH and they can also propagate pro-oxidant effects. The obvious alternative, the induction of PGC-1α levels also has strong caveats, as demonstrated by studies where over-expression of PGC-1α resulted in the loss of metabolic plasticity. For example, the tolerance of a tissue to hypoxia depends on its ability to sustain a glycolytic non-oxidative metabolism, and forced mitochondrial activity would result in mitochondrial induced cell death.

Author disclosure statement

No competing financial interests exist.

Acknowledgements

This work was supported by grants from the Spanish "Ministerio de Economía y Competitividad" (Grant numbers SAF2015-63904-R and SAF2015-71521-REDC).

References

[1] S. Bellentani, G. Saccoccio, F. Masutti, L.S. Croce, G. Brandi, F. Sasso, G. Cristanini, C. Tiribelli, Prevalence of and risk factors for hepatic steatosis in Northern Italy, Ann. Intern. Med. 132 (2000) 112–117.
[2] J.D. Browning, L.S. Szczepaniak, R. Dobbins, P. Nuremberg, J.D. Horton, J.C. Cohen, S.M. Grundy, H.H. Hobbs, Prevalence of hepatic steatosis in an urban population in the United States: impact of ethnicity, Hepatology 40 (2004) 1387–1395.
[3] J.M. Navarro-Jarabo, E. Ubina-Aznar, L. Tapia-Ceballos, C. Ortiz-Cuevas, M.A. Perez-Aisa, F. Rivas-Ruiz, R.J. Andrade, E. Perea-Milla, Hepatic steatosis and severity-related factors in obese children, J. Gastroenterol. Hepatol. 28 (2013) 1532–1538.
[4] P. Angulo, Nonalcoholic fatty liver disease, N. Engl. J. Med. 346 (2002) 1221–1231.
[5] A. Lonardo, S. Ballestri, G. Marchesini, P. Angulo, P. Loria, Nonalcoholic fatty liver disease: a precursor of the metabolic syndrome, Dig. Liver Dis. 47 (2015) 181–190.
[6] S. Desroches, B. Lamarche, The evolving definitions and increasing prevalence of the metabolic syndrome, Appl. Physiol. Nutr. Metab. 32 (2007) 23–32.
[7] S.H. Koo, Nonalcoholic fatty liver disease: molecular mechanisms for the hepatic steatosis, Clin. Mol. Hepatol. 19 (2013) 210–215.

[8] M. Persico, A. Iolascon, Steatosis as a co-factor in chronic liver diseases, World J. Gastroenterol. 16 (2010) 1171–1176.
[9] E.E. Powell, J.R. Jonsson, A.D. Clouston, Steatosis: co-factor in other liver diseases, Hepatology 42 (2005) 5–13.
[10] A. Nocito, A.M. El-Badry, P.A. Clavien, When is steatosis too much for transplantation? J. Hepatol. 45 (2006) 494–499.
[11] C.C. Jadlowiec, T. Taner, Liver transplantation: current status and challenges, World J. Gastroenterol. 22 (2016) 4438–4445.
[12] R. Vetelainen, A. van Vliet, D.J. Gouma, T.M. van Gulik, Steatosis as a risk factor in liver surgery, Ann. Surg. 245 (2007) 20–30.
[13] M.J. Chu, R. Premkumar, A.J. Hickey, Y. Jiang, B. Delahunt, A.R. Phillips, A.S. Bartlett, Steatotic livers are susceptible to normothermic ischemia-reperfusion injury from mitochondrial complex-I dysfunction, World J. Gastroenterol. 22 (2016) 4673–4684.
[14] M. Selzner, H.A. Rudiger, D. Sindram, J. Madden, P.A. Clavien, Mechanisms of ischemic injury are different in the steatotic and normal rat liver, Hepatology 32 (2000) 1280–1288.
[15] W. Liu, S.S. Baker, R.D. Baker, L. Zhu, Antioxidant mechanisms in nonalcoholic fatty liver disease, Curr. Drug Targets 16 (2015) 1301–1314.
[16] P. Caraceni, M. Domenicali, G. Vendemiale, I. Grattagliano, A. Pertosa, B. Nardo, A.M. Morselli-Labate, F. Trevisani, G. Palasciano, E. Altomare, M. Bernardi, The reduced tolerance of rat fatty liver to ischemia reperfusion is associated with mitochondrial oxidative injury, J. Surg. Res. 124 (2005) 160–168.
[17] V.G. Grivennikova, A.D. Vinogradov, Generation of superoxide by the mitochondrial complex I, Biochim. Biophys. Acta 1757 (2006) 553–561.
[18] C.E. Murry, R.B. Jennings, K.A. Reimer, Preconditioning with ischemia: a delay of lethal cell injury in ischemic myocardium, Circulation 74 (1986) 1124–1136.
[19] K.S. Gurusamy, H.D. Gonzalez, B.R. Davidson, Current protective strategies in liver surgery, World J. Gastroenterol. 16 (2010) 6098–6103.
[20] G. Datta, B.J. Fuller, B.R. Davidson, Molecular mechanisms of liver ischemia reperfusion injury: insights from transgenic knockout models, World J. Gastroenterol. 19 (2013) 1683–1698.
[21] A.P. Rolo, J.S. Teodoro, C. Peralta, J. Rosello-Catafau, C.M. Palmeira, Prevention of I/R injury in fatty livers by ischemic preconditioning is associated with increased mitochondrial tolerance: the key role of ATPsynthase and mitochondrial permeability transition, Transpl. Int. 22 (2009) 1081–1090.
[22] Q. Liu, M.L. Izamis, H. Xu, T. Berendsen, M. Yarmush, K. Uygun, Strategies to rescue steatotic livers before transplantation in clinical and experimental studies, World J. Gastroenterol. 19 (2013) 4638–4650.
[23] M.J. Chu, R. Vather, A.J. Hickey, A.R. Phillips, A.S. Bartlett, Impact of ischaemic preconditioning on experimental steatotic livers following hepatic ischaemia-reperfusion injury: a systematic review, HPB 17 (2015) 1–10.
[24] M.J. Reiniers, R.F. van Golen, T.M. van Gulik, M. Heger, Reactive oxygen and nitrogen species in steatotic hepatocytes: a molecular perspective on the pathophysiology of ischemia-reperfusion injury in the fatty liver, Antioxid. Redox Signal 21 (2014) 1119–1142.
[25] K. Sun, Z.S. Liu, Q. Sun, Role of mitochondria in cell apoptosis during hepatic ischemia-reperfusion injury and protective effect of ischemic postconditioning, World J. Gastroenterol. 10 (2004) 1934–1938.
[26] K. Richter, T. Kietzmann, Reactive oxygen species and fibrosis: further evidence of a significant liaison, Cell Tissue Res. 365 (2016) 591–605.
[27] A.J. Vardanian, R.W. Busuttil, J.W. Kupiec-Weglinski, Molecular mediators of liver ischemia and reperfusion injury: a brief review, Mol. Med. 14 (2008) 337–345.
[28] M. Elias-Miro, M.B. Jimenez-Castro, J. Rodes, C. Peralta, Current knowledge on oxidative stress in hepatic ischemia/reperfusion, Free Radic. Res. 47 (2013) 555–568.
[29] H. Jaeschke, Reactive oxygen and mechanisms of inflammatory liver injury: present concepts, J. Gastroenterol. Hepatol. 26 (Suppl 1) (2011) 173–179.
[30] T.C. Nichols, NF-kappaB and reperfusion injury, Drug News Perspect. 17 (2004) 99–104.
[31] P. Mukhopadhyay, B. Horvath, Z. Zsengeller, S. Batkai, Z. Cao, M. Kechrid, E. Holovac, K. Erdelyi, G. Tanchian, L. Liaudet, I.E. Stillman, J. Joseph, B. Kalyanaraman, P. Pacher, Mitochondrial reactive oxygen species generation triggers inflammatory response and tissue injury associated with hepatic ischemia-reperfusion: therapeutic potential of mitochondrially targeted antioxidants, Free Radic. Biol. Med. 53 (2012) 1123–1138.
[32] E. Alchera, C. Dal Ponte, C. Imarisio, E. Albano, R. Carini, Molecular mechanisms of liver preconditioning, World J. Gastroenterol. 16 (2010) 6058–6067.
[33] T. Miyashita, S. Nakanuma, A.K. Ahmed, I. Makino, H. Hayashi, K. Oyama, H. Nakagawara, H. Tajima, H. Takamura, I. Ninomiya, S. Fushida, J.W. Harmon, T. Ohta, Ischemia reperfusion-facilitated sinusoidal endothelial cell injury in liver transplantation and the resulting impact of extravasated platelet aggregation, Eur. Surg. 48 (2016) 92–98.
[34] M. Bockhorn, M. Goralski, D. Prokofiev, P. Dammann, P. Grunewald, M. Trippler, A. Biglarnia, M. Kamler, E.M. Niehues, A. Frilling, C.E. Broelsch, J.F. Schlaak, VEGF is important for early liver regeneration after partial hepatectomy, J. Surg. Res. 138 (2007) 291–299.
[35] A.R. Knudsen, A.S. Kannerup, H. Gronbaek, K.J. Andersen, P. Funch-Jensen, J. Frystyk, A. Flyvbjerg, F.V. Mortensen, Effects of ischemic pre- and postconditioning on HIF-1alpha, VEGF and TGF-beta expression after warm ischemia and reperfusion in the rat liver, Comp. Hepatol. 10 (2011) 3.
[36] J. Tanaka, P.S. Malchesky, S. Omokawa, J.B. Goldcamp, H. Harasaki, D.P. Vogt, T.A. Broughan, Y. Nose, Effects of prostaglandin I2, superoxide dismutase, and catalase on ischemia-reperfusion injury in liver transplantation, ASAIO Trans. 36 (1990) M600–603.
[37] F. Amersi, R. Buelow, H. Kato, B. Ke, A.J. Coito, X.D. Shen, D. Zhao, J. Zaky, J. Melinek, C.R. Lassman, J.K. Kolls, J. Alam, T. Ritter, H.D. Volk, D.G. Farmer, R.M. Ghobrial, R.W. Busuttil, J.W. Kupiec-Weglinski, Upregulation of heme oxygenase-1 protects genetically fat Zucker rat livers from ischemia/reperfusion injury, J. Clin. Investig. 104 (1999) 1631–1639.
[38] K. Kudoh, H. Uchinami, M. Yoshioka, E. Seki, Y. Yamamoto, Nrf2 activation protects the liver from ischemia/reperfusion injury in mice, Ann. Surg. 260 (2014) 118–127.
[39] B. Ke, X.D. Shen, Y. Zhang, H. Ji, F. Gao, S. Yue, N. Kamo, Y. Zhai, M. Yamamoto, R.W. Busuttil, J.W. Kupiec-Weglinski, KEAP1-NRF2 complex in ischemia-induced hepatocellular damage of mouse liver transplants, J. Hepatol. 59 (2013) 1200–1207.
[40] J. St-Pierre, S. Drori, M. Uldry, J.M. Silvaggi, J. Rhee, S. Jager, C. Handschin, K. Zheng, J. Lin, W. Yang, D.K. Simon, R. Bachoo, B.M. Spiegelman, Suppression of reactive oxygen species and neurodegeneration by the PGC-1 transcriptional coactivators, Cell 127 (2006) 397–408.
[41] I. Valle, A. Alvarez-Barrientos, E. Arza, S. Lamas, M. Monsalve, PGC-1alpha regulates the mitochondrial antioxidant defense system in vascular endothelial cells, Cardiovasc Res. 66 (2005) 562–573.
[42] C. Sanchez-Ramos, A. Tierrez, O. Fabregat-Andres, B. Wild, F. Sanchez-Cabo, A. Arduini, A. Dopazo, M. Monsalve, PGC-1alpha regulates translocated in liposarcoma activity: role in oxidative stress gene expression, Antioxid. Redox Signal 15 (2011) 325–337.
[43] V. Krajka-Kuzniak, J. Paluszczak, W. Baer-Dubowska, The Nrf2-ARE signaling pathway: an update on its regulation and possible role in cancer prevention and treatment, Pharmacol. Rep. 69 (2016) 393–402.
[44] J. Rao, X. Qian, G. Li, X. Pan, C. Zhang, F. Zhang, Y. Zhai, X. Wang, L. Lu, ATF3-mediated NRF2/HO-1 signaling regulates TLR4 innate immune responses in mouse liver ischemia/reperfusion injury, Am. J. Transplant. 15 (2015) 76–87.
[45] S. Summermatter, C. Handschin, PGC-1alpha and exercise in the control of body weight, Int. J. Obes. 36 (2012) 1428–1435.
[46] S. Herzig, F. Long, U.S. Jhala, S. Hedrick, R. Quinn, A. Bauer, D. Rudolph, G. Schutz, C. Yoon, P. Puigserver, B. Spiegelman, M. Montminy, CREB regulates hepatic gluconeogenesis through the coactivator PGC-1, Nature 413 (2001) 179–183.
[47] E. Barroso, R. Rodriguez-Calvo, L. Serrano-Marco, A.M. Astudillo, J. Balsinde, X. Palomer, M. Vazquez-Carrera, The PPARbeta/delta activator GW501516 prevents the down-regulation of AMPK caused by a high-fat diet in liver and amplifies the PGC-1alpha-Lipin 1-PPARalpha pathway leading to increased fatty acid oxidation, Endocrinology 152 (2011) 1848–1859.
[48] M. Aharoni-Simon, M. Hann-Obercyger, S. Pen, Z. Madar, O. Tirosh, Fatty liver is associated with impaired activity of PPARgamma-coactivator 1alpha (PGC1alpha) and mitochondrial biogenesis in mice, Lab Investig. 91 (2011) 1018–1028.
[49] C. Sanchez Ramos, I. Prieto, A. Tierrez, J. Laso, M.P. Valdecantos, R. Bartrons, J. Rosello-Catafau, M. Monsalve, PGC-1alpha downregulation in the steatotic liver enhances ischemia-reperfusion injury and impairs ischemic preconditioning, Antioxid. Redox Signal (2017).
[50] J.A. Funk, R.G. Schnellmann, Accelerated recovery of renal mitochondrial and tubule homeostasis with SIRT1/PGC-1alpha activation following ischemia-reperfusion injury, Toxicol. Appl. Pharmacol. 273 (2013) 345–354.
[51] R.C. Gehrau, V.R. Mas, C.I. Dumur, J.L. Suh, A.K. Sharma, H.P. Cathro, D.G. Maluf, Donor hepatic steatosis induce exacerbated ischemia-reperfusion injury through activation of innate immune response molecular pathways, Transplantation 99 (2015) 2523–2533.
[52] Y. Luo, W. Zhu, J. Jia, C. Zhang, Y. Xu, NMDA receptor dependent PGC-1alpha up-regulation protects the cortical neuron against oxygen-glucose deprivation/reperfusion injury, J. Mol. Neurosci. 39 (2009) 262–268.
[53] Z.P. Evans, B.S. Mandavilli, J.D. Ellett, D. Rodwell, M.W. Fariss, R.N. Fiorini, R.G. Schnellmann, M.G. Schmidt, K. Chavin, Vitamin E succinate enhances steatotic liver energy status and prevents oxidative damage following ischemia/reperfusion, Transplant. Proc. 41 (2009) 4094–4098.
[54] D. Tello, E. Balsa, B. Acosta-Iborra, E. Fuertes-Yebra, A. Elorza, A. Ordonez, M. Corral-Escariz, I. Soro, E. Lopez-Bernardo, E. Perales-Clemente, A. Martinez-Ruiz, J.A. Enriquez, J. Aragones, S. Cadenas, M.O. Landazuri, Induction of the mitochondrial NDUFA4L2 protein by HIF-1alpha decreases oxygen consumption by inhibiting Complex I activity, Cell Metab. 14 (2011) 768–779.
[55] S. Movafagh, S. Crook, K. Vo, Regulation of hypoxia-inducible factor-1a by reactive oxygen species: new developments in an old debate, J. Cell Biochem. 116 (2015) 696–703.
[56] R. Cursio, C. Miele, N. Filippa, E. Van Obberghen, J. Gugenheim, Liver HIF-1 alpha induction precedes apoptosis following normothermic ischemia-reperfusion in rats, Transplant. Proc. 40 (2008) 2042–2045.
[57] M.A. Zaouali, I. Ben Mosbah, E. Boncompagni, H. Ben Abdennebi, M.T. Mitjavila, R. Bartrons, I. Freitas, A. Rimola, J. Rosello-Catafau, Hypoxia inducible factor-1alpha accumulation in steatotic liver preservation: role of nitric oxide, World J. Gastroenterol. 16 (2010) 3499–3509.
[58] B. Nath, I. Levin, T. Csak, J. Petrasek, C. Mueller, K. Kodys, D. Catalano, P. Mandrekar, G. Szabo, Hepatocyte-specific hypoxia-inducible factor-1alpha is a determinant of lipid accumulation and liver injury in alcohol-induced steatosis in mice, Hepatology 53 (2011) 1526–1537.
[59] L. Zhu, Q. Wang, L. Zhang, Z. Fang, F. Zhao, Z. Lv, Z. Gu, J. Zhang, J. Wang, K. Zen, Y. Xiang, D. Wang, C.Y. Zhang, Hypoxia induces PGC-1alpha expression and mitochondrial biogenesis in the myocardium of TOF patients, Cell Res. 20 (2010) 676–687.
[60] J. Shoag, Z. Arany, Regulation of hypoxia-inducible genes by PGC-1 alpha, Arterioscler. Thromb. Vasc. Biol. 30 (2010) 662–666.
[61] A. Rimessi, M. Previati, F. Nigro, M.R. Wieckowski, P. Pinton, Mitochondrial reactive oxygen species and inflammation: molecular mechanisms, diseases and

promising therapies, Int. J. Biochem. Cell Biol. 81 (2016) 281–293.
[62] H.Y. Tan, N. Wang, S. Li, M. Hong, X. Wang, Y. Feng, The reactive oxygen species in macrophage polarization: reflecting its dual role in progression and treatment of human diseases, Oxid. Med. Cell Longev. 2016 (2016) 2795090.
[63] H. Sasaki, H. Yamamoto, K. Tominaga, K. Masuda, T. Kawai, S. Teshima-Kondo, K. Rokutan, NADPH oxidase-derived reactive oxygen species are essential for differentiation of a mouse macrophage cell line (RAW264.7) into osteoclasts, J. Med. Investig. 56 (2009) 33–41.
[64] H.K. Choi, T.H. Kim, G.J. Jhon, S.Y. Lee, Reactive oxygen species regulate M-CSF-induced monocyte/macrophage proliferation through SHP1 oxidation, Cell Signal 23 (2011) 1633–1639.
[65] C.J. Hall, L.E. Sanderson, K.E. Crosier, P.S. Crosier, Mitochondrial metabolism, reactive oxygen species, and macrophage function-fishing for insights, J. Mol. Med. 92 (2014) 1119–1128.
[66] P. Czubkowski, P. Socha, J. Pawlowska, Oxidative stress in liver transplant recipients, Ann. Transplant. 16 (2011) 99–108.
[67] K. Muffak-Granero, C. Olmedo, T. Villegas, A. Comino, A. Becerra, J.M. Villar, Y. Fundora, D. Garrote, P. Bueno, J.A. Ferron, Perioperative values of glutathione peroxidase activity and malondialdehyde levels in enolic cirrhotic recipients of a liver transplant, Transplant. Proc. 44 (2012) 2071–2073.
[68] T. Villegas, C. Olmedo, K. Muffak-Granero, A. Comino, D. Garrote, P. Bueno, J.A. Ferron, Perioperative levels of glutathione reductase in liver transplant recipients with hepatitis C virus cirrhosis, Transplant. Proc. 44 (2012) 1542–1544.
[69] L. Hassan, P. Bueno, I. Ferron-Celma, J.M. Ramia, D. Garrote, K. Muffak, A. Garcia-Navarro, A. Mansilla, J.M. Villar, J.A. Ferron, Time course of antioxidant enzyme activities in liver transplant recipients, Transplant. Proc. 37 (2005) 3932–3935.
[70] V.S. Augusto, A.J. Rodrigues, G.S. Reis, A.P. Silveira, O. de Castro e Silva Jr., E.D. Mente, A.A. Jordao Jr., P.R. Evora, Evaluation of oxidative stress in the late postoperative stage of liver transplantation, Transplant. Proc. 46 (2014) 1453–1457.
[71] H. Tashiro, S. Kuroda, Y. Mikuriya, H. Ohdan, Ischemia-reperfusion injury in patients with fatty liver and the clinical impact of steatotic liver on hepatic surgery, Surg. Today 44 (2014) 1611–1625.
[72] V. Defamie, R. Cursio, K. Le Brigand, C. Moreilhon, M.C. Saint-Paul, M. Laurens, D. Crenesse, B. Cardinaud, P. Auberger, J. Gugenheim, P. Barbry, B. Mari, Gene expression profiling of human liver transplants identifies an early transcriptional signature associated with initial poor graft function, Am. J. Transplant. 8 (2008) 1221–1236.
[73] Y.F. Tsai, F.C. Liu, W.C. Sung, C.C. Lin, P.C. Chung, W.C. Lee, H.P. Yu, Ischemic reperfusion injury-induced oxidative stress and pro-inflammatory mediators in liver transplantation recipients, Transplant. Proc. 46 (2014) 1082–1086.
[74] M.J. Chu, R. Vather, A.J. Hickey, A.R. Phillips, A.S. Bartlett, Impact of ischemic preconditioning on outcome in clinical liver surgery: a systematic review, Biomed. Res. Int. 2015 (2015) 370451.
[75] P.A. Clavien, M. Selzner, H.A. Rudiger, R. Graf, Z. Kadry, V. Rousson, W. Jochum, A prospective randomized study in 100 consecutive patients undergoing major liver resection with versus without ischemic preconditioning, Ann. Surg. 238 (843–850) (2003) (discussion 851-842).
[76] P.A. Clavien, S. Yadav, D. Sindram, R.C. Bentley, Protective effects of ischemic preconditioning for liver resection performed under inflow occlusion in humans, Ann. Surg. 232 (2000) 155–162.
[77] O. Hahn, A. Blazovics, L. Vali, P.K. Kupcsulik, The effect of ischemic preconditioning on redox status during liver resections–randomized controlled trial, J. Surg. Oncol. 104 (2011) 647–653.
[78] H.A. Zapata-Chavira, P. Cordero-Perez, A. Casillas-Ramirez, M.M. Escobedo-Villarreal, E. Perez-Rodriguez, L. Torres-Gonzalez, C. Camara-Lemarroy, M.A. Hernandez-Guedea, E. Caballero-Mendoza, L.E. Munoz-Espinosa, Is ischemic preconditioning a useful therapeutic strategy in liver transplantation? Results from the first pilot study in Mexico, Arch. Med. Res. 46 (2015) 296–302.
[79] P. Andreani, E. Hoti, S. de la Serna, D. degli Esposti, M. Sebagh, A. Lemoine, P. Ichai, F. Saliba, D. Castaing, D. Azoulay, Ischaemic preconditioning of the graft in adult living related right lobe liver transplantation: impact on ischaemia-reperfusion injury and clinical relevance, HPB 12 (2010) 439–446.
[80] J.C. Bucuvalas, F.C. Ryckman, S. Krug, M.H. Alonso, W.F. Balistreri, U. Kotagal, Effect of treatment with prostaglandin E1 and N-acetylcysteine on pediatric liver transplant recipients: a single-center study, Pediatr. Transplant. 5 (2001) 274–278.
[81] A.W. Khan, B.J. Fuller, S.R. Shah, B.R. Davidson, K. Rolles, A prospective randomized trial of N-acetyl cysteine administration during cold preservation of the donor liver for transplantation, Ann. Hepatol. 4 (2005) 121–126.
[82] M. Aliakbarian, S. Nikeghbalian, S. Ghaffaripour, A. Bahreini, M. Shafiee, M. Rashidi, Y. Rajabnejad, Effects of N-acetylcysteine addition to University of Wisconsin solution on the rate of ischemia-reperfusion injury in adult orthotopic liver transplant. Exp. Clin. Transplant. (2015).
[83] S.M. Robinson, R. Saif, G. Sen, J.J. French, B.C. Jaques, R.M. Charnley, D.M. Manas, S.A. White, N-acetylcysteine administration does not improve patient outcome after liver resection, HPB 15 (2013) 457–462.
[84] S. Jegatheeswaran, A.K. Siriwardena, Experimental and clinical evidence for modification of hepatic ischaemia-reperfusion injury by N-acetylcysteine during major liver surgery, HPB 13 (2011) 71–78.
[85] M.A. Barros, P.R. Vasconcelos, C.M. Souza, G.M. Andrade, M.O. Moraes, P.E. Costa, G.R. Coelho, J.H. Garcia, L-alanyl-glutamine attenuates oxidative stress in liver transplantation patients, Transplant. Proc. 47 (2015) 2478–2482.
[86] A. Nickkholgh, H. Schneider, M. Sobirey, W.P. Venetz, U. Hinz, H. Pelzl le, D.N. Gotthardt, A. Cekauskas, M. Manikas, S. Mikalauskas, L. Mikalauskene, H. Bruns, M. Zorn, M.A. Weigand, M.W. Buchler, P. Schemmer, The use of high-dose melatonin in liver resection is safe: first clinical experience, J. Pineal Res. 50 (2011) 381–388.
[87] P. Schemmer, A. Nickkholgh, H. Schneider, M. Sobirey, M. Weigand, M. Koch, J. Weitz, M.W. Buchler, PORTAL: pilot study on the safety and tolerance of preoperative melatonin application in patients undergoing major liver resection: a double-blind randomized placebo-controlled trial, BMC Surg. 8 (2008) 2.
[88] Y.F. Tsai, C.C. Lin, W.C. Lee, H.P. Yu, Propofol attenuates ischemic reperfusion-induced formation of lipid peroxides in liver transplant recipients, Transplant. Proc. 44 (2012) 376–379.
[89] R.H. Bhogal, S.M. Curbishley, C.J. Weston, D.H. Adams, S.C. Afford, Reactive oxygen species mediate human hepatocyte injury during hypoxia/reoxygenation, Liver Transpl. 16 (2010) 1303–1313.
[90] R. Adam, V. Delvart, V. Karam, C. Ducerf, F. Navarro, C. Letoublon, J. Belghiti, D. Pezet, D. Castaing, Y.P. Le Treut, J. Gugenheim, P. Bachellier, J. Pirenne, P. Muiesan, Eltr contributing centres, t. E. L. I. T. A., Compared efficacy of preservation solutions in liver transplantation: a long-term graft outcome study from the European liver transplant registry, Am. J. Transplant. 15 (2015) 395–406.
[91] M.A. Zaouali, H. Ben Abdennebi, S. Padrissa-Altes, I. Alfany-Fernandez, A. Rimola, J. Rosello-Catafau, How Institut Georges Lopez preservation solution protects nonsteatotic and steatotic livers against ischemia-reperfusion injury, Transplant. Proc. 43 (2011) 77–79.
[92] D. Hide, M. Ortega-Ribera, A. Fernandez-Iglesias, C. Fondevila, M.J. Salvado, L. Arola, J.C. Garcia-Pagan, A. Mancini, J. Bosch, J. Gracia-Sancho, A novel form of the human manganese superoxide dismutase protects rat and human livers undergoing ischaemia and reperfusion injury, Clin. Sci. 127 (2014) 527–537.
[93] J.V. Guarrera, S.D. Henry, B. Samstein, R. Odeh-Ramadan, M. Kinkhabwala, M.J. Goldstein, L.E. Ratner, J.F. Renz, H.T. Lee, R.S. Brown Jr., J.C. Emond, Hypothermic machine preservation in human liver transplantation: the first clinical series, Am. J. Transplant. 10 (2010) 372–381.
[94] S.D. Henry, E. Nachber, J. Tulipan, J. Stone, C. Bae, L. Reznik, T. Kato, B. Samstein, J.C. Emond, J.V. Guarrera, Hypothermic machine preservation reduces molecular markers of ischemia/reperfusion injury in human liver transplantation, Am. J. Transplant. 12 (2012) 2477–2486.
[95] B.G. Bruinsma, H. Yeh, S. Ozer, P.N. Martins, A. Farmer, W. Wu, N. Saeidi, S. Op den Dries, T.A. Berendsen, R.N. Smith, J.F. Markmann, R.J. Porte, M.L. Yarmush, K. Uygun, M.L. Izamis, Subnormothermic machine perfusion for ex vivo preservation and recovery of the human liver for transplantation, Am. J. Transplant. 14 (2014) 1400–1409.